STRESS and STRAIN

А. П. ЦЕЛИКОВ

Теория расчета усилий в прокатных станах

ИЗДАТЕЛЬСТВО «МЕТАЛЛУРГИЯ»
МОСКВА

A. TSELIKOV

in METAL ROLLING

Translated from the Russian
by
W. U. SIRK

MIR PUBLISHERS • MOSCOW 1967

UDC 621.771.2 (075.8) = 20

Revised from the Russian 1962 Edition

RUSSIAN ALPHABET WITH TRANSLITERATION

Аа	a	Рр	r
Бб	b	Сс	s
Вв	v	Тт	t
Гг	g	Уу	u
Дд	d	Фф	f
Ее	e	Хх	kh
Жж	zh	Цц	ts
Зз	z	Чч	ch
Ии	i	Шш	sh
Йй	y	Щщ	shch
Кк	k	Ъъ	″
Лл	l	Ыы	y
Мм	m	Ьь	′
Нн	n	Ээ	é
Оо	o	Юю	yu
Пп	p	Яя	ya

На английском языке

Contents

I

Theory of Stress and Strain

1. STRESS TENSOR

The forces which must be applied to a solid when it is deformed under pressure are determined not only by the natural properties of this solid. They also depend on the conditions under which the process of deformation is taking place, and, in particular, on the stresses which arise in the solid as its shape is being altered.

The direction of a stress vector on a given surface can vary: hence it is convenient to decompose it into two vectors, the one being normal and the other being tangential to the surface in question. The first vector is called *the vector of normal stress* and is denoted by the letter σ, whilst the other is called *the vector of tangential* or *shear stress* and is denoted by the letter τ.

In an orthogonal coordinate system, when one of the axes is perpendicular to the surface being considered and hence coincides with the direction of the normal stress, the vector of total stress for this surface is specified by the two projections parallel to the remaining two coordinate axes. Consequently, the total stress vector is determined by one normal stress vector and two tangential stress vectors.

In view of the fact that three mutually perpendicular surfaces corresponding to the coordinate axes XYZ (Fig. 1) have to be consid-

ered for the analysis of the state of stress of any solid, the state of stress is specified by the nine quantities

$$T = \begin{vmatrix} \sigma_x \tau_{xy} \tau_{xz} \\ \tau_{yx} \sigma_y \tau_{yz} \\ \tau_{zx} \tau_{zy} \sigma_z \end{vmatrix} \tag{I.1}$$

These nine quantities, which are dependent on the orthogonal coordinate system employed, constitute *a stress tensor.*

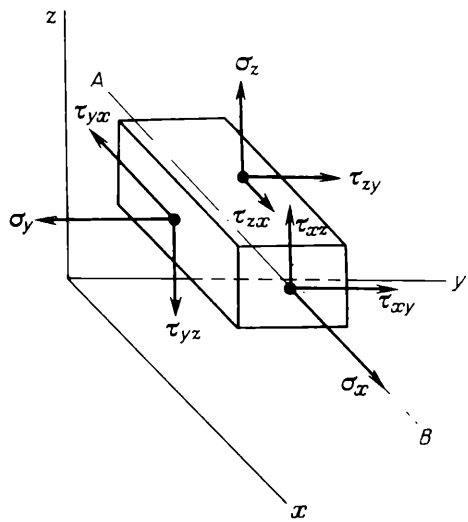

Fig. 1. The nine stress vectors for a given orthogonal coordinate system

In effect the tensor consists not of nine but six quantities, since the values of the tangential stresses disposed symmetrically about its main diagonal are the same, i.e.,

$$\tau_{xy} = \tau_{yx} \quad \tau_{xz} = \tau_{zx} \quad \tau_{yz} = \tau_{zy} \tag{I.2}$$

This can easily be verified if one considers the equilibrium of the parallelepiped shown in Fig. 1. Since the moment of the forces acting on the parallelepiped must be zero about the AB axis, then

$$\tau_{yz}\, dx\, dy\, dz - \tau_{zy}\, dx\, dy\, dz = 0$$

or

$$\tau_{yz} = \tau_{zy}$$

where dx, dy and dz are the sides of the parallelepiped.

The remaining two equations (I.2) can be proved in a similar manner.

2. PRINCIPAL AXES OF STRESS

We shall show that in a three-dimensional state of stress there exist three mutually perpendicular surfaces on which the tangential stresses are zero.

The normal stress on an arbitrarily chosen surface (Fig. 2) can be represented in terms of the total stress s and its projections s_x, s_y

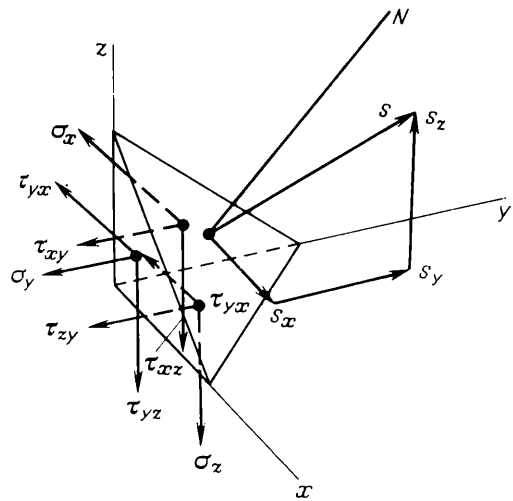

Fig. 2. The stresses on the faces of a tetrahedron

and s_z on the coordinate axes by the expression

$$\sigma = s\cos(s,\ N) = s_x l + s_y m + s_z n \tag{I.3}$$

where l, m and n are the cosines of the angles which the coordinate axes make with the normal N to the given surface.

Considering the equilibrium of the tetrahedron formed by an inclined plane and the three planes passing through the coordinate axes we find that

$$s_x F = \sigma_x F_x + \tau_{yx} F_y + \tau_{zx} F_z$$

where F_x, F_y, F_z and F are the areas of the faces of the tetrahedron.

Since

$$F_x = Fl \quad F_y = Fm \quad \text{and} \quad F_z = Fn$$

then

$$s_x = \sigma_x l + \tau_{yx} m + \tau_{zx} n \tag{I.3a}$$

Projecting the forces acting on the tetrahedron on the other two coordinate axes, we have

$$s_y = \sigma_y m + \tau_{xy} l + \tau_{zy} n \tag{I.3b}$$

and

$$s_z = \sigma_z n + \tau_{xz} l + \tau_{yz} m \tag{I.3c}$$

We substitute these values of s_x, s_y and s_z into equation (I.3):

$$\sigma = \sigma_x l^2 + \tau_{yx} ml + \tau_{zx} nl + \sigma_y m^2 + \tau_{xy} lm + \tau_{zy} nm + \sigma_z n^2 + \\ + \tau_{xz} ln + \tau_{yz} mn$$

or, noting equations (I.2),

$$\sigma = \sigma_x l^2 + \sigma_y m^2 + \sigma_z n^2 + 2\tau_{xy} lm + 2\tau_{xz} ln + 2\tau_{yz} mn \tag{I.4}$$

In the same system of coordinates we draw a straight line r from the origin, parallel to the normal N, and of length

$$r = \sqrt{\frac{C}{\sigma}}$$

where C is an arbitrary constant.

Denoting the projections of the straight line r on the coordinate axes by x, y and z, we obtain

$$l = \frac{x}{r} \quad m = \frac{y}{r} \quad n = \frac{z}{r}$$

When these values are substituted into equation (I.4) it will acquire the following form:

$$\sigma_x x^2 + \sigma_y y^2 + \sigma_z z^2 + 2\tau_{xz} xz + 2\tau_{xy} xy + 2\tau_{yz} yz = C \tag{I.5}$$

This is the equation of an ellipsoid whose centre is at the origin, but whose principal axes do not coincide with the coordinate axes.

When the coordinate axes are rotated relative to the ellipsoid so as to coincide with its principal axes, equation (I.5) assumes the form

$$\sigma_x x_1^2 + \sigma_y y_1^2 + \sigma_z z_1^2 = C$$

and the following coefficients become zero:

$$\tau_{xy} = \tau_{xz} = \tau_{yz} = 0$$

From this it follows that in a three-dimensional state of stress *only normal stresses act on three mutually perpendicular planes, the shear stresses being zero.*

The normal stresses on these planes are called *principal normal stresses.*

Principal normal stresses are usually denoted by σ_1, σ_2 and σ_3.

3. GRAPHICAL REPRESENTATION OF STRESSES IN A THREE-DIMENSIONAL STRESS STATE

We shall determine the relation between the normal and tangential stresses which arise on a plane inclined at an angle to the principal axes of stress.

Let us express the normal and shear stresses on the inclined plane of the tetrahedron (Fig. 2) in terms of the principal normal stresses, when these are directed parallel to the coordinate axes:

$$\sigma = \sigma_1 l^2 + \sigma_2 m^2 + \sigma_3 n^2 \tag{I.6}$$

$$\tau^2 = s^2 - \sigma^2 = \sigma_1^2 l^2 + \sigma_2^2 m^2 + \sigma_3^2 n^2 - (\sigma_1 l^2 + \sigma_2 m^2 + \sigma_3 n^2)^2 \tag{I.7}$$

To these equations must be added the equation

$$l^2 + m^2 + n^2 = 1 \tag{I.8}$$

Solving for l, m and n we have:

$$l^2 = \frac{\tau^2 + (\sigma - \sigma_2)(\sigma - \sigma_3)}{(\sigma_1 - \sigma_2)(\sigma_1 - \sigma_3)} \tag{I.9}$$

$$m^2 = \frac{\tau^2 + (\sigma - \sigma_1)(\sigma - \sigma_3)}{(\sigma_2 - \sigma_1)(\sigma_2 - \sigma_3)} \tag{I.10}$$

$$n^2 = \frac{\tau^2 + (\sigma - \sigma_1)(\sigma - \sigma_2)}{(\sigma_3 - \sigma_1)(\sigma_3 - \sigma_2)} \tag{I.11}$$

We number the principal normal stresses so that the inequality

$$\sigma_1 \geqslant \sigma_2 \geqslant \sigma_3$$

holds.

For real values of l, m and n satisfying equations (I.9), (I.10) and (I.11), the numerators in equations (I.9) and (I.11) must be positive, whilst the numerator in (I.10) must be negative, i.e.,

$$\tau^2 + (\sigma - \sigma_2)(\sigma - \sigma_3) \geqslant 0 \tag{I.12}$$

$$\tau^2 + (\sigma - \sigma_1)(\sigma - \sigma_2) \geqslant 0 \tag{I.13}$$

and

$$\tau^2 + (\sigma - \sigma_1)(\sigma - \sigma_3) \leqslant 0 \tag{I.14}$$

As a particular case of these conditions we obtain the equations of circles whose centres are located on the σ-axis (Fig. 3):

$$\tau^2 + (\sigma - \sigma_2)(\sigma - \sigma_3) = 0 \tag{I.15}$$

$$\tau^2 + (\sigma - \sigma_1)(\sigma - \sigma_2) = 0 \tag{I.16}$$

$$\tau^2 + (\sigma - \sigma_1)(\sigma - \sigma_3) = 0 \tag{I.17}$$

The geometrical significance of these equations can be shown by simple transformations. For example, if we add $\left(\frac{\sigma_2-\sigma_3}{2}\right)^2$ to both sides of equation (I.15), we obtain

$$\tau^2+\left(\sigma-\frac{\sigma_2+\sigma_3}{2}\right)^2=\left(\frac{\sigma_2-\sigma_3}{2}\right)^2$$

i.e., the equation for a circle whose radius equals $\frac{\sigma_2-\sigma_3}{2}$, and whose centre is located on the σ-axis the distance $\frac{\sigma_2+\sigma_3}{2}$ from the origin.

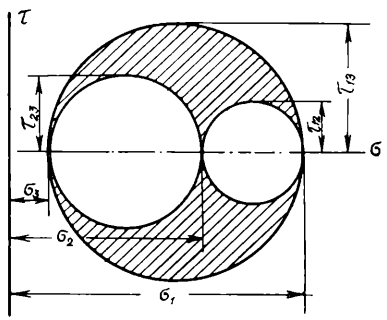

Fig. 3. The circles of stress

The left-hand side of the expressions (I.12) and (I.13) can be zero or greater than zero, whilst the expression (I.14) can be less than zero. Accordingly, σ and τ must lie outside the circles constructed on the diameters $\sigma_1-\sigma_2$ and $\sigma_2-\sigma_3$, and at the same time they must lie inside the circle constructed on the diameter $\sigma_1-\sigma_3$ (Fig. 3), i.e., the normal and shear stresses are specified by a point lying within the shaded area shown in Fig. 3.

By using the stress circle diagram for a three-dimensional state of stress, we can find the limiting values of the normal and shear stresses. This graphical representation of stresses was suggested by Mohr.

Two important conclusions can be drawn from the stress circle diagram.

1. The value of the normal stress on any plane lies between the limits σ_1 and σ_3, i.e., one of the principal stresses, σ_1, is the maximum, and the other, σ_3, the minimum normal stress.

2. There are three extremal values of shear stress, equal to the radii of the stress circles

$$\tau_{12}=\frac{\sigma_1-\sigma_2}{2} \qquad \tau_{13}=\frac{\sigma_1-\sigma_3}{2} \qquad \tau_{23}=\frac{\sigma_2-\sigma_3}{2} \tag{I.18}$$

the greatest of which (τ_{13}) occurs on the plane where the normal stress

$$\sigma = \frac{\sigma_1 + \sigma_3}{2}$$

These three values of shear stresses, τ_{12}, τ_{13} and τ_{23}, are termed *principal shear stresses.*

4. DETERMINATION OF THE ORIENTATION OF THE PLANES OF PRINCIPAL SHEAR STRESS

The orientation of the planes of principal shear stress is determined from equations (I.9), (I.10) and (I.11), by substituting the appropriate values

$$\sigma = \frac{\sigma_1 + \sigma_3}{2} \quad \text{and} \quad \tau = \frac{\sigma_1 - \sigma_3}{2}$$

from which the orientation of the plane where the shear stress attains a maximum value is found relative to the principal axes of stress:

$$l^2 = \frac{\left(\frac{\sigma_1 - \sigma_3}{2}\right)^2 + \left(\frac{\sigma_1 + \sigma_3}{2} - \sigma_2\right)\left(\frac{\sigma_1 + \sigma_3}{2} - \sigma_3\right)}{(\sigma_1 - \sigma_2)(\sigma_1 - \sigma_3)} = \frac{1}{2}$$

or

$$l = \pm \frac{1}{\sqrt{2}} \quad \alpha_x = 45°$$

and

$$m^2 = \frac{\left(\frac{\sigma_1 - \sigma_3}{2}\right)^2 + \left(\frac{\sigma_1 + \sigma_3}{2} - \sigma_1\right)\left(\frac{\sigma_1 + \sigma_3}{2} - \sigma_3\right)}{(\sigma_2 - \sigma_1)(\sigma_2 - \sigma_3)} = 0$$

or

$$\alpha_y = 0$$

where α_x and α_y are the angles between the normal to the required plane and the principal axes of stress.

Thus the plane on which the shear stress attains its greatest value is inclined at an angle of 45° to the direction of the stresses σ_1 and σ_3, and is parallel to the direction of the stress σ_2 (Fig. 4*a*). There are two such planes. They are equally inclined to the σ_1-axis and include an angle of 90° between themselves.

The orientations of the remaining two principal shear stresses are found in a similar manner (Fig. 4*b* and *c*).

Bearing in mind that to each plane we can asign another one parallel to it in such a way that the stresses on these planes balance each other, the planes of action of all three principal shear stresses

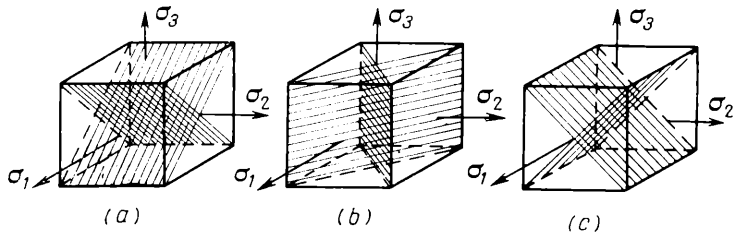

Fig. 4. Orientation of the planes of principal shear stress:

(a) $\tau_{13}=\frac{\sigma_1-\sigma_3}{2}$; b) $\tau_{12}=\frac{\sigma_1-\sigma_2}{2}$; (c) $\tau_{23}=\frac{\sigma_2-\sigma_3}{2}$

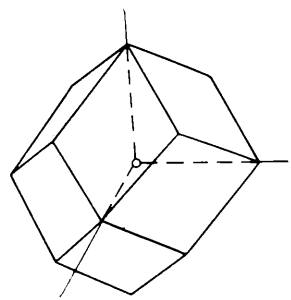

Fig. 5. The rhombic dodecahedron formed by the planes of principal shear stress

may be represented in the form of a rhombic dodecahedron (Fig. 5). For this reason principal shear stresses are also called *dodecahedral stresses.*

5. OCTAHEDRAL STRESSES

The stresses on a plane which makes the same angle with the three principal axes of stress are called *octahedral*, since there are eight such planes in all and together they form an octahedron (Fig. 6).

Octahedral stresses, like principal normal and shear stresses, possess certain characteristic properties.

The angle between a plane of the octahedron and a principal stress axis is found from the equation

$$l^2+m^2+n^2=1$$

Since

$$l = m = n$$

then obviously

$$l = m = n = \frac{1}{\sqrt{3}} \quad (\alpha \approx 55^\circ)$$

We determine the normal octahedral stress from equation (I.6), substituting the values of l, m and n:

$$\sigma_{oct} = \frac{\sigma_1 + \sigma_2 + \sigma_3}{3} \tag{I.19}$$

that is, the normal octahedral stress is equal to the mean of the principal stresses at a given point.

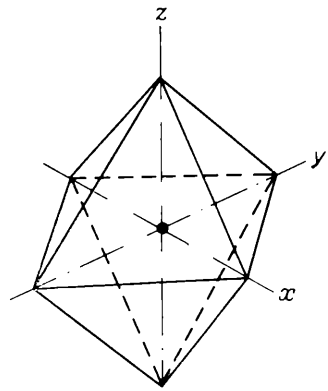

Fig. 6. An octahedron

This stress is also called *the mean hydrostatic pressure.* Since a plastic strain results only from a change in the shape (not volume) of the body, this stress does not give rise to a plastic strain. It produces only a change in volume (dilatation) and a corresponding elastic strain.

We determine the shear stress from equation (I.7):

$$\tau_{oct}^2 = s_{oct}^2 - \sigma_{oct}^2 = \frac{\sigma_1^2 + \sigma_2^2 + \sigma_3^2}{3} - \left(\frac{\sigma_1 + \sigma_2 + \sigma_3}{3}\right)^2$$

Simplifying this expression we obtain

$$\tau_{oct}^2 = \frac{2}{9}(\sigma_1^2 + \sigma_2^2 + \sigma_3^2 - \sigma_1\sigma_2 - \sigma_1\sigma_3 - \sigma_2\sigma_3) \tag{I.20}$$

or

$$\tau_{oct} = \frac{1}{3}\sqrt{(\sigma_1 - \sigma_2)^2 + (\sigma_1 - \sigma_3)^2 + (\sigma_2 - \sigma_3)^2} \tag{I.21}$$

Expressing τ_{oct} in terms of the principal shear stresses we have

$$\tau_{oct} = \frac{2}{3}\sqrt{\tau_{12}^2 + \tau_{13}^2 + \tau_{23}^2} \tag{I.22}$$

In contrast to the octahedral normal stress, this octahedral shear stress does not produce a volume change but leads to deformation of the body.

This stress is of great importance in the study of plastic deformation, and it will be shown later that it is proportional to that part of the potential energy of elastic strain which tends to deform the body without producing volume changes.

6. THIRTEEN SPECIAL PLANES OF STRESS

It was shown above that in a three-dimensional state of stress there are three mutually perpendicular planes with principal normal stresses acting on them. These three planes, together with three other

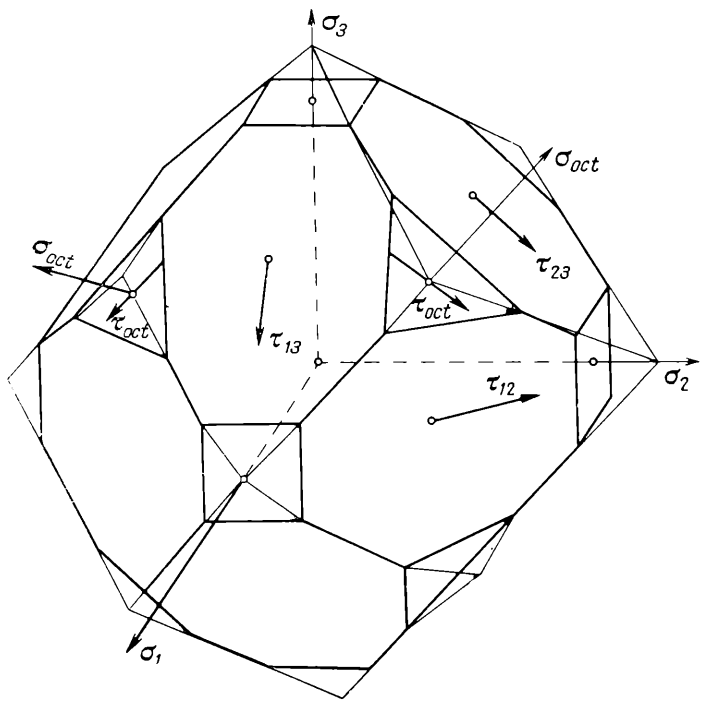

Fig. 7. A twenty-six sided solid showing the thirteen stress planes

planes which are parallel to them and which carry opposing stresses, can be represented conveniently in the form of a cube whose faces are perpendicular to the principal axes of stress.

For this reason principal normal stresses are also called *cubic stresses.*

The six planes of principal shear stress, as was mentioned above, can be represented by a dodecahedron (see Fig. 5).

Adding the four planes of octahedral stress to the three planes of principal normal stress and the six planes of principal shear stress enumerated above, we have altogether thirteen planes of stress which have a number of interesting properties.

These thirteen planes, taken together with other thirteen which are parallel to them, can be represented conveniently in the form of a 26-faced solid, a hexaicosahedron (Fig. 7).

7. STRESS INVARIANTS AND MEAN STRESS

Let us consider the equation of equilibrium of the tetrahedron shown in Fig. 2, when the inclined face coincides with one of the planes of principal normal stress. Then equations (I.3a) to (I.3c) assume the following form:

$$s_x = \sigma l = \sigma_x l + \tau_{yx} m + \tau_{zx} n$$

$$s_y = \sigma m = \sigma_y m + \tau_{xy} l + \tau_{zy} n$$

$$s_z = \sigma n = \sigma_z n + \tau_{xz} l + \tau_{yz} m$$

where σ is the stress acting on the inclined plane of the tetrahedron

s_x, s_y and s_z are projections of this stress on the coordinate axes (Fig. 8).

These three equations are supplemented by

$$l^2 + m^2 + n^2 = 1$$

We express σ by the components of the stress tensor, i.e., we eliminate l, m and n from these four equations. We thus obtain

$$\sigma^3 - (\sigma_x + \sigma_y + \sigma_z)\,\sigma^2 + (\sigma_x\sigma_y + \sigma_x\sigma_z + \sigma_y\sigma_z - \tau_{xy}^2 - \tau_{xz}^2 - \tau_{yz}^2)\,\sigma - \\ - (\sigma_x\sigma_y\sigma_z + 2\tau_{xy}\tau_{xz}\tau_{yz} - \sigma_x\tau_{yz}^2 - \sigma_y\tau_{xz}^2 - \sigma_z\tau_{yx}^2) = 0 \quad \text{(I.23)}$$

The three roots of this cubic equation will give the three values of principal normal stress $\sigma = \sigma_1$, $\sigma = \sigma_2$ and $\sigma = \sigma_3$. The values of the principal normal stress do not depend on the coordinate axes;

consequently, the values of the coefficients for a given point will be constant for any direction of the coordinate axes. For this reason

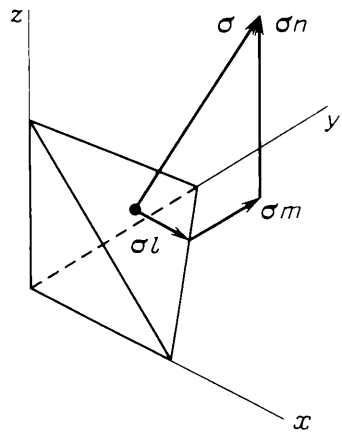

Fig. 8. The equilibrium of a tetrahedron

these coefficients are called *stress invariants*, and they can also be expressed in terms of the principal normal stresses. We have:

the linear invariant

$$\sigma_x + \sigma_y + \sigma_z = \sigma_1 + \sigma_2 + \sigma_3 \tag{I.24}$$

the quadratic invariant

$$\sigma_x\sigma_y + \sigma_x\sigma_z + \sigma_y\sigma_z - \tau_{xy}^2 - \tau_{xz}^2 - \tau_{yz}^2 = \sigma_1\sigma_2 + \sigma_1\sigma_3 + \sigma_2\sigma_3 \tag{I.25}$$

and the cubic invariant

$$\sigma_x\sigma_y\sigma_z + 2\tau_{xy}\tau_{xz}\tau_{yz} - \sigma_x\tau_{yz}^2 - \sigma_y\tau_{xz}^2 - \sigma_z\tau_{xy}^2 = \sigma_1\sigma_2\sigma_3 \tag{I.26}$$

The first two stress invariants have a definite physical meaning. The linear invariant divided by three equals the mean stress, which is also termed *the hydrostatic pressure* or *octahedral normal stress* (I.19):

$$\frac{\sigma_x + \sigma_y + \sigma_z}{3} = \frac{\sigma_1 + \sigma_2 + \sigma_3}{3} = \sigma_m \tag{I.27}$$

It characterizes the change in the volume of the body being strained, i.e., its elastic strain.

Using the quadratic and linear invariants in a modified form, as will be shown later, we can find an expression for that part of the potential energy of elastic strain which tends to change the shape of the body being strained.

8. EXPRESSION OF SMALL STRAINS IN TERMS OF PARTIAL DERIVATIVES

Let us study the deformation of a body by means of an infinitely small parallelepiped $dxdydz$ belonging to it (Fig. 9). As a result of the deformation, the parallelepiped is displaced, and the point A takes up the position of the point A_1 (Fig. 10). We denote the displacement of this point along the coordinate axes by u, v and w.

If as a result of the deformation the point A has been displaced along the x-axis by an amount u, then as a result of the deformation of the section dx the point B is displaced by the amount

$$u + \frac{\partial u}{\partial x} dx$$

where $\frac{\partial u}{\partial x}$ is the increment of the function u in the direction of the x-axis.

Since the increment of an element of length dx is $\frac{\partial u}{\partial x} dx$, the normal strain in the direction of the x-axis is

$$\varepsilon_x = \frac{\partial u}{\partial x} \tag{I.28}$$

Analogous expressions for the normal strains in the direction of the y- and z-axes are:

$$\varepsilon_y = \frac{\partial v}{\partial y} \quad \text{and} \quad \varepsilon_z = \frac{\partial w}{\partial z} \tag{I.29}$$

As a result of shear deformation the sides AB and AC of the parallelepiped need not be parallel to the coordinate axes. The sum of the angles of rotation of these sides will obviously be the expression for the shear deformation in the plane of the x- and y-axes:

$$\gamma_{xy} = \alpha + \beta$$

To determine the angle α we find the displacement of the point B in the direction of the y-axis. If the point A has been displaced an amount v in the direction of the y-axis, then the point B must be displaced by the amount

$$v + \frac{\partial v}{\partial x} dx$$

where the partial derivative indicates the variation of the function v in the direction of the x-axis. The angle α can then be expressed by the difference in the displacements of the points B_1 and A_1 in the

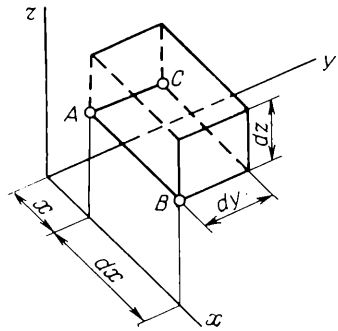

Fig. 9. Deformation of a parallelepiped

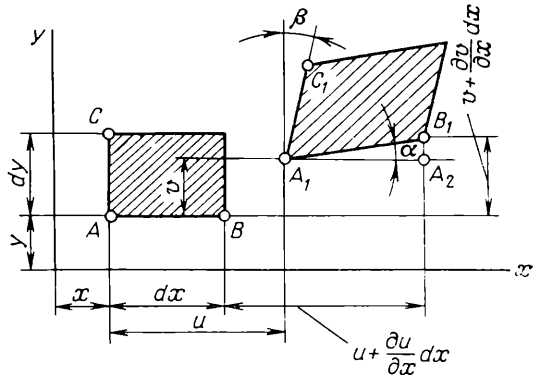

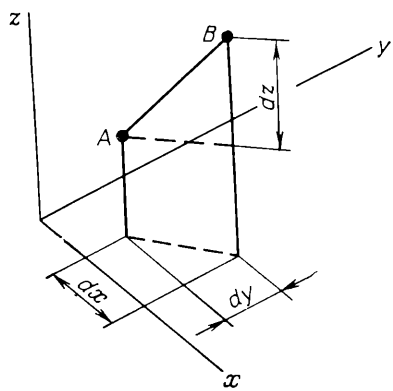

Fig. 10. Deformation of a line segment

direction of the y-axis, divided by A_1A_2:

$$\tan\alpha = \frac{v + \frac{\partial v}{\partial x}\,dx - v}{u + \frac{\partial u}{\partial x}\,dx - u + dx}$$

Bearing in mind that in the present case small deformations are considered, and that the quantity $\frac{\partial u}{\partial x}\,dx$ is small in comparison with dx, we obtain

$$\alpha = \frac{\partial v}{\partial x}$$

and furthermore

$$\gamma_{xy} = \frac{\partial u}{\partial y} + \frac{\partial v}{\partial x} \tag{I.30}$$

In the same way we find the shear strain in the remaining two planes:

$$\gamma_{xz} = \frac{\partial u}{\partial z} + \frac{\partial w}{\partial x} \qquad \gamma_{yz} = \frac{\partial v}{\partial z} + \frac{\partial w}{\partial y} \tag{I.31}$$

9. PRINCIPAL AXES OF STRAIN

Let us consider the deformation of the line segment AB (Fig. 10). As a result of the deformation the points A and B will be displaced by different amounts. If the displacement components of the point A equal u, v and w, then the displacement components of the point B will be

$$u_1 = u + du \qquad v_1 = v + dv \qquad w_1 = w + dw$$

or

$$u + du = u + \frac{\partial u}{\partial x}\,dx + \frac{\partial u}{\partial y}\,dy + \frac{\partial u}{\partial z}\,dz$$

$$v + dv = v + \frac{\partial v}{\partial x}\,dx + \frac{\partial v}{\partial y}\,dy + \frac{\partial v}{\partial z}\,dz$$

$$w + dw = w + \frac{\partial w}{\partial x}\,dx + \frac{\partial w}{\partial y}\,dy + \frac{\partial w}{\partial z}\,dz$$

After the deformation we can express the length of the segment AB (with its initial length taken to be unity) as follows, having projected it on the coordinate axes:

$$(1+\varepsilon)^2 = (dx + du)^2 + (dy + dv)^2 + (dz + dw)^2 =$$

$$= \left(dx + \frac{\partial u}{\partial x}\,dx + \frac{\partial u}{\partial y}\,dy + \frac{\partial u}{\partial z}\,dz\right)^2 + \left(dy + \frac{\partial v}{\partial x}\,dx + \right.$$

$$\left. + \frac{\partial v}{\partial y}\,dy + \frac{\partial v}{\partial z}\,dz\right)^2 + \left(dz + \frac{\partial w}{\partial x}\,dx + \frac{\partial w}{\partial y}\,dy + \frac{\partial w}{\partial z}\,dz\right)^2 \tag{I.32}$$

Denoting the cosines of the angles between the segment AB and the coordinate axes by l, m and n respectively, we find that $dx = l$, $dy = m$ and $dz = n$.

After substituting these values into equation (I.32) we have

$$(1+\varepsilon)^2 = \left[l\left(1+\frac{\partial u}{\partial x}\right) + m\frac{\partial u}{\partial y} + n\frac{\partial u}{\partial z} \right]^2 + \left[m\left(1+\frac{\partial v}{\partial y}\right) + l\frac{\partial v}{\partial x} + n\frac{\partial v}{\partial z} \right]^2 + \left[n\left(1+\frac{\partial w}{\partial z}\right) + l\frac{\partial w}{\partial x} + m\frac{\partial w}{\partial y} \right]^2$$

Neglecting the squares of the quantities ε, $\frac{\partial u}{\partial x}$, $\frac{\partial v}{\partial y}$ and $\frac{\partial w}{\partial z}$, and also their products, and assuming at the same time that

$$l^2 + m^2 + n^2 = 1$$

we obtain

$$\varepsilon = l^2\frac{\partial u}{\partial x} + lm\frac{\partial u}{\partial y} + ln\frac{\partial u}{\partial z} + m^2\frac{\partial v}{\partial y} + lm\frac{\partial v}{\partial x} + mn\frac{\partial v}{\partial z} + n^2\frac{\partial w}{\partial z} + ln\frac{\partial w}{\partial x} + mn\frac{\partial w}{\partial y} \qquad \text{(I.33)}$$

or

$$\varepsilon = l^2\varepsilon_x + m^2\varepsilon_y + n^2\varepsilon_z + lm\gamma_{xy} + ln\gamma_{xz} + mn\gamma_{yz} \qquad \text{(I.34)}$$

Equation (I.34), being analogous to equation (I.4), is easily transformed into an equation for an ellipsoid.

We draw from the origin a straight line of length r, parallel to the segment AB (see Fig. 10), where the length r is given by

$$r = \sqrt{\frac{C}{\varepsilon}}$$

Then

$$\varepsilon = \frac{C}{r^2} \quad l = \frac{x}{r} \quad m = \frac{y}{r} \quad n = \frac{z}{r} \qquad \text{(I.35)}$$

where x, y and z are the projections of the section r on the coordinate axes.

After substituting the values of l, m and n from equation (I.35) into equation (I.34) we obtain

$$\varepsilon_x x^2 + \varepsilon_y y^2 + \varepsilon_z z^2 + \gamma_{xy}xy + \gamma_{xz}xz + \gamma_{yz}yz = C \qquad \text{(I.36)}$$

This equation, like (I.5), is an equation of an ellipsoid whose centre is at the origin, but whose principal axes do not coincide with the coordinate axes. Thus, there must be three mutually perpendicular directions along which the terms γ_{xy}, γ_{xz} and γ_{yz}

become zero in equation (I.36), i.e., the shear strain is absent.

These three mutually perpendicular directions are called *the principal axes of strain.* Along these principal axes of strain only tension or compression takes place; at the same time along one of the axes the value of the strain at a given point is a maximum, and along another it is a minimum.

Comparing the result just obtained with the results concerning principal normal stresses (see Chapter I, Section 2) we conclude that the principal axes of strain coincide with the axes of principal normal stress.

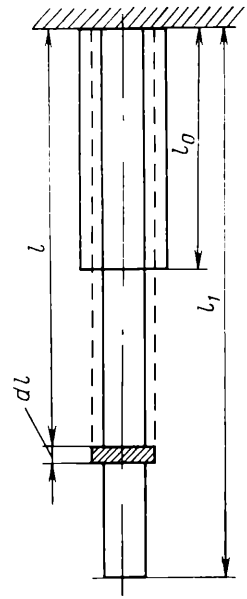

Fig. 11. Deformation of a rod

10. EXPRESSION OF LARGE STRAINS

The ratio of a linear deformation to the original dimension in the case of large strains does not characterize the true strain. In this connection let us consider the elongation of a rod, when its length l_1 after deformation is considerably greater than the original length l_0.

The infinitely small strain of the rod, when there is an intermediate length between l_0 and l_1, will be (Fig. 11):

$$d\varepsilon = \frac{dl}{l} \tag{I.37}$$

Then the total strain of the rod, as it elongates from l_0 to l_1, can be expressed as follows:

$$\varepsilon_l = \int_{l_0}^{l_1} \frac{dl}{l} = \log_e \frac{l_1}{l_0} \tag{I.38}$$

Consequently, the true strain should be expressed not by the ratio of the linear deformation to the original length but by the natural logarithm of the ratio of the final length to the original length.

If a rod of rectangular cross section or a parallelepiped is deformed, the depth of the cross section being reduced from h_0 to h_1 and the width from b_0 to b_1, the strain in the h and b directions can be represented by the following expressions:

$$\varepsilon_h = \log_e \frac{h_1}{h_0} \quad \text{and} \quad \varepsilon_b = \log_e \frac{b_1}{b_0} \tag{I.39}$$

If at the same time the volume of the body remains constant, then the sum of the strains must be zero:

$$\varepsilon_l + \varepsilon_h + \varepsilon_b = 0 \tag{I.40}$$

or

$$\log_e \frac{l_1}{l_0} + \log_e \frac{h_1}{h_0} + \log_e \frac{b_1}{b_0} = 0 \tag{I.41}$$

This can easily be verified if we recall that

$$l_0 h_0 b_0 = l_1 h_1 b_1$$

or

$$\frac{l_1}{l_0} \frac{h_1}{h_0} \frac{b_1}{b_0} = 1$$

After taking logarithms we obtain equation (I.40).

11. PLANE STRAIN

Plane strain is the name given to a strain which takes place in a single plane when the dimensions of the body in the direction perpendicular to this plane remain unchanged, i.e.,

$$\varepsilon_z = 0$$

If at the same time the volume of the body is not altered, then

$$\varepsilon_x + \varepsilon_y = 0 \tag{I.42}$$

or, when b = const.,

$$\log_e \frac{l_1}{l_0} = \log_e \frac{h_0}{h_1} \tag{I.43}$$

For the dimensions of the body to remain unchanged in the direction perpendicular to the plane in which the strain takes place, due to the phenomenon established by Poisson, the stress must be equal to the mean stress:

$$\sigma_z = \frac{\sigma_x + \sigma_y}{2} = \frac{\sigma_1 + \sigma_3}{2} \tag{I.44}$$

This result is an immediate consequence of

$$\varepsilon_z = \frac{1}{E} [\sigma_z - \mu (\sigma_x + \sigma_y)] = 0 \tag{I.45}$$

where $\mu = 0.5$ because the volume is constant.

The case of plastic deformation just described is widespread in practice. Many processes of shaping by pressure correspond to this

process of plastic deformation, in particular the rolling of wide strips when the edge effect—where a strain is observed in the direction of the width of the strip—can be neglected.

12. STRESSES IN PLASTIC STRAIN

As a result of experimental studies of the extrusion of metals through dies of different shapes, the French scientist Tresca concluded as long ago as 1864 that the onset of a plastic strain is not determined by the absolute value of the normal stresses, but by their difference, or the maximum value of the shear stress. This conclusion played an important role in the development of the theory of plastic strain, and it retains much of its significance at the present time.

Subsequently the results of the investigations by Tresca were developed by Saint-Venant (France) in 1870-1872, who proposed that in the case of plastic strain (under static conditions) the stresses should be expressed by the ratio

$$\tau_{max} = \frac{\sigma_1 - \sigma_3}{2} = \frac{\sigma_s}{2} \tag{I.46}$$

where σ_s is the yield stress which is usually defined as the stress arising in the test piece at the onset of a notable plastic deformation, when the test piece is subjected to tension under static conditions.

When the effects of temperature, strain rate and work hardening on the yield stress are allowed for, the relation (I.46) can be written as follows:

$$\sigma_1 - \sigma_3 = \sigma_a \tag{I.47}$$

where σ_a is the actual yield stress for a linear strain (a simple compression or tension), after the effects of temperature, strain rate and work hardening have been allowed for.

This quantity is often denoted by k_f. In terms of σ_s it is approximated by the equation

$$\sigma_a = n_t n_{wh} n_v \sigma_s \tag{I.48}$$

where n_t, n_{wh} and n_v are coefficients which allow for the effects of temperature, work hardening and strain rate on the resistance to deformation.

In a three-dimensional state of stress, when there are three values of the principal normal stresses σ_1, σ_2 and σ_3, the condition (I.47)

is expressed by the three inequalities:

$$\left.\begin{aligned} |\sigma_1 - \sigma_3| &\leqslant \sigma_a \\ |\sigma_1 - \sigma_2| &\leqslant \sigma_a \\ |\sigma_2 - \sigma_3| &\leqslant \sigma_a \end{aligned}\right\} \tag{I.49}$$

At the same time the necessary and sufficient condition for a plastic strain corresponds to one of the three differences of principal normal stresses shown above attaining $-\sigma_a$ or $+\sigma_a$. The same condition can also be written as follows:

$$|\tau_{12}| \leqslant \frac{\sigma_a}{2} \quad |\tau_{13}| \leqslant \frac{\sigma_a}{2} \quad |\tau_{23}| \leqslant \frac{\sigma_a}{2} \tag{I.50}$$

In a rectangular system of coordinates τ_{12}, τ_{13} and τ_{23} these inequalities can be represented in the form of a space bounded by the six planes given by the equations

$$\tau_{12} = \pm \frac{\sigma_a}{2} \quad \tau_{13} = \pm \frac{\sigma_a}{2} \quad \text{and} \quad \tau_{23} = \pm \frac{\sigma_a}{2}$$

The surface of the cube thus obtained, with its centre located at the origin and with a side equal to σ_a, will be the limiting surface corresponding to plastic strain being associated with one of the stresses τ_{12}, τ_{13} and τ_{23} (Fig. 12).

Bearing in mind that

$$\tau_{12} + \tau_{13} + \tau_{23} = 0 \tag{I.51}$$

instead of the limiting surface we obtain a closed contour, the result of the intersection of the cube with the plane given by equation (I.51). This contour is a regular hexagon with side equal to $\frac{\sigma_a}{\sqrt{2}}$ (see Fig. 12).

R. von Mises (Germany, 1913) drew attention to the circumstance that at the corner points of the hexagon two principal shear stresses attain their greatest value, equal to $\frac{\sigma_a}{2}$, whilst at the same time the third shear stress is zero. Thus, the condition for plastic strain given above does not take into account the effect of the third principal shear stress. Because of this von Mises suggested that the hexagon be replaced by a simpler figure, that is, by a circumscribed circle.

In this case the cube is replaced by a sphere whose equation is

$$\tau_{12}^2 + \tau_{13}^2 + \tau_{23}^2 = \frac{\sigma_a^2}{2} \tag{I.52}$$

This equation specifies the relationship between the stresses which holds for plastic strain according to modern theory.

The same equation can also be derived by considering the inequalities (I.49) in a rectangular system of coordinates σ_1, σ_2 and σ_3.

According to the inequalities (I.49), the condition for plastic strain can be represented by the limiting surface of a body bounded by the six planes:

$$\sigma_1 - \sigma_3 = \pm\, \sigma_a \quad \sigma_1 - \sigma_2 = \pm\, \sigma_a \quad \sigma_2 - \sigma_3 = \pm\, \sigma_a \qquad \text{(I.53)}$$

A body formed by these six planes is a regular hexagonal prism of infinite height. The axis of this prism passes through the origin

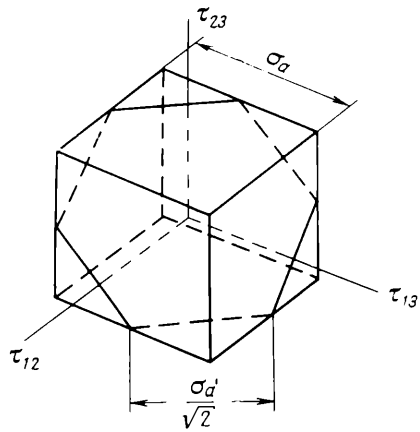

Fig. 12. The cube formed by the planes $\tau_{12} = \pm \frac{\sigma_a}{2}$; $\tau_{13} = \pm \frac{\sigma_a}{2}$ and $\tau_{23} = \pm \frac{\sigma_a}{2}$ and its intersection with the plane $\tau_{12} + \tau_{13} + \tau_{23} = 0$

and forms the same angle with all three coordinate axes (Fig. 13). The distance between opposite planes of this prism is given by $a = \sqrt{\sigma_a^2 + \sigma_a^2} = \sigma_a \sqrt{2}$, and its side by $\sigma_a \sqrt{\frac{2}{3}}$.

In order to eliminate the discontinuity when a given point passes from one face of the prism to another, this prism is replaced, according to G. Hencky (Germany), by a circumscribed cylinder with radius equal to $\sigma_a \sqrt{\frac{2}{3}}$.

When the cylinder is cut by a plane passing through the σ_1- and σ_2-axes, corresponding to $\sigma_3 = 0$, we have an ellipse whose centre is at the origin. The equation of this ellipse is

$$A\sigma_1^2 + B\sigma_2^2 + C\sigma_1\sigma_2 = 1 \qquad \text{(I.54)}$$

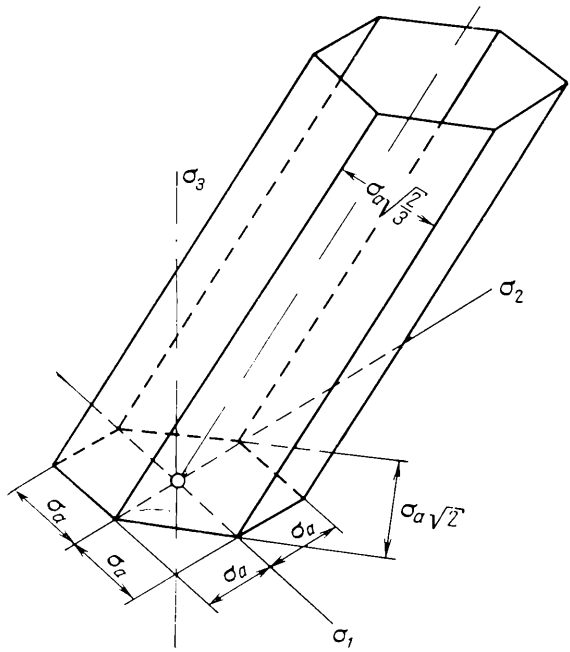

Fig. 13. The hexagonal prism formed by the six planes corresponding to equations (I.53)

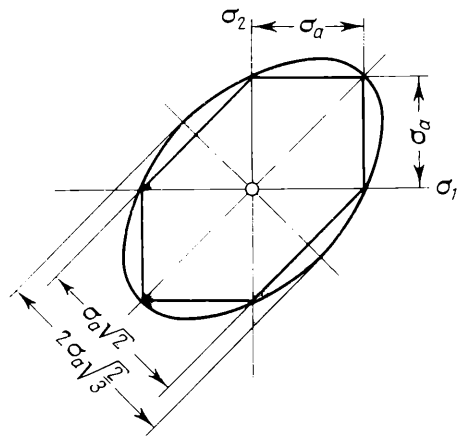

Fig. 14. Hexagon and circumscribing ellipse obtained from the intersection of hexagonal prism and cylinder with the plane $\sigma_3=0$

Since the ellipse constitutes a contour which contains the prism in the plane $\sigma_3 = 0$ (Fig. 14), the coefficients in equation (I.54) can be determined from the following conditions:
when $\sigma_1 = 0$, $\sigma_2 = \sigma_a$

$$B = \frac{1}{\sigma_a^2}$$

when $\sigma_2 = 0$, $\sigma_1 = \sigma_a$

$$A = \frac{1}{\sigma_a^2}$$

when $\sigma_1 = \sigma_2 = \sigma_a$

$$C = -\frac{1}{\sigma_a^2}$$

Equation (I.54) then assumes the form

$$\sigma_1^2 - \sigma_1\sigma_2 + \sigma_2^2 = \sigma_a^2 \tag{I.55}$$

Since the cylinder is located symmetrically relative to all three coordinates, it is obvious that when $\sigma_3 \neq 0$ the expression (I.55) gives the equation of the cylinder:

$$\sigma_1^2 + \sigma_2^2 + \sigma_3^2 - \sigma_1\sigma_2 - \sigma_1\sigma_3 - \sigma_2\sigma_3 = \sigma_a^2 \tag{I.56}$$

Multiplying both sides by 2 we obtain

$$(\sigma_1 - \sigma_2)^2 + (\sigma_1 - \sigma_3)^2 + (\sigma_2 - \sigma_3)^2 = 2\sigma_a^2 \tag{I.57}$$

This equation repeats equation (I.52), and it may also be obtained if in (I.52) the principal shear stresses are replaced by the principal normal stresses.

Equation (I.52), or (I.57), is the fundamental equation of plasticity characterizing the relationship between the principal shear or principal normal stresses for plastic deformation for any state of stress.

This equation of plasticity can also be obtained if we assume that *in a plastic deformation, for any state of stress, the octahedral shear stress equals*

$$\tau_{oct} = \frac{\sqrt{2}}{3}\sigma_a \approx 0.47\sigma_a \tag{I.58}$$

Substituting this value of τ_{oct} into equation (I.21), or (I.22), we obtain equation (I.57), or (I.52).

13. DEPENDENCE OF STRESSES ON THE POTENTIAL ENERGY OF ELASTIC DISTORTION

The quantity of potential energy stored in a body during its elastic deformation does not specify the beginning of plastic deformation. For example, in the case of pressure from all sides this energy can be very considerable, but the body will not be subjected to plastic deformation.

M. Huber (Poland, 1904) suggested that the criterion determining the stress relationships in plastic deformation should be not the total elastic strain energy, but only that part which is expended on changing the shape of the body; that part of the potential energy which is expended on changing the volume of the body is to be disregarded. But the suggestion of Huber remained unnoticed for a long time, and it was only after 1924, when this problem was studied in detail by H. Hencky, that this criterion for determining the boundary between purely elastic and plastic strains became generally accepted.

It follows that the potential energy stored during the elastic deformation which tends to change the shape of a given body without changing the volume must be a completely defined quantity independent of the nature of the state of stress.

The potential energy of elastic distortion A_d is found as the difference:

$$A_d = A_t - A_v \tag{I.59}$$

where A_t and A_v are, respectively, the total potential energy of elastic strain, and that part tending to produce volume change.

Let us refer these values of potential energy to a unit volume of the body being deformed.

The total elastic strain energy in the case of a complex state of stress is determined from the equation

$$dA_t = \sigma_x\, d\varepsilon_x + \sigma_y\, d\varepsilon_y + \sigma_z\, d\varepsilon_z + \tau_{xy}\, d\gamma_{xy} + \tau_{xz}\, d\gamma_{xz} + \tau_{yz}\, d\gamma_{yz}$$

Substituting the values of the elastic strains

$$\left.\begin{aligned}
\varepsilon_x &= \frac{1}{E}\left[\sigma_x - \mu\left(\sigma_y + \sigma_z\right)\right] \\
\varepsilon_y &= \frac{1}{E}\left[\sigma_y - \mu\left(\sigma_x + \sigma_z\right)\right] \\
\varepsilon_z &= \frac{1}{E}\left[\sigma_z - \mu\left(\sigma_x + \sigma_y\right)\right] \\
\gamma_{xy} &= \frac{1}{G}\,\tau_{xy} \\
\gamma_{xz} &= \frac{1}{G}\,\tau_{xz} \\
\gamma_{yz} &= \frac{1}{G}\,\tau_{yz}
\end{aligned}\right\}. \tag{I.60}$$

we obtain

$$A_t = \frac{1}{2E}[\sigma_x^2 + \sigma_y^2 + \sigma_z^2 - 2\mu(\sigma_x\sigma_y + \sigma_x\sigma_z + \sigma_y\sigma_z)] + \frac{\tau_{xy}^2}{2G} + \frac{\tau_{xz}^2}{2G} + \frac{\tau_{yz}^2}{2G} \quad (I.61)$$

The energy tending to produce volume change is

$$A_v = \frac{p\Delta V}{2} \quad (I.62)$$

where p is the mean pressure (stress), and
ΔV is the change in the volume.
Since according to (I.27)

$$p = \sigma_m = \frac{\sigma_x + \sigma_y + \sigma_z}{3}$$

and the volume dilatation ΔV can be expressed in terms of the stresses from equations (I.60):

$$\Delta V = \varepsilon_x + \varepsilon_y + \varepsilon_z = \frac{1-2\mu}{E}(\sigma_x + \sigma_y + \sigma_z)$$

we obtain

$$A_v = \frac{1-2\mu}{E} \times \frac{(\sigma_x + \sigma_y + \sigma_z)^2}{3} \quad (I.63)$$

Substituting these values of A_v and A_t into equation (I.59) we have:

$$A_d = \frac{1}{2E}[\sigma_x^2 + \sigma_y^2 + \sigma_z^2 - 2\mu(\sigma_x\sigma_y + \sigma_x\sigma_z + \sigma_y\sigma_z)] + \frac{1}{2G}(\tau_{xy}^2 + \tau_{xz}^2 + \tau_{yz}^2) - \frac{1-2\mu}{6E}(\sigma_x + \sigma_y + \sigma_z)^2$$

Taking the term $\frac{1+\mu}{3E}$ outside the brackets, and noting that

$$\frac{1}{2G} = \frac{1+\mu}{E}$$

we obtain

$$A_d = \frac{1+\mu}{3E}[\sigma_x^2 + \sigma_y^2 + \sigma_z^2 - \sigma_x\sigma_y - \sigma_x\sigma_z - \sigma_y\sigma_z + 3(\tau_{xy}^2 + \tau_{xz}^2 + \tau_{yz}^2)] \quad (I.64a)$$

This value for the potential energy of elastic distortion, for given mechanical properties of the metal, must be fully defined and independent of the stress state during plastic deformation. That is, the value of A_d for a particular metal must be the same to produce plastic strain, both under a complex state of stress and, for example, under a simple compression or tension, when $\sigma_x = \sigma_a$ and the remaining stresses σ_y, σ_z, τ_{xy}, τ_{xz} and τ_{yz} vanish, so that equation (I.64a)

assumes the form

$$A_d = \frac{1+\mu}{3E}\sigma_a^2 \tag{I.64b}$$

Equating the right-hand sides of equations (I.64a) and (I.64b) and multiplying them by two, we obtain the fundamental equation of plasticity, which is analogous to (I.52) and (I.57) obtained above:

$$(\sigma_x-\sigma_y)^2+(\sigma_x-\sigma_z)^2+(\sigma_y-\sigma_z)^2+6(\tau_{xy}^2+\tau_{xz}^2+\tau_{yz}^2)=2\sigma_a^2 \tag{I.65}$$

When the normal stresses appearing in this equation are directed along the principal axes of stress, the equation becomes identical with equation (I.57).

The evaluation of the potential energy of the elastic distortion testifies to the fact that the fundamental equations of plasticity (I.52), (I.57) and (I.65) have a well-defined physical meaning.

The criterion constituted by these equations is thus based on *the potential energy of elastic strain which tends to produce a change in shape*; *when this potential energy reaches a certain value plastic strain will take place.*

14. ANALYSIS OF THE FUNDAMENTAL EQUATION OF PLASTICITY

The main advantage of equation (I.52), or (I.57), in comparison with equation (I.47) which represents the maximum shear stress theory, consists in the fact that it takes into account the effect of σ_2, i.e., the effect of the intermediate principal stress proceeding from the assumption that

$$\sigma_1 \geqslant \sigma_2 \geqslant \sigma_3$$

In order to clarify to what extent σ_2 has an influence on the stress relationships for a plastic strain, we introduce into equation (I.57) the auxiliary quantity:

$$\xi = \frac{\sigma_2 - \frac{\sigma_1+\sigma_3}{2}}{\frac{\sigma_1-\sigma_3}{2}} \tag{I.66}$$

Since σ_2 can vary from σ_3 to σ_1, the quantity ξ lies between the limits -1, when $\sigma_2 = \sigma_3$, and $+1$, when $\sigma_2 = \sigma_1$.

From equation (I.66) we find

$$\sigma_2 = \xi\frac{\sigma_1-\sigma_3}{2}+\frac{\sigma_1+\sigma_3}{2}$$

We substitute this value of σ_2 into equation (I.57).

Then the equation of plasticity can be represented in the following form:

$$\frac{(3+\xi^2)}{2}(\sigma_1-\sigma_3)^2 \quad 2\sigma_a^2 \tag{I.67}$$

or

$$\sigma_1-\sigma_3 = \frac{2\sigma_a}{\sqrt{3+\xi^2}} \tag{I.68}$$

Depending on ξ, the coefficient $\frac{2}{\sqrt{3+\xi^2}}$ varies along a parabolic curve (Fig. 15). When $\xi = -1$ or $\xi = +1$ this coefficient is unity, and when $\xi = 0$ it attains the maximum, equal to $\frac{2}{\sqrt{3}} \approx 1.15$.

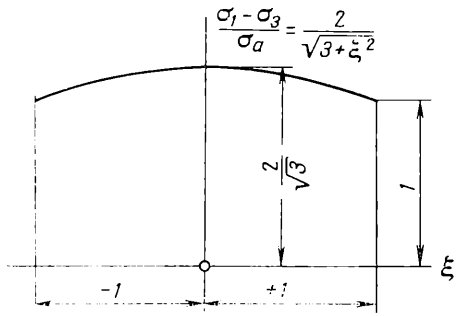

Fig. 15. Effect of σ_2 or ξ on $\frac{\sigma_1-\sigma_3}{\sigma_a}$

The following three important conclusions may be drawn from this analysis:

(1) when $\sigma_2 = \sigma_3$ or $\sigma_2 \quad \sigma_1$, the fundamental equation of plasticity coincides with the equation obtained from the maximum shear stress theory:

$$\sigma_1-\sigma_3 = \sigma_a$$

(2) the intermediate principal stress has only a slight effect on the relationship between the stresses for plastic strain, the ratio of the stresses lying within the limits of 1 and $\frac{2}{\sqrt{3}}$ (i.e., 1 and 1.15);

(3) in a simplified form the fundamental equation of plasticity can be expressed as follows:

$$\sigma_1-\sigma_3 = \frac{2}{\sqrt{3+\xi^2}}\sigma_a$$

where the coefficient ξ is calculated as dependent on σ_2 according to equation (I.66).

To determine the coefficient $\frac{2}{\sqrt{3+\xi^2}}$ the graph shown in Fig. 15 can also be used.

15. THE EQUATION OF PLASTICITY FOR A PLANE STRAIN

In this case we assume that there is no strain in the direction of the z-axis. Then

$$\tau_{xz} = \tau_{yz} = 0$$

$$\sigma_z = \frac{\sigma_x + \sigma_y}{2}$$

We substitute these values of the stresses into equation (I.65):

$$(\sigma_x - \sigma_y)^2 + 4\tau_{xy}^2 = \frac{4}{3}\sigma_a^2 = 4k^2 \tag{I.69}$$

or

$$\boxed{\sqrt{\left(\frac{\sigma_x - \sigma_y}{2}\right)^2 + \tau_{xy}^2} = k} \tag{I.70}$$

where

$$k = \frac{\sigma_a}{\sqrt{3}} \approx 0.57\sigma_a \tag{I.71}$$

When the direction of the stresses σ_x and σ_y coincides with the principal axes of stress, the equation of plasticity assumes the following form:

$$\boxed{\sigma_1 - \sigma_3 = 2k} \tag{I.72}$$

In the case when $\sigma_x = -\sigma_y$ the normal stresses are zero on the planes of maximum shear stress. This particular case of plane strain is called *pure shear*.

Substituting this value of σ_y and $\tau_{xy} = 0$ into equation (I.69), we obtain

$$\sigma_x = \frac{\sigma_a}{\sqrt{3}} = k$$

Hence it follows that in the case of pure shear plastic strain occurs when the shear stress equals

$$\boxed{\tau = \frac{\sigma_a}{\sqrt{3}} \approx 0.57\,\sigma_a}$$

In view of the fact that this quantity has a definite physical meaning, we shall subsequently use it to characterize the resistance of different metals to plastic strain.

In particular, the resistance to strain in the case of two-dimensional simple compression equals $2k$, i.e., twice the value of the resistance to the pure shear.

16. THE INFLUENCE OF THE MEAN STRESS ON THE SHEAR STRENGTH

The equations given above characterizing the stress relationships for plastic strain are based on the convention that the fundamental criterion for evaluating this stress relationship is the *attainment of a definite energy of distortion.* Thus, the above stress relationship for a plastic strain depends only on octahedral shear stresses, whilst the octahedral normal stress does not affect it. This conclusion is supported by numerous experimental investigations.

But according to the investigations of P. Bridgman, as well as L. Vereshchagin and E. Zubova, in cases where the mean stress considerably exceeds the resistance to strain, the shear strength increases with further increases in the mean stress. Thus P. Bridgman discovered that the limiting shear strength for steel 1045, when the mean compressive stress was 72 kg/mm^2, increased by 19.3%; when the mean stress was 250 kg/mm^2, it increased 5.35 times. For lead the limiting shear strength increased from 0.9 to 3.7 kg/mm^2, i.e., 4.1 times, for a mean compressive stress of 250 kg/mm^2.

The results of the investigations of P. Bridgman into the shear strength of a number of metals under pressures of 50,000 kg/cm^2 and 25,000 kg/cm^2 are shown in Table 1. For most metals the shear strength is 5 to 10 times greater, when deformed under a pressure of 50,000 kg/cm^2, than when deformed under the usual conditions under atmospheric pressure.

L. Vereshchagin and E. Zubova, whilst investigating the shear strength of different metals, drew attention to the fact that under high pressures the shear strength depends not only on the value of the pressure but also on the ordinal number Z of the metal. From their experiments they inferred that the shear strength under high pressures depends only on the number of outer electrons, and not on their total number in the atom; it does not depend on the type of the crystal lattice.

To take into account the effect of the mean stress on the shear strength when calculating the stresses for plastic strain (two-dimen-

Table 1

Shear Strength of Different Metals Under Pressures of 50,000 and 25,000 kg/cm²

Metal	Limiting shear strength, kg/cm², under a given pressure, kg/cm²		Breaking strength under atmospheric pressure, divided by 2, kg/cm²
	50,000	25,000	
Aluminium	3,100	1,800	300
Lead	680	370	90
Cadmium	1,900	1,100	320
Cobalt	6,300	3,200	1,230
Iron	12,000	6,600	1,230
Gold	4,500	2,400	700
Copper	4,900	3,000	1,050
Magnesium	870	730	980
Nickel	8,700	4,000	1,050
Silver	4,700	2,600	650
Zinc	1,800	1,050	880
Tin	770	510	130

sional) we have to use an equation of the form

$$\sigma_1 - \sigma_3 = [2k + (\sigma_1 + \sigma_3) \tan \alpha] \qquad (I.73)$$

where α is the angle characterizing the increase in the shear strength (Fig. 16) for an increase in the mean stress, which is determined on the basis of experimental data.

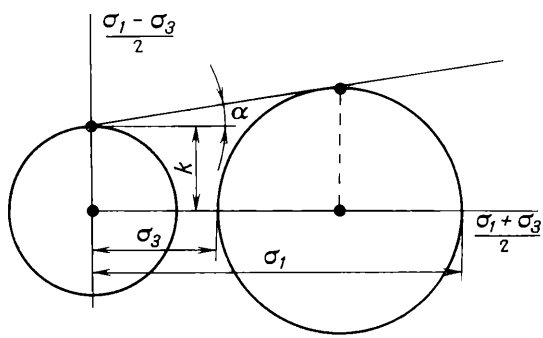

Fig. 16. Effect of mean stress on shear strength

But this equation cannot be recommended for practical calculations owing to the fact that adequate experimental data for the coefficient α are lacking.

17. DIFFERENTIAL EQUATIONS OF EQUILIBRIUM

Let us isolate from the body being deformed an element in the form of a rectangular parallelepiped with the sides equal to dx, dy and dz, and let us consider its equilibrium (Fig. 17). If the faces of this parallelepiped do not coincide with the planes of action of the principal normal stresses, then the stresses on each face are expressed

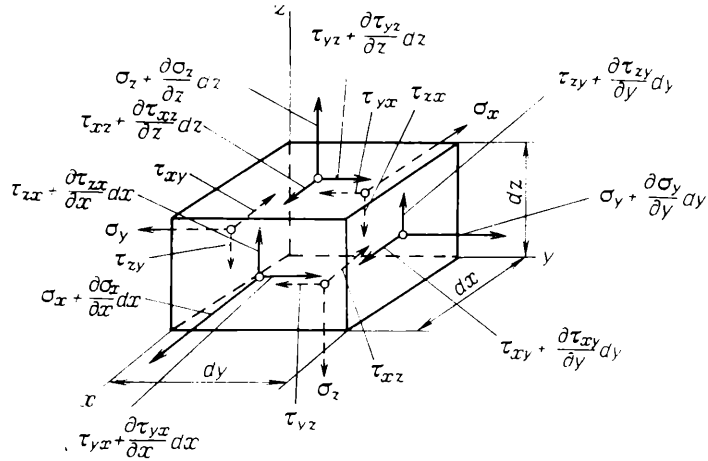

Fig. 17. The stresses acting on a parallelepiped

in the form of three vectors orientated parallel to the coordinate axes: one vector expressing the normal stress and the two remaining vectors, the components of the shear stress.

The variation of the stresses over the sides dx, dy and dz of the parallelepiped can be expressed by means of the partial derivatives. Thus, for example, if on the face of the parallelepiped coinciding with the plane yz the normal stress is equal to σ_x, then on the opposite face, at a distance dx from the origin, the normal stress is

$$\sigma_x + \frac{\partial \sigma_x}{\partial x}\, dx$$

The remaining stresses acting on the faces of the parallelepiped at distances dx, dy and dz from the origin may be found in a similar way (see Fig. 17).

Projecting the forces acting on the parallelepiped on to the x-axis we obtain

$$\left(\sigma_x + \frac{\partial \sigma_x}{\partial x}\, dx\right) dy\, dz - \sigma_x\, dy\, dz + \left(\tau_{xy} + \frac{\partial \tau_{xy}}{\partial y}\, dy\right) dx\, dz -$$

$$- \tau_{xy}\, dx\, dz + \left(\tau_{xz} + \frac{\partial \tau_{xz}}{\partial z}\, dz\right) dx\, dy - \tau_{xz}\, dx\, dy = 0$$

Simplifying this (removing the parentheses and cancelling $dxdydz$, the volume of the element considered) we obtain the equation of equilibrium:

$$\frac{\partial \sigma_x}{\partial x} + \frac{\partial \tau_{xy}}{\partial y} + \frac{\partial \tau_{xz}}{\partial z} = 0 \tag{I.74}$$

The remaining two equations are obtained similarly:

$$\frac{\partial \sigma_y}{\partial y} + \frac{\partial \tau_{xy}}{\partial x} + \frac{\partial \tau_{yz}}{\partial z} = 0$$

$$\frac{\partial \sigma_z}{\partial z} + \frac{\partial \tau_{xz}}{\partial x} + \frac{\partial \tau_{yz}}{\partial y} = 0$$

If one of the normal stresses, say σ_z, is constant, so that we have a two-dimensional or plane state of stress, then

$$\frac{\partial \tau_{xz}}{\partial z} = \frac{\partial \tau_{yz}}{\partial z} = 0$$

and the third equation becomes an identity. The equations of equilibrium in this case are

$$\left.\begin{aligned} \frac{\partial \sigma_x}{\partial x} + \frac{\partial \tau_{xy}}{\partial y} &= 0 \\ \frac{\partial \sigma_y}{\partial y} + \frac{\partial \tau_{xy}}{\partial x} &= 0 \end{aligned}\right\} \tag{I.75}$$

18. SIMULTANEOUS SOLUTION OF THE EQUATIONS OF EQUILIBRIUM AND THE EQUATION OF PLASTICITY

To investigate the distribution of stresses in the case of two-dimensional plastic strain we make use of three equations:

(1) the two differential equations of equilibrium [see equations (I.75)]:

$$\frac{\partial \sigma_x}{\partial x} + \frac{\partial \tau_{xy}}{\partial y} = 0$$

and

$$\frac{\partial \sigma_y}{\partial y} + \frac{\partial \tau_{xy}}{\partial x} = 0$$

(2) the equation of plasticity [see equation (I.70)]:

$$\left(\frac{\sigma_x - \sigma_y}{2}\right)^2 + \tau_{xy}^2 = k^2$$

In these three equations the unknown quantities are σ_x, σ_y and τ_{xy}. Thus, *the study of the stress distribution for two-dimensional strain is a problem which, in principle, is statistically determinate,*

and for an ideally plastic solid it can be solved without taking the deformations into account.

To solve these equations we introduce a quantity φ which indicates the orientation of the plane of the greatest shear stress relative to the coordinate axis.

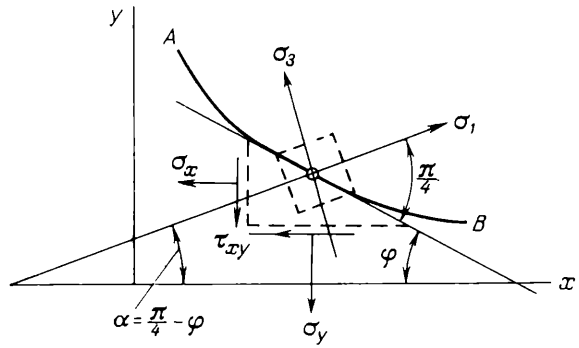

Fig. 18. Trajectory of maximum shear stress

We assume that in the deformed body the trajectory of the greatest shear stress (Fig. 18) is expressed in the form of a cylindrical surface

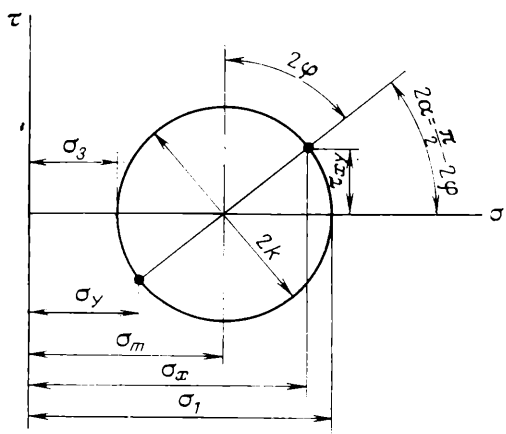

Fig. 19. The stress circle

AB. The stresses which arise in the elemental triangular prism touching the trajectory of the greatest shear stress are expressed by equation (I.70) in terms of the angle φ between the tangent to the curve AB and the x-axis.

The stress circle is drawn using the coordinates σ and τ (Fig. 19).

The radius of this circle equals the quantity k, since it represents the maximum shear stress for a two-dimensional strain, whilst the distance of the centre of the circle from the origin equals the mean stress:

$$\sigma_m = \frac{\sigma_x + \sigma_y + \sigma_z}{3} = \frac{\sigma_x + \sigma_y}{2} \quad \frac{\sigma_1 + \sigma_3}{2} \tag{I.76}$$

The diametral line drawn at the angle $2\alpha = \frac{\pi}{2} - 2\varphi$ to the x-axis gives the value of the stresses on the surface of the triangular prism:

$$\left.\begin{aligned} \sigma_x &= \sigma_m + k\cos 2\alpha = \sigma_m + k\sin 2\varphi \\ \sigma_y &= \sigma_m - k\cos 2\alpha = \sigma_m - k\sin 2\varphi \\ \tau_{xy} &= k\sin 2\alpha = -k\cos 2\varphi \end{aligned}\right\} \tag{I.77}$$

We find the partial derivatives of these stresses:

$$\left.\begin{aligned} \frac{\partial\sigma_x}{\partial x} &= \frac{\partial\sigma_m}{\partial x} + 2k\frac{\partial\varphi}{\partial x}\cos 2\varphi \\ \frac{\partial\sigma_y}{\partial y} &= \frac{\partial\sigma_m}{\partial y} - 2k\frac{\partial\varphi}{\partial y}\cos 2\varphi \\ \frac{\partial\tau_{xy}}{\partial x} &= 2k\frac{\partial\varphi}{\partial x}\sin 2\varphi \\ \frac{\partial\tau_{xy}}{\partial y} &= 2k\frac{\partial\varphi}{\partial y}\sin 2\varphi \end{aligned}\right\} \tag{I.78}$$

Substituting these partial derivatives into the equations of equilibrium (I.75), we obtain the equations of Lévy (France, 1871):

$$\left.\begin{aligned} \frac{\partial\sigma_m}{\partial x} + 2k\left(\frac{\partial\varphi}{\partial x}\cos 2\varphi + \frac{\partial\varphi}{\partial y}\sin 2\varphi\right) &= 0 \\ \frac{\partial\sigma_m}{\partial y} + 2k\left(\frac{\partial\varphi}{\partial x}\sin 2\varphi - \frac{\partial\varphi}{\partial y}\cos 2\varphi\right) &= 0 \end{aligned}\right\} \tag{I.79}$$

For a system of coordinates x and y, these equations give the value of the angle φ, i.e., the direction of the greatest shear stresses.

19. CHARACTERISTICS AND SLIP LINES AS A METHOD OF DETERMINING STRESSES

Both equations (I.79) contain the two unknown quantities σ_m and φ; hence there exist sufficient conditions for determining the stresses. But the solution of these equations, since they involve partial derivatives, is a difficult matter. For this reason in solving these equations their characteristics have to be determined.

This method of determining the characteristics is highly appropriate, since the characteristics in question—as will be shown later—have an important property: they coincide with the trajectories of the greatest shear stress.

This circumstance is very important since plastic strain mainly becomes apparent in shear or slip along the planes of action of the greatest shear stress. This statement may be proved experimentally by using a polished cylinder under tension. As plastic strain begins the surface of the cylinder shows shear or slip lines inclined at 45° to its axis; these lines are called the Lüders-Chernov lines. Consequently, the characteristics of equations (I.79) indicate not only the position of the trajectory of the greatest shear stress, but also the position of these shear or slip lines (surfaces).

In photoelastic investigations these characteristics are defined by the isochromatics.

One possible method of integrating equations (I.79) is to find their characteristics by the method suggested by S. Khristianovich (U.S.S.R., 1938).

Using this method, following V. Sokolovsky and L. Leibenzon, we assume that the equation of the trajectory of the maximum shear stress has the form:

$$y = f(x) \tag{I.80}$$

Along this curve the following differential relations must hold:

$$\left.\begin{aligned} d\sigma_m &= \frac{\partial \sigma_m}{\partial x}\,dx + \frac{\partial \sigma_m}{\partial y}\,dy \\ d\varphi &= \frac{\partial \varphi}{\partial x}\,dx + \frac{\partial \varphi}{\partial y}\,dy \end{aligned}\right\} \tag{I.81}$$

We solve equations (I.79) and (I.81) for the four partial derivatives:

$$\frac{\partial \sigma_m}{\partial x} \quad \frac{\partial \sigma_m}{\partial y} \quad \frac{\partial \varphi}{\partial x} \quad \frac{\partial \varphi}{\partial y}$$

The auxiliary notations are introduced:

$$\left.\begin{aligned} N_1 &= d\sigma_m\,dy\cos 2\varphi - d\sigma_m\,dx\sin 2\varphi - 2k\,dy\,d\varphi \\ N_2 &= d\sigma_m\,dy\sin 2\varphi - d\sigma_m\,dx\cos 2\varphi + 2k\,dx\,d\varphi \\ N_3 &= -\frac{d\sigma_m dy}{2k} + d\varphi\,dx\sin 2\varphi + d\varphi\,dy\cos 2\varphi \\ N_4 &= \frac{d\sigma_m dx}{2k} + d\varphi\,dx\cos 2\varphi + d\varphi\,dy\sin 2\varphi \end{aligned}\right\} \tag{I.82}$$

$$D = 2\,(dy\cos\varphi - dx\sin\varphi)\,(dy\sin\varphi + dx\cos\varphi) \tag{I.83}$$

Then the required derivatives are

$$\frac{\partial \sigma_m}{\partial x} = \frac{N_1}{D} \quad \frac{\partial \sigma_m}{\partial y} = \frac{N_2}{D} \quad \frac{\partial \varphi}{\partial x} = \frac{N_3}{D} \quad \frac{\partial \varphi}{\partial y} = \frac{N_4}{D} \tag{I.84}$$

If in these equations the numerator and denominator simultaneously become zero, then along the curve expressed by equation (I.80) the values of the derivatives become indeterminate, i.e., not unique, and the curve $y = f(x)$ will be *the characteristic of the system of equations of Lévy* (I.79).

In order to find these characteristics we determine the conditions for which both the denominator and numerator in equations (I.84) simultaneously become zero.

Equation (I.83) will be zero for the two conditions:

$$\frac{dy}{dx} = \tan \varphi \quad \text{or} \quad \frac{dy}{dx} = -\cot \varphi \tag{I.85}$$

The first condition expresses the fact that the tangent to the characteristics forms an angle φ with the x-axis, i.e., the same angle as does the tangent to the trajectories of the greatest shear stress. This means that the characteristics run parallel to these trajectories, and since they can be drawn at any distance from each other, it may be concluded that *the characteristics of the differential equations (I.79) coincide with the trajectories of the greatest shear stress, i.e., the slip lines or surfaces.*

The second condition indicates that there are two families of characteristics intersecting each other at an angle of $\frac{\pi}{2}$. This second family of characteristics obviously coincides with slip lines inclined to the principal axes of stress at an angle of 45° in the opposite direction.

We substitute the value $\frac{dy}{dx} = \tan \varphi$ from equation (I.85) into equations (I.82) and equate them to zero:

$$N_1 = d\sigma_m\, dx \tan \varphi\, (2 \cos^2 \varphi - 1) - d\sigma_m\, dx\, 2 \sin \varphi \cos \varphi - \\ - 2k\, dx \tan \varphi\, d\varphi = 0$$

or

$$N_1 = -2k \tan \varphi dx d \left(\frac{\sigma_m}{2k} + \varphi \right) = 0$$

Similarly for the remaining three numerators we have:

$$N_2 = 2k\, dx d \left(\frac{\sigma_m}{2k} + \varphi \right) = 0$$

$$N_3 = -\tan \varphi dx d \left(\frac{\sigma_m}{2k} + \varphi \right) = 0$$

$$N_4 = dx d \left(\frac{\sigma_m}{2k} + \varphi \right) = 0$$

It follows from these equations that N_1, N_2, N_3 and N_4 are simultaneously zero when

$$d\left(\frac{\sigma_m}{2k} \quad \varphi\right) = 0 \tag{I.86}$$

If we put the value $\frac{dy}{dx} \quad -\cot\varphi$, also from equation (I.85), in equations (I.82) and then equate them to zero, then

$$d\left(\frac{\sigma_m}{2k} - \varphi\right) = 0 \tag{I.87}$$

From equations (I.86) and (I.87) there follows a very important conclusion:
along slip lines the quantities

$$\frac{\sigma_m}{2k} + \varphi = \text{const.} \quad \text{and} \quad \frac{\sigma_m}{2k} - \varphi = \text{const.} \tag{I.88}$$

remain constant, i.e., along the characteristic or slip line the dependence of σ_m *on the angle of rotation is specified by the quantity* $\pm 2k\varphi$, where φ is the angle of rotation of the slip line.

This interesting property of slip lines or trajectories of greatest shear stress was discovered by G. Hencky in 1923.

20. PROPERTIES OF SLIP LINES

The interesting property of slip lines considered in the preceding section, consisting in the fact that σ_m varies along the lines with their angle of rotation, can also be proved directly with the aid of the equations of Lévy (I.79).

For this we transfer the coordinate axes xy so that they coincide with the tangents drawn at any point, suppose, at point A of the intersection of two mutually perpendicular slip lines (Fig. 20). Then in equations (I.79) $\varphi = 0$; after substituting α and β for the coordinates x and y chosen arbitrarily, we obtain

$$\left.\begin{aligned} \frac{\partial\sigma_m}{\partial\alpha} + 2k\frac{\partial\varphi}{\partial\alpha} &= 0 \\ \frac{\partial\sigma_m}{\partial\beta} - 2k\frac{\partial\varphi}{\partial\beta} &= 0 \end{aligned}\right\} \tag{I.89}$$

The left-hand sides of these equations are zero when

$$\sigma_m + 2k\varphi = \text{const.} \tag{I.90}$$

and

$$\sigma_m - 2k\varphi = \text{const.} \tag{I.91}$$

Thus along the slip lines σ_m depends on the angle of rotation of these lines.

The other interesting property of slip lines is a geometrical one. This is sometimes called the first theorem of Hencky.

Let us isolate from the network of slip lines a four-cornered element $ABDC$ (Fig. 21) consisting of the two branches AB and CD of the slip lines of the family α, which satisfy equation (I.90), and the two branches AC and BD from the family β, corresponding to equation (I.91).

Let us calculate the angles formed as a result of rotation of the slip lines between the tangents drawn to the isolated element at pthe oints A, B, C and D.

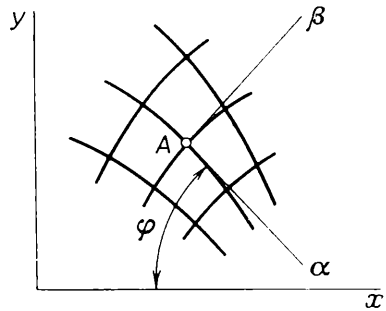

Fig. 20. Transformation of coordinate axes to coincide with the tangents to the slip lines at the point A

If we move from point A along the isolated element (in doing so it is necessary to turn through a total angle of 2π) in a clockwise direction, then, noting that at each point B, C, D and A we must make a turn of $\frac{\pi}{2}$, we can write the following equation:

$$2\pi = \varphi_{AB} + \frac{\pi}{2} + \varphi_{BD} + \frac{\pi}{2} - \varphi_{CD} + \frac{\pi}{2} - \varphi_{AC} + \frac{\pi}{2}$$

or

$$\varphi_{AB} - \varphi_{CD} = \varphi_{AC} - \varphi_{BD} \tag{I.92}$$

Consider these angles, calculating by two methods the difference of the mean stresses between the points A and D according to equations (I.90) and (I.91). If we proceed from point A to point D via point B, the difference of the values of the mean stress is

$$\sigma_{mA} - \sigma_{mD} = (\sigma_{mA} - \sigma_{mB}) + (\sigma_{mB} - \sigma_{mD}) = 2k(\varphi_{AB} - \varphi_{BD})$$

and if we proceed from point A to point D via point C, then

$$\sigma_{mA} - \sigma_{mD} = (\sigma_{mA} - \sigma_{mC}) + (\sigma_{mC} - \sigma_{mD}) = 2k(-\varphi_{AC} + \varphi_{CD})$$

Since in both cases the difference must be the same, then

$$\varphi_{AB} - \varphi_{BD} = \varphi_{CD} - \varphi_{AC}$$

or

$$\varphi_{AB} - \varphi_{CD} = \varphi_{BD} - \varphi_{AC}$$

Comparing this equation with equation (I.92) we obtain

$$\varphi_{AB} = \varphi_{CD} \quad \text{and} \quad \varphi_{AC} = \varphi_{BD}$$

This important property of slip lines can be formulated in the following manner: *the angle between the two tangents* ($\Delta\varphi$), *drawn*

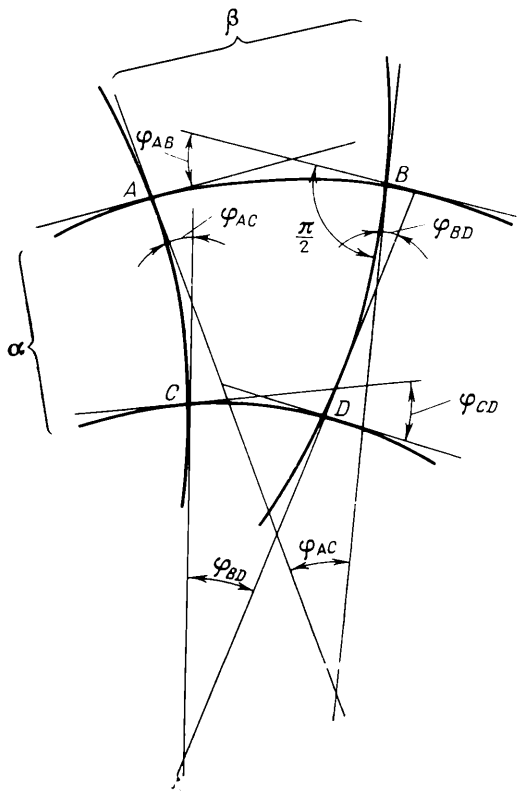

Fig. 21. An element of a slip line network

to two adjacent slip lines at the point of their intersection with any slip line of another family, perpendicular to them both, remains constant over the entire length of these two slip lines (Fig. 22).

The third interesting property of slip lines is also a geometrical one. It was also obtained by G. Hencky.

The length of an element of a slip line of the family α (Fig. 23), bounded by two slip lines of the family β, can be expressed as follows:

$$a = r_\alpha \Delta\varphi$$

where r_α is the radius of curvature of the element a of the arc, and $\Delta\varphi$ is the angle between two tangents to the slip lines β.

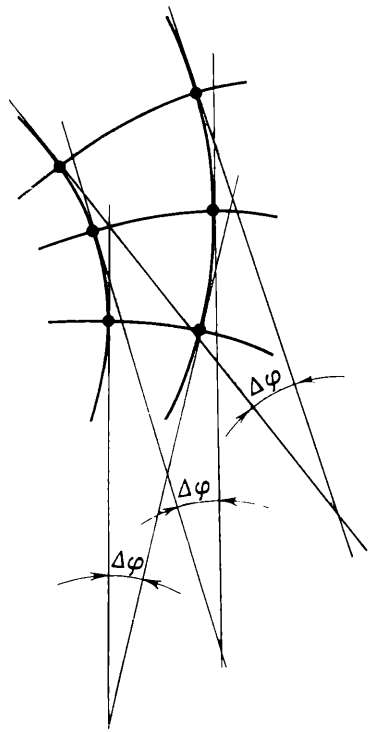

Fig. 22. The tangents drawn to two slip lines at their intersections with the other slip line family, showing the constant angle $\Delta\varphi$ between them

We differentiate this equation with respect to b:

$$\frac{\partial}{\partial b}(r_\alpha \Delta\varphi) = \frac{\partial a}{\partial b}$$

The derivative of the right-hand side of this equation (see Fig. 22) is

$$\frac{\partial a}{\partial b} = -\Delta\varphi$$

Differentiating, we take the quantity $\Delta\varphi$ as a constant in front of the differentiation sign and divide both sides by it. We then obtain

$$\frac{\partial r_\alpha}{\partial b} = -1 \tag{I.93}$$

By means of similar derivations we can also write the equation for r_β, the radius of curvature of the element b of an arc:

$$\frac{\partial r_\beta}{\partial a} = -1 \tag{I.94}$$

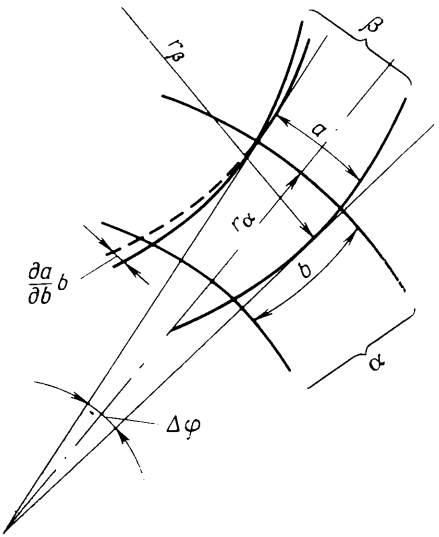

Fig. 23. Dependence of the length of slip line elements on the angle $\Delta\varphi$ and the radius of curvature

For a greater clarity these relationships are conveniently written in the following form:

$$\left.\begin{aligned}\Delta r_\alpha &= -\Delta b\\ \Delta r_\beta &= -\Delta a\end{aligned}\right\} \tag{I.95}$$

where Δr_α and Δr_β are the increments of the radii of curvature, whilst

Δa and Δb are the increments of the distances between the points of intersection of two adjacent slip lines with the other family of slip lines.

These two equations confirm that the radii of curvature of slip lines of one family are proportional to the distances between the

points of intersection with the slip lines of the other family. Thus, for example, if in moving along a slip line we arrive at a section with a smaller radius of curvature, then this means that the slip lines of the second family will intersect with it more often.

The three properties of slip lines just considered greatly facilitate their construction and enable us to study and determine the stress distribution in many cases of two-dimensional strain.

21. BOUNDARY CONDITIONS AND THE CONSTRUCTION OF SLIP LINES

Let us consider the form of the slip lines at the surface of a deformed body.

If this surface is free, and not in contact with the tool so that no external forces of any kind act on it, then obviously the normal to this surface will represent the direction of the minimum principal normal stress σ_3, which is equal to zero in the given case.

Consequently, the slip lines will be directed to the free surface at an angle of 45°. Here two cases are possible when compressive or tensile forces act along the surface (Fig. 24*a* and *b*).

In the case of contact with the tool many different states of stress are possible. Let us consider the characteristic ones.

1. Along the contact surface a slip takes place without friction. In this case the slip lines will also intersect the surface at an angle of 45° (Fig. 24*c* and *d*).

2. A slip occurs along the contact surface, but owing to the fact that the specific friction forces are greater than the shear strength ($p\mu \geqslant k$), the surface layers adhere to the plane of the tool. In this case near the surface of the body one of the directions of the greatest shear stresses is parallel to the contact plane. Consequently, one of the families of slip lines is tangential to the surface, whilst the other is perpendicular to it (Fig. 24*e* and *f*).

3. Friction forces less than the quantity k act along the contact surface. A slip can occur in this case, but also a complete adhesion may be observed. Such a case of interaction with the tool is used very frequently in shaping metals by pressure.

Making use of the stress circle diagram we shall determine the direction of the greatest shear stresses relative to the direction of the contact friction forces. It is obvious that on the contact surface one of the values of the normal stress will be equal to the specific pressure p, whilst the shear stress τ will be equal to the specific friction force (Fig. 25).

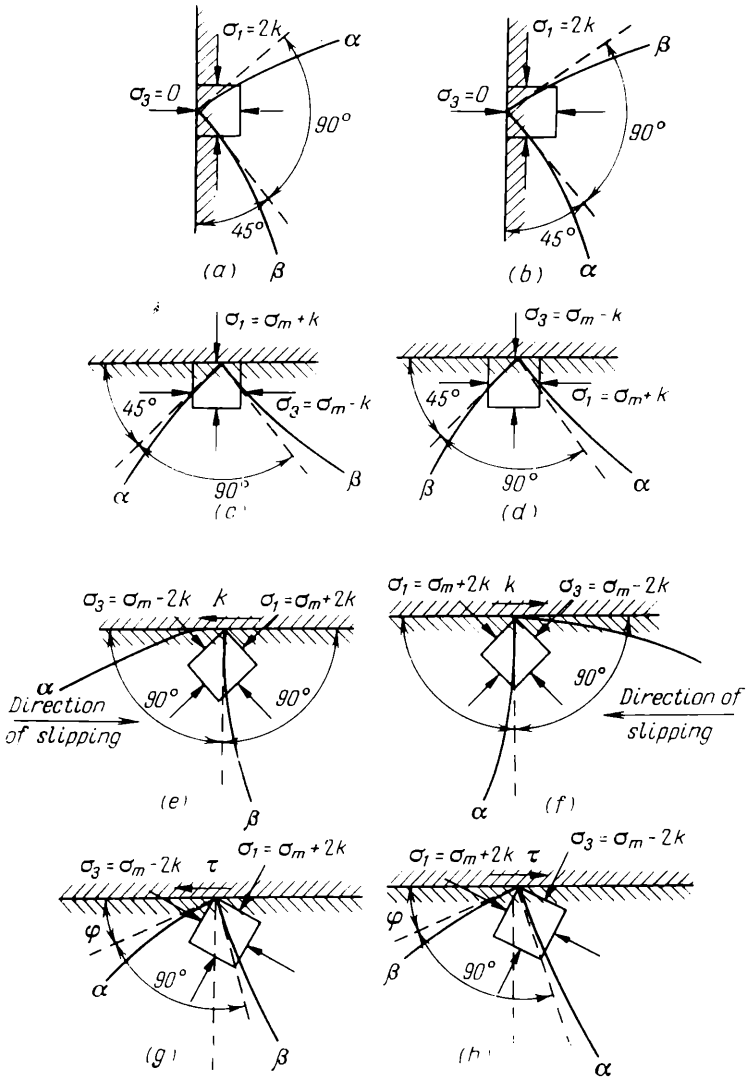

Fig. 24. Different forms assumed by slip lines at the surface of a deformed body: (*a*) and (*b*) free surface; (*c*) and (*d*) tool surface in contact without friction; (*e*) and (*f*) the same, but with sticking of surface layers adjacent to the tool plane; (*g*) and (*h*) the same, but with surface friction forces $\tau < k$

From this it follows that the angle between the contact surface and the direction of one system of slip lines is

$$\varphi = 0.5 \cos^{-1} \frac{\tau}{k} \tag{I.96}$$

When $\tau = 0$, $\varphi = 45°$, and when $\tau = k$, $\varphi = 0$.

Thus, depending on the ratio $\tau : k$, the angle of inclination of a slip line varies within limits from zero to 45° (Fig. 24*g* and *h*).

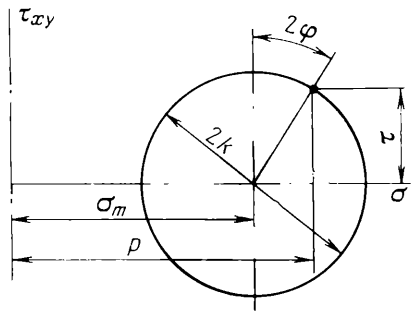

Fig. 25. Stress diagram determining the angle φ between surface friction force τ and slip line (p is the specific pressure on the contact surface)

The mean stress, i.e., the distance from the centre of the stress circle to the origin, in accordance with Fig. 25, is

$$\sigma_m = p - k \sin 2\varphi \tag{I.97}$$

This case of slip lines intersecting the surface is commonest.

When $\tau = k$ the surface layers adhere to the contact surface, the angle φ becomes zero and the case becomes that illustrated by Fig. 24*g*.

If $\tau = 0$, the angle φ becomes equal to 45° and the case becomes that shown in Fig. 24*c*.

22. DETERMINATION OF THE PRESSURE FOR AN INDENTING PLANE DIE

Using the slip lines method let us consider the stresses which arise when a die indents a plastically deformed body whose dimensions in the direction opposite to the p'ane in contact with the die (Fig. 26) are infinite

We assume that the deformation is two-dimensional. The width *AB* of the die is assumed to be relatively small, so that the friction force along the contact surface can be neglected.

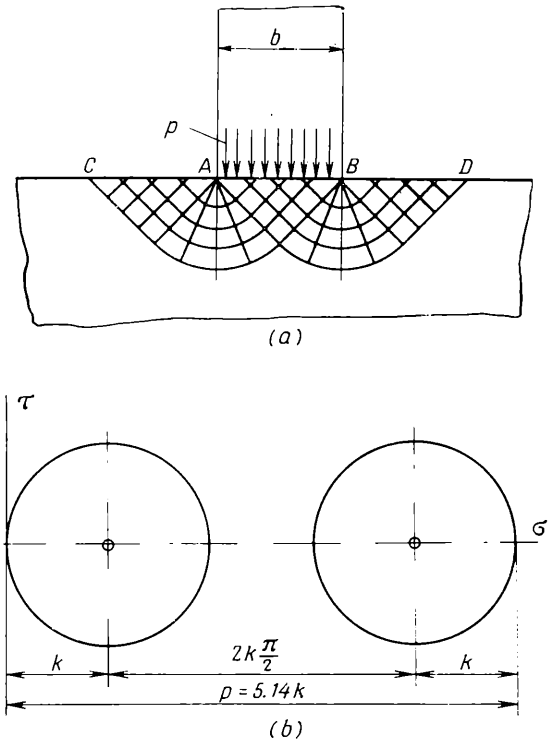

Fig. 26. Slip lines for the indentation of a die into a body extending to infinity on one side of a plane (*a*), and the position of the stress circle for the portions AC and AB (*b*)

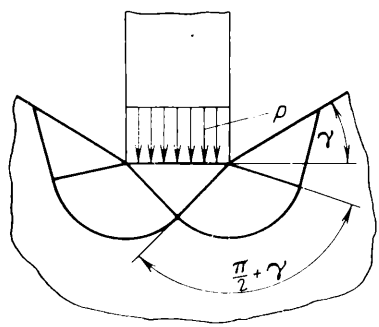

Fig. 27. The angle of rotation of a characteristic emerging from the contact surface to the free zone

In accordance with the case considered above (Fig. 24*c*), the slip lines approach the contact surface at an angle of 45°. Owing to the fact that the strain extends to the zones AC and BD adjoining the die, the slip lines will also occur in these zones, and, according to the scheme shown in Fig. 24*a*, they must approach the free surface also at an angle of 45°. Joining all three parts AB, AC and BD of the slip lines into a single system, we obtain the network of lines shown in Fig. 26*a*.

The stress circle for the parts AC and BD touches the τ-axis (Fig. 26*b*) and, consequently, $(\sigma_m)_{AC} = k$. In passing from the free surface to the contact surface the slip lines rotate through $\frac{\pi}{2}$, and accordingly on the part AB the mean stress increases by $2k\frac{\pi}{2}$:

$$(\sigma_m)_{AB} = (\sigma_m)_{AC} + 2k\frac{\pi}{2}$$

and the centre of the stress circle is displaced along the σ-axis correspondingly by πk. From this it follows that the specific pressure along the contact surface is:

$$p = k + \pi k + k = k(2 + \pi) \approx 5.14k \tag{I.98}$$

This result is of great practical importance; it testifies to the considerable effect of the outer zones, i.e., the zones located close to the contact surface, on the resistance to deformation during compression.

In the process of conventional upsetting, if the effect of the contact friction is neglected, the resistance to strain would be $2k$. In this case, owing to the presence of the deformed portions AC and BD the resistance to deformation is 2.57 times greater:

$$p \left(1 + \frac{\pi}{2}\right) 2k \approx 2.57\,(2k) \tag{I.99}$$

This result largely explains why the hardness of metals, obtained from indentation tests by a sphere (equal to the specific pressure on the contact surface), is on the average 2.5 to 3 times higher than the yield stress.

In the case where the die is indented in a plane located in a hollow as shown in Fig. 27, the angle of rotation of the characteristic when it passes from the contact surface to the free portion is increased with a corresponding increase in the specific pressure:

$$p = 2k\left(1 + \frac{\pi}{2} + \gamma\right) \tag{I.100}$$

where γ is the additional angle of rotation of the characteristic (Fig. 27).

II

Internal and Surface Stresses in Rolled Metal

1. DISTRIBUTION OF THE STRESS AND STRAIN ACROSS THE THICKNESS OF A ROLLED STRIP

Many experimental and theoretical investigations have studied the distribution of stress and strain across the thickness of a rolled strip.

As a result of all these investigations we may confidently assert the non-uniform distribution of the strains, stresses and velocities of motion of a rolled strip across its section. The theory of plane sections, which arose out of the theory of rigid ends and which is widely used in scientific literature, was found to be untenable as a result of this work.

The results of these investigations also showed that the stresses and strains extend over certain portions of the rolled strip, over the so-called zones, which are adjacent to the geometrical zone of strain both on the entry side to the rolls and on the exit side.

We consider the problem of stress and strain distribution across the thickness of the strip being rolled, assuming that the rolling takes place between smooth rolls, and that the strip is very broad in relation to the length of the arc of contact and to the depth of the strip.

Consequently, the effect of spread may be neglected and the problem can be considered as two-dimensional.

The solution of this problem assumes two different forms dependent on the ratio of the arc of contact l to the mean depth h_m of the cross section of the rolled strip. When the ratio $l : h_m > 0.5$ to 1.0, the nature of the non-uniformity in the distribution of stress and strain

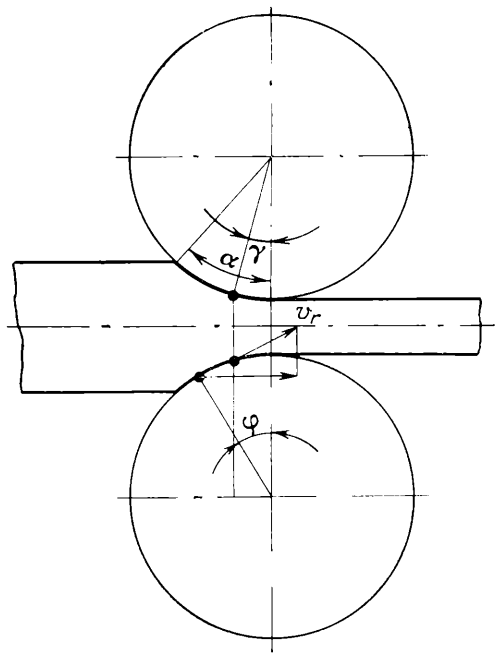

Fig. 28. Horizontal projection of the peripheral roll velocity

across the thickness of the strip differs considerably from rolling with the ratio $l : h_m < 0.5$, when the compressive strain does not penetrate the entire cross section of the metal being rolled. Let us consider both these cases.

The first case: the ratio $l : h_m > 0.5$ to 1.0. The depth of the strip being rolled is not very great in comparison with the arc of contact and the compressive strain extends over the entire depth of the cross section.

This case of rolling, for the angles of contact used in practice (not more than 30 to 35°), is characterized by the fact that the horizontal projection of the peripheral velocity of any point on the surface of the roll within the limits $\varphi = \gamma$ to α (Fig. 28) is greater than the mean

velocity of motion of the strip (v_{xm}), i.e.,

$$v_r \cos \varphi > v_{xm} \tag{II.1}$$

where v_r is the peripheral velocity of the rolls,
and when $\varphi = \gamma$ the horizontal projection will equal v_{xm}.

This can be verified by investigating the ratio

$$\frac{v_r \cos \varphi - v_{xm}}{v_{xm}}$$

We make the following substitution in this ratio:

$$v_{xm} = \frac{h_n v_r \cos \gamma}{h_x} = \frac{h_n v_r \cos \gamma}{h_n + D(\cos \gamma - \cos \varphi)} \tag{II.2}$$

where h_n is the depth of the rolled strip at the neutral section
h_x is the depth of the strip at a given section
D is the diameter of the rolls.

After certain simple transformations

$$\frac{v_r \cos \varphi - v_{xm}}{v_{xm}} = \frac{(D \cos \varphi - h_n)(\cos \gamma - \cos \varphi)}{h_n \cos \gamma} \tag{II.3}$$

Since for the case considered, when the ratio $l : h_m > 0.5$ to 1.0, practical considerations indicate that

$$D \cos \varphi > h_n \tag{II.4}$$

must hold, it follows that for $\varphi > \gamma$ the numerator of the above ratio will be positive, which verifies the inequality (II.1).

Consequently, the friction forces arising between the strip being rolled and the rolls tend to impart higher velocity to the zones of this strip adjacent to the rolls at the sections $\varphi = \gamma$ to α than to the middle portion of the strip; the latter must inevitably, although very slightly, lag behind (Fig. 29).

As a result of such an action of the contact friction forces a non-uniformity in the stress distribution arises across the depth of strip, and, consequently, a non-uniformity in the distribution of strains and velocities.

Thus, this non-uniformity in the distribution of the stresses, strains and velocities of the metal across the depth of the cross section of the strip must, in principle, be a consequence of the action of the contact friction forces, whether the metal slips along the surface of the rolls or not.

It would be therefore incorrect to assume that the non-uniformity of strains mentioned above exists only because of the presence of zones of sticking. Even if we assume that there are no zones of sticking, it does not mean that the above non-uniformity in the distribution of stresses and strains across the depth of the strip cannot be observed.

This non-uniformity in the distribution of strains is strongly resisted by the outer portion of the strip being rolled which is not subjected to deformation and where, in consequence, the velocity of motion across the section of the strip is distributed perfectly uniformly. Between this unstrained zone and the contact zone of deformation there is a zone, located outside the contact, over which we observe a gradual increase in the non-uniformity of the distribution of stresses, strains and velocities across the section of the strip.

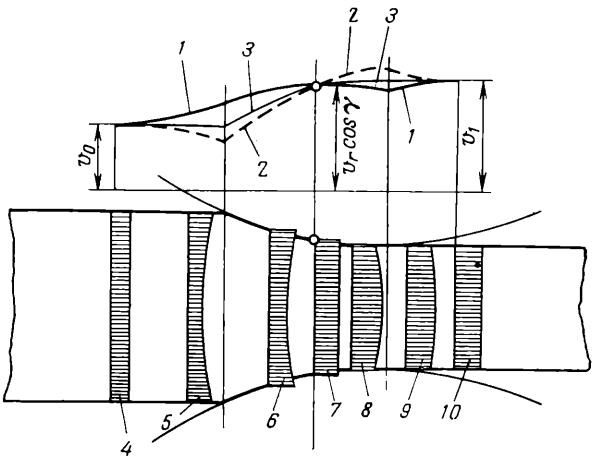

Fig. 29. Above: diagram showing the velocity of a rolled strip at different points in its cross section as it passes through the deformation zone. Below: diagrams showing the velocity distribution for different cross-sectional depths ($l : h_m \geq 0.5$ to 1.0):

1—the velocity of the outer portions of the strip cross section; *2*—the velocity of the middle portions of the strip cross section; *3*—the mean velocity of the strip cross section; *4*—velocity diagram for the unstrained zone; *5*—velocity diagram for the deformation zone at the entry, away from the contact zone; *6*—velocity diagram for the zone of backward slip; *7*—velocity diagram for the neutral zone; *8*—velocity diagram for the zone of forward slip; *9*—velocity diagram for the deformation zone at the exit, away from the contact zone; *10*—velocity diagram for the unstrained zone at the exit

Since the velocity across the section of the strip in the unstrained zone is distributed uniformly, whilst in the contact zone of deformation the outer layers of the metal, touching the rolls, tend to move faster than the inner layers, it follows that in the non-contact zone of deformation, at the cross section where the metal enters the rolls, there will appear longitudinal stresses. These stresses in the outer portion of the cross section are tensile, whilst in the central portion they are compressive (Fig. 30).

At the neutral section the velocity of motion of the rolled metal is equal to the horizontal projection of the peripheral velocity of the rolls, and, consequently, we can assume that along this cross section the stresses, strains and velocities will be distributed uniformly (see Fig. 29).

Beyond the limits of this section, in the zone of forward slip, the horizontal projection of the peripheral velocity of the rolls is smaller than the mean velocity of the metal being rolled, i.e.,

$$v_r \cos \varphi < v_{xm} \qquad \text{(II.4a)}$$

The validity of this inequality can be tested, as for inequality (II.1), by analyzing the ratio (II.3).

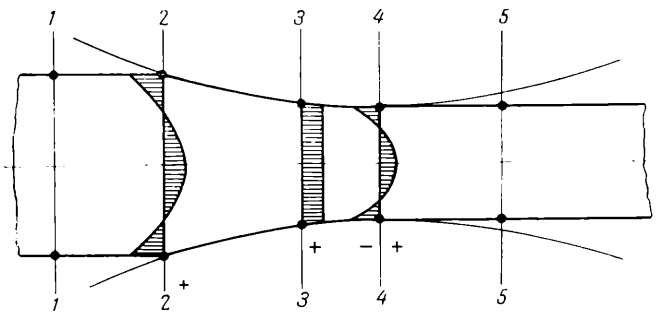

Fig. 30. Diagrams of normal stress for different cross-sectiona depths, $l : h_m > 0.5$ to 1.0 (a negative sign denotes tensile stress, a positive sign denotes compressive stress):

1-1 and *5-5*—sections at which the stresses are zero; *2-2*—section at the entry; *3-3*—neutral section; *4-4*—section at the exit

When $\varphi < \gamma$ the numerator of this ratio becomes negative (when $D \cos \varphi > h_n$) which verifies the inequality (II.4a).

Owing to the fact that the mean velocity of the metal in the zone of forward slip is greater than the horizontal projection of the peripheral velocity of the rolls, the latter play the role of a brake over this portion of the arc of contact. Consequently, the zones of the strip being rolled, adjacent to the rolls, have a smaller velocity than its middle part which always precedes them a little and gives rise to a non-uniformity in the distribution of stresses, strains and velocities across the depth of cross section of the strip (see Fig. 29).

Just as in the zone of backward slip, this non-uniformity in the strain distribution across the depth of the strip in the zone of forward slip interacts with the outer unstrained zone and gives rise to additional stresses.

Tensile stresses arise in the outer layers of the strip, both at the exit from the rolls and at the entry to the rolls, whilst compressive stresses arise in its middle part (see Fig. 30). Over the zone of deformation which is not in contact, these stresses and the corresponding longitudinal strains gradually diminish towards the exit, and become zero when the unstrained zone at the exit is reached.

The pattern mentioned above regarding the distribution of stresses and strains across the depth of the strip at the entry and at the exit is one of the basic laws of the theory of longitudinal rolling. It was first formulated and theoretically confirmed in 1933 by N. Sobolevsky (U.S.S.R.). But this viewpoint for a long time found no support in scientific literature, and, consequently, was little used and developed. Only comparatively recently, as a result of experimental investigations into the distribution of deformations across the thickness during longitudinal rolling, carried out by filming the zone of deformation, first by O. Muzalevsky and then by A. Kolpashnikov, have the patterns been discovered confirming the correctness of the theoretical conclusions of N. Sobolevsky.

This viewpoint received further development owing to the investigations by I. Tarnovsky, A. Pozdeyev and V. Lyashkov who studied the change of form of a coordinate network. They also established a considerable non-uniformity in the strain distribution across the depth of the cross section of the strip being rolled. The changes in the form of individual elements in a given section relative to each other far surpass in magnitude the strain approaching elastic strain, and, in connection with this large non-uniformity in the strain distribution, the character of the slip of the metal along the rolls is altered.

The most interesting part of these investigations was represented in the form of graphs showing the variation of deformation, over the arc of contact, of individual elements of the cross section of the strip, near the contact surfaces and in the middle of the strip. One such graph is shown in Fig. 31. The strain is plotted as ordinates; it is expressed by $\log_{10} \frac{h_0}{h_x}$, where h_0 and h_x represent the height of the elements of the coordinate network prior to entering the rolls and at any section respectively.

As is seen from this graph, at the beginning of the arc of contact the strain of the elements located close to the contact surfaces is more intensive than that of elements inside the cross section of the strip. This testifies not only to the non-uniformity in the distribution of strain over the cross section of the strip, but also to the motion of the outer layers having a higher velocity in comparison with the inner layers. This confirms the validity of the law of velocity distribution along the cross section mentioned above (see Fig. 29).

The point of intersection of the curves on the graph obviously corresponds to the position of the neutral section. To the other side of it the opposite phenomenon can be observed: the inner elements of the cross section of the strip experience a greater tension, and hence have also a higher velocity than the elements next to the rolls. This is also confirmed by the diagrams of Fig. 29 showing the distribution of velocities across the depth of the cross section of the strip being rolled.

In the middle portion of the arc of contact—curve *1* (see Fig. 31)—there is a segment of considerable length lying parallel to the axis

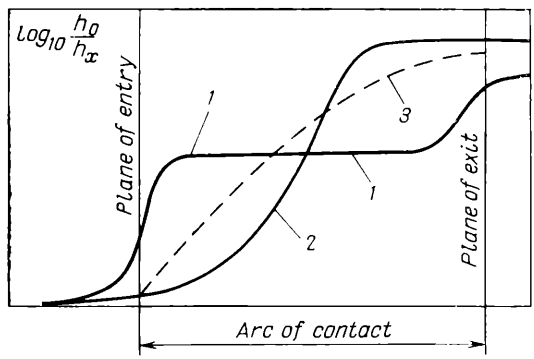

Fig. 31. Graph showing the variation of the strain: $\log_{10}\frac{h_0}{h_x}$ of an element of the cross section along the arc of contact (I. Tarnovsky): *1*—near the contact surfaces; *2*—in the middle of the strip cross section; *3*—for uniform deformation of the entire strip cross section

of abscissas. This signifies that the deformation of the cross-sectional elements close to the central portion of the arc of contact is slowed down. Over this part of the arc no slip occurs, and, consequently, a zone of sticking exists. This is the second very important conclusion, which is based on the results of experimental investigations by I. Tarnovsky and others, viz., that the non-uniformity in the strain distribution across the depth of the strip is considerable, so that a zone of sticking appears in the middle portion of the arc of contact.

The second case: the ratio $l : h_m < 0.5$ to 1.0. As the ratio of the arc of contact to the mean thickness of the cross section of the rolled strip diminishes, the effect of the outer zones on the deformation process becomes more active, and, particularly, the degree of non-uniformity increases in the distribution of stresses across the depth of the cross section of the strip.

Observations and investigations by a number of Soviet scientists have established that when the ratio of the arc of contact to the mean depth of the cross section of the strip being rolled becomes less than 0.5 to 1.0, the compressive strain does not penetrate the whole cross section of the strip, but is localized in the zones adjacent to the contact surfaces and in the non-contact zones situated close to the former.

In view of the fact that the final elongation of the rolled strip, i.e., the overall elongation of the metal emerging from the rolls,

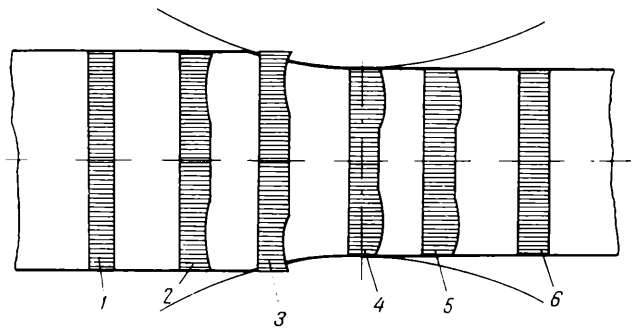

Fig. 32. The variation of velocity with depth in the rolled strip shown at various points along its length, with $l : h_m < 0.5$ to 1.0 and $D \cos \alpha > h_n$:

1—in the unstrained zone; *2*—in the deformation zone at the entry, away from the contact zone; *3*—in the zone of backward slip; *4*—in the zone of forward slip; *5*—in the zone of deformation at the exit, away from the contact zone; *6*—in the undeformed zone

is nearly the same in both its upper and lower layers and in the middle, a considerable stretching of the inner portion of the strip takes place as a result of the elongation during rolling of the parts adjacent to the rolls. The tensile stresses then appearing will often lead to the formation of internal cracks and cavities.

At the entry to the rolls tensile stresses will cause a slight increase in the velocity of motion of the inner portions of the strip, but at the exit, conversely, they will cause a slight slowing down.

If at the same time $D \cos \alpha > h_n$, then the phenomenon described in the first case of rolling will be partially obscured; that is, the tendency of the top and bottom layers of the strip to have a somewhat higher velocity when approaching the rolls and, conversely, to have a lower velocity, when leaving them, will be less marked.

Typical diagrams of the velocity distribution of the metal being rolled for the second case are shown in Fig. 32.

Over the sections located between the undeformed zones and the geometrical zone the strains increase strongly at the entry, whilst the large longitudinal stresses die down at the exit. Over the central

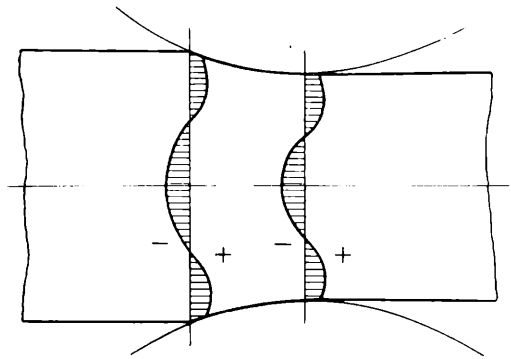

Fig. 33. The distribution of normal stresses across the sections at the entry to the rolls and at the exit from the rolls, with $l : h_m < 0.5$ to 1.0 and $D \cos\alpha > h_n$ (a negative sign denotes tensile stress; a positive sign denotes compressive stress)

portion of the strip these stresses will be tensile, but in the top and bottom layers (which balance these stresses) they are compressive (Fig. 33). Here it is of interest to note the two opposing processes when longitudinal stresses arise at the entry and exit on the actual surface of the rolled strip. When $D \cos\alpha > h_n$ tensile stresses must arise owing to the fact that $v_r \cos\alpha$ is higher than the mean entry

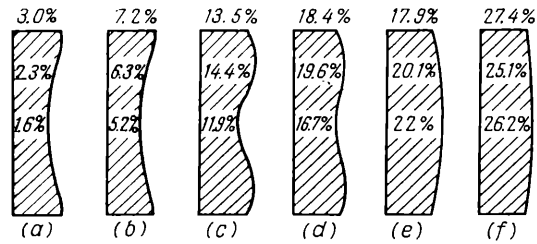

Fig. 34. The distribution of strain with depth when hot rolling a slab of alloy Д16 with different reductions and different ratios of $l : h_m$ (A. Kolpashnikov):

Index	*a*	*b*	*c*	*d*	*e*	*f*
$\frac{\Delta h}{h_0}$, %	2.8	6.7	12.2	16.9	20.4	25.3
$l : h_m$	0.3	0.45	0.6	0.92	1.0	1.25

velocity of the metal into the rolls. But at the same time there is a tendency for compressive stresses to appear as a result of the metal being displaced from the contact surfaces, as happens when a die is pressed into the surface of a large solid.

These trends in the distribution of strains across the depth of the cross section of the strip being rolled, as already mentioned above, have been obtained on the basis of a number of experimental investigations. As an example Fig. 34 gives the data on the strain distribution over the depth of the cross section of the strip obtained by A. Kolpashnikov using high speed photography of the rolling of a coordinate network marked on the side surface of a slab of alloy Д16. The slab was rolled in a hot condition with reductions of 2.8, 6.7, 12.2, 16.9, 20.4 and 25.3%. The results of these tests confirm that over the whole range of these reductions the strains over the depth of the strip are distributed non-uniformly. For a reduction within the limits of 2.8 to 16.9%, when the ratio $l : h_m \approx 0.3$ to 0.92, the deformation of the central portion of the strip is less than that of the outer layers. This corresponds to the case shown in Fig. 32. But when the reduction equals 20.4 and 25.3%, with the ratio $l : h_m \approx 1.0$ and 1.25, the deformation of the inner parts will be greater than that of the outer layers, and this case of rolling will correspond to the case shown in Fig. 29.

2. A SIMPLIFIED FORM OF THE DIFFERENTIAL EQUATION OF SPECIFIC PRESSURE

From the analysis considered above concerning the distribution of strains across the depth of the cross section of the strip being rolled we can determine only the laws for the qualitative variation of stresses. Up to now no analytical relationships for stresses dependent on the factors having an influence on them have been established. Hence the problem concerning the influence of the state of stress on the specific pressure must be solved by approximation.

We shall consider the case of rolling where the length of the arc of contact exceeds the mean depth of the cross section of the strip being rolled. At the same time we shall assume that the rolls are cylindrical and the width of the strip being rolled is several times the length of the arc of contact. Accordingly the problem can be considered as two-dimensional.

Let us isolate from the strip being rolled a certain element *abdc* (Fig. 35) bounded by the cylindrical surfaces of both rolls and by two planes perpendicular to the direction of rolling and separated from each other by an infinitely small distance dx. We consider the conditions of equilibrium of this element; accordingly we project

all the forces acting on the element on to the direction of rolling.

On the right-hand side of the strip the element is acted on by the force

$$\sigma_x h_x$$

where σ_x is the mean normal compressive force arising in the section bd of the strip being rolled, and

h_x is the depth of the cross section.

Suppose that in the plane ac the mean normal stress is $\sigma_x + d\sigma_x$, and the depth of the cross section is $h_x + dh_x$. Then on the left-hand side of the strip the isolated element is acted on by the force

$$(\sigma_x + d\sigma_x)(h_x + dh_x)$$

We shall first consider the equilibrium of the element when it is closer to the point A than to the point B, i.e., this element is located

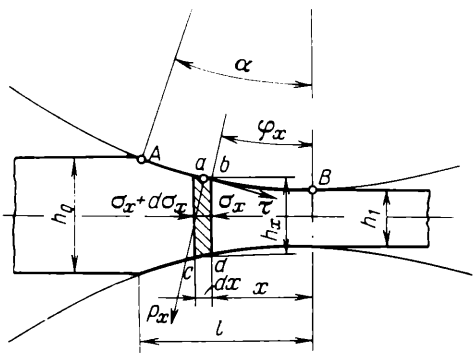

Fig. 35. Elementary forces acting on the rolled metal in the zone of backward slip

in the zone of backward slip, and its particles, touching the rolls, tend to slip along them in the direction opposite to the rotation of the rolls. The horizontal projection of the forces acting on the element from the direction of the rolls can clearly be expressed as follows:

$$2\left(p_x \frac{dx}{\cos \varphi_x} \sin \varphi_x - \tau_x \frac{dx}{\cos \varphi_x} \cos \varphi_x\right)$$

where p_x is the specific roll pressure on the metal being rolled

φ_x is the angle between the tangent to the arc ab and the horizontal plane

τ_x is the shear stress acting on the contact surfaces which is caused by the friction forces arising between the strip and the surface of the rolls.

The sum of the horizontal projections of all the forces acting on the element is

$$\sum X = (\sigma_x + d\sigma_x)(h_x + dh_x) - \sigma_x h_x - 2p_x \tan \varphi_x dx + 2\tau_x dx = 0 \quad \text{(II.5)}$$

The quantities dx and $\tan \varphi_x$ entering this equation can be expressed as

$$dx = \frac{dh_x}{2 \tan \varphi_x}$$

If we substitute this value of dx into equation (II.5) and neglect the infinitely small quantities of the second order, we obtain

$$d\sigma_x - (p_x - \sigma_x)\frac{dh_x}{h_x} + \frac{\tau_x}{\tan \varphi_x}\frac{dh_x}{h_x} = 0 \quad \text{(II.6a)}$$

When the element *abdc* is close to the point B, i.e., in the zone of forward slip, then the particles touching the rolls tend to slip along the surface of the rolls in the direction of the rotation of the rolls. The conditions of equilibrium of this element obviously remain the same as for the zone of backward slip, only the friction forces are directed the other way. The equation of equilibrium for the zone of forward slip in this case can be expressed as follows:

$$d\sigma_x - (p_x - \sigma_x)\frac{dh_x}{h_x} - \frac{\tau_x}{\tan \varphi_x}\frac{dh_x}{h_x} = 0 \quad \text{(II.6b)}$$

To solve equations (II.6a) and (II.6b) it is necessary to find the relationship between the specific pressure p_x and the stress σ_x. For this purpose we use the equation of plasticity derived above for a two-dimensional strain [see equation (I.70)]:

$$\left(\frac{\sigma_x - \sigma_y}{2}\right)^2 + \tau^2_{xy} = k^2$$

Taking the vertical and horizontal stresses σ_1 and σ_3 as the principal stresses, we may write

$$\sigma_1 - \sigma_3 = 2k \quad \text{(II.7)}$$

where

$$\sigma_1 = \left(p_x \frac{dx}{\cos \varphi_x} \cos \varphi_x \pm \tau \frac{dx}{\cos \varphi_x} \sin \varphi_x\right)\frac{1}{dx}$$

The second term of the right-hand side of this equation can obviously be neglected owing to its smallness in comparison with the first term. Then

$$\sigma_1 = p_x \quad \text{and} \quad \sigma_3 = \sigma_x$$

From this, according to equation (II.7),

$$p_x - \sigma_x = 2k \quad \text{(II.8)}$$

Substituting this value of $p_x - \sigma_x$ into equations (II.6a) and (II.6b) we obtain the fundamental differential equation for the specific pressure:

$$d(p_x - 2k) = \left(2k \mp \frac{\tau_x}{\tan \varphi_x}\right) \frac{dh_x}{h_x} \qquad \text{(II.9)}$$

The minus sign in front of the second term on the right-hand side of this equation refers to the zone of backward slip, whilst the plus sign refers to the zone of forward slip.

The constants obtained as a result of integrating equation (II.9) are determined from the initial conditions. For this we find the specific pressure at the points A and B. We take the more general case, when the strip being rolled is subjected to tension at the entry to the rolls and at the exit from them, which in practice is often observed with cold rolling, and also when rolling is carried out in continuous mills. The tensile stresses arising in the strip as a result of its tensioning are denoted by σ_A at the entry to the rolls, i.e., when $x = l$, and by σ_B at the exit from the rolls, when $x = 0$. Then, in accordance with equation (II.8), the specific pressures are:

at point A,

$$\left.\begin{aligned} p_A &= 2k - \sigma_A = \xi_0 2k \\ p_B &= 2k - \sigma_B = \xi_1 2k \end{aligned}\right\} \qquad \text{(II.10)}$$

at point B.

When tension is absent the specific pressures at the points A and B are equal to the quantity $2k$.

The subsequent solution of equation (II.9) may be carried out in two ways: (1) the value of k varies along the arc of contact, and (2) the value of this quantity is constant. A variation of the quantity k along the contact surface during the rolling is possible owing to the hardening of the metal, the different strain rates at the beginning and the end of the arc of contact, and, consequently, the strength, as well as the variation of the temperature of the rolled metal in the direction towards the point B.

V. Smirnov has considered the solution of the equation of specific pressure, assuming that the variation of the quantity k, due to the cold working, is according to the equation

$$p_x - \sigma_x \approx \nu 2k \left(\frac{h_0}{h_x}\right)^n$$

where ν and n are coefficients depending on the hardening characteristics of the metal.

Having made a detailed analysis of the results of his solution V. Smirnov arrived at the conclusion that if instead of the variable

value of k its average value is taken, i.e.,

$$k = \frac{k_A + k_B}{2} \tag{II.11}$$

where k_A and k_B are the values of k at the beginning and end of the arc of contact,

then the accuracy of the solution of the equation is not substantially altered.

Taking into consideration this circumstance, let us solve equation (II.9) with a constant value of k along the arc of contact as given by equation (II.11). Then in accordance with equation (II.8)

$$d\sigma_x = dp_x$$

The differential equation of specific pressure is

$$dp_x = \left(2k \mp \frac{\tau_x}{\tan \varphi_x}\right) \frac{dh_x}{h_x} \tag{II.12}$$

The general solution of this equation in exact form gives rise to difficulties owing to the inadequate definition of the relationship between p_x and τ_x. Below we shall consider certain characteristic cases of friction arising between the metal being rolled and the surface of the rolls.

3. SPECIFIC PRESSURE IN THE CASE OF SLIP WITH DRY FRICTION

In the case when the metal being rolled slips along the surface of the rolls with dry friction the force of friction can be expressed as follows:

$$\tau = \mu p_x$$

After substituting this value of τ into equation (II.12) we obtain the equation of von Kármán:

$$dp_x = \left(2k \mp \frac{\mu p_x}{\tan \varphi_x}\right) \frac{dh_x}{h_x} \tag{II.13}$$

The variable quantities h_x and φ_x appearing in this equation are determined by the coordinates of the arc of contact (Fig. 36). The equation of a circle which represents the cross section of the roll is

$$x^2 + (y - a)^2 = r^2$$

where y and a are the distances along the vertical, from the axis of the rolled strip to any point on the surface of the roll and to its axis respectively (Fig. 36), and

r is the radius of the roll.

From this we find

$$x = \sqrt{r^2 - (y-a)^2}$$

$$dx = \frac{(y-a)\,dy}{\sqrt{r^2-(y-a)^2}}$$

$$\tan\varphi_x = \frac{dy}{dx} = \frac{\sqrt{r^2-(y-a)^2}}{y-a}$$

After substituting this value of $\tan\varphi_x$ into equation (II.13), and noting that $\frac{h_x}{2} = y$, we obtain

$$dp_x = \frac{2k\,dy}{y} \mp \frac{\mu p_x (y-a)\,dy}{y\sqrt{r^2-(y-a)^2}} \qquad \text{(II.14)}$$

This equation can be solved if we introduce the integrating factor

$$e^{\pm\int \frac{\mu(y-a)\,dy}{y\sqrt{r^2-(y-a)^2}}}$$

Subsequently, however, the integral

$$\int \frac{1}{y} e^{\mu \sin^{-1}\frac{y-a}{r} - \frac{a\mu}{\sqrt{a^2-r^2}}\sin^{-1}\left(\frac{a^2-r^2}{ry}-a\right)} dy$$

appears in the equation, and can be evaluated only by expanding the integrand in a series. The final results obtained thereby are cumbersome and not completely accurate.

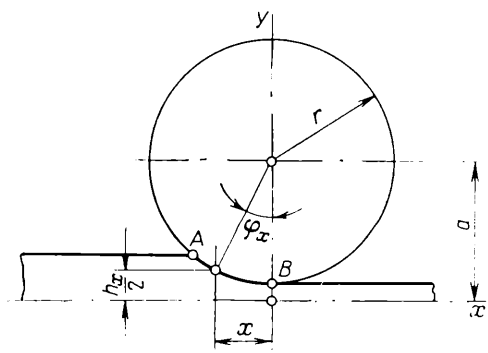

Fig. 36. Determination of x and $\frac{h_x}{2}$

Since the angle of contact of the metal in a majority of cases does not exceed 20 to 30° for hot rolling and 4 to 8° for cold rolling, it can with sufficient accuracy be equated to a curve for which the solution of equation (II.13) is simplified.

This method of solution should also be chosen because in cold rolling, owing to the high specific pressure, the rolls are subjected to a considerable local compressive strain, with the result that in practice the arc of contact will not be an arc of a circle.

Below we shall consider the two simplest solutions of this equation: in the first case we equate the arc of contact to a parabola; in the second we equate it to a chord.

For practical calculations both of these solutions may be considered as completely accurate.

We equate the arc of contact to a parabola whose vertex is located at point B and whose side passes through point A (see Fig. 36).

The equation of this parabola has the form

$$h_x = ax^2 + b$$

When the curve passes through points A and B, the constant coefficients a and b will be

$$a = \frac{\Delta h}{l^2} = \frac{1}{r} \quad \text{and} \quad b = h_1$$

where l is the horizontal projection of the arc of contact, and
Δh is the linear reduction.

We further find that

$$dh_x = 2ax\,dx = \frac{2\Delta h}{l^2}\,x\,dx = \frac{2x\,dx}{r}$$

$$\tan\varphi_x = \frac{dh_x}{2dx} = ax$$

We substitute these values of h_x, dh_x and $\tan\varphi_x$ into equation (II.13):

$$dp_x = (2akx \pm \mu p_x)\frac{2dx}{ax^2+b} \tag{II.15}$$

We introduce the new variable u:

$$x = \sqrt{\frac{b}{a}}\tan u$$

Then

$$u = \tan^{-1}x\sqrt{\frac{a}{b}} \qquad du = \sqrt{\frac{a}{b}}\,\frac{dx}{1+\frac{a}{b}x^2}$$

whence

$$\frac{dx}{ax^2+b} = \frac{du}{\sqrt{ab}}$$

After substituting the value of u into equation (II.15) we obtain

$$dp_x - 4k \tan u \, du \pm \frac{2\mu p_x}{\sqrt{ab}} du = 0 \qquad \text{(II.16)}$$

Instead of p_x we introduce two new variables:

$$p_x = vt$$

Then

$$dp_x = t \, dv + v \, dt$$

Substituting these values of p_x and dp_x into equation (II.16), and also denoting

$$\frac{2\mu}{\sqrt{ab}} = m$$

we obtain

$$t \, dv + v \, dt - 4k \tan u \, du \pm mvt \, du = 0 \qquad \text{(II.17)}$$

We assume that the variable quantity t just introduced satisfies the condition

$$dt + mt \, du = 0 \qquad \text{(II.18)}$$

Then

$$\log t = -mu$$

or

$$t = e^{-mu} \qquad \text{(II.19)}$$

Substituting the expressions (II.18) and (II.19) into equation (II.17) we obtain

$$e^{-mu} \, dv = 4k \tan u \, du$$

After integration we have

$$v = 4k \int e^{mu} \tan u \, du + C$$

or

$$p_x = e^{-mu} \left[4k \int e^{mu} \tan u \, du + C \right] \qquad \text{(II.20)}$$

The integral in this equation can be calculated only approximately, as a result of expanding one of the integrands in a series.

For low and medium reductions, when Δh does not exceed h_1 and $u < 1$, we obtain the convergent series for $\tan u$:

$$\tan u = u + \frac{u^3}{3} + \frac{2u^5}{3 \times 5} + \ldots$$

Substituting this value of $\tan u$ into equation (II.20), p_x can be calculated by means of term by term integration with any accuracy, depending on the number of terms of the series used.

In the given case we confine ourselves to a calculation of $\tan u$ for small reductions, when the convergence of the series obtained

is so rapid that we can limit ourselves to its first term. Then equation (II.20)
for the zone of backward slip assumes the form

$$p_x = C_0 e^{-mu} - \frac{4k}{m^2}(1 - mu) \tag{II.21}$$

whilst for the zone of forward slip this expression is

$$p_x = C_1 e^{mu} - \frac{4k}{m^2}(1 + mu) \tag{II.22}$$

The constant quantities C_0 and C_1 in these equations are determined from the initial conditions.

At the point A, where $x = l$,

$$p_x = 2k - \sigma_A$$

$$u = u_0 = \tan^{-1}\sqrt{\frac{\Delta h}{h_1}}$$

at the point B, where $x = 0$,

$$p_x = 2k - \sigma_B$$

$$u = 0$$

Substituting these values of p_x and u into equations (II.21) and (II.22) we obtain

$$C_0 = 2k\left[\xi_0 + \frac{2}{m^2}(1 - mu_0)\right] e^{mu_0}$$

$$C_1 = 2k\left(\xi_1 + \frac{2}{m^2}\right)$$

where

$$\xi_0 = 1 - \frac{\sigma_A}{2k} \quad \text{and} \quad \xi_1 = 1 - \frac{\sigma_B}{2k}$$

After substituting these values of C_0 and C_1 into equations (II.21) and (II.22) we obtain the final expression for the specific pressure in the zone of backward slip:

$$p_x = 2k\left\{\left[\xi_0 + \frac{2}{m^2}(1 - mu_0)\right] e^{m(u_0 - u)} - \frac{2}{m^2}(1 - mu)\right\} \tag{II.23}$$

whilst in the zone of forward slip

$$p_x = 2k\left[\left(\xi_1 + \frac{2}{m^2}\right) e^{mu} - \frac{2}{m^2}(1 + mu)\right] \tag{II.24}$$

where

$$m = \frac{2\mu l}{\sqrt{h_1 \Delta h}}$$

$$u_0 = \tan^{-1}\sqrt{\frac{\Delta h}{h_1}}$$

and

$$u = \tan^{-1}\left(\sqrt{\frac{\Delta h}{h_1}}\,\frac{x}{l}\right)$$

According to these equations the minimum specific pressure is observed at the points A and B; towards the neutral section this pressure increases (Fig. 37). The maximum specific pressure occurs close to the neutral section where both the pressure curves expressed by equations (II.23) and (II.24) intersect.

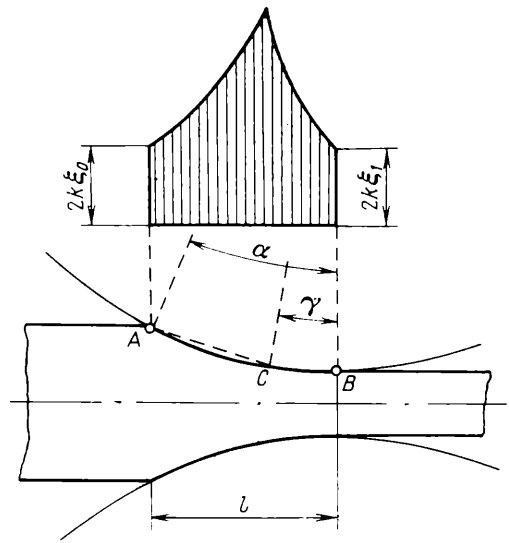

Fig. 37. The distribution of the specific pressure along the arc of contact during slipping with dry friction $\tau = \mu p_x$

Tselikov's equation. If the arc of contact is equated to a chord passing through the points A and B (Fig. 37), or to two chords (AC for the zone of backward slip, and BC for the zone of forward slip), the solution of equation (II.13) is considerably simplified. The final results obtained in this case are simpler and hence more suitable for practical calculations. The discrepancies arising from this assumption—as comparative calculations have shown—are quite insignificant. In particular, for medium and high reductions, and also for angles of contact which are less than the angle of friction, this method of solution gives considerably more accurate results than calculations based on equations (II.23) and (II.24).

In conjunction with this, taking in equation (II.13)

$$\tan \varphi_x = \tan \frac{\alpha + \gamma}{2}$$

for the segment AC, and

$$\tan \varphi_x = \tan \frac{\gamma}{2}$$

for the segment BC,
we obtain

$$dp_x = (2k - \delta_0 p_x) \frac{dh_x}{h_x} \tag{II.25}$$

for the zone of backward slip, and

$$dp_x = (2k + \delta_1 p_x) \frac{dh_x}{h_x} \tag{II.26}$$

for the zone of forward slip,
where

$$\delta_0 = \frac{\mu}{\tan \frac{\alpha + \gamma}{2}} \qquad \delta_1 = \frac{\mu}{\tan \frac{\gamma}{2}} \tag{II.27}$$

After integration we obtain

$$p_x = C_0 h_x^{-\delta_0} + \frac{2k}{\delta_0} \tag{II.28}$$

for the zone of backward slip, and

$$p_x = C_1 h_x^{\delta_1} - \frac{2k}{\delta_1} \tag{II.29}$$

for the zone of forward slip.

The initial conditions are:

$$p_x = \xi_0 2k$$

when $h_x = h_0$, and

$$p_x = \xi_1 2k$$

when $h_x = h_1$.
From this we find C_0 and C_1:

$$C_0 = 2k \left(\xi_0 - \frac{1}{\delta_0} \right) h_0^{\delta_0} \tag{II.30a}$$

$$C_1 = 2k \left(\xi_1 + \frac{1}{\delta_1} \right) h_1^{-\delta_1} \tag{II.30b}$$

Substituting these values of C_0 and C_1 into equations (II.28) and (II.29) we obtain the final expressions for determining the specific pressure:

$$p_x = \frac{2k}{\delta_0} \left[(\xi_0 \delta_0 - 1) \left(\frac{h_0}{h_x} \right)^{\delta_0} + 1 \right] \tag{II.31}$$

for the zone of backward slip, and

$$p_x = \frac{2k}{\delta_1}\left[(\xi_1\delta_1 + 1)\left(\frac{h_x}{h_1}\right)^{\delta_1} - 1\right] \tag{II.32}$$

for the zone of forward slip,
where

$$\delta_0 = \frac{\mu}{\tan\frac{\alpha+\gamma}{2}} \qquad \delta_1 = \frac{\mu}{\tan\frac{\gamma}{2}} \tag{II.33}$$

If the metal is rolled without tension and no external forces, with the exception of that of the rolls, act on the strip, then the values of σ_A and σ_B, where $h_x = h_0$ and $h_x = h_1$, are zero. Then equations (II.31) and (II.32) assume the form:

$$p_x = \frac{2k}{\delta_0}\left[(\delta_0 - 1)\left(\frac{h_0}{h_x}\right)^{\delta_0} + 1\right] \tag{II.34}$$

for the zone of backward slip, and

$$p_x = \frac{2k}{\delta_1}\left[(\delta_1 + 1)\left(\frac{h_x}{h_1}\right)^{\delta_1} - 1\right] \tag{II.35}$$

for the zone of forward slip.

It follows from the analysis of the preliminary law describing the distribution of the specific pressure along the arc of contact that this pressure depends on a number of factors: the coefficient of external friction, the depth of the strip being rolled, reduction, the diameter of the rolls and, finally, the tension of the strip being rolled at the entry to the rolls and at the exit from them. To illustrate the nature of the influence of these factors on the specific pressure Figs. 38, 39, 40 and 41 show diagrams giving the distribution of this pressure over the arc of contact; these have been plotted from the data calculated from equations (II.31) and (II.32), (II.34) and (II.35).

Fig. 38 shows the theoretical distribution curve of the specific pressure along the arc of contact (under its horizontal projection l) in the case of rolling of wide strips with the same reduction of 30% but with different coefficients of friction (0.075, 0.1, 0.15, 0.2, 0.3 and 0.4). As is seen from this curve, the coefficient of the external friction exerts a very great influence on the specific pressure. The greater the coefficient of friction the greater the increase in the specific pressure in the direction of the neutral section, and, consequently, the greater the overall pressure of the metal on the rolls during the rolling.

Figs. 39 and 40 show similar curves, but representing the distribution of the specific pressure along the arc of contact in the case of rolling a wide strip with different reductions and with rolls of differ-

ent diameters (i.e., with different $\frac{h_1}{D}$ ratios) under otherwise identical conditions. Analyzing these curves we note that as the length of the arc of contact increases (when its length is greater than the mean depth of the cross section of the strip being rolled) and as the depth of the strip diminishes, the mean specific pressure will increase.

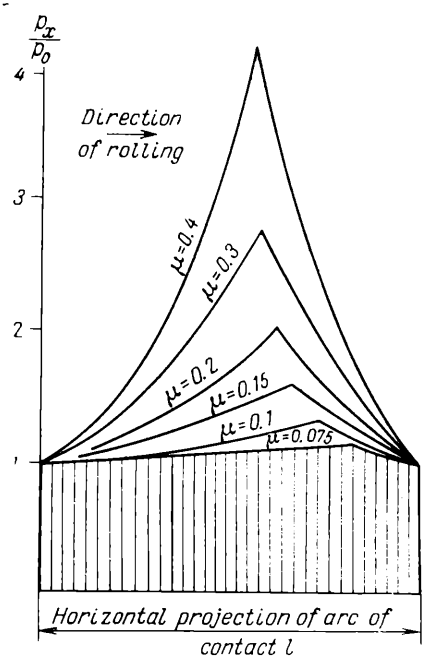

Fig. 38. Theoretical distribution curves of the specific pressure along the arc of contact (with $\tau = \mu p_x$) for two-dimensional rolling with different coefficients of friction $\left(\frac{\Delta h}{h_0} = 30\%;\ \alpha = 5°40'\right.$ and $\left.\frac{h_1}{D} = 1.16\%\right)$

Consequently, the overall pressure of the metal on the rolls in this case will increase not only as a result of the increase in the area of contact between the metal and the rolls, but also as a result of an increase in the specific pressure itself.

This preliminary law for the distribution of the specific pressure along the arc of contact also enables very important conclusions to be drawn about the effect of the back and front tension of the strip on the pressure of the metal on the rolls during the rolling. To illustrate the character of this effect Fig. 41 shows the theoretical distri-

bution curves of the specific pressure along the arc of contact when wide strips are rolled with different tension [for $\sigma = 0$; 0.2 ($2k$) and 0.5 ($2k$)]. These have been plotted from the data calculated from the formulas (II.31) and (II.32). Fig. 41*a* shows the curves when the tension acts on the rolled strip only from the side of its exit from the rolls, whilst Fig. 41*b* shows the case where the rolled strip is subjected

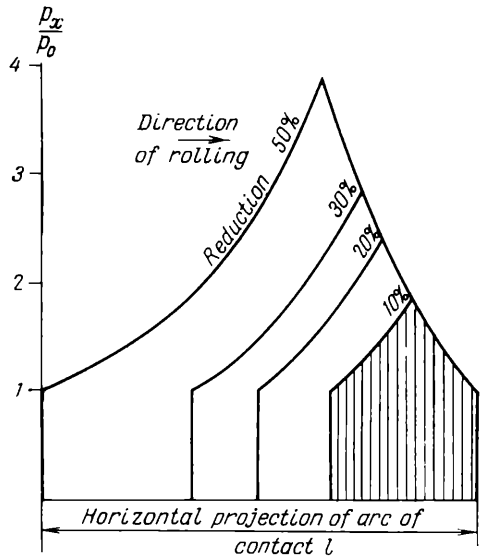

Fig. 39. Theoretical distribution curves of the specific pressure over the arc of contact (with $\tau = \mu p_x$) for two-dimensional rolling with different reductions $\left(\frac{\Delta h}{h_0} = 0.1,\ 0.2,\ 0.3 \text{ and } 0.5\right)$; otherwise conditions are identical and work hardening is absent $\left(\frac{h_1}{D} = 0.5\% \text{ and } \mu = 0.2\right)$

to tension from both sides: from the side of the entry to the rolls and from the side of the exit. Comparing the individual curves we notice that when the rolled strip is tensioned the specific pressure is considerably reduced. At the same time the greater the tension which is applied to the metal being rolled the lower will be the pressure of the metal on the rolls. It should also be noted that the tension from the side of the metal entering the rolls causes a reduction in the specific pressure, as does the tension from the exit side of the rolls.

In reality (in particular, when hard metals are rolled) the reduction in the pressure of the metal on the rolls due to tension will be yet more considerable than that shown in Fig. 40, owing to the reduc-

tion in the local elastic compression of the rolls (contact compression) due to tension, and to a certain shortening of the actual length of the arc of contact in connection with this.

Equations (II.31) and (II.32), in the derivation of which the arc of contact was equated to a chord, are simpler and hence more convenient than equations (II.23) and (II.24). The error incurred thereby is very small and has no practical importance, except in

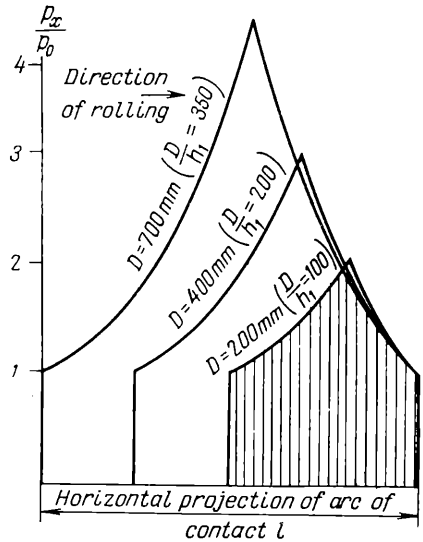

Fig. 40. Theoretical distribution curves of the specific pressure along the arc of contact (with $\tau = \mu p_x$) for two-dimensional rolling with rolls of different diameters $\left(\frac{D}{h_1} = 100,\ 200 \text{ and } 350\right)$ and a reduction of 30% ($\mu = 0.3$)

cases where the specific pressure and the specific friction forces are analyzed for various contact angles whose value is close to the angle of friction or exceeds it. Under these conditions the stress σ_x varying along the rolled strip will strongly depend not only on the contact friction forces, but also on the variation of the horizontal projection of p_x. Accordingly calculations of this kind should be carried out using equation (II.23), or the arc of contact should be divided into several sections (suppose 4 to 6), on each of which the arc is equated to a small chord and the calculation is carried out using equations (II.31) and (II.32), with different values of δ for each section. The curves of the distribution of the specific pressure along the arc of contact thus calculated—when the angles of contact are greater than the angle of friction—have an interesting feature: over the

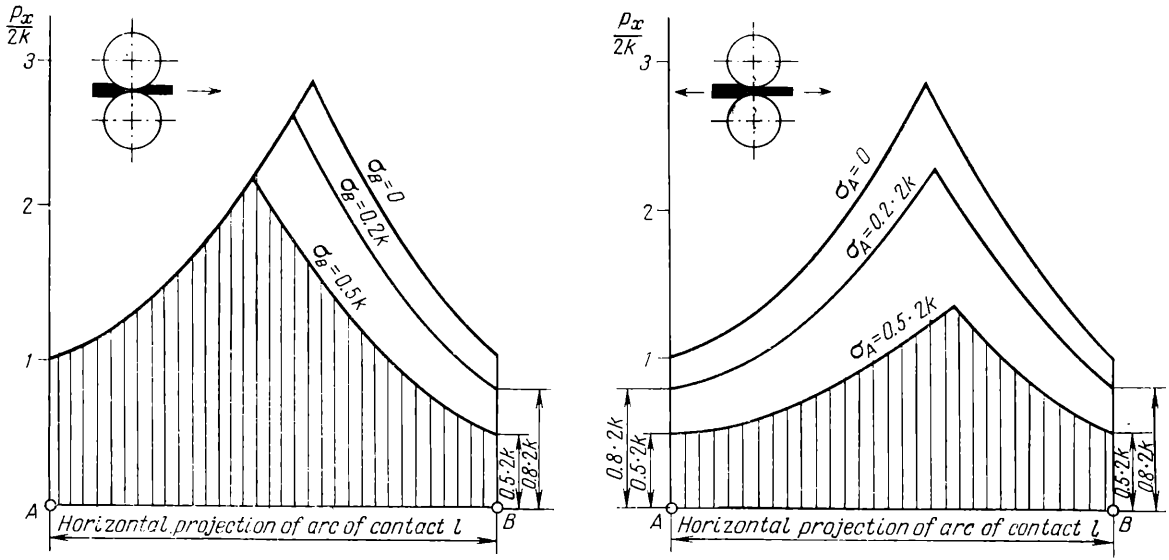

Fig. 41. Theoretical distribution curves of the specific pressure along the arc of contact (with $\tau = \mu p_x$) in the case of two-dimensional rolling with different tensions $\left[\sigma = 0;\ 0.2\,(2k) \text{ and } 0.5\,(2k) \text{ and a reduction of } 30\% \left(\alpha = 30°5';\ \mu = 0.2;\ \frac{h_1}{D} = 0.5\% \text{ and } \delta = 6\right)\right]$:

(*a*) tension at front end only; (*b*) tension at both front and back ends

segment where

$$\tan \varphi_x > \mu$$

the coefficient δ is negative and accordingly the curves of the specific pressure on the section from point A in the direction of rolling are characterized not by a rise, as usual, but by a fall (Fig. 42).

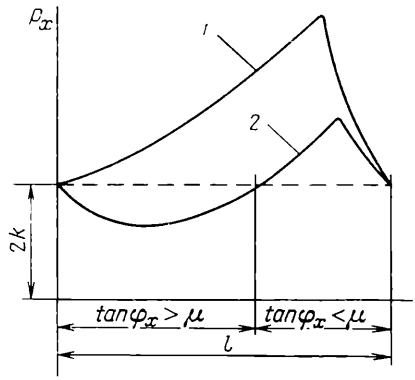

Fig. 42. Theoretical distribution curves of the specific pressure along the arc of contact (with $\tau = \mu p_x$) in the case of two-dimensional rolling with different arcs of contact but with the same horizontal projection of the arc of contact:
1—$\tan \varphi_x < \mu$ along the entire arc of contact; *2*—$\tan \varphi_x > \mu$ at the beginning of the arc of contact

From this we can conclude that if the angle of contact is greater than the angle of friction or close to it, the specific pressure is less than in the case where for the same extent of the arc of contact the rolling takes place for angles φ_x which are less than the angle of friction.

4. SPECIFIC PRESSURE IN THE CASE WHERE FRICTION FORCES ARE CONSTANT OVER THE ARC OF CONTACT

In the given case it is assumed that the specific friction force is constant and approximately equal to

$$\tau = \text{const.} \approx \mu 2k$$

This value of the friction force was suggested by Siebel.

For this condition the solution of equation (II.12) is considerably simplified. As before, we equate the arc of contact to parabolic arc. Then

$$h_x = ax^2 + b$$

$$dh_x = 2ax\,dx \quad \text{and} \quad \tan \varphi_x = ax$$

where

$$a = \frac{\Delta h}{l^2} \quad \text{and} \quad b = h_1$$

After substituting these values of h_x, dh_x and $\tan \varphi_x$ into equation (II.12) we have

$$dp_x = \frac{4k\,ax}{ax^2 + b}\,dx \mp \frac{2\tau\,dx}{ax^2 + b} \tag{II.36}$$

Denoting x by $\sqrt{\frac{b}{a}}\,z$ and then integrating we find the specific pressure

$$p_x = 2k \log_e (z^2 + 1) - \frac{\tau}{\sqrt{ab}} \tan^{-1} z + C_0 \tag{II.37}$$

for the zone of backward slip, and

$$p_x = 2k \log_e (z^2 + 1) + \frac{\tau}{\sqrt{ab}} \tan^{-1} z + C_1 \tag{II.38}$$

for the zone of forward slip.

From the initial conditions when $z = z_0$ and $z = 0$ we find the constants C_0 and C_1:

$$C_0 = 2k [\xi_0 - \log_e (z_0^2 + 1)] + \frac{\tau}{\sqrt{ab}} \tan^{-1} z_0 \tag{II.39}$$

$$C_1 = 2k\xi_1 \tag{II.40}$$

According to equations (II.37) and (II.38) the specific pressure is

$$p_x = 2k \left(\xi_0 - \log_e \frac{z_0^2 + 1}{z^2 + 1} \right) + 2\tau \sqrt{\frac{r}{h_1}} \tan^{-1} \frac{z_0 - z}{1 + z_0 z} \tag{II.41}$$

for the zone of backward slip, and

$$p_x = 2k [\xi_1 + \log_e (z^2 + 1)] + 2\tau \sqrt{\frac{r}{h_1}} \tan^{-1} z \tag{II.42}$$

for the zone of forward slip,
where

$$z = \sqrt{\frac{a}{b}}\,x = \sqrt{\frac{\Delta h}{h_1}}\,\frac{x}{l}$$

$$z_0 = \sqrt{\frac{\Delta h}{h_1}}$$

According to this theory the character of the curves giving the distribution of the specific pressure over the arc of contact is approximately the same as that given by the theory of the specific pressure when $\tau = \mu p_x$, considered above, except that the rise of the specific

pressure curves towards the neutral section takes place less steeply (Fig. 43). This is explained by the fact that the friction forces are assumed to be smaller in this theory than in the preceding theory.

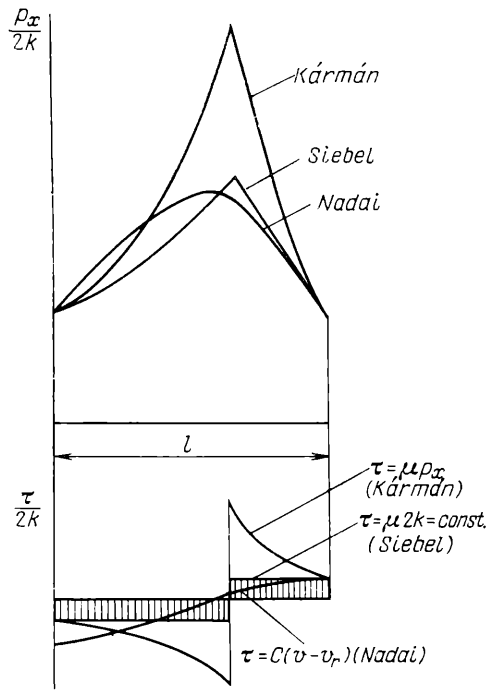

Fig. 43. The distribution of specific pressure and specific friction forces along the arc of contact during two-dimensional rolling according to different theories: dry friction (von Kármán); constant friction force (Siebel), and viscous friction (Nadai)

To illustrate this statement a diagram has been constructed in the lower part of Fig. 43, showing the value of specific external friction forces in accordance with the theories of Siebel, von Kármán and Nadai.

5. SPECIFIC PRESSURE IN THE CASE OF SLIP WITH VISCOUS FRICTION (NADAI'S THEORY)

We shall consider the distribution of the specific pressure over the arc of contact, starting from the assumption that a slip with liquid or viscous friction takes place between the metal being rolled and the rolls. This case of rolling is unlikely in practice, but neverthe-

less it is of a certain interest, since during the cold rolling of metal with lubricated, well polished rolls, and with high rolling velocities (10 to 30 m/s), the friction on individual portions of the contact surface can be expected to approximate liquid friction.

This assumption is also based to a great extent on the fact that the viscosity of lubricants strongly increases with pressure. Accordingly, despite the high specific pressures observed during cold rolling, a partial persistence of the oil film is entirely possible.

In the case of viscous friction the specific friction force, according to Newton's law, can be expressed as follows:

$$\tau = \eta \frac{dv}{dy} \tag{II.43}$$

where η is the viscosity, and

$\frac{dv}{dy}$ is the gradient of the velocity in the direction perpendicular to the plane of slip.

If the thickness of the oil film is denoted by Δ, the velocity gradient can approximately be written as:

$$\frac{dv}{dy} = \frac{v_x - v_r}{\Delta} \tag{II.44}$$

where v_x is the velocity of motion of the metal being rolled in a given section, and

v_r is the peripheral velocity of the rolls.

The velocities v_x and v_r, derived from the fact that the volume per second of the metal being rolled is constant, are

$$v_x = v_1 \frac{h_1}{h_x}$$

$$v_r = v_1 \frac{h_1}{h_n}$$

where v_1 is the exit velocity of the rolled metal from the rolls, and

h_n is the depth of the cross section of the rolled metal in the neutral plane.

If we substitute these values of the velocities into equations (II.44) and (II.43), the specific friction force

$$\tau = \mp \frac{\eta v_1 h_1}{\Delta} \left(\frac{1}{h_x} - \frac{1}{h_n} \right) \tag{II.45}$$

where the minus sign refers to the zone of backward slip, and the plus sign refers to the zone of forward slip.

The quantity $\frac{\eta v_1}{\Delta}$ in this equation is obviously the specific friction force for the velocity of slip equal to the exit velocity of the metal

from the rolls. We denote this quantity by

$$\tau_0 = \frac{\eta v_1}{\Delta} \tag{II.46}$$

Then the force τ, in accordance with equation (II.45), can be expressed as

$$\tau = \mp \tau_0 h_1 \left(\frac{1}{h_x} - \frac{1}{h_n} \right) \tag{II.47}$$

After substituting this value of τ into equation (II.12) we obtain

$$\frac{dp_x}{dx} - \frac{2k}{h_x} \times \frac{dh_x}{dx} - 2\tau_0 \left(\frac{1}{h_x} - \frac{1}{h_n} \right) \frac{h_1}{h_x} = 0 \tag{II.48}$$

The sign $\mp$ in front of the friction force disappears, and thus the equation of the specific pressure is common for both zones of backward and forward slip.

To solve this equation we equate the arc of contact with an arc of a parabola, as it was done above. Then

$$h_x = ax^2 + b \quad \text{and} \quad \tan \varphi_x = ax$$

where

$$a = \frac{\Delta h}{l^2} \quad \text{and} \quad b = h_1$$

Denoting

$$x = \sqrt{\frac{b}{a}}\, z$$

we obtain

$$h_x = 2b\,(1 + z^2)$$

We substitute these values of x and h_x into equation (II.48):

$$\frac{dp_x}{dz} - \frac{4kz}{1 + z^2} - \frac{A\tau_0}{1 + z^2} \left(\frac{1}{1 + z^2} - \frac{1}{1 + z_n^2} \right) = 0 \tag{II.49}$$

where z_n is a quantity depending on the position of the neutral section, i.e., when $h_x = h_n$

$$A = \frac{1}{\sqrt{ab}} = \frac{2l}{\sqrt{h_1 \Delta h}}$$

After integration we have

$$p_x = 2k \log_e (1 + z^2) + \frac{A\tau_0}{2} \left(\frac{z}{1 + z^2} - \frac{1 - z_n^2}{1 + z_n^2} \tan^{-1} z \right) + C \tag{II.50}$$

The constant C can be found from the initial conditions, if we put $z = 0$:

$$C = \xi_1 2k$$

The unknown quantity z_n in equation (II.50) can be eliminated assuming that when $x = l$ and correspondingly when $z = z_0$, the specific pressure

$$p = \xi_0 2k$$

Then the specific pressure

$$p_x = 2k \left[\xi_1 + \log_e (1 + z^2) + \frac{A\tau_0}{2} \left(\frac{z}{1+z^2} - B \tan^{-1} z \right) \right] \qquad \text{(II.51)}$$

where

$$B = \frac{1 - z_n^2}{1 + z_n^2} = \frac{\frac{4k}{A\tau_0} [\xi_1 - \xi_0 + \log_e (1 + z_0^2)] + \frac{z_0}{1+z_0^2}}{\tan^{-1} z_0} \qquad \text{(II.52)}$$

$$z = \frac{1}{l} \sqrt{\frac{\Delta h}{h_1}}\, x$$

$$z_0 = \sqrt{\frac{\Delta h}{h_1}}$$

It follows from this that for slip with liquid friction the curves for the specific pressure distribution for both zones (backward and forward slip) can be expressed by a single equation. We shall find the equation characterizing the variation of the friction forces over the arc of contact. For this we express the quantities h_x and h_n in equation (II.47) by z and z_n:

$$\tau = \mp \tau_0 \left(\frac{1}{1+z^2} - \frac{1}{1+z_n^2} \right) \qquad \text{(II.53)}$$

We determine the unknown z_n from equation (II.52):

$$z_n = \sqrt{\frac{1-B}{1+B}} \qquad \text{(II.54)}$$

Then

$$\tau = \mp \frac{\tau_0}{2} \left(\frac{2}{1+z^2} - B - 1 \right) \qquad \text{(II.55)}$$

Using this equation we can find the position of the neutral section, i.e., assuming that when $z = z_n$ the value $\tau = 0$. It should be pointed out that the position of the neutral section does not coincide with the maximum specific pressure. This can be verified by using equation (II.51), according to which when $z = z_n$ the derivative $\frac{dp_x}{dz}$ does not equal zero.

The very character of the specific pressure curve in this case will be completely different from those for other forms of friction. Instead of the sharp peak of the curve of specific pressure at the neutral section we now have a domed top.

To compare the theory of Nadai with the other two theories of specific pressure with $\tau_x = \mu p_x$ and $\tau_x = \text{const.}$, Fig. 43 represents curves showing the variation of the specific pressure and the specific friction forces along the arc of contact in accordance with the three theories. All these curves have been plotted for the case of rolling when $h_0 = 2$ mm, $h_1 = 1$ mm, $D = 200$ mm and $\xi_0 = \xi_1 = 1$. At the same time the forces of friction in accordance with the theory of Nadai have been calculated with the assumption that when $z = 0$ the value of the friction forces is the same as for the other theories, i.e.,

$$\tau = \mu 2k = 0.2 \times 2k$$

6. DISTRIBUTION OF FRICTION FORCES OVER THE ARC OF CONTACT

The three theories concerning the distribution of the specific pressure along the arc of contact which were considered above are based on the assumption that the metal being rolled slips along the surface of the rolls over the whole extent of the arc of contact. In the zone of backward slip the metal slips in the direction opposite to the rotation of the rolls, whilst in the zone of forward slip this takes place in the direction of the rotation of the rolls.

Depending on the character of slip assumed in these theories the contact friction forces are determined differently and so are the stress states caused by these forces. In the first theory, suggested by von Kármán, the friction forces are assumed to be proportional to the specific pressure, and accordingly it became known as *the theory of dry friction.*

Similar results were derived by E. Siebel. But in his results the friction forces were constant over the whole arc of contact, and equal to $\mu 2k$.

Considerably later Nadai proposed a theory of specific pressure according to which the friction forces were taken as proportional to the velocity of slip. This theory was worked out for cold rolling of metal with lubrication, starting from the assumption that viscous friction is possible between the metal and the rolls.

All these theories are associated with the rolling theory which prevailed more than 25 years ago. The basic shortcomings of the theory are the absence of a sufficient justification for the values of the contact friction forces adopted in them, the existence of a total slip over the arc of contact, and the limitation to certain particular cases of rolling when the effect of the outer zones is insignificant.

In contrast to this assumption of slip over the entire arc of contact there is another view stated in 1933 by N. Sobolevsky (U.S.S.R.),

according to which the metal being rolled does not necessarily slip along the surface of the rolls. This view, although it has not received a general approval, nevertheless deserves the closest attention and is doubtlessly correct under certain conditions of rolling. For example, there are grounds to believe that in the case of rolling thick strips, when the length of the arc of contact is small, the slip between the metal and the rolls is absent.

At the same time it would also be erroneous to deny completely the existence of slip between the metal and the rolls. For example, in the case of rolling of thin strips with a long length of the arc of contact the slip undoubtedly exists.

Analyzing both these views we can say that in the deformation region there is yet another zone besides the two zones of slip (the zones of backward and forward slip) where there is no slip between the metal being rolled and the rolls. In contrast to the zones of slipping we call this *the zone of sticking*. Thus, according to this new theory the boundary between the zones of backward and forward slip, where the direction of motion changes, is not a line but a certain zone over which the backward slip has ceased but the forward slip has not yet begun.

As no slip of the metal takes place over the surface of the rolls in the sticking zone, the condition of deformation in this zone, and hence the distribution law of the specific friction forces, are different from those in the zones of slipping.

Taking into consideration this circumstance, we begin the consideration of the problem of calculating the specific pressure by determining the law of distribution of the contact friction forces over the arc of contact, i.e., we consider the contact shear forces in conjunction with the most characteristic case of longitudinal rolling.

From the viewpoint of the methods of calculating the contact friction forces, practical cases of rolling wide strips with smooth rolls (bearing in mind two-dimensional strain) are conveniently divided into four types of rolling, which differ from each other by a different ratio of the length of the arc of contact to the mean depth of the rolled strip.

Type of rolling	The approximate value of the ratio $l : h_m$
I	5
II	2-5
III	0.5-2
IV	<0.5

The deformations for the above four types of rolling differ considerably in character, and accordingly, different methods must be used to calculate the contact friction forces and hence the specific pressure for these types of rolling. But the boundaries between these four types of rolling have not yet been established exactly; they depend not only on the ratio $l : h_m$ but also on other factors and, in particular, on the coefficient of friction, the reduction and the angle of contact. Accordingly the values of the ratio $l : h_m$ stated above should be regarded only as very tentative.

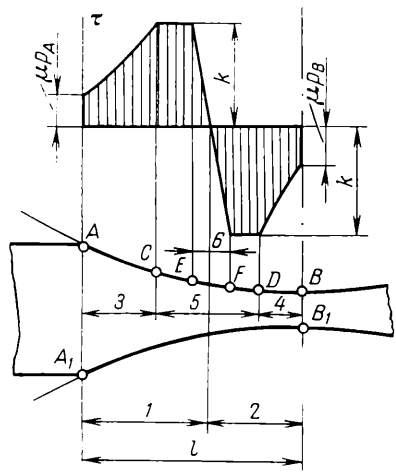

Fig. 44. The distribution of friction forces along the arc of contact when the ratio $l : h_m > 5$:

1—zone of backward slip; *2*—zone of forward slip; *3*—region of slipping in the zone of backward slip; *4*—region of slipping in the zone of forward slip; *5*—zone of sticking; *6*—zone of reduced deformation

I. When the ratio $l : h_m > 5$ there are zones on the arc of contact where the friction forces follow different laws.

At the beginning and at the end of the arc of contact, when its length considerably exceeds the depth of the cross section of the rolled strip, the metal undoubtedly slips along the surface of the rolls. This circumstance is confirmed by the data of numerous experimental investigations. Therefore, we can assume that on these regions, i.e., over the zones of slipping (Fig. 44), the friction forces are distributed according to the law of dry friction:

$$\tau = \mu p_x \qquad \text{(II.56)}$$

If at the beginning of the arc of contact $\tan \varphi_x > \mu$ then on this region of the arc, as was mentioned above, a reduction in the spe-

cific pressure (see Fig. 42) is observed, and, consequently, a reduction in the specific friction forces (Fig. 45).

Since the quantity p_x increases towards the centre of the arc of contact and, consequently, the quantity μp_x increases, the friction force can attain the value:

$$\tau \quad k \tag{II.57}$$

where k is the resistance to pure shear.

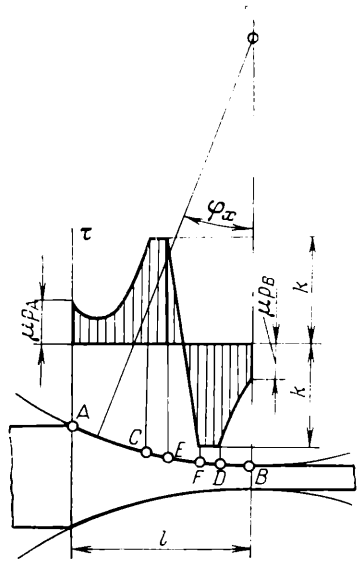

Fig. 45. The distribution of friction forces along the arc of contact when initially $\tan \varphi_x > \mu$

The friction cannot attain any higher value since when the resistance to slip along the contact surface is higher than k, internal slip or shear occurs in the metal next to the contact surface. Consequently, whenever the friction force on the contact surface reaches k (at points C and D in Figs. 44 and 45), the metal ceases to slip along the surface of the rolls so that on the rest of the segment CD of the arc of contact a zone of sticking is observed.

Over the portions of this zone close to the points C and D the friction forces are equal to k, i.e., for k = const. their value is constant.

On the middle portion of the zone of sticking close to the neutral section there appears a region where the plastic deformation is slowed down or is absent altogether. This region is also called *the region of stagnation.*

The presence of such a region of stagnation is confirmed by a number of experimental investigations, according to which a region is observed, close to the middle portion of the arc of contact, where there is no deformation along the arc, and in the case of a two-dimensional strain, where there is also no deformation in the radial direction. Certain investigators assume that in the case of large ratios $b_m : h_m$ (where b_m is the mean width of the rolled strip) the zone of sticking does not exist, in particular, when $l : h_m > 2.4$. But the tests conducted by I. Tarnovsky and V. Trubin provide evidence that the variation of this ratio of width to depth of the rolled strip over very wide limits ($b_m : h_m \approx 0.85$ to 3.4) shows no substantial influence on the extent of the zone of sticking. In all their tests on rolling lead pieces of various width, the extent of the zone of sticking at the mid-width of the strip was considerable and on the average equalled $l_{st} = (0.69 \text{ to } 0.73)l$. I. Tarnovsky and V. Trubin assume that the zone of sticking is somewhat larger in the middle of the test piece than at the sides, where the tensile stresses due to the increased zone of sticking are reduced. At the same time they considered the fact that in rolling lead test pieces the zone of sticking sharply contracts as the ratio $l : h_m$ increases to more than 1.85, and for a further increase of this ratio disappears altogether. This fact is doubtlessly of interest, and it shows the great difference in two-dimensional rolling processes, when the ratio $l : h_m > \sim 2$ (the first two types of rolling) and when $l : h_m < < \sim 2$ (the third and fourth types of rolling).

When the ratio $l : h_m > \sim 2$ the tendency of the metal to slip over the arc of contact increases sharply. As a consequence of this, as was already mentioned above, the zones of slipping AC and DB will appear (see Fig. 44). Simultaneously with the increase in slip the difference

$$v_r \cos \varphi - v_{xm}$$

in the inequality (II.1) must diminish, and, consequently, the non-uniformity in the distribution of the deformation across the depth of the strip becomes less severe. In this case the methods of investigation used by I. Pavlov and Ezhi Bazan (the method of imprints), and also by I. Tarnovsky and V. Trubin (the method of analyzing the coordinate network) are not sufficiently accurate for discovering small plastic strains (less than 1 to 2%). Because of this, the disappearance of the zone of sticking noted in these investigations when rolling test pieces having the ratio $l : h_m$ roughly in excess of 2 to 2.4 can rather be explained by the imperfections of the measuring equipment than by its actual absence.

The law for the distribution of contact shear stresses or friction forces in the region of stagnation of the zone of sticking has not yet

been determined in exact form. It can be established approximately on the basis of the analysis of experimental data on the distribution of the specific pressure over the arc of contact. For this we use equation (II.12), from which it follows that

$$\tau \quad \mp \left(\frac{h_x}{2} \times \frac{dp_x}{dx} - 2k \tan \varphi_x \right) \tag{II.58}$$

The derivative $\frac{dp_x}{dx}$ represents the tangent of the angle of slope of the specific pressure curve, and therefore the first term of this equation varies within a wide range over the middle portion of the arc of contact. But owing to the domed peak of the curve this variation is gradual. At the point of the maximum pressure the tangent of the angle of slope equals zero. On one side of this point it increases smoothly, whilst on the other side it decreases. The second term of equation (II.58) varies little over the middle portion of the arc of contact; accordingly it has no substantial effect on the value of τ. Hence we can draw the conclusion that the domed peak of the diagram of the specific pressure measured on the arc of contact signifies a smooth variation of the friction forces close to the neutral section, where their value is zero. On both sides of this section the absolute value of the friction forces increases approaching its extremal values only gradually.

In the recent years this has been verified experimentally by A. Chekmarev and P. Klimenko from simultaneous measurements of the projection of the specific pressure and friction forces by two load cells set in the body of the roll at an angle of 45° to the contact surface and positioned on different sides. One of the diagrams of the distribution of the normal and shear forces along the arc of contact thus obtained is shown in Fig. 46. Later O. Muzalevsky and A. Grishkov arrived at the same result, measuring directly the contact friction forces by a load cell especially designed by them for this purpose.

Thus the zone of sticking consists of three regions: two regions of internal slip, located close to the points C and D where the friction forces equal μk, and a middle region EF (see Figs. 44 and 45) where plastic strain is slowed down and the contact friction forces vary from zero in the neutral section to the maximum values given by equation (II.56) or (II.57), both in the zone of backward slip, and in the zone of forward slip.

Approximately, if we assume that the friction forces on the region of stagnation vary according to a law which is approximately linear, then

$$\tau \approx k \frac{h_x - h_n}{EF \tan \varphi_{EF}} = \frac{h_x - h_n}{2 \tan \varphi_{EF}} \eta \tag{II.58a}$$

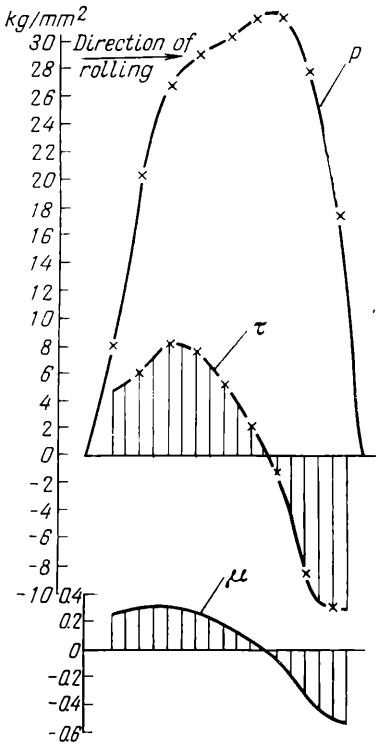

Fig. 46. Distribution of the normal and contact shear stresses and the ratio $\tau : p$ during the hot rolling (1,050° C) of 08 rimmed steel ($h_0 = 5.5$ mm; $h_1 = 4.7$ mm; $b_0 = 50$ mm; $\Delta h = 0.8$ mm; $v_r = 0.4$ m/s; $D = 270$ mm and $l : h_m \approx 2.0$)

where η is a coefficient characterizing the intensity of the variation of τ on the region EF and which is equal to the ratio $\frac{2k}{EF}$.

To determine the quantity η in equation (II.58a) it is necessary to know the extent of the stagnation region EF. The extent of this region depends on a large number of factors and in the first instance on the depth of the cross section of the rolled strip over the region EF, i.e., on h_n, and on the coefficient of contact friction. When h_n and μ increase, the extent of the region EF increases as well. In view of the absence of theoretical and experimental data concerning the extent of the region EF, we must tentatively put for its value

$$l_0 \approx (0.5 \text{ to } 2)\, h_m$$

for hot rolling, and

$$l_0 \approx (0.3 \text{ to } 1.0)\, h_m$$

for cold rolling,

where h_m is the mean depth of the cross section of the rolled strip.

From the analysis of the distribution of specific friction forces along the arc of contact we can conclude that the division of the arc of contact into two zones—the zones of backward and forward slip—specifies only the direction of deformation of the rolled metal relative to the rolls. This division says nothing about the character of the displacement of the metal relative to the surface of the rolls.

When the ratio $l : h_m$ roughly exceeds 5 the arc of contact should be divided into three parts, of which the two end ones are zones of slipping, whilst the middle one is a zone of sticking, which in its turn consists of three regions: two regions of internal slipping, and a middle region where deformation is slowed down, the latter being located simultaneously in the zones of backward and forward slip.

II. When the ratio $l : h_m \approx 2$ to 5 the regions CE and FD, where the friction forces are constant, can disappear (Fig. 47). This takes place because the friction forces on the regions AC and DB, owing to the reduction in the length of the arc of contact, cannot increase up to the value of k, since the law governing the variation of the friction forces on the region EF of the diminishing deformation becomes effective.

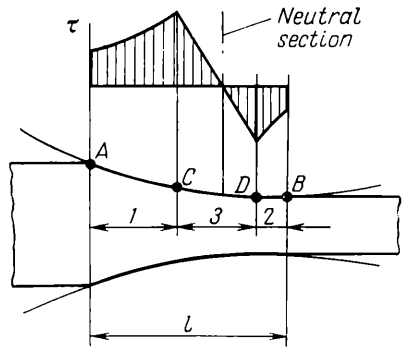

Fig. 47. Distribution of the friction forces along the arc of contact when the ratio $l : h_m \approx 2$ to 5. No sections show constant friction forces:
1 and *2*—zones of slipping; *3*—zone of sticking

Thus, for the ratio $l : h_m$ stated the zone of sticking consists only of a single region where the deformation is diminished (see Fig. 45).

For the remaining three regions AC, CD and DB the specific friction forces are clearly determined by the equations (II.56) and (II.58) given above.

III. When the ratio $l : h_m \approx 0.5$ to 2 the length of the arc of contact relative to the height of the cross section becomes so small that there is no room for the zones of slipping, and the zone of sticking begins to spread out over the entire arc of contact. The diagram for the distribution of the specific friction forces will in this case be expressed by two triangles (Fig. 48*a*). The magnitude of the friction forces can approximately be determined from equation (II.58a). By the quantity EF appearing in this equation in the given case is meant the ideal extent of the zone of sticking, equal to the agreed section over which the friction force undergoes a full range of variation: from $-k$ to zero and then to $+k$.

IV. When the ratio $l : h_m < 0.5$ the compressive strain does not penetrate the whole cross section of the strip being rolled, and the side edges are usually concave at mid-thickness. The zone of

sticking in this case spreads out over the entire arc of contact, just as in the preceding case, only the tendency of the metal to slip will become very slight and accordingly the contact friction forces will be quite small. Their diagram is given approximately by two triangles of small height (Fig. 48*b*).

The analysis of contact friction forces just carried out shows that their value and the law according to which they vary along the arc

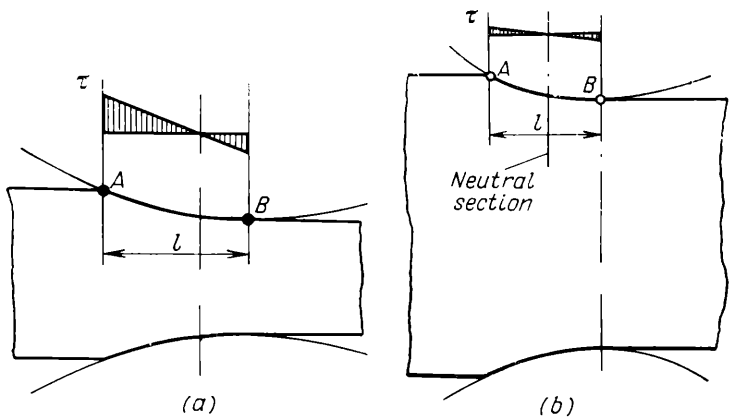

Fig. 48. Distribution of friction forces along the arc of contact: (*a*) $l : h_m \approx 0.5$ to 2; (*b*) $l : h_m < 0.5$

of contact are not the same for different conditions of longitudinal rolling, and that to a large extent they are determined by the ratio of length of the arc of contact to the mean thickness of the cross section of the strip being rolled.

There are four most characteristic cases of the distribution of contact shear stresses or friction forces: (1) $l : h_m > 5$ (see Figs. 44 and 45); (2) $l : h_m \approx 2$ to 5 (Fig. 47); (3) $l : h_m \approx 0.5$ to 2 (Fig. 48*a*); (4) $l : h_m < 0.5$ (Fig. 48*b*).

7. THE LOCATION OF THE MAXIMUM SPECIFIC PRESSURE RELATIVE TO THE NEUTRAL SECTION

In considering this problem we first define more precisely the fundamental features of the neutral section and the section passing through the point located on the arc of contact where the specific pressure attains the maximum value. We shall call the latter the section of maximum pressure.

The first section is characterized by the fact that an isolated element of the metal being rolled moves with a mean velocity equal

to the horizontal projection of the velocity of the rolls, and has the same tendency to deform towards the zone of backward slip and towards the zone of forward slip. From this it follows that the contact friction forces acting on this element must be zero.

The section of maximum pressure is characterized by the fact that the mean pressure, and, consequently, the mean longitudinal compressive stress in the metal attain a maximum value in this

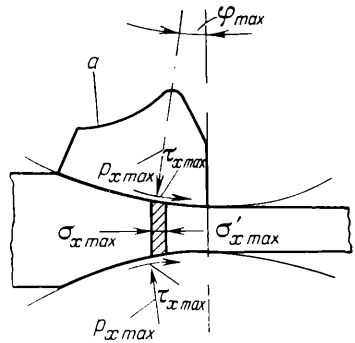

Fig. 49. The conditions of equilibrium of an element at the section characterized by maximum specific pressure (*a*—specific pressure diagram)

section. Accordingly, an isolated element of the metal at this section is subjected to longitudinal compressive stresses from both sides, having the same value (Fig. 49):

$$\sigma_{x\,max} = \sigma'_{x\,max}$$

Bearing in mind this precise definition, proceeding from the condition of equilibrium of the two elements mentioned above and assuming that the pressure p_x is considerably higher than the longitudinal stress σ_x, we can draw the following conclusions:

(1) the element isolated at the neutral section (Fig. 50) has the values of the longitudinal stresses on either side (σ_{xn} and σ'_{xn}) which are not the same, since from the condition of equilibrium it is necessary that

$$\sigma_{xn} > \sigma'_{xn}$$

and, consequently, the neutral section does not satisfy the conditions for the section of maximum pressure;

(2) the element isolated at the section of maximum pressure must have friction forces acting along its contact surfaces; otherwise, when $\sigma_{x\,max} = \sigma'_{x\,max}$ the conditions of equilibrium would not be satisfied. It is not difficult to see that these friction forces must act in the direction of rotation of the rolls. The value

of the specific friction forces τ_{max} can be found from the equation of equilibrium:

$$\tau_{max} = (p_x - \sigma_x) \tan \varphi_{max} \approx 2k \tan \varphi_{max} \qquad (II.59)$$

where φ_{max} is the angle characterizing the position of the section of maximum specific pressure.

It follows that the contact friction forces τ are not zero at the section of maximum specific pressure. Thus, this section does not satisfy the conditions of equilibrium of the neutral section.

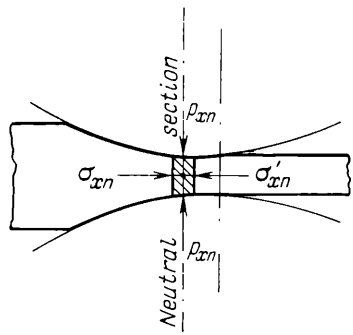

Fig. 50. The conditions of equilibrium of an element at the neutral section, where $\sigma_{xn} > \sigma'_{xn}$

From this analysis of the conditions of equilibrium of isolated elements at the two selected sections we arrive at a positive conclusion: *the neutral section must not coincide with the section of maximum pressure.* This conclusion was made by A. Nadai in analyzing the theory of specific pressure (in the case of slipping with viscous friction), and in a more general form by A. Korolev.

Since the contact friction forces at the section of maximum pressure are in the direction of rotation of the rolls, it follows that this section is located in the zone of backward slip, and the neutral section is displaced from it (obviously by a very small amount) towards the exit of the metal from the rolls.

The correctness of the conclusion that the maximum specific pressure does not coincide with the neutral section can be verified not only on the basis of the analysis of the conditions of equilibrium of elements isolated between plane sections. Similar results are obtained if the neutral section and the section of maximum pressure are represented not by a plane, but, say, by a cylindrical surface perpendicular to the surfaces of the rolls (Fig. 51). It is not difficult to see that if friction forces are absent on the con-

tact surfaces, then for the condition of equilibrium it is necessary that $\sigma_{xn} > \sigma'_{xn}$, and, conversely, if σ_{xn} σ'_{xn}, then for equilibrium it is necessary that the friction forces on the contact surfaces are nonzero. Thus, the above conclusion that the neutral section does not coincide with the location of the maximum specific pressure is confirmed.

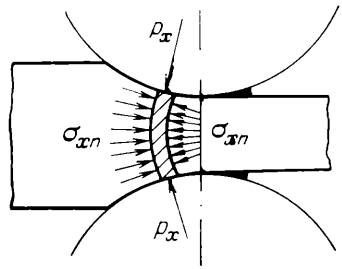

Fig. 51. The conditions of equilibrium at the neutral section, using cylindrical coordinates

In concluding we shall attempt to explain this result from a physical standpoint. When metal is compressed between two inclined plates (Fig. 52) or rolls, it can deform more readily in the direction of the greater distance between the plates. Hence, in order to deform

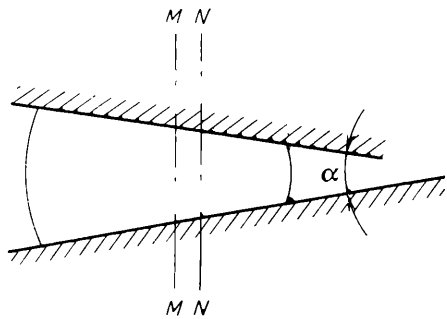

Fig. 52. The relative locations of the maximum specific pressure *MM* and the neutral section *NN* for metal compressed between inclined plates

in both directions which correspond to the neutral section, it is obviously necessary that at the given site the horizontal compressive stresses on the side of the diverging space are somewhat larger than those on the side of the converging space. In the case where these stresses are equal, which corresponds to the maximum specific pressure, the metal deforms only in the direction of the diverging space.

It is clear that the smaller the angle α between the plates, the nearer to the position of the maximum specific pressure will be the neutral section. When the plates are parallel the position of the neutral section and the location of the maximum specific pressure coincide.

8. MODERN THEORY CONCERNING THE DISTRIBUTION OF THE SPECIFIC PRESSURE ALONG THE ARC OF CONTACT

As has already been mentioned above, the distribution of the specific pressure along the contact surface is to a large extent determined by the law of distribution of the friction forces. Consequently, the existing theories of specific pressure (see Chapter II, Sections 3 to 5) differ from each other not in the method of accounting for the effect of the state of stress on the specific pressure, but only in the method used to calculate the friction forces.

The detailed analysis of contact friction forces carried out in Section 6 of Chapter II shows that the actual patterns of their distribution differ in principle from the patterns assumed in deriving the existing theories of specific pressure.

Since these theories do not reflect the actual law of distribution of the contact friction forces, we shall attempt to outline the modern theory of specific pressure for longitudinal two-dimensional rolling.

The law of distribution of the specific pressure over the arc of contact will be considered in the same way as for the case of contact friction forces, that is, separately for four cases of rolling differing from each other in the ratio of the length of the arc of contact to the depth of the cross section of the strip being rolled. The curves of the distribution of the specific pressure for the four cases of rolling, like the curves of the contact friction forces, will differ considerably from each other, and hence different methods of calculation must be used.

When the ratio $l : h_m > 5$, at the beginning and at the end of the arc of contact, over the regions AC and DB (see Fig. 44) the friction force is determined from equation (II.56). Therefore, for calculating the variation of the specific pressure in these regions, equation (II.13) may be used, i.e., the equation of von Kármán, and also equations (II.23) and (II.24), or equations (II.31) and (II.32) of the author:

$$p_x = \frac{2k}{\delta_{AC}} \left[(\xi_0 \delta_{AC} - 1) \left(\frac{h_0}{h_x} \right)^{\delta_{AC}} + 1 \right] \qquad \text{(II.60)}$$

for the region AC, and

$$p_x = \frac{2k}{\delta_{DB}} \left[(\xi_1 \delta_{DB} + 1) \left(\frac{h_x}{h_1} \right)^{\delta_{DB}} - 1 \right] \qquad \text{(II.61)}$$

for the region DB,
where

$$\xi_0 = 1 - \frac{\sigma_0}{2k} \quad \xi_1 = 1 - \frac{\sigma_1}{2k} \quad \delta_{AC} = \mu : \tan \varphi_{AC} \quad \delta_{DB} = \mu : \tan \varphi_{DB}$$

σ_0 and σ_1 are the mean tensile stresses in the regions AA_1 and BB_1

φ_{AC} and φ_{DB} are the angles the chords AC and DB make with the axis of the strip being rolled (see Fig. 44).

If at the beginning of the arc of contact $\tan \varphi_x > \mu$, then, as has already been stated, we should either use equation (II.23) or we should divide the arc AC into two or three regions and calculate p_x from equation (II.60) for each region, using the appropriate value of δ_{AC} dependent on the angle of inclination φ_x of the tangent to the axis of the strip being rolled (see Fig. 45).

In the subsequent regions of the arc of contact, CE and FD (see Fig. 44), the friction forces equal k, and accordingly the specific pressure can be calculated from the theory of constant friction forces, taking $\mu = 0.5$.

But assuming that over these regions of the arc of contact the contact friction forces $\tau_x = k$, the direction of the normal stresses p_x considerably deviates from the principal normal stress, and accordingly the equations of equilibrium (II.6a) and (II.6b) must be solved simultaneously with (I.70) rather than (II.8), i.e.,

$$\left(\frac{p_x - \sigma_x}{2}\right)^2 + \tau_x^2 = k^2$$

Putting $\tau_x = k$ in it we obtain

$$p_x - \sigma_x = 0$$

whence, in accordance with equations (II.6a) and (II.6b), it follows that

$$dp_x = \mp \frac{k}{\tan \varphi} \times \frac{dh_x}{h_x} \tag{II.62}$$

After integration, in order to simplify the calculation, we replace p_x, without introducing appreciable error in the arc of contact over the regions CE and FD, and obtain

$$p_x = p_C + \frac{k}{\tan \varphi_{CE}} \log_e \frac{h_C}{h_x} \tag{II.63}$$

for the region adjacent to the point C, and

$$p_x = p_D + \frac{k}{\tan \varphi_{DF}} \log_e \frac{h_x}{h_D} \tag{II.64}$$

for the region adjacent to the point D respectively,

where p_C and p_D are the specific pressures at the points C and D, calculated from equations (II.60) and (II.61)

φ_{CE} and φ_{DF} are the angles between the axis of the rolled strip and the chords CE and DF

h_C and h_D are the thicknesses of the rolled section at the points C and D.

Equation (II.64) can also be easily solved when tan φ is varying, i.e., without equating the arc of contact to a chord. This exact solution can be of interest in the case of large angles of contact, when tan φ is close to the coefficient of friction, i.e., close to 0.5. In equation (II.64) we denote

$$\tan\varphi = \frac{dh_x}{2dx} \quad \text{and} \quad h_x \approx h_1 + \frac{x^2}{r}$$

then

$$dp_x = \mp \frac{2k\,dx}{h_1 + \frac{x^2}{r}}$$

After integration we find p_x for the zone of backward slip:

$$p_x = p_C + 2k\sqrt{\frac{r}{h_1}}\left(\tan^{-1}\frac{x_C}{\sqrt{rh_1}} - \tan^{-1}\frac{x}{\sqrt{rh_1}}\right) \qquad \text{(II.65)}$$

whilst for the zone of forward slip

$$p_x = p_D + 2k\sqrt{\frac{r}{h_1}}\left(\tan^{-1}\frac{x}{\sqrt{rh_1}} - \tan^{-1}\frac{x_D}{\sqrt{rh_1}}\right) \qquad \text{(II.66)}$$

According to the initial conditions, when $x = x_C$ (Fig. 53*a*), $p_x = p_C$, and when $x = x_D$ the quantity $p_x = p_D$.

The specific pressure over the regions CE and DF will increase towards the neutral section, but not so rapidly as over the regions AC and DB (Fig. 53*a*).

To determine the specific pressure over the middle region of the zone of sticking, i.e., over the region EF, it is necessary to substitute the value of the friction forces for this region from equation (II.58a) into equation (II.12).

Noting that

$$\tan\varphi = \tan\varphi_{EF}$$

we obtain

$$dp_x = k\left[2 - \frac{\eta(h_x - h_n)}{2k\tan^2\varphi_{EF}}\right]\frac{dh_x}{h_x} \qquad \text{(II.67)}$$

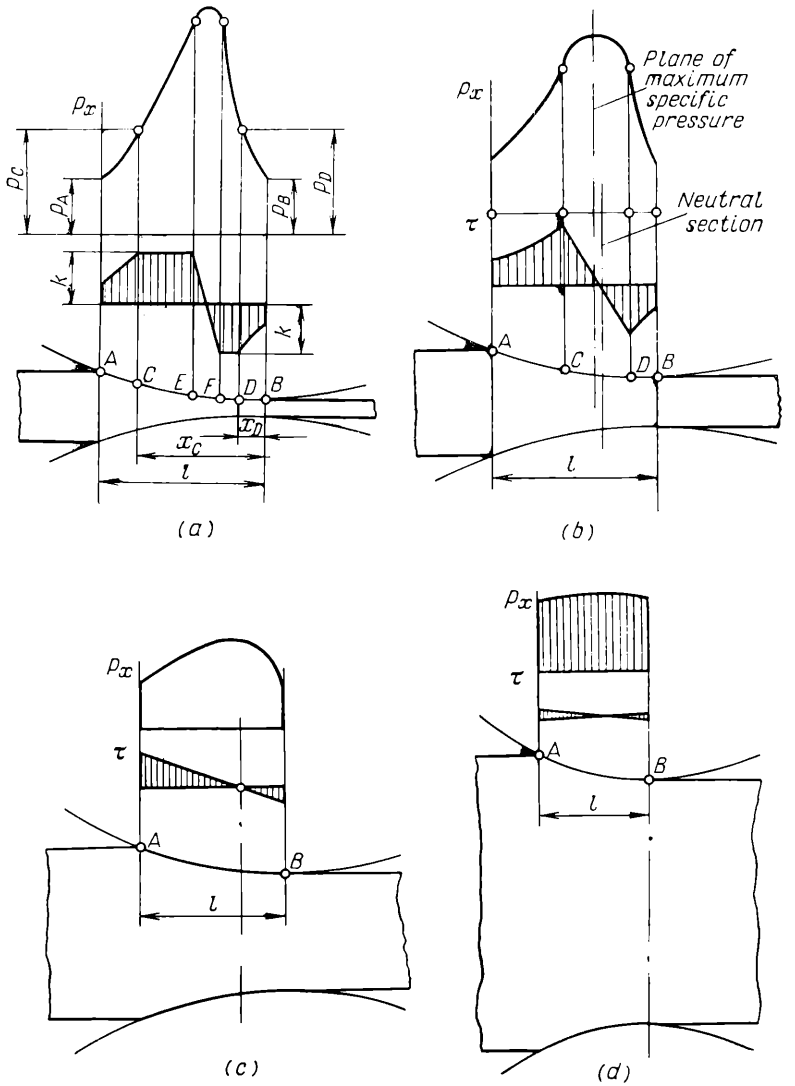

Fig. 53. Variation of the specific pressure and specific friction forces along the arc of contact for two-dimensional rolling with different $l : h_m$ ratios:
(*a*) $l : h_m > 5$; (*b*) $l : h_m \approx 2$ to 5; (*c*) $l : h_m \approx 0.5$ to 2; (*d*) $l : h_m < 0.5$

The other sign in front of the second term inside the brackets vanishes, since equation (II.58a) gives the friction force for the whole region EF, including that part of it which is located in the zone of forward slip.

After integrating between the points EF we have

$$p_x = p_E + k\left[A(h_E - h_x) - (2 + Ah_n)\log_e \frac{h_E}{h_x}\right] \qquad \text{(II.68)}$$

where p_E is the specific pressure at the point E, determined from equation (II.63) or (II.65)

h_E is the depth of the cross section of the strip at the point E

A is a constant for the region EF, given by the equation

$$A = \frac{1}{EF \tan^2 \varphi_{EF}} = \frac{\eta}{2k \tan^2 \varphi_{EF}} \qquad \text{(II.69)}$$

The quantity h_n entering equation (II.68) can be found from the condition that the values of the specific pressures, given by equations (II.66) and (II.68) for the point F, must be the same:

$$h_n = \frac{\frac{p_E - p_F}{k} + A(h_E - h_F)}{A \log_e \frac{h_E}{h_F}} - \frac{2}{A} \qquad \text{(II.70)}$$

where p_E and p_F are the specific pressures at the points E and F determined from equations (II.65) and (II.66) respectively.

Thus, for the region EF the specific pressure on both sides of the neutral section is expressed by a single common equation. The dome-like peak of the specific pressure curve (Fig. 53*a*) obtained from equation (II.68) fully corresponds to the experimental results of W. Lueg, A. Korolev and others. The oscillograms taken during their investigations, showing the variation of the specific pressure during the rolling process, as a rule have rounded peaks which cannot be explained merely by the width of the probe transmitting the pressure of the metal to the load cell. It is certain that the dome-like peaks of these specific pressure curves are obtained as a result of the presence of a zone of sticking between the two zones of slipping.

This circumstance is supported in a particularly striking manner by the investigations into the specific pressure, conducted with this specific aim in view, by A. Korolev, N. Svedo-Shvets and A. Tselikov. Owing to the fact that these investigations were carried out on a mill with rolls of large diameter (900 mm), the arc of contact during the rolling was many times greater than the diameter of the measuring probe which was 3 mm. As a result, the effect of the

diameter of the probe on the radius of curvature of the oscillogram was eliminated.

The location of the maximum specific pressure can be determined if we equate the derivative given by equation (II.68) to zero:

$$\frac{dp_x}{dh_x} = k\left[-A + (2 + Ah_n)\frac{1}{h_x}\right] = 0$$

i.e., the maximum specific pressure will be observed when

$$h_x = h_n + \frac{2}{A}$$

Consequently, the point of maximum specific pressure is displaced a little relative to the neutral section in the direction of the entry of the metal into the rolls, the amount of this displacement being proportional to tan φ_{EF}, which agrees with the conclusions drawn in the preceding section.

When the ratio $l : h_m \approx 2$ to 5 the regions where the value of the friction force is constant, and, consequently, the regions of the specific pressure diagram corresponding to them can vanish (Fig. 53*b*). For the remaining three regions of the diagram (*AC*, *CD* and *DB*) the specific pressure will obviously be determined from equations (II.60), (II.61) and (II.68).

When the ratio $l : h_m \approx 0.5$ to 2 the zone of sticking, as previously mentioned, occupies the entire arc of contact and therefore the graph showing the specific pressure distribution is in the form of an externally convex curve over the whole arc of contact (Fig. 53*c*). Then the specific pressure is determined by equation (II.68), if by the region *EF* in equation (II.69) we understand, as before, the ideal extent of the zone of sticking, equal to the agreed region over which the value of the friction force can vary from $-k$ to $+k$.

When the ratio $l : h_m \leqslant 0.5$ the specific pressure curve—owing to the fact that the magnitude of contact friction is small—is characterized by a slight rise at the middle portion of the arc of contact, and in practice its value may be taken as constant (Fig. 53*d*). The character of the specific pressure curve is similar to that of the curve for the preceding case (Fig. 53*c*), located close to the neutral section. But owing to the low value of the ratio $l : h_m$ the specific pressure is in this case affected considerably by the outer zones. As a result of the phenomenon considered in Chapter I, Section 22, the specific pressure at the points *A* and *B*, and hence also over the entire arc of contact, will be higher than in the cases of rolling represented by Fig. 53*a*, *b* and *c*. This problem will be considered in detail in Section 10.

Summing up the above analysis of the patterns of the specific pressure distribution over the arc of contact for the four typical

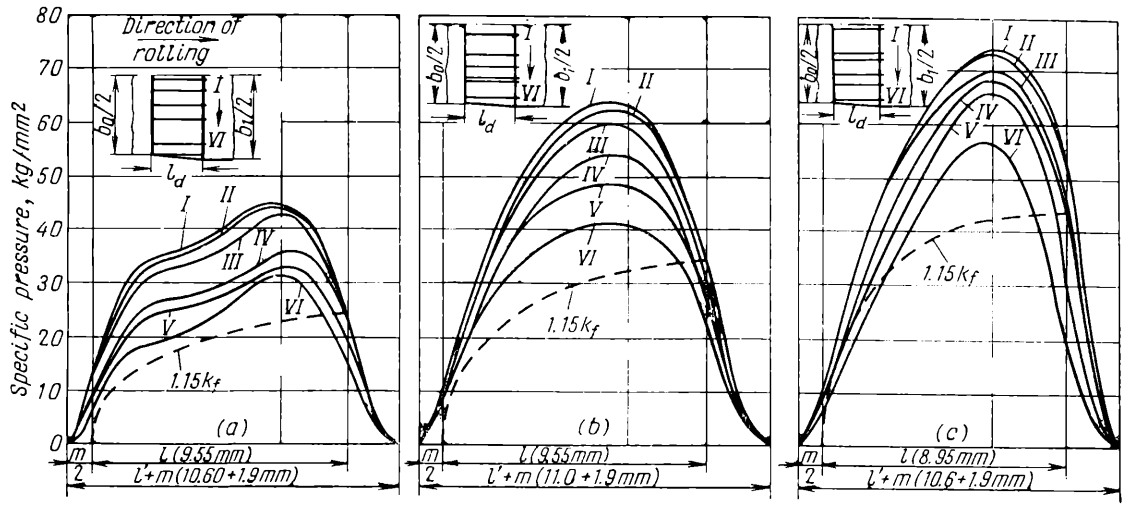

Fig. 54. Variation of the specific pressure along the arc of contact during the cold rolling of copper strips (width 30 mm approx.) for different strip thicknesses and different distances from the axis of the strip (W. Lueg):

(*a*) $h_0 = 8$mm, $\Delta h = 1$ mm and $l : h_m \approx 1.41$; (*b*) $h_0 = 4$ mm, $\Delta h = 1$ mm and $l : h_m \approx 3.15$; (*c*) $h_0 = 2$ mm, $\Delta h = 0.9$ mm and $l : h_m \approx 6.9$ (l and l' are the calculated and measured lengths of the arc of contact and m is the thickness of the load cell probe)

cases of rolling, we may conclude that in solving this problem different approaches must be used depending on the ratio $l : h_m$. As was shown above, this enables the contact friction forces to be found more correctly, and hence their influence on the specific pressure to be taken into account. But it must be taken into consideration that the classification of specific pressure diagrams into four basic types (Fig. 53) does not precisely differentiate between the cases of rolling mentioned above. Actually the boundaries are not solely determined by the ratio $l : h_m$. They also depend on the coefficient of friction, the reduction and the angle of contact, and accordingly the values of the ratio $l : h_m$ given above should only be regarded as approximate.

9. EXPERIMENTAL RESULTS FOR THE DISTRIBUTION OF THE SPECIFIC PRESSURE ALONG THE ARC OF CONTACT

The specific pressure distribution over the arc of contact has been subjected to repeated experimental investigation, in which the

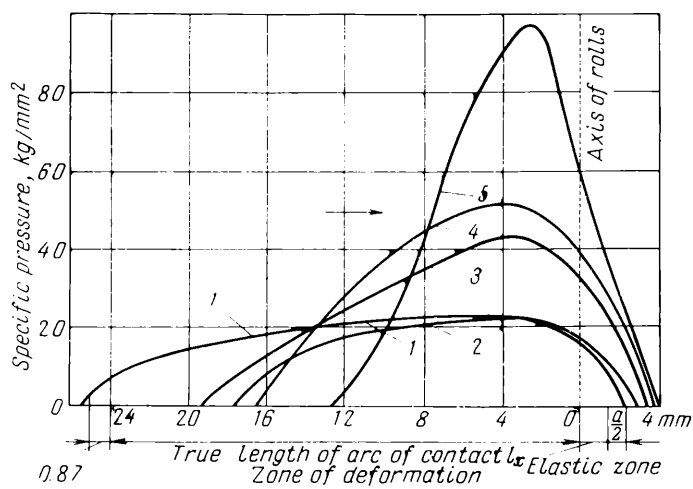

Fig. 55. Variation of the specific pressure along the arc of contact for hot rolling of strips of steel Ст. 3 with different strip thicknesses and different reductions; a—diameter of the load cell probe:

Curve No.	h_0, mm	$\frac{\Delta h}{h_0}$	l, mm	$l : h_m$
1	15	0.28	25	1.94
2	11.6	0.28	16.5	1.65
3	5.0	0.54	18.3	5.0
4	4.3	0.46	15.7	4.8
5	2.3	0.43	11.2	6.2

actual pressure of the metal being rolled was measured by the probe of a special load cell installed in the body of the roll. The form of all experimental specific pressure curves for rolling wide strips with smooth rolls is very close to the form of the curves plotted from the theoretical results presented above (Fig. 53).

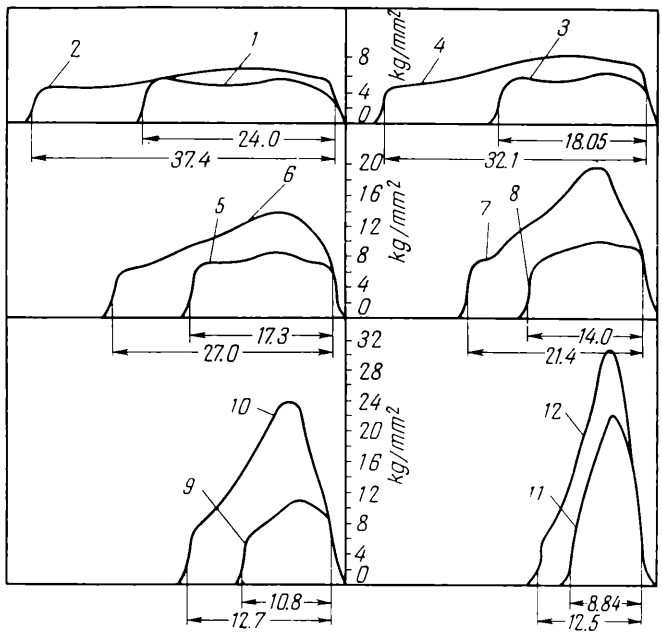

Fig. 56. Variation of the specific pressure along the arc of contact at the strip axis in the rolling of 50-mm wide lead strips with different thicknesses and different reductions:

Curve No.	h_0, mm	Δh, mm	$l : h_m$	Curve No.	h_0, mm	Δh, mm	$l : h_m$
1	22	4.4	1.21	*7*	6.1	1.5	2.61
2	22	10.8	2.25	*8*	5.9	3.5	5.15
3	15.9	2.5	1.22	*9*	4.0	0.9	3.02
4	15.9	7.9	2.74	*10*	3.9	2.4	6.55
5	10.1	2.3	1.97	*11*	2.1	0.6	4.9
6	9.8	5.6	3.85	*12*	2.0	1.2	11.8

As an example we present the specific pressure diagrams measured by W. Lueg (Fig. 54) for cold rolled copper, by A. Korolev (Fig. 55) for hot rolled steel, and by A. Chekmarev, L. Kapturov and P. Klimenko (Fig. 56) for rolled lead test pieces. In all these cases test pieces of different cross-sectional depths were rolled, using different reductions, i.e., different $l : h_m$ ratios.

Comparing the curves presented in each of these figures we notice that as the ratio $l : h_m$ increases the slope of the curve over the region close to the neutral section becomes steeper, and the peak of the curve grows more pronounced. When the ratio $l : h_m$ is approximately equal to two, for example, the curves of Fig. 54*a* and also the curves *1* and *2* of Fig. 55 and the curves *1* to *5* of Fig. 56 resemble the curves shown in Fig. 53*c* and *d*, whilst the curves shown in Fig. 54*c* and the curve *5* of Fig. 55, and the curves *10*, *11* and *12* of Fig. 56 are generally similar to the curve shown in Fig. 53*a*.

10. THE INFLUENCE OF THE OUTER ZONES ON THE SPECIFIC PRESSURE

Experimental investigations into the forces arising during the longitudinal rolling of strips of considerable depth of cross section, when the ratio $l : h_m < 0.5$, show that the specific pressure in this case is higher than in the case of rolling where $l : h_m \approx 1$ to 2, where also the effect of external friction is greater. The author together with V. Smirnov explained this phenomenon by the influence of the outer zones, i.e., the zones adjacent to the geometrical range of deformation; as a result of their action the resistance to deformation is considerably increased in the case of a small arc of contact and large depth of the cross section of the rolled strip.

In deriving equation (I.98)

$$p = k(2 + \pi)$$

this problem was considered theoretically for the case of a flat die indenting a semi-infinite body. This case of deformation can be identified with the rolling, for example, of large ingots in plate mills in the first passes, which are characterized by small reductions when the depth of the cross section of the ingot is many times greater than the length of the arc of contact. But equation (I.98) for this case of deformation is scarcely applicable *in toto*, since the ingot being rolled is ultimately subjected to a general stretching, although metal located on its axis is deformed to a small extent.

To determine the effect of the outer zones on the resistance to deformation V. Smirnov and afterwards V. Pushkarev conducted a series of experimental investigations.

V. Smirnov subjected test pieces of rolled lead, steel, aluminium and copper to compression, using the two set-ups shown in Fig. 57. The first set-up is for compression of rectangular test pieces with the dimensions l, h and b between parallel faces, whilst the second is intended for the local compression of test pieces of

a considerably greater length, over a portion limited by the length l. The test pieces being compared had the same depth h and width b.

For test pieces of each dimension the mean specific pressures were calculated at the same deformation for schemes I (p') and

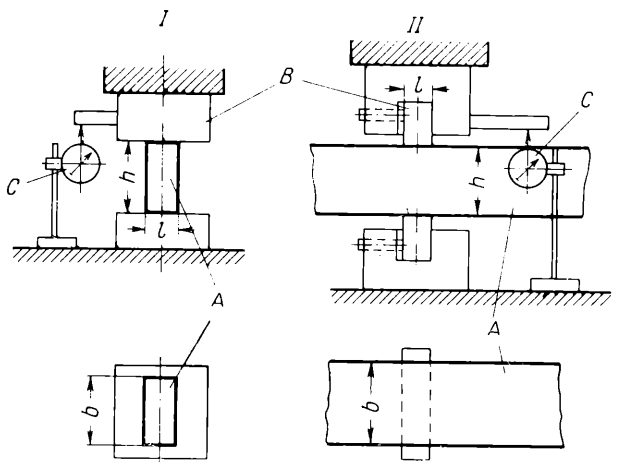

Fig. 57. Two methods (*I* and *II*) of compressing test pieces to determine the effect of the outer zones of the strip on the resistance to deformation:
A—test pieces; *B*—compression faces; *C*—dial indicator

II (p); the influence of the outer zones on the magnitude of the mean specific pressure was evaluated via the coefficient of the state of stress

$$n''_\sigma = \frac{p}{p'} = f\left(\frac{l}{h}\right) \qquad \text{(II.71)}$$

The main test pieces were made of lead (Table 2); specimens of other metals were tested to establish the relation between n''_σ and the kind of material.

The different dimensions of the lead test pieces enabled n''_σ to be determined for different absolute values of l and h, using the same ratio so as to establish the effect of the scale factor.

The test pieces were compressed in a hydraulic press at the rate of 1 mm/min. The forces during the test were recorded by the manometer of the hydraulic press, whilst the deformations were read off from a dial indicator (Fig. 57).

The results of the tests showed that the coefficient n''_σ depends only slightly on plastic deformation the maximum value of which during the tests amounted to 18 to 20%. The fluctuations of the

Table 2

The Results of Testing Different Specimens to Determine the Effect of the Outer Zones on the Resistance to Deformation

Test piece dimensions, mm*		Ratio $l:h$	Coefficient n''_σ	Test results			
				Set-up I		Set-up II	
h	l			number of test pieces	p' kg/mm²	number of test pieces	p kg/mm²
			Lead				
30	30	1.000	1.00	5	1.62	4	1.66
30	15	0.500	1.40	3	1.42	3	1.96
30	10	0.333	1.60	7	1.40	3	2.28
30	7.5	0.250	1.73	3	1.44	4	2.48
30	5	0.167	2.20	3	1.41	4	2.98
30	2.5	0.0835	2.70	—	—	3	3.83
30	1.25	0.0417	3.60	—	—	3	4.90
30	0.5	0.0167	4.70	—	—	3	6.50
22.5	30	1.333	1.03	3	1.70	2	1.78
22.5	15	0.166	1.17	3	1.53	2	1.80
22.5	10	0.444	1.42	3	1.49	5	2.10
22.5	7.5	0.333	1.50	3	1.55	3	2.30
22.5	5	0.222	1.80	3	1.49	3	2.70
22.5	2.5	0.111	2.40	—	—	3	3.68
15	30	2.000	1.05	3	1.97	4	2.09
15	15	1.000	1.08	3	1.75	6	1.95
15	10	0.666	1.16	4	1.68	3	2.00
15	7.5	0.500	1.30	3	1.65	4	2.15
15	5	0.333	1.52	4	1.60	4	2.54
15	2.5	0.167	2.15	—	—	4	3.24
			Steel				
30	15	0.500	1.37	4	32.1	3	42.5
30	10	0.333	1.54	3	33.9	7	51.1
30	7.5	0.250	1.66	—	—	5	57.0
30	5	0.167	2.19	—	—	4	74.2
			Aluminium				
30	15	0.500	—	2	16.0	—	—
30	10	0.333	1.62	4	15.9	4	27.0
30	5	0.167	2.30	—	—	3	36.8
			Copper				
30	10	0.333	1.62	4	23.1	3	39.2
30	5	0.167	2.22	—	—	3	53.3

* Width of test pieces is 45 mm.

coefficient n''_σ within the range of deformations tested did not exceed 10 to 15%. Accordingly Table 2 shows the mean values of n''_σ. As the test data show, no substantial influence of the scale factor and the kind of material is observed on the relation (II.71).

Over the interval $0.05 < \frac{l}{h} < 1$ this relation can with a sufficient accuracy be expressed by the following equation (Fig. 58):

$$n''_\sigma = \left(\frac{l}{h}\right)^{-0.4} \tag{II.72}$$

For values of the ratio $l : h > 1$ the coefficient n''_σ can with a sufficient accuracy be taken to be unity. For values of the ratio

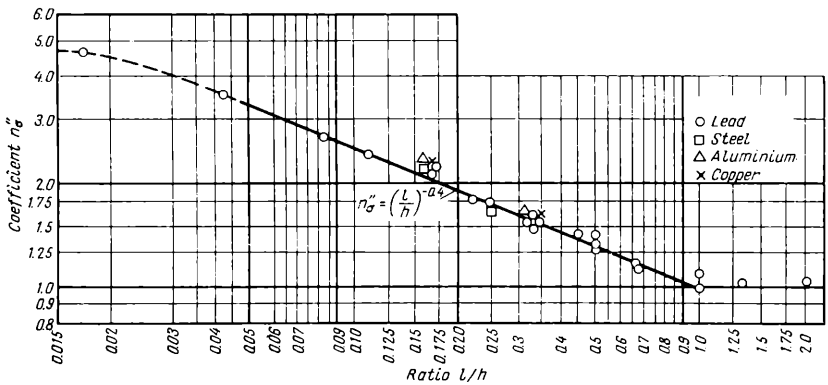

Fig. 58. Dependence of coefficient n''_σ on the ratio $l : h$

$l : h < 0.05$ this coefficient was not investigated since the corresponding processes have no practical application. It may be assumed that for small values of the ratio $l : h$ the coefficient will increase to a certain finite value; this, however, exceeds in practice the quantity corresponding to equation (I.98) which was derived for the problem of a flat die being indented into a semi-infinite solid.

In Table 2 the particular values of p and p' are given for the strain $\varepsilon = 7\%$ (for which the curves showing the dependence of p' and p on the magnitude of strain become flat).

To illustrate the physical meaning of the coefficient n''_σ, curves $p' = f\left(\frac{l}{h}\right)$ and $p = f\left(\frac{l}{h}\right)$ were plotted from these results for lead specimens of height $h = 22.5$ mm (Fig. 59).

The rise of the curve of p' when the ratio $l : h$ increases clearly reflects the increase in the specific pressure as a result of the external friction whose influence is taken into account by introducing the

coefficient n''_σ. Consequently,

$$p' = 2kn''_\sigma \tag{II.73}$$

where k is determined from equations (I.48) and (I.71).

Solving simultaneously equations (II.71) and (II.73) we obtain

$$p = 2kn'_\sigma n''_\sigma \tag{II.74}$$

Since the value of the mean specific pressure occurring during rolling is usually expressed in the general form by the equation

$$p = 2kn_\sigma \tag{II.75}$$

where n_σ is the coefficient of the state of stress,

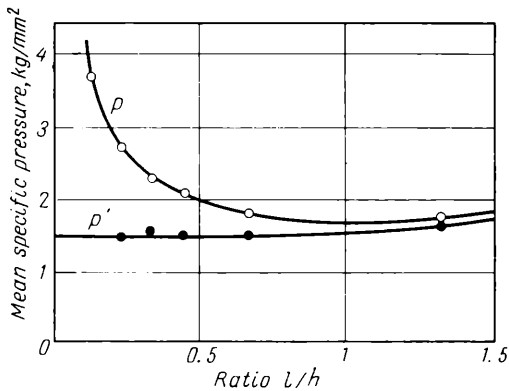

Fig. 59. The relations $p = f\left(\frac{l}{h}\right)$ and $p' = f\left(\frac{l}{h}\right)$ for lead test pieces of height $h = 22.5$ mm for a strain $\varepsilon = 7\%$

the tests carried out enable us to split this general coefficient into its component parts, representing it in the form

$$n_\sigma = n'_\sigma n''_\sigma n'''_\sigma \tag{II.76}$$

where n'''_σ is the coefficient reflecting the effect of tension on the specific pressure.

In the general form the effect of the value of the ratio $l : h$ on the specific pressure can be represented diagrammatically by curves (Fig. 60), from which, when appropriate values of n''_σ are used for the case of rolling, we may draw the following practical conclusions:

(a) when rolling is carried out without tension and with small reductions, and when the ratio $l : h < 1$, the effect of the external friction is small and it can be neglected (for example, during the first passes in plate and blooming mills); in this case the mean

specific pressure is given by the portion AB of the curve (Fig. 60), and it can be calculated from the formula

$$p = 2kn''_{\sigma} \tag{II.77}$$

(b) conversely, when rolling is carried out without tension, using large reductions, and when the ratio $l : h > 1$, the effect of the outer

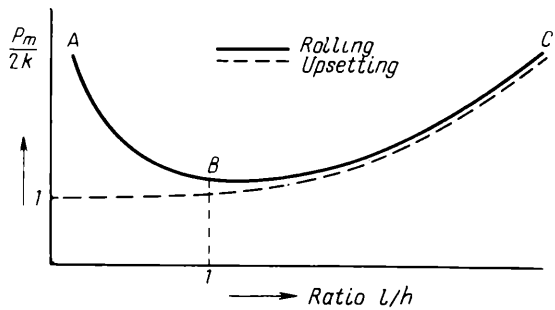

Fig. 60. Variation of the resistance to deformation with the ratio $l : h$ for rolling and upsetting

zones is practically absent, whilst the influence of the external friction becomes considerable; the portion BC of the curve corresponds to this case, and the specific pressure can be determined from the well-known relation

$$p = 2kn'_{\sigma}$$

V. Lugovskoi, considering the two-dimensional deformation of a plate compressed from both sides by narrow dies (Fig. 61), when the slip lines intersect the entire cross section of the plate, arrived at the conclusion that the specific pressure depending on the ratio can be expressed by the equation

$$p = 2k\left(1.25\frac{l}{h} + 1.25\log_e\frac{h}{l} - 0.25\right) \tag{II.78}$$

This equation is valid when the ratio $l : h$ varies in the range $1 > \frac{l}{h} > 0.118$. When the ratio $l : h = 0.118$ the slip lines cease to intersect the cross section of the plate, the slip line field of each die becomes independent, and in this case equation (II.78) gives the same value of p as the equation of Prandtl (I.99).

A comparison of the values of p calculated from equation (II.78) with the experimental data gives good agreement, and hence this equation can be recommended for the calculation of n''_{σ} along with equation (II.72).

V. Pushkarev has investigated the effect of the outer zones on the specific pressure during the rolling of special test pieces which consisted of two parts joined together by an interlay. One part of the test pieces was made shorter so that for a given

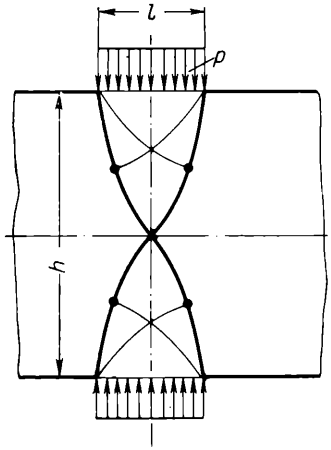

Fig. 61. Compression of a thick plate between two narrow dies

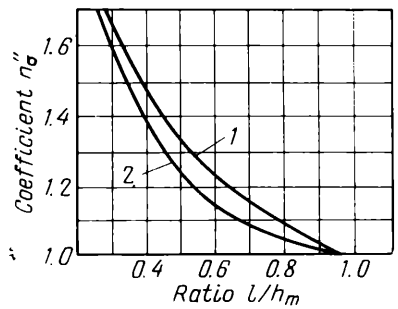

Fig. 62. Variation of the coefficient n''_σ with the ratio $l : h_m$:

1—compression (A. Tselikov and V. Smirnov); *2*—rolling (V. Pushkarev)

reduction when the metal filled the geometrical zone of deformation there were no outer zones.

The results of these tests substantiated the conclusions given above: the outer zones cause an increase in the specific pressure when the ratio $l : h$ becomes smaller than 0.5 to 1. But at the same time a very important phenomenon was established: the effect of the outer zones on the increase in the pressure is less during the rolling of the metal than when a part of the strip is compressed (Fig. 62). It should be noted that this phenomenon is a fundamental feature of the process. As was pointed out above, during rolling when $D \cos \alpha > h_n$ there is a tendency for longitudinal tensile stresses to appear at the surface of the strip at the entry and exit sides of the rolls. As a consequence a partial localization of the compressive stresses takes place at the point of entry and exit, with the result that the increase in the resistance to deformation caused by the outer zones will be less pronounced than that occurring when a part of the strip is compressed.

The influence of the outer zones on the pressure of the metal on the rolls during the rolling of billets was investigated for the first time by E. Rokotyan.

In analyzing the results of his detailed measurements of the metal pressure on the rolls of blooming mills, he noted that the specific pressure during the first passes is higher than during the subsequent ones, when the ratio $l : h$ becomes higher. E. Rokotyan represented

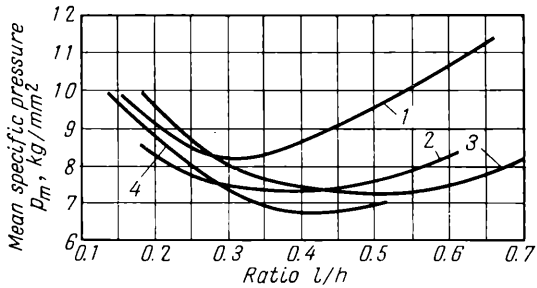

Fig. 63. Variation of the mean specific pressure with $l : h_m$ when rolling blooms of different cross sections and different steels:
1—blooms, 160 × 160 mm and 170 × 170 mm, weighing 6.5 tons, steel Ст. 6; *2*—bloom, 255 × 310 mm, weighing 3.1 tons, steel Ст. 3; *3*—bloom, 170 × 170 mm, weighing 6.5 tons, steel Ст. 4; *4*—bloom, 160 × 160 mm

the results of these investigations in the form of graphs, one of which is shown in Fig. 63. According to these investigations the minimum specific pressure during the rolling of blooms occurs not when $l : h \approx \approx 1$, as was the case with compression, but in the interval $l : h =$

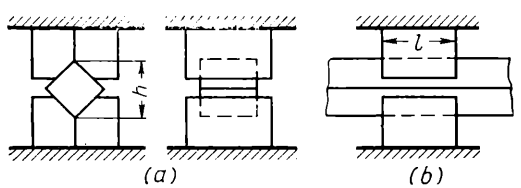

Fig. 64. Diagrams for compressed test pieces with $l : h = 0.08$ to 1.0:
(*a*) neglecting the effect of the outer zones; (*b*) including the effect of the outer zones

$= 0.3$ to 0.55. A. Chekmarev and others arrived at these results whilst investigating the pressure of the metal on the rolls of blooming mill 1150.

In order to clarify the influence of the outer zones on the resistance to deformation during rolling in section mills, we can use the results of the experimental investigations of M. Brovman. He compressed lead test pieces between two dies of square, rhombic, round and flat form. In order to determine the effect of the outer zones, he compressed both short test pieces whose length was less than the length of the dies (Fig. 64*a*) and long test pieces. In the latter case the

test pieces were compressed by dies of various length so that the ratio $l : h$ varied from 0.08 to 1.0.

The results of these investigations given in Fig. 65 show that the effect of the outer zones for square, round and rhombic sections

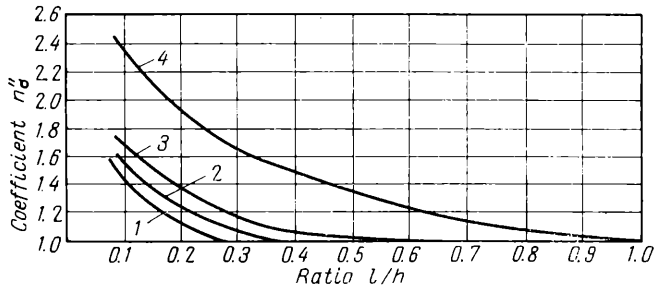

Fig. 65. Variation of the coefficient n''_σ (the effect of the outer zones) with the ratio of the length of the arc of contact l to the depth of rolled section h (M. Brovman):
1—strip of square cross section; *2*—strip of round cross section; *3*—strip of rhombic cross section; *4*—strip of flat cross section

is considerably smaller than for the compression of a rectangular section whose width is considerably greater than the depth.

11. POSITION OF THE NEUTRAL SECTION

In the textbook treatment the position of the neutral section, and, consequently, the magnitude of the forward slip are determined from the condition that the specific pressure and friction forces are uniformly distributed over the arc of contact, when the sign of the latter changes at the neutral section.

The analysis of the contact friction forces and pressure presented above (see Figs. 44, 45, 46 and 53) confirms that whilst averaging the specific pressure is still permissible to a good approximation, the assumption that the specific friction forces are constant, both over the zone of backward slip and over the zone of forward slip, is far from reality. This method of calculation is particularly far from the truth in the case of rolling with the ratio $l : h_m < 2$, when over the entire arc of contact the friction forces vary approximately as two triangles.

This circumstance was considered in 1952 by V. Smirnov, and he suggested that in determining the neutral section the effect of the zone of sticking be taken into account.

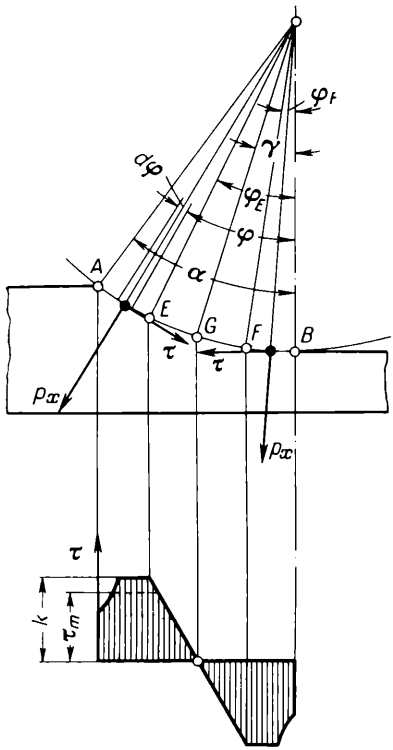

Fig. 66. Forces acting on the rolled metal and the distribution of contact friction forces

We shall determine by a similar method the position of the neutral section in the diagrams of friction forces shown in Figs. 44, 47 and 48, i.e., for the case of rolling which is characterized by a well developed zone of sticking.

To solve this problem we shall set up the equation of equilibrium. We project all the forces applied to the metal being rolled on to the direction of its motion (Fig. 66). Then

$$\sum X = -\int_0^{\alpha} p_x \sin\varphi r\, d\varphi + \int_{\varphi_E}^{\alpha} \tau \cos\varphi r\, d\varphi + \int_{\varphi_F}^{\varphi_E} \eta r (\sin\varphi - \sin\gamma)\cos\varphi r d\varphi - \int_0^{\varphi_F} \tau \cos\varphi r\, d\varphi \quad (II.79)$$

where

$$\eta = \frac{2k}{r(\sin\varphi_E - \sin\varphi_F)}$$

and γ is the angle of the neutral section.

To simplify the subsequent solution of this equation we assume that $p_x = p_m = \text{const}$. and that τ over the segments $\varphi = 0$ to φ_F and $\varphi = \varphi_E$ to α equals the mean friction force for these segments: $\tau = \tau_m = \text{const}$.

Then

$$-p_m(1-\cos\alpha) + \tau_m(\sin\alpha - \sin\varphi_E - \sin\varphi_F) + \frac{\eta r}{4}(\cos 2\varphi_F - \cos 2\varphi_E) - \eta r \sin\gamma(\sin\varphi_E - \sin\varphi_F) = 0 \quad (II.80)$$

Subsequently assuming that $\tau_m \approx k$ we obtain the equation for calculating the angle of neutral section:

$$\sin\gamma = \frac{1}{2}(\sin\alpha - \sin\varphi_E - \sin\varphi_F) + \frac{1}{4} \times \frac{\cos 2\varphi_E - \cos 2\varphi_F}{\sin\varphi_E - \sin\varphi_F} - \frac{p_m}{2\tau_m}(1-\cos\alpha) \quad (II.81)$$

After studying the extent of the zone of sticking where deformation is slowed down, and discovering simple methods for determining its boundaries, i.e., the angles φ_E and φ_F, this equation should have a practical use for a more exact calculation of the angle of neutral section and forward slip.

If the ratio of the angle of contact to the mean thickness of the rolled strip is much greater than 3 to 4, the effect of the region where deformation is slowed down and friction forces vary as a triangle may be neglected. In this case

$$\varphi_E \approx \varphi_F \approx \gamma$$

and then equation (II.80) assumes the form

$$\sin\gamma = \frac{\sin\alpha}{2} - (1-\cos\alpha)\frac{p_m}{2\tau_m} \qquad \text{(II.82)}$$

and if we assume that $\tau_m = \mu p_m$, it transforms into the expanded equation of S. Ekelund:

$$\sin\gamma = \frac{\sin\alpha}{2} - \frac{1-\cos\alpha}{2\mu} \qquad \text{(II.83)}$$

In this case if, on the contrary, the ratio of the arc of contact to the mean depth of the cross section of the rolled section is small ($l : h_m < 2$), then the region where deformation is slowed down will occupy the entire arc of contact (Fig. 48), i.e.,

$$\varphi_E = \alpha \quad \text{and} \quad \varphi_F = 0$$

Substituting these values of the angle into equation (II.80) we can determine the angle of neutral section from the equation

$$\sin\gamma = \frac{\sin\alpha}{2} - (1-\cos\alpha)\frac{p_m}{\eta r \sin\alpha} \qquad \text{(II.84)}$$

The quantity $\eta r \sin\alpha$ in this formula represents the sum of the friction forces at the points A and B, i.e., $\eta r \sin\alpha = \tau_A + \tau_B$. Then equation (II.84) assumes the following form:

$$\sin\gamma = \frac{\sin\alpha}{2} - (1-\cos\alpha)\frac{p_m}{\tau_A+\tau_B} \qquad \text{(II.85)}$$

Correspondingly the extent of the zone of forward slip is given by

$$l_{fs} = r\sin\gamma = 0.5\left(\sqrt{r\Delta h} - \Delta h\frac{p_m}{\tau_A+\tau_B}\right) \qquad \text{(II.86)}$$

If we put $\tau_A + \tau_B = 2\mu p_m$ in this equation it coincides with the equation of S. Ekelund and gives the extent of the zone of forward slip when the friction forces have a constant value over the entire arc of contact:

$$l_{fs} \quad 0.5\left(\sqrt{r\Delta h} - \frac{\Delta h}{2\mu}\right) \qquad \text{(II.87)}$$

12. FORWARD SLIP

Forward slip is the excess of the exit velocity of the rolled strip over the peripheral velocity of the rolls. It is of great importance when continuous mills are being designed, not only as regards their draught and the rotational speeds of the rolls, but also the torques required for their rotation and the forces tensioning the strip between the roll stands.

The magnitude of the forward slip may be expressed by the ratio

$$s = \frac{v_1 - v_r}{v_r} \tag{II.88}$$

where v_1 is the exit velocity of the metal, and
v_r is the peripheral velocity of the rolls.

In practice the forward slip is usually determined by measuring the difference of the distances l_1 and l_r between the impressions of two

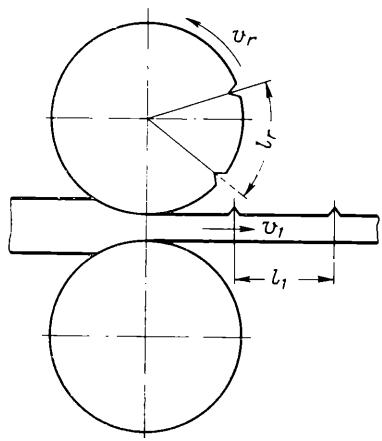

Fig. 67. Measurement of the forward slip using marks on the roll surface

marks on the strip being rolled and between the marks on the rolls respectively (Fig. 67). Since the time of rotation of the roll through an angle formed between the marks equals the time taken for the metal to pass through the distance l_1, the forward slip on the basis of equation (II.88) can be expressed by the equation

$$s = \frac{l_1 - l_r}{l_r} \tag{II.89}$$

In the case of hot rolling, when l_1 is measured after the metal has cooled down, a correction must be made for the temperature

shrinkage:

$$l_1 = l_0 [1 + \alpha (\vartheta_1 - \vartheta_0)]$$

where ϑ_1 and ϑ_0 are the temperatures during the rolling and measuring respectively, and

α is the coefficient of linear expansion due to temperature rise.

For a carbon steel the value of this coefficient can be taken as follows:

Temperature interval, °C	Coefficient α
0-1,200	(15 to 20) 10^{-6}
0-1,000	(13.5 to 17.5) 10^{-6}
0-800	(13.5 to 17) 10^{-6}

Theoretically the magnitude of forward slip can be found dependent on the position of the neutral section. Considering the problem as two-dimensional and proceeding from the condition that the volume of metal per second is constant, we have

$$h_n v_r \cos \gamma = h_1 v_1$$

where h_n is the thickness of the rolled strip at the neutral section.

Substituting the ratio $v_1 : v_r$, obtained from this equation, into equation (II.88), we get

$$s = \frac{h_n \cos \gamma}{h_1} - 1 \qquad \text{(II.90)}$$

Since

$$h_n = h_1 + 2r (1 - \cos \gamma)$$

$$s = \frac{h_1 + 2r (1 - \cos \gamma)}{h_1} \cos \gamma - 1$$

Substituting

$$1 - \cos \gamma = 2 \sin^2 \frac{\gamma}{2}$$

into this equation we obtain

$$s = \left(\frac{2r}{h_1} \cos \gamma - 1 \right) 2 \sin^2 \frac{\gamma}{2} \qquad \text{(II.91)}$$

Since $\cos \gamma$ in practice is close to unity, and $\sin^2 \frac{\gamma}{2} \approx \frac{\gamma^2}{4}$, then

$$s = \left(\frac{r}{h_1} - 0.5 \right) \gamma^2 \qquad \text{(II.92)}$$

In rolling thin strips, where r is considerably larger than h_1, the second term in this equation may be neglected in view of the

fact that it is small in comparison with the first, which gives the formula of D. Dresden:

$$s = \frac{r}{h_1} \gamma^2 \tag{II.93}$$

This formula has widely been used to calculate the forward slip. But when the value of the ratio $r : h_1$ is about 0.5, the formula yields inaccurate results, and accordingly in these cases it is advisable to use equation (II.92).

We shall now consider the effect on the forward slip of a non-uniform distribution of the velocity of motion of the metal across the section and the presence of a zone of sticking, a consequence of which is that the forward slip continues beyond the limits of the geometrical zone of deformation.

The non-uniform distribution of the exit velocity of the rolled metal across the section of the strip and the effect of this phenomenon on the forward slip were first pointed out by A. Rodzevich-Belevich, A. Golovin and A. Vinogradov. Subsequently this problem was investigated in detail by N. Sobolevsky.

We assume that the rolling is two-dimensional, that is, it takes place between smooth rolls, and the strip is characterized by a considerable width in comparison with the length of the arc of contact so that the effect of spread may be neglected. The thickness of the rolled strip relative to the arc of contact is not very large and the reduction of the metal extends completely over the entire thickness of its cross section.

Since in the middle portion of the arc of contact there is a zone where the slip of the metal over the rolls is absent, the velocity of motion of any point A (Fig. 68) of the metal being rolled, located on the contact surface in the zone of sticking, will be equal to the peripheral velocity of the rolls v_r.

The horizontal projection of this velocity is

$$v_{xA} = v_r \cos \varphi_x \tag{II.94}$$

where φ_x is the angle between the line connecting the centres of the rolls and the radius drawn to the point A.

When this point A emerges from the zone of sticking its speed, because of forward slip, begins to exceed the peripheral velocity of the rolls, and in the next zone of deformation extending beyond the limits of the contact surface, this velocity will increase further owing to the stretching of the surface layers of the metal, until the velocity

$$v_1 = (s + 1) v_r \tag{II.95}$$

or

$$v_1 = \frac{h_n}{h_1} v_r \cos \gamma \tag{II.96}$$

has been reached,

where s is the final value of the forward slip
h_n is the depth of the neutral section
h_1 is the depth of the section of the metal at the exit
γ is the angle of neutral section.

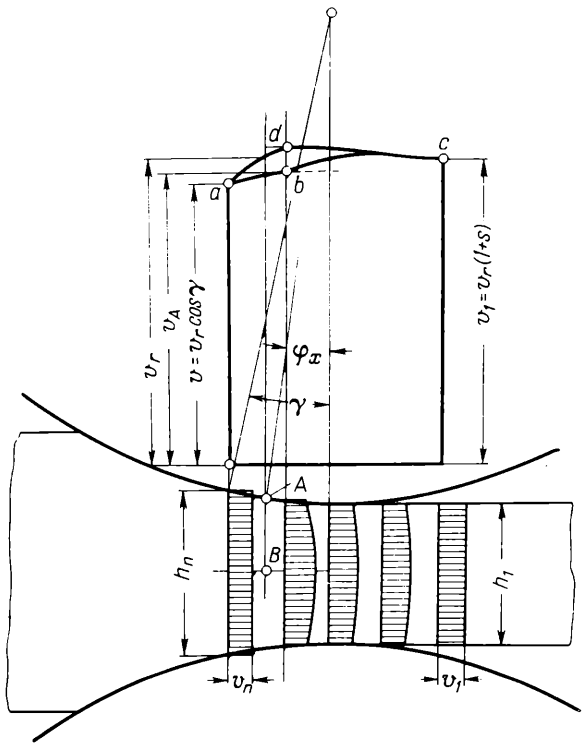

Fig. 68. Velocity distribution of the metal across the thickness of the strip for forward slip, and the variation of the velocity in the external deformation zone of the strip (*abc*) and in the internal zone (*adc*)

In Fig. 68 this variation of the velocity of the surface particles (not sides) of the metal is represented by the curve *abc*.

Let us consider the velocity of motion of the metal at the middle portion of the cross section of the strip at the neutral section on the basis of its definition. We may assume that the velocity of motion

of the rolled metal across its thickness is distributed uniformly and is equal to

$$v_A = v_r \cos \gamma$$

The volume per second of the rolled metal passing through any section, including the neutral section, must be constant and equal to

$$V = h_n v_n = h_1 v_1 = \int_{-\frac{h_x}{2}}^{\frac{h_x}{2}} v_x \, dy = h_x v_{xm} \qquad (II.97)$$

where h_x is the depth of the section x-x, and
v_{xm} is the mean velocity of motion at this section.

Taking into consideration that

$$h_x v_r \cos \varphi_x < h_n v_r \cos \gamma$$

as remarked already, the mean velocity of the rolled metal in sections to the right of the neutral section is higher than the velocity of a point touching the rolls:

$$v_{xm} > v_r \cos \varphi_x$$

Thus, to the right of the neutral section the velocity of the inner portion of the rolled strip is higher than the velocity of the outer layers:

$$v_{xB} > v_{xA}$$

If the law of distribution of the velocity across the thickness of the strip is known, $v_{xy} = f(y)$, then the value of this velocity could be found from the equation

$$\int_{-\frac{h_x}{2}}^{\frac{h_x}{2}} f(y) \, dy = h_n v_n$$

For example, if we assume that the velocity across the thickness of the strip varies along a parabola, then

$$v_x = f(y) = v_{xB} - 4 \frac{v_{xB} - v_{xA}}{h_x^2} y^2$$

Substituting this value of $f(y)$ into equation (II.97) we obtain

$$\int_{-\frac{h_x}{2}}^{\frac{h_x}{2}} \left[v_{xB} - 4 \frac{v_{xB} - v_{xA}}{h_x^2} y^2 \right] dy = h_n v_n$$

or

$$\frac{h_x}{3}(2v_{xB} + v_{xA}) = [h_1 + 2r(1 - \cos\varphi)]\, v_r \cos\gamma$$

where r is the radius of the roll.

From this the velocity of the metal at the centre of the cross section of the rolled strip is

$$v_{xB} = \left[\frac{3}{2} \times \frac{h_1 + 2r(1 - \cos\gamma)}{h_1 + 2r(1 - \cos\varphi_x)} \cos\gamma - \frac{1}{2}\cos\varphi_x\right] v_r \qquad \text{(II.98)}$$

It is not difficult to see that, independently of the selected functional law of velocity variation across the thickness of the strip, as we move away from the neutral section the difference of the velocity of motion of the metal particles at the centre of the cross section of the strip and at the points where it touches the rolls increases, reaching a maximum at the boundary of the zone of sticking. In Fig. 68 the character of the increase in the velocity of the motion of the central portion of the strip is shown by the curve *ad*. When the zone of sticking approaches the plane passing through the axis of the rolls, and, if we assume that in equation (II.98)

$$\varphi_x = 0 \quad \text{and} \quad \frac{2r}{h_1}(1 - \cos\gamma) \approx s$$

then the exit velocity of the metal at the central portion of the strip is

$$v_{1B} = v_r(1 + 1.5s)$$

Since in this case the exit velocity of the outer layers of the strip touching the rolls equals v_r, their velocity will be considerably lower than the exit velocity of the central portion of the strip.

Over the last region of deformation, i.e., over the contactless zone of deformation at the exit, as has been mentioned above, the equalization of the velocities of the central and outer layers of the strip takes place. During the equalization of the velocities the outer layers of the strip are subjected to tension, whilst the inner layers are subjected to compression and at the same time to deceleration, so that their velocity is approximately reduced

$$\text{from } v_r(1 + 1.5s) \text{ to } v_r(1 + s)$$

At the other boundary of the zone of contactless deformation at the exit the equalization of the velocities is complete, and the final value of the forward slip of the outer and inner layers of the strip is the same.

On the basis of the analysis of the relationship of the exit velocities of the metal at the surface of the rolls and at the centre of the cross section of the strip, we can thus draw the conclu-

sion that at the plane of exit the forward slip of the inner layers is greater than that of the outer layers. The ratio $l : h_m$ exerts great influence on the difference of the forward slips. In the case where this ratio is large (more than four) the difference of the forward slips is very small, but if this ratio is small (less than two) and the zone

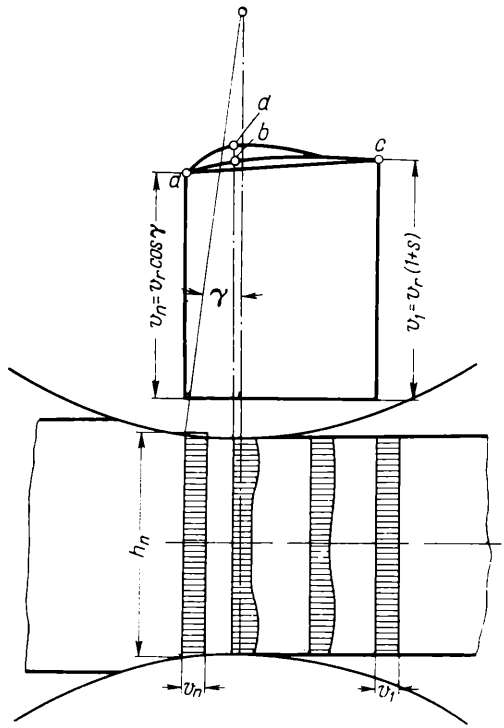

Fig. 69. Velocity variation of the metal across the thickness of the strip for forward slip when the compressive strain does not extend into the entire cross section. The upper part of the figure shows the velocity variation in the external deformation zone (*abc*), the central zone (*ac*) and in the intermediate zone (*adc*)

of sticking begins to occupy the entire zone of forward slip (Fig. 53*c*), then the forward slip in the plane of exit of the central layers of the strip will be nearly 1.5 times as large as the final overall forward slip, whilst the forward slip of the outer layers will be zero. In this case the forward slip is greatly intensified in the contactless zone at the exit, where an acceleration of the outer layers of the strip takes place owing to tension, whilst the inner layers are decelerated owing to compression.

A similar phenomenon, i.e., a non-uniform distribution of the forward slip across the thickness of the strip is observed also when $l : h_m < 0.5$ to 1 and the compression does not affect the whole cross section. The results obtained for the outer layers of the strip touching the rolls remain completely valid for this case of rolling.

The velocity of the inner layers of the strip, however, follow a completely different law. Owing to the fact that the compressive strain does not penetrate the whole cross section of the strip, an elongation of its middle portion takes place as a result of a pull by the layers subjected to the compression. Accordingly, on the right-hand side of the neutral section (if we assume that the velocity distribution in it is uniform), the velocity of the inner layers of the contact zone of deformation must be less than the velocity of those portions of the strip which are subjected to the deformation. In the next zone of deformation (contactless) these velocities are equal, having the value

$$v_1 = v_r (1 + s)$$

Fig. 69 shows an approximate distribution of the velocities of motion of the metal across the thickness of the strip and the graphs of the velocity variation over the zone of deformation: in the outer layers of the strip (curve *abc*), in the layers located on the axis (curve *ac*) and in the intermediate layers (curve *adc*).

13. THE EFFECT OF TENSION ON FORWARD SLIP

Tension has the greatest effect on forward slip in comparison with other technological parameters. This circumstance considerably simplifies the control of continuous mills which operate with tension between the roll stands, and at the same time has a practical interest in the study of the effect of this factor on the forward slip.

The forward slip with the effect of tension taken into account can be calculated from equation (II.92), if the angle γ in this equation is determined from equation (II.79), taking into consideration the variation of the normal and shear contact stresses caused by the tension.

However, such an approach to the problem is complicated, since when the variable value p_x is substituted into equation (II.79) with the effect of the tension taken into consideration, cumbersome expressions appear which are ill suited for practical calculations. Because of this we shall solve the problem in a simplified form, assuming that:

(1) the specific pressure over the entire arc of contact is expressed by only two equations: one for the zone of backward slip and the other for the zone of forward slip;

(2) the same applies to the contact friction forces;

(3) the neutral section is located very close to the maximum specific pressure, and the difference of the positions of these two sections may be neglected.

With such premises the position of the neutral section can be found as the point of intersection of the curves expressing the specific pressure in the zones of forward and backward slip.

If we consider the case of hot rolling, then the friction forces acting over the regions of slipping are close to the quantity k. Then with a degree of approximation we can assume that from the equations of specific pressure given above (II.63) and (II.64) or (II.65) and (II.66) will be the most appropriate for the given case.

We find the position of the neutral section, assuming that when $h_x = h_n$ the values of the specific pressure p_x determined by equations (II.63) and (II.64) are the same, that is,

$$2k - \sigma_A + \frac{k}{\tan\frac{\alpha+\gamma}{2}} \log_e \frac{h_0}{h_n} = 2k - \sigma_B + \frac{k}{\tan\frac{\gamma}{2}} \log_e \frac{h_n}{h_1}$$

where σ_A and σ_B are the tensile stresses at the entry and at the exit respectively.

Defining δ_0 and δ_1 by the expressions

$$\frac{0.5}{\tan\frac{\alpha+\gamma}{2}} = \delta_0 \quad \text{and} \quad \frac{0.5}{\tan\frac{\gamma}{2}} = \delta_1 \tag{II.99}$$

we obtain

$$\frac{h_n}{h_1} = e^{\frac{\xi_0-\xi_1}{\delta_0+\delta_1}} \left(\frac{h_0}{h_1}\right)^{\frac{\delta_0}{\delta_0+\delta_1}} \tag{II.100}$$

where $\xi_0 = \frac{2k-\sigma_A}{2k}$ and $\xi_1 = \frac{2k-\sigma_B}{2k}$.

Since in calculating the ratio $\frac{h_n}{h_1}$ from this equation the angle γ is as yet unknown, an approximate value of this angle γ $\left(\text{say, } \frac{\alpha}{3} \text{ or } \frac{\alpha}{4}\right)$ should be substituted into equation (II.99).

If the arc of contact is equated to a single chord, then $\delta_0 \approx \delta_1 \approx \approx \frac{l}{\Delta h}$ and equation (II.100) assumes the following form:

$$\frac{h_n}{h_1} = e^{(\xi_0-\xi_1)\frac{\Delta h}{2l}} \sqrt{\frac{h_0}{h_1}} \tag{II.100a}$$

It is interesting to note that when $\sigma_B = \sigma_A$

$$\frac{h_n}{h_1} = \sqrt{\frac{h_0}{h_1}}.$$

Knowing the ratio $\frac{h_n}{h_1}$ we can determine the angle of neutral section:

$$\frac{h_n - h_1}{2} = r \sin\gamma \tan\frac{\alpha}{2}$$

or

$$\sin\gamma = \frac{h_1}{\sqrt{r\Delta h}}\left(\frac{h_n}{h_1} - 1\right) \qquad \text{(II.101)}$$

Substituting the value of $\sin\gamma \approx \gamma$ into equation (II.92), we obtain

$$s = \left(\frac{r}{h_1} - 0.5\right)\frac{h_1^2}{r\Delta h}\left(\frac{h_n}{h_1} - 1\right)^2 \qquad \text{(II.102)}$$

In the case of cold rolling (more precisely, when the position of the neutral section is calculated) instead of equations (II.65) and (II.66) we can use equations (II.31) and (II.32), i.e., when $\tau_x = \mu p_x$.

As in the preceding case, we assume that when $h_x = h_n$ the values of the specific pressure calculated from both the equations will be the same, i.e.,

$$\frac{2k}{\delta_0}\left[(\xi_0\delta_0 - 1)\left(\frac{h_0}{h_n}\right)^{\delta_0} + 1\right] = \frac{2k}{\delta_1}\left[(\xi_1\delta_1 + 1)\left(\frac{h_n}{h_1}\right)^{\delta_1} - 1\right]$$

For the sake of simplification we assume that

$$\delta_0 \approx \delta_1 \approx \delta = \frac{\mu}{\tan\frac{\alpha}{2}}$$

and rewrite this equation in the following form

$$(\xi_1\delta + 1)\left(\frac{h_n}{h_1}\right)^{2\delta} - 2\left(\frac{h_n}{h_1}\right)^{\delta} - (\xi_0\delta - 1)\left(\frac{h_0}{h_1}\right)^{\delta} = 0$$

whence we obtain

$$\frac{h_n}{h_1} = \left\{\frac{1 + \sqrt{1 + (\xi_0\delta - 1)(\xi_1\delta + 1)\left(\frac{h_0}{h_1}\right)^{\delta}}}{\xi_1\delta + 1}\right\}^{\frac{1}{\delta}} \qquad \text{(II.103)}$$

where $\xi_0 = \frac{2k - \sigma_A}{2k}$ and $\xi_1 = \frac{2k - \sigma_B}{2k}$.

After the ratio $\frac{h_n}{h_1}$ has been calculated the angle of the neutral section and the forward slip are calculated in the same way as in the preceding case, that is, from equations (II.101) and (II.102).

Curves plotted from equations (II.102) and (II.103) are given in Fig. 70, showing the effect of front tension on the forward slip during rolling with different coefficients of friction. It is seen from the figure that when the coefficient of friction diminishes the forward slip becomes sensitive to tension.

Experimental investigations have been carried out by a number of scientists into the effect of tension on the forward slip. The results

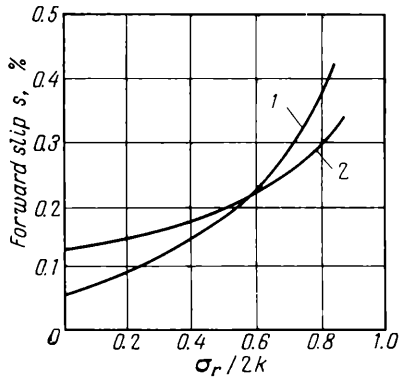

Fig. 70. The Effect of the front tension σ_B on the forward slip when rolling with different coefficients of friction $\left(\frac{\Delta h}{h_0} = 0.5 \text{ and } \frac{h_1}{D} = 0.005\right)$:
(1) $\mu = 0.1$; (2) $\mu = 0.2$

of these investigations confirm the correctness of the equations (II.102) and (II.103) derived above (Figs. 71 and 72).

When the tension varies within the limits used in practice (approximately $\frac{\sigma_B}{2k} = 0$ to 0.4) the forward slip can be expressed by a linear law; this was pointed out by D. Morozov and N. Druzhinin:

$$s = s_0 + \alpha\sigma_B$$

where s_0 is the forward slip when tension is absent, and
α is a coefficient characterizing the angle of inclination of the straight line to the horizontal axis in Figs. 71 and 72.

Expressing the forward slip in this equation in terms of the velocity we obtain

$$v_1 = v_r\left(1 + s_0 + \frac{\alpha}{Q_1} T_1\right)$$

where v_r is the peripheral velocity of the rolls
T_1 is the total tension ($T_1 = \sigma_{ex} Q_1$)
Q_1 is the cross section of the rolled strip at the exit from the rolls.

The investigation carried out by N. Druzhinin on a three-high continuous mill into the effect of the simultaneous action of the front and back tensions on the forward slip is of great interest. On the basis of the test results he arrived at the conclusion that in practice the forward slip can be expressed not only as dependent

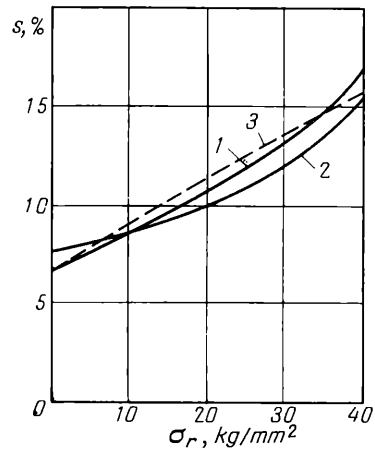

Fig. 71. The effect of the front tension on the forward slip when cold rolling steel band (N. Druzhinin):
1—experimental curve; *2*—curve plotted according to equations (II.102) and (II.103); *3*—straight line

on the front tension, but also as dependent on the difference between the two tensions (front and back) when they act simultaneously (see Fig. 72). Accordingly, when the tension does not exceed approximately (0.6 to 0.7) $2k$ the forward slip can, in practice, be expressed as dependent on the front and back tensions (T_1 and T_0 respectively), thus:

$$s = s_0 + \alpha \frac{T_1 - T_0}{Q_1} \qquad \text{(II.104)}$$

where s_0 is the forward slip when tension is absent
α is the tangent of the angle of slope of the straight line to the horizontal axis
Q_1 is the cross section of the strip at the exit from the rolls.

Then the exit velocity of the metal from the rolls is given by

$$v_1 = (s + 1)\, v_r = \left(1 + s_0 + \alpha \frac{T_1 - T_0}{Q_1}\right) v_r \qquad \text{(II.105)}$$

To simplify the calculation of the forward slip when the effect of tension is taken into consideration Y. Fainberg proposed a for-

mula based on equation (II.78), but in solving it he introduced a number of assumptions.

In the first place, in the same way as in deriving the formula of Ekelund (II.83), the assumption was made that the value of the contact normal and shear stresses is constant over the arc of contact,

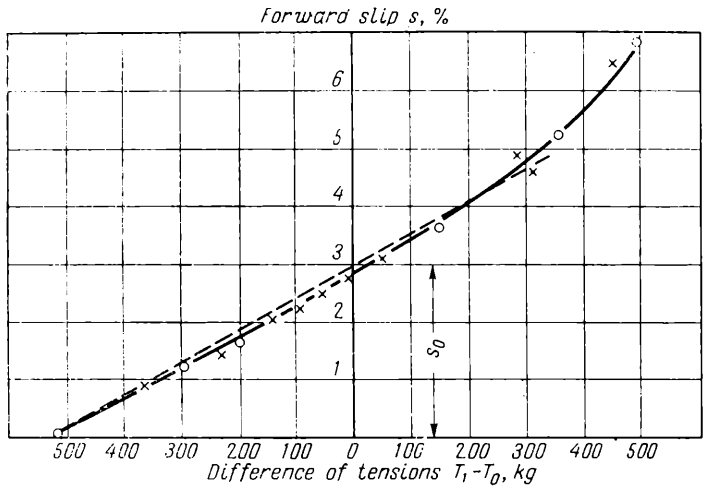

Fig. 72. Dependence of the forward slip on the difference between the front and back tensions ($T_1 - T_0$) when cold rolling steel strip, with $h_0 = 1.44$ mm; $\frac{\Delta h}{h_0} = 0.27$ and $b = 15$ to 20 mm (N. Druzhinin):
crosses—test results; circles—equations (II.102) and (II.103); the straight line is shown by dash line

but their sign changes at the neutral section. Furthermore, Y. Fainberg assumed that tension does not lead to a change in the specific pressure. With such assumptions, noting that $\sum X = \frac{T_1 - T_0}{2}$, equation (II.79) after integration and cancelling assumes the following form:

$$\cos\alpha - 1 + \mu \sin\alpha - 2\mu \sin\gamma = \frac{T_1 - T_0}{2bp_m r}$$

from which

$$\sin\gamma = \frac{\sin\alpha}{2} - \frac{1-\cos\alpha}{2\mu} + \frac{T_1 - T_0}{4\mu r b p_m} \qquad \text{(II.106a)}$$

or, according to (II.87),

$$\sin\gamma = \frac{1}{2r}\left(\sqrt{r\Delta h} - \frac{\Delta h}{2\mu}\right) + \frac{T_1 - T_0}{4\mu r b p_m} \qquad \text{(II.106b)}$$

where r is the radius of the rolls
b is the width of the rolled strip
p_m is the mean specific pressure.

In reality the specific pressure depends strongly on the tension, and in the case where the front and back tensions differ much from each other, the values of the specific pressure in the zones of backward and forward slip are also unequal. In this case calculations based on equations (II.106a) and (II.106b) can lead to inaccurate results.

14. STRESSES ON CONTACT SURFACES MOVING WITH DIFFERENT VELOCITIES

We shall consider two-dimensional rolling of a strip between smooth rolls rotating with different peripheral velocities. In this case the rolling process becomes unsymmetric relative to both rolls: the roll possessing the higher peripheral velocity acquires additional activity, whilst the other roll is transformed into a brake. In solving this problem we proceed as we did in Section 2 (see Chapter II), i.e., we isolate an element from the rolled metal between two planes drawn parallel to the plane passing through the axes of the rolls, and consider its equilibrium. If the element is located in the zone where the rolls tend to slip along it in the opposite directions, then the friction forces will act in different directions. Hence

$$\sum X = (\sigma_x + d\sigma_x)(h_x + dh_x) - \sigma_x h_x - 2p_x \tan\varphi\, dx + \tau\, dx - \tau\, dx = 0 \qquad \text{(II.107)}$$

or

$$d\sigma_x - (p_x - \sigma_x)\frac{dh_x}{h_x} = 0$$

Separating the variables we obtain

$$\frac{d\sigma_x}{p_x - \sigma_x} = \frac{dh_x}{h_x}$$

If we assume that

$$p_x - \sigma_x = 2k \quad \text{and} \quad d\sigma_x = dp_x$$

then after integration we have

$$\frac{p_x}{2k} = \log_e h_x + C \qquad \text{(II.108)}$$

We put $p_x = p_A$ and $h_x = h_A$ in the initial section passing through the point A where the friction forces begin to act in differ-

ent directions. Then

$$p_x = p_A - 2k \log_e \frac{h_A}{h_x} \qquad \text{(II.109)}$$

From this equation it follows that, over the region where the friction forces are directed oppositely, the specific pressure does not undergo large changes and will vary little when h_x diminishes. In this connection it is interesting to follow the variation of the specific pressure curve as the difference of the peripheral velocities

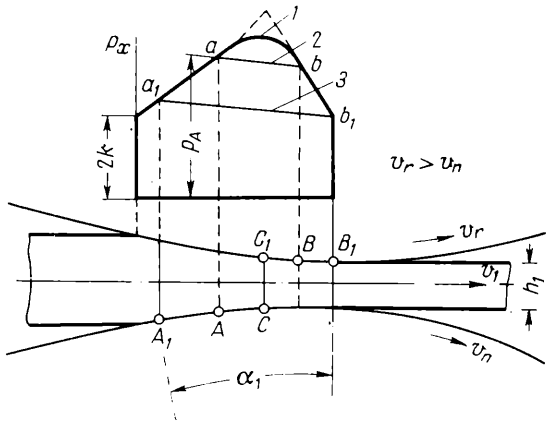

Fig. 73. Variation of the specific pressure due to difference between the peripheral velocities of the two rolls:
(1) $v_r = v_n$; (2) $v_r > v_n$, where v_r equals the mean velocity of the metal in the section at point B, and v_n is the velocity of the metal in the section at point A; (3) the same ($v_r > v_n$) but with $v_r = v_1$; v_n is the velocity of the metal in the section at point A_1

of the two rolls increases. If the rolls have the same peripheral velocity and the rolling process is symmetrical, then the specific pressure may approximately be expressed by the diagram shown in Fig. 73. When the velocity of the lower roll diminishes, the zone of forward slip on it will increase, and the point determining the beginning of this zone will be displaced from the neutral section to the point A. Then, beginning from this point, the specific pressure can evidently be expressed by equation (II.109), i.e., by the curve ab. The diagram will thus be cut off, whilst the zone of forward slip on the upper roll will diminish and the point C_1 will be displaced from the neutral section to the point B. For a further reduction in the velocity of the lower roll the point B will be displaced further and it can occupy the position of the point B_1; thus the zone of forward slip on the upper roll will disappear altogether. In this case the curve constructed from equation (II.109) passes through the

points b_1 and a_1, and the specific pressure reduces to a minimum. The zone of forward slip on the lower roll will increase and its boundary with the zone of backward slip will be determined by the point A_1.

Thus from what has been said we may conclude that with the appearance of a difference in the velocities of the two rolls the specific pressure is substantially reduced whilst the contact friction forces are increased. At the same time the specific pressure diminishes until the zone of forward slip disappears from the roll having the higher velocity, as shown in Fig. 73. This limiting difference in the roll velocities can clearly be found from the equation

$$v_n \cos \alpha_1 h_{A_1} = v_r h_1$$

i.e.,

$$\frac{v_r}{v_n} = \frac{h_{A_1} \cos \alpha_1}{h_1} \tag{II.110}$$

This method of determining the specific pressure can also be used in the design of mills for the longitudinal rolling of tubes, when they are deformed between a roll and a moving or stationary mandrel.

15. DISTRIBUTION OF CONTACT STRESSES ACROSS THE WIDTH OF A ROLLED STRIP AND SPREADING

If we assume that $\sigma_1 = p$, then from equation (I.68), the specific pressure is

$$p = \frac{2\sigma_a}{\sqrt{3+\xi^2}} + \sigma_3$$

where σ_3 is the stress in the metal being rolled, perpendicular to the vector p.

Thus, the distribution of p across the width of the rolled strip is dependent on the variation of the stress σ_3 across the width of its cross section, and, consequently, on the distribution of deformations.

In this connection it is necessary to consider the spreading in order to determine the contact stresses. The spreading, like the distribution of deformations across the thickness of the rolled strip (which has been discussed above), is greatly affected by the outer zones.

The action of the outer zones of the strip on the spreading consists in a tendency to equalize the stretch, i.e., the deformations in the longitudinal direction of the central and side portions of the rolled strip. Because of this action of the outer zones the longitudinal tensile stresses arise not only in the side portions of the strip in the contact zone of deformation, but also in the side portions of the

strip which are located in the contactless zones of deformation both at the entry and at the exit. In the zones next to them longitudinal compressive stresses arise; in all the sections considered in the outer zones of the strip these stresses are balanced by tensile stresses.

Experimental investigations have established that owing to the phenomenon just described the outer zones cause a considerable reduction in the spreading; in particular, at the ends of the strip, as,

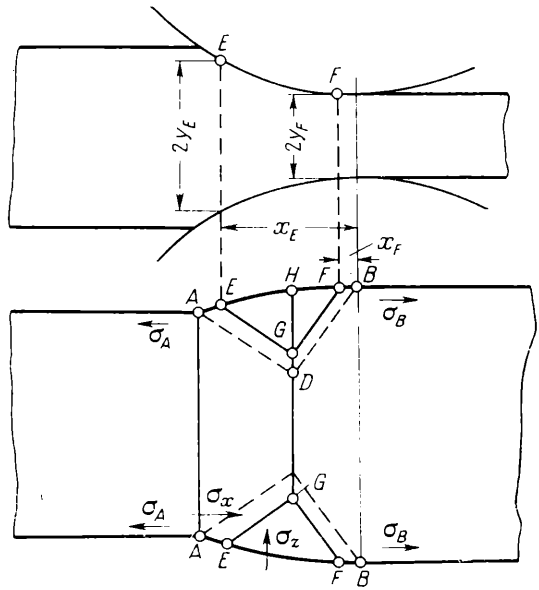

Fig. 74. Displacement of zones (shown dotted) where metal is spread by the action of the outer zones

for example, A. Chekmarev and I. Pavlov pointed out, the spreading is always greater than over its main portion.

In this connection we attempt to elucidate the cause of the effect which the longitudinal tensile and compressive stresses in the outer zones have on the spreading.

We denote the longitudinal stresses acting at the points A and B (Fig. 74) by σ_A and σ_B.

Since tensile stresses arise as a result of the influence of external friction, the compressive stresses σ_x in the zone of deformation are greatly reduced and owing to this the lines where the longitudinal and lateral stresses σ_x and σ_z are equal will not pass through the points A, D and B; they are displaced a little from the outer zones and take up approximately the position of the lines EG and GF (Fig. 74).

Thus, the influence of the outer zones is exhibited by the reduction of the regions where the metal tends to spread, as a result of which the spread itself is considerably reduced.

Similar effects on the spread are shown also by the back and front tensions which are used in cold rolling; as they are stepped up the spread is reduced.

If the stresses σ_A and σ_B become sufficiently large and the maximum specific pressure does not exceed the quantity $2k$, then the regions

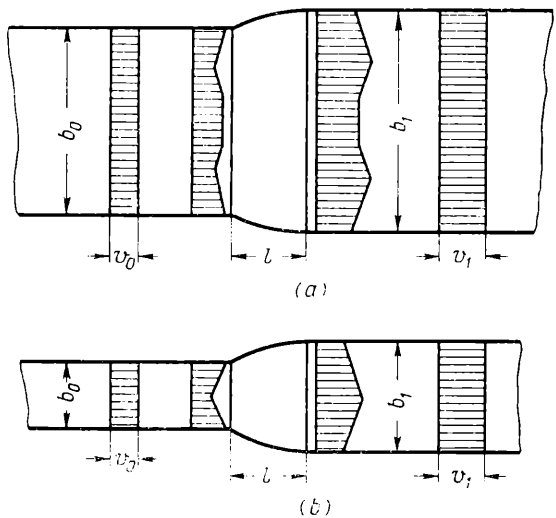

Fig. 75. Variation of metal velocity across the strip width:
(*a*) wide strip; (*b*) narrow strip

where the metal tends to spread vanish and spreading is nearly completely absent. This phenomenon was, for example, observed by the author in developing multiple-roll mills for cold rolling of strip, where owing to a considerable tension and a small roll diameter spreading was almost completely absent, and in certain cases even became negative.

From the analysis of the effect of the outer zones on spreading and from the conclusion that in connection with the tensile stresses the zone of spreading diminishes, it follows that the outer zones greatly affect both the distribution of stresses and strains across the width of the rolled strip and the spreading process itself. The outer zones, preventing the development of spread, are at the same time subjected to the action of considerable stresses which equalize the elongation of the middle portion of the strip as well as of the

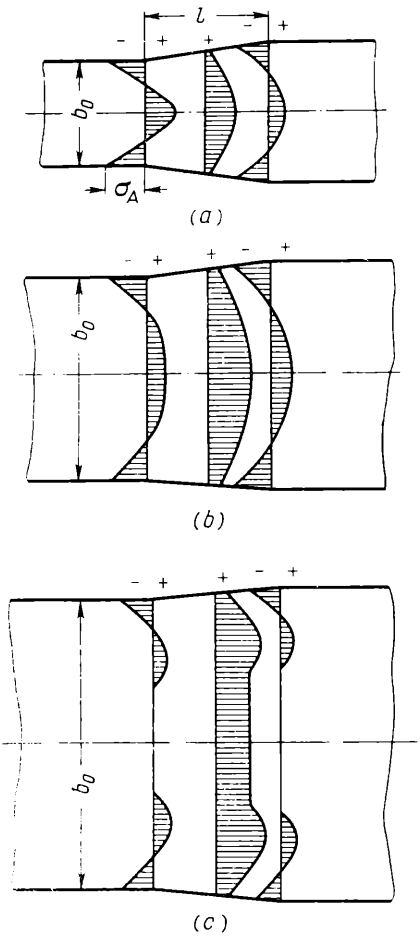

Fig. 76. Variation of the longitudinal stress σ_x across the rolled strip width at entry, in mid-course and at exit for different $b_m : l$ ratios (compressive stress denoted by a positive sign, tensile stress by a negative sign):

(a) $\frac{b_m}{l} < \sim 1$; (b) $\frac{b_m}{l} \approx 1$ to 4; (c) $\frac{b_m}{l} > 4$

edges. Accordingly the value of the tensile stress which arises in the edges as a result of spreading must be the greatest on the boundaries of the contact zone of deformation with the outer zones, i.e., close to the points A and B (see Fig. 74). In the zone of spreading itself these stresses are obviously less; they are partially localized by the external friction.

Tests carried out by the author in rolling test pieces covered with lacquer show that, in deed, along the edges of the outer zones, over a distance more than half the length of the arc of contact, considerable tensile stresses appear.

The appearance of tensile stressesat the edges of the outer zones allows us to assume that the velocities of motion of the metal across the width of the strip are distributed approximately according to the diagrams shown in Fig. 75*a* and *b*. But as the spread requires an additional volume of the metal, at the edges of the strip we observe an increase in the velocity at the entry and a decrease in the velocity at the exit. These velocities are completely equalized at a certain distance from the rolls, which does not exceed the approximate thickness of the strip.

We can assume that the longitudinal tensile and compressive stresses arising in the planes of entry and exit as a result of the action of the outer zones are distributed across the width of the strip approximately as shown in Fig. 76. In doing so we must distinguish between three typical cases:

(1) a narrow strip ($b_m < \sim l$): owing to the small width of the strip the compressive stress at its middle is in the form of a narrow triangle (Fig. 76*a*);

(2) a strip of medium width [$b_m \approx (1 \text{ to } 4)l$]: the compressive stress is distributed over a wider portion at the middle of the strip (Fig. 76*b*);

(3) a wide strip ($b_m > \sim 4l$): the compressive stress which equilibrates the tensile stress does not extend over the whole central portion of the strip owing to the large width of the latter, but is localized in the regions adjacent to the zones of tensile stress (Fig. 76*c*).

Following these patterns for the distribution of longitudinal stresses across the width of the rolled strip we may also represent the distribution of the specific pressure across its width, using equation (I.68) (Fig. 77). Here we also distinguish between three types of specific pressure diagram which correspond to the cases of rolling with the different $b_m : l$ ratios shown in Fig. 76. At the same time the boundaries between these cases must be determined, which depend not only on the ratio $b_m : l$, but also on the reduction, the angle of contact, the coefficient of friction, and still other factors.

The characteristic feature of all these diagrams is that at the edges of the strip the specific pressure is considerably less than in its middle portion; at the points A of entry and B of exit (Fig. 77) the specific pressure at the edges of the strip is less than $2k$, owing to the presence of longitudinal tensile stresses.

Numerous experimental investigations have been carried out to determine the actual distribution of specific pressure across the width of a rolled strip. All of these have been based on measuring the specific pressure over the arc of contact at different distances from the edges of the rolled strip. From the results of these measurements a three-dimensional diagram has been constructed characterizing the variation of the specific pressure both over the arc of contact and across the width of the rolled strip. One such diagram is shown in Fig. 78.

The results of these experimental investigations agree with the theoretical data given above concerning the distribution of the specific pressure across the width of the rolled strip. Close to the edges of the strip the specific pressure is considerably less than in its middle portion, and not only in the region adjoining the neutral section but also at the entry and at the exit.

Experimental investigations carried out by I. Astakhov into the distribution of the specific pressure across the width of the rolled strip showed that the maximum pressure is not always located in the middle of the strip. When wide strips are rolled (with a width slightly exceeding $5\sqrt{r\Delta h}$) two pressure maxima appear,

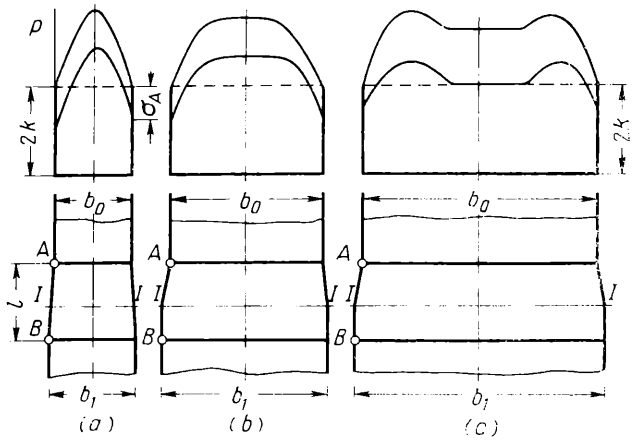

Fig. 77. Variation of specific pressure across the rolled strip width: lower curves—in the plane of entry at A; upper curves—in the central portion of the arc of contact, in the plane I-I; (a) b_m: $l < \sim 1$; (b) b_m : $l \approx 1$ to 4; (c) b_m : $l > 4$

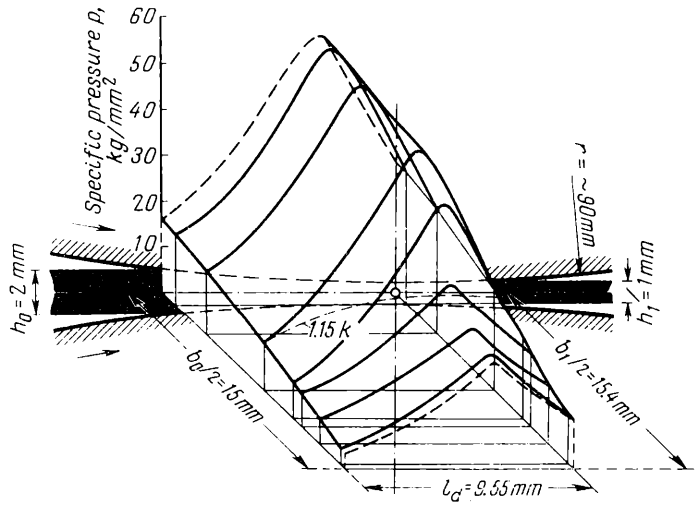

Fig. 78. Three-dimensional specific pressure diagram, plotted from cold rolling test results for aluminium, with $h_0 = 2$ mm; $\Delta h = 1$ mm; $b_0 = 30$ mm and $D = 180$ mm (W. Lueg)

located approximately (1.5 to 2.5) $\sqrt{r\Delta h}$ from the side edge (Fig. 79). The investigations of I. Astakhov thus confirm the correctness of the theoretical results given above (see Fig. 77).

I. Astakhov also carried out experimental investigations into the effect of the non-uniformity of elongation on the distribution of the specific pressure across the width of the rolled strip. He rolled test pieces of different form and with a different character of the elongation distribution across their width. In all cases a reduction in the specific pressure was observed at those points of the test

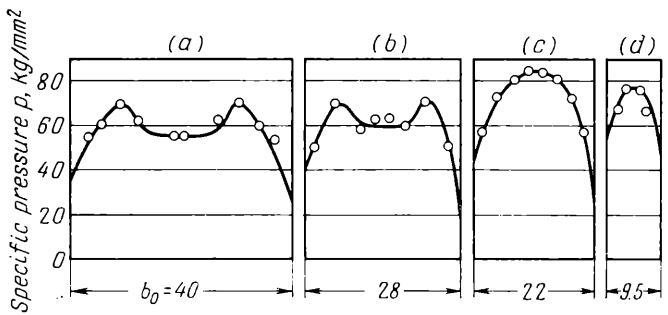

Fig. 79. Variation of the specific pressure across the width of rolled specimens in the plane p_{max} for different ratios of $b_0 : l$, with $D = 150$ mm; $h_0 = 1.4$ mm and $\frac{\Delta h}{h_0} = 0.22$ (I. Astakhov):
(a) $b_0 : l \approx 8.3$; (b) $b_0 : l \approx 5.8$; (c) $b_0 : l \approx 4.6$; (d) $b_0 : l \approx 2$

piece where the elongation was less than the mean value and where, consequently, longitudinal tensile stresses appeared owing to the influence of the outer zones (Fig. 80). At those points of the test piece where the elongation was greater than the mean value, conversely, an increase in the specific pressure was observed because of additional longitudinal compressive stresses.

The zones where the metal tends to spread, shown in Fig. 74, do not characterize the actual volume of metal displaced in the direction of the edges of the strip. Owing to the influence of the outer zones, which has previously been mentioned, a part of the metal of the strip located in the edge zones deforms in the longitudinal direction, and, conversely, owing to the longitudinal compressive stresses arising along the edges of the rolled strip (Fig. 81), the displacement of a certain volume of metal will obviously take place, spreading beyond the limits of the side zones.

But the investigations carried out by B. Bakhtinov and in more detail by the author, and afterwards by A. Grishkov, showed that these side zones—in spite of their provisional nature—nevertheless

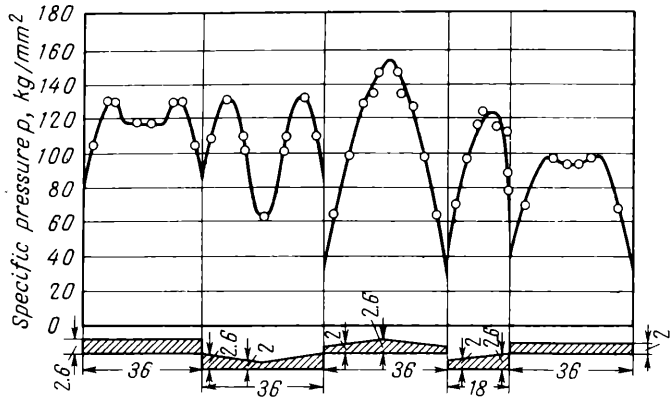

Fig. 80. Variation of the specific pressure across the width of rolled specimens of different cross-sectional shapes (see lower part of figure) (I. Astakhov)

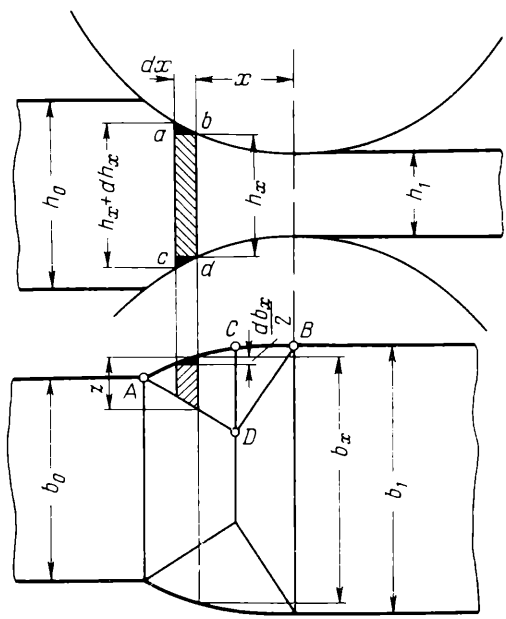

Fig. 81. The arbitrary elementary volume at the strip edge which contributes to the spreading

provide a starting point for calculations of the actual spreading. In the first place, we may show how the formula for spreading is deduced, and not merely drawn from empirical data, which is very important for educational purposes. In the second place, it enables a more accurate formula to be obtained in comparison with existing ones.

We assume that the entire volume contained within the boundaries of the side zone ABD (Fig. 81) is deformed in the direction of spreading; we may then assume that when the section ac, located at the distance $x + dx$ from the exit, is displaced by the amount dx, i.e., when it is displaced into the position bd, the following equation must hold for the elementary displaced volumes:

$$\frac{1}{2} h_x \, dx \, \frac{db_x}{2} = -\frac{1}{2} z \, dx \, dh_x \qquad \text{(II.111)}$$

where dh_x and db_x are the reduction in the depth h_x of the cross section of the rolled strip and the increment of its width b_x respectively when the section ac is displaced, whilst

z is the distance from edge of the strip to the assumed boundary of the edge zone at the section bd.

The minus sign in the right-hand side of the equation shows that b_x increases with decreasing h_x.

This equation is clearly valid whether the spreading takes place as a result of lateral slip or whether the side surfaces are transformed into the contact surfaces, as reported by P. Polukhin.

From equation (II. 111) we find that

$$db_x = -2z \frac{dh_x}{h_x} \qquad \text{(II.112)}$$

The relation between z and h_x can be found from the condition that on the boundaries of a side zone, on the one hand, and on those of the zones of backward and forward slip, on the other hand, the values of the mean lateral stresses σ_z and the mean longitudinal stresses σ_x across the thickness of the strip must approximately be equal.

Every variation of σ_z will at the same time be met by an equal variation of σ_x at the corresponding point of the boundary of the zones. Thus, if over the entire boundary of the zones $\sigma_z = \sigma_x$, then along this boundary their differentials must also be equal: $d\sigma_z = d\sigma_x$.

According to equation (II.9) $d\sigma_x$ can approximately be expressed as

$$d\sigma_x = \left(2k \mp \frac{\tau_x}{\tan \varphi}\right) \frac{dh_x}{h_x} \qquad \text{(II.113)}$$

where k is the resistance to pure shear, and
τ_x is the friction force acting on the contact surfaces in the longitudinal direction.

In a similar manner we find $d\sigma_z$, assuming that $\tan \varphi = 0$ in equation (II.113):

$$d\sigma_z = \frac{2\tau_z}{h_z} dz \qquad \text{(II.114)}$$

where τ_z is the specific friction force acting on the contact surfaces in the lateral direction, and
h_z is the depth of the cross section of the rolled strip, which, when any point located on the boundary of the zones is considered, in contrast to h_x remains constant over the shaded portion (Fig. 82).

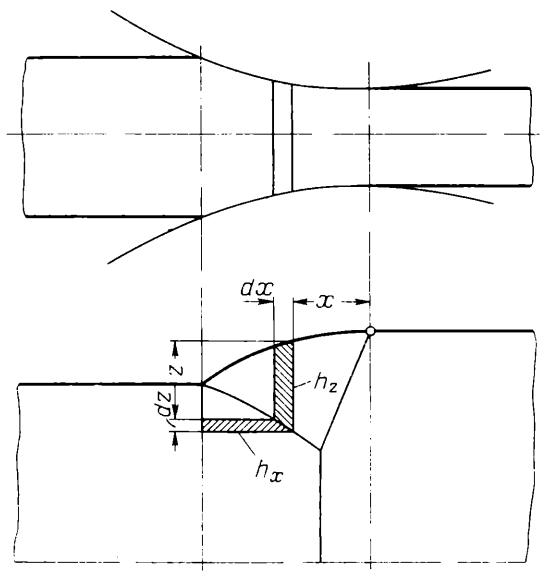

Fig. 82. Ranges of values of the quantities h_x and h_z occurring in equations (II.113) and (II.114)

Equating the right-hand sides of equations (II.113) and (II.114) we obtain

$$dz = \frac{1}{2}\left(\frac{2k}{\tau_z} \mp \frac{\tau_x}{\tau_z \tan \varphi}\right) h_z \frac{dh_x}{h_x} \qquad \text{(II.115)}$$

For an approximate solution of this equation and for simpler final results, we may assume that

$$\tau_z \approx \mu 2k \quad \text{and} \quad \tau_x \approx \tau_z$$

In addition, in determining the boundaries of the edge zone with the zones of backward and forward slip we equate the arc of contact to a chord. Then

$$\tan\varphi = \frac{\Delta h}{2l} \quad \text{and} \quad dz = \left(\frac{1}{2\mu} \mp \frac{l}{\Delta h}\right) h_z \times \frac{dh_x}{h_x} \qquad \text{(II.116a)}$$

and after substituting $h_x = h_1 + \frac{\Delta h}{l} x$ we obtain

$$dz = \left(\frac{\Delta h}{2l\mu} \mp 1\right) h_z \frac{dx}{h_1 + \frac{\Delta h}{l} x} \qquad \text{(II.116b)}$$

After integrating this equation, substituting the value of z thus obtained into equation (II.112) and once more integrating we obtain the equation which specifies the variation of b_x dependent on x.

The results of this derivation as carried out by the author confirm that the spreading, in the main, develops up to the neutral section; over the portion of the edge zones adjacent to the zones of forward slip the spreading is negligible.

Accordingly in a practical calculation of the spreading that part of it which occurs in the zone of forward slip may be neglected.

Integrating equation (II.116b) we obtain

$$z = \left(\frac{l}{\Delta h} - \frac{1}{2\mu}\right) h_z \log_e \frac{h_0}{h_1 + \frac{\Delta h}{l} x} \qquad \text{(II.117a)}$$

After substituting z into equation (II.112)

$$db_x = \frac{2}{\Delta h}\left(l - \frac{\Delta h}{2\mu}\right) \log_e \frac{h_1 + \frac{\Delta h}{l} x}{h_0} dh_x \qquad \text{(II.117b)}$$

The quantities h_x and h_z appearing in equations (II.112) and (II.117a) may be cancelled out since their values along the line AD are the same.

We express dh_x in terms of dx:

$$h_x = h_1 + 2r(1 - \cos\varphi) = h_1 + 4r\sin^2\frac{\varphi}{2} \approx h_1 + \frac{x^2}{r} \qquad \text{(II.118)}$$

Then

$$dh_x = \frac{2x}{r} dx$$

We substitute the value of dh_x just found into equation (II.117b) and find the width of the strip in the region of deformation at a distance x from the plane passing through the axes of the rolls:

$$b_x = \frac{4}{l^2}\left(l - \frac{\Delta h}{2\mu}\right) \int x \log_e \frac{h_1 + \frac{\Delta h}{l} x}{h_0} dx \qquad \text{(II.119)}$$

The quantity $l - \frac{\Delta h}{2\mu}$ in this equation represents the doubled length of the zone of forward slip. Hence it follows that the spreading is proportional to this zone.

We shall use the following substitution in equation (II.119):

$$\frac{h_1 + \frac{\Delta h}{l} x}{h_0} \quad y$$

Then

$$x = \frac{l}{\Delta h}(h_0 y - h_1) \quad \text{and} \quad dx = \frac{l h_0}{\Delta h} dy$$

After substituting these values of x and dx into equation (II.119) and integrating, we have for the region AC (Fig. 81):

$$b_x \quad \left(l - \frac{\Delta h}{2\mu}\right) \frac{4h_0 h_1}{\Delta h^2} y \left[\left(0.5 \frac{h_0}{h_1} y - 1\right) \log_e y - \right.$$

$$\left. - 0.25 \frac{h_0}{h_1} y \quad 1 \right] + C \quad \text{(II.120)}$$

We find the quantity C from the condition that when $x \quad l$, $b_x = b_0$ and $y \quad 1$.

Then

$$b_x - b_0 = \left(l - \frac{\Delta h}{2\mu}\right) \frac{4h_0 h_1}{\Delta h^2} \left[y \left(0.5 \frac{h_0}{h_1} y - 1\right) \log_e y - \right.$$

$$\left. - 0.25 \frac{h_0}{h_1} (y^2 - 1) + y - 1 \right] \quad \text{(II.121)}$$

This equation shows how the width of the strip being rolled varies in the zone of deformation dependent on x, without the influence of the outer zones being taken into consideration.

Fig. 83 represents the variation of the width of the strip in the zone of deformation; this has been calculated from the above equation for the case of rolling of a strip ($h_0 \quad 100$ mm and $h_1 = 60$ mm) between smooth rolls with a diameter of 720 mm and different coefficients of friction ($\mu = 0.3$, 0.4 and 0.5). For the zone of forward slip the variation of the width may be calculated from an equation analogous to equation (II.121), which is derived for this zone.

From Fig. 83 it follows that the spreading in the zone of forward slip is very small, as has been pointed out above, and that in practical calculations of the overall magnitude of the spreading not only the variation of b_x may be neglected over this region, but we can assume that equation (II.121) is valid for the entire arc of contact.

Substituting $y = \frac{h_1}{h_0}$ (for $x = 0$) into equation (II.121) we obtain the theoretical formula from which the spreading may be calculated

without the effect of the outer zones being taken into consideration:

$$\Delta b = \left(\sqrt{r\Delta h} - \frac{\Delta h}{2\mu}\right) f\left(\frac{\Delta h}{h_0}\right) \qquad \text{(II.122)}$$

where

$$f\left(\frac{\Delta h}{h_0}\right) = 2\left(\frac{h_1}{\Delta h}\right)^2 \log_e \frac{h_0}{h_1} - \frac{2h_1}{\Delta h} + 1 \qquad \text{(II.123)}$$

Owing to the fact that the right-hand side of this equation contains the difference of similar quantities, particularly, when small

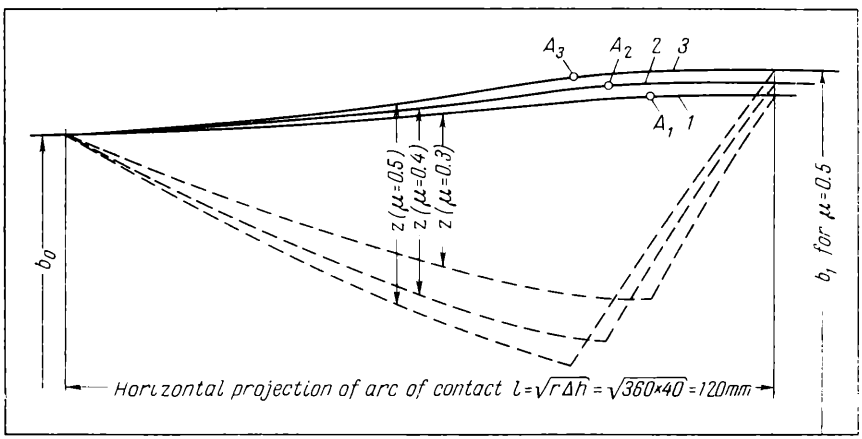

Fig. 83. Variation of the spreading in the deformation zone in the absence of the effect of the outer zones, as predicted by equation (II.121) and the analogous equation for the zone of forward slip (h_0 = 100 mm; h_1 = 60 mm and D = 720 mm) when various coefficients of friction are considered. The points of inflexion A_1, A_2 and A_3 refer to the position of the neutral section:
(1) $\mu = 0.3$; (2) $\mu = 0.4$; (3) $\mu = 0.5$

reductions are used, computations in it must be carried out with an accuracy of several decimal places.

When the reduction $\frac{\Delta h}{h_0} < 0.9$ the value $f\left(\frac{\Delta h}{h_0}\right)$ can also be approximated by the equation:

$$f\left(\frac{\Delta h}{h_0}\right) \approx 0.276\left(\frac{\Delta h}{h_0}\right)^2 - 0.646\,\frac{\Delta h}{h_0} \qquad \text{(II.124)}$$

The formula (II.123) can also be simplified by the following transformation. Multiplying and dividing the last two terms of the right-hand side of this formula by $\frac{2\Delta h}{2h_1 + \Delta h}$ we obtain:

$$\frac{-2h_1}{\Delta h} + 1 = \frac{-4h_1^2 + \Delta h}{2\Delta h^2} \times \frac{2\Delta h}{2h_1 + \Delta h}$$

The second term in this equation can, with sufficient accuracy, be represented as:

$$\frac{2\Delta h}{2h_1 + \Delta h} \approx \log_e \frac{h_0}{h_1}$$

After substituting this into equation (II.123) and cancelling we obtain

$$f\left(\frac{\Delta h}{h_0}\right) \approx 0.5 \log_e \frac{h_0}{h_1}$$

then equation (II.122) for the spreading can be represented as follows:

$$\Delta b = 0.5\left(\sqrt{r\Delta h} - \frac{\Delta h}{2\mu}\right) \log_e \frac{h_0}{h_1} \qquad \text{(II.125)}$$

that is, when the effects of the width and tension are not taken into account the spreading equals the product of the length of the zone of forward slip by the deformation:

$$\log_e \frac{h_0}{h_1}$$

The theoretical calculation of the effect of the width of the rolled strip constitutes an extremely complex problem which as yet remains completely unsolved. We shall give here merely the basic propositions concerning the spreading of narrow and wide rolled strips.

When the width of the rolled strip is approximately equal to the length of the arc of contact or less than it, the zones of deformation where the metal tends to spread will meet from both sides of the strip (Fig. 84). In this case over the region C_1D_1 the quantity z, entering equation (II.112), will be equal to

$$z = \frac{b_x}{2}$$

the spreading over the region C_2D_2 can approximately be expressed as

$$\frac{db_x}{b_x} \approx -\frac{dh_x}{h_x} \qquad \text{(II.126)}$$

or

$$\log_e b_x \approx -\log_e h_x + C$$

We find the quantity C from the condition that at the point C_1 the width of the rolled strip equals b_C whilst the depth is h_C.

After substitution we obtain

$$\log_e \frac{b_x}{b_C} \approx \log_e \frac{h_C}{h_x} \qquad \text{(II.127)}$$

This equation can also be obtained from the law of constant volume if we assume that over the region C_2D_2 the deformation of the strip in the direction of its length is absent:

$$b_x \approx b_C \frac{h_C}{h_x} \tag{II.128}$$

The variation of the width of the strip over the region AC_2 (Fig. 84), in the case of rolling of a narrow strip, can be found from

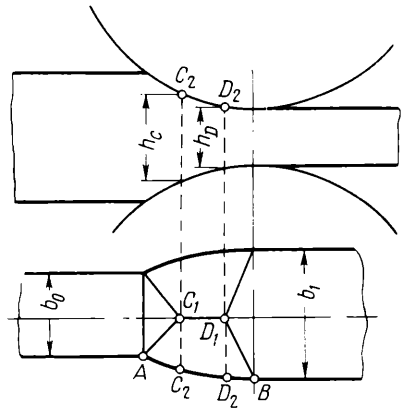

Fig. 84. Zones where the deformation of the metal tends to spread when a narrow strip is rolled

equation (II.121) derived above, if we assume that for this region

$$y = 1 + \frac{\Delta h}{lh_1} x_C$$

In the same way we can find the variation of the width of the strip over the region D_2B, assuming that

$$y_n = 1 + \frac{\Delta h}{lh_1} x_D$$

Here x_C and x_D are the distances of the points C_1 and D_1 from the plane passing through the axes of the rolls.

The position of these points can be found from equations (II.116b) and (II.117a), if we assume that
in the zone of backward slip

$$z = b_C \quad \text{and} \quad h_x = h_C \approx h_1 + \frac{x_C^2}{r}$$

and in the zone of forward slip

$$z = b_D \quad \text{and} \quad h_x = h_D \approx h_1 + \frac{x_D^2}{r}$$

The diagram of the zones where the metal tends to spread, given in Fig. 84, confirms that when the width of the strip is reduced to slightly less than the length of the arc of contact, the spreading diminishes.

In the case where the width of the rolled strip slightly exceeds the length of the arc of contact, the action of the longitudinal stresses σ_A and σ_B (see Fig. 74) arising in the edges of the rolled strip becomes more effective.

These stresses, as has been shown above, reduce the spreading. Consequently, as the width of the rolled strip is increased further the spreading will diminish, but there is clearly a certain limit after which the stresses σ_A and σ_B cease to increase with the width.

The effect of tension on the spreading during hot rolling was first experimentally investigated by V. Kalinin. Strips of various cross sections (rectangle, angle and channel) were rolled in the mill and subjected during the rolling process to either front or back tension by means of a hydraulic cylinder provided for this purpose.

A low carbon steel served as the material for the rolled strips. The rolling temperature was 950°C. The tension varied from 0 to 8.6 kg/mm²; at higher values of the tension a break occurred in the strip.

As a result of these investigations it was established that front tension exerts no significant influence on the spreading, even at tensions causing a break in the rolled strip.

Back tension, on the other hand, exerts a very considerable influence on the spreading, causing a necking of the rolled strip. It has been established that at the approach of the metal to the rolls a zone of necking appears where the width and depth of the cross section of the rolled strip are slightly reduced (Fig. 85).

Owing to the presence of this zone the actual width of the strip entering the rolls will be less than b_0. For this reason the overall value of spreading $b_0 - \Delta b_y$ obtained is considerably smaller than when rolling the metal without back tension:

$$\Delta b < \Delta b_0$$

The results of these investigations, obtained by rolling strips of rectangular cross section and dimensions 15 × 25 mm made out of steel Ст. 3 and using a reduction of 5 mm (33%) at temperatures of 900 to 950°C are shown in the diagram (Fig. 86). It follows from this diagram that the preliminary necking at the approach of the metal to the rolls, Δb_y, appears when $\sigma_0 > 3$ kg/mm², and when $\sigma_0 \approx 7$ kg/mm² it reaches approximately 1.5 mm. The overall necking, i.e., the reduction in the spreading due to tension,

$$\Delta b_y = \Delta b_0 - \Delta b$$

appears at once when tension is applied, and when $\sigma_0 \approx 7$ kg/mm² it increases up to 4.5 mm; then the spreading is reduced from 5.6 to 1.1 mm, i.e., about 5 times.

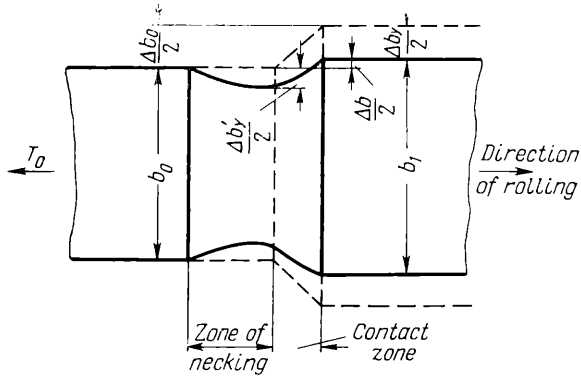

Fig. 85. Zone of necking of a section when rolling with the back tension T_0 (V. Kalinin)

Similar results were obtained by V. Kalinin in rolling carbon steel strip and channel sections with tension.

The conclusions presented above, concerning the influence of the outer zones on the spreading, as well as the results of experimental

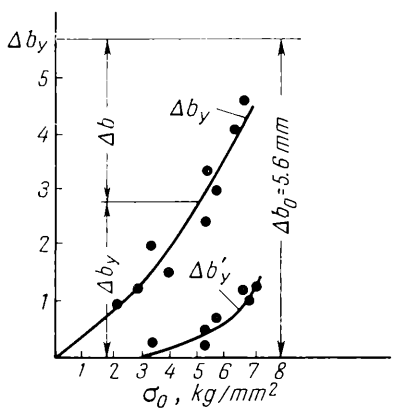

Fig. 86. Effect of back tension on necking when a rectangular section of steel Ст. 3 is rolled at 900 to 950°C (V. Kalinin)

investigations, confirm the complexity of this problem. This problem can, however, be solved in a simplified form, if we take the formula (II.125) as a basis, which takes into account the effect of a number of factors on the spreading, such as: reduction, roll diameter, coef-

ficient of friction and others; the influence of the strip width and tension can be taken into account if we introduce appropriate coefficients into this equation.

Consequently, the following formula may be recommended for the calculation of spreading:

$$\Delta b = 0.5 C_b C_\sigma \left(\sqrt{r\Delta h} - \frac{\Delta h}{2\mu} \right) \log_e \frac{h_0}{h_1} \qquad \text{(II.129)}$$

where C_b and C_σ are coefficients taking into account the influence of the width and tension of the strip.

On the basis of the theoretical data and the results of experimental investigations the effect of the width on the spreading during the rolling of rectangular sections in smooth rolls may approximately be represented as a coefficient dependent on the ratio $\frac{b_0}{\sqrt{r\Delta h}}$, in accordance with the curve shown in Fig. 87.

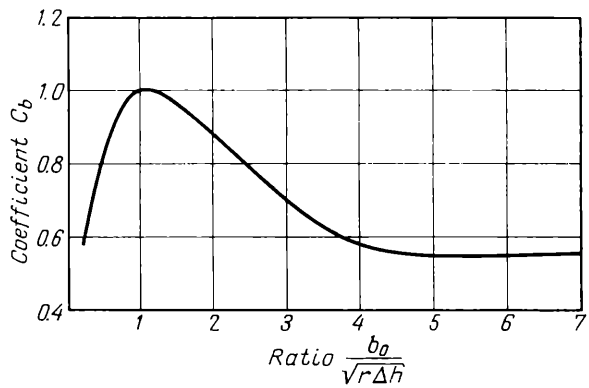

Fig. 87. Variation of the coefficient C_b with the ratio of strip width to the length of the arc of contact

For the calculation of this coefficient the following approximate formula may also be recommended:

$$C_b = 1.34 \left(\frac{b_0}{\sqrt{r\Delta h}} - 0.15 \right) e^{0.15 - \frac{b_0}{\sqrt{r\Delta h}}} + 0.5 \qquad \text{(II.130)}$$

A. Grishkov gives more accurate values of this coefficient, basing them on his experimental studies, where he established that the coefficient C_b depends not only on the ratio $\frac{b_0}{\sqrt{r\Delta h}}$ but partly on the reduction as well. At the same time the maximum value

of the coefficient is close to $\frac{b_0}{\sqrt{r\Delta h}} = 1$ only for small reductions (about 15%). As the reduction increases it is displaced towards the left (Fig. 88). Furthermore, it was discovered that when $\frac{b_0}{\sqrt{r\Delta h}} > \sim 3.5$ the coefficient C_b becomes equal to the relative reduction.

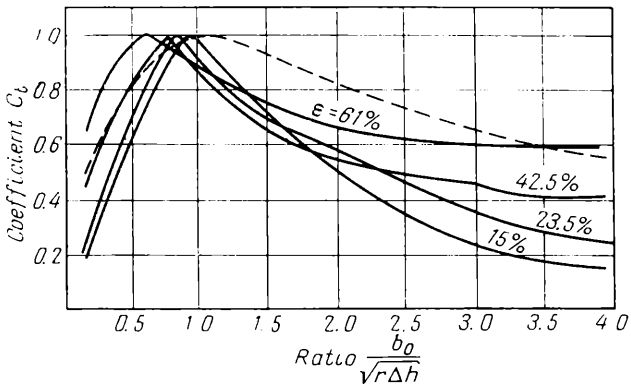

Fig. 88. Variation of the coefficient C_b with the ratio of the strip width to the length of the arc of contact when rolling with different reductions (A. Grishkov)

In connection with the above A. Grishkov recommends the following formula for the determination of C_b:

$$C_b = 4(1-\varepsilon)\left(\frac{b_0}{\sqrt{r\Delta h}} - 0.15\right) e^{1.5\left(0.15-\frac{b_0}{\sqrt{r\Delta h}}\right)} + \varepsilon \qquad \text{(II.131)}$$

where ε is the relative reduction.

In determining from Fig. 86 the second coefficient, which takes into account the effect of back tension, we can start from the condition that when $\sigma_0 = 0$ the value of C_σ is unity, and when $\sigma_0 \approx \sigma_a$, $C_\sigma = 0$. Equating the curve showing increase in necking as the tension increases (Fig. 89) to a straight line over the region of integration, we obtain

$$C_\sigma \Delta b_0 = \Delta b_0 - \frac{2\sigma_0}{\sigma_a} \tan\alpha$$

where α is the angle between the straight line and the horizontal axis.

From this

$$C_\sigma = 1 - \frac{2\sigma_0}{\sigma_a} \times \frac{\tan\alpha}{\Delta b_0} \qquad \text{(II.132)}$$

in approximate calculations we can obviously assume that

$$C_\sigma = 1 - \frac{2\sigma_0}{\sigma_a} \qquad \text{(II.133)}$$

Besides these formulas, which have been derived theoretically, there exists a large number of other formulas, in the main empirical or derived from rough assumptions as to the displaced volumes.

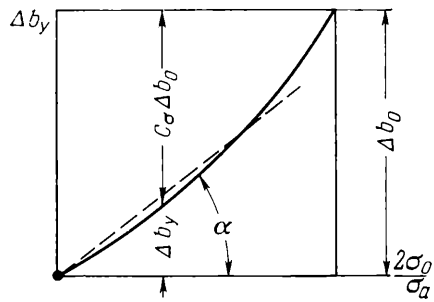

Fig. 89. Determination of the coefficient C_σ

In deriving these formulas and in developing the calculation theory of spreading in general four basic stages should be pointed out:

(1) in the last century the spreading was calculated as proportional to the linear reduction;

Geuze's formula:

$$\Delta b = C_G \Delta h$$

(2) at the beginning of this century the spreading of steel was calculated as not only proportional to reduction, but also to the length of the arc of contact;

Petrov's formula (1917):

$$\Delta b = C_P \frac{\Delta h}{h_1} \sqrt{r\Delta h}$$

Siebel's formula (1927):

$$\Delta b = C_S \frac{\Delta h}{h_0} \sqrt{r\Delta h}$$

(3) the spreading is not proportional to the entire arc of contact but only to the zone of forward slip;

Bakhtinov's formula (1950):

$$\Delta b = 1.15 \frac{\Delta h}{2h_0} \left(\sqrt{r\Delta h} - \frac{\Delta h}{2\mu} \right)$$

and Gubkin's formula (1947):

$$\Delta b = \left(1 + \frac{\Delta h}{h_0} \right) \mu \left(\sqrt{r\Delta h} - \frac{\Delta h}{2\mu} \right) \frac{\Delta h}{h_0}$$

(4) the spreading is calculated theoretically; it depends also on the extent of the zone of forward slip, and, in addition, on the logarithm of strain, the width and tension of the strip [the formula (II.93) of the author, and the formula (II.98) simplified by A. Grishkov].

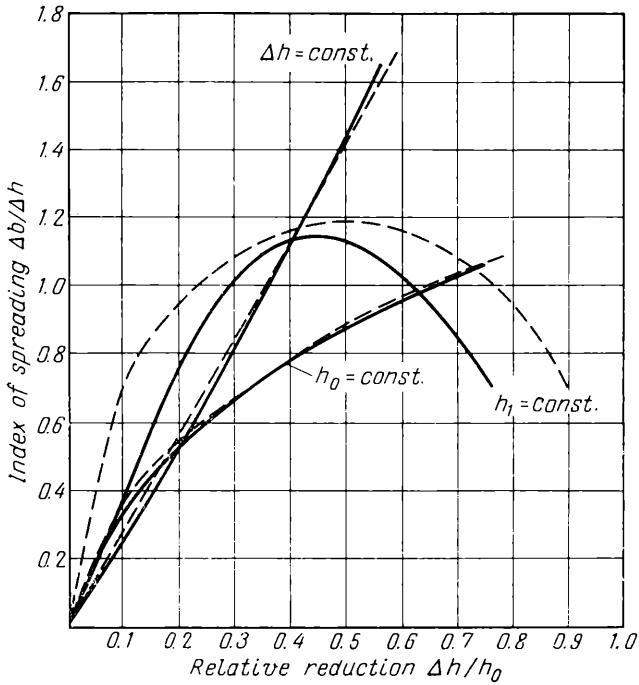

Fig. 90. Variation of the index of spreading $\frac{\Delta b}{\Delta h}$ with $\frac{\Delta h}{h_0}$ when Δh const.; h_0 const. and h_1 const.:
continuous lines: Chizhikov; dash lines: Siebel's formula with $C = 0.53$

There are also other methods of assessing the existing formulas for calculating the spreading. Some of them are not justified. Thus, for example, Y. Chizhikov in his writings evaluates a number of existing formulas for calculating the spreading, the criterion being to what extent the results of calculation, obtained from this formula or other, coincide with the three typical curves shown in Fig. 90. These curves were constructed by him, varying the index of spreading, $\frac{\Delta b}{\Delta h}$, in accordance with the relative reduction, when either Δh is kept constant (first curve), or h_0 is kept constant (second curve), or h_1 is kept constant (third curve). This method of analysis is incorrect since a number of other factors, strongly affecting the

spreading, are not taken into consideration, particularly the diameter of the rolls, the angle of contact, the coefficient of friction, the ratio $b_0 : \sqrt{r\Delta h}$ and others. It was shown above (see Fig. 88) that as the ratio $b_0 : \sqrt{r\Delta h}$ varies the spreading can increase fivefold, keeping the quantities Δh, h_0 and h_1 constant. But if on the graph (Fig. 90) curves, calculated from Siebel's formula for $C_S = 0.53$, are plotted showing the variation of the ratio $\Delta b : \Delta h$ with the reduction, then these curves nearly coincide with the curves of Y. Chizhikov.

Thus, the analysis of the formula for calculating the spreading, recommended by Y. Chizhikov, is essentially based on Siebel's formula which has long been superseded in the theory of spreading.

III

Resistance to Linear Deformation and Pure Shear

1. BASIC FACTORS AFFECTING RESISTANCE TO DEFORMATION

The normal stress, arising at the contact surface of the material being worked and the tool, also called *the specific pressure*, is affected by a large number of factors. All these factors may be divided into two groups.

The first group consists of those factors which affect the mechanical properties of the material, i.e., the resistance to linear (simple) deformation, σ_a, or the resistance to pure shear, k. Apart from the natural properties of the metal itself, this group also includes such factors as temperature, work hardening and strain rate. To the second group belong the factors which influence the state of stress of the metal as it is worked, i.e., the contact friction forces, the outer zones, the tension and other such factors.

In this chapter only the factors of the first group will be considered, i.e., those which determine σ_a (k_f) or k as dependent on the yield point.

According to Nadai's equation, the effect of these factors can in the general case be expressed as:

$$d\sigma = \frac{\partial\sigma}{\partial T}\,dT + \frac{\partial\sigma}{\partial\varepsilon}\,d\varepsilon + \frac{\partial\sigma}{\partial t}\,dt + \frac{\partial\sigma}{\partial u}\,du \qquad \text{(III.1)}$$

The first term of this equation takes into account the effect of the temperature T on the resistance to deformation, the second takes account of the work hardening resulting from the deformation ε, the third takes account of the relaxation with the time t, and the fourth takes into account the increase in the stresses σ with the strain rate when the viscosity of the metal is considered.

The laws necessary for the solution of this equation are as yet little studied, and therefore in practice the effect of these factors must be taken into account by introducing corresponding coefficients. In the case of a linear state of stress the actual yield stress in simple compression or tension (k_f) may be determined from equation (I.48), i.e.,

$$\sigma_a = n_t n_{wh} n_v \sigma_s \qquad \text{(III.2)}$$

where n_t, n_{wh} and n_v are the coefficients accounting for the effect of temperature, work hardening and strain rate on the resistance to deformation, and

σ_s is the yield stress for the metal when tested under static conditions, i.e., by means of the usual testing machines.

When σ_s is substituted into equation (I.48) or (III.2) it must be remembered that for certain metals the resistance to plastic compression is higher than the resistance to tension. In particular, according to the investigations by E. Siebel and A. Pomp, the stresses for plastic compression of steel are approximately 10% higher than for tension, whilst for the compression and tension of copper and aluminium these stresses are nearly the same.

It follows from this that in calculating σ_a for steel in the case of compressive strain, which also includes rolling, when the yield stress σ_s is determined in tension, this stress must be increased by 10%.

When the strain is two-dimensional, the resistance to deformation should be determined not from σ_a, i.e., the actual resistance to simple compression or tension, but from the resistance to pure shear k [see equation (I.71)]:

$$k = \frac{\sigma_a}{\sqrt{3}} \approx 0.57 n_t n_{wh} n_v \sigma_s \qquad \text{(III.3)}$$

2. THE EFFECT OF THE TEMPERATURE OF THE METAL ON THE RESISTANCE TO DEFORMATION

To calculate the forces arising during hot rolling the effect of temperature on the yield stress or ultimate strength must be known. According to certain experimental investigations the dependence

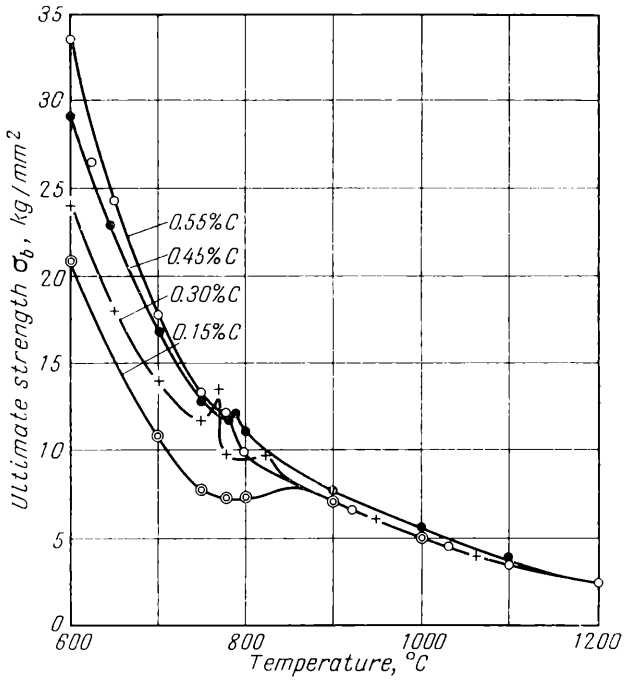

Fig. 91. Variation of the ultimate strength of a steel containing 0.15 to 0.55% C with the temperature (M. Vratsky and I. Frantsevich)

of the mechanical properties of metals (ultimate strength and hardness) on temperature, in the interval between phase transformations can be expressed in exponential form:

$$P = Me^{-mT} \qquad \text{(III.4)}$$

where P refers to the mechanical properties of the metal (ultimate strength, hardness, outflow pressure, etc.)
T is the absolute temperature, and
M, m are constants depending on the nature of the given metal.

This law was established for the first time by K. Ito from investigations into the hardness of various metals at different temperatures. Subsequently this law was confirmed and used in practical cases by a number of other investigators; it was then found that the temperature dependence of the yield point and the ultimate strength can also be expressed in an exponential form. According to this law, if the logarithm of hardness or ultimate strength is plotted

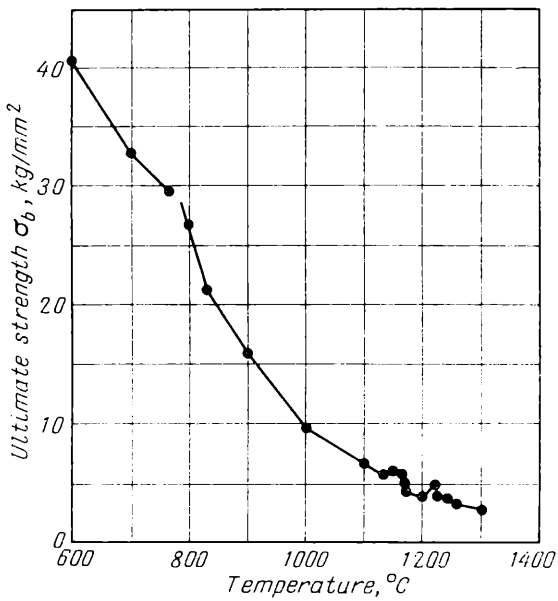

Fig. 92. Variation of the ultimate strength of stainless steel (0.2% C; 0.3% Si; 0.45% Mn; 0.015% P; 0.01% S; 8.2% Ni and 17.2% Cr) with the temperature (M. Vratsky et al.)

as the ordinate and the temperature as the abscissa, the relationship between the hardness or the ultimate strength and the temperature in the intervals between phase transformations is expressed graphically by a straight line.

This law is of great interest for the theory of shaping metals by pressure; from it we can assess the temperature effect on the hardness and the ultimate strength, and, consequently, on the resistance to deformation. But this law has not yet received practical application in determining the mechanical properties of metals at different temperatures. At present this problem is solved by using data obtained from corresponding laboratory tests.

The results of investigations referring to a carbon hypoeutectoid steel with 0.15 to 0.55% C are shown in Fig. 91. The essential feature in the variation of the ultimate strength of hypoeutectoid steels with temperature, as seen from this diagram, consists in a certain reduction in the strength when the temperature is reduced in the interval between the critical points, Ac_3 to Ac_2, i.e., in the case of β-iron. In addition, the ultimate strength of a carbon steel at temperatures higher than 900°C is nearly independent of variations in the carbon content between the limits from 0.15 to 0.55%.

Similar results were obtained by M. Zaikov when investigating the ultimate strength of steel with the carbon content varying within somewhat wider limits (0.12 to 1.19%).

Special steels possess the most diverse mechanical properties which depend on their composition. As a rule, the tensile strength of special steels during hot rolling is higher than that of a carbon steel. In certain cases the strength of special steels in a hot state can be 4 to 5 times higher than the strength of a carbon steel.

A rough idea as to the effect of the alloying elements on the mechanical properties of special steels at high temperatures is given by the investigations, whose results are presented in Table 3 and Figs. 92, 93 and 94.

The data on the effect of temperature on non-ferrous metals are presented in Table 4. The dependence of the resistance to deforma-

Table 3

Tensile Strength of Alloy Steels vs Temperature (After V. Vratsky and I. Frantsevich)

Temperature, °C	Tensile strength of steel, kg/mm²				Temperature, °C	Tensile strength of steel, kg/mm²			
	Э3	Э10	ЭХ2	chrome-molybdenum		Э3	Э10	ЭХ2	chrome-molybdenum
20	62	100	92	55	950	7.2	—	—	—
600	25	27	55	34	1,000	6.3	6.0	5.8	5.7
700	15	19	19	19	1,050	—	—	—	—
750	14	16	17.3	12	1,100	4.5	4.1	4.2	3.7
800	12	13	13	12	1,150	3.7	—	—	3.2
850	10	11	—	10.6	1,200	3.0	2.8	2.6	2.5
900	8.8	9.2	9.0	9.0					

Note. The chemical composition of steel Э3: 0.1% C; 0.3% Si; 0.3% Mn; 0.9% Cr; 0.025% S; 0.035% P and 3.15% Ni; steel Э10: 0.34% C; 0.24% Si; 0.30% Mn; 0.02% S; 0.025% P; 1.65% Cr and 3.3% Ni; steel ЭХ2: 0.95% C; 0.5% Si; 0.25% Mn; 0.02% S; 0.035% P and 1.5% Cr; chrome-molybdenum steel: 0.26% C; 0.2% Si; 0.30% Mn; 0.016% S; 0.037% P; 0.70% Cr and 0.12% Mo.

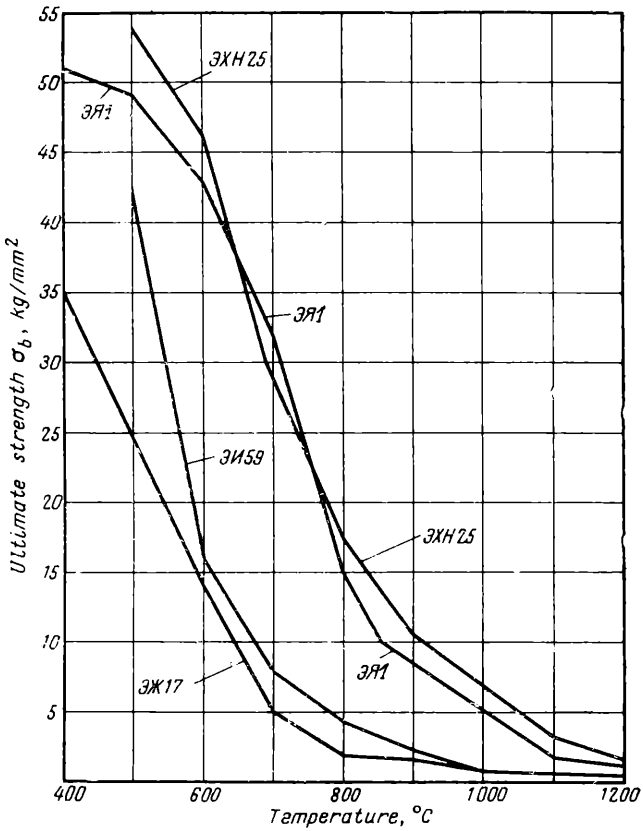

Fig. 93. Variation of the ultimate strength of a refractory steel with temperature (N. Pik):

ЭЖ17 (0.12% C; 0.74% Si; 0.39% Mn; 0.01% P; 0.005% S; 0.16% Ni and 17.00% Cr); ЭИ59, furodite (0.15% C; 0.9% Si; 0.3% Mn; 0.01% P; traces of S; 0.17% Ni and 30.3% Cr); ЭЯ1 (0.13% C; 0.58% Si; 0.5% Mn; 0.01% P; 0.02% S; 9.42% Ni and 18.27% Cr); ЭХН25 (0.23% C; 0.9% Si; 0.6% Mn; 25.0% Ni and 21.0% Cr)

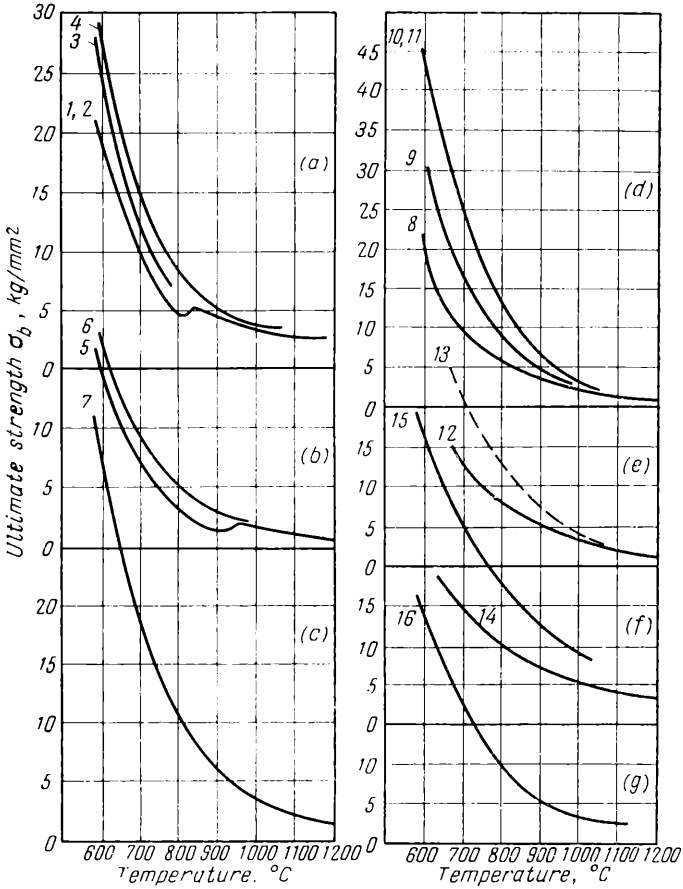

Fig. 94. Ultimate strength of chrome steels and alloys in static tests; $u = 2 \times 10^{-4}$ sec^{-1} (M. Zaikov):

(*a*) and (*b*) low carbon steel with 0.1 to 0.17% C (*1*—steels 15X, 21X; *2*—steel containing 5% Cr; *3*—steel containing 9.6% Cr; *4*—steel 2X13; *5*—X17; *6*—X25 to X30); (*c*) medium carbon steel with 0.3 to 0.5% C (*7*—steels 40X, ШХ10, 3Х18, 3Х25); (*d*) and (*e*) high carbon steel with 0.7 to 1% C (*8*—steel 70; *9*—steel 7Х3; *10*—steel containing 11% Cr; *11*—steel Х28; *12*—9Х and ШХ15; *13*—Х12); (*f*) high carbon steel with 1.5% C (*14*—steel Х12; *15*—Х28); (*g*) high chrome cast iron with 2.25% C (*16*—cast iron Х34)

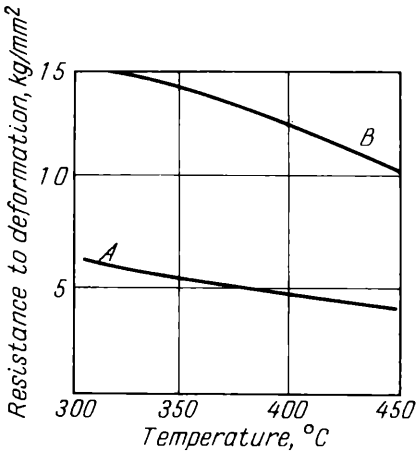

Fig. 95. Effect of temperature on the resistance to deformation of aluminium (*A*) and duralumin (*B*) when external frictional forces are small during rolling (O. Emicke and K. Lukas)

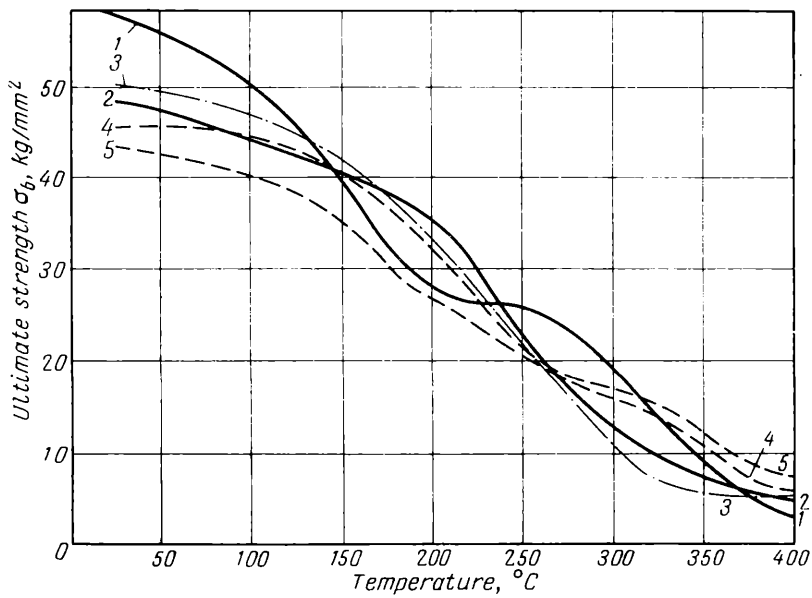

Fig. 96. Variation of the ultimate strength of aluminium alloy forgings, used in the U.S.A., with temperature:

1—alloy 7075-T6 (1.6% Cu and 2.5% Mg); *2*—alloy 2024-T4 (4.5% Cu; 0.65% Mn and 1.5% Mg); *3*—alloy 2014-T6 (4.5% Cu; 0.9% Si; 0.8% Mn and 0.5% Mg); *4*—alloy 2618-T61 (2.2% Cu; 1.1% Fe; 1.6% Mg; 1.05% Ni and 0.07% Ti); *5*—alloy X2219-T6 (6% Cu; 0.3% Mn; 0.1% V and 0.15% Zn)

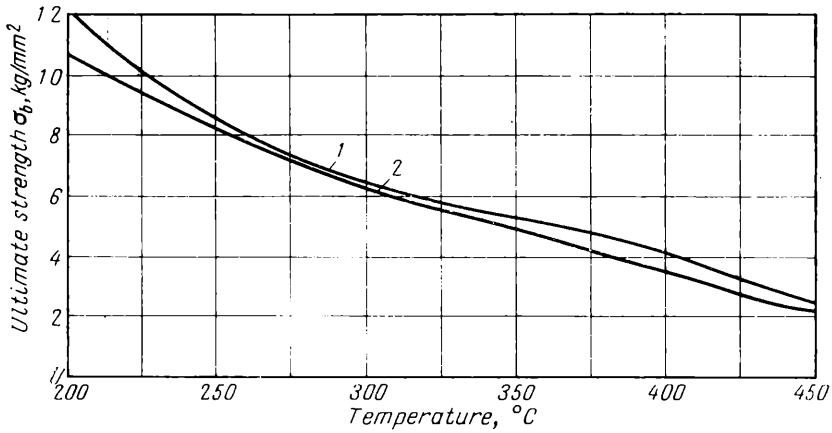

Fig. 97. Variation of the ultimate strength of magnesium alloys with tempera ture, when $u = 1 \times 10^{-3}$ sec^{-1} (S. Gubkin):
1—alloy МАГ (3.5% Al; 0.5% Zn and 0.3% Mn); *2*—alloy МАЗ (6% Al; 1% Zn and 0.3% Mn)

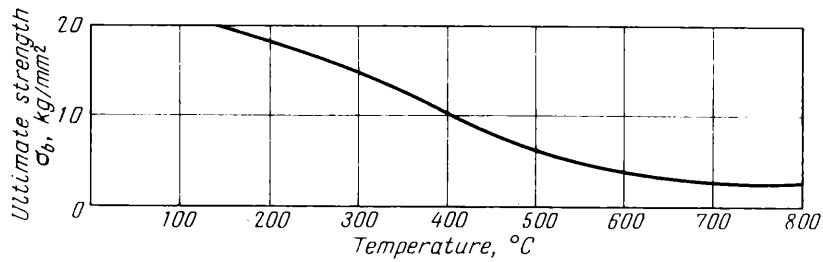

Fig. 98. Variation of the ultimate strength of copper (99.9% Cu) with temper- ature (A. Geleji)

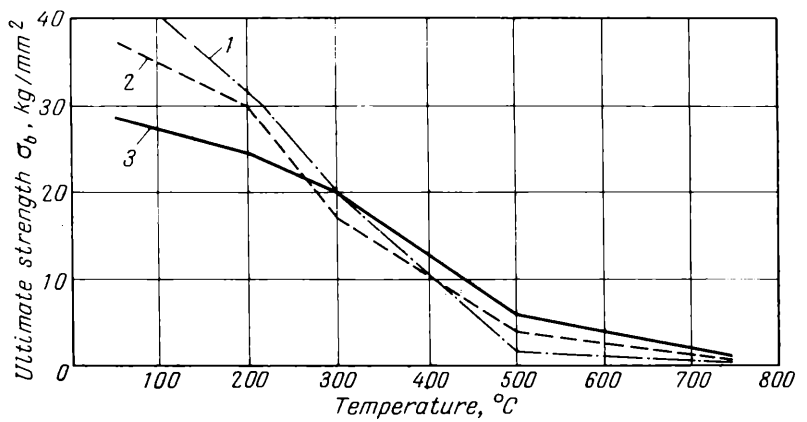

Fig. 99. Variation of the ultimate strength of brass with temperature (A. Geleji):
1—MS54; *2*—MS60; *3*—MS70

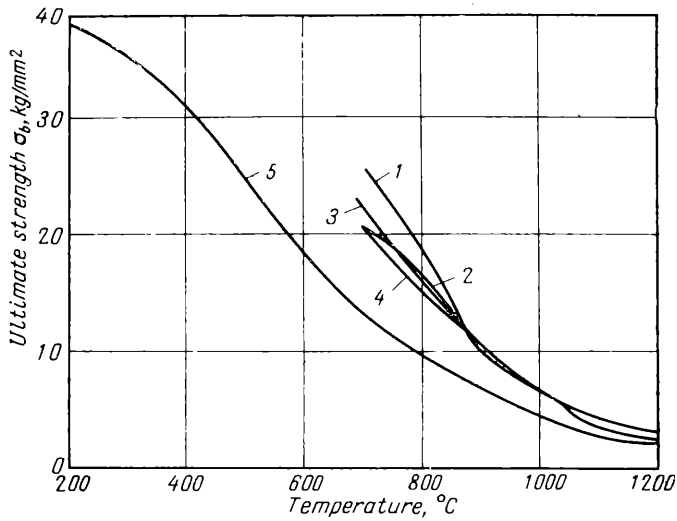

Fig. 100. Variation of the ultimate strength of nickel alloys with temperature:

1—hot rolled alumel НМЦАКГ-Г-1 (1.8 to 2.2% Mn; 1.8 to 2.5% Al and 0.85 to 1.15% Si); *2*—cast НМЦАКГ-Г-1; *3*—hot rolled НМЦ5; *4*—manganese cast nickel НМЦ5 (92.6 to 95.4% Ni + Co and 4.6 to 5.4% Mn); *5*—cast nickel Н-1 (99.5% Ni + Co)

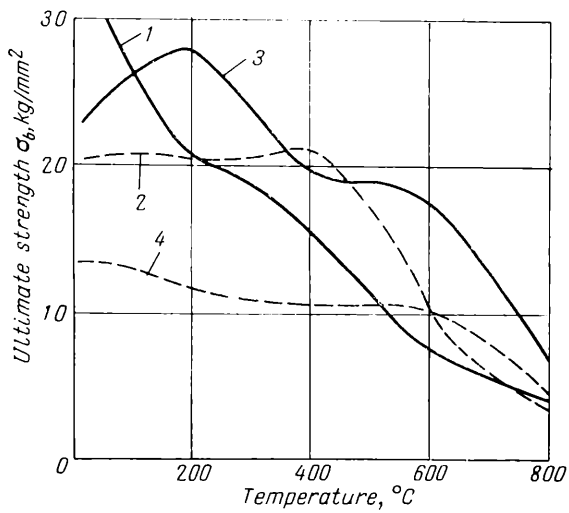

Fig. 101. Variation of the ultimate strength of beryllium with temperature:

transverse (*1*) and longitudinal (*2*) pressed test pieces; longitudinal (*3*) and transverse (*4*) cast test pieces

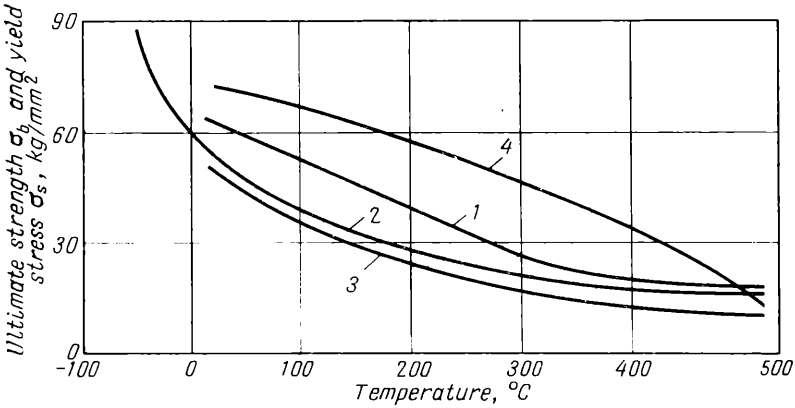

Fig. 102. (*1*) variation of the ultimate strength; (*2-4*) variation of the yield point of titanium with temperature:
1—baked at 1,200°C, cold forged and annealed in vacuum (2 hours) at 800°C; *2*—hot rolled bar; *3*—annealed bar; *4*—cold rolled strip

Table 4

Mechanical Properties of Non-Ferrous Metals at Different Temperatures (After P. Ludwik)

Metal	Temperature, °C		Ultimate strength, kg/mm²	Metal	Temperature, °C		Ultimate strength, kg/mm²
	preliminary annealing	test			preliminary annealing	test	
Aluminium	350	20	11.6	Nickel	900	455	30.2
		75	10.0			593	20.6
		135	7.65			800	9.20
		310	2.60			1,000	4.00
		403	1.25			1,100	2.50
		510	0.55	Brass	500	20	32.4
		600	0.35			200	26.9
Lead	100	20	1.35			400	11.8
		82	0.80			600	2.8
		150	0.50			800	0.5
		195	0.40	Zinc	200	20	11.30
		265	0.20			112	7.25
Copper	600	20	22.8			150	5.00
		160	18.4			247	2.25
		300	13.2			330	1.25
		555	4.85			405	0.03
		650	3.30	Tin	50	20	2.73
		793	1.90			53	1.79
		970	0.80			100	1.05
Nickel	900	20	49.3			153	0.65
		195	44.8			180	0.45
		300	44.8			207	0.25

tion of aluminium and duralumin on temperature for rolling with small reductions, when the effect of the external friction is negligible, is shown in Fig. 95.

Figs. 96 to 102 present curves showing the effect of temperature on the ultimate strength of aluminium and magnesium alloys, copper, brass, nickel alloys, beryllium and titanium.

3. CALCULATION OF THE TEMPERATURE VARIATION OF THE METAL DURING ROLLING

The temperature of the metal when it emerges from the preheating furnace and during its passage between the rolls of the rolling mill changes due to:

(1) the loss of heat to the surrounding medium by radiation;

(2) the loss of heat by convection;

(3) the loss of heat (by conduction) to the rolls, guides, rollers of the roller table and other parts of the mill with which the metal being rolled comes into contact;

(4) the acquisition of heat resulting from the energy expended on the plastic deformation of the metal.

Of these four items in the heat balance of the metal being rolled the first is the most important, since at temperatures higher than 200 to 300°C the cooling of steel is primarily by radiation. At these temperatures the loss of heat by the metal by convection is so small in comparison with radiation that it can be neglected. This has been shown by a special investigation into the heat transfer from metal to rolls, carried out by G. Ivantsov. Consequently, in practical calculations of the temperature drop of the metal during rolling only two of the above items in the heat balance need be taken into consideration, viz., the loss of heat due to radiation and the gain of heat as a result of plastic deformation.

The amount of heat which is lost by the rolled metal to the external medium by radiation is expressed, according to the Stefan-Boltzmann law, by the following formula:

$$Q = FtC\left[\left(\frac{T}{100}\right)^4 - \left(\frac{T'}{100}\right)^4\right] \qquad \text{(III.5)}$$

where F is the surface giving off heat, m^2

t is the time of cooling, hr

T and T' are the absolute temperatures of the surface of the cooling body, and the surrounding medium, °K

C is the radiation constant of the cooling body, cal $100^4/m^2$ hr $(1°K)^4$.

The quantity C can be determined from the formula

$$C = \varepsilon C_s$$

where C_s is the radiation constant of an absolutely black body equal to (4.88 to 5.2) cal $100^4/m^2$ hr $(1°K)^4$

ε is a coefficient depending on the character of the surface (when a carbon steel is rolled, this is taken as approximately equal to 0.8).

Hence

$$C = 4 \text{ cal } 100^4/m^2 \text{ hr } (1° K)^4$$

The quantity of heat which as a result of radiation is transferred during the time dt from the cooling metal into the surrounding medium is

$$dQ = FC \left[\left(\frac{T}{100} \right)^4 - \left(\frac{T'}{100} \right)^4 \right] dt \qquad \text{(III.6)}$$

If we assume that the difference of the temperature of the inner portion of the strip and that of its surface during the period considered remains unchanged, then

$$dQ = Gc\, dT \qquad \text{(III.7)}$$

where G is the weight of the cooling metal, kg

c is the thermal capacity, cal/kg °C.

Since the temperature of the surrounding medium is considerably less than the temperature of the cooling metal, we discard the second term in the brackets of equation (III.6) in order to simplify the calculation. Then for a time dt the reduction dT of the temperature can be found from the equation

$$dT = \frac{FC}{Gc} \left(\frac{T}{100} \right)^4 dt \qquad \text{(III.8)}$$

from this the temperature drop of the metal over the time t is determined as follows:

$$t = \frac{Gc}{FC} \int_{T_1}^{T_0} \left(\frac{100}{T} \right)^4 dT \qquad \text{(III.9)}$$

or

$$t = 0.033 \frac{Gc}{FC} \left[\left(\frac{1{,}000}{T_1} \right)^3 - \left(\frac{1{,}000}{T_0} \right)^3 \right] \qquad \text{(III.10)}$$

Hence we find that the reduction of the temperature $(T_0 - T_1)$ for the time interval t is

$$T_0 - T_1 = T_0 - \frac{10}{\sqrt[3]{\frac{30FCt}{Gc} + \left(\frac{1,000}{T_0}\right)^3}} \qquad \text{(III.11)}$$

where t is the time in hours.

Substituting $C = 4$ cal 100^4/m^2 hr $(1\,^\circ\text{K})^4$ and $c = 0.166$ cal/kg °C into this equation we obtain

$$T_0 - T_1 = T_0 - \frac{10}{\sqrt[3]{\frac{Ft_{\text{sec}}}{5G} + \left(\frac{1,000}{T_0}\right)^3}} \qquad \text{(III.12)}$$

where t_{sec} is the time in seconds, and
F and G are the area and weight respectively of 1 metre of the rolled section.

If the time interval is not large and the temperature drop during this interval is small, the calculation may be carried out by means of the formula (III.8), giving the mean value T_m as the temperature of the metal over the given time interval. The temperature drop is then given by

$$\Delta T = \frac{FC}{Gc}\left(\frac{T_m}{100}\right)^4 \Delta t_{\text{hr}} \qquad \text{(III.13)}$$

where Δt_{hr} is the time in hours.
For steel

$$\Delta T = 0.0067\,\frac{F}{G}\left(\frac{T_m}{100}\right)^4 \Delta t_{\text{sec}} \qquad \text{(III.14)}$$

where Δt_{sec} is the time in seconds.

The increase in the temperature of the rolled metal during its passage between the rolls, which results from the deformation, can be determined from the equation

$$\Delta T = \frac{A(1-\alpha)}{427Gc} \qquad \text{(III.15)}$$

where A is the work required to deform the metal, kgm
α is a coefficient specifying the proportion of the energy expended on the deformation that is lost in heating the rolls and dissipated in the surrounding medium.

The quantity A may be found by various methods (see Chapter VI below). The commonest method for its determination uses experimental curves of the specific energy expended during rolling, taking into account the loss of part of this energy in the rolling mill mechanisms so that it is not utilized in deforming the metal:

$$A = 270\,(a_1 - a_0)\,G\eta \text{ kgm}$$

where $a_1 - a_0$ is the specific expenditure of energy per given pass determined from the curves, hp hr/t
G is the weight, kg
η is the efficiency of the mill.

Substituting this value of A into equation (III.15) we have, taking c 0.166 cal/kg °C:

$$\Delta T \quad 3.8\,(1-\alpha)\,\eta\,(a_1 - a_0) \qquad \text{(III.16)}$$

4. THE EFFECT OF WORK HARDENING ON THE RESISTANCE TO DEFORMATION

During cold rolling of metals, i.e., when the temperature is below the recrystallization temperature or when the rate of recrystallization is less than the rate of deformation, hardening of the

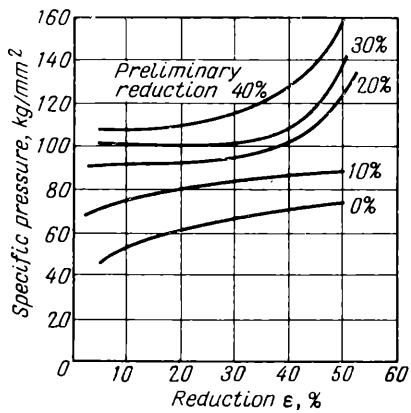

Fig. 103. Variation of the specific pressure with reduction for cold rolled strip (0.1% C) previously rolled with reductions of 0, 10, 20, 30, and 40% ($h_0 \approx 2$ mm; b = 30 mm and D = 185 mm; lubricant: emulsion) (W. Lueg and A. Pomp)

metal takes place, with the result that its resistance to deformation is increased. In practice one must give due consideration to this phenomenon when metals are cold worked, the only exceptions being lead and tin, whose recrystallization temperature does not exceed room temperature.

To illustrate the effect of strain or work hardening on the resistance to deformation Fig. 103 shows the relationship between the specific roll pressure and the reduction during cold rolling of a steel strip with different preliminary reductions. From this diagram it is seen that the specific pressure in rolling a strip reduced by

40% is 1.5 to 2 times greater than when rolling without a preliminary reduction.

Owing to the absence of detailed data on the effect of work hardening on the specific pressure during the rolling of different metals, this effect is usually judged from the variation of the yield stress of the metal in question, as the reduction in the cold state is varied. This variation for each metal is different; as a rule, the hardening

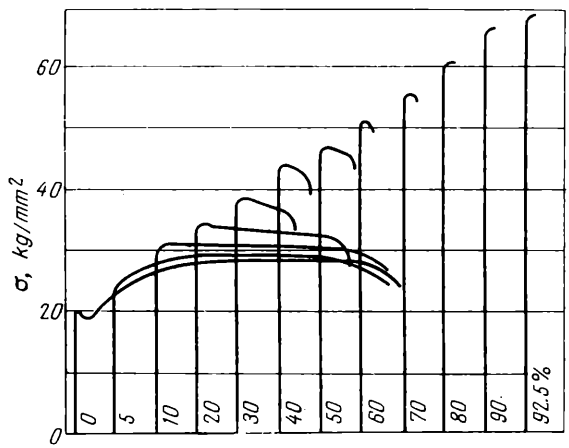

Fig. 104. The effect of the reduction during the cold rolling of mild steel on the form of the fracture test diagram

of pure metals is less than that of alloys, and brass and austenitic steel are particularly susceptible to hardening. The yield stress increases more rapidly as compared with the ultimate strength as the reduction increases, and for high reduction it is nearly equal to the ultimate strength (Fig. 104).

P. Bridgman, from his investigations into the hardening of steel and other metals at large deformations, arrived at the conclusion that the relation between the yield stress and the true deformation is linear (Fig. 105). By true deformation is meant the deformation expressed in natural logarithms (see Chapter I, Section 10). Thus, the effect of strain hardening may be expressed in the general form as:

$$\sigma_a = \sigma_s + a \log_e \frac{l_1}{l_0} \qquad \text{(III.17)}$$

where a is a coefficient equal to the tangent of the angle of inclination of the straight line of strain hardening to the horizontal axis (Fig. 105).

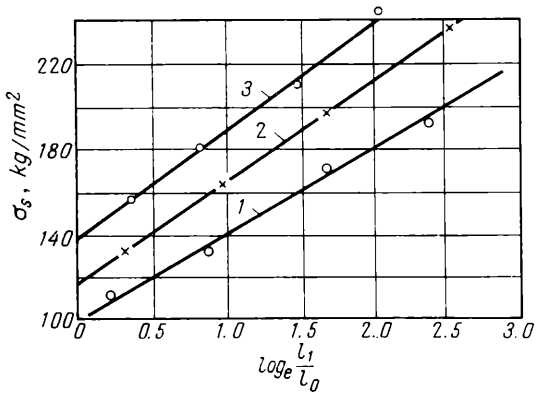

Fig. 105. Strain hardening curves (variation of the yield point with true deformation) for various steels:
1—SAE1315 (manganese), annealed, *HRC* = 21.1; *2*—AE2320 (nickel), annealed, *HRC* = 29.1; *3*—AE4140 (chrome), annealed, *HRC* = 34.5 (P. Bridgman)

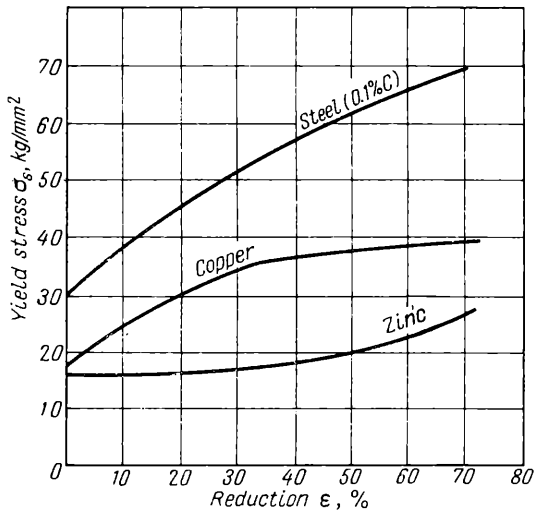

Fig. 106. The effect of the reduction during cold rolling on the yield point of steel (0.1% C), copper, and zinc (E. Rokotyan)

Then the coefficient of work hardening is given by

$$n_{wh} = 1 + \frac{a}{\sigma_s} \log_e \frac{l_1}{l_0}$$

Since equation (III.17) has been little studied with reference to different metals the value of the yield stress as a function of deformation is determined in practice from suitable experimental data.

The effect of reduction on the yield stress during cold rolling of different metals was investigated by Soviet scientists. The results of these investigations are shown in Figs. 106 to 110 together with

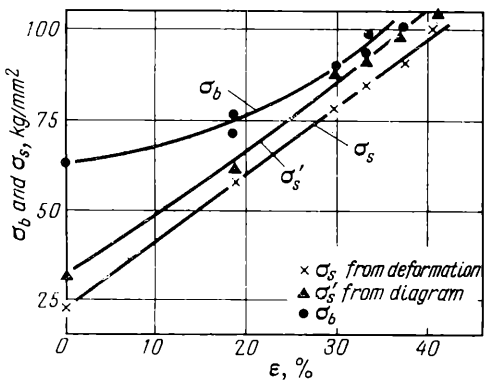

Fig. 107. The conditional yield stress and the ultimate strength of steel 1X18H9; σ_s and σ_s' are the conditional yield stresses for a residual strain of 0.2%, measured by test diagram and mechanical tensometer (A. Tretyakov)

values of the ultimate strengths of various metals. In these investigations the yield stress at which the specimen under tension received a residual elongation equal to 0.2% of its initial length was termed the yield strength:

$$\sigma_{02} \quad \frac{P_{02}}{F_0}$$

where P_{02} is the load, kg, corresponding to the residual strain of 0.2%

F_0 is the cross-sectional area of the test piece, mm².

Figs. 111 to 113 show how the values of the yield stress of titanium, zirconium, niobium, tantalum and molybdenum depend on the deformation (from data supplied by various investigators), whilst Fig. 114 gives the ultimate strength of tungsten.

A. Tretyakov and E. Albrekht have investigated the influence of reduction in cold rolling on the variation in the mechanical

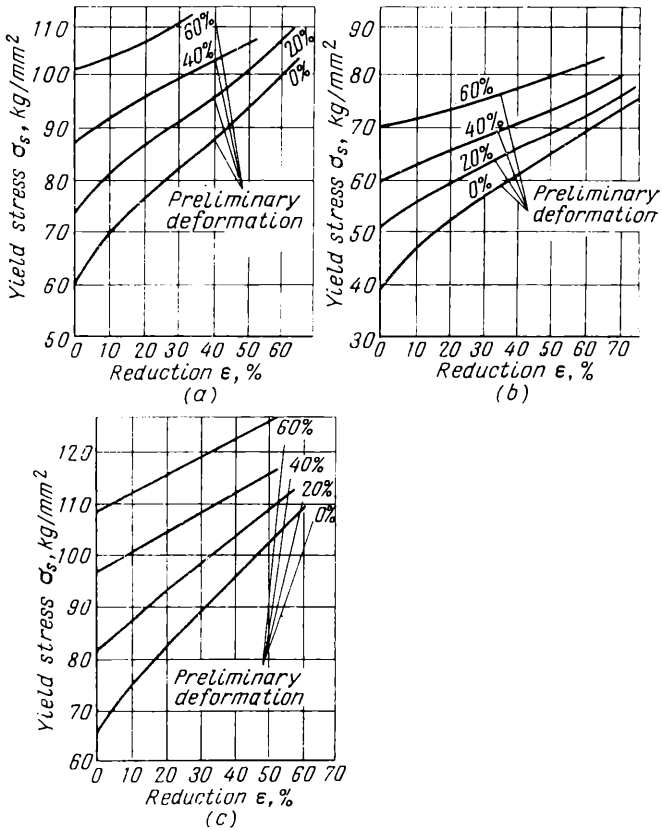

Fig. 108. Variation of the yield point with reduction during the cold rolling of a steel strip having different preliminary reductions (A. Tretyakov):

(a) 0.63% C and 0.62% Mn; (b) 0.10% C and 0.45% Mn; (c) 0.93% C and 0.62% Mn

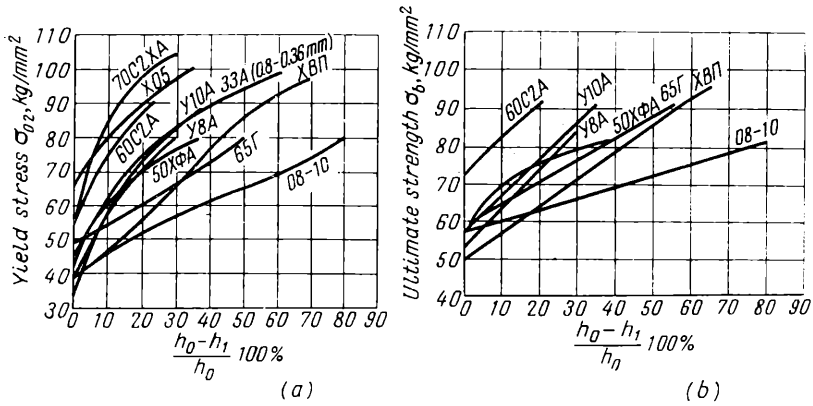

Fig. 109. Variation of the yield strength (*a*) and the ultimate strengths (*b*) of different steels with the reduction during cold rolling (N. Pavlov)

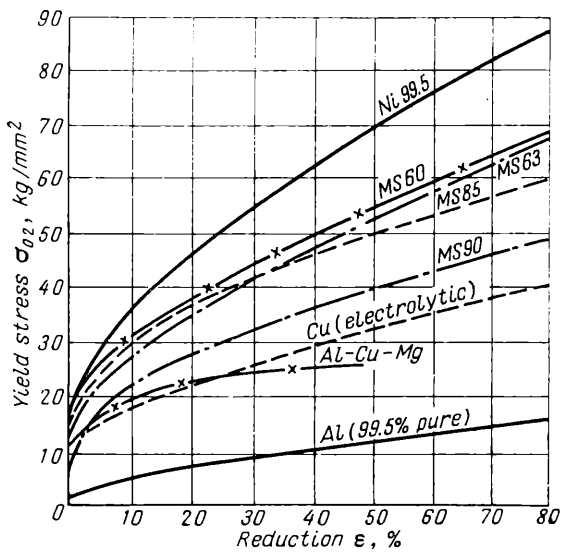

Fig. 110. Variation of the yield stresses of various metals with strain (A. Geleji)

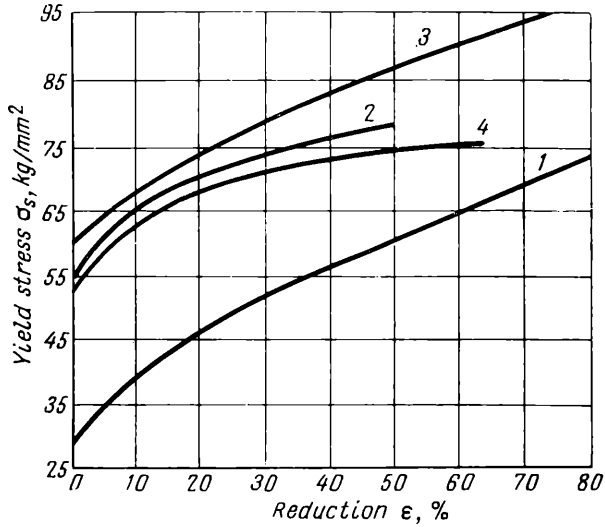

Fig. 111. Variation of the yield stress with reduction during the cold working of titanium:

1—iodide titanium (V. Yeremenko); *2*—magnesium thermal titanium; *3*—calcium thermal titanium; *4*—commercial titanium

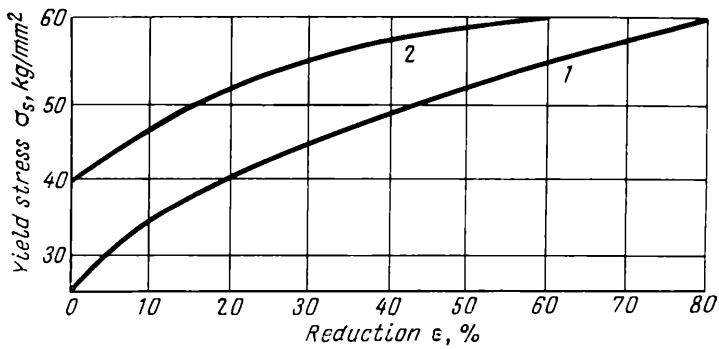

Fig. 112. Variation of the yield stress with reduction during the cold working of zirconium:

1—iodide zirconium, $h_0 = 1.5$ mm (E. Demin); *2*—after hot rolling at 650°C

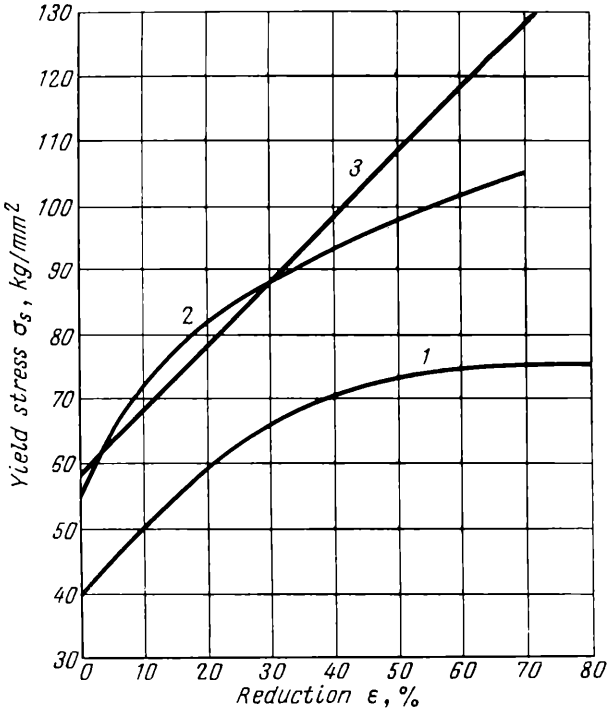

Fig. 113. Variation of the yield stress with reduction during cold working:

1—niobium (E. Demin); *2*—tantalum (E. Demin); *3*—molybdenum (A. Tatarenkov)

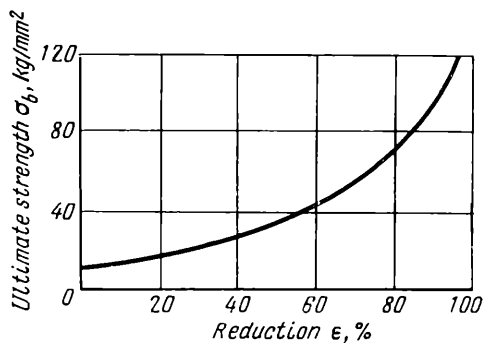

Fig. 114. Variation of the ultimate strength of tungsten with deformation during forging and wire drawing; diameter of initial section 6.2 mm, diameter of final section 0.029 mm (Jeffreys)

properties of steel and alloys of aluminium and copper. From their analysis they were able to establish empirical formulas for these metals which can be used to determine how σ_{02} and σ_b depend on the reduction (Table 5).

Table 5

The Empirical Formulas of Tretyakov and Albrekht for Determining the Dependence of σ_{02} and σ_b on Reduction

Metal group	Metal	Formula
1	Low carbon steel with 0.1 to 0.45% C	$\sigma_{02} = \sigma_{02\,orig} + 1.4\varepsilon^{0.6}$
2	Quality carbon steel (08 rimmed; 08 killed; 35; 45 to 50)	$\sigma_b = \sigma_{b\,orig} + 2.4\varepsilon^{0.64}$
3	Quality carbon steel (У8А; У10; У12)	$\sigma_b = \sigma_{b\,orig} + 1.8\varepsilon^{0.8}$ $\sigma_{02} = \sigma_{02\,orig} + 2.9\varepsilon^{0.72}$
4	Aluminium and its alloys (aluminium, 99.5 to 99.99% pure; АМЦ; АМ2; Д1)	$\sigma_b = \sigma_{b\,orig} + 0.1\varepsilon$ $\sigma_{02} = \sigma_{02\,orig} + 0.7\varepsilon^{0.6}$
5	Brass (Л68; Л69; Л59)	$\sigma_b = \sigma_{b\,orig} + 0.6\varepsilon$ $\sigma_{02} = \sigma_{02\,orig} + 1.4\varepsilon^{0.57}$

Note. Reduction ε expressed as percentage.

5. DETERMINATION OF STRAIN RATE

The derivative of strain with respect to time is called the strain rate, thus

$$u = \frac{d\varepsilon}{dt} \tag{III.18}$$

Since

$$d\varepsilon = \frac{dh}{h}$$

the strain rate is

$$u = \frac{dh}{dt}\,\frac{1}{h} \tag{III.19}$$

The derivative $\frac{dh}{dt}$ is the linear rate of reduction, i.e., the velocity of motion of the tool in the direction of the deformation:

$$v_h = \frac{dh}{dt}$$

whilst h is the instantaneous depth of the body being deformed.

Substituting this value of the derivative into equation (III.19) we obtain

$$u = \frac{v_h}{h} \tag{III.20}$$

To determine the mean strain rate in longitudinal rolling the following formulas have extensively been used in the literature:

$$u_m \approx \frac{\Delta h}{h_0 t} \text{ sec}^{-1} \tag{III.21}$$

or

$$u_m \approx \frac{2v_r \sqrt{\frac{\Delta h}{r}}}{h_0 + h_1} \tag{III.22}$$

where Δh is the linear reduction

h_0 and h_1 are the depths of cross section of the strip being rolled before entry into the rolls and after exit respectively

t is the time during which the metal remains in the zone of deformation, sec

v_r is the peripheral velocity of the roll

r is the radius of the roll.

In formula (III.21) the mean strain rate was taken as equal to the ratio of the strain to the time during which the metal remains in the zone of deformation. Such a representation of the strain rate is obviously inaccurate and accordingly calculations using the formula (III.21) do not yield the correct value of the strain rate.

In formula (III.22), derived on the basis of experimental work carried out by S. Ekelund in 1927 to 1929, the value of the mean strain rate is taken equal to the ratio of the vertical component of the peripheral velocity of the rolls, applied at the mid-point of the arc of contact, to the mean depth of the cross section, which is taken equal to $\frac{h_0 + h_1}{2}$.

Since in reality the strain rate variation over the extent of the arc of contact is not expressed by a straight line, formula (III.22) also does not yield the correct value of the mean strain rate. This shortcoming of the formula was pointed out by N. Kreindlin, and in connection with this he introduced

the new formula:

$$u_m = \frac{2h_1 v_r \lambda \left[(h_1 + D) \frac{\Delta h}{h_0 h_1} + \log_e \frac{h_0}{h_1 \cos \alpha} \right]}{(h_1 + D)^2 \alpha} \qquad \text{(III.23)}$$

where λ is the tension
D is the diameter of the rolls
α is the angle of contact, radians.

In this the actual variation of the strain rate is taken into consideration over the extent of the arc of contact and the mean strain rate is determined by integration as the mean ordinate. Accordingly Kreindlin's formula should be accepted as completely accurate.

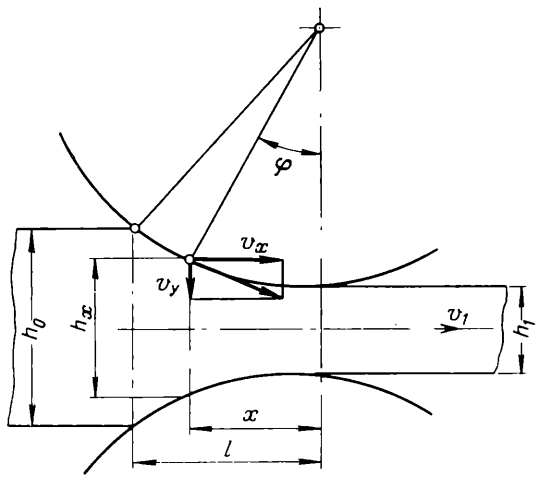

Fig. 115. Determination of the mean strain rate

The drawback of this formula consists only in that it is somewhat cumbersome and, in addition, gives the mean strain rate over the arc of contact, and not over its horizontal projection. The latter would be more correct when solving problems concerned with the calculation of the pressure of the metal on the rolls.

Bearing in mind what has been said, let us try to eliminate the shortcomings of this formula.

During rolling the strain rate at any section of the zone of deformation, located at a distance x from the line connecting the centres of the rolls (Fig. 115), according to equation (III.20), can be expressed as:

$$u_x = \frac{2v_y}{h_x} \qquad \text{(III.24)}$$

The velocity of the metal displaced in the vertical direction is found from the condition that the volume per second is constant, the effect of spreading being neglected:

$$v_y = v_x \tan \varphi = v_1 \frac{h_1}{h_x} \tan \varphi \qquad \text{(III.25)}$$

where v_1 is the exit velocity of the metal.

Substituting this value of v_y into equation (III.24) we obtain

$$u_x = 2v_1 h_1 \frac{\tan \varphi}{h_x^2} \qquad \text{(III.26)}$$

The value of the strain rate can be determined as the mean value of u_x over the segment l:

$$u_m = \frac{1}{l} \int_0^l u_x \, dx \qquad \text{(III.27)}$$

or, after substitution for u_x from equation (III.26),

$$u_m = \frac{2v_1 h_1}{l} \int_0^l \frac{\tan \varphi}{h_x^2} \, dx \qquad \text{(III.28)}$$

Expressing

$$\tan \varphi = \frac{dh_x}{2dx}$$

we obtain

$$u_m = \frac{v_1 h_1}{l} \int_{h_1}^{h_0} \frac{dh_x}{h_x^2} = \frac{v_1 h_1}{l} \left(\frac{1}{h_1} - \frac{1}{h_0} \right)$$

or

$$u_m = \frac{v_1 l}{r h_0} = \frac{v_1}{l} \frac{\Delta h}{h_0} \qquad \text{(III.29)}$$

where v_1 is the exit velocity of the metal
l is the horizontal projection of the arc of contact
r is the radius of the roll
h_0 is the depth of the strip being rolled at the entry into the rolls.

This formula was used in the literature for approximate calculation of strain rate. The results given above indicate that it may be recommended for a completely accurate determination of the mean strain rate in longitudinal rolling (neglecting the effect of spreading).

This formula gives a value of the mean strain rate which differs little from the value obtained using Kreindlin's formula; it is, however, more convenient for practical calculations.

6. THEORETICAL RESULTS RELATING TO THE EFFECT OF VELOCITY ON THE RESISTANCE TO DEFORMATION

On the average the strain rate during rolling is usually within the limits of 1 to 10^3 sec^{-1}.

The effect of strain rate on the pressure of the metal on the rolls during rolling has so far been little studied so that there is as yet no analytical formula which expresses accurately the relation between velocity and resistance to deformation. At present it is known only that resistance to deformation increases with strain rate.

One of the explanations of this phenomenon is based on the assumption that plastically deformed metal may be compared with a viscous fluid, and is thus subject to its laws of motion. If we proceed from the Newton-Stokes law, according to which the increase of the internal friction in the motion of a viscous fluid is proportional to the viscosity and the velocity of the relative slip of its particles, then the relation between the resistance to deformation and the strain rate may be expressed by the equation

$$\sigma_u = \sigma_0 + \eta w \tag{III.30}$$

where σ_0 and σ_u are the yield stresses for static and dynamic deformation

η is the viscosity of the body being deformed

w is the strain rate.

This assumption, however, does not coincide with the relaxation theory of Maxwell. Furthermore, experimental investigations do not confirm a linear relation between the resistance to deformation and the strain rate. According to test data an increase in the resistance to deformation with the strain rate takes place more slowly than would be expected from a linear relation. Because of this instead of equation (III.30) a number of other formulas has been introduced, of which the formula of Siebel and Pomp should be mentioned:

$$\sigma_u = \sigma_0 + Bu^n \tag{III.31}$$

where B and n are coefficients depending on the material, with $n < 1$, and in particular, for steel not exceeding 0.3.

We should also mention Nadai's formula

$$\sigma_u = \sigma_0 + m \log_e \frac{u}{u_0} \tag{III.32}$$

where m is a coefficient depending on the material.

These formulas, although they agree better with the test data than formula (III.30), are little suited for practical calculations in view of inadequate information about their coefficients.

It is more accurate to take into account the effect of strain rate on the resistance to deformation analytically, considering two processes that take place simultaneously: work hardening and relaxation. The intensity of work hardening as a function of deformation will clearly be characterized at any given instant by the tangent of the angle of inclination of the tangent line to the strain hardening curve (Fig. 116). In accordance with the investigations of P. Bridgman, for most metals in compression the relation

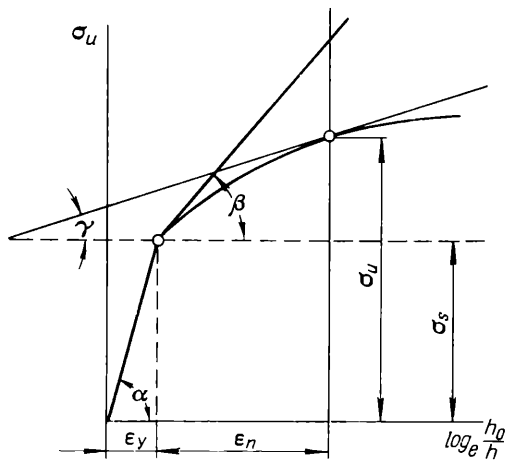

Fig. 116. Strain hardening diagram

between the stresses and the actual deformation, expressed as the natural logarithm of $\frac{h_0}{h}$, is linear. Consequently, the intensity of work hardening for any stage of deformation can be expressed by the same modulus of hardening D.

As for the relaxation, we assume that it is proportional to the time of deformation and to the increase in stress due to work hardening. This agrees with the results of an investigation into the relaxation process which show that the stresses do not fall to zero but only to a certain value σ_0. Consequently, the fall in stress should not be taken as proportional to σ_u but to $\sigma_u - \sigma_0$.

The above discussions lead to the following equation:

$$d\sigma_u = D\,d\varepsilon - A\,(\sigma_u - \sigma_0)\,dt \qquad \text{(III.33)}$$

where A is a coefficient of proportionality, representing the rate of relaxation, sec^{-1}.

Transforming this with due allowance for the strain rate $u = \frac{d\varepsilon}{dt}$ we obtain

$$\frac{d\sigma_u}{d\varepsilon} = D - A\frac{\sigma_u - \sigma_0}{u} \qquad \text{(III.34)}$$

In the strain hardening diagram the first term of the right-hand side of this equation represents the intensity of hardening (tan β) for the case of no relaxation, i.e., for an infinitely large strain rate, whilst the second term represents the intensity of relaxation, i.e., tan β — tan γ.

If the strain rate during the given period is assumed to be constant, then after integration we obtain

$$-\frac{u}{D}\log_e\left(\frac{Du}{A} - \sigma_u - \sigma_0\right) = \varepsilon + C \qquad \text{(III.35)}$$

Neglecting the elastic deformation because of its smallness we find the integration constant C from the condition that for the residual strain $\varepsilon = 0$:

$$\sigma_u = \sigma_0 = \sigma_s$$

We thus obtain the following equation:

$$\sigma_u = \sigma_0 + D\frac{u}{A}\left(1 - e^{-A\frac{\varepsilon}{u}}\right) \qquad \text{(III.36)}$$

This equation accounts for the simultaneous effect of two factors on the resistance to deformation: the rate and amount of deformation. In order to account also for the influence of internal friction when the strain rate is varied, we assume that, as suggested by A. Ilyushin,

$$\sigma_0 = \sigma_{st} + 3\eta u$$

After substituting σ_0 into equation (III.36) we obtain

$$\sigma_u = \sigma_{st} + 3\eta u + D\frac{u}{A}\left(1 - e^{-A\frac{\varepsilon}{u}}\right) \qquad \text{(III.37)}$$

where σ_{st} is the yield stress obtained by static tests, kg/mm^2
η is the viscosity, kg sec/mm^2
u is the mean strain rate, sec^{-1}.

Using the results derived above we can readily obtain the equation of Maxwell, provided we neglect the hardening, i.e., we assume that $D = 0$ and that the intensity of the relaxation is proportional to σ_u, and not to $\sigma_u - \sigma_0$. In comparison with the equation of Maxwell the essential advantage of equation (III.36) or (III.37) is that it simultaneously accounts for the process of relaxation and work hardening.

Using the curves given in Fig. 117 we can compare the data obtained from the formula (III.36) with the experimental data of E. Siebel and A. Pomp, assuming that for lead $D = 4.6$ kg/mm^2; $A = 1/50$ sec^{-1}; $\sigma_0 = 1$ kg/mm^2, as follows from the analysis of these experiments.

Applying equation (III.36), given above to any two experimental points for which the stress and the degree of deformation are known, we can determine the constants D and A for the metal

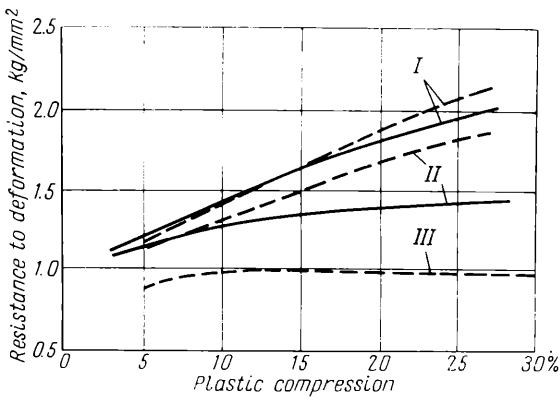

Fig. 117. The resistance to deformation of lead at different strain rates:
I—1.25%/sec; *II*—0.20%/sec; *III*—0.0003%/sec; continuous curves refer to formula (III.36); dash curves refer to the experimental results of E. Siebel and A. Pomp

in question at a given temperature. Knowing these constants we can calculate from equation (III.36) the stresses for other velocities and deformations.

This method has been subsequently developed by V. Persiyantsev for the case of a variable rate of deformation.

Owing to the fact that the rate of relaxation is strongly affected by temperature Vitman and Zlatin suggested, as a result of their tests, the following formula for the determination of σ_u:

$$\log_e \frac{\sigma_u}{\sigma_{st}} = m\,(T - T_0) \log_e \frac{u}{u_0} \qquad \text{(III.38)}$$

where m and T are constants

T_0 is the temperature at which the deformation takes place, °K.

7. RESULTS OF EXPERIMENTAL INVESTIGATIONS INTO THE EFFECT OF VELOCITY ON THE RESISTANCE TO DEFORMATION

To determine the effect of the strain rate on the forces required several experimental investigations have been carried out; these may be divided into two basic groups: the investigations of the first group are conducted directly on a rolling mill when rolling metal with different velocities, whilst the investigations of the

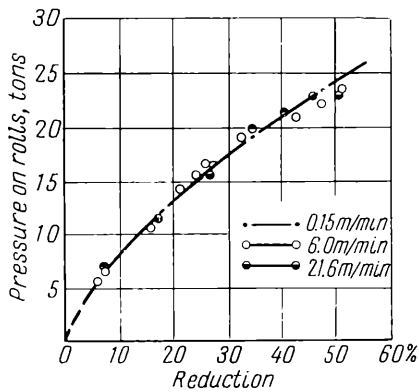

Fig. 118. Variation of the pressure exerted by the metal on the rolls with reduction during the cold rolling of steel (0.1% C) with different velocities (0.15, 6.0 and 21.6 m/min); h_0 = 2 mm; b_0 = =30 mm and D = 185 mm; emulsion lubrication (W. Lueg and A. Pomp)

second group are carried out on testing machines by extending or compressing test pieces with various strain rates.

Comparatively few investigations have been conducted so far into the effect of velocity on the resistance to deformation when metal is rolled in a rolling mill.

In most of these investigations the metal is rolled in cold state; it emerges that during cold rolling the strain rate has a very slight effect on the pressure of the metal on the rolls. We can easily convince ourselves of this, if we consider Fig. 118 which shows the measured pressure of the metal on the rolls during the cold rolling of steel (0.17% C) with different velocities (0.15, 6.0 and 21.6 m/min). The points shown in this diagram indicate that an increase in the velocity from 0.15 to 21.6 m/min, i.e., about 140 times, did not give rise to an increased pressure of the metal on the rolls.

It may be assumed that if the velocity of rolling is increased still further (for example, up to 600 m/min), it would have a con-

siderable effect on the pressure of the metal on the rolls. At the same time it is necessary to take into consideration that there are other factors in cold rolling which, as the velocity increases, decrease rather than increase the pressure of the metal on the rolls. Among these factors are, in the first place, a reduction in heat transfer to the rolls with an increase in the rolling speed (the heat being released in the metal as a result of its plastic deformation) and a reduction in work hardening due to this; in the second place, when the rolling speed is increased the conditions of lubrication of the rolled metal are improved owing to the increased hydrodynamic pressure in the lubricant film. As a result of this the effect of the external friction on the specific pressure is reduced.

This statement was proved by N. Druzhinin and V. Khotulev who investigated the effect of the rolling speed on the expenditure of energy when the speed varied over a very wide range; the maximum speed was 14.05 m/s, nearly 40 times higher than in the tests of W. Lueg and A. Pomp. N. Druzhinin and V. Khotulev concluded that the rolling speed has little effect on the energy expenditure (Fig. 119).

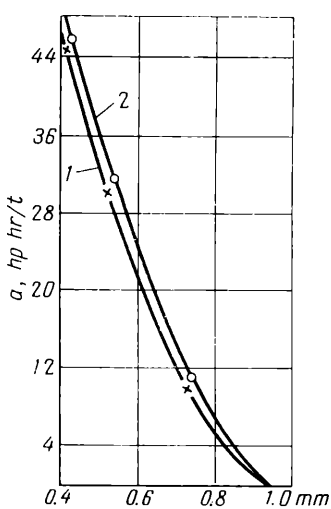

Fig. 119. Variation of the specific energy consumption in the cold rolling of 1010 mild steel strip for various rolling velocities; h_0 = 0.93 mm; $\frac{\Delta h}{h_0}$ = 0.22 to 0.25; b = 13.9 mm and D = 60 mm:
1—0.627 m/s (adjusted velocity); 2—14.05 m/s

The investigations carried out by H. Ford and afterwards by D. Christopherson and B. Parsons indicated that the effect of strain rate depends on the reduction of the metal during rolling. In the case of high reductions a comparatively small increase is observed in the resistance to deformation as the rolling speed increases (Fig. 120). The laws obtained by them, however, refer to low rolling speeds (up to 2.8 m/s).

The effect of velocity on the resistance to deformation in the hot state has been investigated mainly on testing machines. As a result of these investigations a considerable effect of velocity on the resistance to deformation was noted at temperatures exceeding the recrystallization point. In certain cases the ultimate tensile strength at high velocities increases roughly 5 to 7 times in comparison with deformations carried out under static conditions (Fig. 121).

During rolling the strain rate varies within a very wide range: from 0.5 to 5 sec^{-1} for upsetting mills and up to 100

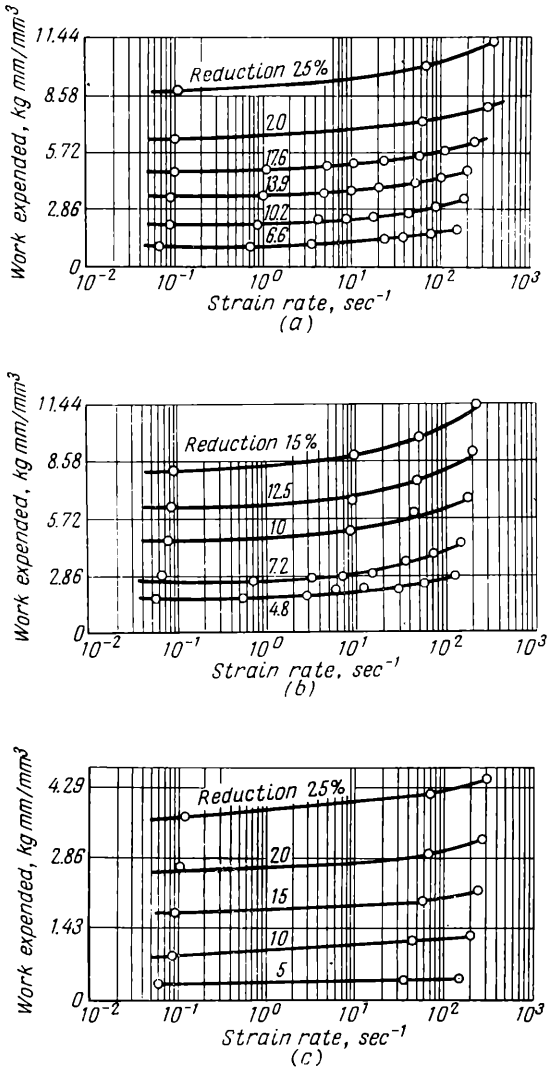

Fig. 120. Variation of the energy consumption with strain rate during cold rolling with various reductions (D. Christopherson and B. Parsons):

(*a*) copper; (*b*) aluminium; (*c*) mild steel

to 400 sec^{-1} for continuous thin strip and wire mills. To determine more accurately the effect of the strain rate, within the limits of 0.5 to 20 sec^{-1}, on the resistance to deformation of low carbon steel at different temperatures, Fig. 122 shows a portion of the diagram of Fig. 121 on a larger scale.

It has also been established that the effect of velocity on the resistance to deformation depends to a large extent on the amount

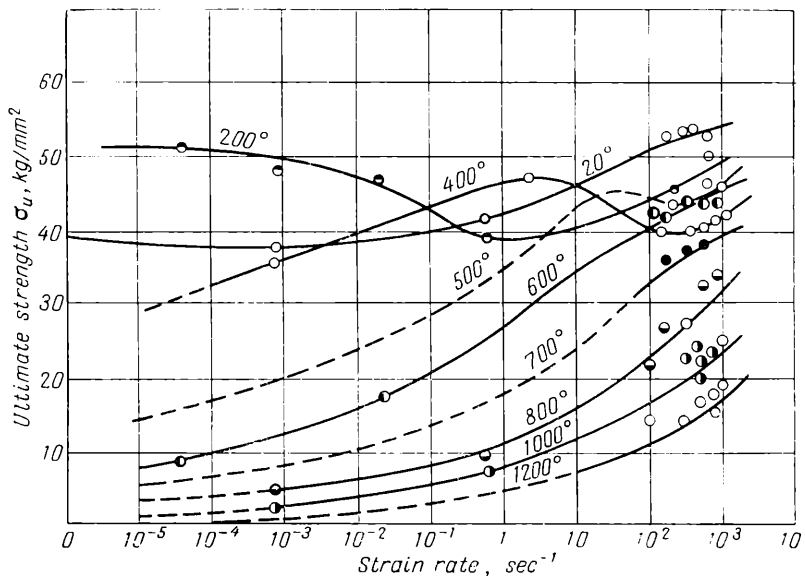

Fig. 121. Variation of the ultimate strength of mild steel with strain rate at various temperatures (A. Nadai and M. Manjone)

of deformation. This phenomenon has been noted above when deriving equation (III.36).

Detailed experimental investigations of the problem were carried out by P. Cook, A. Dinnik and others. They made many measurements of the resistance to deformation of test pieces of various steels, as a function of the deformation at different velocities and temperatures. P. Cook carried out his tests on a testing machine, plastometer, especially constructed by him for this purpose; by means of a cam upsetting was effected with a given constant strain rate despite the change of the height of the test piece during the upsetting process. The test pieces had cylindrical form and were prepared from previously annealed round rolled bars. The dimensions were: (1) $h_0 = 25$ mm and $d_0 = 18$ mm; (2) $h_0 = 25$ mm and $d_0 = 12$ mm; (3) $h_0 = 12.7$ mm and $d_0 = 9.53$ mm. Test pieces

of smaller dimensions were used for high strain rates and were prepared from high grade alloy steel, since the limiting load of the plastometer amounted to 10 tons. The maximum value of the strain equalled $\log_e \frac{h_0}{h_1} = 0.7$, which corresponds to the ratio $h_1 : h_0 = 0.5$. At the

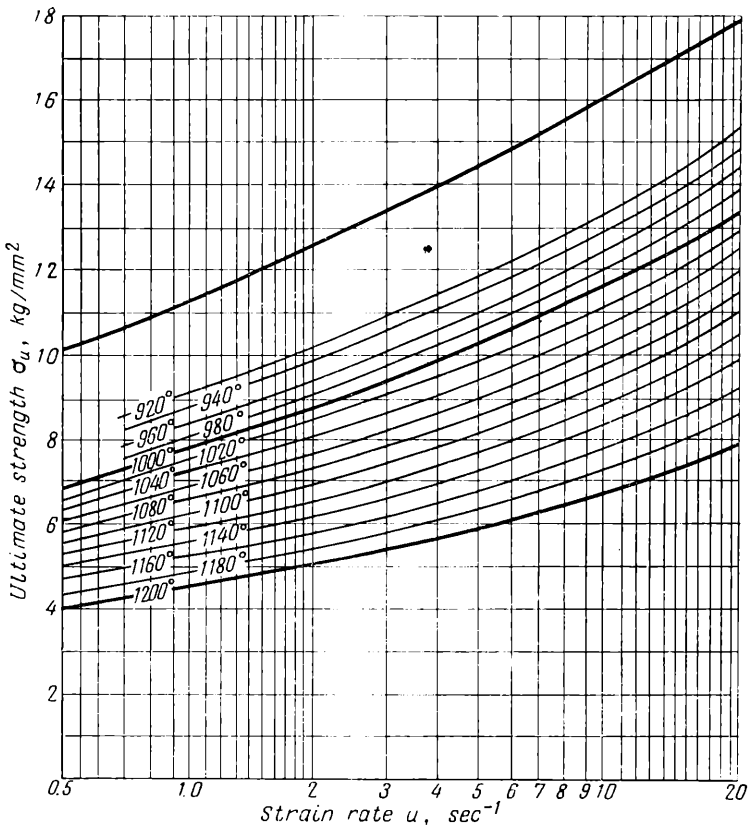

Fig. 122. The ultimate strength of mild steel at different temperatures as a function of strain rate variation in the range from 0.5 to 20 sec^{-1}; curves obtained by enlargement of portion of Fig. 121

same time the cylindrical form of the test pieces was retained, which showed a good approximation to a linear state of stress. To reduce the effect of the external friction glass as a lubricant was used which prior to heating was applied to the ends of the test pieces in the form of a suspension of glass dust in spirit. This enabled the friction force between the contact surfaces of the test pieces

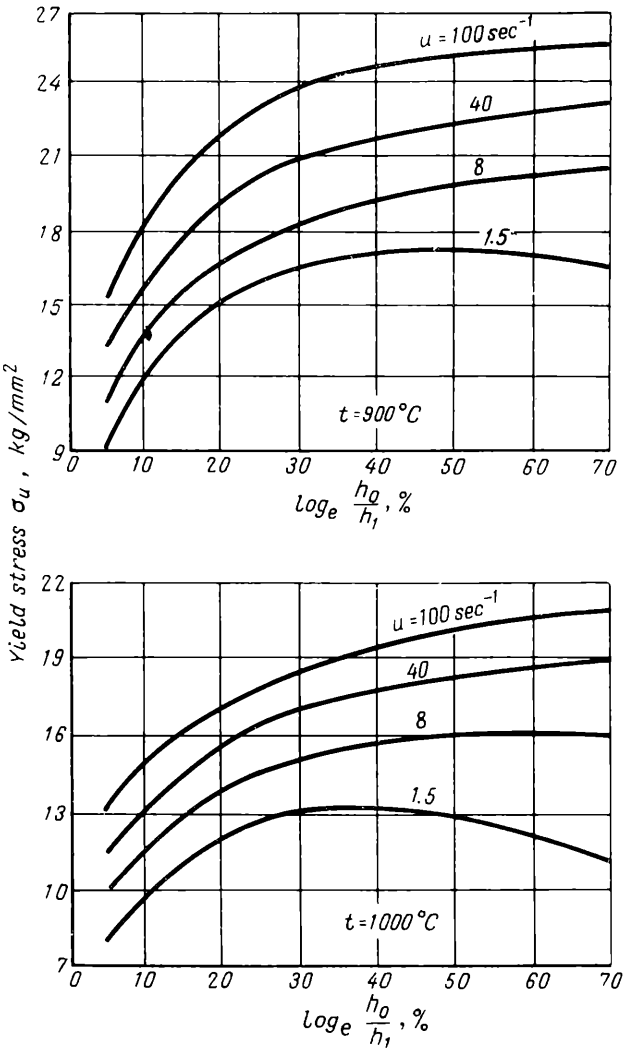
Yield stress σ_u, kg/mm^2
27
24
21
18
15
12
9
0
10
20
30
40
50
60
70
$u = 100\ sec^{-1}$
40
8
1.5
t = 900°C
$\log_e \frac{h_0}{h_1}$, %
22
19
16
13
10
7
$u = 100\ sec^{-1}$
40
8
1.5
t = 1000°C
$\log_e \frac{h_0}{h_1}$, %

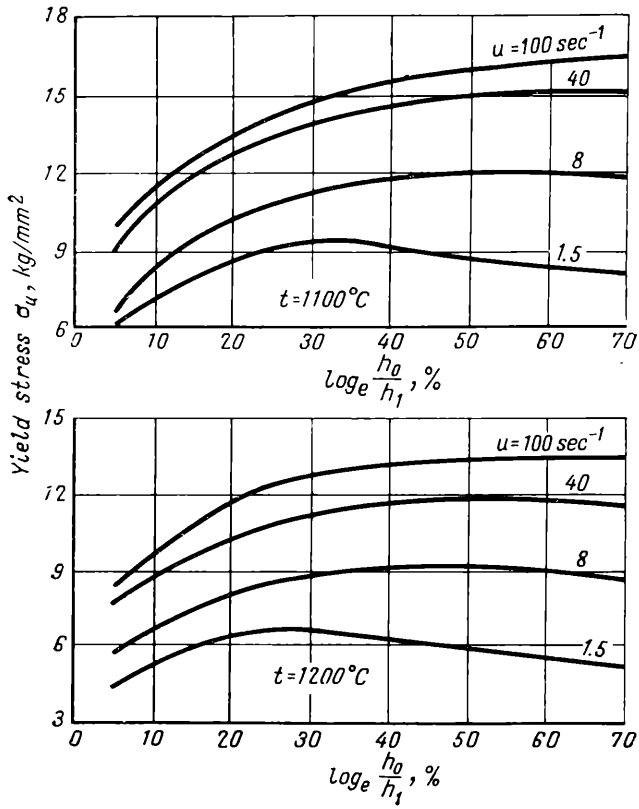

▲

◀ **Fig. 123.** Variation of the yield stress with reduction of a low carbon steel with 0.15% C (see Table 6) at various strain rates and temperatures (P. Cook)

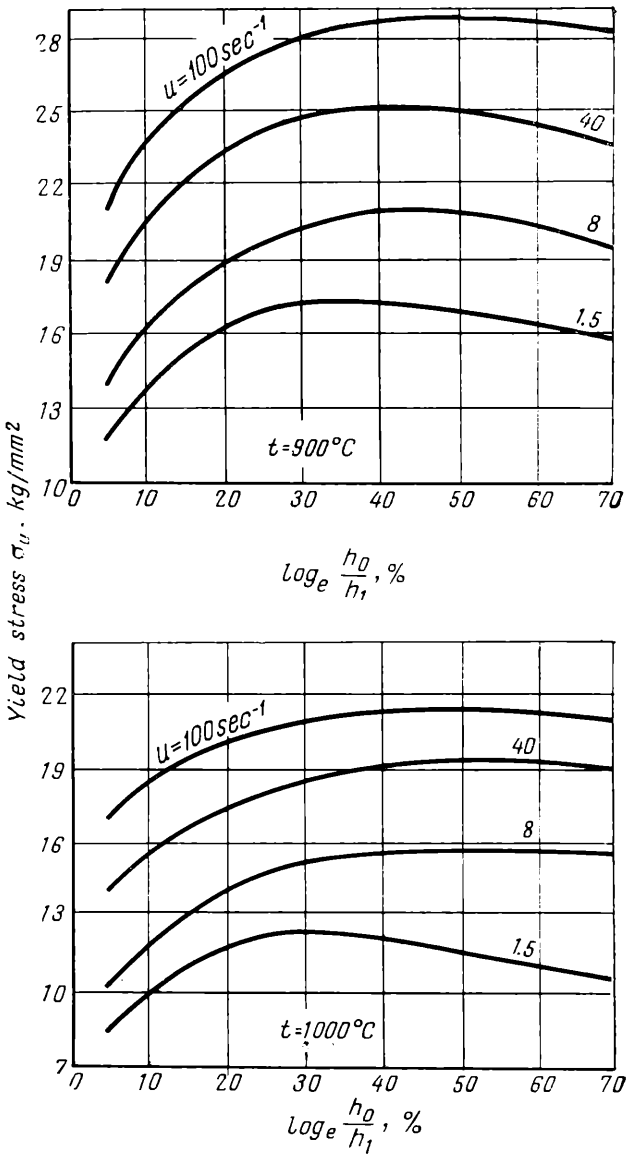
Yield stress σ_u, kg/mm²
28
25
22
19
16
13
10
0
10
20
30
40
50
60
70
$u=100\,sec^{-1}$
40
8
1.5
t=900°C
$\log_e \frac{h_0}{h_1}$, %
22
19
16
13
10
7
$u=100\,sec^{-1}$
40
8
1.5
t=1000°C
$\log_e \frac{h_0}{h_1}$, %

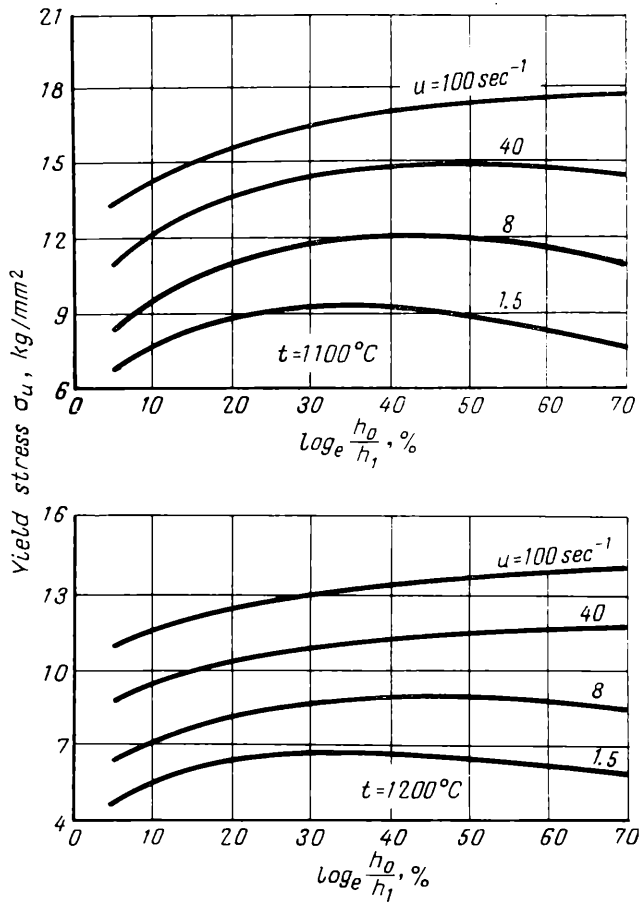

▲

◀ Fig. 124. Variation of the yield stress with reduction of a medium carbon steel with 0.56% C (see Table 6) at various strain rates and temperatures (P. Cook)

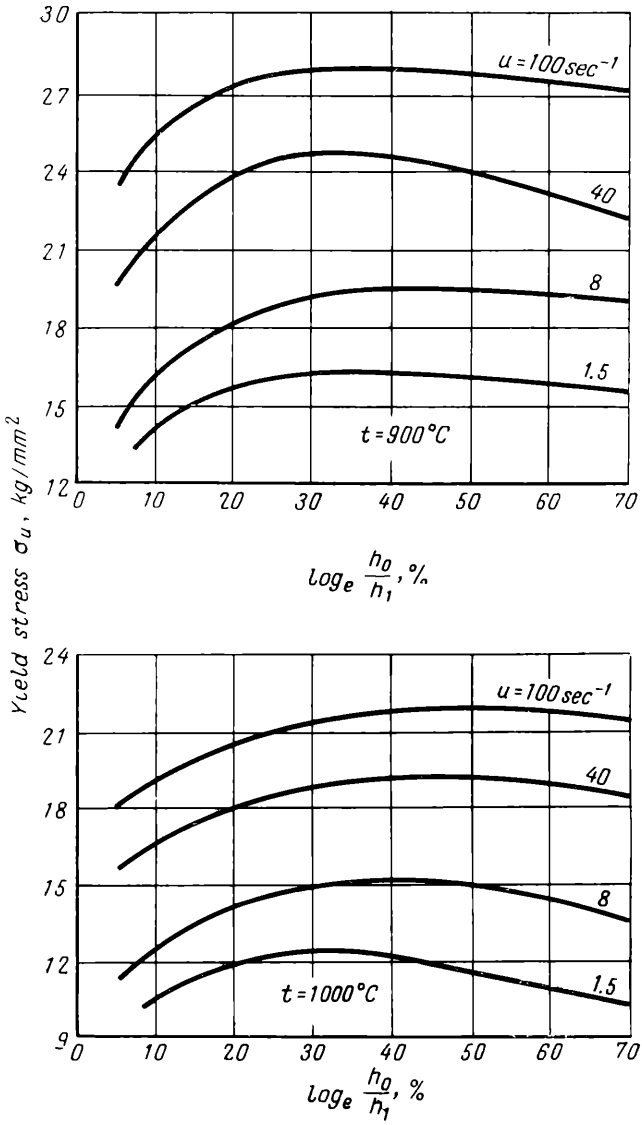
30
27
24
21
18
15
12
0
10
20
30
40
50
60
70
$u = 100\,sec^{-1}$
40
8
1.5
$t = 900°C$
Yield stress σ_u, kg/mm^2
$\log_e \frac{h_0}{h_1}$, %
24
21
18
15
12
9
0
10
20
30
40
50
60
70
$u = 100\,sec^{-1}$
40
8
1.5
$t = 1000°C$
$\log_e \frac{h_0}{h_1}$, %

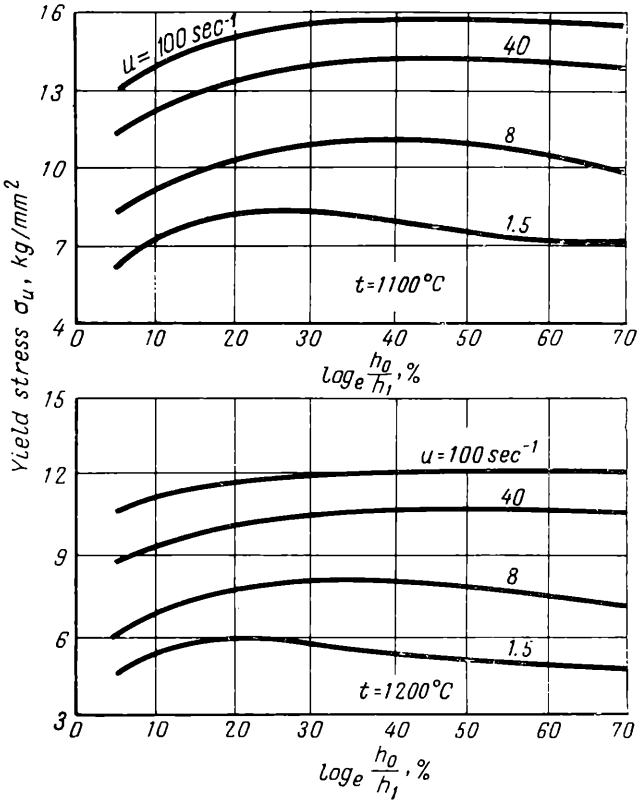

▲

◀ Fig. 125. Variation of the yield stress with reduction of a high carbon steel with 1.0% C (see Table 6) at various strain rates and temperatures (P. Cook)

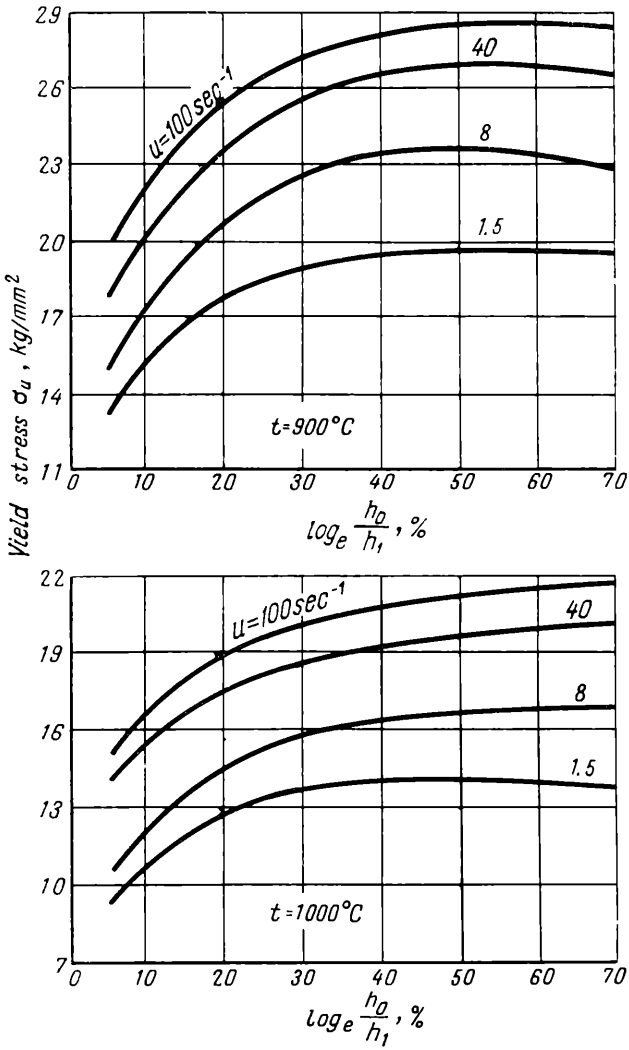
Yield stress σ_u, kg/mm²
29
26
23
20
17
14
11
0
10
20
30
40
50
60
70
u=100 sec⁻¹
40
8
1.5
t=900°C
$\log_e \frac{h_0}{h_1}$, %
22
19
16
13
10
7
u=100 sec⁻¹
40
8
1.5
t=1000°C
$\log_e \frac{h_0}{h_1}$, %

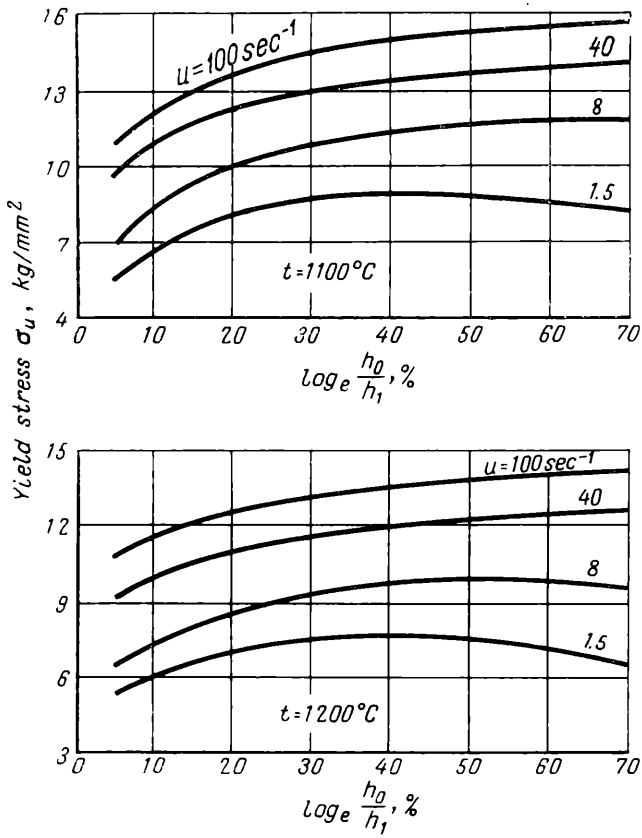

Fig. 126. Variation of the yield stress of a molybdenum-manganese steel (see Table 6) with reduction at various strain rates and temperatures (P. Cook)

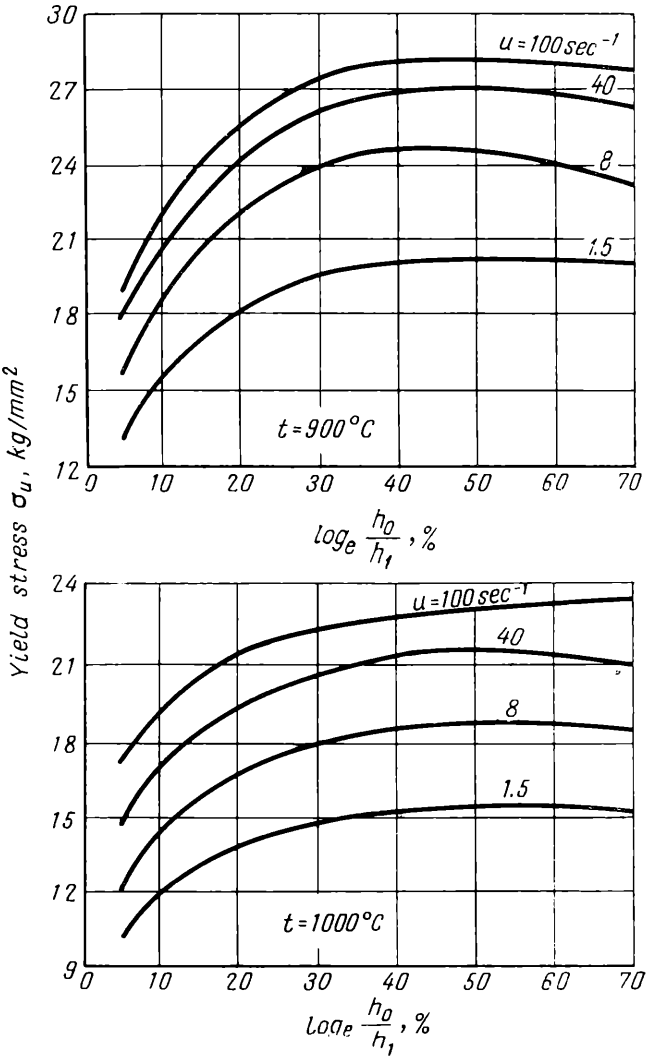
Yield stress σ_u, kg/mm²
30
27
24
21
18
15
12
0
10
20
30
40
50
60
70
$u = 100\,sec^{-1}$
40
8
1.5
$t = 900°C$
$\log_e \frac{h_0}{h_1}$, %
24
21
18
15
12
9
$u = 100\,sec^{-1}$
40
8
1.5
$t = 1000°C$
$\log_e \frac{h_0}{h_1}$, %

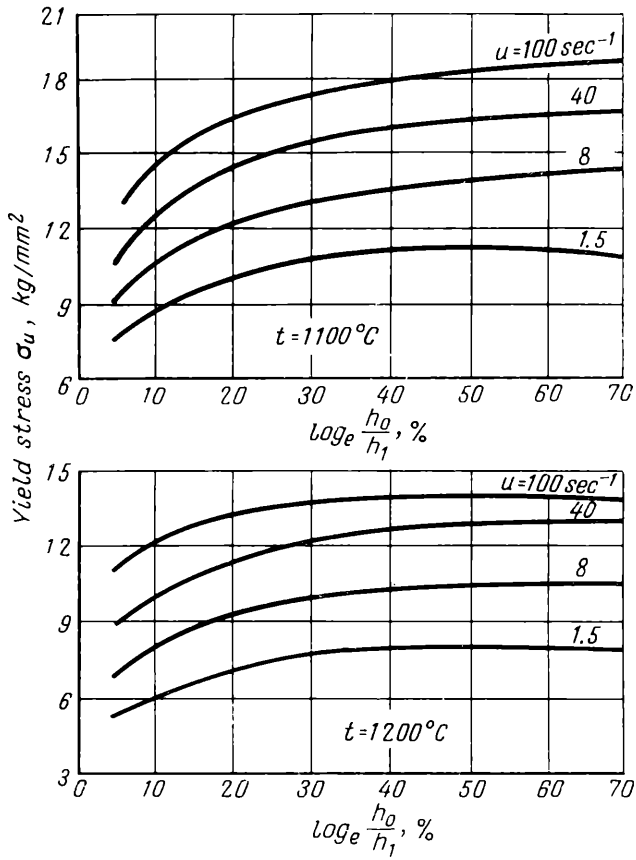

▲

◀ Fig. 127. Variation of the yield stress of a chrome-nickel-molybdenum steel (see Table 6) with reduction at various strain rates and temperatures (P. Cook)

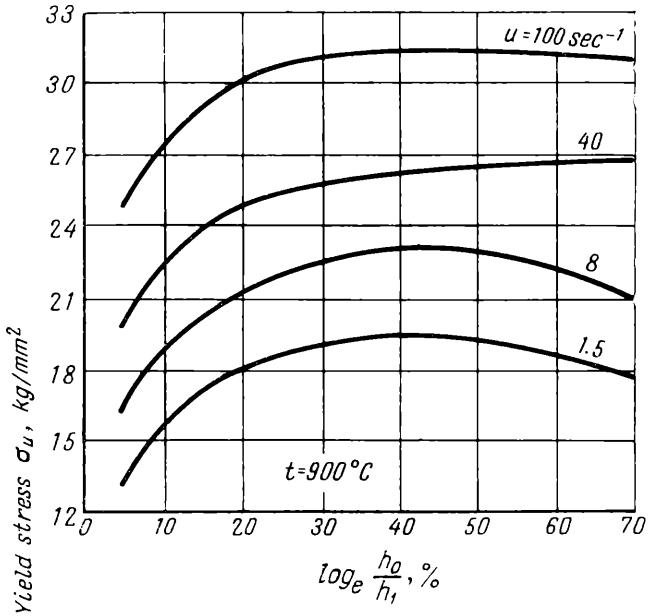
33
30
27
24
21
18
15
12
0
10
20
30
40
50
60
70
u = 100 sec⁻¹
40
8
1.5
t = 900 °C
Yield stress σu, kg/mm²
log_e h0/h1, %

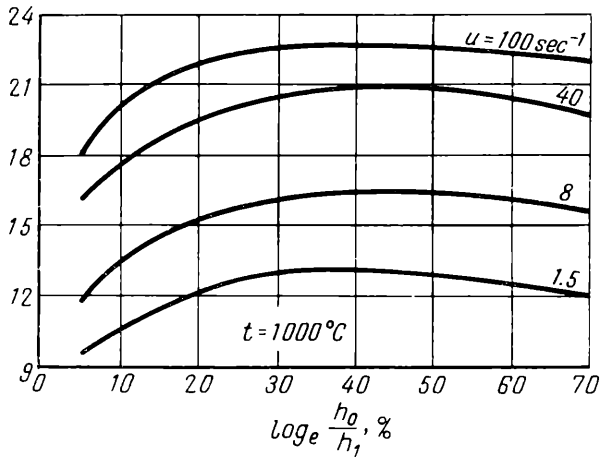
24
21
18
15
12
9
0
10
20
30
40
50
60
70
u = 100 sec⁻¹
40
8
1.5
t = 1000 °C
log_e h0/h1, %

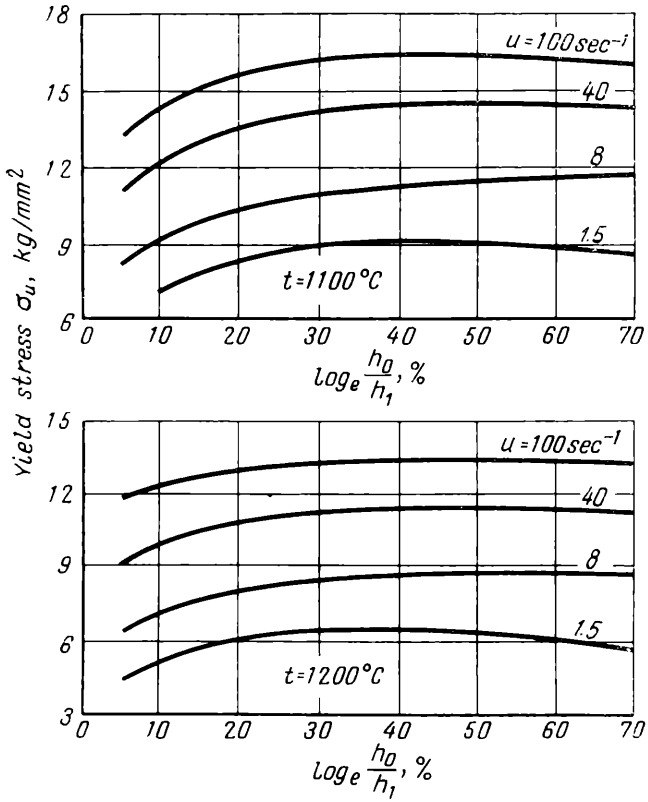

▲

◀ Fig. 128. Variation of the yield stress of a chrome steel with 0.41% Cr (see Table 6) with reduction at various strain rates and temperatures (P. Cook)

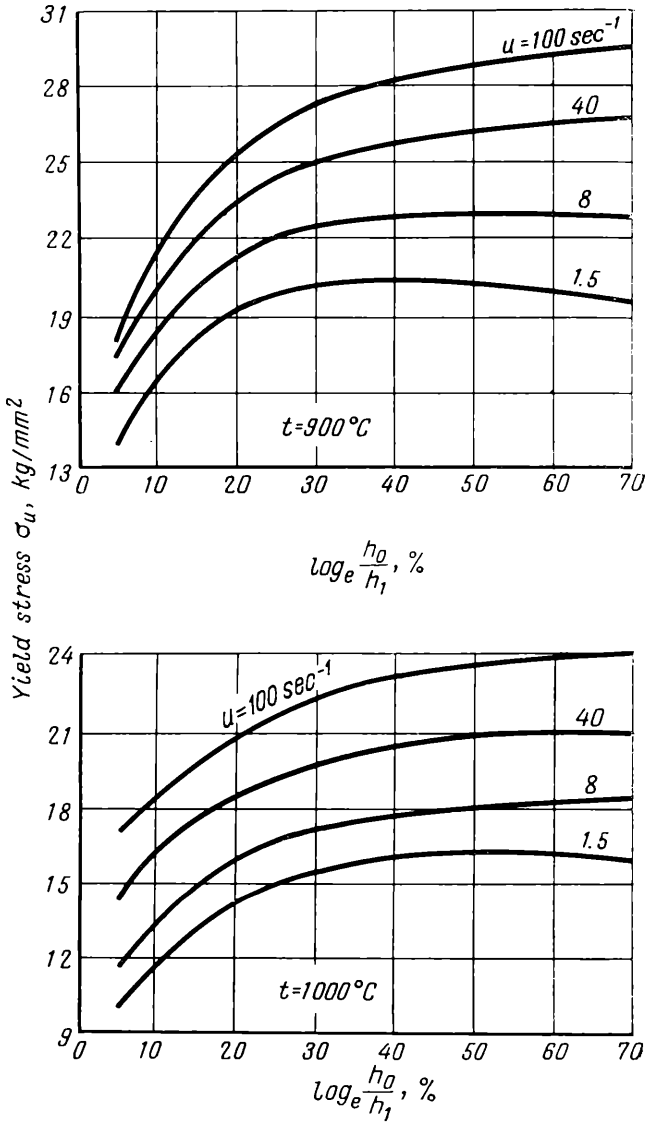
31
28
25
22
19
16
13
0
10
20
30
40
50
60
70
u = 100 sec⁻¹
40
8
1.5
t=900°C
Yield stress σu, kg/mm²
log_e h0/h1, %
24
21
18
15
12
9
u=100 sec⁻¹
40
8
1.5
t=1000°C
log_e h0/h1, %

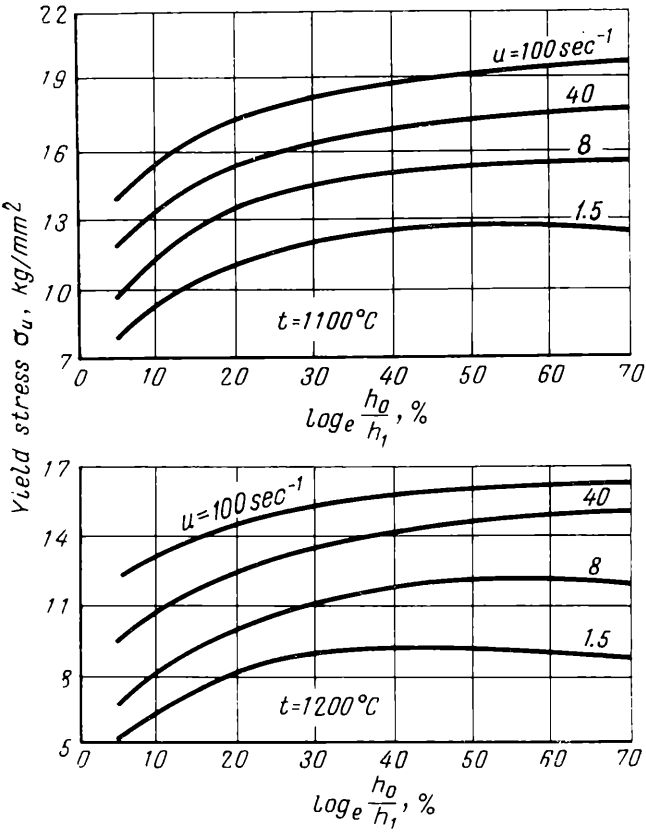

▲

◀ Fig. 129. Variation of the yield stress of a chrome-molybdenum steel (see Table 6) with reduction at various strain rates and temperatures (P. Cook)

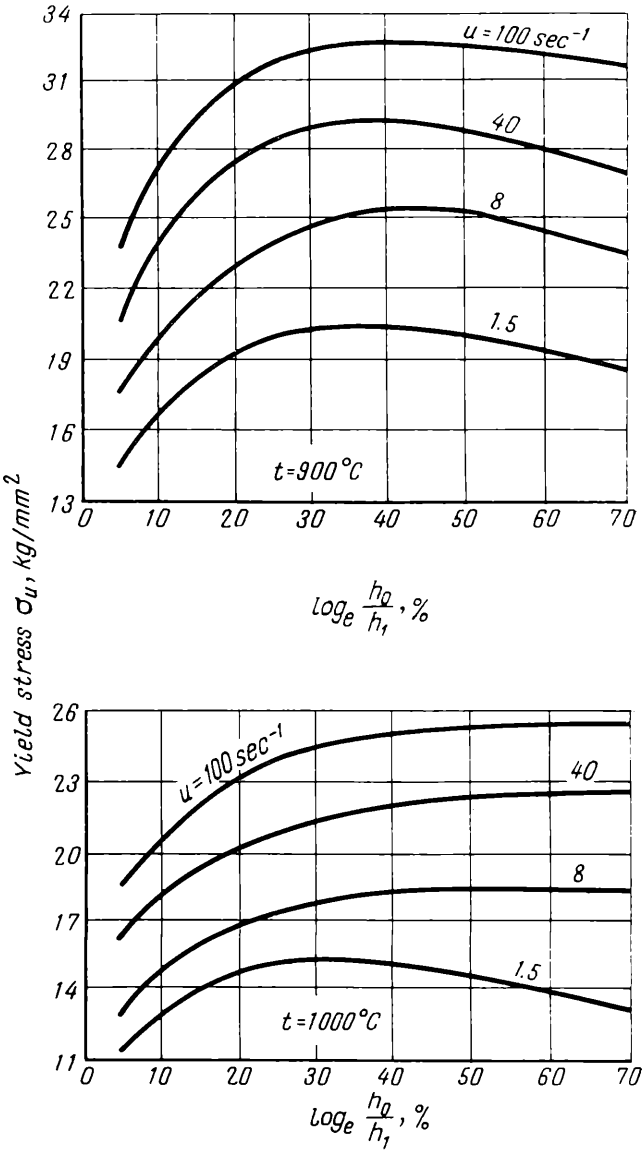
34
31
28
25
22
19
16
13
0
10
20
30
40
50
60
70
u = 100 sec⁻¹
40
8
1.5
t=900°C
Yield stress σu, kg/mm²
log_e h0/h1, %
26
23
20
17
14
11
u=100 sec⁻¹
40
8
1.5
t=1000°C
log_e h0/h1, %

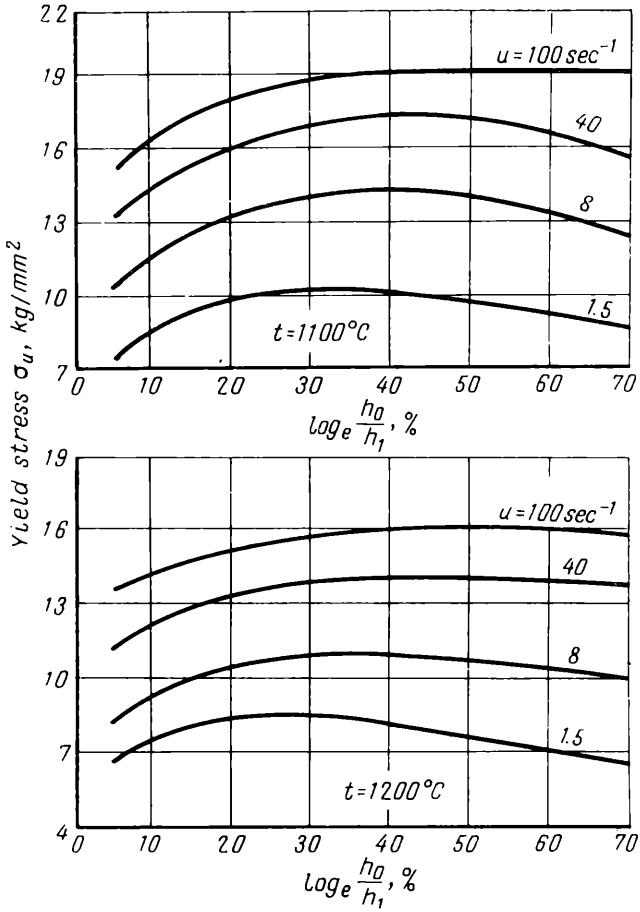

▲

◀ **Fig. 130.** Variation of the yield stress of a silico-manganese steel (see Table 6) with reduction at various strain rates and temperatures (P. Cook)

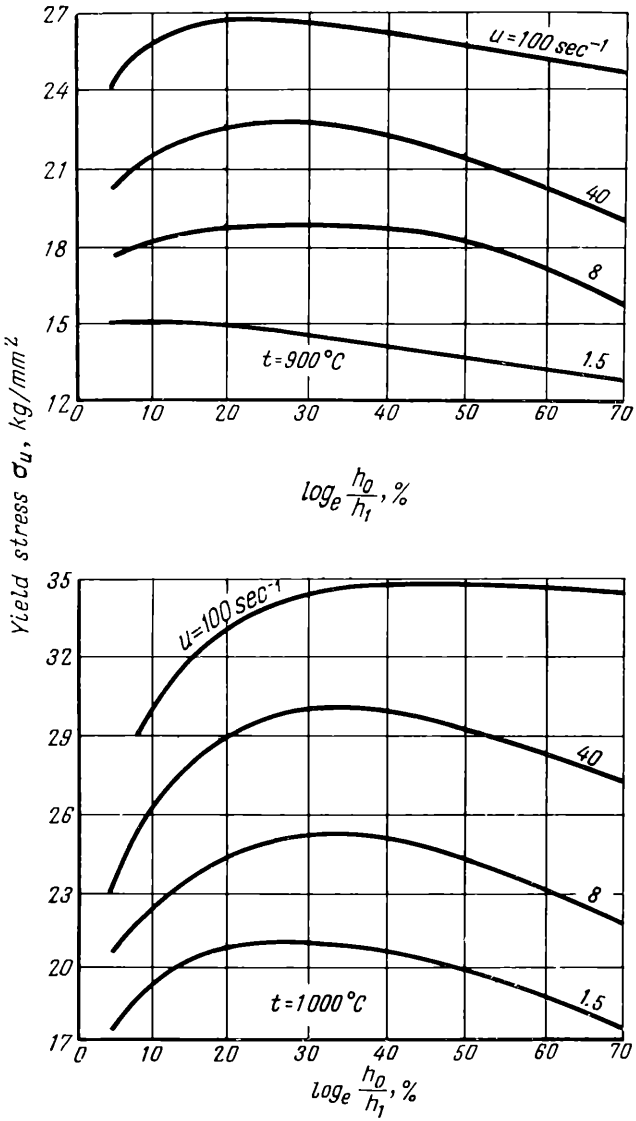
Yield stress σ_u, kg/mm²
27
24
21
18
15
12
0
10
20
30
40
50
60
70
u=100 sec⁻¹
40
8
1.5
t=900°C
$\log_e \frac{h_0}{h_1}$, %
35
32
29
26
23
20
17
u=100 sec⁻¹
40
8
1.5
t=1000°C
$\log_e \frac{h_0}{h_1}$, %

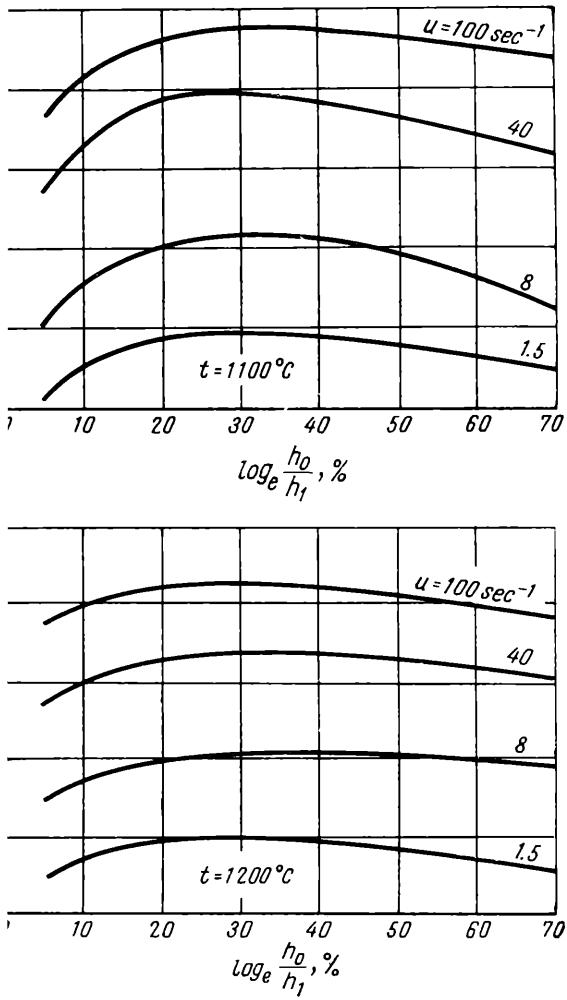

. Variation of the yield stress of a silico-chrome
e Table 6) with reduction at various strain rates
peratures (P. Cook)

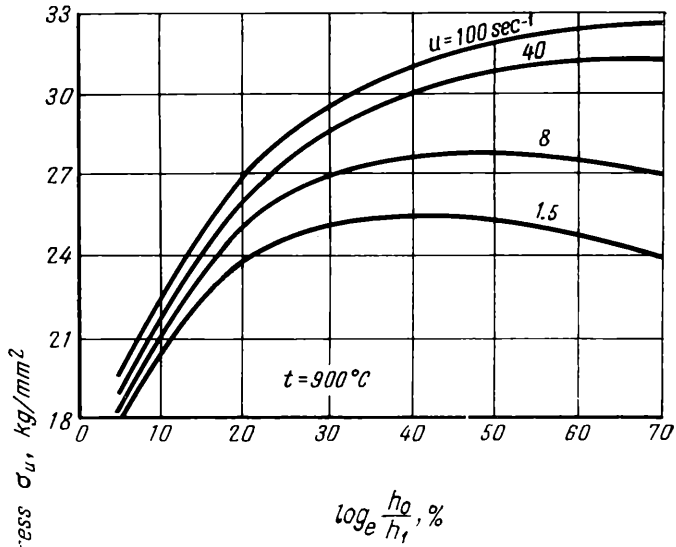
33
30
27
24
21
18
0
10
20
30
40
50
60
70
u = 100 sec⁻¹
40
8
1.5
t = 900 °C
Yield stress σu, kg/mm²
log_e h0/h1, %

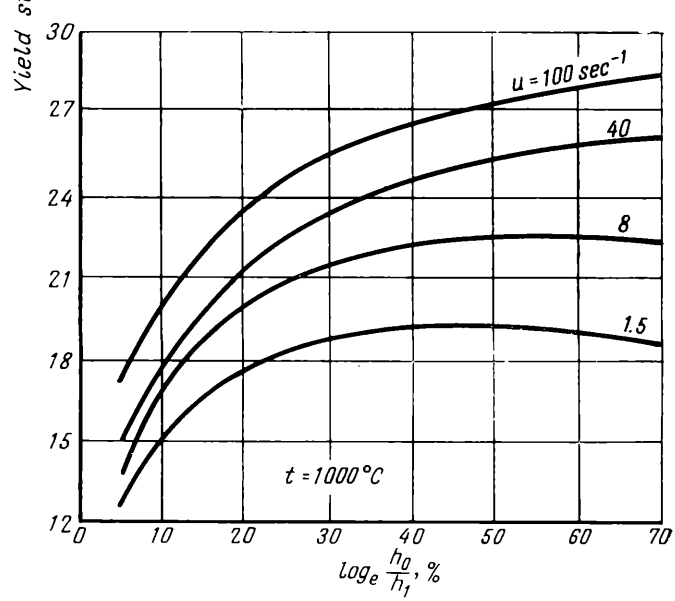
30
27
24
21
18
15
12
0
10
20
30
40
50
60
70
u = 100 sec⁻¹
40
8
1.5
t = 1000 °C
log_e h0/h1, %

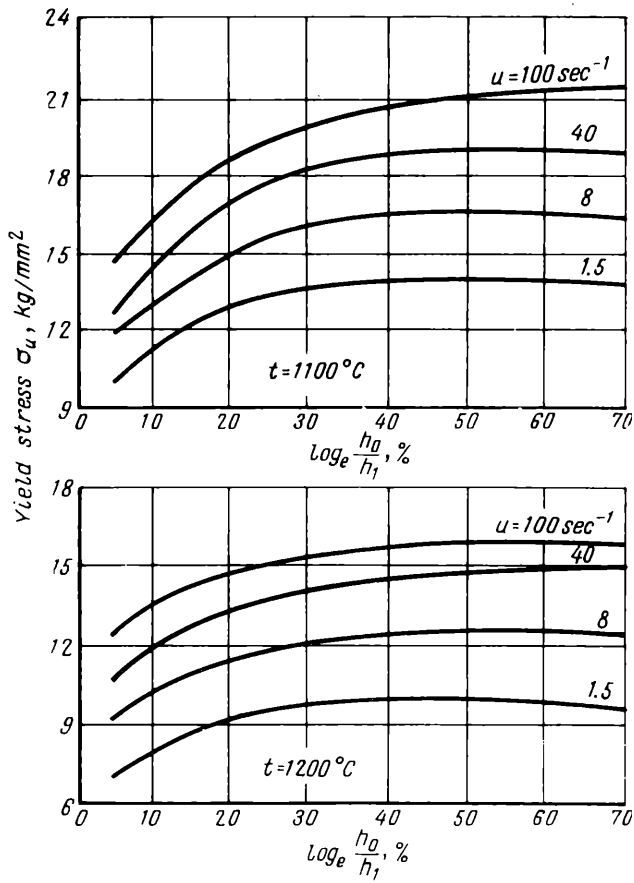

▲

◀ Fig. 132. Variation of the yield stress of an 18-8 stainless steel (see Table 6) with reduction at various strain rates and temperatures (P. Cook)

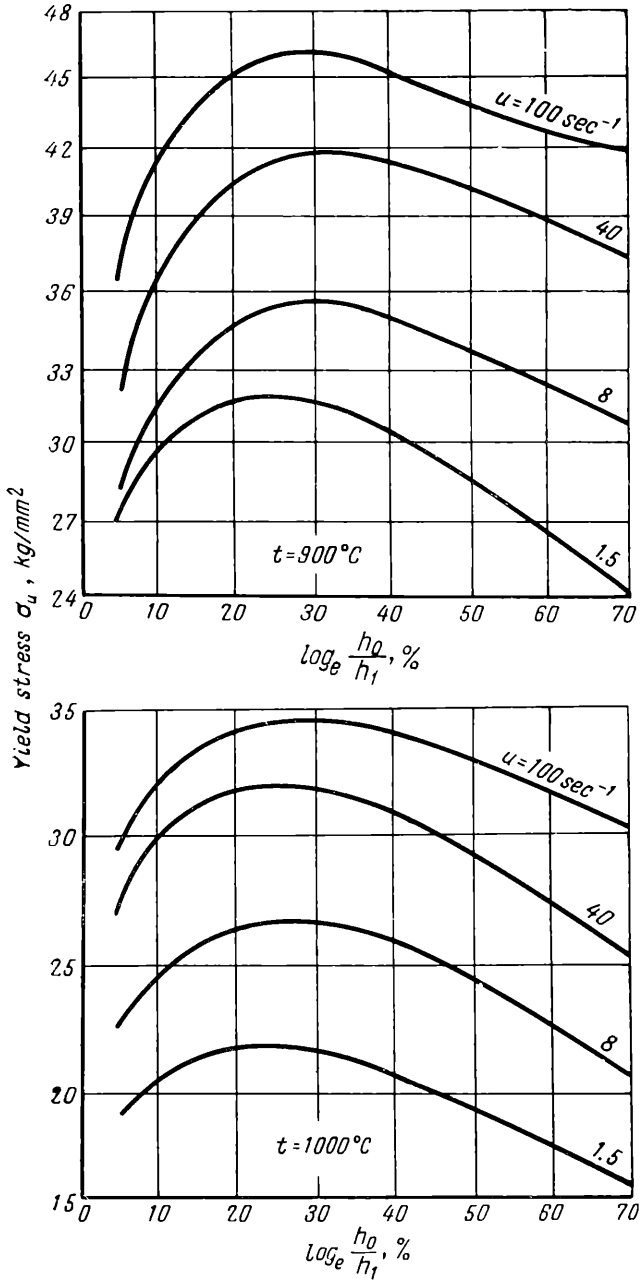
Yield stress σ_u, kg/mm^2
48
45
42
39
36
33
30
27
24
0
10
20
30
40
50
60
70
$\log_e \frac{h_0}{h_1}$, %
u = 100 sec^{-1}
40
8
1.5
t = 900°C
35
30
25
20
15
t = 1000°C

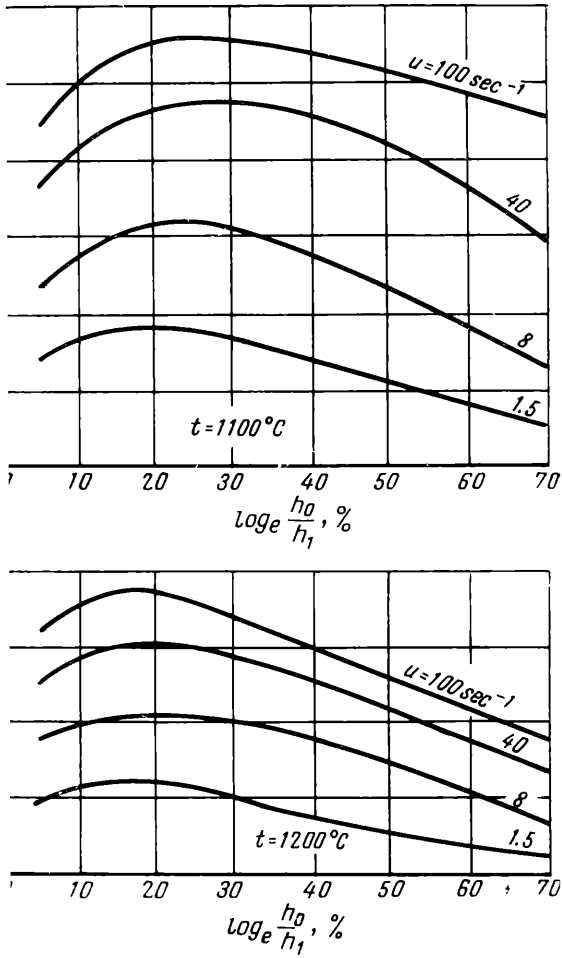

3. Variation of the yield stress of a high chrome th 13% Cr (see Table 6) with reduction at various ates and temperatures (P. Cook)

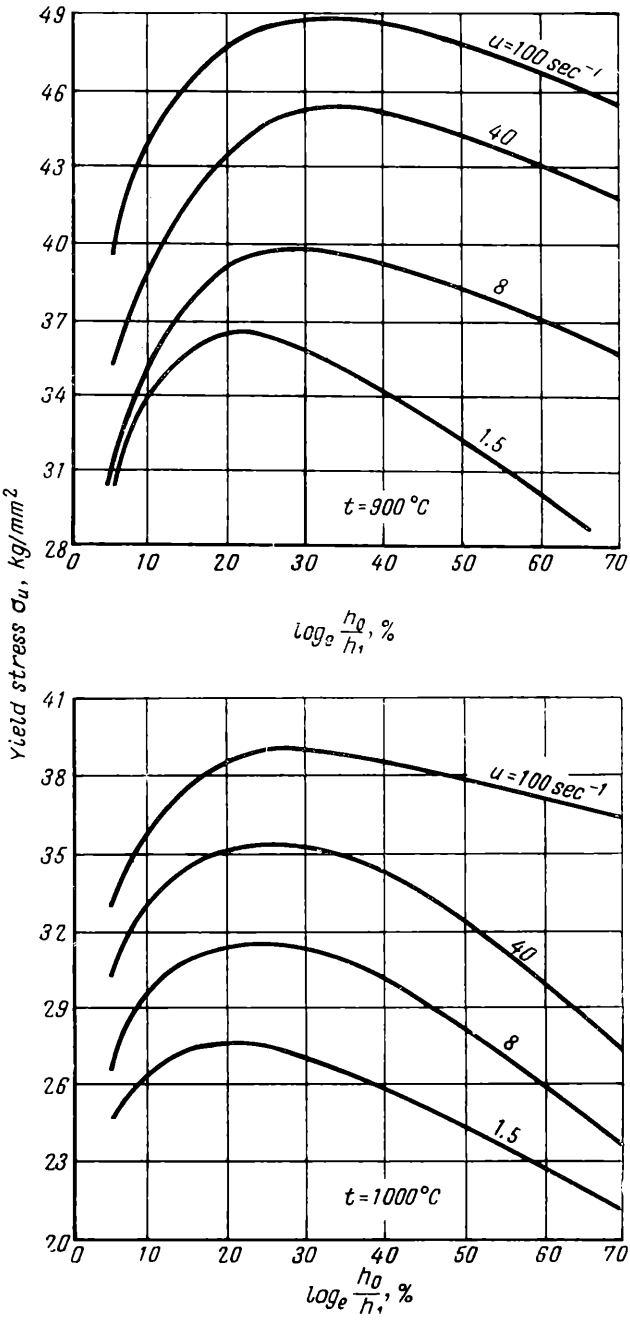
49
46
43
40
37
34
31
28
0
10
20
30
40
50
60
70
u=100 sec⁻¹
40
8
1.5
t=900°C
Yield stress σu, kg/mm²
log_e h0/h1, %
41
38
35
32
29
26
23
20
u=100 sec⁻¹
40
8
1.5
t=1000°C
log_e h0/h1, %

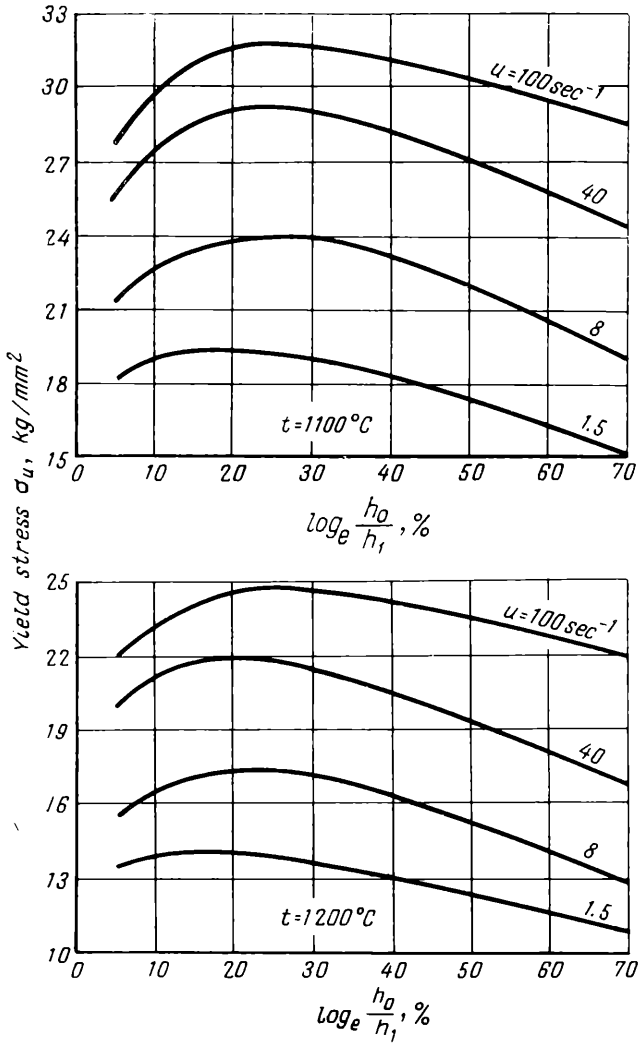

▲

◀ Fig. 134. Variation of the yield stress of an 18-4-1 high speed steel (see Table 6) with reduction at various strain rates and temperatures (P. Cook)

and the platens of the plastometer to be held to a minimum. The strain rate $u = \frac{d\varepsilon}{dt}$ during the tests was 1.5; 8; 40 and 100 sec^{-1}, whilst the temperature was 900; 1,000; 1,100 and 1,200°C. The results of these tests have been presented in the form of diagrams (Figs. 123 to 134) which show the variation of the yield stress with the degree of deformation.

The chemical composition of the steels in question is given in Table 6.

Table 6

Chemical Composition of Steel (for Figs. 123 to 134) (After P. Cook)

Steel	Composition, %									
	C	Si	Mn	S	P	Cr	Ni	Mo	W	V
Low carbon	0.15	0.12	0.68	0.034	0.025	—	—	—	—	—
Medium carbon	0.56	0.26	0.28	0.014	0.013	0.12	0.09	—	—	—
High carbon	1.00	0.19	0.17	0.027	0.023	0.10	0.09	—	—	—
Molybdenum-manganese	0.35	0.27	1.49	0.041	0.037	0.03	0.11	0.28	—	—
Chrome-nickel-molybdenum	0.35	0.27	0.66	0.023	0.029	0.59	2.45	0.59	—	—
Chrome	0.06	0.22	0.46	0.019	0.031	0.41	0.17	—	—	—
Chrome-molybdenum	0.26	0.35	0.57	0.009	0.023	3.03	0.29	0.49	—	—
Silico-manganese	0.61	1.58	0.94	0.038	0.035	0.12	0.27	0.06	—	—
Silico-chrome	0.47	3.74	0.58	—	—	8.20	0.20	—	—	—
Stainless 18-8	0.07	0.43	0.48	—	—	18.60	7.70	—	—	—
High chrome (13% Cr; 2.25% C)	2.23	0.43	0.37	—	—	13.10	0.33	—	—	—
High speed 18-4-1	0.80	0.28	0.32	—	—	4.30	0.18	0.55	18.40	1.54

Analyzing the diagrams (Figs. 123 to 134) we notice that in the case of small strains (on average up to 20-30%) the yield stress strongly increases as the strain increases. For medium strains (more than 30%) the rate of increase in the yield stress is reduced, and in a number of cases the yield stress decreases when the strain is increased still further. If the results of these tests are represented in the form of a diagram, with the strain rate on a logarithmic scale along the abscissa and the yield stress on the ordinate with the same scale, then the dependence of the yield stress on the strain rate is expressed by a straight line (Fig. 135).

The results of the investigation into the effect of strain rate on the yield stress carried out by A. Dinnik are also of great interest; he investigated this effect for 15 grades of steel. In the same way as in the tests by P. Cook the test pieces were compressed at a rate

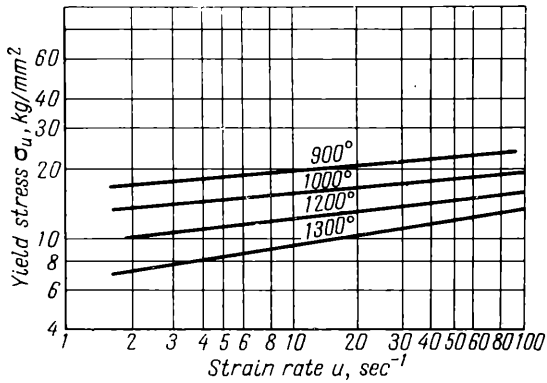

Fig. 135. Variation of the yield stress of a mild steel with 0.15% C (see Table 6) with the strain rate when $\log_e \frac{h_0}{h_1} = 0.3$ for various temperatures (P. Cook)

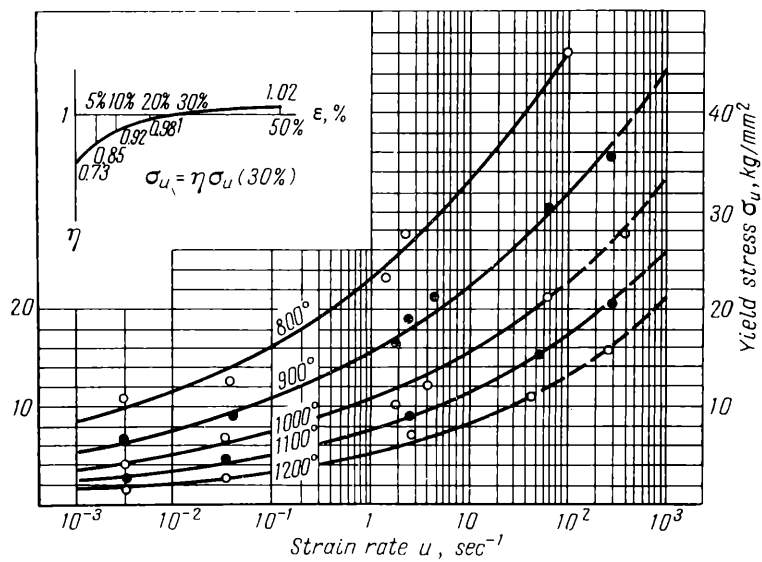

Fig. 136. Variation of the yield stress of ball bearing steel ШХ15 (1.0% C; 0.31% Mn; 0.24% Si; 1.54% Cr; 0.1% Cu; 0.018% S and 0.017% P) with the strain rate at various temperatures for a reduction of 0.3. See the upper part of the diagram for the value of the correction factor corresponding to the reduction (A. Dinnik)

u = (2 to 41) sec^{-1} in a mechanical press, and at a rate u = (40 to 100) sec^{-1} in a drop hammer of the Amsler type. From the results of these tests he constructed diagrams one of which is shown in Fig. 136. The tests by A. Dinnik also showed that the effect of strain rate on the yield stress strongly depends on the reduction; in contrast to P. Cook's results, all his tests showed an increase in the yield stress as the strain rate increased. The way the yield stress varied with the reduction is represented in the form of an additional diagram in the top left-hand portion of Fig. 136, giving the value of the correction factor η.

The yield stress σ_u for different reductions is then given by

$$\sigma_u = \eta \sigma_{u30}$$

where σ_{u30} is the yield stress for 30% reduction determined from the main diagram (see Fig. 136).

I. Tarnovsky and others have investigated the resistance of metal to deformation by extending and compressing of cylindrical test pieces made of steel of 16 grades, as a function of deformation at four different velocities and at different temperatures (800 to 1,200°C).

The tension tests were carried out at rates of ~0.007 and 0.05 sec^{-1} in an experimental press, where also the compression tests were carried out at a rate of 0.05 sec^{-1}. Compression at a rate of 7.5 sec^{-1} was carried out in a friction press, whilst a drop hammer was used for a rate of ~150 sec^{-1}. For all steels investigated a considerable increase in the resistance to deformation was established for increased velocities both at small and large strains (confirming observations of previous investigators). It was also pointed out that, when the velocity was increased, the increase in the resistance to deformation was greater for large reductions than for small reductions.

8. DETERMINATION OF THE RESISTANCE TO LINEAR DEFORMATION, TAKING INTO ACCOUNT TEMPERATURE, WORK HARDENING AND VELOCITY

During cold rolling the resistance to linear deformation, σ_a, depends mainly on work hardening. The temperature and strain rate have a slight effect on σ_a, and in practice the coefficients n_t and n_v in equation (III.2), allowing for the temperature and velocity, may be taken as $n_t \approx 1$ and $n_v \approx 1$.

At the same time it should be noted that in the case of high reductions a slight increase occurs in the resistance to deformation as the velocity is increased. These results, however, refer to small veloci-

ties; at high velocities, as shown by the tests of N. Druzhinin and V. Khotulev (see Fig. 119), the velocity has an insignificant effect on the resistance to deformation.

Then for cold rolling equation (III.2) assumes the following form:

$$\sigma_a = n_{wh}\sigma_s = \frac{\sigma_{s0} + \sigma_{s1}}{2\sigma_s}\sigma_s \qquad \text{(III.39)}$$

where σ_{s0} and σ_{s1} are the yield stresses before and after the rolling process.

During hot rolling the resistance to linear deformation depends mainly on the temperature and velocity. Work hardening or strain affects the resistance to deformation alongside the velocity, and accordingly this effect is more conveniently taken into account by the appropriate value of the velocity coefficient n_v. Owing to this, equation (III.2) in the case of hot rolling assumes the following form:

$$\sigma_a = n_t n_v \sigma_s \qquad \text{(III.40)}$$

For determining the coefficients n_t and n_v three basic methods may be recommended.

The first method should be used for the rolling of those metals for which data exist concerning the effect of velocity on the yield stress and deformation at hot working temperatures. Then the values of these coefficients can be obtained from the diagrams constructed from the test data (see Figs. 123 to 136). Since the effect of velocity on the resistance to strain depends on the temperature, then from these diagrams we find not the value of each of the above-mentioned coefficients, but the value of their product:

$$\sigma_a = n_t n_v \sigma_s = \sigma_u \qquad \text{(III.41)}$$

where σ_u is the yield stress obtainable from the diagrams (see Figs. 123 to 136) or from the data of other experimental investigations for the given rolling conditions: strain rate, temperature and reduction. The quantity σ_u refers to the resistance to linear deformation at the beginning and the end of the arc of contact. Accordingly for the strain rate, temperature and reduction we must also take mean values over the arc of contact.

The corresponding strain rate must be calculated from equation (III.29), whilst for the determination of the mean reduction the following method may be used.

The relative reduction in any section of the deformation zone is

$$\varepsilon_x = \frac{h_0 - h_x}{h_0} \qquad \text{(III.42)}$$

The mean value of the relative reduction may be determined as its mean value over the length l, where l is the horizontal projection

of the arc of contact (see Fig. 115):

$$\varepsilon_m = \frac{1}{l} \int_0^l \frac{h_0 - h_x}{h_0} \, dx \tag{III.43}$$

The quantity h_x appearing in this equation can be expressed as:

$$h_x = h_1 + \frac{\Delta h}{l^2} x^2$$

Then

$$\varepsilon_m = \frac{\Delta h}{l h_0} \int_0^l \left(1 - \frac{x^2}{l^2}\right) dx \tag{III.44}$$

or

$$\varepsilon_m = \frac{2}{3} \frac{\Delta h}{h_0} \tag{III.45}$$

When the curves of Figs. 123 to 135 are used, the mean reduction found from this equation must subsequently be recalculated as the mean strain, i.e., as the strain expressed as a natural logarithm:

$$\left(\log_e \frac{h_0}{h_1}\right)_m \approx \log_e \frac{1}{1 - \frac{2}{3} \frac{\Delta h}{h_0}} \tag{III.46}$$

The second method of determining the coefficients in equation (III.40) is less accurate. It can be recommended in the case where the appropriate curve, i.e., a curve of the type shown in Figs. 123 to 136, is missing for the metal in question or the given conditions of rolling, and only data are available concerning the effect of velocity on the resistance to deformation without the effect of the reduction being taken into account, i.e., curves of the type shown in Figs. 121 and 122.

In this case a correction, accounting for the effect of the mean reduction on the resistance to linear deformation, is introduced into the product $n_t n_v$ found from the curves mentioned above. It should be noted that, as follows from the relevant experimental data, the effect of the reduction on the yield stress is comparatively small. In particular, V. Valorinta, comparing the resistance to deformation of certain steels (stainless steel X18H9, valve steel 3X14H14B2M and carbon steel 35) at different strain rates (from 0.01 to 0.1 sec^{-1}), arrived at the conclusion that a variation in the reduction from 0.25 to 0.9 influences the deviation of the mean value of the resistance to deformation by not more than 10% when $\varepsilon = 0.35$ (Fig. 137).

An analysis of the curves obtained by P. Cook (see Figs. 123 to 135) and A. Dinnik confirms that for the majority of steels the reduction affects the yield stress most when it varies from 0.15

to 0.2%. In particular, according to the data of A. Dinnik, when the reduction varies from 0.2 to 0.5% the yield stress of the steels investigated by him increases from 4 to 9%, whilst for a variation of the reduction from 5 to 20% the yield stress increases from 13 to 32%. Hence we may conclude that if data are available concerning the effect of velocity on the resistance to deformation for a given reduction, then it will not lead to large errors if these data are used for another reduction with a small correction for the difference. For

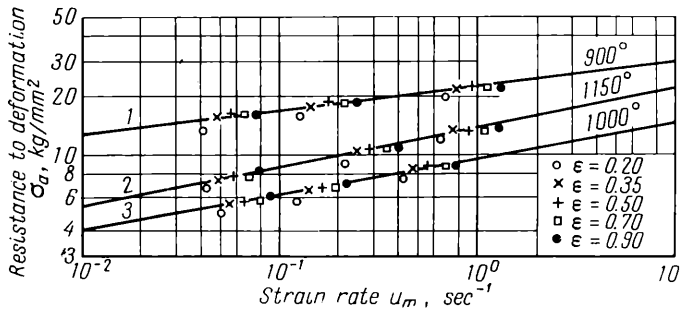

Fig. 137. Variation of the resistance to deformation of steels of the grades X18H9 (*1*), 3X14H14B2M (*2*) and 35 (*3*) with velocity at various temperatures and reductions; the reductions are shown at the bottom right

reductions exceeding 20 to 30% this correction must be expressed by a coefficient exceeding unity ($\eta = 1.05$ to 1.1), whilst for reductions less than 20 to 30% a coefficient approximately equal to 0.7 to 0.85 should be used. If the data concerning the effect of velocity on the yield stress are obtained by tensile tests (see Figs. 121 and 122) then, as was mentioned above, the calculated value of σ_a for steel must be increased by 10%.

The third method may be recommended for approximate determination of σ_a only. It must sometimes be resorted to when the metal pressure on the rolls has to be calculated for the rolling of a metal for which there are no test results available concerning the effect of velocity on the resistance to deformation.

In this case both the coefficients in equation (III.40) must be determined separately. The coefficient n_t is found from the equation

$$(\sigma_s)_t = n_t \sigma_s$$

where $(\sigma_s)_t$ is the yield stress of the metal in question, determined from the curves (see Figs. 91 to 102) or from the results of other tests.

The coefficient n_v is determined approximately, following the test results on the effect of velocity on the resistance to deformation of a metal which is closest to the given metal in its properties, but for which test results are available, i.e.,

$$n_v = \frac{(\sigma_s)_u}{(\sigma_s)_0}$$

where $(\sigma_s)_u$ is the yield stress at the given velocity, temperature and reduction

$(\sigma_s)_0$ is the yield stress in static tests at the given temperature.

9. BASIC SPECIFIC PRESSURE

The calculation of the forces acting on the rolls may not be based on the quantity σ_a, found by testing the metals under conditions of tension or compression, but directly on the quantity k which is obtained by measuring the contact normal stresses during rolling.

This method of determining the quantity k was suggested by A. Tselikov and was worked out by V. Pushkarev.

The distinctive feature of this method is that for the initial characteristic of the true resistance to deformation of the metal it uses, instead of the yield stress or σ_a, the mean specific pressure p_0 during the rolling of standard test pieces under standard conditions.

The conditions of two-dimensional strain are taken as the standard conditions; they exclude the effect of spreading, whereby the effect of the longitudinal stresses on the resistance to deformation is, as far as possible, reduced to a minimum. These conditions are to a considerable extent fulfilled by the rolling of test pieces of rectangular cross section, when

$$b_m \approx 5\sqrt{r\Delta h} \text{ and } h_m \approx \sqrt{r\Delta h}$$

Owing to the fact that the ratio of the length of the arc of contact to the mean depth of the cross section of the test piece is unity, the effect of external friction and outer zones is reduced to a minimum, and accordingly we may assume that $p_0 \approx 2k$.

Tests for determining p_0 for different metals and temperatures have been carried out on a duo mill with rolls with a diameter of 174 mm. To comply with the above rolling conditions, test pieces with the dimensions $h_0 = 12$ mm and $b_0 = 50$ mm were rolled with the reduction $\frac{\Delta h}{h_0} = 0.1$ to 0.13 or $\log_e \frac{h_0}{h_1} \approx 0.1$ to 0.14 ($\Delta h = 1.46$ mm). The strain rate is $u_m = 5.8$ to 6.4 sec^{-1}.

The results of the investigation into the basic specific pressure for different steels and temperatures, carried out by V. Pushkarev, are given in Table 7.

Table 7

Basic Specific Pressure in Rolling Steel of Various Grades at Different Temperatures

Grade of steel	Basic specific pressure, kg/mm², at temperatures, °C										
	20	200	400	500	600	700	800	900	1,000	1,100	1,200
30	80.9	64.4	70.8	78.6	59	39.7	27.7	23.1	18.2	11.2	8.8
30ХГСА	66.4	55.1	61.2	68.5	47	33.9	22.2	19.6	15.5	13.5	9.6
45	108.6	84.7	89.4	96.8	73.7	48.8	35.9	27.2	18	11.4	8.3
50	142.3	112	107	104.5	76.6	50	32.3	23.9	18	11.5	8.2
65Г	157.5	126.7	112.4	107.9	86.0	60.6	35.6	22.4	19.0	12.5	8.3
У9	—	—	145.8	128.0	98.5	67.4	33.3	24.5	17.5	10.9	8.3

In determining the quantity k by this method the accuracy of the calculation is increased due to the fact that the yield stress does not always correctly characterize the true resistance to deformation. In addition, in this case it may be more accurate to take into account also the strain rate, since without doubt it is not equal for compression or tension and for rolling. Subsequently, when the method of the basic specific pressure is supplemented by experimental data concerning the effect of strain rate and reduction, this method becomes the most exact one.

If data are only available concerning the basic specific pressure for any single strain rate, the following method may be recommended for the determination of the quantity k.

For cold rolling, in analogy with equation (III.39),

$$k = \frac{p_0}{2} \times \frac{\sigma_{s0} + \sigma_{s1}}{2\sigma_{s12}} \qquad \text{(III.47)}$$

where p_0 is the basic specific pressure (for $\frac{\Delta h}{h_0} \approx 0.12$)

σ_{s0} and σ_{s1} are the yield stresses before and after rolling

σ_{s12} is the yield stress (for $\frac{\Delta h}{h_0} = 0.12$).

For hot rolling

$$k = \frac{p_0}{2} \times \frac{\sigma_{u\Sigma}}{\sigma_{012}} \qquad \text{(III.48)}$$

where $\sigma_{u\Sigma}$ is the yield stress at the given strain rate and the given reduction Σ

σ_{012} is the yield stress when the rate and amount of the strain are the same as during rolling when the pressure is p_0.

The values of these yield stresses are found from the curves shown in Figs. 123 to 136.

In the case where data are available only on the effect of velocity on the resistance to deformation without the effect of the reduction being taken into account (see Figs. 121 and 122), the following equation may be recommended for the determination of k:

$$k = \frac{p_0}{2} \times \frac{\sigma_u}{\sigma_0} \eta_{12} \qquad \text{(III.49)}$$

where σ_u and σ_0 are the yield stresses at the given strain rate and at the same amount of strain as during rolling when the pressure is p_0

η_{12} is a correction factor for the given reduction in relation to $\frac{\Delta h}{h_0} = 0.12$, at which p_0 was determined.

The value of this coefficient can be found approximately, by determining the same coefficient for a metal which, in composition and properties, is closest to the given one, and for which the curves shown in Figs. 123 to 136 are available.

IV

Direction of the Forces Acting on the Rolls During Rolling

1. DIRECTION OF THE FORCES DURING A SIMPLE ROLLING PROCESS

We shall first consider the most common case of rolling; no forces, with the exception of the forces applied by the rolls, act on the metal being rolled; the motion of the metal at the entry and exit is uniform; both rolls are driven and the rolling process is completely symmetrical with respect to both rolls, i.e., the rolls have the same peripheral velocities and diameters; and the metal is homogeneous as regards mechanical properties. This case is called *the simple rolling process.*

It follows from the laws given above concerning the distribution of the specific friction forces and pressure over the arc of contact that the elementary forces, applied by the roll to the metal being rolled, can be represented by three resultant forces: a force N acting normally to the roll surface, and two friction forces T_1 and T_2 directed tangentially in the opposing directions, one from the zone of backward slip, and the other from the zone of forward slip (Fig. 138).

Since the rolling process is symmetrical relative to both rolls, the interaction of the rolled metal with the other roll can be expressed in the form of three similar forces.

In accordance with the assumption, only the forces from the rolls are applied to the metal being rolled and its motion at entry and exit is uniform. That portion of the metal which is located in the geometrical zone of deformation, however, has an acceleration, the mean of which amounts to $j = \frac{v_1 - v_0}{\Delta t}$, where Δt is the time during which the metal is located in the geometrical zone of deformation. But the inertial forces caused by this phenomenon are very small in comparison with the metal pressure on the rolls and may

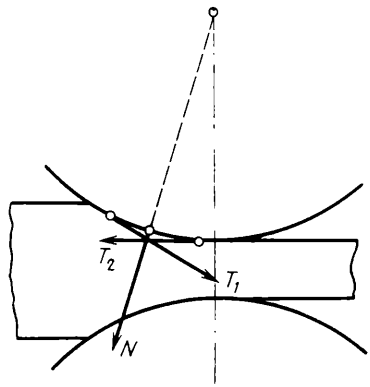

Fig. 138. Resultants of the elementary forces exerted by the roll on the rolled metal

be neglected. Then obviously the six forces mentioned above, acting on the metal from the top and bottom rolls, must be balanced out, i.e., their vector sum must be zero. This is possible only under the condition that the overall resultant P_1 of the three forces applied by one roll (Fig. 139) is equal and opposite to the force P_2, the overall resultant of the other three forces applied by the other roll. Since, in accordance with the symmetry conditions, the point A, where the overall resultant force P_1 of one system of three forces is applied, must be located at the same distance as the point B from the plane passing through the axes of the rolls, B being the point where the resultant force P_2 of the other three, mirror image forces is applied; thus $AC = BD$.

Hence we may conclude that the resultant of the roll pressure on the metal, including the friction forces, must be directed parallel to the line connecting the centres of the two rolls, i.e., it must be vertical, as shown in Fig. 139.

Taking into consideration that the metal being rolled exerts on the rolls the same pressure as the rolls do on the metal, we arrive

at the conclusion that the resultant P of the overall pressure of the rolled metal on the rolls, i.e., the normal pressure and the friction forces, is also directed parallel to the line connecting the centres O_1 and O_2 of the rolls (Fig. 140).

Let us find the torque necessary to rotate the roll, without taking into account the friction loss in its bearings. This torque is equal

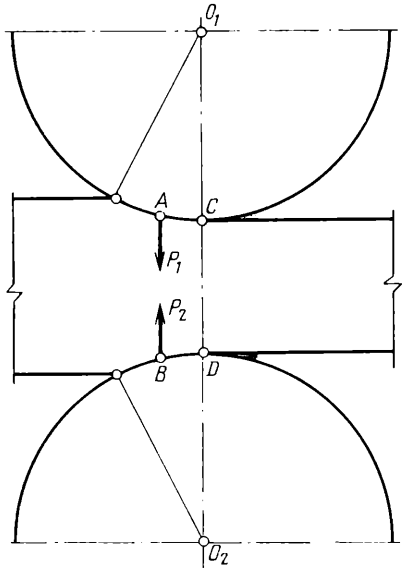

Fig. 139. Direction of overall resultant forces exerted by the roll on the rolled metal in a simple rolling process

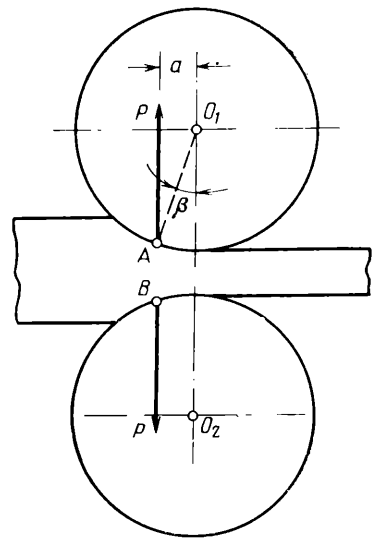

Fig. 140. Direction of the resultant forces applied to the rolls in a simple rolling process

to the product of the force P by its lever arm about the axis of the roll, i.e.,

$$M_1 = Pa \tag{IV.1}$$

or

$$M_1 = P\frac{D}{2}\sin\beta \tag{IV.2}$$

where D is the diameter of the rolls, and

β is the angle characterizing the point of application of the resultant of the metal pressure on the rolls.

The torque required for the rotation of both the rolls obviously is equal to $2M_1$, i.e.,

$$M = 2Pa \tag{IV.3}$$

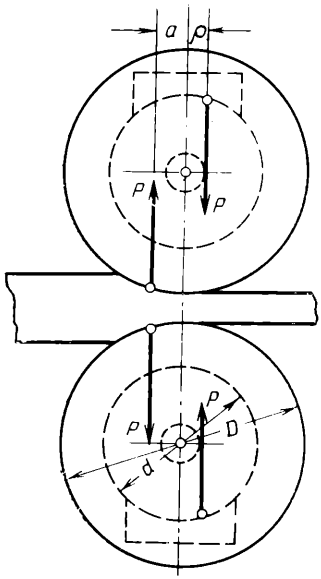

Fig. 141. Direction of the resultant forces acting on the rolls in a simple rolling process when the effect of the friction in the bearings is included

or

$$M = PD \sin \beta \qquad \text{(IV.4)}$$

Let us determine the direction of the reactions of the bearings of the roll and the torque necessary to rotate them, taking into consideration the inevitable friction losses in the journals.

From the condition of equilibrium of the roll it is obvious that the reaction of its bearings is directed parallel to the resultant of the pressure of the metal on the rolls, and will produce a torque about the axis of the roll which equals the torque of the friction forces in the bearings. In the case of a simple rolling process and when the journals or the necks of the roll are located on both sides of the roll barrel these conditions will be satisfied only when the reaction of the bearings of each roll equals the resultant of the pressure of the metal on the roll, i.e., the force P, and is directed vertically along the tangent to the friction circle, as represented in Fig. 141.

The couple of the forces P, with the lever arm of $a + \rho$, which acts on the rolls will be balanced by the torque required to rotate the roll and equal to

$$M_1 = P(a + \rho)$$

where ρ is the radius of the friction circle.

The torque required to rotate both the rolls when the friction losses in the bearings are taken into account is

$$M = 2P(a + \rho) \qquad \text{(IV.5)}$$

or

$$M = P(D \sin \beta + d\mu) \qquad \text{(IV.6)}$$

where d is the diameter of the journal or the neck of the roll, and
μ is the coefficient of friction in the journals.

In practice, however, the set of conditions corresponding to the case of a simple rolling process is not always satisfied (see above), so that the resultant of the pressure of the metal on the rolls is not

directed vertically. Thus, for example, the following variants are possible:

(1) in addition to the forces applied by the rolls, there are still other forces (tensioning of the metal by the preceding or following stand in continuous mills, or by the reeler in mills for cold rolling) acting on the rolled metal;

(2) the motion of the metal being rolled is non-uniform (reversible mills, considering the period when the metal is gripped by the rolls);

(3) in the rolling process the symmetry conditions between the top and bottom rolls are not satisfied; in particular, only a single roll is driven (thin strip two-high mills);

(4) the rolls rotate with different peripheral velocities (rolling carried out in section mills with top or bottom pressure);

(5) different roll diameters (mills of the Lauth type);

(6) the metal being rolled is inhomogeneous in its mechanical properties (rolling of bimetal or unevenly heated metal);

(7) different coefficients of friction of the two rolls;

(8) different width of the upper and lower portions of the rolled strip.

In all the cases enumerated above and in similar cases the resultant of the pressure of the metal on the rolls is not vertical so that the bearings of the rolls are subjected to lateral forces. When the rolling process becomes unsymmetrical with respect to both rolls, the torques necessary to rotate each roll are unequal as well.

Below we shall consider the most characteristic of these cases of rolling, when the resultant of the pressures of the metal on the rolls deviates from the vertical.

2. DIRECTION OF THE FORCES WHEN EXTERNAL LONGITUDINAL FORCES ARE APPLIED TO THE ROLLED METAL

We assume that the metal is rolled under the same conditions as for a simple rolling process, but additional forces R_0 and R_1 are applied to the rolled strip at entry to the rolls and at exit; the forces act along the axis of the strip. The forces can be either tensile (Fig. 142) or compressive. In practice such cases of rolling are often observed.

Rolling with tension is extensively used in continuous mills (particularly when strips are cold rolled and when tubes are reduced), and also in mills provided with coiling and tensioning drums. Rolling with the application of thrust or rolling with pressure head is encountered when the metal is forced into the rolls or when it

meets an additional resistance in passing through the rolls or when it emerges from the rolls; for example, the mandrel in automatic tube rolling mills, turning and guiding devices, etc.

We shall assume that the forces R_0 and R_1 have positive signs when they are tensile forces.

Let us suppose that $R_0 < R_1$. In order to determine the direction of the resultant of the pressures the metal exerts on the rolls, just as in the preceding cases, we shall first consider the conditions of

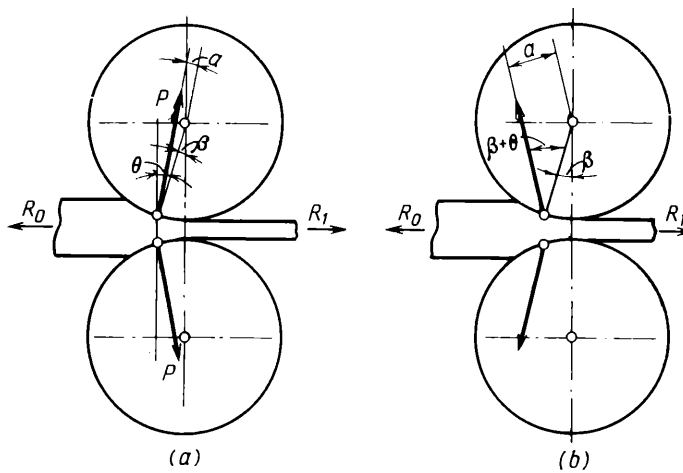

Fig. 142. Direction of the forces acting on the rolls during rolling with tension:
(a) $R_0 < R_1$; (b) $R_0 > R_1$

equilibrium of the metal being rolled. For equilibrium it is obviously necessary that the sum of the horizontal projections of the pressure resultants on the rolls and on the metal being rolled be equal to

$$\sum X = R_1 - R_0$$

Since the rolling process is symmetrical with respect to the top and bottom rolls, i.e., the deformation of the metal effected by the top and bottom rolls is the same, the horizontal projections of the resultants of the roll pressure on the metal being rolled must be the same. Then

$$X = \frac{R_1 - R_0}{2} \qquad \text{(IV.7)}$$

where X is the horizontal projection of the force P, i.e., the resultant of the roll pressure on the metal being rolled.

It follows from this that in rolling where external longitudinal forces are applied to the metal the resultant P of the metal pressure

on the rolls is vertical only if $R_0 = R_1$. In the majority of cases $R_0 \neq R_1$ so that the force X is not zero and the resultant of the pressure of the metal on the rolls is inclined towards the direction of rolling, when $R_0 < R_1$ (Fig. 142*a*), or it is inclined away from the direction of rolling, if $R_0 > R_1$ (Fig. 142*b*).

We denote the angle between the vertical line and the direction of the force P by θ; then the torque required to drive both the rolls is

$$M = 2Pa = PD \sin(\beta \mp \theta) \qquad \text{(IV.8)}$$

where D is the diameter of the rolls.

The angle θ in this equation can be determined from the condition (IV.7), i.e.,
for the case $R_0 < R_1$:

$$\sin\theta = \frac{R_1 - R_0}{2P} \qquad \text{(IV.9)}$$

and for the case $R_0 > R_1$:

$$\sin\theta = \frac{R_0 - R_1}{2P} \qquad \text{(IV.10)}$$

It follows from (IV.8) that when $R_0 < R_1$ (Fig. 142) the torque necessary to drive the rolls diminishes as the angle θ increases, but when this angle increases as far as $\theta = \beta$, then $M = 0$. The force P in this case passes through the centre of the roll, and the entire rolling process takes place as a result of the front tension (or, more precisely, because $R_1 > R_0$). In practice this type of rolling process is used in wire drawing benches, when the die is made up of free-running rolls.

If at the same time the effect of the friction forces of the rolls in the bearings is taken into consideration, then the resultants of the pressures on the rolls, when the latter are free-running, must pass along the tangent to the friction circles, as shown in Fig. 143.

In this case the angle θ of the inclination of the force P to the vertical can be found from the triangle ABO:

$$\theta = \beta + \theta_1$$

where θ_1 is the angle between the force P and the radius OA.

This angle can be determined from the equation

$$\sin\theta_1 = \frac{2\rho}{D} = \frac{d}{D}\mu \qquad \text{(IV.11)}$$

where ρ is the radius of the friction circle of the bearings of the roll
D is the roll diameter
d is the diameter of the journal
μ is the coefficient of friction in the bearings.

The forces necessary for pulling the metal through the free-running rolls or so-called roll dies, dependent on the overall pressure on

them, can be found from the equation

$$R_1 - R_0 = 2P \sin(\beta + \theta_1) \qquad \text{(IV.12)}$$

The results obtained above concerning the direction of the forces are applicable not only for rolling between two rolls as shown in Fig. 142 but are also valid for rolling and wire drawing in stands with three or four rolls (Fig. 144). In this case the overall pressure of the metal on all rolls must be substituted for $2P$ in equations (IV.8), (IV.9), (IV.10) and (IV.12).

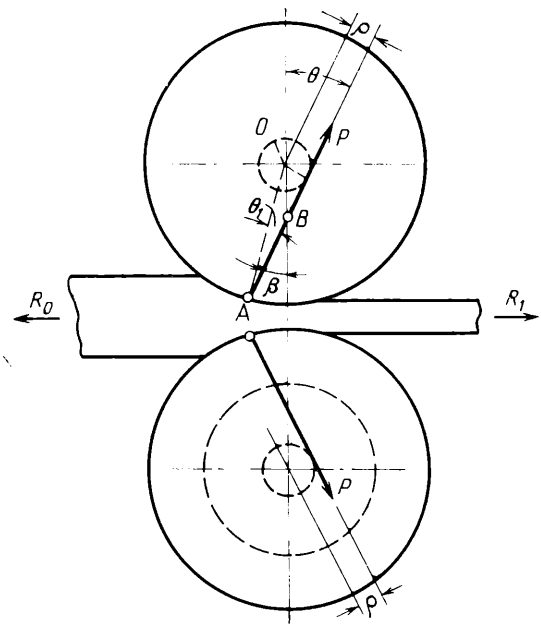

Fig. 143. Direction of the forces acting on free-running rolls

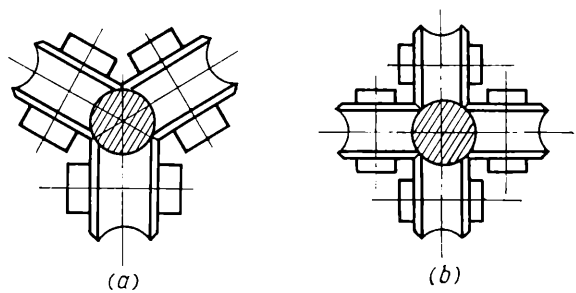

Fig. 144. Three- and four-roll working arrangements

3. DIRECTION OF THE FORCES WHEN THE METAL BEING ROLLED MOVES NON-UNIFORMLY

Let us suppose that the rolls rotate non-uniformly, with the result that the rolled strip emerges from the rolls with a certain acceleration, which we denote by j. In other respects we assume that all the conditions of the simple process of rolling are satisfied (see above).

We denote the weight of the strip by G.

According to d'Alembert's theorem the rolled strip can be considered as being at rest if the corresponding inertial force U is added to the system of forces acting on it.

The overall length of the rolled strip, after it emerges from the rolls, is denoted by l_1, whilst the elongation which it receives during its passage is denoted by λ. Let us assume that at the instant in question the strip has emerged from the rolls to a distance x (Fig. 145). Then the weight of the portion of the strip located at this instant on the other side of the rolls equals

$$\frac{G}{l_1}(l_1 - x)$$

The acceleration of this rear portion of the strip is $\frac{j}{\lambda}$. Then the inertial force U of the entire strip, located in the front and back of the rolls, can be found from the equation

$$U = \frac{G}{gl_1}\left[(l_1 - x)\frac{j}{\lambda} + xj\right] \qquad \text{(IV.13)}$$

where g is the acceleration of free fall.

To determine the direction of the resultants of the metal pressure on the rolls, as in the preceding cases, we consider first the conditions of equilibrium of the strip being rolled. For equilibrium it is obviously necessary that the sum of the horizontal projections of the resultants of the roll pressure on the rolled strip be equal to

$$2X = U \qquad \text{(IV.14)}$$

where X is the horizontal projection of the force P, the resultant of the roll pressure on the strip.

Since the force P has a horizontal projection, the resultant of the pressure of the metal on the rolls departs from the vertical. For a positive acceleration it will be inclined away from the direction of motion of the strip (Fig. 145*a*), whilst for a negative acceleration, i.e., for a deceleration, it will be inclined towards the direction of motion of the strip (Fig. 145*b*).

In practice the angle of inclination of the resultant of the metal pressure on the rolls is usually not large, since the tangential ac-

celeration of the rolls even in reversing mills does not exceed 5 to 8 m/s², and as a result of this the inertial forces arising are insignificant in comparison with the pressure of the metal on the rolls. Of this we can convince ourselves from the following example.

Example. Determine the maximum side pressure of the metal on the rolls and their bearings for a blooming mill when a billet

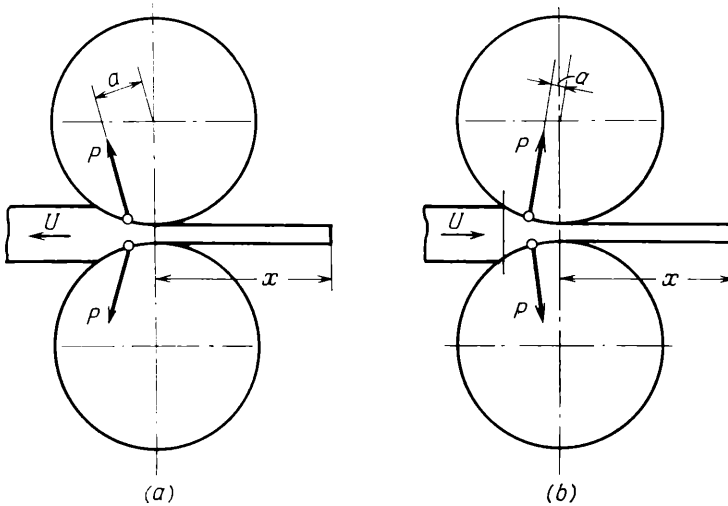

Fig. 145. Direction of the forces acting on the rolls during non-uniform motion of the rolled metal:
(*a*) accelerating motion; (*b*) decelerating motion

weighing 10 tons is rolled. At the end of the pass the rolls rotate with a deceleration of 120 revolutions per minute per second. The working diameter of the rolls is 1,150 mm.

The maximum side pressure will be observed at the end of the pass. Neglecting the forward slip we assume that the deceleration of the strip emerging from the rolls is

$$j = \frac{1.15\pi}{60} 120 = 7.25 \text{ m/s}^2$$

Using equations (IV.13) and (IV.14) we determine the side pressure on one roll:

$$X = \frac{1}{2} \times \frac{10{,}000}{9.8} 7.25 \approx 3{,}700 \text{ kg}$$

For blooming mills 1150 the overall pressure on the rolls reaches 1,200 to 2,000 tons. Thus the effect of a non-uniform velocity of motion of the rolled metal on the direction of the force resultants is insignificant.

4. FORCES ACTING ON THE METAL AT THE ENTRY TO THE ROLLS, AND THE CONDITION FOR GRIPPING

The inertial forces arising during a non-uniform motion of the rolled strip can in certain cases attain a considerable magnitude (when the strip is gripped by the rolls).

We shall consider the case of a strip being gripped when it is fed to the rolls with a velocity considerably less than the velocity of gripping.

We denote the feed velocity of the strip by v_0, and the entry velocity of the strip into the rolls during steady state motion by v. When $v_0 < v$ the entire mass of the strip being rolled receives a considerable acceleration during the period of gripping, and its velocity is thereby increased from v_0 to v. In practice for the majority of rolling mills the feed velocity v_0 is usually less than the velocity v, and consequently at the instant when the strip is gripped by the rolls inertial forces arise. The velocities v_0 and v are found to be equal in continuous mills (with the exception of the first stand), with the result that inertial forces are absent during the gripping period.

Let us attempt to calculate the possible value of the inertial forces arising at the instant when the strip is gripped by the rolls. We denote the acceleration with which the strip is gripped during the time interval in question by j.

Then the gripping is counteracted by the inertial force

$$U = \frac{G}{g} j$$

Two normal forces N and two tangential friction forces T (Fig. 146) are applied to the metal from the side of the rolls. The forces acting on the metal being rolled from the side of the guides, rolls of the roller table, etc., will be neglected in view of their smallness. Then the sum of the projections of the forces N and T on the direction of motion must be equal to the force

$$U = 2T \cos \alpha - 2N \sin \alpha \qquad \text{(IV.15)}$$

We express the tangential force T in terms of the torque M_{gr} applied by the motor to both rolls to rotate them during the gripping period (the friction forces in the bearings of the rolls are neglected):

$$T = \frac{M_{gr}}{D}$$

We denote the coefficient of friction between the roll and the strip being rolled by μ. Then equation (IV.15) assumes the follow-

ing form:

$$U = \frac{2M_{gr}\cos\alpha}{D}\left(1 - \frac{\tan\alpha}{\mu}\right) \qquad \text{(IV.16)}$$

It follows from this equation that for the same M_{gr} the inertial force increases as the angle of contact diminishes. The maximum value of this force is limited by the ratio

$$U_{max} < \frac{M_{gr}}{\frac{D}{2}}$$

In practice the greatest value of the force U is observed during unexpected interruptions in the rolling process, which are sometimes

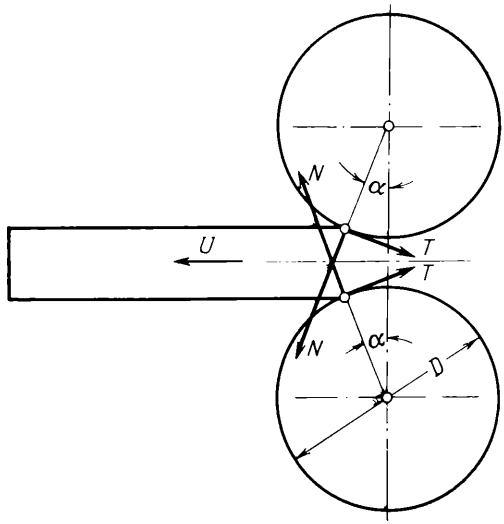

Fig. 146. Forces exerted on the rolled metal when rolls first take hold

seen to occur when the rolls, as a result of a random, but sharp drop in the coefficient of friction, begin to slip on the rolled strip and then instantaneously grip it anew. A phenomenon of this kind is observed, in rare cases, during the first passes in slab mills and in the roughing stands in strip mills. When rolling takes place with high angles of contact, then, as metal with a softer skin gets between the rolls, a short-timed slipping of the rolls on the metal can take place, after which the metal is again gripped by the rolls. The magnitude of the inertial forces arising at this instant is considerable, and as a result a breakdown can occur.

The conditions for the gripping of the metal being rolled by the rolls, when an external force R acts in the direction of the motion and promotes increased gripping, can be expressed by the following equation:

$$T\cos\alpha - N\sin\alpha + \frac{R-U}{2} = 0 \qquad \text{(IV.17)}$$

Taking into account that

$$T \leqslant N\mu$$

we obtain the condition for gripping

$$\mu \geqslant \tan\alpha - \frac{R-U}{2N\cos\alpha} \qquad \text{(IV.18)}$$

If we neglect the effect of the force U when the force R is absent, then

$$\mu \geqslant \tan\alpha \qquad \text{(IV.19)}$$

i.e., in this case the angle of contact must not exceed the angle of friction.

For a steady state rolling process the maximum possible angle of contact may also be determined from the equation of equilibrium. We project all the forces on the metal being rolled on the direction of its motion. In so doing we neglect the effect of spreading. Then (Fig. 147):

$$\sum X = -\int_0^{\alpha} p_x \sin\alpha_x r\, d\alpha_x + \int_{\gamma}^{\alpha} \tau_x \cos\alpha_x r\, d\alpha_x - \int_0^{\gamma} \tau_x \cos\alpha_x r\, d\alpha_x + \frac{R_1 - R_0}{2b} = 0 \qquad \text{(IV.20)}$$

where p_x is the specific pressure
τ_x is the specific friction force
r is the radius of the roll
b is the width of the rolled strip.

If for the sake of simplification we assume that the value of the specific pressure is constant over the arc of contact and equal to p_m, and the friction force $\tau_x = \mu p_m$, then the equation of equilibrium and, consequently, the condition of gripping is

$$-\frac{1-\cos\alpha}{\mu} + \sin\alpha - 2\sin\gamma + \frac{R_1 - R_0}{2p_m\mu br} = 0 \qquad \text{(IV.21)}$$

Let us analyze equation (IV.21) for the case where $R_0 = R_1 = 0$. For this we find the derivative $\frac{d(\sin\gamma)}{d\alpha}$ and equate it to zero:

$$\frac{d(\sin\gamma)}{d\alpha} = \frac{\cos\alpha}{2} - \frac{\sin\alpha}{2\mu} = 0$$

It follows from this equation that the maximum value of the angle γ is observed in the case where $\alpha = \mu$. With a subsequent increase of the angle α the angle γ diminishes, and, consequently, the friction forces diminish over the zone of forward slip, i.e., the

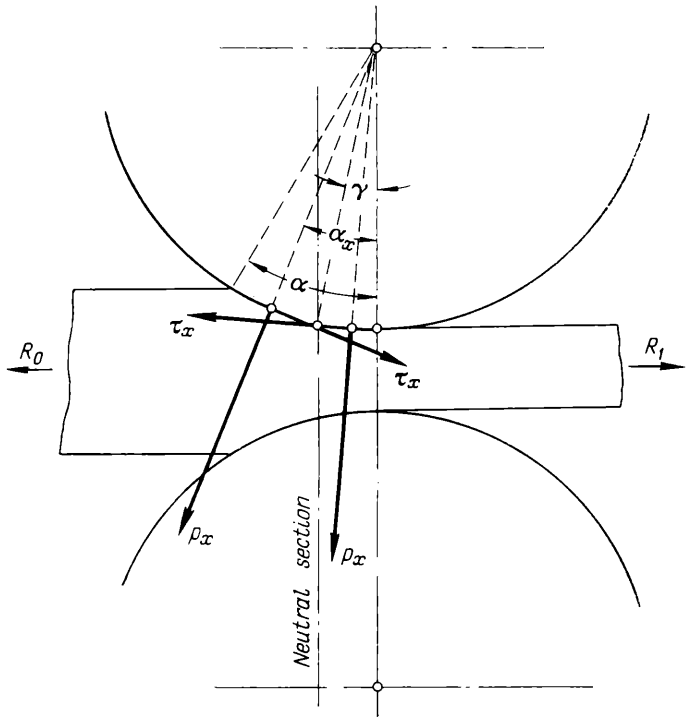

Fig. 147. Forces acting on the rolled metal during steady state motion

friction forces in the zone of forward slip, being a kind of reserve friction force, are exhausted when the angle γ diminishes, and the rolling process becomes less stable.

Finally, when $\gamma = 0$ the angle of contact reaches the theoretical maximum and if this value of γ is substituted into equation (IV.21), then for $R_0 = R_1$ we obtain

$$\frac{1 - \cos \alpha_{max}}{\mu} = \sin \alpha_{max}$$

or

$$\frac{1}{\mu} 2 \sin^2 \frac{\alpha_{max}}{2} = 2 \sin \frac{\alpha_{max}}{2} \cos \frac{\alpha_{max}}{2}$$

From this

$$\tan \frac{\alpha_{max}}{2} = \mu$$

From the above we arrive at the generally known result that when $p_x = \text{const.}$, $\tau_x = \mu p = \text{const.}$ and $R_0 = R_1 = 0$

$$\alpha_{max} \leqslant 2\varphi$$

In practice, however, the maximum possible angle of contact in the steady state motion is always less than the doubled angle of friction during gripping. This is explained, in the first place, by the fact that rolling with forward slip or with $\gamma = 0$ is practically impossible; in the second place, the coefficient of friction during a steady state motion is less than during gripping, and, in the third place, the specific friction forces over the arc of contact, as mentioned above, are distributed non-uniformly and close to the neutral section their value is less than μp_x. In view of these circumstances the maximum angle of contact is less than 2φ during a steady state motion.

5. DIRECTION OF THE FORCES WHEN ROLLING WITH ONE DRIVEN ROLL

This case is observed when only one roll is driven by the motor (the bottom one, for example), whilst the other rotates only as a result of the friction arising between the metal being rolled and the surface of this free-running roll. Such a method of driving the rolls is often used for thin strip two-high mills.

Let us suppose that the other conditions correspond to the case of a simple rolling process (see above). The action of the rolled metal on the top roll, expressed in the form of the elementary forces applied to the arc of contact, can be represented by a single resultant force P applied, say, at the point A (Fig. 148). If we neglect the friction forces in the bearings, then this resultant of the pressure of the metal on the top roll must pass through its axis, since, in accordance with the condition of uniform rotation of the roll, equilibrium is possible only when the sum of the moments of all the forces acting on the roll about its axis is zero.

Since action is equal to reaction, the resultant of the pressure of the top roll on the metal is obviously $P_1 = P$, and is directed normally to the roll surface as shown in Fig. 148*b*.

Let us determine the direction of the resultant P_2 of the pressure of the bottom roll on the metal being rolled. Since in accordance with the condition assumed only the forces from the rolls act on the

metal being rolled and its motion is uniform, then obviously the force P_2 must balance the force P_1. This is possible only if $P_2 = P_1$ and the force P_2 is directed to the opposite side, being in the same straight line as the force P_1 (Fig. 148*b*).

The resultant P of the pressure of the rolled metal on the bottom roll is equal to the force P_2 and is directed to the opposite side,

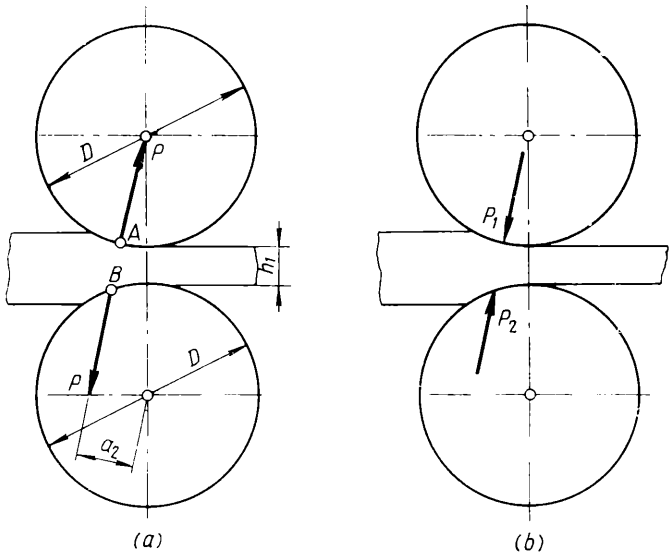

Fig. 148. Direction of the forces acting on the rolls (*a*) and on the rolled metal (*b*) when only the bottom roll is driven

being also in the same straight line with the force P_1 (Fig. 148*a*).

Thus we may conclude that if only one roll is driven and the other rotates only as the result of the friction arising between the rolled metal and the rolls, then resultants of the pressure of the metal on the rolls are equal to each other and depart from the vertical. On the free-running roll the pressure resultant is directed radially to the roll, whilst on the driven roll this resultant is directed along the line drawn through the centre of the free-running roll and the point of application of the resultant of the pressure of the metal on the rolls.

The torque necessary to rotate the bottom, i.e., the driven roll, is equal to the product of the force P by its lever arm a_2, i.e.,

$$M_2 = Pa_2 \qquad \text{(IV.22)}$$

In view of the fact that

$$a_2 = (D + h_1) \sin \beta_1$$

where β_1 is the angle characterizing the point of application of the resultant of the pressure of the metal on the free-running roll,

M_2 can also be expressed as:

$$M_2 = P(D + h_1) \sin \beta_1 \qquad \text{(IV.23)}$$

Comparing this equation with equation (IV.2) we see that the torque which in the case of one driven roll must be applied to this roll to rotate it is roughly twice the torque which must be applied to each roll when both the rolls are driven. This is fully understandable since in one case the total torque necessary for rolling is applied to one roll, whilst in the other case it is applied to two.

When the friction forces in the journals of the roll are taken into account, the direction of the resultants of the metal pressure on the rolls is altered somewhat. We denote (Fig. 149) the diameter of roll journal by d, and the coefficient of friction of the journal in the bearing by μ. The torque of the friction forces on the top roll can then be expressed by the equation

$$M_{fr} = P\mu \frac{d}{2}$$

Since the top roll is free-running, it follows from the condition of equilibrium that this torque must balance the torque produced by the resultant of the pressure of the rolled metal on the top roll. Therefore, when the friction forces in the journals of the rolls are taken into account, the resultant of the pressure of the rolled metal on the top roll passes not through the centre of the latter, but is directed along the tangent to the friction circle as shown in Fig. 149, i.e.,

$$P\mu \frac{d}{2} = P\rho$$

where ρ is the radius of the friction circle.

As for the resultant of the pressure of the rolled metal on the bottom roll, it lies, as in the case considered above, on the same straight line as the force P which is applied to the top roll (Fig. 149).

The torque which must be applied to the bottom roll to rotate both the rolls is

$$M_2 = P\left(a_2 + \mu \frac{d}{2}\right) \qquad \text{(IV.24)}$$

The lever arm a_2 can be found from the equation

$$a_2 = BO_2 - \rho$$

where BO_2 is a perpendicular dropped from the centre of the bottom roll to the line passing through the centre of the top roll parallel to the force P.

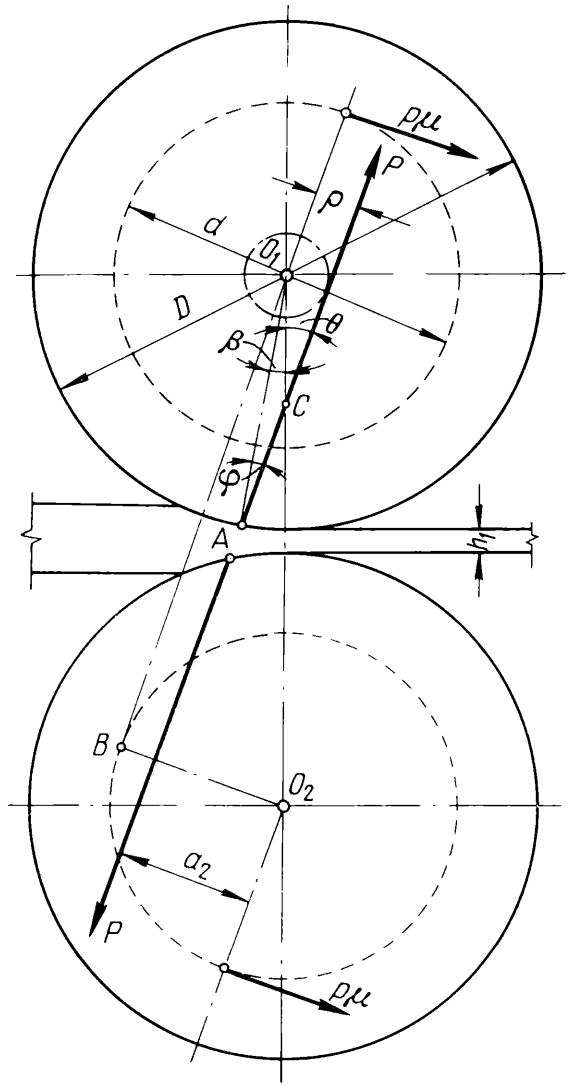

Fig. 149. Direction of the forces acting on the rolls, taking account of friction in the bearings, when only the bottom roll is driven

If the angle of inclination of the force P to the line connecting the centres of the rolls is denoted by 0, the length of the line segment BO_2 is

$$BO_2 = (D + h_1) \sin \theta$$

From the triangle ACO_1 it follows that $\theta = \beta + \varphi$. The angle β is determined by the point A at which the resultant of the pressure on the top roll is applied, whilst the angle φ, i.e., the angle between the radius drawn from the centre of the top roll to the point A and the direction of the force P, can be found from the equation

$$\sin \varphi = \frac{2\rho}{D} = \frac{d}{D} \mu \qquad \text{(IV.25)}$$

Then the lever arm a_2 can be determined from the equation

$$a_2 = (D + h_1) \sin (\beta + \varphi) - \rho$$

Substituting this value of a_2 into equation (IV.24) and noting that $\rho = \mu \frac{d}{2}$ we find the torque required to rotate the bottom roll when the friction forces in the journals of both rolls are taken into account:

$$M_2 = P (D + h_1) \sin (\beta + \varphi) \qquad \text{(IV.26)}$$

where the angle φ is determined from equation (IV.25).

By a similar method we can find the direction of the forces for other arrangements of rolling with a free-running roll. In particular, a problem of this type was solved by A. Zvyagintsev in connection with a rolling mill for wheels.

6. DIRECTION OF THE FORCES FOR DIFFERENT PERIPHERAL VELOCITIES OF THE ROLLS

We shall consider rolling with so-called top or bottom pressure. This case is often encountered in rolling structural sections. In this case the peripheral velocities and the diameters of the rolls are different; otherwise we assume that all the conditions of the simple rolling process are satisfied.

Let us assume that in the given case the diameter D_1 of the top roll is a little larger than the diameter D_2 of the bottom roll (Fig. 150). For equal angular velocities of the two rolls their peripheral velocities are not the same. As a result of the difference in the peripheral velocities the emergent end of the rolled metal (if the

difference in diameters is not very large) does not tend to go in the horizontal direction, but will tend to curve towards the roll with the lower peripheral velocity, i.e., in the present case towards the bottom roll. In order to prevent this motion of the strip, guides are installed at the exit side of the bottom roll.

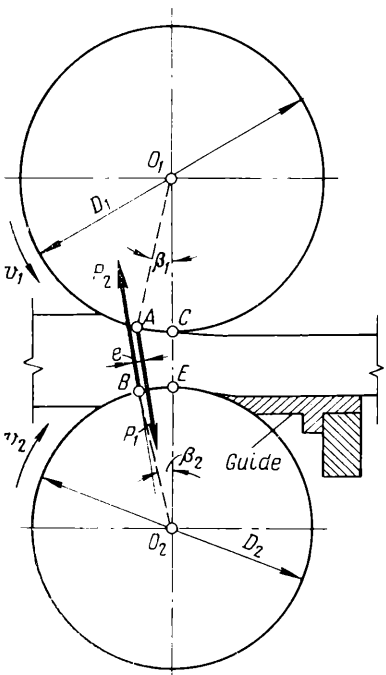

Fig. 150. Forces acting on the rolled metal when the peripheral velocity of the top roll exceeds the peripheral velocity of the bottom roll

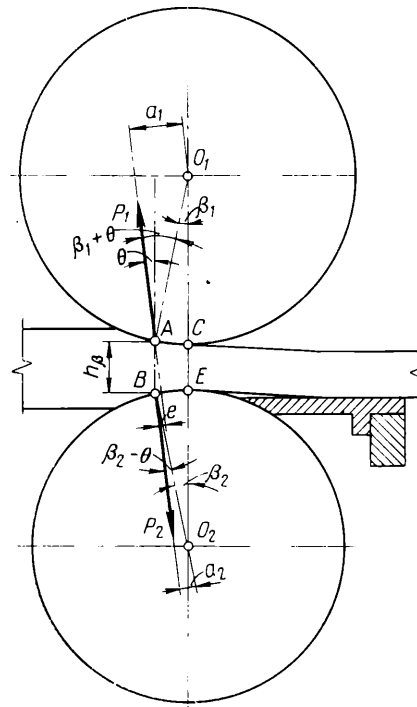

Fig. 151. Forces acting on the rolls during rolling with top pressure

By means of the guides the strip is straightened out at the exit from the rolls; in connection with this the action of the guides on the strip can approximately be expressed in the form of a bending moment

$$M_b = \sigma_s W \qquad \text{(IV.27)}$$

where σ_s is the yield stress of the rolled metal, and
W is the section modulus of the rolled strip for plastic bending.

To determine the direction of the forces acting in this case on the rolls, let us first consider the conditions of equilibrium of the rolled strip.

We denote the resultant of the pressure of the top roll on the metal by P_1, and the resultant of the pressure of the bottom roll by P_2. In view of the fact that besides the forces only the bending moment M_b acts on the rolled strip, both forces P_1 and P_2 must obviously be equal to each other and be directed in such a way that they form a couple equal to M_b (Fig. 150):

$$P_1 e = M_b \tag{IV.28}$$

where e is the lever arm of the forces P_1 and P_2.

It follows from this equation that the larger M_b the longer must be the lever arm e. This lever arm can be increased by increasing the distances from the plane passing through the axes of the rolls to the points A and B where the forces P_1 and P_2 are applied, and also depends on the inclination of these forces to the horizontal.

Since the magnitudes of AC and BE are very close to each other, owing to the relative smallness in the diameters of the rolls and the angle of contact is nearly the same for both rolls, the forces P_1 and P_2 are not vertical (Fig. 151). Thus, when rolling is carried out by top or bottom pressure, lateral forces arise acting on the rolls and their bearings. Owing to the fact that the forces P_1 and P_2 are equal and parallel, the lateral forces acting on the bearings of the top or bottom roll are the same, but are directed to opposite sides. The roll with the smaller diameter exerts side pressure on the bearings in the direction of motion of the rolled metal, whilst the roll with the larger diameter exerts it in the opposite direction.

If the angle of inclination of the forces P_1 and P_2 to the vertical is denoted by θ, then the value of the side pressure on the bearings is

$$X = P_1 \sin \theta \tag{IV.29}$$

Here the angle θ can be found from the equation

$$\sin \theta = \frac{e}{h_\beta} \tag{IV.30}$$

where h_β is the depth of the cross section of the rolled strip in the section AB.

Substituting this value of $\sin \theta$ into equation (IV.29) and expressing $P_1 e$, in accordance with equation (IV.28), in terms of M_b, we obtain

$$X = \frac{M_b}{h_\beta} \tag{IV.31}$$

Let us determine the torques necessary to drive the rolls. Dropping perpendiculars from the centres O_1 and O_2 of the rolls on to the

direction of the forces P_1 and P_2 and denoting their lengths by a_1 and a_2, we find the torques

$$M_1 = P_1 a_1 \tag{IV.32}$$

and

$$M_2 = P_2 a_2 \tag{IV.33}$$

We denote the angles AO_1C and BO_2E, specifying the points of application of the forces P_1 and P_2, by β_1 and β_2.

Then the angle between the force P_1 and the radius O_1A equals $\beta_1 + \theta$, and the angle between the force P_2 and the radius O_2B is $\beta_2 - \theta$. The lever arms a_1 and a_2 in this case can be expressed as:

$$a_1 = \frac{D_1}{2} \sin (\beta_1 + \theta)$$

$$a_2 = \frac{D_2}{2} \sin (\beta_2 - \theta)$$

where D_1 and D_2 are the diameters of top and bottom rolls.

Substituting these values of a_1 and a_2 into equations (IV.32) and (IV.33) we obtain

$$M_1 = P_1 \frac{D_1}{2} \sin (\beta_1 + \theta) \tag{IV.34}$$

and

$$M_2 = P_2 \frac{D_2}{2} \sin (\beta_2 - \theta) \tag{IV.35}$$

Since in practice $D_1 \approx D_2$ and correspondingly $\beta_1 \approx \beta_2$, it follows from these equations that $M_1 > M_2$.

Thus, the torque is distributed unequally between the two rolls when applying top or bottom pressure. For the roll which rotates with the greater peripheral velocity a larger torque is required than for the other roll. From Fig. 151 it is also seen that $P_1 a_1 > > P_2 a_2$.

When the difference in the peripheral velocities of the rolls is considerably increased, it can happen that the angle θ equals the angle β_2; then the force P_2 passes through the bottom roll and $M_2 = 0$. In this case the torque necessary for rolling must be applied only to the other roll which moves with the higher velocity. If, however, $\theta > \beta_2$, then the force P_2 will pass above the point O_2, and in this case the bottom roll will act as a brake.

For the top and bottom pressures used in practice the torque applied to the roll having the lower peripheral velocity is usually not equated to zero; it is, as a rule, less than the torque necessary to drive the other roll.

To determine tentatively the difference in the torques applied to the top and bottom rolls, assuming for simplicity that the angles

$\beta_1 \approx \beta_2 \approx \beta$ and the diameters $D_1 \approx D_2 \approx D$, we can use the following equations:

$$M_1 - M_2 = PD \sin\theta \cos\beta \qquad \text{(IV.36)}$$

or

$$M_1 - M_2 = \frac{M_b}{h_\beta} D \cos\beta \qquad \text{(IV.37)}$$

The effect of the difference in the peripheral velocities on the distribution of the torques necessary to drive the two rolls has been experimentally investigated by a number of scientists. These investigations confirm the conclusions drawn above that if one of the rolls rotates with a higher peripheral velocity, then the torque applied to this roll must be greater than the torque applied to the second roll. At the same time it was noted that even a comparatively small difference in the peripheral velocities of the rolls causes a considerable inequality of the torques of the rolls (Fig. 152). Also it was discovered that the side walls of the section rolls greatly affect the distribution of the torques between the two rolls. The appearance of friction forces on the side surfaces of the section roll had an effect similar to the increase of the peripheral velocity of the roll.

When rolling with closed section rolls the main part of the torque necessary to drive both rolls is often taken up by the roll with the groove. Because of this phenomenon we often observe a very great non-uniformity in the distribution of the torques between the two rolls of actual mills intended for rolled section material, and sometimes the ratio approaches 1:5 or even 1:10.

It follows from the above that the inequality of the peripheral velocities of the two rolls is undesirable as regards the work of the drive mechanism of the rolling mill (shafts and gear stand), since it leads to a considerable increase in the load on one of the shafts, usually constituting the weakest link in a rolling mill. For example, in slabbing mills and in four-high mills, when the roll barrel is of considerable length (more than 2,000 mm), the permissible reductions and, consequently, the productivity in the majority of cases are limited by the strength of the joint between the shaft and the roll, the size of which is limited by the minimum centre distance between the rolls. In addition, the inequality of the peripheral roll velocities can lead to a considerable increase of the load on the gear stand when the thickness of the rolled strip is small.

Unequal peripheral velocities of the rolls are in a number of cases inadmissible also for the process of rolling. Thus, for example, in hot rolling thin strips and wire the top roll is often made free-running in order to achieve almost absolutely equal peripheral velocities of both rolls; the top roll is driven as a result of the fric-

tion of the metal on the roll. It must always be taken into consideration that, owing to the difference in the peripheral velocities of the two rolls, the end of the emergent rolled strip does not tend to move in the horizontal direction, but will bend towards the roll with the lower peripheral velocity. Therefore, different peripheral veloci-

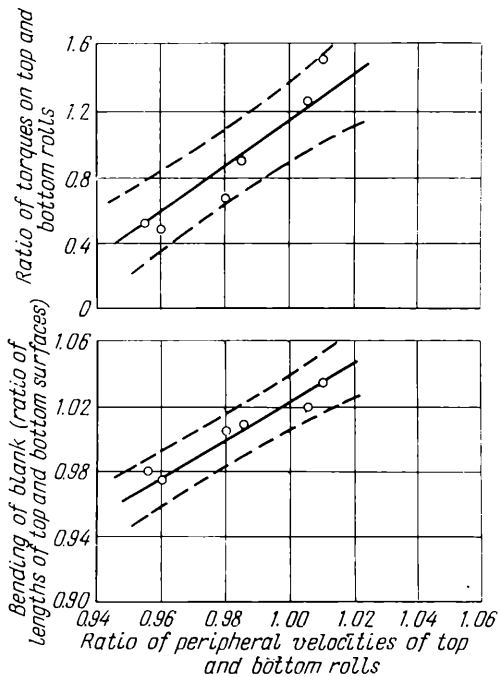

Fig. 152. Effect of the difference in the peripheral velocities of the two rolls on the torque ratio for top and bottom rolls and on the form of the bent blank when it emerges from the rolls (G. Kennedy and F. Slamar)

ties are permissible only in those cases where this bending of the strip emerging from the rolls is allowable or is required by the rolling process itself.

This effect of unequal roll velocities on the exit characteristics of the rolled strip is in practice widely utilized in slabbing and section mills. In particular, in blooming mills the diameter of the bottom roll is usually 10 mm larger than the diameter of the top roll, whilst in section mills, conversely, the diameter of the top roll often is taken larger than the diameter of the bottom roll.

Unequal peripheral velocities of the rolls are sometimes also utilized in cold rolling of a thin strip or sheets. In this case this inequality is not chosen from the considerations of the flexure of the strip at the exit, but is used only to reduce the pressure on the rolls and to reduce their local compressive deformation (flattening) over the contact surfaces. In this connection it is of interest to mention the rolling process under the conditions where the difference in the

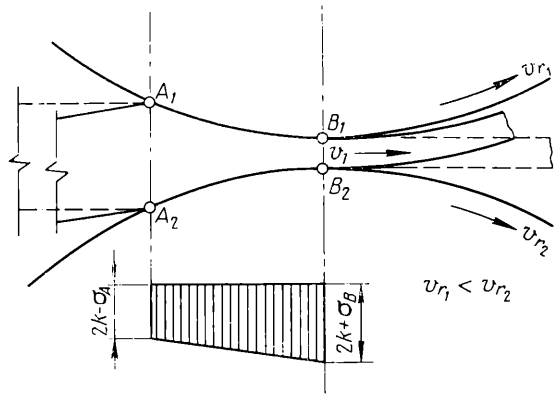

Fig. 153. Distribution of the specific pressure on the bottom roll when its peripheral velocity v_{r_2} exceeds the velocity v_1 of the rolled metal as it emerges from the rolls

peripheral velocities of the rolls is so great that the peripheral velocity of one of the rolls, v_{r_1}, exceeds the exit velocity v_1 of the metal. During rolling under such conditions the rolled metal slips along the roll having the higher velocity, the slip taking place over the entire arc of contact in the same direction. Consequently, there is no zone of forward slip on the contact surface of this roll, and the zone of backward slip extends over the entire arc of contact. The character of the specific pressure diagram in this case must be completely different in comparison with the usual rolling process. There is no increase in the specific pressure in the middle of the arc of contact as a result of the external friction, and the specific pressure diagram must have a form close to a trapezium (Fig. 153; see also Fig. 73). In view of the fact that the rolled metal tends to acquire the higher velocity at the point A_2 (in comparison with the point A_1) at the entry, and at the point B_2 (in comparison with the point B_1) at the exit, we can assume that in the region of the point A_2 tensile stresses σ_A arise, whilst in the region of the point B_2 compressive stresses σ_B arise. Consequently, even if the effect of work

hardening is not taken into account, the specific pressure diagram will be trapezoidal. But independently of this phenomenon the mean specific pressure on the roll with the higher velocity, for $v_{r_2} > v_1$, must be less than when rolling with equal peripheral velocities.

It follows from the foregoing that the problem concerning the effect of unequal peripheral velocities on the forces in the rolling mill must be considered together with the resulting deformation of the metal. In particular, it is necessary to take into account the inevitable flexure of the rolled strip at the entry and exit of the rolls owing to their unequal peripheral velocities. As a result of this flexure the contact surfaces on the rolls will be unsymmetrical,

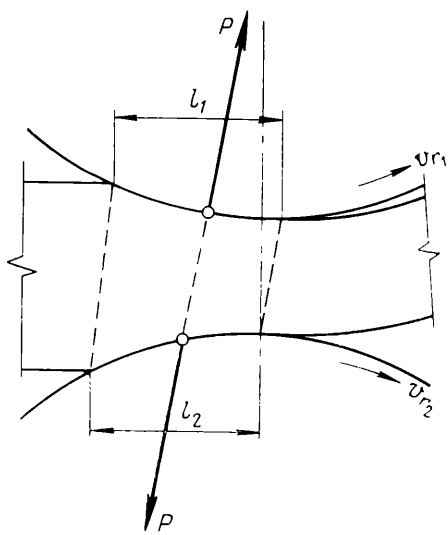

Fig. 154. Displacement of the contact surfaces arising from unequal peripheral velocities of the rolls, also showing the direction of the resultant forces

and the planes of entry and exit will not be parallel to the plane passing through the axes of the rolls.

The approximate diagram presented in Fig. 154 which gives the layout of the contact surfaces on both rolls indicates that the point of application of the resultant of the pressure on the roll which has the lower peripheral velocity must be closer to the line connecting the roll centres than the corresponding point on the roll which is characterized by the higher peripheral velocity. As

a consequence the resultant of the pressure of the metal on the roll with the higher peripheral velocity will be inclined to meet the direction of motion of the rolled metal.

7. DIRECTION OF THE FORCES WHEN ROLLING WITH DIFFERENT COEFFICIENTS OF FRICTION ON THE TWO ROLLS

In certain cases rolling can take place with different coefficients of friction on the two rolls. In practice this is observed in both hot and cold rolling; in the first case because of a possible

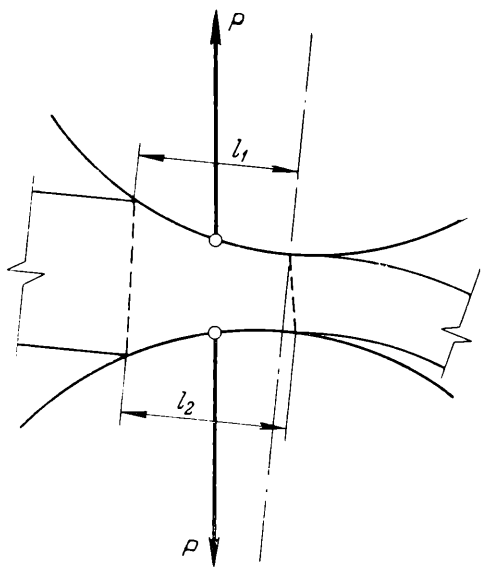

Fig. 155. Displacement of the contact surfaces due to the difference in the coefficients of friction of the two rolls, also showing the direction of the resultant forces (coefficient of friction of top roll exceeds that of the bottom one)

difference in the skin at the top and bottom surfaces of the rolled strip, and in the second case because of different lubrication conditions.

In measuring the torque on both the shafts of blooming mills E. Rokotyan established that in certain cases, in spite of the somewhat larger diameter of the bottom roll, and, consequently, its higher peripheral velocity, and also in spite of the uniform temper-

ature of the rolled strip, the torque on the top roll can be considerably higher than that on the bottom roll.

The investigations into this phenomenon carried out by E. Rokotyan showed a considerable influence of the unequal coefficients of friction (because of the different state of the skin on the two rolls) on the distribution of the torque. For the roll characterized by the higher coefficient of friction on the contact surface a larger torque is necessary than for the other roll. N. Kirilin came to similar conclusions whilst experimentally investigating the torque distribution for cold rolling with different lubrication conditions on the top and bottom surfaces of the rolled strip. This phenomenon is explained by the fact that when the coefficient of friction increases the zone of forward slip increases, and, consequently, the particles of metal located close to the roll with the higher coefficient of friction tend to emerge from the rolls with a higher velocity than the particles touching the other roll. The unequal coefficients of friction on each roll have roughly the same effect on the character of the metal emerging from the rolls as do unequal peripheral velocities. The contact surfaces on both rolls will not be symmetric and the resultant forces of pressure on the rolls deviate from the vertical (Fig. 155).

The problem concerning the direction of the forces during rolling for different coefficients of friction has not yet been worked out theoretically, and therefore it is not possible to recommend any analytical relation for the dependence of the inclination of the forces P on the difference in the coefficients of friction.

8. DIRECTION OF THE FORCES WHEN THE ROLLS HAVE DIFFERENT DIAMETERS

We shall consider the case where the peripheral velocity of both rolls is the same, but the diameter of one roll is considerably larger than the diameter of the other roll. Otherwise the same conditions apply as for the case of a simple rolling process.

In practice this case is encountered in strip mills of the Lauth type and in combined mills for cold rolling thin strip (mills of type Y). The ratio of the roll diameters sometimes reaches 2 : 1 and more.

Owing to the fact that the rolled metal is homogeneous as regards its mechanical properties and its pressure on both rolls is the same, we may assume that for the same width of the strip (Fig. 156), over its entire thickness, the arcs CF and DG are equal to each other. We assume further that the distribution of the specific pressure for

the strip being rolled is the same over the arc CF as it is over the arc DG. In this case the point A, where the resultant of the pressure of the rolled strip on the top roll is applied, must be located at the same distance from the point F as the point B from the point G, B

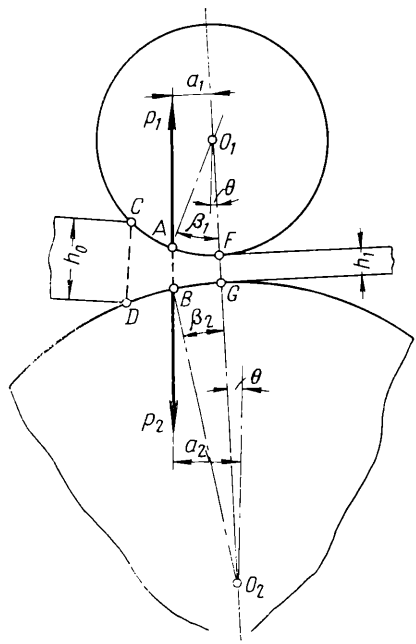

Fig. 156. Forces acting on rolls of different diameters

being the point of application of the resultant of the pressure exerted on the bottom roll; thus,

$$AF = BG$$

We drop perpendiculars (Fig. 157) from the points A and B on to the plane passing through the axes of both rolls. Since $\beta_1 > \beta_2$, it is obvious that

$$AH < BK$$

the point A is located closer to the plane passing through the roll axes than the point B.

Since it is given that only the forces applied by the rolls act on the strip, it is clear that the two resultants of the pressure exerted by the top and bottom rolls on the metal must balance each other, that is, their vector sum will be zero. This is possible only if these

forces are equal and have opposite directions. The resultants of the pressure exerted by the metal on the rolls (see Fig. 156) are expressed in the form of two forces (P_1 and P_2) which are equal and opposite. Thus, the resultants of the pressures exerted by the metal on the rolls lie in the same straight line. This straight line must obviously pass through points A and B and will be slightly inclined towards

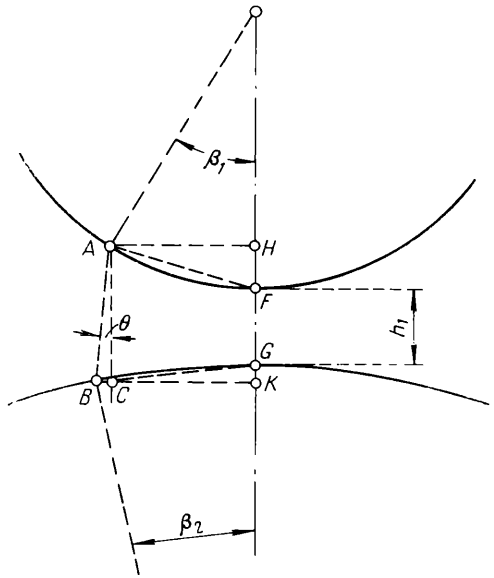

Fig. 157. Determination of the direction of the forces acting on rolls of different diameters

the plane passing through the axes of both rolls (see Fig. 156). We shall denote this angle of inclination by θ.

As is seen from Fig. 156, the lever arms of the two forces are different, and accordingly the torques necessary to rotate the rolls are also unequal:

$$M_1 = P_1 a_1 < M_2 = P_2 a_2 \qquad \text{(IV.38)}$$

where

$$a_1 = \frac{D_1}{2} \sin (\beta_1 - \theta) \qquad \text{(IV.39)}$$

and

$$a_2 = \frac{D_2}{2} \sin (\beta_2 + \theta) \qquad \text{(IV.40)}$$

The angle θ can be found approximately from the triangle ABC (see Fig. 157), where the segment AC is parallel to the plane passing

through the axes of the rolls:

$$\tan\theta = \frac{BC}{AC}$$

or

$$\theta = \tan^{-1}\frac{D_2\sin\beta_2 - D_1\sin\beta_1}{2h_1 + D_2(1-\cos\beta_2) + D_1(1-\cos\beta_1)} \qquad \text{(IV.41)}$$

9. DIRECTION OF THE FORCES WHEN ROLLING NON-UNIFORMLY HEATED METAL AND BI-METALLIC STRIPS

We shall consider the influence exerted by the non-uniformity of the mechanical properties of the rolled metal on the direction of the forces acting on the rolls during rolling. We assume that a strip the top layer of which is heated to a higher temperature than the bottom layer is rolled, the other conditions being the same as in the case of a simple rolling process. Consequently, the resistances of the top and bottom layers of the strip are different, and obviously the angle of contact for the top roll is greater than that for the bottom roll. We denote (Fig. 158) the mean specific pressure exerted by the strip on the top roll by p_1, and that exerted on the bottom roll by p_2. We correspondingly denote the angle of contact on the top and bottom rolls by α_1 and α_2. We assume that the width of the rolled strip is constant over its depth, and denote it by b. In accordance with the condition that the pressures exerted by the rolled metal on the top and bottom rolls are equal, we can write the following equation:

$$p_1 b\frac{D}{2}\sin\alpha_1 \quad p_2 b\frac{D}{2}\sin\alpha_2$$

or

$$\frac{p_1}{p_2} \quad \frac{\alpha_2}{\alpha_1}$$

We assume that the specific pressure distribution over the arc of contact is the same for the top and bottom rolls.

Denoting the angles between the plane passing through the axes of rolls and the

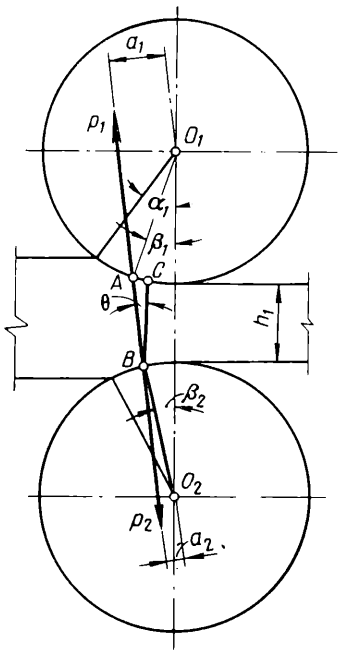

Fig. 158. Forces acting on the rolls during the rolling of non-uniformly heated metal

radii drawn to the points A and B, where the resultants of the pressure exerted by the rolled strip on the top and bottom rolls are applied, by β_1 and β_2 (see Fig. 158) respectively, we obtain

$$\frac{p_1}{p_2} = \frac{\beta_2}{\beta_1}$$

from which it follows that $\beta_1 > \beta_2$.

We assume that no other forces besides those applied by the rolls act on the rolled metal. Then the two resultants of the pressure exerted by the rolls on the metal, which we denote by P_1 and P_2, must balance, i.e., their vector sum must be zero.

It is not difficult to see that, as in the preceding case, these two forces balance only if $P_1 = P_2$ and they have opposite directions. The resultants of the pressure exerted by the rolled metal are expressed in the form of the same forces with the reversed directions. The straight line with which the direction of the forces P_1 and P_2 coincide must obviously pass through the points A and B (see Fig. 158).

Since this straight line is inclined to the plane passing through the axes of the rolls (as in the preceding case), forces arise acting on the rolls in the horizontal direction, and the lever arms of the two forces P_1 and P_2 are unequal.

To rotate the roll in contact with the more heated portion of the strip a somewhat greater torque is needed than to rotate the other roll:

$$M_1 = P_1 a_1 > M_2 = P_2 a_2 \qquad \text{(IV.42)}$$

The lever arms a_1 and a_2 can be determined in terms of the angles β_1 and β_2.

We denote the angle of inclination of the forces P_1 and P_2 to the vertical by θ (see Fig. 158). The angle between the direction of the force P_1 and the radius AO_1 is then equal to $\beta_1 + \theta$, and the angle between the direction of the force P_2 and the radius BO_2 is $\beta_2 - \theta$, from which

$$a_1 = \frac{D}{2} \sin(\beta_1 + \theta)$$

and

$$a_2 = \frac{D}{2} \sin(\beta_2 - \theta)$$

When the possible flexure of the strip as it emerges from the rolls is neglected the angle θ can be determined from the triangle ABC, where the segment BC is parallel to the line O_1O_2:

$$\tan\theta = \frac{AC}{BC}$$

$$\theta = \tan^{-1} \frac{\sin\beta_1 - \sin\beta_2}{\frac{2h_1}{D} + 2 - \cos\beta_1 - \cos\beta_2} \qquad \text{(IV.43)}$$

The same method can obviously be used also for determining the direction of the forces which act on the rolls when bi-metallic strips or strips with different widths of the top and bottom portions are rolled, i.e., in the case where the lateral dimensions of the surfaces of the strip in contact with the top and bottom rolls are different.

10. DIRECTION OF THE FORCES ACTING ON THE ROLLS OF RING ROLLING MILLS

We shall consider the most common case when the outer and inner surfaces of a ring or tyre are worked by the two rolls *1* and *2*, the axes of which are parallel with the axis of the ring (Fig. 159). For this the inner roll *1* is usually made free-running, whilst the outer roll *2* is driven.

Since the inner roll is free-running, the resultant P of the pressure exerted by the metal on it must be directed along the tangent to the friction circle of the journals of the roll (Fig. 159). As for the resultant of the pressure on the outer roll, it is in line with the force P acting on the inner roll.

The torque which must be applied to the outer roll to rotate both rolls is

$$M = P(a_2 + \rho_2) \qquad \text{(IV.44)}$$

where a_2 is the lever arm of the force P relative to the centre of the outer roll

ρ_2 is the radius of the friction circle of the journal of the outer roll.

From Fig. 159 it follows that

$$a_2 = AO_2 - \rho_1$$

where ρ_1 is the radius of the friction circle of the journal of the inner roll

AO_2 is the perpendicular dropped from the centre of the outer roll on to the line passing through the centre of the inner roll parallel to the forces P.

If the angle of inclination of the forces P to the line connecting the roll centres is denoted by θ, the length of the segment AO_2 can be determined from the equation

$$AO_2 = (r_1 + r_2 + h_1) \sin \theta$$

where r_1 and r_2 are the radii of the inner and outer rolls. The angle θ can be found by the same method as in the case concerning the direction of the forces when rolling with one free-running

roll (see Fig. 149):

$$\theta = \beta_1 + \varphi_1$$

where

$$\sin \varphi_1 = \frac{\rho_1}{r_1} \qquad \text{(IV.45)}$$

Then the lever arm is

$$a_2 = (r_1 + r_2 + h_1) \sin (\beta_1 + \varphi_1) - \rho_1$$

We substitute this value of a_2 into equation (IV.44); then the torque which must be applied to the outer roll to rotate both rolls.

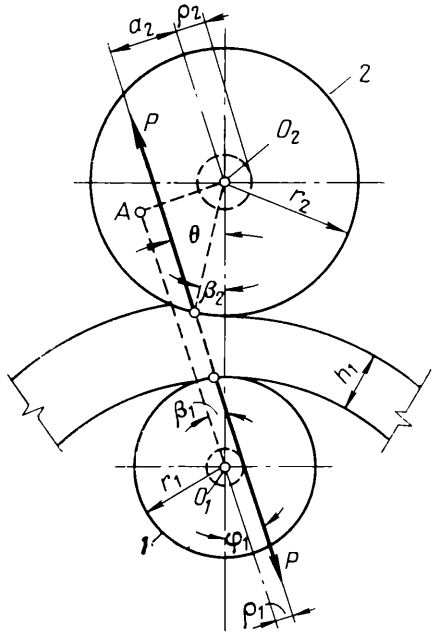

Fig. 159. Direction of the forces acting on the rolls of a ring rolling mill:
1—non-driven roll; *2*—driven roll

when the friction forces in the journals are taken into account, can be expressed by the equation

$$M = P\,[(r_1 + r_2 + h_1) \sin (\beta_1 + \varphi_1) - \rho_1 + \rho_2] \qquad \text{(IV.46)}$$

where β_1 is the angle between the line connecting the roll centres and the radius drawn from the point of application of the resultant of the pressure exerted by the metal on the free-running roll.

If the rolls in the mill are arranged as cantilevers then the friction forces in the bearings, which are correspondingly increased, are represented by the appropriate values of the radii of the friction circles:

$$\rho_1 = \frac{A\rho_A + B\rho_B}{P}$$

and

$$\rho_2 = \frac{C\rho_C + E\rho_E}{P}$$

where A and B are the loads on the bearings of the inner roll
C and E are the loads on the bearings of the outer roll
ρ_A, ρ_B, ρ_C and ρ_E are the radii of the friction circles of the bearings.

Let us consider the case when the outer roll has the form of a ring (die) and the rolling takes place between its inner surface and the

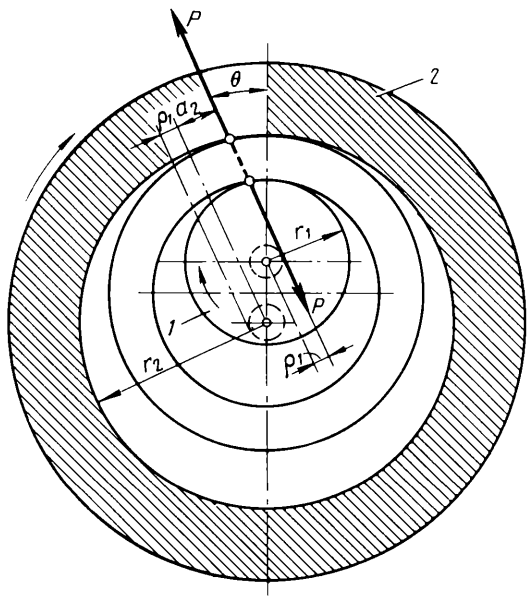

Fig. 160. Direction of the forces acting on the rolls during the rolling of a ring between the inner roll *1* and the roll *2*, made in the form of a die

roll located in it (Fig. 160). The direction of the forces acting on the rolls will be the same as for the setup just considered, and the resultants of the pressures exerted by the metal on the rolls must lie on the same straight line. If the inner roll is free-running as well,

then obviously this straight line will touch the friction circle of its bearings as shown in Fig. 160. The torque necessary to rotate the driven roll can be determined from equation (IV.44) or (IV.46).

11. DIRECTION OF THE FORCES ACTING ON THE ROLLS OF FOUR-HIGH MILLS

When metal is rolled on four-high mills two fundamentally different cases are possible as regards the direction of the forces acting on the rolls: the first occurs when the mill is driven by the motor via the working rolls, and the second when it is driven via

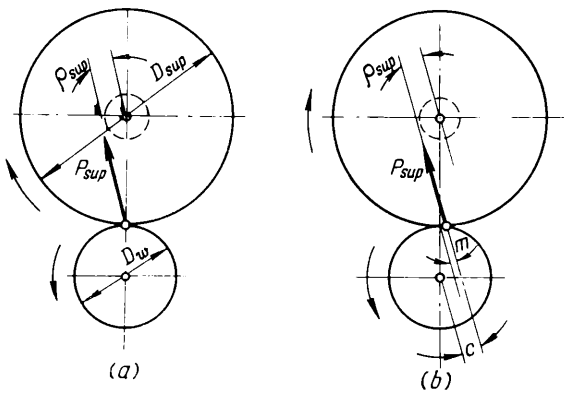

Fig. 161. Direction and point of application of the resultant of the pressure exerted by the working roll on the support roll:
(*a*) without the rolling friction between the rolls taken into account;
(*b*) with the rolling friction taken into account

the support rolls. In the first case the support rolls are free-running and rotate as a result of the friction forces arising on the contact surfaces between the working and support rolls, and in the second case, conversely, from the drive the motion is transferred to the shafts of the support rolls, whilst the working rolls are free-running.

Let us consider the direction of the forces acting on the rolls in both these cases.

In the first case it is necessary to begin with the determination of the conditions of equilibrium of the support rolls. Since these rolls are driven the resultant of the pressure exerted by the working roll on the support roll, P_{sup}, must be directed along the tangent to the friction circle of its bearings (Fig. 161*a*), in order to balance the reaction of the bearings, also directed along the tangent to this circle. If the rolling friction is neglected we can assume that the point of application of the force P_{sup} lies on the line connecting the

roll centres as shown in Fig. 161*a*. But when rolling friction is taken into account the point of application of the force P_{sup} is displaced from the line of the centres by the length of the lever arm m of the rolling friction (Fig. 161*b*). This displacement of the point of application of the force P_{sup} takes place as a result of rotation of the rolls during which the contact surface is located asymmetrically relative to the line connecting the centres of the two rolls, being a little displaced towards the motion of the metal. Theoretically this problem has been investigated by N. Glagolev.

The directions and the points of application of the forces acting on the support rolls do not depend on the direction of the forces applied to the working roll, and, consequently, on the ratio between the back and front tensions in the rolled metal.

To rotate the support rolls it is necessary to apply to the working roll the torque (Fig. 162),

$$M_{sup} = P_{sup} c \qquad \text{(IV.47)}$$

or

$$M_{sup} = P_{sup} \left(\frac{D_w}{2} \sin \alpha + m \right) \qquad \text{(IV.48)}$$

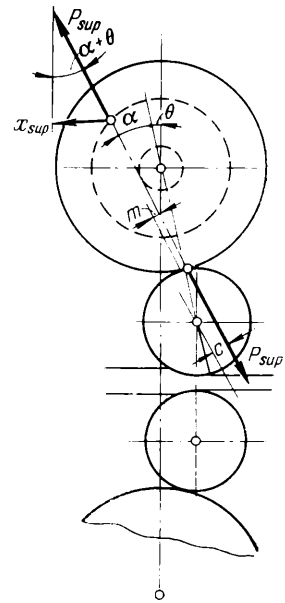

Fig. 162. Forces acting on the bearings of the support roll, with the force acting on the working roll over the contact surface between the support rolls

where c is the lever arm of the force P_{sup} relative to the working roll
D_w is the diameter of the working roll
m is the lever arm of the rolling friction
α is the angle between the force P_{sup} and the line connecting the roll centres.

At the same time the angle α can be determined from the expression

$$\sin \alpha = 2 \frac{\rho_{sup} + m}{D_{sup}} \qquad \text{(IV.49)}$$

where D_{sup} is the diameter of the support roll
ρ_{sup} is the radius of the friction circle of the support roll.

Substituting the value of sin α into equation (IV.48) we obtain the final formula for M_{sup}:

$$M_{sup} = P_{sup} \left[\frac{D_w}{D_{sup}} \rho_{sup} + m \left(1 + \frac{D_w}{D_{sup}} \right) \right] \qquad \text{(IV.50)}$$

In this equation the first term corresponds to the friction losses in the bearings of the support roll, whilst the second term corresponds to the friction losses due to the rolling of the working roll on the support roll.

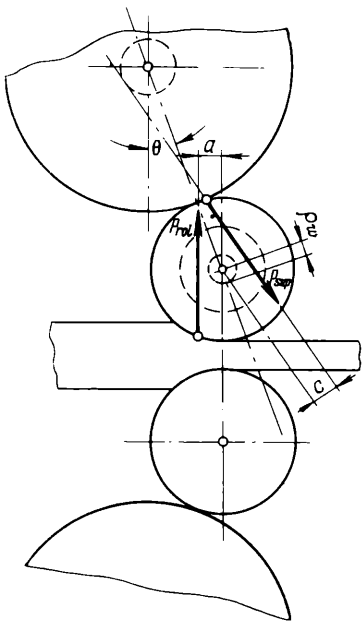

Fig. 163. Forces acting on the working roll during rolling without tension or when $R_0 = R_1$

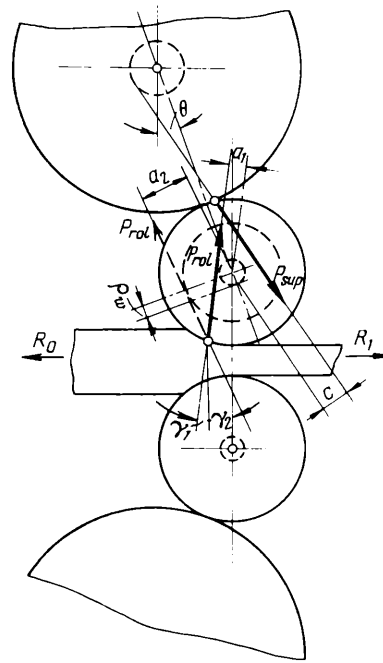

Fig. 164. Forces acting on the working roll during rolling with tension (the direction of the force P_{rol} is shown by the continuous line for $R_0 < R_1$, and by the dash line for $R_0 > R_1$)

The horizontal component of the pressure on the bearings of the support roll is found from the expression

$$X_{sup} = P \sin (\alpha \pm \theta) \qquad \text{(IV.51)}$$

where θ is the angle between the vertical plane and the line connecting the centres of the support and working rolls.

The plus sign in this expression corresponds to the displacement of the working rolls from the line connecting the centres of the support rolls in the direction of rolling, as shown in Fig. 162, whilst the minus sign signifies the displacement in the opposite direction.

From equation (IV.51) it is already possible to draw the fundamental conclusion about the greater stability of the position of the support roll in relation to the working roll when the angle θ has the positive sign, i.e., when the working rolls are displaced in the direction of rolling.

Let us now consider the conditions of equilibrium of the working roll.

The torque necessary to rotate the working roll is a sum of three torques (Figs. 163 and 164):

$$M_w = M_{rol} + M_{sup} + M_{fr} \tag{IV.52}$$

where M_{rol} is the rolling torque, equal to the product of the resultant of the pressure exerted by the metal on the roll, P_{rol}, by its lever arm a

M_{sup} is the torque used to rotate the support roll, defined by equation (IV.50)

M_{fr} is the torque of the friction forces in the bearings of the working roll.

In equation (IV.52) the only unknown quantity is M_{fr}, which is equal to the product of the resultant of the pressure on the bearings of the working roll, T, by the radius of the friction circle of the journals of the working roll, ρ_w.

Thus the following form can be given to equation (IV.52):

$$M_w = P_{rol}a + P_{sup}\left[\frac{D_w}{D_{sup}}\rho_{sup} \quad m\left(1 + \frac{D_w}{D_{sup}}\right)\right] + T\rho_w \tag{IV.53}$$

Since the working roll is carried by the support roll and its bearings have vertical guides, the resultant of the pressure on the bearings of the working roll, T, must be directed horizontally.

Projecting the two remaining forces P_{rol} and P_{sup} acting on the working roll on to this direction we obtain:

(a) for rolling without tension when the resultant of the pressure exerted by the rolled metal on the rolls is directed vertically (see Fig. 163)

$$T = X = P_{sup}\sin\alpha \tag{IV.54}$$

(b) when the front tension R_1 exceeds the back tension R_0 (see Fig. 164)

$$T = P_{sup}\sin\alpha + P_{rol}\sin\gamma_1 \tag{IV.55}$$

(c) when $R_0 > R_1$

$$T = P_{sup}\sin\alpha - P_{rol}\sin\gamma_2 \tag{IV.56}$$

where γ_1 and γ_2 are the angles between the force P_{rol} and the line connecting the centres of the working rolls.

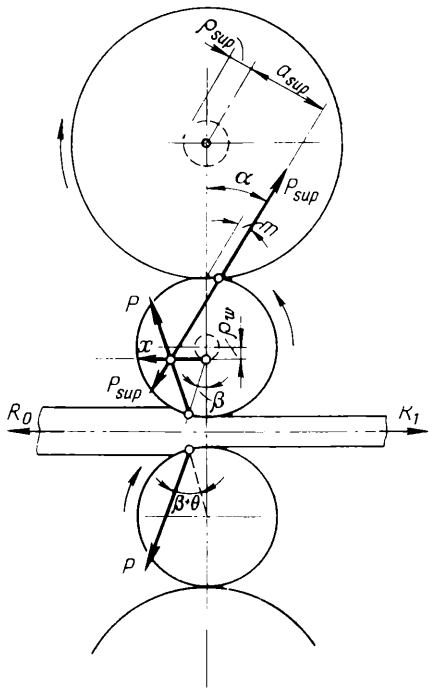

Fig. 165. Direction of forces acting on the rolls of a four-high mill when the support rolls are driven and the working rolls are free-running

The value of the pressure on the support roll, P_{sup}, appearing in equations (IV.54), (IV.55) and (IV.56) can be found by projecting the forces on the working roll on to the vertical direction:

when $R_0 = R_1$

$$P_{sup} = P_{rol} \frac{1}{\cos(\alpha + \theta)} \quad \text{(IV.57)}$$

when $R_0 < R_1$

$$P_{sup} = P_{rol} \frac{\cos \gamma_1}{\cos(\alpha + \theta)} \quad \text{(IV.58)}$$

when $R_0 > R_1$

$$P_{sup} = P_{rol} \frac{\cos \gamma_2}{\cos(\alpha + \theta)} \quad \text{(IV.59)}$$

The interaction of the forces between the working and support rolls of four-high mills just considered, when the friction circles and the rolling friction are taken into account, gives a clear and simple idea about the true forces acting on the rolls.

In the second case, when the support rolls are the driven ones, the analysis of the direction of the forces should be commenced with determining the conditions of equilibrium of the working roll. Since this roll is free-running, the reaction of the support roll must be directed towards it so that the sum of the moments of the forces acting on the working roll is equal to zero.

Assuming that the rolling process is symmetrical with respect to both working rolls and that external longitudinal forces act on the metal being rolled (see Fig. 142), and, consequently, that the rolling torque can be expressed by equation (IV.48) we obtain (Fig. 165):

$$P \frac{D_w}{2} \sin(\beta \pm \theta) + X\rho_w = P_{sup} \left(\frac{D_w}{2} \sin \alpha - m \right) \quad \text{(IV.60)}$$

where P is the overall pressure exerted by the metal on the working roll

X is the pressure on the bearings of the working roll

ρ_w is the radius of the friction circle of the bearings of the working roll

α is the angle between the direction of the force P_{sup} and the line connecting the centres of the working and support rolls.

In accordance with the equilibrium condition of the working roll, all of the three forces P, P_{sup} and X acting on it intersect at a single point as shown in Fig. 165. At the same time the force X runs tangentially to the friction circle and is directed horizontally, because the bearings of the working rolls are arranged usually so that they move in vertical guides, and, consequently, can take up only forces directed horizontally. It follows that the force X will be equal to the horizontal projection of the forces P and P_{sup}:

$$X = P \sin \varphi + P_{sup} \sin \alpha$$

Substituting this value of the force X into equation (IV.60) we find the angle of inclination of the force P_{sup} to the line connecting the roll centres:

$$\sin \alpha = \frac{\frac{P}{P_{sup}} \left[\frac{D_w}{2} \sin (\beta \pm 0) + \rho_w \right] + m}{\frac{D_w}{2} - \rho_w} \qquad \text{(IV.61)}$$

Having determined the angle α we find the torque necessary to rotate the support roll:

$$M_{sup} = P_{sup} (a_{sup} + \rho_{sup}) \qquad \text{(IV.62)}$$

or

$$M_{sup} = P_{sup} \left(\frac{D_{sup}}{2} \sin \alpha + m + \rho_{sup} \right) \qquad \text{(IV.63)}$$

If we neglect the friction forces in the bearings of the working roll and the rolling friction of the working roll on the support roll, then after substituting the value of sin α from equation (IV.61) we obtain

$$M_{sup} = P \frac{D_{sup}}{2} \sin (\beta \pm \theta) \qquad \text{(IV.64)}$$

i.e., the torque defined by equation (IV.8) increases proportionally with the diameter of the driven roll.

The problem concerning the torques necessary to rotate the support rolls of four-high mills has also been considered by A. Filatov and A. Tretyakov.

12. DIRECTION OF THE FORCES ACTING ON THE ROLLS OF MULTI-ROLL MILLS

The method considered above can also be used to determine the direction and magnitude of the forces acting on the rolls of multi-roll mills with the number of support rolls more than two.

As an example let us determine these forces for a 12-roll mill (Fig. 166) in which the working rolls *1* are free-running, whilst the intermediate support rolls *2* and *3* are driven.

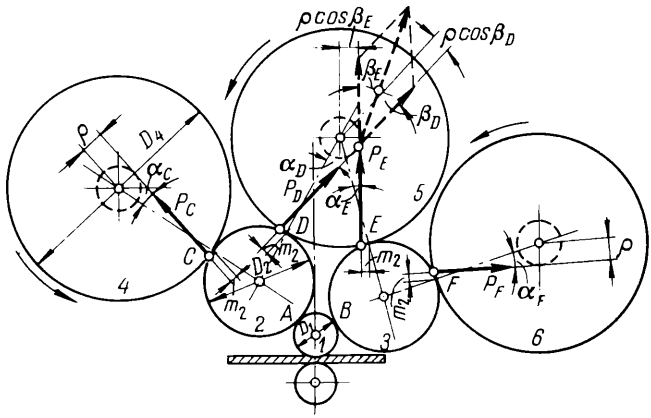

Fig. 166. Forces acting on the principal support rolls of a 12-roll mill

We denote the points of contact of the rolls by the letters A, B, C, D, E and F, and the forces at the points of contact of the rolls by P_A, P_B, P_C, P_D, P_E and P_F respectively.

We shall first find the direction of the forces acting on the principal support rolls *4*, *5* and *6*. The angle between the force P_C and the line connecting the centres of the support rolls *2* and *4* can be determined from the expression

$$\sin \alpha_C = 2 \frac{\rho + m_2}{D_4} \qquad \text{(IV.65)}$$

where D_4 is the diameter of the support roll *4*

ρ is the radius of the friction circle of the journals of the support roll

m_2 is the lever arm of the rolling friction arising between the principal support rolls and the intermediate rolls.

Similarly we can find the direction of the forces P_D, P_E and P_F acting on the support rolls *5* and *6*, where in calculating the angles for roll *5* we must substitute into equation (IV.65) the quantities

$\rho \cos \beta_D$ and $\rho \cos \beta_E$, corresponding to the actual forces P_D and P_E relative to the centre of the roll 5, instead of the radius ρ of the friction circle (Fig. 166). The direction of the forces acting on the

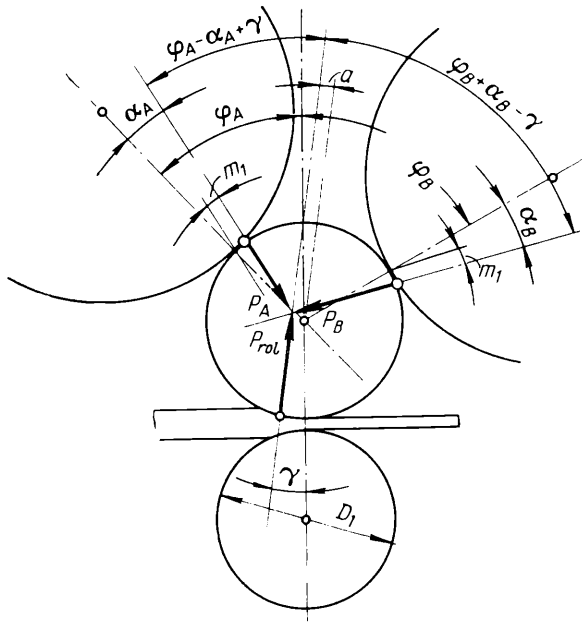

Fig. 167. Forces acting on the working roll of a 12-roll mill

working roll is determined from the condition that moments of the forces applied to it by the rolled metal and the support rolls are equal (Fig. 167):

$$P_{rol}a = P_A\left(\frac{D_1}{2}\sin\alpha_A - m_1\right) + P_B\left(\frac{D_1}{2}\sin\alpha_B - m_1\right) \quad \text{(IV.66)}$$

where m_1 is the lever arm of the rolling friction arising between the working and support rolls.

If we assume that $\alpha_A \approx \alpha_B$, then

$$\sin\alpha_A = \frac{P_{rol}a + (P_A + P_B)m_1}{P_A + P_B} \times \frac{2}{D_1} \quad \text{(IV.67)}$$

The torque required to rotate the intermediate support roll 2 is determined from the expression (Fig. 168):

$$M_2 = P_A\left(\frac{D_2}{2}\sin\alpha_A + m_1\right) + P_C\left(\frac{D_2}{2}\sin\alpha_C + m_2\right) + P_D\left(\frac{D_2}{2}\sin\alpha_D + m_2\right) \quad \text{(IV.68)}$$

Assuming for the sake of simplicity that

$$\alpha_C = \alpha_D = \alpha_E = \alpha_F$$

$$D_4 = D_5 = D_6$$

$$\rho \approx \rho \cos \beta_D \approx \rho \cos \beta_E$$

and substituting the values of $\sin \alpha_C$ and $\sin \alpha_A$ from equations (IV.65) and (IV.67), we obtain the formula for the calculation of

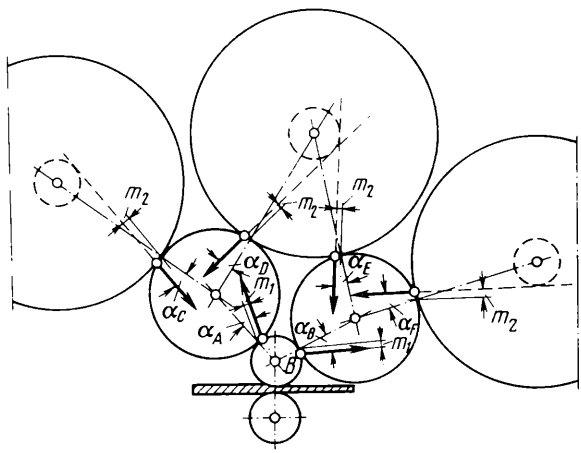

Fig. 168. Forces acting on the intermediate (driven) support rolls of a 12-roll mill

the torque which must be applied to both the driven rolls of a 12-roll mill:

$$M = P_{rol} a \frac{D_2}{D_1} + (P_A + P_B)\left(1 + \frac{D_2}{D_1}\right) m_1 + (P_C + P_D + P_E + P_F) \times \left[\frac{D_2}{D_4}\rho + \left(1 + \frac{D_2}{D_1}\right) m_2\right] \qquad \text{(IV.69)}$$

The first term of this equation represents half the rolling torque referred to the driven support rolls, the second term is the torque expended on the rolling friction of the working roll along the driven support rolls, and the third term is the torque required to overcome the friction in the bearings of the principal support rolls and the rolling friction between them and the driven support rolls.

Having determined the direction of the forces P_A, P_B, P_C, P_D, P_E and P_F, let us calculate their magnitudes.

We shall consider the conditions of equilibrium of the working roll. Projecting the forces P_A and P_B on to the direction of the resultant of the pressure P_{rol} exerted by the rolled metal on the working roll (Fig. 167), we obtain

$$P_{rol} = P_A \cos(\varphi_A - \alpha_A + \gamma) + P_B \cos(\varphi_B + \alpha_A - \gamma) \quad \text{(IV.70)}$$

But since the projections of the forces P_A and P_B on to the line perpendicular to the direction of the forces P_{rol} must be equal to each other, then

$$P_A \sin(\varphi_A - \alpha_A + \gamma) = P_B \sin(\varphi_B + \alpha_A - \gamma) \quad \text{(IV.71)}$$

Solving equations (IV.70) and (IV.71) for the forces P_A and P_B we find

$$P_A = P_{rol} \frac{\sin(\varphi_B + \alpha_A - \gamma)}{\sin(\varphi_A + \varphi_B)} \quad \text{(IV.72)}$$

and

$$P_B = P_{rol} \frac{\sin(\varphi_A - \alpha_A + \gamma)}{\sin(\varphi_A + \varphi_B)} \quad \text{(IV.73)}$$

Proceeding from the conditions of equilibrium of the intermediate support rolls we obtain analogous formulas for the forces P_C, P_D, P_E and P_F acting on the principal support rolls.

The method just considered can also be used to determine the direction of the forces in multi-roll mills with other numbers of rolls, and, specifically, in 20-roll mills. In the latter case it is necessary to bear in mind that usually four out of the six intermediate support rolls, being in contact with the principal support rolls, are the driven rolls.

13. DIRECTION OF THE FORCES IN ROLLER MILLS

For cold rolling of thin-walled tubes use has been made in the recent years of mills of VNIIMETMASH (All-Union Research Institute for the Construction of Metallurgical Machinery) system, developed under the leadership of V. Nosal, in which the metal *1* is compressed by the rollers *2* resting on support planes *3* (Fig. 169). When the support plane moves in the direction indicated in the figure the roller touches the metal being worked and, as a result of the inclination of this plane, is pushed into the metal, thus compressing it.

Since the rollers are free-running and the rolling is effected only as a result of the movement of the support plane in the horizontal direction, the resultant of the pressure P_1 which the metal exerts on the roller must be balanced by the pressure P_2 which the support

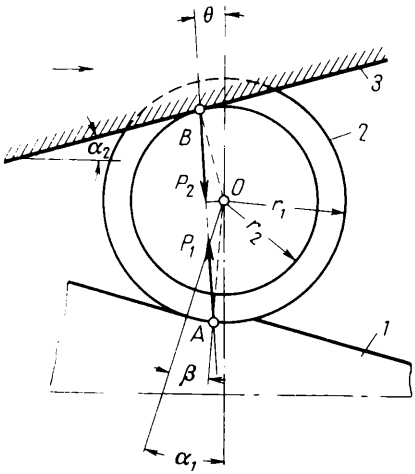

Fig. 169. Direction of the forces acting on the roller of a roller mill, neglecting the rolling friction loss:
1—rolled metal; *2*—roller; *3*—support plane

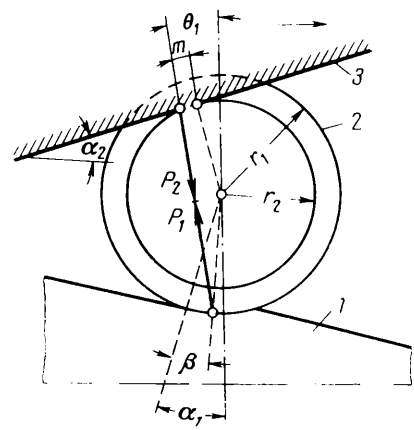

Fig. 170. Direction of the forces acting on the roller of a roller mill, including the rolling friction loss of the roller *2* on the support plane *3* (*1*—rolled metal)

plane exerts on the roller, as shown in Fig. 169. The angle of inclination θ of the force P_1 to the vertical can be found from the condition that the two segments are equal:

$$r_1 \sin(\alpha_1 - \beta + \theta) = r_2 \sin(\alpha_2 - \theta) \qquad \text{(IV.74)}$$

where r_1 and r_2 are the radii of the roller along the working and support surfaces respectively

α_1 and α_2 are the angles between the vertical and the perpendiculars dropped from the centre O of the roller on to the surface of the rolled metal and on to the support plane

β is the angle characterizing the position of the point A, at which the resultant of the pressure exerted by the metal on the roller is applied.

Assuming that $\sin \alpha_2 \approx \alpha_2$, etc., in view of the smallness of the angles in equation (IV.74), we obtain

$$\sin \theta = \frac{r_2 \sin \alpha_2 - r_1 \sin(\alpha_1 - \beta)}{r_1 + r_2} \qquad \text{(IV.75)}$$

Having determined the angle θ we find the force which is necessary to move the support plane in the horizontal direction:

$$X = nP_1 \sin \theta \tag{IV.76}$$

where n is the number of rollers.

If the friction losses occurring when roller *2* rolls over the support plane *3* are taken into account the point of application of the force P_2 must be displaced by m opposite to the motion (Fig. 170). In this case the angle of inclination θ_1 of the force P_1 to the vertical can be found from the condition

$$r_1 \sin (\alpha_1 - \beta + \theta) = r_2 \sin (\alpha_2 - \theta) + m \tag{IV.77}$$

Then the angle θ_1 can be determined from the equation assuming, in view of the smallness of the angles, that $\sin \alpha_1 \approx \alpha_1$, etc.:

$$\sin \theta_1 = \frac{r_2 \sin \alpha_2 - r_1 \sin (\alpha_1 - \beta) + m}{r_1 + r_2} \tag{IV.78}$$

The force which is required to move the support plane in the horizontal direction is found from equation (IV.76), putting $\theta = \theta_1$ in accordance with equation (IV.78).

V

Pressure Exerted by the Metal on the Rolls During Longitudinal Rolling

1. THE FACTORS DETERMINING THE PRESSURE OF THE METAL ON THE ROLLS

When the magnitude of the resultant of the pressure exerted by the metal on the rolls is determined attention should be concentrated on the calculation of the force P which is directed parallel to the line connecting the roll centres. This force is the main component of the overall pressure exerted by the metal on the rolls. The other component of the force, X, which is perpendicular to the main component, and which is dependent on the direction of the resultant of the force, is found from the equations given in Chapter IV.

If we neglect the variation of the contact stresses over the width of the rolled strip and if we take the width as equal to unity, the force P can be expressed in the general form by the equation (Fig. 171):

$$P = \int_0^{\alpha} p_x \frac{dx}{\cos \alpha_x} \cos \alpha_x + \int_{\gamma}^{\alpha} \tau_x \frac{dx}{\cos \alpha_x} \sin \alpha_x - \int_0^{\gamma} \tau_x \frac{dx}{\cos \alpha_x} \sin \alpha_x$$

The second and third terms of this equation may be neglected in view of their smallness as compared with the first term. The

pressure of the metal is then

$$P = \int_0^l p_x \, dx$$

In practice this quantity is usually calculated as the product

$$P = F p_m \tag{V.1}$$

where F is the projection of the contact area between the metal and the roll; this is also called the contact area on the plane normal to the direction of the force P.

The symbol p_m denotes the mean specific pressure given by the equation

$$p_m = \frac{1}{F} \int_0^l p_x \, dx \tag{V.2}$$

Thus the determination of the pressure which the metal exerts on the rolls during rolling reduces to the solution of the two basic problems:

(1) the calculation of the contact area between the metal being rolled and the rolls, or, more precisely, the projection of this area on to a plane normal to the direction of the force P;

(2) the determination of the mean specific pressure on the rolls.

The quantity F appearing in this equation can, in the majority of cases, be found comparatively simply, as it depends on the geometrical dimensions of the rolls and the rolled strip before it enters the rolls and after it emerges from them.

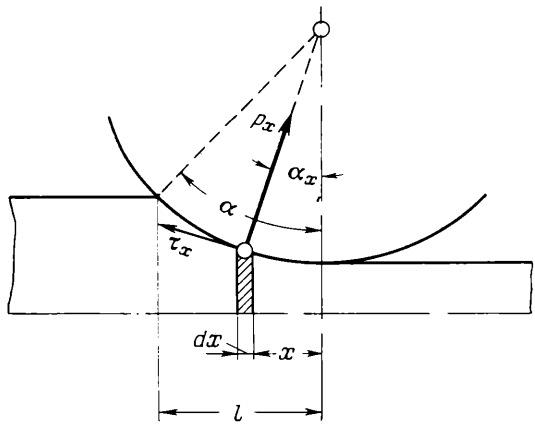

Fig. 171. Forces acting on the roll

On the other hand, the determination of a quantity required for the calculation of the overall pressure on the rolls, viz., p_m, may offer considerable difficulties in a number of cases.

This quantity, as has already been mentioned (see Chapter III, Section 1), depends on a large number of different factors, which are divided into two groups. The first group is made up of those factors which affect the mechanical properties of the rolled metal, whilst the second group consists of factors which influence the character of the state of stress of the rolled metal, i.e., contact friction forces, outer zones, tension and so on.

The effect of the first group of factors was considered in detail in Chapter III and was in its general form expressed by either equation (III.1) or equation (III.2). The effect of the second group of the factors just mentioned, which determine the specific pressure, can be expressed in the form of a product of two quantities, of which the first takes into account the mean normal stress σ_2, whilst the second factor, n_σ, takes into account the effect of the rest of the stresses on the resistance to deformation:

$$p_m = \frac{2}{\sqrt{3 + \xi^2}} n_\sigma \sigma_a \qquad (V.3)$$

The first term on the right-hand side of this equation (see Chapter I, Section 14) varies from 1 to 1.15 as it depends on the ratio given by equation (I.66).

If the deformation is two-dimensional, that is, when the effect of spreading may be neglected and it may be assumed that $\sigma_2 = \frac{\sigma_1 + \sigma_3}{2}$, then

$$\frac{2}{\sqrt{3 + \xi^2}} = \frac{2}{\sqrt{3}} \approx 1.15$$

The second term in equation (V.3), n_σ, representing a coefficient of the state of stress, often exerts more influence on the specific pressure than the remaining coefficients. As will be shown, depending on the conditions of rolling and the external friction, it can vary between very wide limits (on the average from 0.8 to 8).

This coefficient can in turn be represented in the form of a product of three coefficients, in accordance with equation (II.76):

$$n_\sigma = n'_\sigma n''_\sigma n'''_\sigma \qquad (V.4)$$

where n'_σ is the coefficient taking account of the effect of external friction

n''_σ is the coefficient taking account of the effect of outer zones

n'''_σ is the coefficient taking into consideration the effect of tension.

The first two coefficients n'_σ and n''_σ are usually greater than unity but the third coefficient n'''_σ is less than unity and can reach 0.7 to 0.8 for large tensions.

If we take into account what has just been said and also equation (III.2), then the specific pressure on the rolls is

$$p_m = \frac{2}{\sqrt{3+\xi^2}} n_t n_{wh} n_v n_\sigma \sigma_s \qquad (V.5)$$

or

$$p_m = \frac{2}{\sqrt{3+\xi^2}} n'_\sigma n_\sigma n'''_\sigma \sigma_a \qquad (V.6)$$

In many cases the rolling process can be considered as a two-dimensional deformation; then

$$p_m = n_\sigma 2k \qquad (V.7)$$

where k is the resistance to pure shear, defined by equation (III.3).

2. DETERMINATION OF THE CONTACT AREA BETWEEN THE MATERIAL BEING ROLLED AND THE ROLLS

In order to calculate the pressure on the rolls from equation (V.2) it is necessary to know the area of the contact surface between the rolled metal and the rolls. At the same time it must be remembered that instead of substituting the actual contact area with the rolls into equation (V.2), one should use its projection on to the plane normal to the resultant of the pressure acting on the rolls. This area will be called the contact area. Since in the majority of cases of rolling the resultant of the pressure on the rolls is directed vertically or deviates but little from this direction, in practical calculations the quantity F in equation (V.2) is usually taken to be equal to the horizontal projection of the contact area.

As has been mentioned above, the contact area depends on the geometrical dimensions of the rolls and the rolled strip before it enters the rolls and after it emerges from them. Accordingly, when the reductions are known it can be determined without difficulty.

When sheets, bands, and all kinds of strips with rectangular cross section are rolled, i.e., when the rolls touch the metal being rolled only with their cylindrical surface, the contact area (of one roll) can be calculated from the equation

$$F = lb_m \qquad (V.8)$$

where l is the width of the zone of deformation, equal to AC (Fig. 172), and

b_m is the mean width of the rolled strip over the zone of deformation.

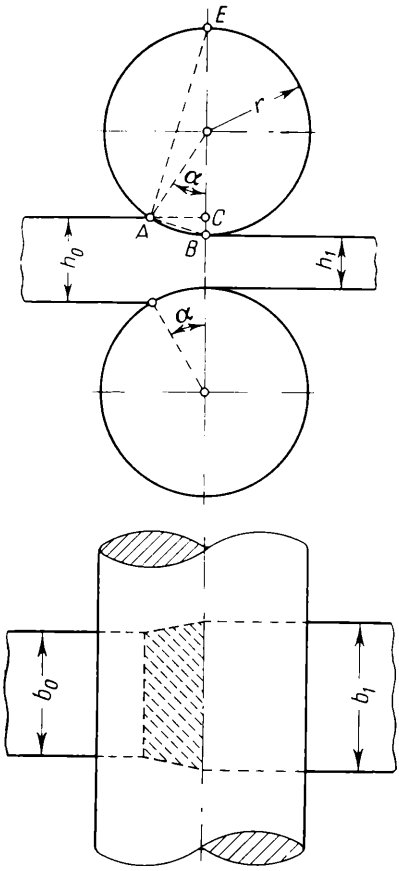

Fig. 172. Area of contact between rolled material and rolls

In the majority of cases we may assume that

$$b_m \approx \frac{b_0 + b_1}{2}$$

where b_0 and b_1 are the widths of the rolled strip at the entry to the rolls and at the exit from them.

If the edge of the rolled strip over the zone of deformation is approximated not by a straight line but by an arc of a parabola, then it will obviously be more accurate to take

$$b_m = b_0 + \frac{2}{3}(b_1 - b_0) \qquad (V.9)$$

When the angle of contact α is known the quantity l can be found from the equation

$$l = r \sin \alpha$$

Let us calculate l in terms of the reduction. From the triangle ABC we find

$$l = AC = \sqrt{AB^2 - BC^2} \qquad (V.10)$$

where

$$BC = \frac{\Delta h}{2}$$

The chord AB is found from the similarity of the triangles ABC and ABE:

$$\frac{AB}{BC} = \frac{BE}{AB}$$

whence

$$AB = \sqrt{r\Delta h}$$

Substituting these values of the segments BC and AB into equation (V.10) we obtain

$$l = \sqrt{r\Delta h - \frac{\Delta h^2}{4}} \qquad (V.11)$$

Since for the angles of contact used in practice the second term of the radicand is very small in comparison with the first one, the quantity l can be determined with sufficient accuracy for practical calculations from the equation

$$l = \sqrt{r\Delta h} \tag{V.12}$$

The contact area then is

$$F = b_m \sqrt{r\Delta h} \tag{V.13}$$

where b_m is the mean width of the section over the zone of deformation
r is the roll radius
Δh is the linear reduction.

If the diameters of the two rolls differ considerably (rolling mills of the Lauth type, for example), then the contact area for each roll is calculated from the equation

$$F = b_m \sqrt{\frac{2r_1r_2}{r_1 + r_2}\Delta h} \tag{V.14}$$

where r_1 and r_2 are the radii of the rolls.

This equation is based on the equality of pressures on the two rolls, and, consequently, the equality of contact areas of both rolls. We shall denote the reduction in the depth of the strip, effected by each roll, by z_1 and z_2. Equating the lengths of the arcs of contact of the rolls in accordance with equation (V.12) we obtain

$$\sqrt{2r_1z_1} = \sqrt{2r_2z_2} \tag{V.15}$$

whence

$$z_1 = \frac{r_2}{r_1} z_2$$

Since

$$z_1 + z_2 = \Delta h$$

then

$$z_1 = \frac{r_2}{r_1 + r_2}\Delta h$$

Substituting this value of z_1 into equation (V.15) we obtain equation (V.14).

When metal is rolled in section mills where the rolls have non-cylindrical working surfaces, for example, when a circle, an oval or a square is rolled into tee-pieces, angles or similar sections, the contact area is determined either graphically or analytically. In the graphical method the section of the roll together with the rolled part located on it is drawn in three projections and, plotting the lines of intersection of the roll and entering strip (Fig. 173), the contact

area is determined. For a more accurate determination of this area it is advisable to draw the section of the roll to an enlarged scale.

The contact area can also approximately be determined, when metal is rolled in non-rectangular section rolls, using equation (V.13) and taking Δh equal to the mean linear reduction over the width of section, i.e.,

$$\Delta h = \frac{Q_0}{b_0} - \frac{Q_1}{b_1} \qquad \text{(V.16)}$$

where Q_0 and Q_1 are the cross-sectional areas of the profile before and after rolling.

In such a calculation the following relations may be recommended for rhombic, square, oval and circular cross sections:

for a rhombus rolled from a rhombus (Fig. 174*a*)

$$\Delta h = (0.55 \text{ to } 0.6)(h_0 - h_1)$$

for an oval rolled from a square (Fig. 174*b*)

$$\Delta h = h_0 - 0.7h_1 \text{ (for a shallow oval)}$$

and

$$\Delta h = h_0 - 0.85h_1 \text{ (for a round oval)}$$

for a square rolled from an oval (Fig. 174*c*)

$$\Delta h = (0.65 \text{ to } 0.7)\, h_0 - (0.55 \text{ to } 0.6)\, h_1$$

for a circle rolled from an oval (Fig. 174*d*)

$$\Delta h = 0.85h_0 - 0.79h_1$$

where h_0 and h_1 refer to the depth of the cross section of the strip before and after the pass (see Fig. 174).

To calculate the contact surface in reducing section mills we can also recommend the formulas proposed by V. Drozd:

for a square rolled from an oval

$$F = 0.75b_1 \sqrt{r_1 (h_0 - h_1)}$$

for an oval rolled from a square

$$F = 0.54 (b_0 + b_1) \sqrt{r_1 (h_0 - h_1)}$$

for a rhombus or square rolled from a rhombus

$$F = 0.67b_1 \sqrt{r_1 (h_0 - h_1)}$$

where h_0 and h_1 are the depth at the middle of the cross section of the rolled strip before and after the pass respectively (see Fig. 174)

b_0 and b_1 are the greatest width of the cross section of the strip before and after the pass respectively

r_1 is the roll radius at the middle of the section.

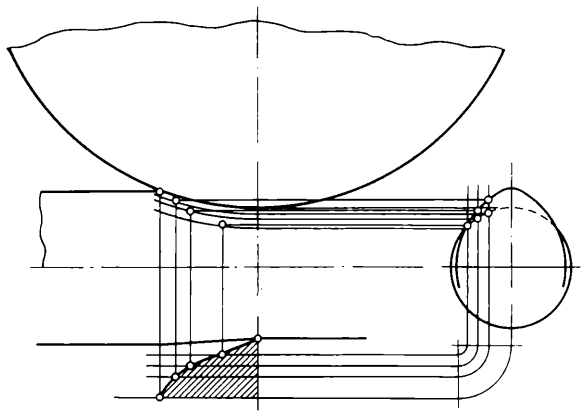

Fig. 173. Graphical determination of the contact area

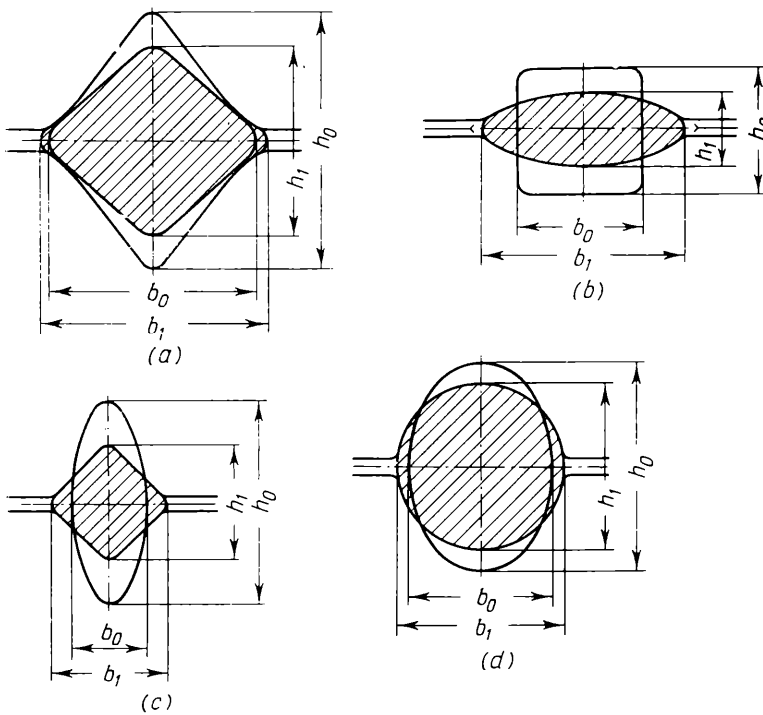

Fig. 174. Types of reduction effected by rolling:
(*a*) a rhombus; (b) an oval from a square; (*c*) a square from an oval; (*d*) a circle from an oval

In addition to these methods of determining the contact area, when rolling is carried out with section rolls having non-cylindrical working surfaces, other methods are used. Amongst these the method of corresponding strip, which has been worked out by N. Pavlov, is of greatest interest.

3. DETERMINATION OF THE CONTACT AREA WHEN THE ELASTIC DEFORMATION OF THE ROLLS AND ROLLED METAL IS TAKEN INTO ACCOUNT

Local elastic deformations of compression arise as a result of the pressure occurring between the rolled metal and the rolls.

During the cold rolling of steel and also other comparatively hard metals this elastic deformation, as a result of the high specific pressure, may be so large that it causes a considerable increase in the length of the arc of contact. This phenomenon has a particularly great significance during cold rolling of thin strips and bands with a small angle of contact.

In this case the formulas given above for the calculation of the contact area, which have been derived for an ideal, i.e., non-deformed roll, are no longer valid.

Let us determine the contact surface, taking into account not only the elastic deformation of the rolls but also that of the rolled metal.

We denote the local elastic deformation of the rolled metal by Δ_1 and that of the rolls by Δ_2, these quantities being measured along the line connecting the centres of both rolls (Fig. 175). For the rolled metal to receive the residual deformation Δh it is necessary that each roll approach the metal by an amount $\Delta_1 + \Delta_2$, and then the contact surface can be expressed by the line A_2B_2C.

The horizontal projection of this line can be found from the triangles A_2DO and B_1CO:

$$l = x_1 + x_2 = \sqrt{r^2 - (r - B_3D)^2} + \sqrt{r^2 - (r - B_1B_3)^2} \qquad (V.17)$$

Removing the parentheses in this equation we neglect the squares of the quantities B_3D and B_1B_3 owing to the fact that they are small in comparison with r. After the substitutions

$$B_3D = \frac{\Delta h}{2} + \Delta_1 + \Delta_2 \text{ and } B_1B_3 = \Delta_1 + \Delta_2$$

we obtain

$$l = x_1 + x_2 \approx \sqrt{2r\left(\frac{\Delta h}{2} + \Delta_1 + \Delta_2\right)} + \sqrt{2r(\Delta_1 + \Delta_2)} \qquad (V.18)$$

or

$$l \approx \sqrt{r\Delta h + x_2^2} + x_2 \qquad \text{(V.19)}$$

where

$$x_2 = \sqrt{2r(\Delta_1 + \Delta_2)} \qquad \text{(V.20)}$$

The magnitudes of the local deformation, Δ_1 and Δ_2, can be found using the known results of the theory of elasticity for the compression of two cylinders. If we neglect the absence of symmetry in the

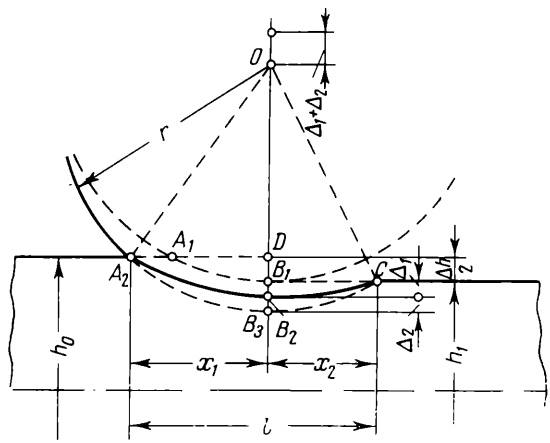

Fig. 175. Effect of the elastic compression of the rolls and the rolled metal on the length of the arc of contact

compression of these cylinders relative to the line which connects the centres, then the deformations Δ_1 and Δ_2 can be expressed as:

$$\Delta_1 = 2q\frac{1-\mu_1^2}{\pi E_1} \qquad \Delta_2 = 2q\frac{1-\mu_2^2}{\pi E_2} \qquad \text{(V.21)}$$

where q is the pressure per unit length of the compressed cylinders

μ_1 and μ_2 are the Poisson ratios of the metal of the roll and the rolled strip

E_1 and E_2 are the moduli of elasticity of the roll and the rolled metal.

Expressing the quantity q in terms of the specific pressure p on the contact surface

$$q = 2x_2 p$$

and substituting the values of Δ_1 and Δ_2 from equations (V.21) into equation (V.20), we obtain an expression from which the con-

tact surface can be determined with the elastic deformation of the rolls and the rolled strip taken into account:

$$x_2 \approx 8p\left(\frac{1-\mu_1^2}{\pi E_1}+\frac{1-\mu_2^2}{\pi E_2}\right)r \qquad (V.22)$$

When this value of x_2 is substituted into equation (V.19) the quantity l can be determined.

If the elastic deformation of the rolled strip is neglected when its thickness is small in comparison with the radii of the rolls, i.e., if we put $E_2 = \infty$ in this equation, we shall obtain the formula for the contact surface taking into consideration only the elastic compression of the rolls, known as the formula of Hitchcock:

$$x_2 = \frac{8(1-\mu^2)}{\pi E} rp \qquad (V.23)$$

where μ is the Poisson ratio of the material of the rolls
E is the modulus of elasticity
r is the radius of the roll
p is the specific pressure which the metal exerts on the rolls.

For steel rolls (if we assume that $E = 2.2 \times 10^4$ kg/mm^2 and $\mu = 0.3$), this equation can be expressed as:

$$x_2 \approx \frac{pr}{9,500}\text{ mm} \qquad (V.24)$$

When the elastic compression of tungsten carbide rolls is determined it is necessary to take into account the fact that their modulus of elasticity is approximately three times higher than that of steel rolls. When $E = 6.64 \times 10^4$ kg/mm^2,

$$x_2 \approx \frac{pr}{28,700}\text{ mm} \qquad (V.25)$$

Correspondingly the elastic compression of tungsten carbide rolls will be less than that of steel rolls.

4. DETERMINATION OF THE CONTACT AREA DURING RING ROLLING

We shall consider the rolling of a cylindrical ring between cylindrical rolls (Fig. 176). We shall assume that the contact area is the same for both rolls.

We denote the inner and outer radii of the original ring by r_i and r_o, and the linear reductions produced by the inner and outer rolls by Δr_1 and Δr_2 respectively. Let us first find the expression

for the arc of contact of the inner roll. From the triangles ABO and ABO_1 (Fig. 176)

$$l = AB = \sqrt{r_i^2 - (r_i - z_1)^2} \tag{V.26}$$

and

$$l = AB = \sqrt{r_1^2 - (r_1 - \Delta r_1 - z_1)^2} \tag{V.27}$$

where

$$z_1 = AO - BO$$

In the same manner from the triangles CEO and CEO_2 we find

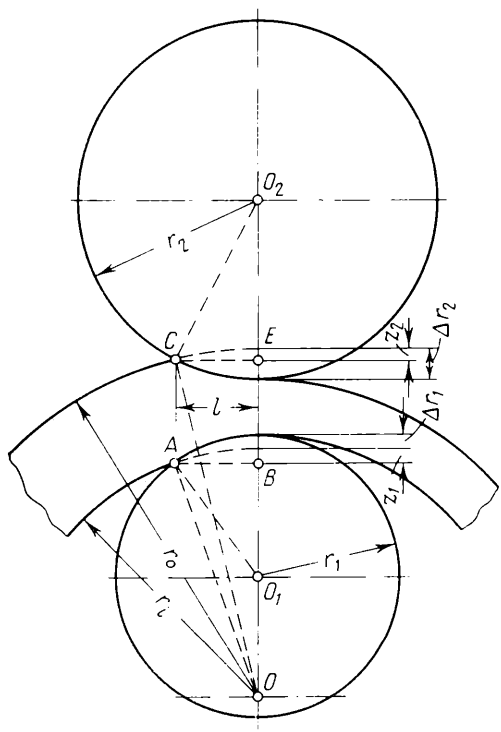

Fig. 176. Determination of the contact area during ring rolling

the expression for the arc of contact of the outer roll:

$$l = CE = \sqrt{r_o^2 - (r_o - z_2)^2} \tag{V.28}$$

and

$$l = CE = \sqrt{r_2^2 - (r_2 - \Delta r_2 + z_2)^2} \tag{V.29}$$

where

$$z_2 = OC - OE$$

To simplify the solution of these equations we neglect the squares of the quantities Δr_1, Δr_2, z_1 and z_2 in view of their smallness in comparison with the radii of the rolled ring and the rolls. Then

$$l = \sqrt{2r_i z_1} = \sqrt{2r_1(\Delta r_1 - z_1)} = \sqrt{2r_o z_2} = \sqrt{2r_2(\Delta r_2 - z_2)}$$

We first eliminate z_1 and z_2 from this equation:

$$l = \sqrt{\frac{2r_i r_1}{r_i - r_1}\Delta r_1} = \sqrt{\frac{2r_o r_2}{r_o + r_2}\Delta r_2} \qquad \text{(V.30)}$$

Taking into consideration that $\Delta r_1 + \Delta r_2 = \Delta h$ we express Δr_1 and Δr_2 in equation (V.30) in terms of Δh. We obtain then the final

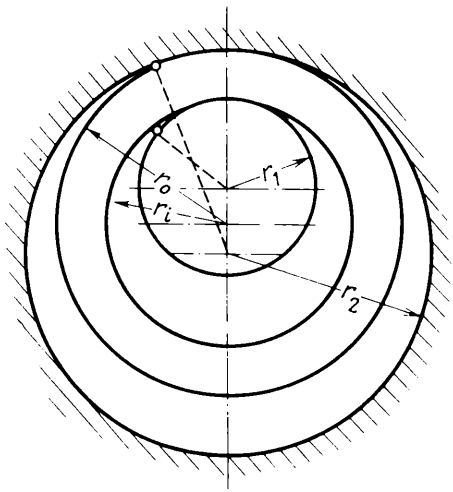

Fig. 177. Rolling a ring in a die

formula for l in the case of ring rolling as shown in Fig. 176:

$$l = \sqrt{\frac{2\Delta h}{\frac{1}{r_1} + \frac{1}{r_o} - \frac{1}{r_i} + \frac{1}{r_2}}} \qquad \text{(V.31)}$$

This formula can also be used to determine the contact surface when the outer roll is made in the form of a ring (die) touching the ring being rolled with its inner cylindrical surface (Fig. 177). This method of rolling is sometimes used in producing races for roller bearings.

In this case the sign of the curvature of the outer roll, $\frac{1}{r_2}$, in the formula (V.31) is obviously replaced by the opposite one. Then for the case of rolling represented in Fig. 177 we can express l as follows:

$$l \quad \sqrt{\frac{2\Delta h}{\frac{1}{r_1}+\frac{1}{r_o}-\frac{1}{r_i}-\frac{1}{r_2}}} \tag{V.32}$$

Comparing this formula with formula (V.31) we notice that, for the same reductions and the same radii of ring and rolls, the contact area for the rolling setup shown in Fig. 177 will be considerably larger than for the rolling setup of Fig. 176.

The formulas (V.12) and (V.14) derived above can also be obtained from equation (V.31) as particular cases. If we assume that

$$r_o = r_i = \infty$$

in this equation, then

$$l = \sqrt{\frac{2r_1r_2}{r_1+r_2}\Delta h}$$

i.e., we have obtained the formula (V.14).

If, however, we assume that $r_1 = r_2$, then we obtain the formula (V.12).

5. THE COEFFICIENT OF FRICTION BETWEEN THE ROLLED METAL AND THE ROLLS

The friction forces arising between the metal being rolled and the rolls have a great influence on the rolling process. Not only the allowed angle of contact and, consequently, the possible reduction depend on these friction forces, but also, as has been mentioned above, the forward slip and spreading depend on them.

On the one hand—when the conditions for the gripping of the rolled metal are considered—the friction forces are positive factors and the ordinary rolling process is not possible without them; on the other hand, with increasing friction forces, i.e., increasing coefficient of friction, the pressure exerted by the metal on the rolls increases, and together with this the expenditure of energy on rolling increases. Accordingly whenever the productivity of the mill is limited by the allowable angle of contact, we try in practice to make the coefficient of friction between the rolled metal and the rolls as high as possible. For this purpose, for example, the surface of the reducing section rolls is deliberately made uneven by knurling or welding on. But in those cases where the reduction is determined

not by the angle of contact but by the allowable pressure exerted by the metal on the rolls, as in cold rolling, for example, the surface of the rolls is polished and is lubricated during rolling.

The coefficient of friction between the rolled metal and the rolls depends not only on the state of the contact surfaces and the contact conditions (the quality of the rolled metal, the rolling temperature, the presence of oxides, the type of lubricant, the specific pressure, and the velocity of rolling) but also on the nature of the slip itself. Accordingly in the rolling process it is necessary to distinguish between three kinds of coefficient of friction, which differ markedly from each other under identical contact conditions and occur, respectively:

(1) during the gripping process;

(2) when the rolls slip over the entire contact surface;

(3) during the steady state motion when the slipping of the metal takes place in opposing directions about the neutral section.

The coefficient of friction during the gripping process is found by experimentally determining the limiting angle of contact, taking

$$\mu_{gr} = \tan \alpha_{max}$$

The coefficient of friction at the instant of gripping was studied by S. Ekelund for hot rolling of steel (0.15% C). He found the limiting angles of contact whilst rolling test pieces with a 10 × 225 mm cross section into a ribbed section using a sharp groove and raised rolls. On the basis of these tests S. Ekelund recommends the following formula for determining the coefficient of friction as a function of temperature (not less than 700°C):

$$\mu_{gr} = 1.05 - 0.0005t \qquad \text{(V.33)}$$

Table 8

The Coefficient of Friction During Hot Rolling of Non-Ferrous Metals at the Instant of Gripping (After A. Presnyakov)

Metal	Temperature, °C	Coefficient of friction
Copper	900	0.52
Brass		
Л62	800	0.45
Л68	800	0.38
German silver		
НМ 81	950	0.4
Nickel	1,100	0.4

For cast iron rolls with a hardened surface S. Ekelund suggests the following formula:

$$\mu_{gr} = 0.8\,(1.05 - 0.0005t) \qquad (V.34)$$

where t is the temperature of the metal during the rolling process.

The coefficients of friction at the instant of gripping during hot rolling of non-ferrous metals are given in Table 8.

According to the investigations of A. Grudev the coefficients of friction during the cold rolling of a low carbon steel (0.08% C) at the instant of gripping are as follows:

Condition of rolling	Coefficient of friction
Dry rolls	0.138 to 0.147
Lubricant:	
paraffin	0.147 to 0.154
emulsion (10% water solution of the commercial emulsifying agent B)	0.126 to 0.134

The surface of the rolls is polished; their peripheral velocity is 0.3 m/s.

According to a number of experimental investigations *the coefficient of friction during slipping and steady state motion* is lower than during gripping. This problem has been studied in detail by A. Grudev. From his test data, for cold rolling of a low carbon steel, the ratio of the coefficients of friction during gripping and slipping is as follows:

Condition of rolling	Mean value of the ratio $\frac{\mu_{gr}}{\mu_{sl}}$
Dry rolls	1.66
Lubricant:	
paraffin	2.85
emulsion	2.30

Comparing these results with the data given previously we notice that lubricant exerts a considerable effect on the coefficient of friction when the metal is in contact over the entire arc, and that it affects slightly the coefficient of friction during gripping.

The ratio of the coefficients of friction during gripping and slipping in the case of hot rolling of metal was investigated by V. Niko-

layev. For steel Ст. 3 at a rolling temperature 1,000 to 1,200°C the above-mentioned ratio obtained by him was

$$\frac{\mu_{gr}}{\mu_{sl}} = 1.25 \text{ to } 2.0$$

A. Presnyakov studied this problem for the hot rolling of non-ferrous metals.

There are three methods for the determination of the coefficient of friction during slipping. All these methods are based on controlling the conditions under which the transition takes place from the steady state rolling process to the process of slipping.

The first two methods consist in a gradual increase in the draft, bringing it up to the limiting value, when the rolls begin to slip along the metal. For this purpose either wedge-shaped test pieces are used or standard test pieces are rolled with simultaneous approach of the rolls to each other until slipping occurs. The coefficient of friction in this case is determined from the equation

$$\mu_{sl} = \tan(\psi\alpha_{max})$$

where α_{max} is the maximum angle of contact at which slipping occurs

ψ is the ratio of the angle β, giving the position of the point of application of the resultant of the pressure exerted by the metal on the rolls, to the angle α_{max}, i.e.,

$$\psi = \frac{\beta}{\alpha_{max}}$$

At the instant of slipping the distribution of the specific pressure over the arc of contact is nearly uniform (see Chapter II, Section 14) (Fig. 178) and therefore $\psi \approx 0.5$.

The third method of determining the coefficient of friction during slipping consists in stopping the rolling process as a result of applying an external force to the rolled metal, opposite to the direction of its motion. This method of determining the friction forces has been suggested by I. Pavlov.

In the third method the friction force is calculated from the equation of equilibrium, projecting all forces acting on the rolled metal on to the direction of its motion:

$$N\mu\cos\beta = N\sin\beta + \frac{R}{2}$$

where N is the normal component of the pressure exerted by the metal on the rolls

R is the braking force.

The third method of determining the coefficient of friction is considerably less accurate as compared with the previous methods, since owing to the presence of the force R there is a large non-uniformity in the distribution of the specific pressure over the arc of contact (over the trapezium) and accordingly $\beta \neq \frac{\alpha}{2}$.

This defect of the above-mentioned method of determining μ_{sl} was also pointed out by A. Korolev.

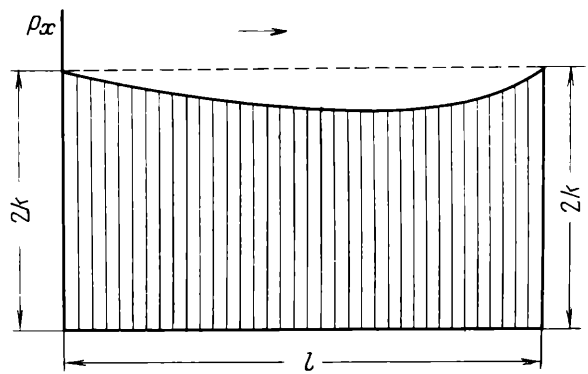

Fig. 178. Distribution of the specific pressure along the arc of contact when the roll slips on the rolled metal

An investigation into the coefficient of friction by the third method was carried out by N. Get for hot rolling of a steel containing 0.5 to 0.8% C. The values of the coefficient of friction obtained by him when $t > 700°C$ can be represented by the equation

$$\mu_{sl} = 0.55 - 0.00024t \qquad \text{(V.35)}$$

The coefficient of friction during steady state motion is determined by an indirect method from the magnitude of the forward slip, or it is determined by measuring directly the tangential forces on the contact surface.

The first of these methods, i.e., the determination of the coefficient of friction in terms of the forward slip, is approximate, since it has two considerable shortcomings:

(1) the law of the distribution of the tangential forces over the arc of contact is not known in its exact form, and consequently the existing formulas for the determination of the coefficient of friction from the forward slip are approximate;

(2) during cold rolling the local elastic compression of the rolls has a strong influence on the extent of the zone of forward slip. This

circumstance also strongly impedes the calculation of the coefficient of friction as dependent on the forward slip.

In spite of these shortcomings the method of determining the coefficient of friction from the forward slip has been widely used, owing to its simplicity.

Table 9 presents the data on the coefficient of friction, obtained by this method for hot rolling of steel.

Table 9

Coefficients of Friction During Hot Rolling of Steel at Different Temperatures and Velocities (After T. Golubev and M. Zaikov)

Temperature, °C	Coefficients of friction at rolling velocity, m/s				
	0.2	0.3-0.5	0.5-1.0	1.0-1.5	1.5-2.5
800	0.53-0.66	0.44-0.49	0.34-0.39	0.29-0.33	0.17-0.20
900	0.50-0.57	0.38-0.46	0.32-0.37	0.24-0.32	0.17-0.24
1,000	0.45-0.54	0.37-0.44	0.28-0.34	0.25-0.29	0.17-0.23
1,100	0.41-0.49	0.33-0.38	0.26-0.34	0.26-0.29	0.18-0.23
1,200	0.40-0.43	0.32-0.38	0.30-0.34	0.22-0.27	0.18-0.21

Several methods have been worked out to measure directly the contact tangential forces. Four of them are of most interest.

1. A simultaneous measurement of the projections of the specific pressure and friction forces by two load cells installed in the body of the roll and inclined in different directions with reference to the contact surface (Fig. 179). The ratio of the friction force to the normal force which is determined from the data of the two load cells can be expressed as:

$$\frac{\tau_x}{p_x} = \frac{P_1 \sin \alpha_1 - P_2 \sin \alpha_2}{P_1 \cos \alpha_1 + P_2 \cos \alpha_2}$$

where P_1 and P_2 are the loads on the load cells.

This method was suggested and used by A. Chekmarev and P. Klimenko. Using this method we can measure not only the value of the ratio of the friction force to the normal force, but we can also establish its distribution over the arc of contact.

2. As in the preceding case, the normal pressure on the roll and the friction forces are measured simultaneously, but a special force measuring roll is used as suggested by D. Piryazev. In this case a small segment is set in the body of the roll; by means of this the normal and tangential forces acting on it are measured as the segment enters the zone of deformation and as it emerges from it.

3. A direct and simultaneous measurement of the specific pressure and friction forces by means of a special load cell set in the body of the roll. This method was suggested and used by O. Muzalevsky and A. Grishkov. It is undoubtedly the most precise one, since using it we obtain the direct value of the friction force, and not only its magnitude and distribution over the arc of contact, but also the magnitude of the component of the friction force in the direction of the width of the rolled strip.

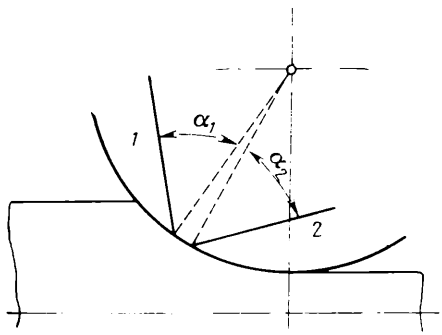

Fig. 179. Two load cells *1* and *2* inserted into the body of the roll, and inclined in different directions with reference to the contact surface (as suggested by A. Chekmarev and P. Klimenko)

4. Measurement of the friction forces from the torque on the roll whilst rolling with the zone of forward slip very close to zero. This method was proposed by D. Bland and H. Ford. The principle is that rolling is carried out with front and back tensions; by gradually increasing the back tension we can arrive at a process where the neutral section reaches the point of exit, with the result that the friction forces will act on the contact surface in the same direction. Measuring in this case the torque (M) on the roll and the resultant (P) of the pressure acting on the roll, its direction being normal to the roll surface, we can determine the coefficient of friction from the equation

$$\mu_{st} = \frac{M}{Pr}$$

where r is the radius of the roll.

This method of measuring friction forces was used by P. Whitton and H. Ford to investigate the coefficient of friction during cold rolling of steel and non-ferrous metals with different lubricants. In carrying out these investigations it was noticed that from the

instant when the forward slip is terminated and to the appearance of the negative value of this quantity (from 0 to —3%) the ratio $M : Pr$ is nearly unaltered (Fig. 180), and hence the results of the measurement are nearly constant. The value of the ratio $M : Pr$ in the

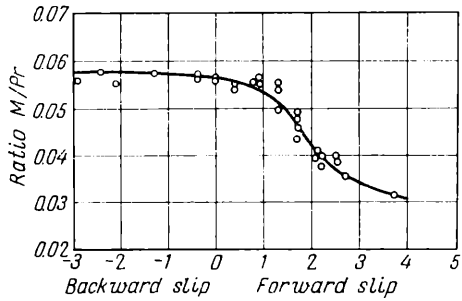

Fig. 180. Variation of the ratio $\frac{M}{Pr}$ with forward slip

right-hand side of the diagram falls owing to the reduced difference between the back and front tensions; here this ratio ceases to be equal to μ_{sl}. Tables 10 to 13 give the data on μ_{sl} during cold rolling of low carbon steel, copper, brass and aluminium obtained from the

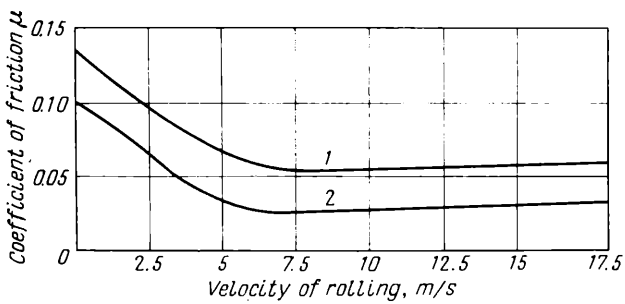

Fig. 181. Variation of the coefficient of friction with the velocity of rolling during the cold rolling of steel:
1—a mineral oil emulsion; *2*—a palm oil emulsion

above-mentioned investigations. The rolling was carried out on a two-high laboratory mill. The rolls are of steel, polished, with the diameter 100 mm; the velocity of rolling is 0.15 m/s.

When using tables 10 to 13 we must bear in mind that as the velocity of rolling increases the coefficient of friction diminishes (Fig. 181).

Table 10

Coefficient of Friction During the Rolling of Annealed Low Carbon Steel Under Different Conditions

Lubricant	No. of pass	Reduction per pass, %	Coefficient of friction
Clean, dry rolls and strip	1	15.0	0.085
Paraffin	1	16.5	0.080
Ditto	2	17.0	0.068
Ditto	3	22.0	0.060
Ditto + 1% stearic acid	1	16.7	0.075
Ditto + 1% stearic acid + 0.6% sulphur	1	17.0	0.071
Ditto + 5% copper stearate	1	16.8	0.063
Ditto + 5% sodium stearate	3	24.0	0.060
Ditto + 5% lead stearate	2	17.3	0.058
Ditto + 5% lead oleate	2	17.4	0.058
Ditto + 1% lauric acid	3	24.3	0.053
Ditto + 1% lauric acid	2	18.8	0.052
Ditto + 5% sodium oleate	4	23.0	0.049
Ditto + 1% palmitic acid	3	22.0	0.043
68/615 graphite in oil	1	15.5	0.072
615 graphite in oil	4	24.5	0.047
Vacuum:			
R0546	1	15.0	0.070
R0950	1	15.6	0.069
R040A	1	17.0	0.061
Shell:			
PE6	3	23.0	0.050
PE6	4	27.9	0.053
Esso Baywest	4	27.5	0.050
Esso Pale 885	3	24.0	0.052
Esso Paranox 108	2	21.4	0.054
Ditto	3	25.9	0.056
Oil:			
olive	2	18.1	0.057
castor	4	23.0	0.045
Lanoline	4	26.5	0.041
Camphor	4	27.2	0.038

Table 11

Coefficient of Friction During the Rolling of Pure Annealed Copper Under Different Conditions

Lubricant	No. of pass	Reduction per pass, %	Coefficient of friction
Clean, dry rolls and strip	1	29.0	0.093
Ditto	3	31.0	0.069
Ditto	4	12.4	0.071
Ditto	4	13.0	0.070

Table 11 (continued)

Lubricant	No. of pass	Reduction per pass, %	Coefficient of friction
Water	1	26.0	0.075
Paraffin	1	23.9	0.067
Ditto	3	31.5	0.068
68/615 graphite in oil	2	32.4	0.061
615 graphite in oil	3	36.8	0.054
Vacuum:			
R0950	1	26.9	0.059
R040A	1	23.7	0.054
R040A	2	35.0	0.056
R040A	3	38.7	0.061
Solvac	1	25.2	0.065
Ditto	2	26.0	0.064
Ditto	2	33.0	0.058
Oil:			
palm	1	26.85	0.076
ditto	1	26.9	0.075
ditto	1	25.1	0.074
ditto	2	28.4	0.066
olive	2	30.2	0.058
castor	3	34.1	0.046

Table 12

Coefficient of Friction During the Rolling of Annealed Brass Л63 Under Different Conditions

Lubricant	No. of pass	Reduction per pass, %	Coefficient of friction
Clean, dry rolls and strip	1	15.1	0.093
Paraffin	1	15.0	0.067
Water	1	29.2	0.061
68/615 graphite in oil	3	38.6	0.055
615 graphite in oil	2	27.8	0.049
Vacuum:			
R0950	4	22.2	0.052
R040A	3	22.4	0.059
Solvac	1	33.4	0.052
Ditto	2	28.8	0.049
Ditto	3	33.1	0.046
Oil:			
olive	1	33.8	0.057
ditto	5	28.0	0.055
Lanoline	6	28.0	0.043

Table 13

Coefficient of Friction During the Rolling of Annealed Aluminium Under Different Conditions

Lubricant	No. of pass	Reduction per pass, %	Coefficient of friction
Clean, dry rolls and strip	1	22.5	0.092
Ditto	2	22.9	0.101
Ditto	2	37.9	0.101
Ditto	2	22.0	0.100
Ditto	3	22.0	0.099
Paraffin	1	24.5	0.081
Ditto	2	21.3	0.087
Ditto	3	29.0	0.071
Ditto	3	28.3	0.069
Ditto+1% oleic acid	1	24.8	0.059
Ditto+5% calcium stearate	4	30.0	0.08
Ditto+5% sodium oleate	3	27.9	0.059
Ditto+5% lead oleate	3	27.5	0.056
Ditto+5% lead oleate+ +0.6% sulphur	2	30.0	0.049
615 graphite in oil	1	33.5	0.055
Vacuum R0546	3	30.0	0.082
Oil:			
palm	1	24.0	0.066
ditto	3	33.4	0.066
ditto	3	38.0	0.064
ditto	4	47.7	0.069
castor	3	21.6	0.057
Lanoline	4	25.4	0.025

6. ACCURATE METHOD FOR DETERMINING THE EFFECT OF EXTERNAL FRICTION ON THE PRESSURE OF THE METAL ON THE ROLLS

The effect of the friction forces arising on the contact surfaces, i.e., the external friction, on the specific pressure is taken into account by the coefficient n'_σ in equation (V.4).

For a two-dimensional deformation, when the effect of the width of the strip is neglected, this coefficient can be determined from the mean ordinate of the specific pressure distribution diagram over the arc of contact, as it depends on the external friction. Thus this problem must be solved by equation (V.2), substituting into it the functional relationship $p_x = f(x)$ in accordance with the theories of specific pressure considered above (see Chapter II, Section 8).

Since the law of distribution of the specific pressure depends on the ratio $l : h_m$, this problem must also be solved separately for different cases of rolling. Let us consider it first for the most complex specific pressure distribution diagram when the ratio $l : h_m > 5$ (see Fig. 53*a*), there being five regions on the arc of contact, characterized by the different laws of the specific pressure distribution.

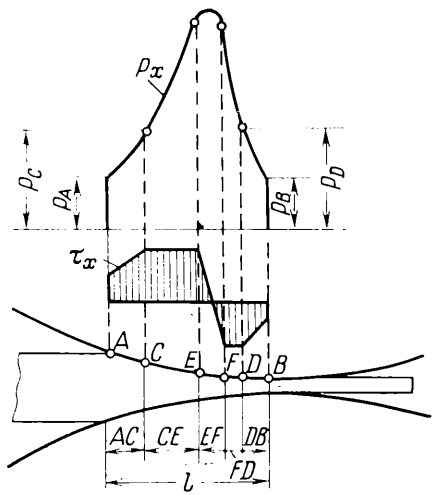

Fig. 182. Specific pressure p_x and contact shear stress τ_x

The coefficient of the stress state for such a specific pressure distribution diagram is found as the mean coefficient of the five regions:

$$n'_\sigma = \frac{n_{AC}AC + n_{CE}CE + n_{EF}EF + n_{FD}FD + n_{DB}DB}{l} \qquad \text{(V.36)}$$

where n_{AC}, n_{CE}, etc., are the partial coefficients of the stress state for the regions AC, CE, etc.

AC, CE, etc., are the lengths of the regions of the arc of contact (Fig. 182).

Each of the partial coefficients can be calculated if the functional relationship $p_x = f(x)$ corresponding to the given region is inserted into equation (V.3).

At the beginning and end of the arc of contact (the regions AC and DB) the quantity p_x is expressed by equations (II.60) and (II.61). After substituting this value into equation (V.3), and taking into consideration that

$$dx = \frac{l}{\Delta h}\, dh_x \quad \xi_0 = \xi_1 = 1$$

we obtain

$$n_{AC} = \frac{p_m}{2k} = \frac{l}{\Delta h \delta_{AC} AC} \int_{h_C}^{h_0} \left[(\delta_{AC} - 1) \left(\frac{h_0}{h_x} \right)^{\delta_{AC}} + 1 \right] dh_x \quad \text{(V.37)}$$

for the region AC, and

$$n_{DB} = \frac{p_m}{2k} = \frac{l}{\Delta h \delta_{DB} DB} \int_{h_1}^{h_D} \left[(\delta_{DB} + 1) \left(\frac{h_x}{h_1} \right)^{\delta_{DB}} - 1 \right] dh_x \quad \text{(V.38)}$$

for the region DB.

After integration

$$n_{AC} = \frac{l h_C}{\Delta h \delta_{AC} AC} \left[\left(\frac{h_0}{h_C} \right)^{\delta_{AC}} - 1 \right] \quad \text{(V.39)}$$

and

$$n_{DB} = \frac{l h_D}{\Delta h \delta_{DB} DB} \left[\left(\frac{h_D}{h_1} \right)^{\delta_{DB}} - 1 \right] \quad \text{(V.40)}$$

where h_C and h_D are the thicknesses of the rolled strip at the points C and D.

When n_{CE} and n_{FD} are to be determined, i.e., for the regions CE and FD, we substitute the value of p_x from equations (II.63) and (II.64) into equation (V.3). Then

$$n_{CE} = \frac{l}{2k \Delta h CE} \int_{h_E}^{h_C} \left(p_C + \frac{k}{\tan \varphi_{CE}} \log_e \frac{h_C}{h_x} \right) dh_x$$

and

$$n_{FD} = \frac{l}{2k \Delta h FD} \int_{h_D}^{h_F} \left(p_D + \frac{k}{\tan \varphi_{FD}} \log_e \frac{h_x}{h_D} \right) dh_x$$

After integration

$$n_{CE} = \frac{l}{\Delta h CE} \left\{ \frac{p_C}{2k} (h_C - h_E) + \frac{1}{2 \tan \varphi_{CE}} \times \right.$$
$$\left. \times \left[h_C - h_E \left(1 + \log_e \frac{h_C}{h_E} \right) \right] \right\} \quad \text{(V.41)}$$

and

$$n_{FD} = \frac{l}{\Delta h FD} \left\{ \frac{p_D}{2k} (h_F - h_D) + \frac{1}{2 \tan \varphi_{FD}} \times \right.$$
$$\left. \times \left[h_D - h_F \left(1 - \log_e \frac{h_F}{h_D} \right) \right] \right\} \quad \text{(V.42)}$$

For the zone of complete sticking EF the coefficient n_{EF} is determined by substituting the value of p_x from the expression (II.68) into equation (V.2):

$$n_{EF} = \frac{l}{2k\Delta hEF} \int_{h_F}^{h_E} \left\{ p_E + k \left[A(h_E - h_x) - (2 + Ah_n) \log_e \frac{h_E}{h_x} \right] \right\} dh_x$$

After integrating

$$n_{EF} \quad \frac{l}{\Delta hEF} \left\{ \left[\frac{p_E}{2k} - 1 - Ah_n + 2A(h_E - h_F) \right] (h_E - h_F) + \right.$$
$$\left. + (1 + Ah_n) h_F \log_e \frac{h_E}{h_F} \right\} \qquad (V.43)$$

Substituting the partial coefficients n_{AC}, n_{DB}, n_{CE}, n_{FD} and n_{EF} found from equations (V.39), (V.40), (V.41), (V.42) and (V.43) into equation (V.36) we calculate the value of the coefficient n'_σ in equation (V.4).

7. SIMPLIFIED METHODS OF DETERMINING THE EFFECT OF THE EXTERNAL FRICTION ON THE PRESSURE

The application of the method of determining n'_σ, which has been considered above, requires lengthy computations. Therefore simplified methods may be recommended for calculating the coefficient n'_σ.

For a ratio of $l : h_m$ somewhat greater than two, and particularly during cold rolling, the region of stagnation (see the region EF in Fig. 182) is comparatively small and the curvature of the specific pressure diagram may be neglected, i.e., we may assume that $EF = 0$ in equation (V.36) and $h_E = h_F = h_n$ in equations (V.41) and (V.42). In addition, if the ratio $l : h_m$ is not too large (not more than 4 to 5) we can also neglect the reduction in the pressure over the region CD in comparison with the results given by the theory of dry friction; for an approximate calculation the value of p_x can be taken over the whole arc of contact according to equations (II.34) and (II.35).

In this case we assume that in equations (V.39) and (V.40)

$$\delta_{AC} = \delta_{DB} = \delta = \mu \frac{\Delta h}{2l} \qquad h_C = h_D = h_n$$

and that after substituting the values of n_{AC} and n_{DB} thus obtained into equation (V.36)

$$n'_\sigma = \frac{h_n}{\delta \Delta h} \left[\left(\frac{h_0}{h_n} \right)^\delta + \left(\frac{h_n}{h_1} \right)^\delta - 2 \right] \qquad (V.44)$$

Expressing $\frac{h_0}{h_n}$ in terms of $\frac{h_n}{h_1}$ and proceeding from the condition that the specific pressures calculated from equations (II.34) and (II.35) are equal at the neutral section, i.e., when $h_x = h_n$, we obtain

$$\frac{1}{\delta}\left[(\delta-1)\left(\frac{h_0}{h_n}\right)^{\delta}+1\right]=\frac{1}{\delta}\left[(\delta+1)\left(\frac{h_n}{h_1}\right)^{\delta}-1\right] \quad \text{(V.45)}$$

from which

$$\left(\frac{h_0}{h_n}\right)^{\delta}=\frac{1}{\delta-1}\left[(\delta+1)\left(\frac{h_n}{h_1}\right)^{\delta}-2\right]$$

Substituting this value of $\frac{h_0}{h_n}$ into equation (V.44) we find that the coefficient which takes into account the effect of the external friction on the pressure exerted by the metal on the rolls can be expressed by the formula suggested by A. Tselikov in 1939:

$$\boxed{n'_{\sigma}=\frac{2h_n}{\Delta h\,(\delta-1)}\left[\left(\frac{h_n}{h_1}\right)^{\delta}-1\right]} \quad \text{(V.46)}$$

The mean specific pressure can be determined if we multiply both sides of this equation by $2k$, assuming that $n''_{\sigma} = n'''_{\sigma} = 1$:

$$p_m=2k\frac{2h_n}{\Delta h\,(\delta-1)}\left[\left(\frac{h_n}{h_1}\right)^{\delta}-1\right] \quad \text{(V.47)}$$

or

$$p_m=2k\frac{2h_1}{\Delta h\,(\delta-1)}\left(\frac{h_n}{h_1}\right)\left[\left(\frac{h_n}{h_1}\right)^{\delta}-1\right] \quad \text{(V.48)}$$

where $k \approx 0.57 n_t n_{wh} n_v \sigma_s$ in accordance with equation (V.5);

$$\delta=\mu\frac{2l}{\Delta h} \quad \text{(V.49)}$$

h_n is the depth of the rolled strip at the neutral section.

The quantity h_n entering into equations (V.46) and (V.48) can be found from equation (V.45). Carrying out certain transformations on it we obtain

$$\frac{h_n}{h_1}=\left\{\frac{1+\sqrt{1+(\delta^2-1)\left(\frac{h_0}{h_1}\right)^{\delta}}}{\delta+1}\right\}^{\frac{1}{\delta}} \quad \text{(V.50)}$$

The value of the ratio $\frac{h_n}{h_1}$ calculated from this equation is shown on the graph of Fig. 183.

To simplify the use of equation (V.46) or (V.47) in calculating the specific pressure, a diagram is shown in Fig. 184, plotted from

these equations and characterizing the dependence of the coefficient n'_σ on δ for different reductions.

According to this diagram the mean specific pressure increases considerably as the reduction, coefficient of friction and roll diameter are increased.

This method of calculation using equation (V.46) can overestimate the value of n'_σ for large coefficients of friction. In the case of hot

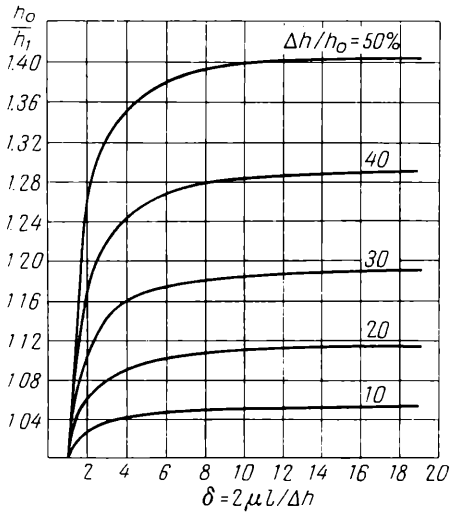

Fig. 183. Ratio $\frac{h_n}{h_1}$ as determined by equation (V.50)

rolling when the ratio $l : h_m$ equals more than 4 to 5, the regions CE and FD (Fig. 182) can be considerable; in this case a lesser error will be incurred in the calculation if we put $\tau_x = k$ and not $\tau_x = \mu p_x$ over the entire arc of contact.

Making these assumptions, we put

$$p_C = p_D = 2k$$

$$h_C = h_0 \qquad h_E = h_F = h_n \qquad h_D = h_1$$

$$\tan \varphi_{CE} = \tan \varphi_{FD} \approx \frac{\Delta h}{2l}$$

in equations (V.41) and (V.42).

We next find the value of h_n from the condition that the specific pressures calculated from equations (II.63) and (II.64) are the same for the neutral section:

$$p_n = 2k + k \frac{2l}{\Delta h} \log_e \frac{h_0}{h_n} = 2k + k \frac{2l}{\Delta h} \log_e \frac{h_n}{h_1}$$

from which

$$h_n = \sqrt{h_1 h_0} \qquad \text{(V.51)}$$

After substituting these values into equations (V.41) and (V.42) and determining n_{CE} and n_{FD} from equation (V.36) we find the

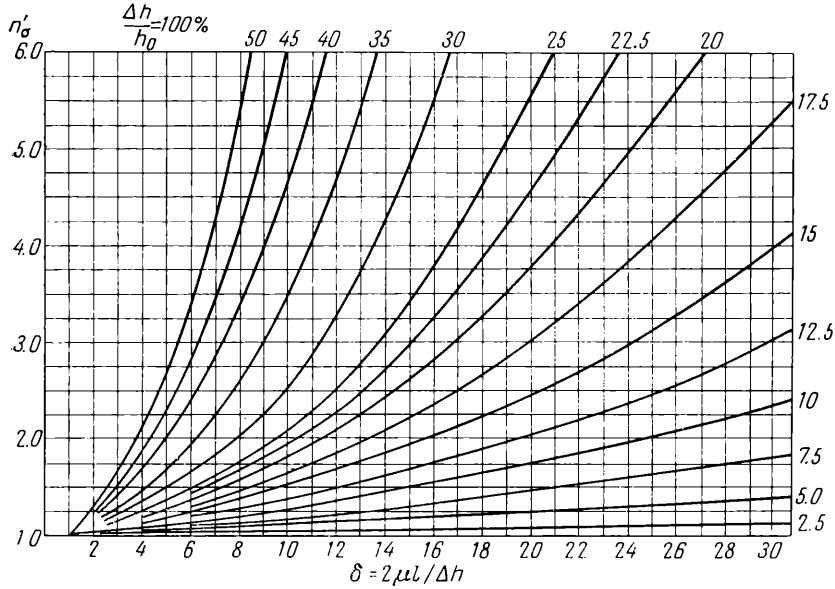

Fig. 184. Variation of the coefficient n'_σ, which determines the effect of external friction on pressure, with δ for various $\frac{\Delta h}{h_0}$

value of the coefficient of the stress state which takes into account the effect of the external friction

$$n'_\sigma = 1 + \frac{2l}{\Delta h} \times \frac{h_1 + \frac{\Delta h}{2} - h_n}{\Delta h} \qquad \text{(V.52)}$$

This equation is Unksov's formula which was derived by him for calculating the force when metal is compressed between two inclined plates.

During hot rolling when the ratio $l : h_m$ is approximately less than 1.5 to 2 the zones of slipping are small. In this case (see Fig. 53*c*) the diagram of the specific pressure will in the main be expressed by equation (II.68).

Then obviously the coefficient of the state of stress must be calculated putting $EF = l$ in equation (V.36); when h_{EF} is determined we must put

$$p_E = 2k \qquad h_E = h_0 \qquad h_F = h_1$$

in equation (V.43).

After substitution we have

$$n'_\sigma = (1 + Ah_n)\frac{h_1}{\Delta h}\log_e\frac{h_0}{h_1} + A(2\Delta h - h_n) \tag{V.53}$$

where, in accordance with equation (II.69),

$$A = \left(\frac{2l}{\Delta h}\right)^2 \frac{\eta}{2k} \tag{V.54}$$

We determine the quantity η from the assumption, recommended by A. Korolev, that at the point of entry the contact shear stress $\tau_x = k$.

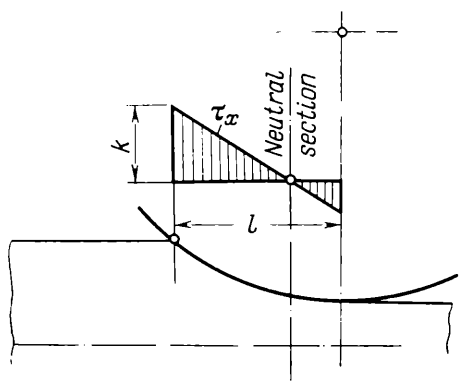

Fig. 185. Assumed distribution of the contact shear stresses during hot rolling when the ratio $l : h_m < \sim 1.5$

We further assume, as in the derivation of equation (II.67), that τ_x varies according to a linear law and at the neutral section $\tau_x = 0$ (Fig. 185).

Then

$$\tau_x = k\frac{h_x - h_n}{h_0 - h_n} \tag{V.55}$$

from which, in accordance with equation (II.58a),

$$\eta = k\frac{\Delta h}{l(h_0 - h_n)} \tag{V.56}$$

and after substituting η into equation (V.54)

$$A = \frac{2l}{\Delta h\,(h_0 - h_n)} \tag{V.57}$$

Substituting this value of A into equation (V.53) we obtain

$$n'_\sigma = \left[\left(1 + \frac{2l}{\Delta h}\,\frac{h_n}{h_0 - h_n}\right)\frac{h_1}{\Delta h}\log_e\frac{h_0}{h_1} + \frac{2l\,(2\Delta h - h_n)}{\Delta h\,(h_0 - h_n)}\right] \tag{V.58}$$

The quantity h_n can be found from the condition that $p_x = 2k$ in accordance with equation (II.68) when $h_x = h_1$.

To simplify the calculation we can with sufficient accuracy assume that

$$h_n = \sqrt{h_1 h_0}$$

It should be noted that for the ratio $\frac{l}{h_m} < 1.5$ to 2 the coefficient of the effect of the external friction is insignificant, and accordingly no large error is incurred if we take a value for this coefficient corresponding to compression of a prism, taking into consideration the similar law for the distribution of the contact shear stresses, i.e., assuming that $\tau_x = k$ at the boundaries and $\tau_x = 0$ at the centre.

Then

$$n'_\sigma = 1 + \frac{\sqrt{r\Delta h}}{3\,(h_0 + h_1)} \tag{V.59}$$

8. THE EFFECT OF THE TENSION ON THE PRESSURE OF THE METAL ON THE ROLLS

The effect of the tension on the pressure, according to the formula (V.6), is taken into account by the coefficient n''_σ. From the equation of plasticity the specific pressure decreases at least by $\frac{\sigma_0 + \sigma_1}{2}$ on the average owing to the tension, where σ_0 and σ_1 are the tensile stresses in the rolled metal at the entry and exit.

The above coefficient can be expressed approximately as:

$$n''_\sigma = C\left(1 - \frac{\sigma_0 + \sigma_1}{2p'_m}\right) \tag{V.60}$$

where p'_m is the mean specific pressure when the tension is absent

C is a coefficient a little less than unity, which takes into account the reduction in the effect of the external friction on the specific pressure owing to the tension.

For rolling, when the ratio $l : h_m$ is in the region of unity and the effect of the external friction on the pressure exerted by the

metal on the rolls is small, $C = 1$ and equation (V.60) may be recommended for practical calculations. At the same time it is necessary to bear in mind that the application of back tension is more effective in reducing the pressure of the metal on the rolls than the application of front tension.

During cold rolling of thin strips the reduction in the pressure, owing to the tension, is more pronounced due to the decrease in the effect of external friction and local elastic compression of the rolls. In this case the coefficient n''_σ should be calculated from the formulas (II.31) and (II.32) for the mean specific pressure.

The pressure exerted by the metal on the rolls, when the effect of the tension is taken into account, can be found from the area of the specific pressure diagram over the arc of contact (see Fig. 41). If the tension and the functional relationship $p_x = f(x)$ are known, then, with the assumptions made in deriving equation (V.46), the mean specific pressure is given by

$$p_m = \frac{2k}{\Delta h \delta}\left\{\int_{h_n}^{h_0}\left[(\xi_0\delta - 1)\left(\frac{h_0}{h_x}\right)^{\delta} + 1\right]dh_x + \right.$$
$$\left. + \int_{h_1}^{h_n}\left[(\xi_1\delta + 1)\left(\frac{h_x}{h_1}\right)^{\delta} - 1\right]dh_x\right\} \qquad (V.61)$$

The solution of this equation was given by the author; it leads, however, to cumbersome final formulas which are unsuitable for practical calculations. To obtain a simpler formula which enables the pressure of the metal on the rolls to be determined with the effect of tension taken into account, let us solve this problem by approximation.

The value p_x, as in the preceding method of solution, will be found from the differential equation derived above [see (II.13)] for the distribution of the specific pressure over the arc when slipping takes place with constant μ, and when the influence of the zone of sticking is neglected. To simplify the solution of equation (II.13) we assume that $2k \approx p_x$ in view of the smallness of $\tan \varphi_x$, and, consequently, of the first term in comparison with the second when thin strips and bands are cold rolled. Then equation (II.13) assumes the following form:

$$\frac{dp_x}{p_x} = (1 \mp \delta)\frac{dh_x}{h_x} \qquad (V.62)$$

where $\delta = \frac{2\mu l}{\Delta h}$.

After integrating we obtain

$$p_x = h_x^{1-\delta} C_0 \qquad (V.63)$$

for the zone of backward slip, and

$$p_x = h_x^{1+\delta} C_1 \tag{V.64}$$

for the zone of forward slip.

The quantities C_0 and C_1 are found from the condition that for $h_x = h_0$

$$p_x = \xi_0 2k$$

and for $h_x = h_1$

$$p_x = \xi_1 2k$$

Then

$$p_x = \xi_0 2k \left(\frac{h_0}{h_x}\right)^{\delta-1} \tag{V.65}$$

for the zone of backward slip, and

$$p_x = \xi_1 2k \left(\frac{h_x}{h_1}\right)^{\delta+1} \tag{V.66}$$

for the zone of forward slip,

where $\xi_0 = 1 - \frac{\sigma_0}{2k}$ and $\xi_1 = 1 - \frac{\sigma_1}{2k}$.

We substitute these values of p_x into equation (V.2):

$$p_m = \frac{2k}{\Delta h}\left[\int_{h_n}^{h_0} \xi_0 \left(\frac{h_0}{h_x}\right)^{\delta-1} dh_x + \int_{h_1}^{h_n} \xi_1 \left(\frac{h_x}{h_1}\right)^{\delta+1} dh_x\right] \tag{V.67}$$

After integrating we obtain the formula for determining the mean specific pressure with the effect of the tension and external friction taken into account:

$$p_m = \frac{2k}{\Delta h}\left\{\xi_0 \frac{h_0}{\delta-2}\left[\left(\frac{h_0}{h_n}\right)^{\delta-2} - 1\right] + \xi_1 \frac{h_1}{\delta+2} \times \right.$$
$$\left. \times \left[\left(\frac{h_n}{h_1}\right)^{\delta+2} - 1\right]\right\} \tag{V.68}$$

The quantity h_n appearing in this equation is found from equations (V.65) and (V.66), proceeding from the condition that for $h_x = h_n$,

$$p_x = \xi_0 2k \left(\frac{h_0}{h_x}\right)^{\delta-1} = \xi_1 2k \left(\frac{h_x}{h_1}\right)^{\delta+1}$$

from which

$$h_n = \sqrt[2\delta]{\frac{\xi_0}{\xi_1} h_0^{\delta-1} h_1^{\delta+1}}$$

If we take into account the effect of work hardening and assume that at the entry $k = k_0$ and at the exit $k = k_1$, then we can calcu-

late the specific pressure approximately from the formula

$$p_m = \frac{1}{\Delta h}\left\{\xi_0 2k_0 \frac{h_0}{\delta-2}\left[\left(\frac{h_0}{h_n}\right)^{\delta-2}-1\right]+\xi_1 2k_1 \frac{h_1}{\delta+2}\times\right.$$
$$\left.\times\left[\left(\frac{h_n}{h_1}\right)^{\delta+2}-1\right]\right\} \qquad (V.69)$$

Using a similar method and various simplifications several formulas have been derived for taking into account the effect of tension on the pressure of the metal on the rolls.

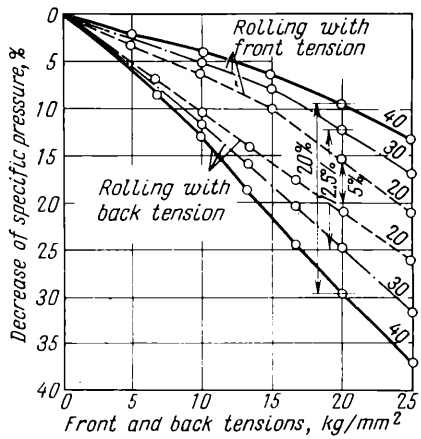

Fig. 186. The effect of back and front tensions on the decrease in the specific pressure during the cold rolling of steel strip for reductions of 20, 30 and 40% (W. Lueg and F. Schultze)

The effect of the tension on the pressure of the metal has been the subject of detailed experimental investigations. The results of these investigations confirm the correctness of the formulas (V.68) and (V.69). When the tension is increased a considerable reduction in the specific pressure is observed; at the same time application of the back tension results in a more effective reduction in the pressure as compared with the front tension (Fig. 186). Further, it is interesting to note that this difference in the effects of the back and front tensions on the pressure increases as the reduction increases, and, conversely, diminishes as the reduction is reduced. It follows from Fig. 187 that for rolling with a reduction of 20% the difference in the reduction of pressure as it depends on the back and front tensions is considerably less (about 5%) than for rolling with a reduction of 40%, when this difference amounts to 20%.

According to the data of W. Hessenberg and R. Sims, the specific pressure of the metal on the rolls, p_m, can be expressed as follows

when the effect of tension is taken into consideration:

$$p_m = p'_m \left(1 - \frac{\sigma_0 + \sigma_1}{4k}\right)$$

where p'_m is the mean specific pressure without tension.

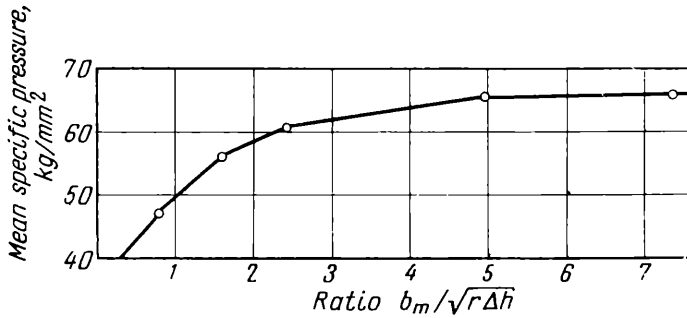

Fig. 187. The mean specific pressure during the cold rolling of steel (0.08% C) with a reduction of 20% for various ratios of the strip width to the length of the arc of contact ($h_0 = 2$ mm and $D = 184.7$ mm; the lubricant: an emulsion). The curve is plotted from the test results of W. Lueg and A. Pomp

Structurally this equation is similar to the equation (V.60) derived above; this confirms the possibility of finding by this method the approximate value of n''_σ, i.e.,

$$n''_\sigma = 1 - \frac{\sigma_0 + \sigma_1}{2p'_m} \qquad \text{(V.70)}$$

9. THE EFFECT OF THE WIDTH OF THE ROLLED STRIP ON THE PRESSURE

The nature of the effect of the width of the rolled strip on the specific pressure was considered in Chapter II, Section 15. From the diagrams of the specific pressure distribution over the width of the rolled strip, given earlier (see Figs. 77, 79 and 80), we can draw the conclusion that the mean specific pressure diminishes as the width is reduced. If the width of the strip is close to its depth or the length of the arc of contact, then obviously the specific pressure will be considerably less.

Thus, as the ratio of the width of the rolled strip to its depth or the length of the arc of contact is reduced, the remaining conditions being the same, the mean specific pressure of the metal on the rolls diminishes.

This phenomenon is confirmed by experimental investigations into the effect of the width of the rolled strip on the overall pressure of the metal on the rolls. During these investigations it was noticed that the effect of the width of the strip on the pressure manifests itself only when the width varies within definite limits and

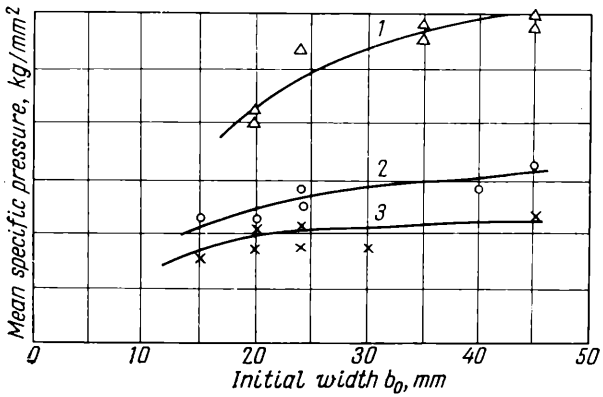

Fig. 188. The mean specific pressure during the hot rolling (1,050°C) of steel 45 with various reductions and for various ratios of the strip width to the length of the arc of contact; h_0 = 15 mm and D = 178 mm (A. Grishkov):

1—a reduction of 42.5%; *2*—a reduction of 23.5%; *3*—a reduction of 15%

when the ratio $b_m : l$ becomes approximately more than five; for a further increase in the width there is no change in the mean pressure (Figs. 187 and 188). In the tests of A. Grishkov (Fig. 188) the length of the arc of contact was:

$\frac{\Delta h}{h_0}$	l, mm
0.15	~14
0.235	~17
0.425	~24

Thus the ratio $b : l$ for a reduction of 15% did not exceed 3.2; for a reduction of 42.5% it did not exceed 1.9. Consequently, the curves could not reach the portion which is parallel to the axis of abscissas, but their character indicates that they are close to this portion.

The effect of the width of the strip on the mean specific pressure is largely explicable in terms of variation in the state of stress. As spreading takes place the specific pressure diminishes due to the

reduction in the stress σ_2 relative to $\frac{p_x + \sigma_x}{2}$ and as a result of the influence of the external friction.

In its general form the effect of the width of the strip can be represented as a product of two new coefficients n_b' and n_b'', supplementing the coefficient n_σ of the state of stress, whose values are less than unity:

$$p_m \quad n_b' n_b'' n_\sigma 2k \tag{V.71}$$

where n_b' takes account of the effect of σ_2
n_b'' takes account of the variation in the effect of the external friction in connection with spreading.

The first of these coefficients, n_b', affects the specific pressure according to equation (V.3) within the limits 1 to 1.15. When strips are rolled with free spreading and when the ratio $b : l \approx 1$, i.e., when there are favourable conditions for the metal to spread,

$$\sigma_2 \approx \sigma_3$$

and, in accordance with equation (V.3), we obtain

$$p_m \approx n_\sigma \sigma_a$$

where

$$p_m \approx \frac{n_\sigma 2k}{1.15}$$

As the width of the strip is increased or as its freedom to spread is reduced, the stress σ_2 increases and the coefficient ξ in equation (V.3) varies accordingly:

$$\xi = \frac{\sigma_2 - \frac{p_x + \sigma_x}{2}}{\frac{p_x - \sigma_x}{2}}$$

For two-dimensional deformation in the limit, σ_2 takes the value given by

$$\sigma_2 = \frac{p_x + \sigma_x}{2}$$

for this p_m increases by 15%.

Consequently, the first of the above-mentioned coefficients can be expressed as:

$$n_b' = \frac{\sqrt{3 + \xi^2}}{2} \tag{V.72}$$

where ξ is found from equation (I.66).

The influence of this coefficient on p_m was analyzed in more detail by A. Grishkov.

The second coefficient, n''_b, affects the mean specific pressure in a similar manner as over the width of a parallelepiped which is being compressed. In connection with this A. Dinnik recommends that the formula of S. Gubkin be used for this purpose, according to which the mean specific pressure during the compression of a parallelepiped is

$$p_m = 2k\left(1 + \frac{3b-a}{6b}\,\frac{\mu a}{h}\right) \tag{V.73}$$

where a and b are the dimensions of the sides of the parallelepiped, with $a < b$.

From this equation, comparing the specific pressure during the compression of the given parallelepiped and a parallelepiped with an infinitely large side b, we obtain approximately for the cases of rolling where $b > l$:

$$n''_b = \frac{1 + \frac{3b-l}{6b}\,\mu\,\frac{l}{h}}{1 + \mu\,\frac{l}{2h}} \tag{V.74}$$

where b and h are the mean width and depth of the cross section of the rolled strip

l is the length of the arc of contact, corrected for the condition under which the compression takes place; it can be determined from the equation

$$l = \sqrt{r\Delta h}\left(1 - \frac{\tan\frac{\alpha}{2}}{\mu}\right) \tag{V.75}$$

As has been mentioned above, for rolling of metal when $l : h_m < 2$ the slip along the surface of the rolls is nearly absent. If we assume as an approximation that

$$\mu = 0.5$$

we obtain

$$n''_b = \frac{1 + \frac{3b-l}{3b}\,\frac{l}{4h}}{1 + \frac{l}{4h}} \tag{V.76}$$

Summarizing the above we must point out that for rolling with free spreading in a smooth barrelled or grooved rolls, when the ratio

$$\frac{b_m}{\sqrt{r\Delta h}} < 5$$

the effect of spreading on the pressure must be taken into account, by reducing the coefficient of the state of stress by multiplying it by n_b' and n_b'', the values of which are found from equations (V.72) and (V.74).

10. EKELUND'S FORMULA

S. Ekelund (Sweden), proceeding from his experimental results, suggested the following formula for the calculation of the specific pressure of the metal on the rolls:

$$p = (1 + m)(2k + \eta u) \text{ kg/mm}^2 \qquad \text{(V.77)}$$

where m is a coefficient characterizing the effect of the external friction on the specific pressure

$2k$ is the specific resistance in static compression, which obviously corresponds to $1.15k_f$, kg/mm^2

η is the viscosity of rolled metal, kg sec/mm^2

u is the strain rate, sec^{-1}.

The first term $(1 + m)$ of this equation takes account of the increase in the resistance to deformation as a result of the friction of the rolled metal along the surface of the rolls. The coefficient m in this term was determined by S. Ekelund from the theory of maximum shear stress, assuming that the specific friction forces in the zone of backward slip are given by $\tau_x = \mu p_x$, whilst in the zone of forward slip they are $\tau_x = k$. To calculate this coefficient he gives the following equation:

$$m = \frac{1.6\mu\sqrt{r(h_0 - h_1)} - 1.2(h_0 - h_1)}{h_0 + h_1} \qquad \text{(V.78)}$$

where r is the radius of the roll.

The second term of equation (V.77) represents the resistance to deformation when external friction in the direction of rolling is absent (when $\sigma_2 = \frac{\sigma_1}{2}$ and $\sigma_3 = 0$); the product ηu in this term takes account of the effect of velocity on the resistance to deformation.

S. Ekelund expressed the strain rate by the formula

$$u \approx \frac{2v\sqrt{\frac{\Delta h}{r}}}{h_0 + h_1} \qquad \text{(V.79)}$$

After substituting the values of m and u found from equations (V.78) and (V.79) into equation (V.77), and multiplying both sides

of the equation by the contact area, we obtain Ekelund's formula in its complete form, which expresses the overall pressure exerted by the metal on the rolls during the rolling process:

$$P = \frac{b_0 + b_1}{2} \sqrt{r(h_0 - h_1)} \left[1 + \frac{1.6\mu \sqrt{r(h_0 - h_1)} - 1.2(h_0 - h_1)}{h_0 + h_1} \right] \times$$

$$\times \left[2k + \frac{2\eta v \sqrt{\frac{h_0 - h_1}{r}}}{h_0 + h_1} \right] \text{ kg} \quad \text{(V.80)}$$

where b_0 and b_1 represent the width of the rolled strip before and after rolling, mm

v is the peripheral velocity of the rolls, mm/s.

The values of $2k$ and η in this equation were determined by S. Ekelund only for heated steel, by comparing the results obtained from this formula with the test data. From this comparison he derived the following empirical formulas for $2k$ and η:

$$2k = (14 - 0.01t)(1.4 + \text{C} + \text{Mn}) \text{ kg/mm}^2 \quad \text{(V.81)}$$

$$\eta = 0.01(14 - 0.01t) \text{ kg sec/mm}^2 \quad \text{(V.82)}$$

where t is the rolling temperature, °C

C is the carbon content, %

Mn is the manganese content, %.

These equations are valid for temperatures $\geqslant 800$°C and manganese content $\leqslant 1\%$.

To calculate the coefficient of friction S. Ekelund recommends the formulas (V.33) and (V.34) derived by him.

Subsequently corrections were introduced into Ekelund's formula, according to which the viscosity was determined from the equation

$$\eta = 0.01(14 - 0.01t)C \text{ kg sec/mm}^2$$

where C is a coefficient depending on the velocity of rolling, the values of which are given below:

Velocity of rolling, m/s	Coefficient C
Up to 6	1
6 to 10	0.8
10 to 15	0.65
15 to 20	0.60

For the calculation of the value of $2k$ a formula is recommended, in which besides the influence of carbon and manganese on the resistance to deformation, the influence of chrome is also taken into account,

$$2k = (14 - 0.01t)(1.4 + C + Mn + 0.3Cr) \qquad (V.83)$$

where Cr is the chrome content, %.

There are, however, no data available on the applicability of this formula. Apparently this formula is suitable for steel containing no more than 2 to 3% Cr.

Ekelund's formula was derived in 1927 and is one of the first serious attempts to express the pressure of the metal on the rolls by a single equation which, as far as possible, would take into account the basic factors affecting this pressure. According to this formula the specific pressure depends not only on the mechanical properties of the rolled metal, but also on the strain rate, coefficient of external friction and the ratio of the length of the arc of contact to the mean depth of the rolled strip.

But in spite of this feature Ekelund's formula should not in any way be regarded as solving the problem of the determination of the pressure of the metal on the rolls. In analyzing the formula itself and its derivation we note that it has a number of shortcomings, due to which results obtained from this formula sometimes deviate markedly from the experimental data.

The shortcomings of Ekelund's formula are the following:

(1) the first term of the formula $(1 + m)$ is calculated approximately, and hence the role of the external friction is not determined with sufficient accuracy;

(2) the effect of the tension on the pressure exerted by the metal on the rolls is not taken into account at all;

(3) the viscosity is determined only tentatively;

(4) the influence of carbon and other constituents on the resistance to deformation of steel is allowed for not quite correctly; for example, the increase in the ultimate strength of the steel with an increase in carbon, obtained from the formula, when the temperature exceeds 900°C, disagrees with the test data given above.

In spite of these shortcomings Ekelund's formula still gives relatively correct results for hot rolling of low carbon structural steel. This is explained mainly by the fact that the quantities $2k$ and η in this formula were calculated from the test data of J. Puppe.

To a certain degree of approximation Ekelund's formula can also be used for the rolling of other metals, if the values of $2k$ and μ corresponding to the given rolling conditions are substituted into the formula.

11. GELEJI'S METHOD

To calculate the pressure exerted by the metal on the rolls during rolling A. Geleji (Hungary) suggested a formula whose original form was the following:

$$k_m = k_f \left(1 + C\mu \frac{l_d}{h} \sqrt[n]{v}\right) \qquad \text{(V.84)}$$

where k_m is the mean specific pressure, kg/mm²
k_f is the resistance to linear deformation (the quantity corresponding to σ_a), kg/mm²
C is an experimental coefficient, initially recommended to be taken as equal to 5.5, but subsequently depending on the $l_d : h$ ratio, and determined from a graph (Fig. 189)
μ is the coefficient of friction
$\sqrt{r\Delta h} = l$ is the length of the arc of contact
n is an index, taken to be equal to four
v is the peripheral velocity of the rolls, m/s.

The value of the coefficient C, shown in Fig. 189, was obtained by A. Geleji by analyzing a series of test results, principally the data of O. Emicke.

For the determination of the value k_f for hot rolling of plain carbon steels A. Geleji recommends the formula

$$k_f = 0.015\,(1{,}400 - t) \text{ kg/mm}^2 \qquad \text{(V.85)}$$

or the use of Ekelund's equation (V.83).

For a more exact determination of k_f A. Geleji also recommends that the graph shown in Fig. 190 be used.

A. Geleji recommends that the coefficient of friction be determined from the equations:

$$\mu = 1.05 - 0.0005t - 0.056v \qquad \text{(V.86)}$$

for steel rolls,

$$\mu = 0.94 - 0.0005t - 0.056v \qquad \text{(V.87)}$$

for hardened cast iron rolls, and

$$\mu = 0.82 - 0.0005t - 0.056v \qquad \text{(V.88)}$$

for polished steel or hardened cast iron rolls,
where v is the peripheral velocity of the rolls, m/s
t is the rolling temperature, °C.

These formulas are valid for $t > 700$°C and $v < 5$ m/s.

Subsequently A. Geleji has suggested an improved method for the determination of the pressure of the metal on the rolls. The main

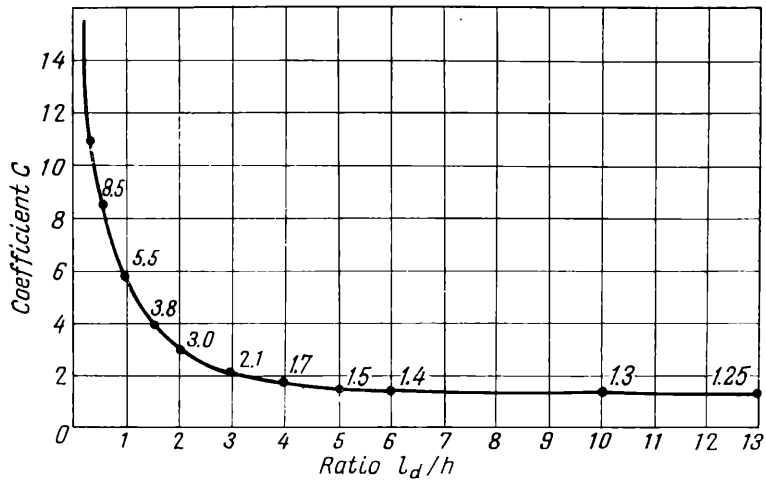

Fig. 189. Variation of the value of the coefficient C in formula (V.84) with the ratio $l_d : h$ (A. Geleji)

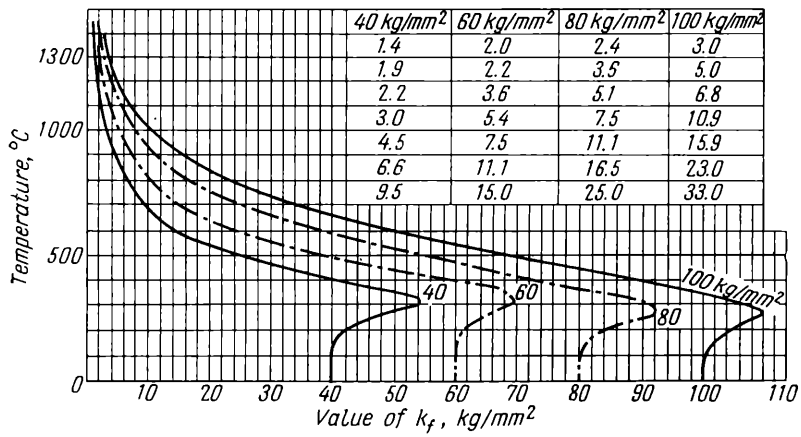

Fig. 190. Variation with temperature of k_f of a plain carbon steel (C $<$ 0.6%; Si $<$ 0.5% and Mn $<$ 0.8%), characterized by ultimate strengths of 40, 60, 80 and 100 kg/mm² in the cold state (A. Geleji)

point of this method is that the value of the pressure is calculated by determining the area of the specific pressure distribution diagram over the arc of contact, dividing it into seven separate elements (Fig. 191) and subsequently summing according to the formula

$$k_m = \frac{T_1 + T_2 + T_3 + T_4 + T_5 + T_6 + T_7}{l_d}$$

where k_m is the mean specific pressure
l_d is the horizontal projection of the arc of contact
T_1, T_2, etc., are the areas of the individual elements of the specific pressure distribution diagram (Fig. 191), given by the equations:

$$\left.\begin{aligned} T_1 &= \frac{k_{f_1} + k_{x_{01}}}{2} x_{01} \\ T_2 &= k_{x_{01}} (x_1 - x_{01}) \\ T_3 &= \frac{2}{3} (k_{x\,max} - k_{x_{01}}) (x_1 - x_{01}) \\ T_4 &= \frac{k_{f_2} + k_{x_{02}}}{2} x_{02} \\ T_5 &= k_{x_{02}} (x_2 - x_{02}) \\ T_6 &= \frac{2}{3} (k_{x\,max} - k_{x_{02}}) (x_2 - x_{02}) \\ T_7 &= k_{sm} l_d \end{aligned}\right\} \quad \text{(V.89)}$$

where x_{01} and x_{02} are the line segments determining the boundaries between the zones of slipping and sticking (Fig. 191)
x_1 and x_2 are the lengths of the zones of backward slip and sticking
k_{f_1} and k_{f_2} are the resistances to linear deformation at entry to the rolls and at exit respectively
$k_{x_{01}}$ and $k_{x_{02}}$ are the resistances to deformation on the boundaries of the zones of slipping and sticking
$k_{x\,max}$ is the maximum value of the resistance to deformation
k_{sm} is the supplementary mean resistance to deformation.

In developing the above method A. Geleji assumed that the total pressure of the metal on the rolls is made up of two parts: the pressure necessary for the proper reduction of the metal and the pressure expended to overcome the internal shear in the metal.

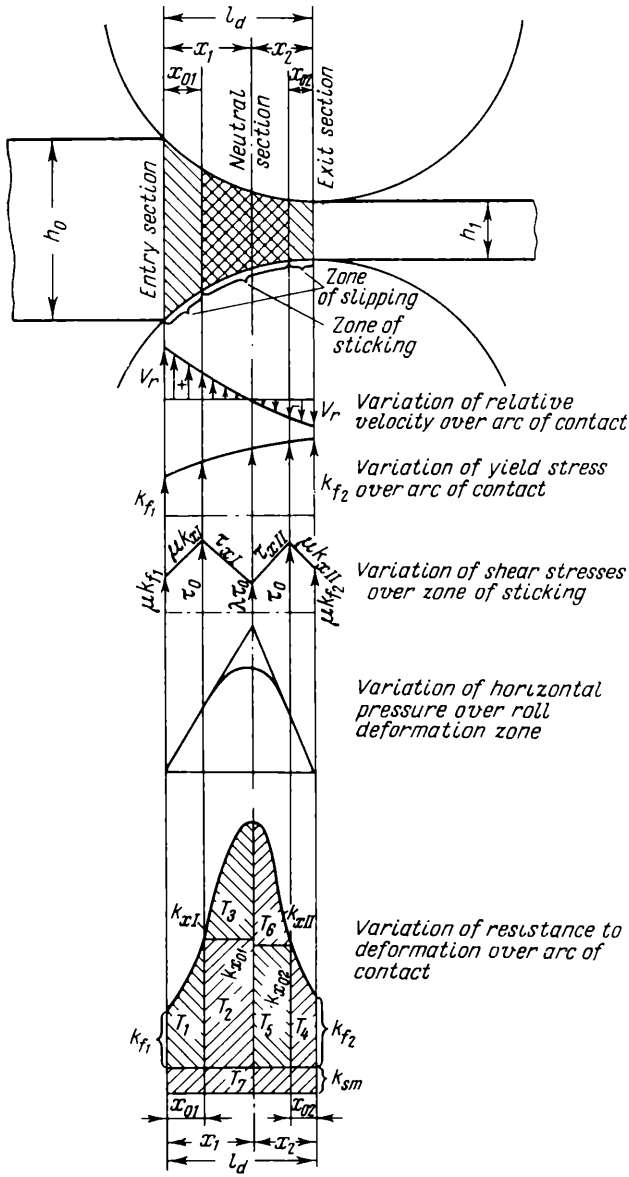

Fig. 191. Determination of the pressure exerted by the metal on the rolls by summing component areas of the specific pressure diagram (A. Geleji)

Therefore, according to A. Geleji, the mean resistance to deformation is

$$k_m = k_{\alpha m} + k_{sm}$$

where $k_{\alpha m}$ is the mean resistance to deformation when the metal is compressed

k_{sm} is the supplementary mean resistance to deformation, caused by "internal shear".

This division of the resistance to deformation into two components is apparently quite arbitrary, and it should be understood that $k_{\alpha m}$ takes account of the resistance to the external friction, and k_{sm} takes account of the supplementary resistance to the internal shear. For the calculation of k_{sm} the formula below is recommended

$$k_{sm} = \frac{2}{3\sqrt{3}} k_f \frac{l_d}{r} \times \frac{h_1}{\Delta h} \qquad \text{(V.90)}$$

where r is the radius of the roll.

The lengths x_{01} and x_{02} are determined from the condition that on the boundaries of the zones of slipping and sticking the shear contact stresses are

$$\tau_0 = k_x \mu = 0.58 k_f$$

The value of k_x (p_x) in the zones of slipping is found in accordance with the theory of dry friction, whilst in the sticking zone it is determined from the linear law of variation of friction forces, shown diagrammatically in Fig. 191. At the same time it is assumed that at the neutral section

$$\tau = \lambda \tau_0 \approx 0.5 \tau_0$$

The remaining quantities appearing in equation (V.89) are found by the usual methods.

It should be pointed out that this method of calculating the pressure suggested by A. Geleji is correct in principle and, indeed, the most precise method, since it takes into account the largest number of factors having an effect on the pressure. We cannot, however, agree with A. Geleji that the maximum specific pressure coincides with the neutral section and that the specific friction forces at this section are non-zero. It has been shown above that the maximum specific pressure is somewhat displaced from the neutral section opposite to the direction of rolling, whilst the friction forces at the neutral section are zero.

12. THE FORMULA OF SIMS

This formula was proposed by Sims (England) in 1954. It is derived by solving the differential equation of equilibrium of an element [see equation (II.5)] isolated from the metal being rolled (see Fig. 35)

$$\frac{d(\sigma_x h_x)}{dx} = 2(p_x \tan\varphi_x \mp \tau_x) \tag{V.91}$$

where the minus sign refers to the zone of backward slip.

The values in this equation are:

$$dx \approx r\,d\varphi \quad \tan\varphi_x \approx \varphi \quad \sigma_x h_x = T_x$$

where T_x is the longitudinal force arising in the metal being rolled as a result of the stress σ_x.

Next we obtain

$$\frac{dT_x}{d\varphi} = 2r p_x \varphi \mp 2r\tau_x \tag{V.92}$$

Proceeding further R. Sims makes two assumptions:

(1) sticking takes place over the entire arc of contact and consequently

$$\tau_x = \pm k$$

when the direction of τ_x changes at the neutral section;

(2) the force T_x, using the results of E. Orowan for a body compressed between two inclined rough plates, is taken equal to

$$T_x = h_x\left(p_x - \frac{\pi}{2}k\right) \tag{V.93}$$

It should be noted that the first assumption gives only an approximate value of the friction forces close to the neutral section; neither is it exactly true for a large $l : h_m$ ratio (roughly > 4) at the beginning and at the end of the arc of contact, where slipping occurs.

The second assumption is in principle analogous to the assumption made in deriving the differential equation of specific pressure (II.12) with the only difference that then the mean value of the stress across the depth of the cross section, from the plasticity equation, was taken equal to [see equation (II.8)]:

$$\sigma_x = p_x - 2k$$

In the given case, in accordance with equation (V.93), Sims assumes that this stress is

$$\sigma_x = \frac{T_x}{h_x} = p_x - \frac{\pi}{4}2k \approx p_x - 0.785(2k) \tag{V.94}$$

Thus for a given value of σ_x, which in the present case depends on the contact stresses τ_x and the boundary conditions, the stress p_x according to the results given above equals

$$p_x = \sigma_x + 2k$$

whilst in his results Sims has taken

$$p_x = \sigma_x + 0.785\,(2k)$$

i.e., 0 to 21.5% less than in the case of simple compression. It is doubtful whether this assumption can be considered well grounded.

It should further be pointed out that the two assumptions made by Sims in the derivation of his formulas are incompatible and contradict each other.

If we assume—as Sims does—that the contact shear stresses are

$$\tau_x = k$$

then in this case the position of the contact surface relative to the direction of the principal axes of stress is given by the top of the circle (see Fig. 19). Consequently, the value of the normal stress (p_x) on this plane and that of the stress (σ_x) perpendicular to it must be the same:

$$p_x = \sigma_x$$

We can arrive at the same result, analyzing the equation of plasticity (I.70) for two-dimensional deformation:

$$\left(\frac{p_x - \sigma_x}{2}\right)^2 + \tau_x^2 = k^2$$

From this it follows that when $\tau_x = k$

$$p_x - \sigma_x = 0$$

i.e., in solving equation (V.92) Sims is not justified in using the result of E. Orowan.

It should have been assumed that

$$T_x = h_x p_x$$

After substituting $\tau_x = k$, T_x from the expression (V.93) and $h_x \approx h_1 + r\varphi^2$ into equation (V.92), and assuming the value of k constant over the arc of contact, we obtain

$$(h_1 + r\varphi^2)\,dp_x + \left(p_x - \frac{\pi}{2}k\right) 2r\varphi\,d\varphi = 2r p_x \varphi\,d\varphi \mp 2rk\,d\varphi$$

or

$$dp_x = \frac{\pi\varphi \mp 2}{h_1 + r\varphi^2}\,rk\,d\varphi \qquad \text{(V.95)}$$

After integrating with the initial conditions $\varphi = 0$, $\varphi = \alpha$ and $p_x = 2k$ we obtain

$$\frac{p_x}{2k} = \frac{\pi}{4} \log_e \frac{h_x}{h_0} + \frac{\pi}{4} + \sqrt{\frac{r}{h_1}} \tan^{-1}\left(\sqrt{\frac{r}{h_1}}\,\alpha\right) - \sqrt{\frac{r}{h_1}} \tan^{-1}\left(\sqrt{\frac{r}{h_1}}\,\varphi\right) \qquad \text{(V.96)}$$

for the zone of backward slip, and

$$\frac{p_x}{2k} = \frac{\pi}{4} \log_e \frac{h_x}{h_1} + \frac{\pi}{4} + \sqrt{\frac{r}{h_1}} \tan^{-1}\left(\sqrt{\frac{r}{h_1}}\,\varphi\right) \qquad \text{(V.97)}$$

for the zone of forward slip.

It should be pointed out that these equations are analogous to equations (II.41) and (II.42) which were published in 1946 by

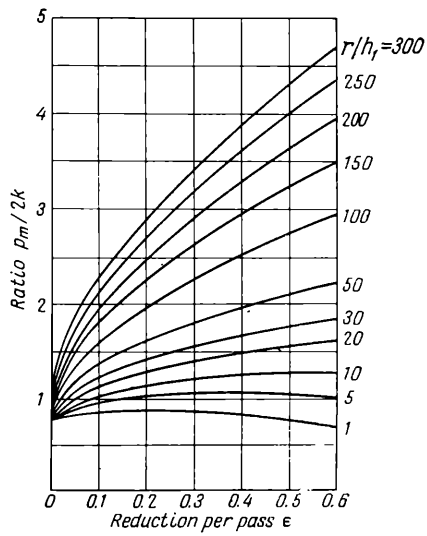

Fig. 192. Variation of the ratio $\frac{p_m}{2k}$ with reduction for various ratios $r : h_1$, according to the formula of Sims (V.99)

A. Tselikov. If in equations (II.41) and (II.42) we put $\xi_0 = \xi_1 = 1$, introduce the factor $\frac{\pi}{4}$ in front of $2k$ and set $\tau = k$, then they will be identical.

Substituting the above values of $\frac{p}{2k}$ into equation (V.2):

$$p_m = \frac{2kr}{F} \int_0^{\alpha} \left(\frac{p}{2k} \right) d\varphi \qquad (V.98)$$

we obtain the formula of Sims for determining the mean specific pressure, i.e., the coefficient of the state of stress:

$$\frac{p_m}{2k} = \left(\frac{\pi}{2} \sqrt{\frac{1-\varepsilon}{\varepsilon}} \tan^{-1} \sqrt{\frac{\varepsilon}{1-\varepsilon}} - \frac{\pi}{4} - \right.$$
$$\left. - \sqrt{\frac{1-\varepsilon}{\varepsilon}} \sqrt{\frac{r}{h_1}} \log_e \frac{h_n}{h_1} + \frac{1}{2} \sqrt{\frac{1-\varepsilon}{\varepsilon}} \sqrt{\frac{r}{h_1}} \log_e \frac{1}{1-\varepsilon} \right) \qquad (V.99)$$

where $\varepsilon = \frac{\Delta h}{h_0}$.

The ratio $\frac{h_n}{h_1}$ in this equation is found from the condition that for $\varphi = \gamma$ and $h_x = h_n$ the values of the specific pressure given by equations (V.96) and (V.97) are the same.

According to the formula of Sims the coefficient of the stress state depends only on the reduction ε and the ratio $\frac{r}{h_1}$. The values of this coefficient calculated from the formula of Sims are shown in Fig. 192.

13. A BRIEF SURVEY OF THE EXPERIMENTAL RESULTS CONCERNING THE PRESSURE OF THE METAL ON THE ROLLS UNDER PRODUCTION CONDITIONS

Thanks to a marked improvement in the methods and devices for force measurement many detailed investigations into the force parameters have been carried out during the last 15 to 20 years on different rolling mills under production conditions. Particularly extensive investigations have been carried out in the U.S.S.R., where they are used not only for obtaining the required test data concerning the actual forces acting on the rolls, but also for increasing the capacity of the mills by intensifying the rolling conditions as a result of a fuller utilization of the power reserves and prolonged service life. Much was done in formulating and working out the methods for these investigations by E. Rokotyan, A. Gurevich, A. Chekmarev and others.

Data on the measured values of the pressure of the metal on the rolls and the torques necessary to rotate them during the normal work of blooming mill 1150 are given below (tables 14, 15 and 16)

Table 14

Force and Power Characteristics of Rolling 320 × 330 mm Blooms from Rimmed Steel Billets (After T. Golubev et al.)

No. of pass	Initial depth of section h_0, mm	Reduction, mm	Degree of strain, %	Temperature of metal, °C	Velocity of rolling, m/s	Rolling force, tons	Specific pressure, kg/mm²	Rolling torque, tm	Specific power consumption, kWh/t
0	690	—	—	—	—	—	—	—	—
I	592	98	14.2	1,155	2.13	1,371	7.0	106.4	0.187
II	542	50	8.4	1,150	2.15	1,492	12.0	118.1	0.270
III	495	47	8.7	1,145	2.15	1,456	11.9	135.2	0.276
IV	448	47	9.5	1,135	2.21	1,415	11.3	127.3	0.337
K*									
V	649	141	17.8	1,130	2.15	797	5.9	149.9	0.372
VI	564	85	13.1	1,120	2.08	771	8.7	152.0	0.456
VII	477	87	15.4	1,110	2.08	789	7.7	146.9	0.506
VIII	411	66	13.8	1,100	2.12	764	8.7	134.0	0.585
K									
IX	388	87	18.3	1,085	2.20	747	8.7	149.9	0.694
X	306	82	21.1	1,070	2.16	889	10.0	141.7	0.780
XI	317 × 330	133	29.0	1,055	2.50	470	6.4	146.8	1.120

* K denotes turnover.

characterizing the forces which arise when blooms and slabs are rolled.

A general idea of the magnitude of the forces arising during the normal use of section mills is given by diagrams showing the overall pressure of the metal on the rolls for each pass, when a rail P-43 and a channel No. 30 are rolled on a rail and bar mill 750-800 (Figs. 193 and 194), and when a rail weighing 24 kg/m, an I-beam No. 20 and a channel No. 20 are rolled on a 540 cross-country mill (Figs. 195, 196 and 197). It follows from these diagrams that the pressure exerted by the metal on the rolls in the majority of cases is sharply reduced with each pass, which proves the imperfection of the roll pass design used.

In sheet-rolling mills intended for hot rolling of steel the pressure under the production conditions was measured by many investigators. According to the data of M. Zaikov and others the overall pressure on the 850-560-850 breakdown stand of a three-high tandem 2150 mill was 380 to 670 tons, when 17- to 25-mm thick sheets were

rolled from 100- to 170-mm thick slabs of 08 to 10 rimmed steel Ст. 3 and steel Ст. 4. For steel 1XB this pressure was 250 to 400 tons; for steel 09Г2 it was 400 to 650 tons, and for steel 1Х18Н9Т it was 450 to 750 tons. On the 850-560-850 finishing stand the pressure was considerably higher, and it strongly depended on the thickness of the sheets being rolled. When 3.5- to 5-mm thick sheets of 08 to 10 rimmed steel Ст. 4 were rolled, the pressure on the average amounted to 1,000 to 1,200 tons; for a thickness from 12 to 20 mm the pressure was 600 to 750 tons. The maximum value of the forces measured in the finishing stand reached 1,865 tons (when 3.5-mm thick sheets were rolled). In the case when 1,800-mm wide and 5.5- to

Table 15

Force and Power Characteristics of Rolling 320 × 330 mm Blooms from Billets of Steel 38ХМЮА (After T. Golubev et al.)

No. of pass	Initial depth of section h_0, mm	Reduction, mm	Degree of strain, %	Temperature, °C	Velocity of rolling, m/s	Rolling force, tons	Specific pressure, kg/mm²	Rolling torque, tm	Specific power consumption, kWh/t
0	690	—	—	—	—	—	—	—	—
I	642	48	7.0	1,180	1.38	1,210	11.0	77.0	0.04
II	597	45	7.0	1,175	2.11	1,400	13.1	151.4	0.24
K*									
III	630	70	10.0	1,170	1.33	1,070	9.4	107.1	0.077
IV	567	63	10.0	1,165	1.83	1,340	12.2	141.5	0.24
V	527	40	7.1	1,160	2.48	1,330	15.1	96.5	0.18
VI	487	40	7.6	1,155	2.25	1,440	16.2	136.2	0.41
VII	463	24	5.0	1,150	2.25	1,360	19.6	151.5	0.34
VIII	447	16	3.5	1,145	2.33	1,580	27.5	165.9	0.28
K									
IX	574	56	8.9	1,140	2.23	945	12.4	147.6	0.31
X	514	60	10.4	1,135	2.07	930	11.6	152.7	0.63
XI	458	56	10.9	1,130	2.17	800	10.3	118.1	0.48
XII	405	53	10.6	1,125	2.17	945	12.1	142.6	0.76
K									
XIII	378	107	22.0	1,120	2.17	700	7.3	143.2	0.67
XIV	305	73	19.3	1,110	2.12	810	9.9	137.9	1.02
K									
XV	322 × 330	108	25.0	1,100	2.52	680	9.2	158.7	1.20

* K denotes turnover.

Table 16

Force and Power Characteristics of Rolling 140 × 650 mm Slabs from Rimming Steel Billets (After T. Golubev et al.)

No. of pass	Initial depth of section h_0, mm	Reduction, mm	Degree of strain, %	Temperature, °C	Velocity of rolling, m/s	Rolling force, tons	Specific pressure, kg/mm²	Rolling torque, tm	Specific power consumption, kWh/t
0	760	—	—	—	—	—	—	—	—
I	707	53	7.0	1,165	1.38	1,150	10.2	77.0	0.081
II	667	40	5.7	1,160	2.26	1,320	13.6	81.6	0.22
K*									
III	587	83	12.4	1,155	1.98	1,370	9.8	166.4	0.28
IV	527	60	10.2	1,145	2.15	1,500	12.5	151.1	0.55
V	469	58	11.0	1,140	1.43	1,350	11.4	151.5	0.185
VI	412	57	12.1	1,130	2.10	1,340	11.5	161.5	0.50
VII	352	60	14.5	1,125	2.21	1,440	12.5	146.3	0.436
VIII	295	57	16.2	1,115	2.10	1,290	11.0	156.7	0.70
K									
IX	648	32	4.7	1,105	2.25	215	5.7	109.4	0.36
X	598	50	7.7	1,095	2.25	355	7.5	84.1	0.41
K									
XI	239	56	19.0	1,090	2.31	1,420	13.6	151.3	0.80
XII	197	42	17.6	1,085	2.87	1,350	15.0	106.5	0.81
XIII	142 × 650	55	28.0	1,085	2.65	1,520	14.1	151.0	1.45

* K denotes turnover.

8-mm thick sheets of steel 1X18H9T were rolled the pressure on the rolls was 800 to 1,400 tons, whilst for a thickness of 24 mm it was 450 to 600 tons.

A. Geleji and others have investigated the forces which arise when metal is rolled in a 3290 × 950-720-950 single-stand three-high plate mill. According to the data of these investigators, the actual overall pressure of the metal on the rolls is distributed very unevenly between the passes (Fig. 198). In the first 12 passes or so, when the temperature of the billet is still high (more than 1,000°C) and its depth is great, the pressure on the average varies from 100 to 600 tons, whilst with the subsequent passes it rises to 1,200 tons.

Detailed data concerning the forces acting on the rolls of continuous strip mills during hot rolling of steel were obtained by E. Rokotyan in investigating the force parameters of the 1680 mill. In the

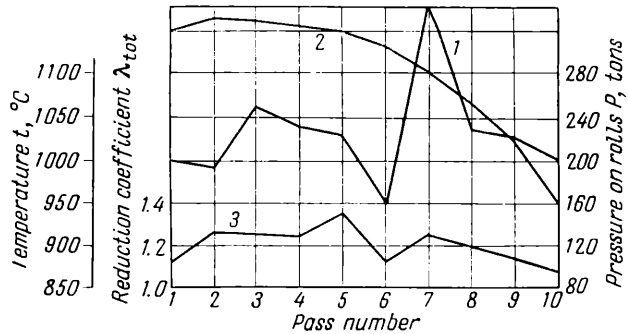

Fig. 193. The pressure of the metal on the rolls of a 750-800 rail and bar mill during the rolling of a P-43 rail (T. Golubev et al.): *1*—pressure of the metal on the roll; *2*—temperature; *3*—reduction ratio per pass

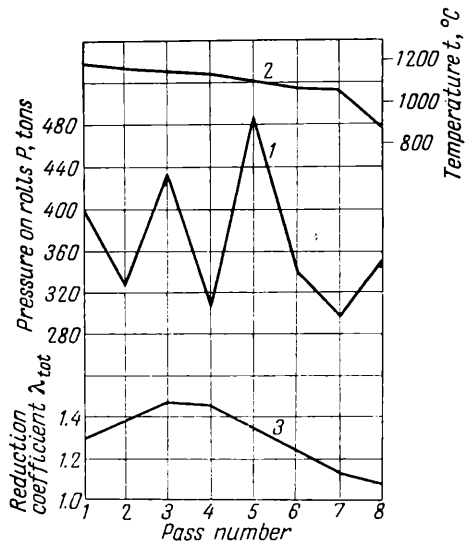

Fig. 194. The pressure of the metal on the rolls of a rail and bar mill during the rolling of a No. 30 channel (notations as in Fig. 193)

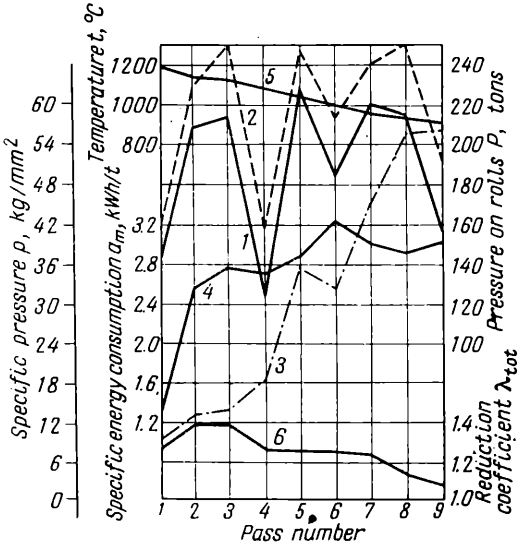

Fig. 195. The pressure of the metal on the rolls during the rolling of a P-24 rail on a 540 cross-country mill:

1—mean pressure; *2*—maximum pressure; *3*—specific pressure; *4*—specific energy consumption; *5* and *6*—temperature and reduction ratio per pass (N. Skorokhodov et al.)

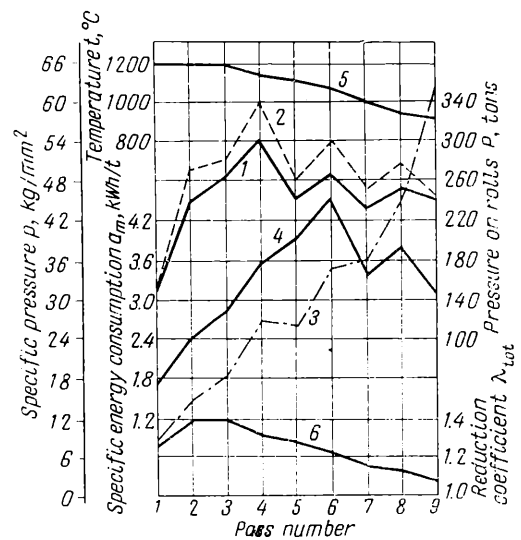

Fig. 196. The pressure of the metal on the rolls during the rolling of a No. 20 beam in a 540 cross-country mill:

1—mean pressure; *2*—maximum pressure; *3*—specific pressure; *4*—specific energy consumption; *5* and *6*—temperature and reduction ratio per pass (N. Skorokhodov et al.)

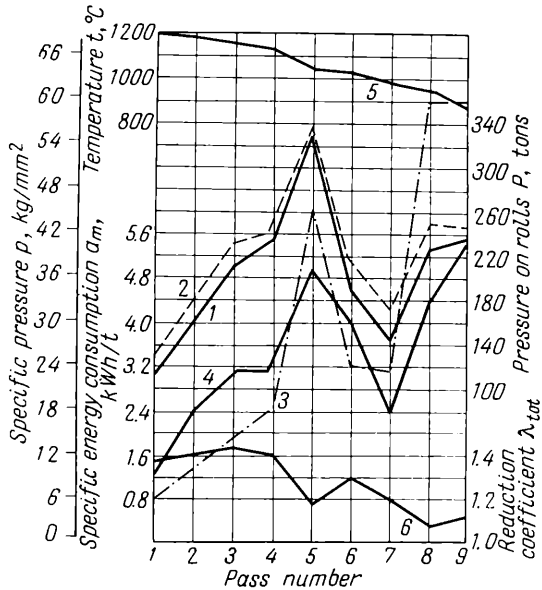

Fig. 197. The pressure of the metal on the rolls during the rolling of a No. 20 channel in a 540 cross-country mill:

1—mean pressure; *2*—maximum pressure; *3*—specific pressure; *4*—specific energy consumption; *5* and *6*—temperature and reduction ratio (N. Skorokhodov et al.)

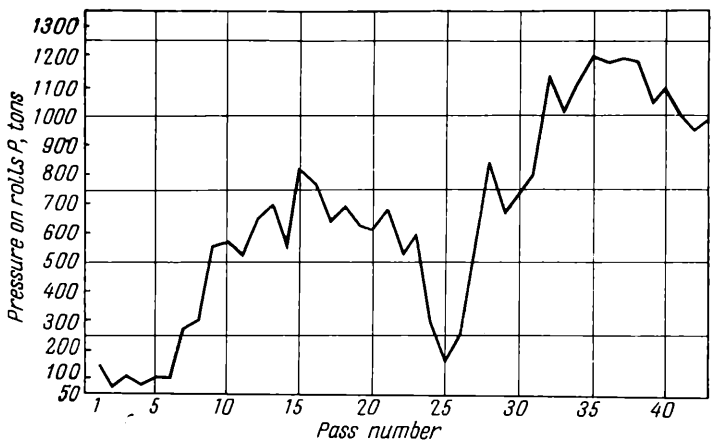

Fig. 198. The pressure of the metal on the rolls of a 3290 single-stand three-high plate mill during the rolling of sheets of steel Ст. 35.21, of dimensions 8.5 × 600 × 5,480 mm, from billets having dimensions 220 × 500 × 1,300 mm

roughing group the maximum pressure of the metal on the rolls was reached in the first, broadside stand, where the roll diameter is 950 mm. When a 2,000- to 2,200-mm long slab was rolled in the lateral direction, the pressure in the first stand amounted nearly to 1,500 tons. In the remaining stands of the roughing group (the diameter of the working rolls being 600 mm) the pressure was markedly less; on the average its magnitude varied from 530 to 1,230 tons (Table 17).

Table 17

The Pressure of Metal on the Rolls in the Roughing Group of a 1680 Continuous Strip Mill (After E. Rokotyan)

Initial cross section of slab, mm	Steel	Reduction in the stand, %				Pressure of metal on the rolls in the stand, tons			
		I	II	III	IV	I	II	III	IV
115×1,040	08 rimmed	26.0	29.2	31.6	34.5	720	550	625	750
110×970	10 killed	27.1	23.2	37.5	33.5	1,180	720	950	980
115×950	15 rimmed	29.5	28.4	38.1	35.3	1,440	800	1,050	1,000
110×970	20 killed	26.4	23.4	38.7	34.2	1,395	740	1,080	1,030
115×1,020	Ст. 2 rimmed	25.2	24.9	34.9	34.7	1,345	770	1,230	1,050
100×970	Ст. 3	25.7	29.6	33.1	37.1	1,400	800	1,065	1,200
100×970	Ст. 3	25.5	35.0	32.5	37.9	1,500	920	950	1,230

The mean specific pressure in the roughing group ranges from 6 to 12.5 kg/mm² for 08 rimmed steel (the lower limit for the stand I and the higher limit for the stand IV), whilst for the rimmed steel Ст. 3 and the steel Ст. 3 it is within the limits 6 to 17 kg/mm².

In the finishing group the first stands, i.e., the stands V to VII, are the ones loaded most, with the pressure of the metal on the rolls reaching 1,000 to 1,420 tons (Table 18).

The mean specific pressure during the rolling of 08 to 10 rimmed steels in the first stands of the roughing group is 22 to 28 kg/mm²; in subsequent stands it increases up to 40 to 50 kg/mm².

The results of the investigations of A. Chekmarev and others, carried out on this 1680 continuous strip mill, are of great interest. In this case the forces were measured in the stands of the finishing group of the mill when sheets of an alloy steel and sheets of width up to 1,510 mm were rolled.

The greatest pressure was also observed in the first stand of the finishing group (i.e., in the stand V), where during the rolling of 1,430-mm wide sheets of a 12X5MA steel it reached 2,840 tons; during the rolling of 1,510-mm wide sheets of 08 rimmed steel it went up to 1,910 tons.

Table 18

The Pressure of Metal on the Rolls in the Finishing Group of a 1680 Continuous Strip Mill (After E. Rokotyan)

Dimensions of workpiece, mm	Dimensions of sheet, mm	Steel	Reduction, %, in stand						Pressure of metal on rolls, tons, in stand					
			V	VI	VII	VIII	IX	X	V	VI	VII	VIII	IX	X
21×940	2.0×940	08 rimmed	54.0	41.8	32.5	30.3	21.2	4.3	1,420	1,410	1,000	920	875	460
20×1,000	2.0×1,000	08 rimmed	47.0	41.5	35.0	31.0	23.0	7.5	1,320	1,230	1,000	910	750	425
22×880	2.5×880	08 rimmed	40.7	36.4	35.3	34.7	16.6	14.2	1,250	1,290	975	970	900	570
23×1,010	3.0×1,000	08 rimmed	39.4	35.1	30.0	33.6	15.8	11.5	1,140	1,270	870	920	780	420
23×932	3.5×932	08 rimmed	37.5	37.4	28.0	28.3	18.4	11.0	1,110	1,090	800	740	740	430
24×100	3.0×1,000	10 rimmed	45.3	36.8	28.4	28.3	21.3	6.7	1,210	1,100	930	850	680	420
23×1,000	3.0×1,000	Ст.2 rimmed	39.9	36.0	29.9	34.5	12.5	16.6	1,240	1,300	1,000	970	850	470
24×1,000	3.5×1,000	Ст.2 rimmed	39.0	39.0	33.6	26.1	17.3	15.3	1,190	1,270	990	900	840	420
27×980	5.5×980	25 rimmed	35.2	32.4	23.1	26.0	10.7	8.5	1,120	925	770	725	550	330
23×1,000	2.5×1,000	Ст.3 rimmed	42.2	37.0	35.0	34.2	11.0	16.3	1,320	1,300	1,040	1,040	970	600
22×1,000	3.0×1,000	Ст.3 rimmed	35.2	38.8	31.5	29.8	16.4	12.2	1,270	1,130	920	900	845	420

During the rolling of alloy steel the specific pressure in the first stands of the roughing group is approximately 30 to 40 kg/mm², whilst in the last stands it is approximately 40 to 70 kg/mm².

On the basis of the results of the investigations by E. Rokotyan and A. Chekmarev we can assume that the maximum pressure in the stands of the finishing group, per millimetre width of the rolled sheet of a low carbon steel, is

$$q = 1.25 \text{ to } 1.5 \text{ t/mm}$$

whilst for an alloy steel

$$q \approx 1.5 \text{ to } 2.0 \text{ t/mm}$$

The pressure of the metal on the rolls during hot rolling of sheets of aluminium alloys under production conditions was investigated in detail by E. Rokotyan on a 2800 four-high mill. He established that the pressure of the metal on the rolls of this mill (diameter of the working rolls is 700 mm), when sheets of aluminium alloys with the approximate width of 2,200 mm are rolled, reaches 2,000 tons, i.e., it is somewhat less than during the rolling of steel.

The forces acting on the rolls under production conditions when wide steel sheets are cold rolled were investigated by E. Rokotyan on a continuous three-stand 1680 × 480-1250 four-high mill. The maximum pressure on the rolls of this mill was observed in the first stand. Thus, for example, in the case of rolling sheets 1,460 mm wide and 1.2 mm thick, from 08 rimmed steel, with three passes from a blank 1.2 mm thick, the overall pressure in the first stand (for a reduction of 37.8%) reached 1,390 tons, in the second stand (for a reduction of 22.4%) it reached 1,060 tons, and in the third stand (for a reduction of 7.76%) it reached 700 tons.

The longitudinal tension of the rolled metal had a great effect on the pressure, which on the average varied from 14 to 21 kg/mm².

14. PRACTICAL DATA ON THE FORCES ARISING DURING LONGITUDINAL ROLLING OF TUBES

The forces arising in tube mills during longitudinal continuous rolling (the forces in the mills during Pilger and helical rolling will be considered below, in chapters VII and VIII) were investigated in two-high mills with a short mandrel (automatic), in continuous mills with a long mandrel, and in reducing mills.

I. Fomichev and V. Ostrenko have measured the pressure of the metal on the rolls and the axial force on the mandrel during the rolling of tubes with the diameter of 168 × 325 mm on a two-high mill (diameter of the rolls being 920 to 960 mm) with a short mandrel,

under normal production conditions. A part of the experimental data obtained by them is given in Table 19.

Table 19

Results of the Measurement of the Forces During the Rolling of Tubes Made of a Low Carbon Steel on a Two-High Mill with a Short Mandrel

Dimensions of tube, mm		Rolling temperature in the pass, °C		Pressure on rolls in the pass, tons		Axial force on mandrel in the pass, tons	
Diameter	Wall thickness	I	II	I	II	I	II
168	7.5	1,110	1,050	215	205	—	—
168	11	1,110	1,060	200	175	48	50
219	8	1,125	1,080	310	307	—	—
273	9	1,100	1,000	350	360	76	74
273	25	1,150	1,120	270	250	—	—
325	10	1,080	1,015	450	464	—	

During the rolling of tubes 86 mm in diameter having a wall thickness of 3 to 8 mm, on a two-high mill with a short mandrel, the pressure on the roll was 65 to 112 tons, whilst the axial pressure on the mandrel was 18 to 32 tons.

According to the data obtained by V. Anisiforov whilst rolling tubes on (140-250) mills with a short mandrel, the ratio between the longitudinal force, Q, acting on the mandrel and the vertical pressure of the metal on the rolls, P, is

$$Q = (0.4 \text{ to } 0.5)\,P$$

for thin-walled tubes, and

$$Q = (0.15 \text{ to } 0.2)\,P$$

for thick-walled tubes.

A detailed investigation into the pressure exerted by the metal on the rolls during the rolling of tubes in continuous mills on a long mandrel was carried out by Y. Vatkin and others under production conditions. They have established that the pressure of the metal on the rolls varies considerably during the motion of the tube being rolled. At the entry of the tube into each pair of the rolls the pressure is large; during the steady state motion it is sharply reduced owing to the tension of the metal between the stands of the mill, whilst at the exit it increases again. Thus, for example, during the rolling of a tube 59 mm in diameter having a wall thickness of 3.25 mm the pressure at its entry into the fourth stand reaches

57 tons; during the steady state motion it falls to 32 tons, whilst at the exit it rises to 46 tons.

In tube reducing mills, as in mills of the preceding type, the pressure of the metal on the rolls strongly depends on the tension. This influence of the tension is particularly marked in three-roll reducing mills of modern design, which work with considerable tension, as a result of which the tube diameter is reduced as well as the wall thickness.

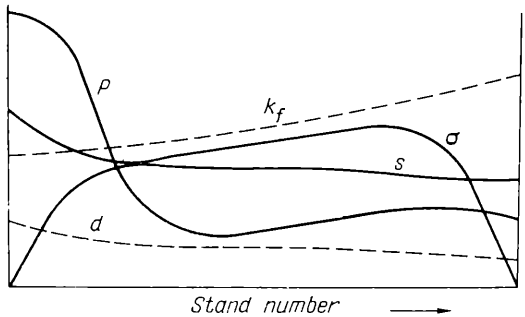

Fig. 199. Variation of k_f (resistance to deformation), d (tube diameter), s (tube wall thickness), P (pressure of the metal on the three rolls of the stand) and σ (tension) in a stretch-reducing mill as the tube passes from stand to stand

Fig. 199 shows a typical graph (obtained experimentally) of the variation of the dimensions of the cross section of the tube being rolled, the pressure of the metal on the rolls and the tension in the stands of the mill. After passing 3 to 4 stands the tension in the tube becomes considerable and the pressure on the rolls drops sharply; before the last stands, in spite of the reduction in the diameter and the wall thickness of the tube, the pressure increases as a consequence of the reduction in the tension.

The firm "Kocks" (FRG), engaged in the design and manufacture of stretch-reducing tube mills, recommends the following formula for calculating the pressure of the metal on the three rolls of a reducing mill:

$$P = 2\pi k_f s \left(1 - \frac{\sigma}{k_f}\right) \sqrt{D_r \Delta r} \qquad \text{(V.100)}$$

where k_f is the resistance to deformation in simple compression
s is the wall thickness of the tube
D_r is the roll diameter
σ is the tension, kg/mm²
Δr is the linear reduction along the radius of the tube.

To determine the mean specific pressure during the reduction of tubes we recommend the formula suggested by V. Anisiforov; this, when the effect of the tension is taken into account, has the following form:

$$p_m = k_f \left(1 - \frac{\sigma}{k_f}\right) n''_\sigma \frac{2s}{r_0 + r_1} \qquad \text{(V.101)}$$

where r_0 and r_1 refer to the mean radius of the tube before and after rolling

n''_σ is the coefficient taking account of the effect of the outer zones on the specific pressure.

From the theoretical solution of the problem concerning the strain of a long tube loaded over a comparatively narrow portion m of its width, and the results of a specially conducted test on tubular test pieces compressed in a press to determine n''_σ, we obtain the formula

$$n''_\sigma \quad 1 \quad 0.9 \frac{d_m}{l} \sqrt{\frac{s}{d_m}} \qquad \text{(V.102)}$$

where l is the width of the loaded portion of the tube, measured along its length

d_m is the mean diameter of the tube.

VI

Torque Required to Drive the Rolls During Longitudinal Rolling

1. BASIC QUANTITIES CONSTITUTING THE LOAD OF THE DRIVE OF THE ROLLS

The torque on the motor shaft, required to drive the rolls of a rolling mill, is composed of the four quantities:

$$M_{mot} = \frac{M_{rol}}{i} + M_{fr} + M_l + M_{dyn} \qquad \text{(VI.1)}$$

where M_{rol} is the rolling torque, i.e., the torque which is needed to overcome the resistance to deformation of the metal being rolled, and to overcome the friction forces of the metal along the surface of the rolls

i is the gear ratio between the rolls and the motor

M_{fr} is the torque of the additional friction forces applied to the motor shaft which arise in the bearings of the rolls, in the transmission and other parts of the mill when the metal being rolled passes between the rolls; it does not include the torque necessary to drive the mill running idle

M_l is the torque of running light, i.e., the torque which is needed when the mill is running idle

M_{dyn} is the dynamic torque on the motor shaft, required to overcome the inertial forces which arise during non-uniform rotation of the rolls.

The first three quantities which form the load of the roll drive constitute the sum of the static torque and are unavoidable for any rolling mill. Of these quantities the rolling torque has the largest magnitude, and only on rare occasions, in particular, in two-high mills of the old type for thin strip, can the torque of the additional friction forces, resulting from large losses in the bearings of the rolls, be larger than the rolling torque.

Of the quantities which make up the static load the rolling torque M_{rol} is the useful load, and the losses due to the friction of the metal over the roll surface, which are included in it, are inevitable. On the other hand, the torques M_{fr} and M_l constitute a harmful load due to the imperfection of the components and mechanisms of the mill.

The ratio of rolling torque, as referred to the motor shaft, to the total static torque is called the efficiency of the rolling mill:

$$\eta = \frac{M_{rol} : i}{\frac{M_{rol}}{i} + M_{fr} + M_l} \tag{VI.2}$$

Depending on the conditions of rolling and the arrangement of the mill (mainly on the construction of the bearings of the rolls) the efficiency of the mill can vary within fairly wide limits; on average $\eta = 0.5$ to 0.95.

The dynamic torque occurs only in certain mills with non-uniform rotation of the rolls: in mills with a flywheel, in mills with a regulated rolling velocity during the pass, including reversible mills. The magnitude of the dynamic torque is found from the formula

$$M_{dyn} = I \frac{\pi}{30} \frac{dn}{dt} \tag{VI.3}$$

where I is the moment of inertia of the rotating parts of the mill, referred to the motor shaft

$\frac{dn}{dt}$ is the angular acceleration, rpm sec.

Expressing I in terms of the flywheel moment, constituting the product of the square of diameter of inertia of the rotating parts and their weight

$$GD^2 = 4gI$$

where g is gravity acceleration,
we obtain the following formula for calculating the dynamic moment:

$$M_{dyn} = \frac{GD^2}{375} \frac{dn}{dt} \tag{VI.4}$$

2. DETERMINATION OF THE ROLLING TORQUE FROM THE VALUE OF THE PRESSURE OF THE METAL ON THE ROLLS

The rolling torque is calculated either from the forces acting on the rolls or from the experimental data on the energy consumption during rolling. The first method gives more accurate results when rectangular sections are rolled, that is: sheets, blooms, slabs, etc.

Using the well-known law concerning the distribution of shear stresses on the contact surface over the arc of contact, and neglecting the variation of these stresses over the width of the rolled strip, i.e., assuming the strain to be two-dimensional, we can express the torque required to rotate the roll as

$$M \quad b \int_{\gamma}^{\alpha} \tau_x r^2 \, d\varphi - b \int_{0}^{\gamma} \tau_x r^2 \, d\varphi \tag{VI.5}$$

where b is the mean width of the rolled strip
α is the angle of contact
γ is the angle of neutral section
r is the radius of the roll.

If we assume that stresses over the arc of contact are constant (equal to τ_m) and their direction changes only at $\varphi = \gamma$, then we obtain the formula suggested by V. Bayukov:

$$M = br^2\tau_m(\alpha - 2\gamma) \tag{VI.6}$$

This formula is, however, unsuitable for practical calculations, since the actual contact shear stresses over the arc of contact undergo considerable changes. Since the law of distribution of these stresses over the contact surface is not sufficiently understood, equation (VI.5) is not recommended for calculation of M.

The method considered above for calculation of the torque in terms of the contact shear stresses has a further disadvantage that the error incurred in the calculation of the angle γ gives rise to a doubled error in the torque.

The most reliable results in determining the torque needed to drive the rolls can be obtained if the direction of the forces acting on the rolls is found by considering the conditions of equilibrium of the rolled material. Using this method, we can determine the direction of the resultants of the forces applied to the rolls, and use the equations derived above (see Chapter IV) to calculate the torques on the rolls for different rolling conditions.

The angle β in these equations is determined by the point of application of the resultant of the pressure of the metal on the rolls,

i.e., mainly by the law of distribution of the normal stresses on the contact surface, which has received more attention than the law of distribution of the shear stresses.

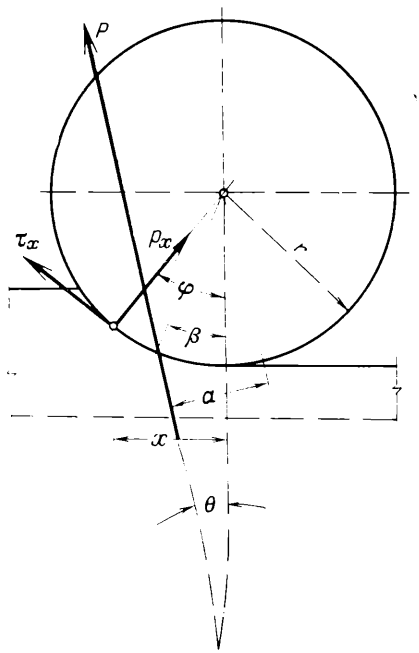

Fig. 200. Diagram of the forces acting on a roll (used in determining the lever arm of the resultant)

Using this method, let us determine the torque for the symmetric case of rolling (Fig. 200), taking b, the width of the material being rolled, to be equal to unity:

$$M = Pa = \int_0^{\alpha} p_x r^2 \sin\varphi \cos\varphi \, d\varphi + \int_{\gamma}^{\alpha} \tau_x r^2 \sin^2\varphi \, d\varphi - \int_0^{\gamma} \tau_x r^2 \sin^2\varphi \, d\varphi - \int_0^{\alpha} p_x r^2 \sin\varphi \cos\varphi \, d\varphi + \int_{\gamma}^{\alpha} \tau_x r^2 \cos^2\varphi \, d\varphi - \int_0^{\gamma} \tau_x r^2 \cos^2\varphi \, d\varphi \qquad (VI.7)$$

At the same time let us consider the equation of equilibrium of the rolled material, projecting all forces on to the direction of its

motion:

$$P \sin \theta = -\int_0^{\alpha} p_x r \sin \varphi \, d\varphi + \int_{\gamma}^{\alpha} \tau_x r \cos \varphi \, d\varphi - \int_0^{\gamma} \tau_x r \cos \varphi \, d\varphi \qquad \text{(VI.8)}$$

Comparing these equations we notice that for relatively small angles φ (approximately within the limits of 30°), when $\cos \varphi = 0.87$ to 1, the last three terms of equation (VI.7) will differ very little from the right-hand side of equation (VI.8). If, for example, in determining the effect of the horizontal forces on the rolling torque we equate the arc of contact to a chord and thus assume that $\cos \varphi = \cos \frac{\alpha}{2}$, $r d\varphi = \frac{dx}{\cos \frac{\alpha}{2}}$, then instead of the last three terms in equation (VI.7) we can write $Pr \sin \theta \cos \frac{\alpha}{2}$.

Further, in equation (VI.7) we can also neglect the difference of the second and third terms. As a result of this simplification

$$M = Pa = \int_0^{\alpha} p_x r^2 \sin \varphi \cos \varphi \, d\varphi + Pr \sin \theta \cos \frac{\alpha}{2} \qquad \text{(VI.9)}$$

whence, denoting $r \sin \varphi = x$, we obtain

$$M = Pa = \int_0^{l} p_x x \, dx + Pr \sin \theta \cos \frac{\alpha}{2} \qquad \text{(VI.10)}$$

We then find the angle β (Fig. 200) from the condition

$$a = r \sin (\beta + \theta) = \frac{\int_0^{l} p_x x \, dx}{P} + r \sin \theta \cos \frac{\alpha}{2} \qquad \text{(VI.11)}$$

In the simple case of rolling, when $\theta = 0$, the equation for the lever arm of the resultant of the pressure exerted by the metal on the rolls will be the following:

$$a = r \sin \beta = \frac{\int_0^{l} p_x x \, dx}{\int_0^{l} p_x \, dx} \qquad \text{(VI.12)}$$

i.e., the lever arm of the resultant of the pressure exerted by the metal on the rolls in the simple case of rolling is practically equal to the distance from the line connecting the centres of the rolls to the centroid of the specific pressure diagram plotted on the horizontal projection of the arc of contact.

The ratio of the angles $\frac{\beta}{\alpha}$ is denoted by ψ; thus

$$\frac{\beta}{\alpha} = \psi$$

We call this ratio the lever arm coefficient for the position of the resultant of the metal pressure on the rolls.

In the simple case of rolling, i.e., when the resultant of the pressure of the metal on the rolls is directed vertically:

$$\beta : \alpha \approx a : l$$

where a is the lever arm of the pressure of the metal on the rolls
l is the length of arc of contact.

The torque required to rotate both rolls in the simple case of rolling equals

$$M_{rol} = 2P\psi l \approx 2P\psi \sqrt{r\Delta h} \qquad \text{(VI.13)}$$

Analytically the values of the lever arm coefficient for various laws of distribution of the contact stresses have been calculated by A. Korolev, N. Spiridonov and N. Kirilin, when the friction forces were proportional to the specific pressure, and by R. Sims for constant friction forces.

In calculating the lever arm coefficient N. Kirilin assumed that the specific pressure of the metal on the rolls is distributed according to Tselikov's equations (II.34) and (II.35) for k = constant. He represented the results of this calculation in the form of a diagram (Fig. 201), where the coefficient ψ is given as a function of $\frac{\mu l}{2\Delta h}$ for different reductions $\varepsilon = \frac{\Delta h}{h_0}$. In so doing k is taken to be constant.

It can be seen from this diagram that as the reduction is increased, and with it δ, the lever arm coefficient diminishes from 0.5, for small reductions, to 0.4-0.45, for reductions close to 0.6.

R. Sims calculated the rolling torque, basing it on his formula (V.99) for the pressure, i.e., he assumed that the friction forces over the arc of contact are constant and equal to $\tau_x = k$ and only change their direction at the neutral section. In calculating the torque for both rolls, when $b = 1$, he recommends the formula

$$M_{rol} = 2rR(2k) f\left(\frac{R}{h_1}, \frac{\Delta h}{h_0}\right) \qquad \text{(VI.14)}$$

where r is the radius of the ideal roll
R is the radius of the deformed roll

$f\left(\frac{R}{h_1}, \frac{\Delta h}{h_0}\right)$ is a function depending on $\frac{R}{h_1}$ and $\frac{\Delta h}{h_0}$.

To determine the value of this function, which, when equation (VI.14) is compared with equation (VI.6), equals

$$f\left(\frac{R}{h_1}, \frac{\Delta h}{h_0}\right) = \frac{\alpha - 2\gamma}{2}$$

the graph of Fig. 202 is recommended. On this graph, as in Fig. 201, k is taken constant over the entire contact surface. In reality k varies both for hot and cold rolling along the arc of contact; accordingly,

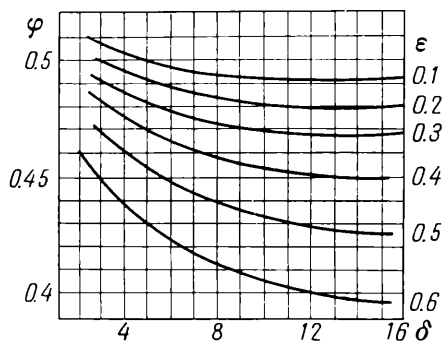

Fig. 201. Variation of the lever arm coefficient $\psi = \frac{M}{2Pl}$ with $\delta = \mu \frac{l}{2\Delta h}$ for various reductions ε

the coefficient of the lever arm should be determined by considering the results of experimental investigations.

In this respect the results of the investigation of E. Rokotyan are of the greatest interest; these were conducted under production conditions on a blooming mill (Fig. 203), a strip mill (Fig. 204) and others. According to his investigations the coefficient of the lever arm depends on the ratio $l : h_m$; as this ratio increases the coefficient ψ diminishes during the rolling of blooms from 0.55-0.5 down to 0.35-0.3, whilst during hot rolling of aluminium alloys it falls from 0.55 to 0.45.

During hot rolling of steel the coefficient of the lever arm was also investigated in detail by G. Walquist on a 340 laboratory mill. He rolled test pieces with rectangular cross section 50 mm wide

and 2.5, 5, 10 and 20 mm thick from 16 different steels, using reductions 10 to 40% at temperatures of 800, 900, 1,000 and 1,100°C. One of G. Walquist's experimental diagrams is given in Fig. 205. For a low carbon steel (Fig. 205*a*) the values of the coefficient ψ

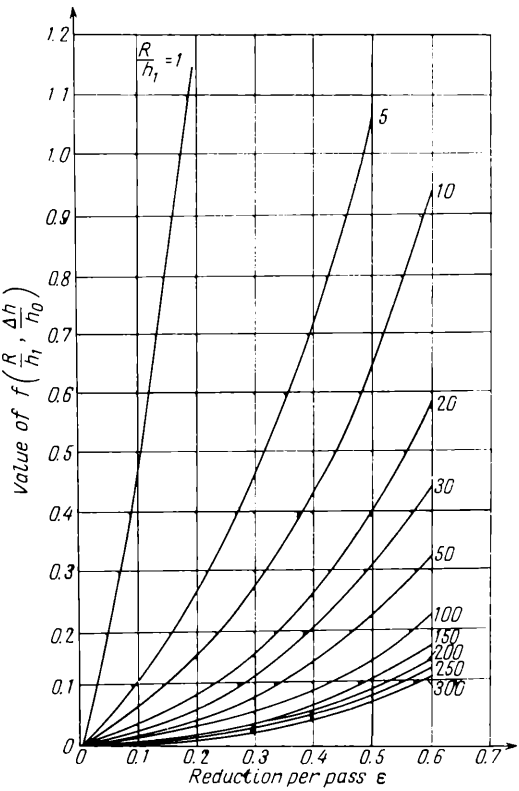

Fig. 202. Variation of $f\left(\frac{R}{h_1}, \frac{\Delta h}{h_0}\right)$ with the reduction $\frac{\Delta h}{h_0}$ for various ratios $R : h_1$; used in determining the rolling torque from the formula (VI.14)

obtained vary from 0.34 to 0.47. A higher value of the coefficient is obtained in rolling thicker test pieces (20 mm). The common difference in the value of the coefficient ψ depending on variation in the thickness of the strip is 0.08. When the temperature is reduced the value of ψ diminishes a little.

For a high carbon steel (Fig. 205*b*), and also for the other steels the character of the diagram is similar, but the variation in the

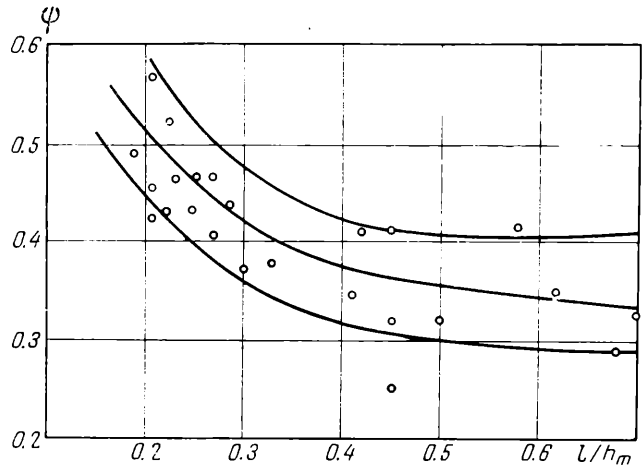

Fig. 203. Variation of the lever arm coefficient ψ with the ratio $l : h_m$ in blooming mill 1000 during the rolling of blooms 160 × 160 mm in cross section from billets weighing 6.5 tons; medium carbon tube steel

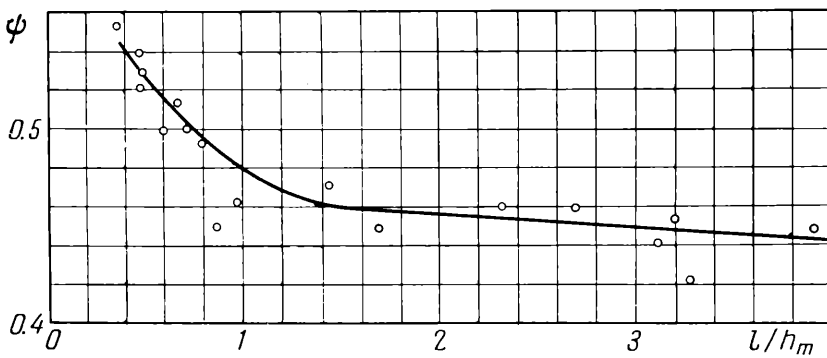

Fig. 204. Variation of the lever arm coefficient ψ with the ratio $l : h_m$ in a 2840 × 700/1350 four-high reversing plate mill during the hot rolling of plates of aluminium alloy Д16; plate thickness 6 mm, and width 1,330-2,160 mm

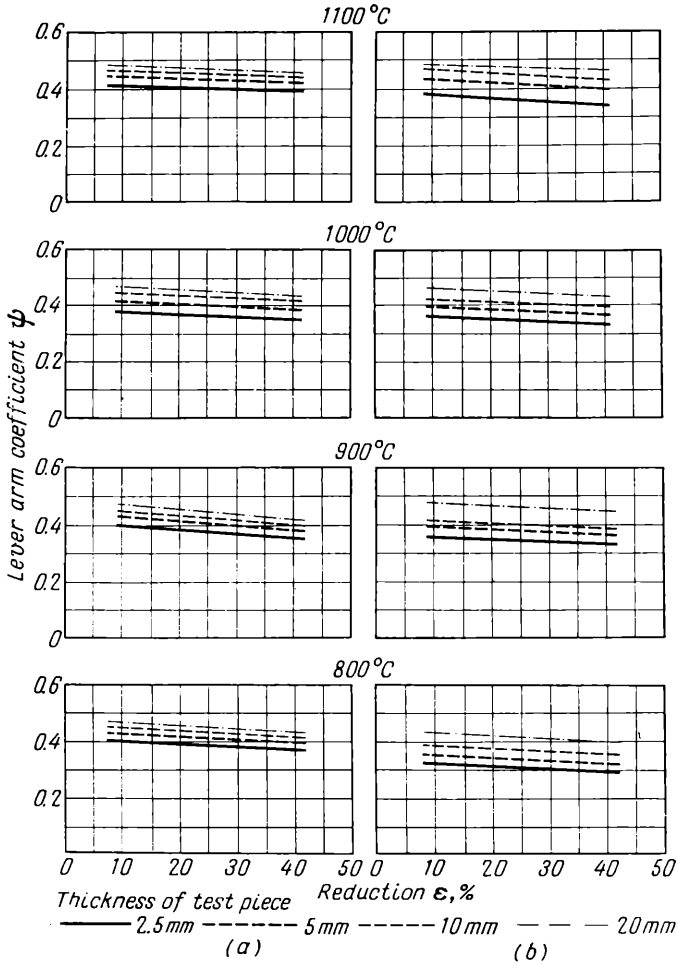

Fig. 205. Variation of the lever arm coefficient ψ with reduction when plain carbon test pieces are rolled at 800, 900, 1,000 and 1,100°C; initial thickness of test pieces: 2.5, 5, 10 and 20 mm: (*a*) 0.1% C; (*b*) 1.03% C

coefficient of the lever arm as a function of the above factors is within wider limits. In particular, for a steel with 1.03% C:

$$\psi = 0.30 \text{ to } 0.49$$

whilst for a high speed steel with 17.8% W and 4.65% Cr

$$\psi = 0.28 \text{ to } 0.56$$

In the U.S.A. the coefficient ψ for hot rolling of blanks of square cross section is taken equal to 0.5, for round sections it is 0.6, for closed grooves 0.7, for sheets in continuous mills in first stands 0.48 is used, and in the last 0.39.

In rolling strips which are not too wide, if their width is commensurable with the length of the arc of contact, the coefficient of the lever arm is strongly affected by spreading, with the result that the resultant of the pressure exerted by the metal on the rolls approaches the plane passing through their axes; consequently, ψ is reduced a little.

When rolling is carried out in grooved rolls the calculation of the lever arm coefficient becomes more difficult owing to the considerable effect of the friction forces which arise between the metal and the side walls of the grooves. In this case more reliable results are obtained from the experimental data concerning the consumption of energy during rolling.

The lever arm coefficient for cold rolling was investigated by E. Rokotyan, A. Korolev, M. Safyan, H. Ford, W. Hessenberg, R. Sims and others. In these investigations the pressure of the metal on the rolls and the rolling torque were measured simultaneously. The lever arm coefficient was found from the ratio

$$\psi = \frac{M_{rol}}{2P\sqrt{r\Delta h}}$$

for ideal (non-deformed) rolls.

According to the data of M. Safyan the lever arm coefficient on the average was 0.19 to 0.24 during the rolling of strips of low carbon steel.

H. Ford investigated the value ψ during the rolling of strips of low carbon steel and high conductivity copper with different initial thicknesses and with different reductions. Some of the initial strips were previously annealed and others upset with different degrees of strain (10, 20, 30, 40 and 50%). The mean values of the lever arm coefficient ψ obtained by him for ideal rolls are given in Table 20.

From the test data of H. Ford it follows that in spite of the different rolling conditions the lever arm coefficient does not

undergo large changes, and, in particular, when copper is rolled with reductions of 0.1 to 0.8 per pass, the lever arm coefficient varies from 0.29 (when $\varepsilon = 0.1$) to 0.37 (when $\varepsilon = 0.6$).

Table 20

Mean Values of the Lever Arm Coefficient ψ

Material	Thickness of strip, mm	Surface of rolls	Mean value of ψ
Carbon steel:			
0.2% C	2.54	Mirror finish	0.40
ditto	2.54	Dull finish	0.32
ditto	2.54	Dull finish; no lubrication *	0.33
0.11% C	1.88	Mirror finish	0.36
0.07% C	1.65	Ditto	0.35
High conductivity copper	2.54	Ditto	0.40
Ditto	1.27	Dull finish	0.40
Ditto	1.9	Ditto	0.32
Ditto	2.54	Ditto	0.33

* In all other cases the rolls were lubricated with vacuum oil 40A

3. THE EFFECT OF THE ELASTIC COMPRESSION OF THE ROLLS AND THE METAL BEING ROLLED ON THE ROLLING TORQUE

The local elastic compressions which occur in the rolls and the metal being rolled during cold rolling owing to the high specific pressure, as has been mentioned previously, have a marked effect on the contact area and the pressure of the metal on the rolls.

Let us consider to what extent the rolling torque and the energy consumption depend on these deformations. For this we shall first determine the effect of the elastic compression on the position of the resultant of the pressure exerted by the metal on the rolls, and on its lever arm relative to the centre of the roll.

During rolling with deformed rolls the resultant of the pressure of the metal on the rolls is obviously applied in the same way as during rolling with ideally rigid rolls: close to the middle of the arc of contact and slightly displaced towards the exit side. But owing to the fact that the increase of the arc of contact as a result of the elastic compression of the rolls and the metal being rolled takes place rather in the direction of exit of the metal from the rolls than in the direction of entry, the point of application of the resultant

of the pressure is still further displaced towards the direction of rolling, as the rolls are deformed.

This displacement of the point of application of the resultant of the metal pressure on the rolls, due to their compression, is shown in Fig. 206. For rigid rolls the resultant of the pressure of the metal on the rolls is applied at point B_1 which is close to the

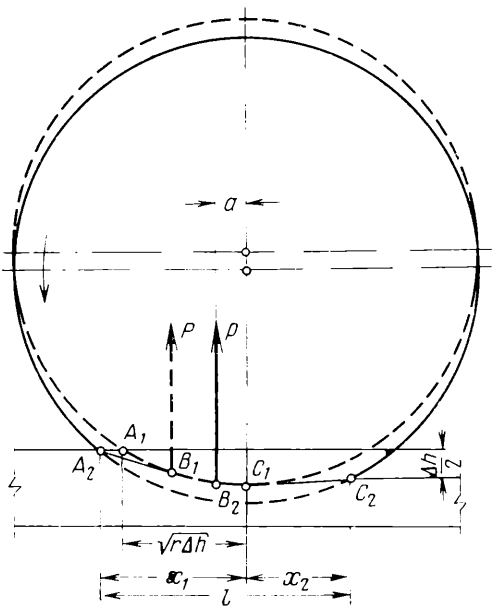

Fig. 206. Displacement of the point of application of the resultant of the metal pressure on the rolls due to the elastic compression of the rolls and the rolled metal

middle of the ideal arc of contact A_1C_1, whilst for deformed rolls it is applied at point B_2 which is located close to the centre of the actual arc of contact A_2C_2.

If we assume (neglecting the elastic deformation of the rolled metal) that the position of the resultant of the pressure for rigid rolls is determined by the equation

$$B_1C_1 = \psi_{rig} A_1C_1 = \psi_{rig} \sqrt{r\Delta h}$$

where ψ_{rig} is the coefficient of the lever arm for rigid rolls, then for the elastically deformed rolls and the rolled metal

$$B_2C_2 = \psi_{rig} A_2C_2 = \psi_{rig} (x_1 + x_2)$$

Owing to the fact that the segment of the arc of contact $C_1C_2 = x_2$, the distance from the point B_2 to the line connecting the centres of the rolls is

$$B_2C_1 = \psi_{rig}\left[x_1 - \left(\frac{1}{\psi_{rig}} - 1\right)x_2\right] \qquad \text{(VI.15)}$$

If the position of the point B_2 is known, the magnitude of the lever arm of the resultant of the pressure can be found relative to the roll centres for various cases of rolling.

In the simple case of rolling where the resultant of the pressure of the metal on the rolls is directed vertically, as shown in Fig. 206, the length of the lever arm [see equation (V.19)] is

$$a = \psi_{rig}\left[\sqrt{r\Delta h + x_2^2} - \left(\frac{1}{\psi_{rig}} - 1\right)x_2\right] \qquad \text{(VI.16)}$$

Taking into consideration the elastic deformation of the rolls and the metal being rolled, the actual coefficient of the lever arm is

$$\psi_{el} = \frac{a}{l} = \psi_{rig} - \frac{x_2}{l} \qquad \text{(VI.17)}$$

where l and x_2 are found from equations (V.19) and (V.22) respectively.

If we assume tentatively that $\psi_{rig} = 0.5$, then the rolling torque from equation (VI.16) is

$$M_{rol} = P\left(\sqrt{r\Delta h + x_2^2} - x_2\right) \qquad \text{(VI.18)}$$

where P is the overall pressure exerted by the metal on the rolls.

We express P in terms of the mean specific pressure p_m and the contact area:

$$P = p_m b\left(x_2 + \sqrt{r\Delta h + x_2^2}\right)$$

where b is the width of the rolled metal.

Substituting this value of P into equation (VI.18) we obtain

$$M_{rol} = p_m b r \Delta h \qquad \text{(VI.19)}$$

Comparing this equation with equation (VI.13), putting $\psi = 0.5$ and expressing P in terms of p_m and the contact area, we conclude that in the case where p_m is maintained constant, elastic deformation of the rolls does not affect the rolling torque.

But in reality, owing to the elastic deformation of the rolls, the specific pressure increases as a result of the effect of the external friction, because of the longer arc of contact.

Elastic deformation of the rolls thus gives rise to an increase in the rolling torque, but only as a result of the increased specific pressure. The energy consumption during rolling in this case is also increased due to the increase in the rolling torque and friction losses in the bearings of the rolls due to the greater pressure.

4. DETERMINATION OF THE ROLLING TORQUE FROM THE ENERGY CONSUMPTION

In a number of cases it is more convenient to determine the rolling torque from the consumption of energy during rolling, since in this field more extensive experimental material has been collected than for the pressure of the metal on the rolls. This method of calculating the torques required to drive the rolls is mostly used when non-rectangular metal sections are rolled, where the determination of the contact area and the pressure of the metal on the rolls is more complicated than when sheets, strips and rectangular sections in general are rolled.

The rolling torque can be expressed as a function of the work A expended during the rolling:

$$M_{rol} = \frac{A}{\varphi} = A \frac{D}{2} \frac{1+s}{L_1} \qquad \text{(VI.20)}$$

where φ is the angle of rotation of the rolls during the passage of the metal, radians
D is the working diameter of the rolls
s is the forward slip during rolling
L_1 is the length of the rolled strip when it emerges from the rolls.

There are numerous formulas for the calculation of the work expended during the rolling process, and they were investigated in detail by I. Pavlov. The formula of Fink (two expressions), and the formula of Timme (U.S.S.R.) can be regarded as amongst the most important ones.

According to the formula of Fink the theoretical amount of work equals

$$A = pV \log_e \frac{h_0}{h_1} \qquad \text{(VI.21)}$$

for rolling without intermediate turnovers, when $b_0 \leqslant b_1$, and

$$A = pV \log_e \frac{L_1}{L_0} \qquad \text{(VI.22)}$$

for rolling with turnover, when $b_0 \geqslant b_1$,
where p is the resistance to deformation calculated from experimental results
V is the volume of the rolled strip
L_0 and L_1 are the lengths of the rolled metal before and after the pass.

According to these formulas the energy consumption is proportional to the displaced volume expressed as the product of the total

volume of the rolled strip and the natural logarithm of deformation, i.e.,

$$V_{dis} = V \log_e \frac{h_0}{h_1} \text{ or } V_{dis} = V \log_e \frac{L_1}{L_0}$$

Graphically this displaced volume is represented by the shaded portion in Fig. 207*a*.

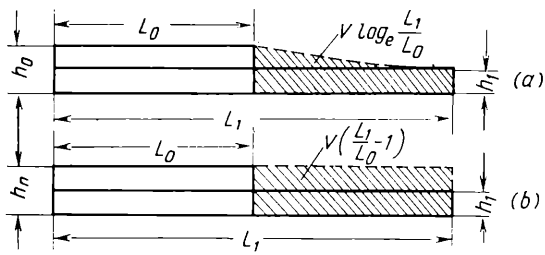

Fig. 207. Volume taken as proportional to energy consumption during rolling (V is the volume of the rolled strip):

(*a*) according to Fink's formula $A = pV \log_e \frac{L_1}{L_0}$; (*b*) according to Timme's formula $A = pV \log_e \left(\frac{L_1}{L_0} - 1\right)$

According to the formula of Timme the energy consumption during rolling is

$$A = G\Delta \left(\frac{L_1}{L_0} - 1\right) \qquad \text{(VI.23)}$$

where G is the weight of rolled strip, tons

Δ is the specific energy consumption, determined from experimental data.

According to this formula the consumption of energy is taken equal to the volume shown in Fig. 207*b*.

To compare the results given by the formulas of Fink and Timme a diagram is shown in Fig. 208 giving the consumption of energy per unit weight of the rolled metal as dependent on the reduction ratio. According to this diagram the results obtained by the two formulas greatly diverge.

Theoretically the formula of Fink should give more correct results, but in certain cases, for example, as a result of a drop of the temperature of the metal being reduced during hot rolling, or when work hardening increases during cold rolling, the formula of Timme can give results which are closer to the truth.

In view of the difficulty of allowing for all the factors that affect the energy consumption during the rolling of this component or

other, the formulas just mentioned give only an approximate idea of the energy consumption for the individual passes as it depends on the reduction ratio.

To obtain more accurate results it is necessary to use the data of experimental investigations, which characterize not only the total energy consumption during the rolling of the given component

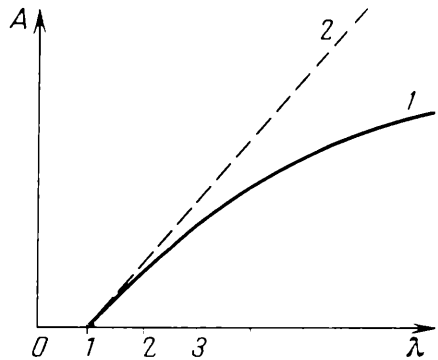

Fig. 208. Variation of energy consumption with total reduction ratio during rolling:
1—according to Fink's formula; *2*—according to Timme's formula

but also characterize the variation of this consumption with the deformation of the metal in each pass.

These results of experimental investigations are usually given in the form of curves expressing the energy consumption per one ton of the rolled product as dependent on the total reduction ratio, i.e., the elongation, or when sheets and strips are rolled, as dependent on the reduction in the thickness of the rolled material. Data of this kind are found in handbooks where curves of the specific energy consumption during rolling are given.

As an example a curve of this type is represented in Fig. 209, where the energy consumption is plotted as the ordinate and the elongation as compared to the length of the initial product is plotted as abscissa (to a logarithmic scale). According to this graph the specific energy consumption per pass of the metal through the rolls equals the difference of the two ordinates a_1 and a_0, which correspond to the ratio of the length of the rolled strip after and before the pass to the initial length. Thus, the energy consumption per pass per one ton amounts to $a_1 - a_0$ hp hr/t.

Then the total quantity of work for the given pass is

$$A = 75 \times 3{,}600\,(a_1 - a_0)\,G \text{ kgm} \qquad \text{(VI.24)}$$

where G is the weight of the rolled strip in tons.

In view of the fact that the energy consumption during rolling is usually measured by the load on the motor, the above curves also include the friction losses in the mechanisms of the rolling

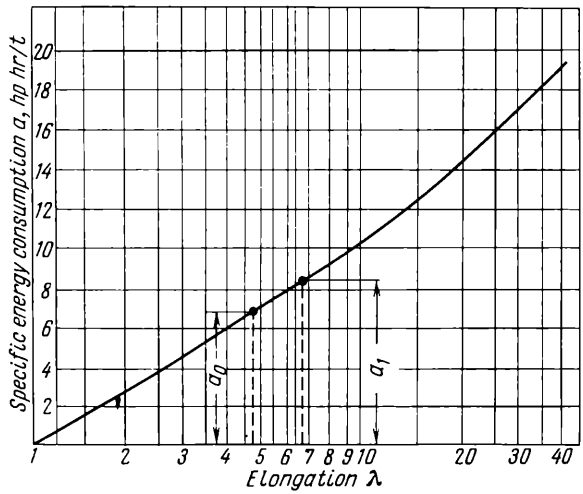

Fig. 209. Variation of energy consumption with overall elongation during the rolling of blooms

mill, but do not include the losses due to the idling of the mill. Accordingly the torque calculated from this energy consumption is the sum of the torques M_{rol} and iM_{fr}.

Using equation (VI.20) we find the torque necessary to rotate the rolls:

$$M_{rol} + iM_{fr} = \frac{75 \times 3{,}600\,(a_1 - a_0)\,GD}{2L_1}(1 - s) \text{ kgm}$$

Expressing the ratio $\frac{G}{L_1}$ in terms of the cross-sectional area of the rolled strip and the specific weight, we obtain

$$M_{rol} + iM_{fr} = 135\,(a_1 - a_0)\,\gamma QD\,(1 - s) \text{ tm} \qquad \text{(VI.25)}$$

where a_0 and a_1 are the specific energy consumption before and after the pass in question, hp hr/t
γ is the specific weight, t/m³
Q is the cross-sectional area of the rolled strip, m²
D is the working diameter of the rolls, m
s is the forward slip.

If the effect of the forward slip is neglected, then for steel with specific weight 7.8 t/m³ we obtain

$$M_{rol} + iM_{fr} = 1{,}050\,(a_1 - a_0)\,QD \text{ tm} \qquad \text{(VI.26)}$$

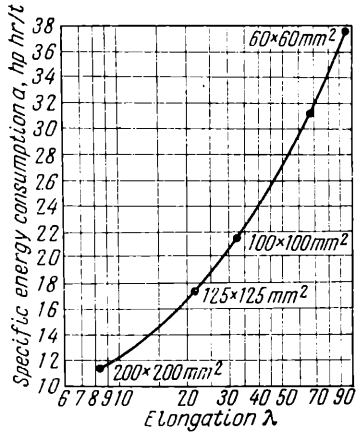

Fig. 210. Variation of energy consumption with elongation during the rolling of blanks having cross sections of 100 × 100 and 60 × 60 mm from blooms having a cross section of 200 × 200 mm; continuous blank mills 630 and 450 were used (Sheiman, Brozgol and Gerasimov)

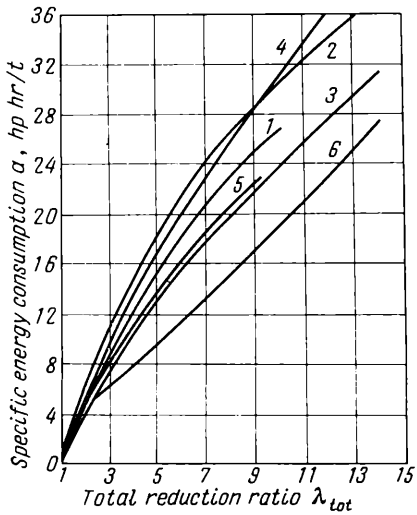

Fig. 211. Variation of energy consumption with overall reduction ratio during the rolling of various sections in cross-country mill 300:

1—square steel with 25-mm side from a 78 × 78 mm blank weighing 0.21 ton; *2*—round steel 24 mm in diameter from a 78 × 78 mm blank weighing 0.21 ton; *3*—40 × 40 × 4 mm angle steel from a 66 × 66 mm blank weighing 0.16 ton; *4*—40 × 40 × 5 mm angle steel from a 66 × 66 mm blank weighing 0.16 ton; *5*—40 × 10 mm strip steel from a 66 × 66 mm blank weighing 0.16 ton; *6*—50 × 6 mm strip steel from a 66 × 66 mm blank weighing 0.16 ton

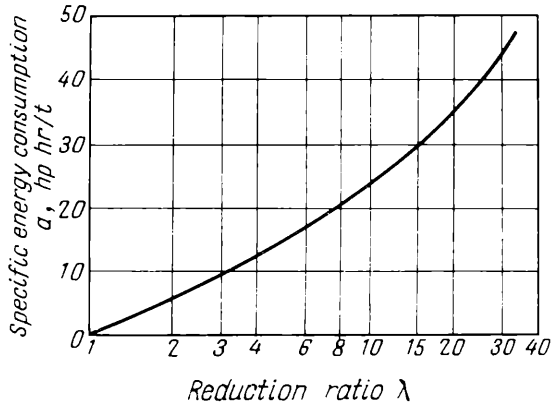

Fig. 212. Variation of energy consumption with overall reduction ratio during the rolling of a 2.5 × 135 mm mild steel strip in continuous strip mill 300. The blank cross section was 106 × 106 mm; temperature 1,200°C (N. Druzhinin and V. Khotulev)

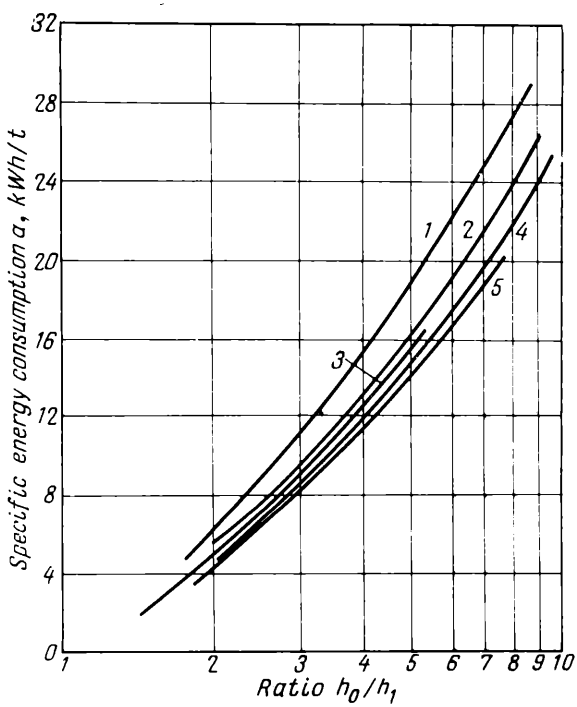

Fig. 213. Variation of energy consumption with $\frac{h_0}{h_1}$ during the rolling of wide mild steel band in the finishing section of continuous band mill 1680 (A. Chekmarev et al.):

1—killed steel Ст. 3 (3.0 × 1,400 mm); *2*—rimmed steel Ст. 3 (3.0 × × 1,400 mm); *3*—20 rimmed steel (5.0 × 1,400 mm); *4*—08 rimmed steel (2.5 × 1,510 mm); *5*—08 rimmed steel (3.5 × 1,400 mm)

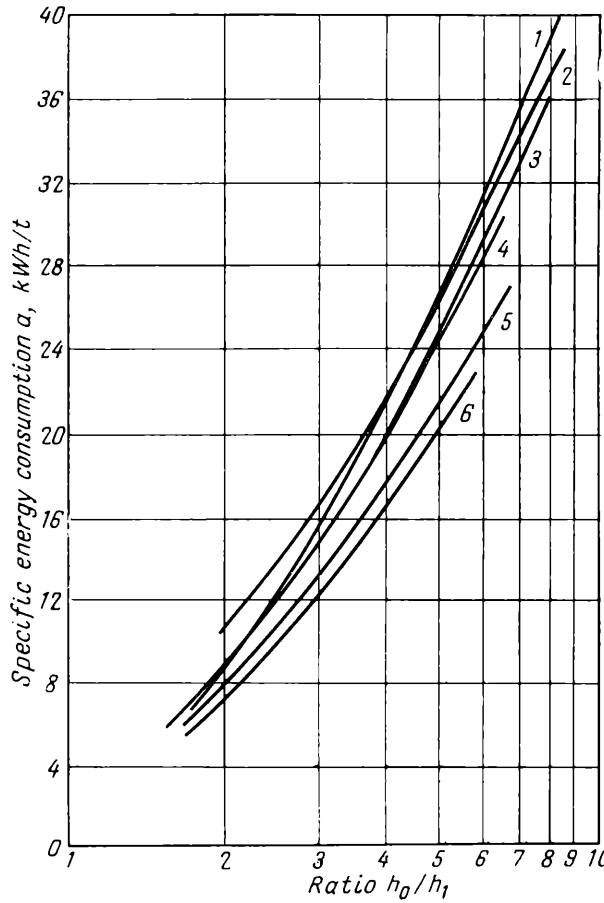

Fig. 214. Variation of energy consumption with $\frac{h_0}{h_1}$ during the rolling of a wide alloy steel band in the finishing section of continuous band mill 1680 (A. Chekmarev et al.):

1—30ХГСА (2.3 × 740 mm); *2*—12Х5МА (3.0 × 1,430 mm); *3*—30ХГСА (3.0 × 1,030 mm); *4*—30ХГСА (3.5 × 1,230 mm); *5*—12Х5МА (4.0 × × 1,030 mm); *6*—30ХГСА (4.0 × 1,280 mm)

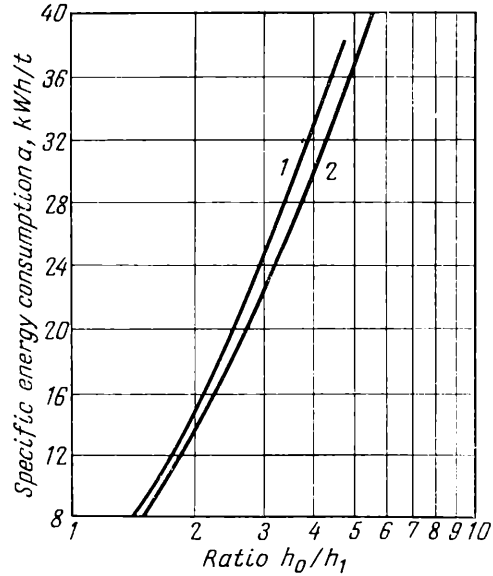

Fig. 215. Variation of energy consumption with $\frac{h_0}{h_1}$ during the rolling of a wide stainless steel band in the finishing section of continuous band mill 1680 (A. Chekmarev et al.):
(*1*) 1X18H9T (4.0 × 1,280 mm); (*2*) 1X18H9T (4.0 × 1,030 mm)

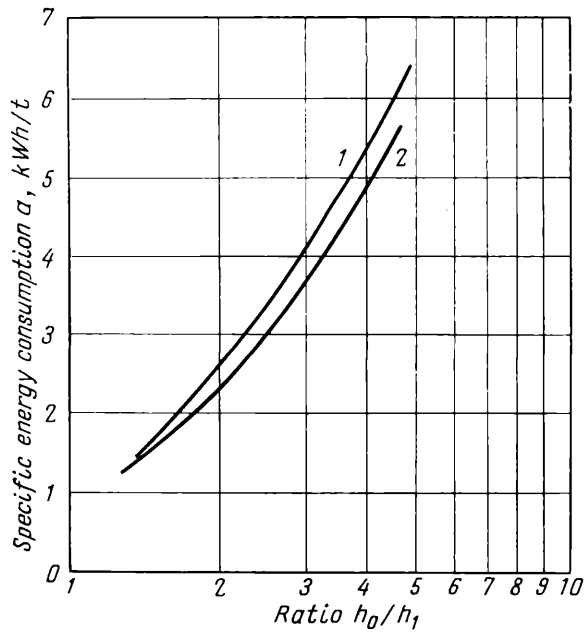

Fig. 216. Variation of the energy consumption with $\frac{h_0}{h_1}$ during the rolling of a wide carbon steel band in the roughing section of continuous band mill 1680. The initial thickness of the slab is 110 to 115 mm (A. Chekmarev et al.):
(*1*) 08 rimmed; (*2*) 3 rimmed, 15 rimmed and 25 rimmed

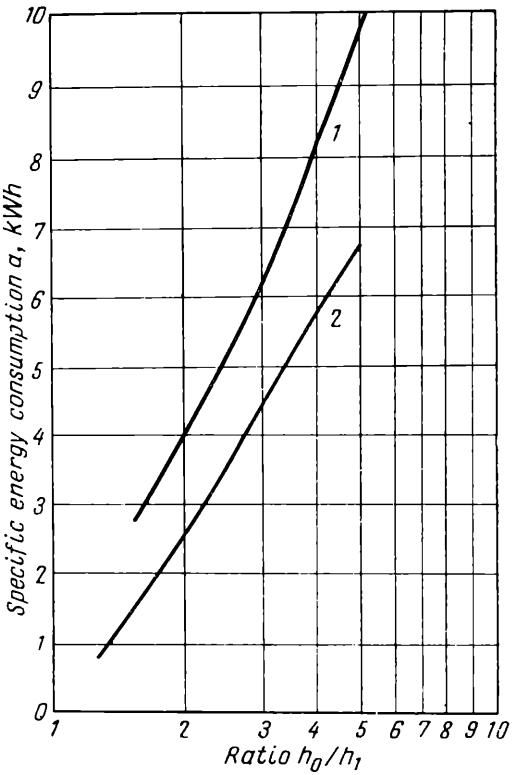

Fig. 217. Variation of energy consumption with $\frac{h_0}{h_1}$ during the rolling of a wide alloy steel band in the roughing section of continuous band mill 1680. The initial thickness of the slab is 110 mm (A. Chekmarev et al.): (*1*) 1Х18Н9Т and 2Х18Н9Т; (*2*) 12Х5МА and 25ХГСА

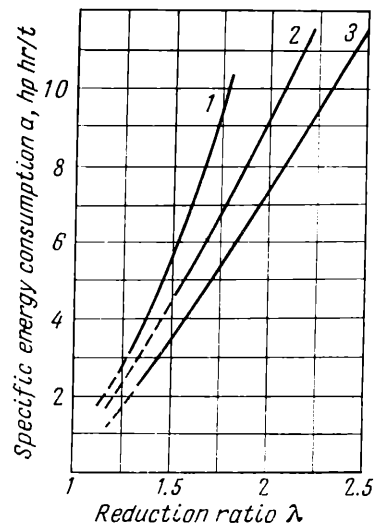

Fig. 218. Variation of energy consumption with λ during the rolling of tubes of carbon steels 1010, 1020 and 1035, with different diameters and wall thicknesses, in an automatic mill with a short mandrel (diameter of the rolls 700-750 mm). Temperature at the beginning of rolling 1,050 to 1,100°C; at the end of rolling 950 to 1,000°C (M. Sonkin):

(*1*) 219 × 8 to 10 mm; (*2*) 152 to 159 × 5 to 6 mm; (*3*) 121 to 127 × × 4.5 mm

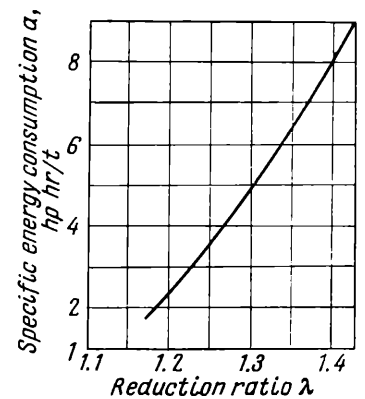

Fig. 219. Variation of energy consumption with λ when tubes of steels 1010, 1020 and 1035 are reduced in a two-high reducing mill. Initial temperature 900°C. Initial dimensions of the tube cross section 83 × 5 and 102 × 11.5 mm (M. Sonkin)

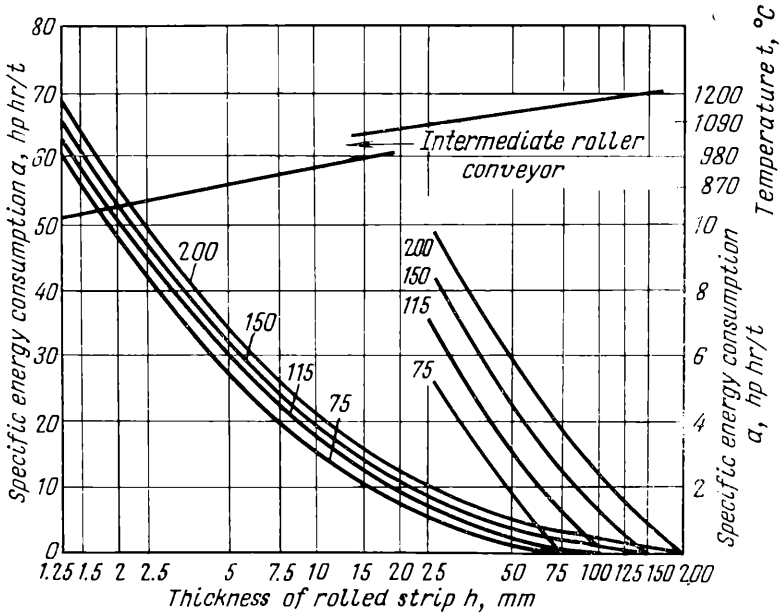

Fig. 220. Variation of energy consumption with h during the hot rolling of a mild steel band from a preheated slab (1,150-1,200°C) in a continuous mill. Thickness of slab: 75, 115, 150 and 200 mm; exit velocity 8.1 m/s

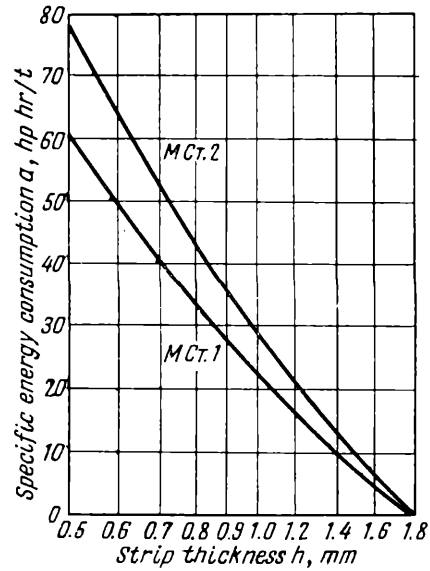

Fig. 221. Variation of energy consumption with h during the cold rolling of steels МСт. 1 and МСт. 2 in a 1450 × 450/1120 continuous mill. Rolling velocity in the last stand 4.1 to 4.25 m/s

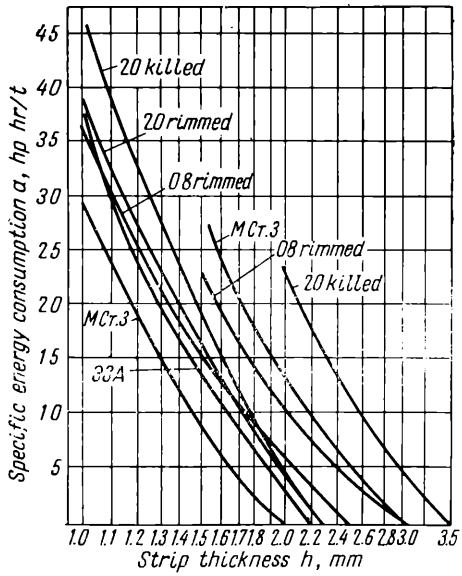

Fig. 222. Variation of energy consumption with h during the cold rolling of strips of different low carbon steels and different initial thicknesses in a 1450×450/1120 continuous mill. Velocity of rolling in the last stand 2.7 to 3.9 m/s

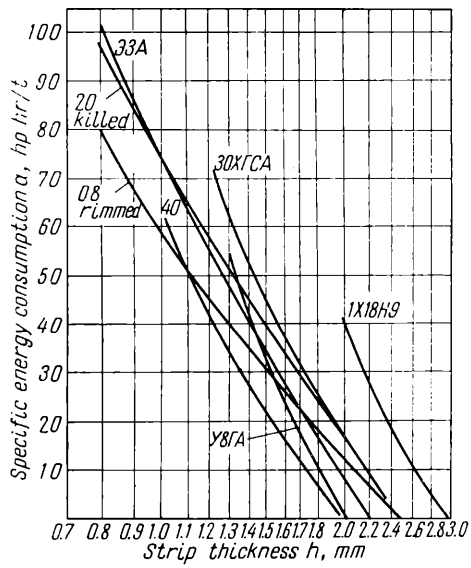

Fig. 223. Variation of energy consumption with h during the cold rolling of strips of low, medium and high alloy steels and of different initial thicknesses in a 740 × 520/1010 continuous mill. Velocity of rolling in the last stand 1.85 to 2.45 m/s

When the quantity of work is calculated from the curves, the required power can be expressed by the following equation:

$$N = \frac{3{,}600\,(a_1 - a_0)}{t} G \text{ hp} \qquad \text{(VI.27)}$$

where t is the time of passage of the metal between the rolls, seconds.

In calculating the energy consumption during rolling from the curves it is necessary in each case to choose the curve which is the closest to the conditions of rolling in question (material, dimensions and the form of section, type of rolling mill, etc.); in each case an elongation equal to unity must be ascribed to the section emerging from the preheating furnace.

Some curves of specific energy consumption plotted from experimental data are shown in Figs. 210 to 219.

Curves of specific energy consumption in rolling sheets and strips are sometimes constructed as a function of variation of the thickness (Figs. 220 to 223) of the rolled material, since the thickness greatly affects the energy consumption.

5. COMPARISON OF THE METHODS OF EVALUATING THE ROLLING TORQUE FROM THE MAGNITUDE OF THE PRESSURE AND THE ENERGY CONSUMPTION

When sheets, strips and other rectangular sections are rolled, i.e., when the contact area is determined by equation (V.13), the rolling torque can also be expressed in terms of the mean specific pressure:

$$M_{rol} = 2P\psi \sqrt{r\Delta h} = 2p_m \psi b_m r \Delta h \qquad \text{(VI.28)}$$

To analyze this equation we use it to calculate the energy consumption necessary for the rolling of strips or sheets of length L_1. According to equation (VI.20):

$$A = M_{rol}\varphi = M_{rol}\frac{L_1}{(1+s)r} = 2p_m\psi b_m \frac{L_1 \Delta h}{1+s} \qquad \text{(VI.29)}$$

where s is the forward slip.

If we tentatively put $\psi \approx 0.5$ in this equation and neglect the effect of the forward slip, then

$$A = 2p_m b_m L_1 \Delta h \qquad \text{(VI.30)}$$

It follows from this equation that the work which is needed for rolling is approximately equal to the product of the mean specific pressure and the volume formed by the contact area when it moves in the direction of rolling over a portion equal to the length of the rolled strip (Fig. 224).

It is not difficult to see that this volume is equal to that shown in Fig. 207*b*; it follows from this that equation (VI.30) expressing approximately the amount of work determined from the pressure

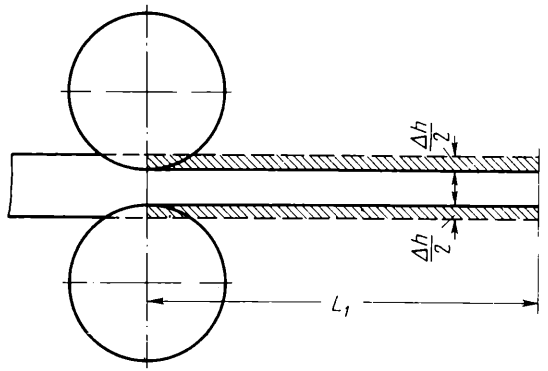

Fig. 224. The volume (shown shaded in the figure) formed by the contact area moving in the direction of rolling a length equal to the length of the rolled strip

of the metal on the rolls, coincides in principle with the formula of Timme (VI.23), and thus, at first glance, seems to contradict the formula of Fink (VI.22).

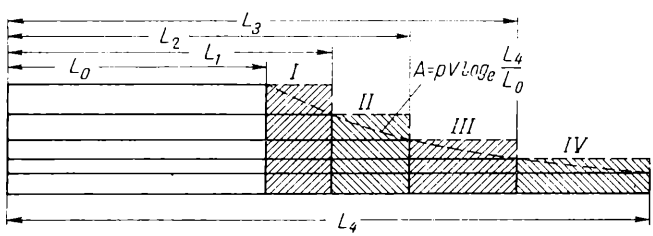

Fig. 225. Comparison of the volumes to which the energy consumption for four passes is taken to be proportional; calculations of the energy consumption are based on approximate formula (VI.30) (sum of the parallelepipeds *I-IV*) and the formula $A = pV \log_e \frac{L_4}{L_0}$

The contradiction is only apparent, however. When the required increase in length of the strip from L_0 to L_4 takes place in several (say, 4) passes, then the volumes to which the amount of work is proportional according to equation (VI.30) can be represented in the form of four parallelepipeds (Fig. 225). The sum of the volumes of these parallelepipeds, which represents the work performed during the four passes, does not differ markedly from the dis-

placed volume $V \log_e \frac{l_4}{l_0}$, to which the work is assumed to be proportional, defined by the formula of Fink. This displaced volume is shown as the dashed curve in Fig. 225.

The correctness of formula (VI.22) can be also confirmed if we determine theoretically the work required for the plastic deformation alone, neglecting the inevitable friction losses of metal along the surfaces of the rolls.

Let us isolate in the deformation zone an element from the metal contained between two vertical planes so that the length of the arc

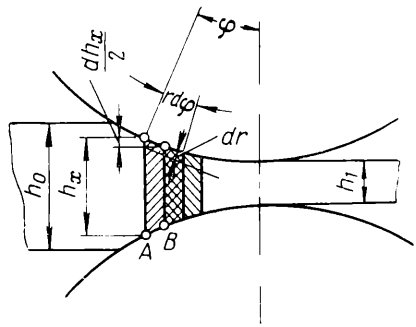

Fig. 226. Determination of the energy consumption during rolling

of contact of this element will be equal to $rd\varphi$. When this element is displaced along the arc of contact by the amount AB, and when it is reduced in the radial direction by the distance dr at top and bottom, the work for $b = 1$ can be expressed as (Fig. 226):

$$dA = 2prd\varphi\, dr \qquad \text{(VI.31)}$$

From the condition that the volume ΔV of this element remains constant when it passes through the rolls it follows that

$$\Delta V = h_x r d\varphi \cos\varphi$$

Substituting the value of $rd\varphi$ obtained from this equation into equation (VI.31) and denoting

$$dr = \cos\varphi \frac{dh_x}{2}$$

we find that

$$dA = p\Delta V \frac{dh_x}{h_x}$$

or

$$A = p\Delta V \log_e \frac{h_0}{h_1} \qquad \text{(VI.32)}$$

or, when spreading is absent,

$$A = p\Delta V \log_e \frac{L_1}{L_0} \tag{VI.33}$$

From equations (VI.32) and (VI.29) it follows that

$$2p_m \psi b_m \frac{L_1 \Delta h}{1+s} = pL_1 h_1 b_m \log_e \frac{h_0}{h_1}$$

if we substitute $p_m = p$, so that

$$\frac{2\psi}{1+s} \frac{\Delta h}{h_1} \approx \log_e \frac{h_0}{h_1}$$

From this

$$\psi = 0.5(1+s) \frac{h_1}{\Delta h} \log_e \frac{h_0}{h_1} \tag{VI.34}$$

If we neglect the effect of forward slip and if $\log_e \frac{h_0}{h}$ is expanded in a series and only the first term of this series is used, i.e.,

$$\log_e \frac{h_0}{h_1} = \log_e \left(1 + \frac{\Delta h}{h_1}\right) \approx \frac{\Delta h}{h_1}$$

then we obtain $\psi \approx 0.5$.

From these results it follows that the formula

$$A = pV \log_e \frac{h_0}{h_1}$$

does not contradict formulas (VI.29) and (VI.30); if in calculating the amount of work from the pressure of the metal on the rolls we take into consideration the forward slip and bear in mind that during the simple rolling process the lever arm coefficient is a little less than 0.5, then the results obtained from formulas (VI.22) and (VI.29) must be identical. At the same time formula (VI.30) may be considered as a simplification of formula (VI.22), when $\log_e \frac{h_0}{h_1}$ is expanded in a series and only the first term of this series is used, the effect of the forward slip is neglected, and it is assumed that $\psi = 0.5$.

As a consequence of what has just been said it is thought advisable to calculate, on the basis of formula (VI.33), the power required during rolling from the equation

$$N = \frac{p_m v_1 Q_1}{102} \log_e \lambda \text{ kW} \tag{VI.35}$$

where p_m is the mean specific pressure, kg/mm²
v_1 is the exit velocity of the metal, m/s
Q_1 is the cross-sectional area of the metal emerging from the rolls, mm².

If this formula, with the rating expressed in horse power, is compared with equation (VI.27), we obtain the following relationship (recommended by E. Rokotyan) between the mean specific pressure and the specific energy consumption during rolling:

$$\frac{p_m v_1 Q_1}{75} \log_e \lambda = \frac{3{,}600\,(a_1 - a_0)}{t} G \text{ hp}$$

Bearing in mind that

$$\frac{G}{t} = \frac{Q_1 v_1 \gamma}{10^6}$$

where Q_1 is the cross-sectional area of the strip as it emerges from the rolls, mm²

v_1 is the exit velocity of the metal, m/s

γ is the specific weight of the metal, t/m³,

we obtain

$$p_m = 0.27\gamma \frac{a_1 - a_0}{\log_e \lambda} \text{ kg/mm}^2$$

where $a_1 - a_0$ is the specific energy consumption for the given pass, determined from the curves of Figs. 210 to 223, but with the energy expended in friction in the mechanisms of the rolling mill subtracted, hp hr/t.

6. THE EFFECT OF TENSION OR THRUST ON THE ENERGY CONSUMPTION AND THE ROLLING TORQUE

In order to establish the effect of tension or thrust on the energy consumption during plastic deformation, we shall consider the simplest case of deformation when two-dimensional upsetting of a prism takes place between two parallel planes, provided that external forces act on the sides of this prism.

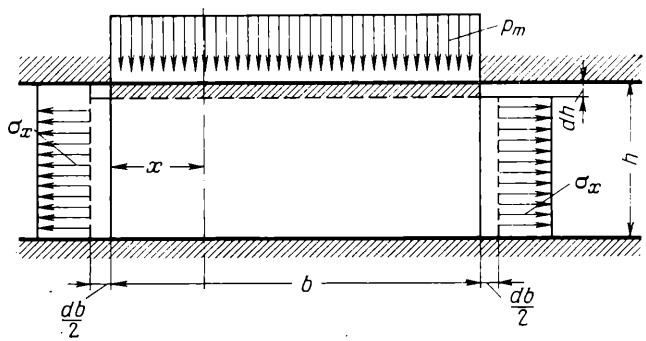

Fig. 227. Compression of a prism with external forces applied to its side surfaces

When the prism is compressed by the amount dh (Fig. 227) the work is equal to the sum of two quantities:

$$dA = p_m F_y \, dh + 2\sigma_x F_x \frac{db}{2} \tag{VI.36}$$

where p_m is the mean specific pressure
σ_x is the stress arising on the side surfaces of the prism
F_x and F_y are the areas where the stresses p_m and σ_x are applied
db is the spreading.

Denoting the volume of the prism by V, and taking its dimension in the direction perpendicular to the plane of the paper equal to unity, we obtain

$$F_y = \frac{V}{h} \quad F_x = \frac{V}{b}$$

After substituting the values of F_y and F_x into equation (VI.36) we have

$$dA = p_m V \frac{dh}{h} + \sigma_x V \frac{db}{b} \tag{VI.37}$$

Since the strain is

$$\frac{dh}{h} = \frac{db}{b}$$

equation (VI.37) assumes the following form:

$$dA = (p_m + \sigma_x) V \frac{dh}{h} \tag{VI.38}$$

The specific pressure on the contact surfaces at a distance x from the edge of the prism is determined from the equation of equilibrium

$$h \, d\sigma_x = 2\tau_x \, dx$$

and the equation of plasticity

$$p_x = 2k - \sigma_x$$

For constant friction forces on the contact surfaces, say, equal to k, the specific pressure is given by

$$dp_x = \frac{2k}{h} dx$$

or

$$p_x = (2k - \sigma_x) + \frac{2k}{h} x \tag{VI.39}$$

From this the mean specific pressure is

$$p_m = 2k \left(1 + \frac{b}{4h}\right) - \sigma_x \tag{VI.40}$$

The first term of the right-hand side of this equation represents the mean specific pressure p'_m when the external stress σ_x on the side surfaces is absent:

$$p_m = p'_m - \sigma_x$$

Substituting this value of p_m into equation (VI.38) we obtain

$$dA = p'_m V \log_e \frac{dh}{h}$$

Hence we may conclude that for obtaining the same deformation the total energy consumption will not depend on the nature of the additional external forces (tension or compression) applied to the side surfaces. Thus we may assume that in rolling with tension or thrust the total energy consumption varies only as a result of a reduction in the friction forces on the contact surfaces.

In practice during cold rolling of metal in rolls with a large $D : h_1$ ratio, the energy consumption is slightly reduced owing to a reduction in the local elastic deformation of the rolls, and, consequently, in the effect of the contact friction forces as a result of tension. In reversing mills with a small $D : h_1$ ratio the energy consumption obviously may not diminish with increasing tension owing to the increased losses during its recovery at the driven coiler drum.

Taking into consideration the above conclusions, let us calculate the rolling torque. It is necessary to bear in mind that if the torque is determined from equation (VI.13), difficulties arise in calculating the lever arm coefficient ψ which is greatly affected by the tension or thrust.

Assuming that the power consumed in rolling does not vary when tension is applied, we can write, using equation (VI.35):

$$N = p'_m v_1 Q_1 \log_e \lambda = M_{rol} \frac{v_1}{1+s} \frac{2}{D} - \sigma_0 Q_0 v_0 + \sigma_1 Q_1 v_1 \text{ kgm/s} \quad \text{(VI.41)}$$

From this we obtain the formula for determining M_{rol}, i.e., the torque required to drive both rolls in order to overcome the resistance to deformation of the metal between the rolls when rolling with tension:

$$M_{rol} = (p'_m \log_e \lambda + \sigma_0 - \sigma_1) \frac{Q_1 D}{2} (1 + s) \text{ kgm} \quad \text{(VI.42)}$$

where p'_m is the mean specific pressure without the effect of the tension taken into account, kg/mm²

λ is the reduction ratio

σ_0 and σ_1 are the tensile stresses, kg/mm²

Q_1 is the cross-sectional area of the strip as it emerges from the rolls, mm²

D is the working diameter of the rolls, m

s is the forward slip.

When metal is rolled with thrust the sign in front of σ_0 and σ_1 must be changed accordingly.

If the mean specific pressure p_m—with the effect of tension taken into account—is known, then according to equation (V.70), when approximate calculations are performed, the following substitution

$$p'_m \approx p_m + \frac{\sigma_0 + \sigma_1}{2} \qquad \text{(VI.43)}$$

must be made in formula (VI.42).

7. DETERMINATION OF THE TORQUE OF THE ADDITIONAL FRICTION FORCES

By the torque of additional friction forces we understand the torque required to overcome the friction forces which arise in the bearings of the rolls and in the drive mechanism of the mill when the metal being rolled passes through the rolls; however, the value of this torque does not contain the torque required to drive the rolls when the mill is running idle.

The major part of the torque of additional friction forces is the torque of the friction forces in the bearings of the rolls. The value of this torque for both rolls is

$$M_{fr1} = P\, d\mu_1 \qquad \text{(VI.44)}$$

where P is the load on the bearings (in the case of the non-overhung arrangement of the rolls this load equals the pressure of the rolled metal on the rolls except in six-roll and multi-roll mills)

d is the journal diameter

μ_1 is the coefficient of friction in the bearings of the rolls.

The construction of the bearings and the working conditions affect the value of the coefficient of friction, which may be taken as given in the table below.

Type of bearing	Coefficient of friction μ_1
Sliding:	
metallic bushes:	
hot rolling	0.07 to 0.1
cold rolling	0.05 to 0.07
plastic bushes	0.01 to 0.03
Fluid friction	0.003
Rolling	0.003

The second component of the torque of additional friction forces is the friction forces in the drive mechanism of the mill, i.e., in gear

stand, in the reduction gear, etc. This quantity depends on the efficiency of the transmission and is usually determined from the equation

$$M_{fr2} = \left(\frac{1}{\eta} - 1\right) \frac{M_{rol} + M_{fr1}}{i} \qquad \text{(VI.45)}$$

where M_{fr2} is the torque of the losses in the transmission, referred to the motor shaft

η is the efficiency of the transmission from the motor to the rolls

i is the gear ratio of this transmission

M_{rol} and M_{fr1} are the rolling torque and the torque of the friction forces in the bearings of the rolls, referred to the latter.

The efficiency of a single stage gear drive is usually taken equal to 0.96 to 0.98, that of a belt drive is taken to be 0.85 to 0.9 and that of a rope drive equal to 0.85.

In four-high mills and in other mills provided with support rolls, a further component of the torque of the additional friction forces is present: this is provided by the rolling friction losses of the working rolls along the support rolls. But because of their smallness these losses are usually not taken into account in calculations.

Thus the total torque of the additional friction forces, referred to the motor shaft, is

$$M_{fr} = \frac{M_{fr1}}{i} + M_{fr2} \qquad \text{(VI.46)}$$

or

$$M_{fr} = \frac{M_{fr1}}{i\eta} + \left(\frac{1}{\eta} - 1\right) \frac{M_{rol}}{i} \qquad \text{(VI.47)}$$

If the mill is provided with idle rolls, then the first term of this equation must be multiplied by the gear ratio between the working and support rolls. Then

$$M_{fr} = \frac{M_{fr1}}{i\eta} \frac{D_w}{D_{sup}} + \left(\frac{1}{\eta} - 1\right) \frac{M_{rol}}{i} \qquad \text{(VI.48)}$$

where D_w and D_{sup} are the diameters of the working and support rolls respectively.

8. IDLE LOAD

The idling torque, i.e., the torque required to drive the main line of a rolling mill in idle periods, is calculated for large mills from the weight of the rotating components and the radii of the friction circles of their bearings.

Let us calculate this torque in a general form for a case where in the main line of the rolling mill a number of components (rolls, shafts, couplings, gears, flywheel, etc.) are of different weight, and rotate with different velocities in bearings with journals of different diameters and different coefficients of friction. The idling torque is obviously equal to the sum of the torques, referred to the motor shaft, which are required to drive each component, i.e.,

$$M_l = \sum M_n \qquad \text{(VI.49)}$$

where M_n is the torque required to drive a particular component, referred to the motor shaft.

Expressing the quantity M_n in terms of the force and the radius of the friction circle of the bearings of the given component, we obtain

$$M_n = \frac{G_n \mu_n d_n}{2i_n} \qquad \text{(VI.50)}$$

where G_n is the weight of the given component (by this the load on the bearings is understood)
μ_n is the coefficient of friction in the bearings
d_n is the journal diameter
i_n is the gear ratio between the motor and the component in question.

Substituting this value of M_n into equation (VI.49) we obtain

$$M_l = \sum \frac{G_n \mu_n d_n}{2i_n} \qquad \text{(VI.51)}$$

The coefficient of friction must be chosen, for the particular type of bearing, from the data given above; in so doing a possible seizure of the bushes must be considered.

When the idling torque is calculated for thin strip cold-rolling mills and certain other mills the initial pressure on the rolls still has to be considered. In this case the load on the bearings of the rolls can be very considerable and will sometimes nearly approach the pressure of the metal on the rolls during rolling. The additional torque of the friction forces so produced can obviously be calculated from equation (VI.44), taking the pressure P equal to the force between the rolls. Then the torque of the additional friction forces should correspondingly be reduced during the working run.

If the mill is provided with a flywheel, the value of the idling torque must be supplemented by the torque dissipated in overcoming the friction of this flywheel against the air. To calculate this item of power consumption, the following empirical formula is often used:

$$N = v^{2.5} D^2 (1 + 5b)\, 10^{-5} \text{ hp} \qquad \text{(VI.52)}$$

where v is the peripheral velocity of the flywheel rim, m/s
D is the outside diameter of the flywheel, m
b is the width of the rim, m.

9. STATIC LOAD DIAGRAMS

To determine the power of the drive, and to calculate the strength of the mill, the magnitude of the load must be supplemented with the knowledge of the graph of the load variation with time. This graph is known as the load diagram.

The preliminary calculations leading to the construction of this diagram first involve the determination of the static load on the drive over the entire rolling cycle of the strip, and also the determination of the duration of the passes and the necessary intermissions between them.

The static load, as was mentioned above, can be calculated from the equation

$$M_{st} = \frac{M_{rol}}{i} + M_{fr} + M_l$$

where $\frac{M_{rol}}{i}$, M_{fr}, M_l denote the rolling torque, the torque of the additional friction forces, and the idling torque, referred to the motor shaft and given by equations (VI.13), (VI.25), (VI.47) and (VI.51).

The duration t of the pass is found from the ratio

$$t \quad \frac{L}{v_1}$$

where L is the length of the rolled strip and
v_1 is the mean exit velocity of the metal.

The length of idle periods between the passes is calculated or assumed dependent on the length of the operations which must be carried out when the strip to be rolled is fed to the rolls, such as: feed along the roller conveyor, turnover, transfer into another groove or into another stand, drop or lift of the top roll, reversal of the mill, etc.

The load diagram is constructed for the entire cycle of a given strip: from the instant it enters the rolls to its departure in the last pass and the feed of the next strip. After each cycle, whose form determines the rhythm of rolling, the load diagram is represented afresh.

The most characteristic static load diagrams of the drive for different rolling mills are shown in Fig. 228. Fig. 228*a* and *b* shows the

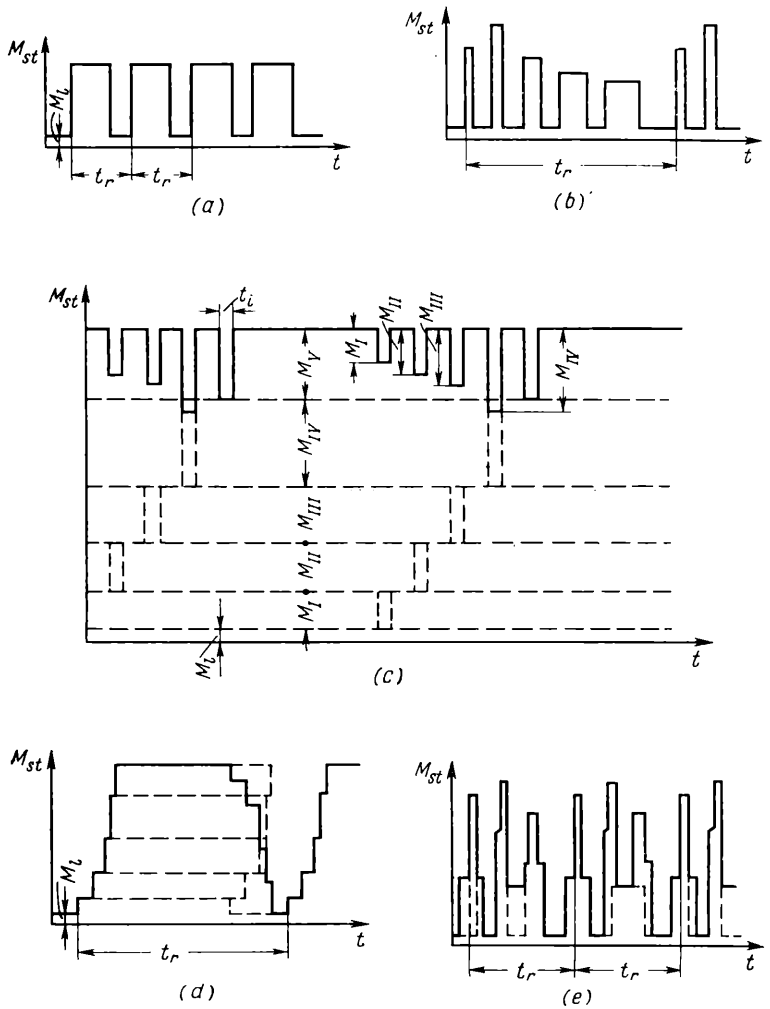

Fig. 228. Static load diagrams for various rolling mills (t_r is the rhythm of rolling):

(*a*) continuous mills with individual drives and other mills which roll a single strip in one pass; (*b*) single-stand mills and other mills which roll a single strip by repeated passes (five shown); (*c*) simultaneous rolling of two or more strips by repeated passes (five shown); (*d*) continuous mills with group drives (five stands) during the simultaneous rolling of a single strip; (*e*) as for *d*, but with the intermission between the feeds of two strips less than the time required by the strip to pass between the stands of the mill (t_i is the length of an intermission)

load diagrams of the drive, where the height of the rectangles corresponds to a single pass, whilst the height of the rectangles of the load diagrams shown in Fig. 228*c*, *d* and *e* corresponds to two or more passes. In this case the load diagram is constructed by adding one set of rectangle to another. The displacement of these rectangles (Fig. 228*d*) along the abscissa depends on the time of the passage of the rolled strip between the stands of the continuous mill and the duration of the idle periods. Often, in order to obtain a greater capacity of the mill, the intermissions are made less than the time necessary for the strip to pass from one stand into another; the ordinate of the load diagram will then be constant, with small gaps in it (Fig. 228*e*).

10. THE EFFECT OF A FLYWHEEL LOAD ON THE DRIVE

To equalize the load on the drive of a rolling mill during the time the rolled metal passes through the rolls and during the idle period, flywheels are used in certain cases.

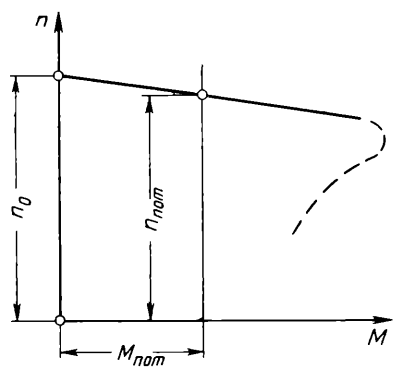

Fig. 229. The relation between the speed n and the load M of an asynchronous electric motor

According to equation (VI.4), the load on the drive shaft, with the effect of the flywheel taken into account, is

$$M_{mo} = M_{st} + \frac{GD^2}{375}\frac{dn}{dt} \qquad \text{(VI.53)}$$

where M_{st} is the torque on the motor shaft due to the static load
GD^2 is the dynamic moment of the flywheel and other rotating parts, referred to the motor shaft
$\frac{dn}{dt}$ is the acceleration of the motor, rpm sec.

The motor load diminishes only when its speed is reduced; the acceleration $\frac{dn}{dt}$ becomes negative and the second term in equation (VI.53), representing the dynamic moment, will have a minus sign.

To solve equation (VI.53) it is necessary to find the relationship between the number of revolutions per minute and the torque or the time. In most cases when a drive with a flywheel is to be calculated, and when an asynchronous electric motor provides the motive power, it is assumed that the speed of the motor is reduced proportionally to the increase in load (Fig. 229), i.e.,

$$n = a - bM_{mo} \tag{VI.54}$$

The constant values of a and b are indicated on the motor nameplate. Denoting the number of revolutions of the motor at zero load by n_0 (synchronous speed) and that at a load equal to the nominal torque M_{nom} by n_{nom}, we obtain

$$a = n_0 \quad b = \frac{n_0 - n_{nom}}{M_{nom}}$$

Then equation (VI.54) can be written as:

$$n = n_0 \left(1 - \frac{n_0 - n_{nom}}{n_0} \frac{M_{mo}}{M_{nom}}\right) \tag{VI.55}$$

The ratio $\frac{n_0 - n_{nom}}{n_0}$ is called the nominal slip of the motor; it is denoted by s_{nom}:

$$s_{nom} = \frac{n_0 - n_{nom}}{n_0}$$

This quantity depends on the characteristics of the electric motor and is usually 3 to 10%.

Let us find from equation (VI.55) the derivative of the speed:

$$\frac{dn}{dt} = -\frac{s_{nom}}{M_{nom}} n_0 \frac{dM_{mo}}{dt}$$

Substituting the value of $\frac{dn}{dt}$ into equation (VI.53), we obtain

$$M_{mo} = M_{st} - \frac{GD^2}{375} \frac{s_{nom}}{M_{nom}} n_0 \frac{dM_{mo}}{dt}$$

and after a transposition

$$\frac{dM_{mo}}{M_{mo} - M_{st}} = -\frac{375 M_{nom}}{GD^2 n_0 s_{nom}} dt$$

Denoting the constant quantity by

$$\frac{GD^2 n_0 s_{nom}}{375 M_{nom}} = T \tag{VI.56}$$

we obtain the basic differential equation for a drive with a flywheel

$$\frac{dM_{mo}}{M_{mo} - M_{st}} = -\frac{1}{T} dt \tag{VI.57}$$

The value of T depends on the dimensions of the flywheel and on the characteristics of the motor; it is called the inertial constant of the motor and flywheel system. This value is measured in time units; it is the product of the nominal slip and the startup time of the flywheel from rest to the speed of n revolutions per minute, provided that during the entire startup time the motor develops the nominal torque M_{nom}, and no static load is applied.

It is not difficult to see this, since $\frac{GD^2}{375} n_0$ is a momentum and $M_{nom} \frac{T}{s_{nom}}$ is the impulse of a force.

After integrating equation (VI.57) we obtain

$$\log_e (M_{mo} - M_{st}) = -\frac{t}{T} + C$$

The constant C is found from the initial conditions, if we assume that for $t = 0$

$$M_{mo} = M_0$$

We then obtain the equation of Gache:

$$M_{mo} = M_{st} - (M_{st} - M_0) e^{-\frac{t}{T}} \tag{VI.58}$$

This equation shows that the drive torque varies as an exponential curve, the asymptote of which is a line parallel to the time axis and passing at a distance from it equal to M_{st} (Fig. 230). At the same time, the greater the inertial constant of the motor and flywheel system, i.e., the dynamic torque of the flywheel or the slip of the motor, the smaller is the slope of the curve in question (see the dotted line in Fig. 231).

For the idle period of the drive, when $M_{st} = M_l$ and $M_0 > M_l$, equation (VI.58) assumes the following form:

$$M_{mo} = M_l + (M_0 - M_l) e^{-\frac{t}{T}} \tag{VI.59}$$

Using formulas (VI.58) and (VI.59) we can construct the load diagram for all passes and idle periods. For a large number of passes the plotting of this diagram by analytical means is time-consuming; hence it is advisable to construct it by means of a stencil.

The stencil is drawn on a thick paper to the scale of the load diagram (Fig. 232) from the equation

$$M' = M'_{st}\left(1 - e^{-\frac{t}{T}}\right) \qquad \text{(VI.60)}$$

where M'_{st} is the static torque, assumed to be approximately equal to the maximum value of M_{st} of the load diagram.

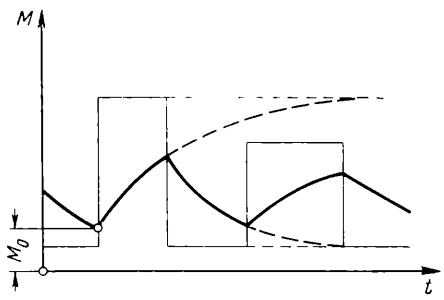

Fig. 230. Time variation of a load on a drive with a flywheel

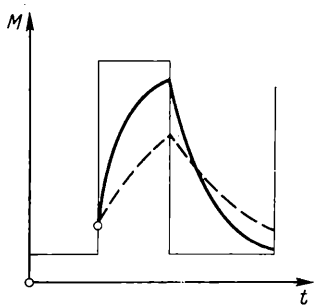

Fig. 231. Time variation of a load on a drive for different values of the inertial constant of the motor-flywheel system

The value of the time in constructing the stencil is taken from $t = 0$ to $t \approx 4T$, after which the curve merges with the asymptote.

In constructing the curves by a stencil the stencil is laid on the static load diagram in such a way that it touches the point where $M = M_0$, and so that its asymptote coincides with the straight line parallel to the time axis and is located from it at a distance equal to M_{st}. Within the limits of a given pass or idle period, the stencil is used to trace the corresponding part of the load diagram (Fig. 233).

We shall prove that it is possible to use one stencil to construct the exponential load curves of the drive for any value of M_{st}.

The equation of the stencil curve passing through the origin of the coordinates M' and t' (Fig. 232) is

$$M' = M'_{st}\left(1 - e^{-\frac{t'}{T}}\right) \qquad \text{(VI.61)}$$

where M'_{st} is the maximum value of the static torque, assumed in constructing the stencil.

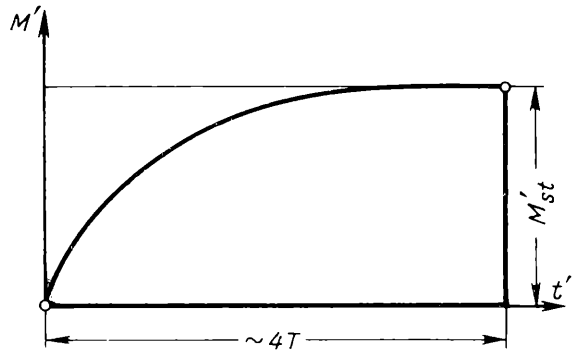

Fig. 232 Construction of stencil curve

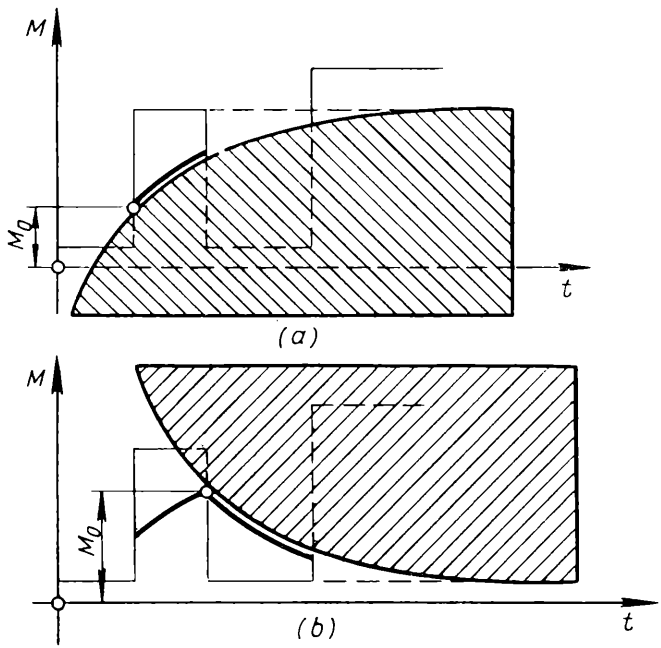

Fig. 233. Method of constructing the load diagram using a stencil in the case of a drive with a flywheel:
(a) $M_{st} > M_{mo}$; (b) $M_{st} < M_{mo}$

We find the equation of this curve in M-t coordinates of the given load diagram, where the curve passes through the point where $t = 0$ and $M = M_0$ and asymptotically approaches the straight

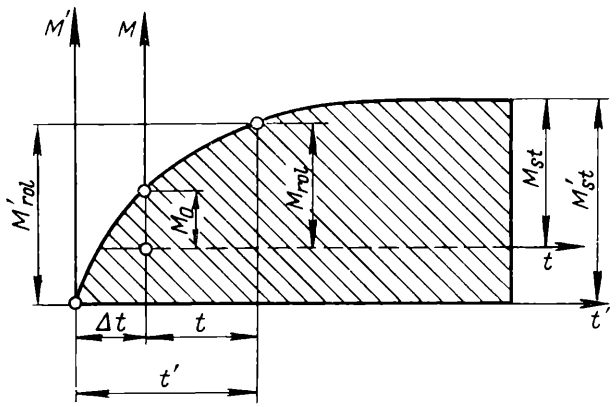

Fig. 234. Position of the stencil in M-t coordinates of the load diagram

line parallel to the abscissa and located from it at a distance equal to M_{st} (Fig. 234). To this end the coordinates of the stencil are expressed in terms of the coordinates of the load diagram:

$$M' = M + (M'_{st} - M_{st})$$
$$t' = t + \Delta t$$

which are then substituted into equation (VI.61):

$$M + (M'_{st} - M_{st}) = M'_{st}\left(1 - e^{-\frac{t+\Delta t}{T}}\right)$$

or

$$M - M_{st} = -M'_{st} e^{-\frac{\Delta t}{T}} e^{-\frac{t}{T}} \qquad \text{(VI.62)}$$

The value of Δt in this equation is found from the condition that for $t = 0$ and $M = M_0$

$$M_{st} - M_0 = M'_{st} e^{-\frac{\Delta t}{T}}$$

After substituting this value into equation (VI.62) we have

$$M = M_{st} - (M_{st} - M_0)\, e^{-\frac{t}{T}}$$

i.e., we obtain the curve which was to be constructed.

11. LOAD ON THE DRIVE OF REVERSING MILLS

In reversing mills the gripping of the metal being rolled takes place at a reduced velocity; afterwards the velocity of the rolls increases, and at the end of the pass it is reduced again (Fig. 235). Thus the time needed for the metal to pass through the rolls is made up of three periods: acceleration, steady state velocity and deceleration.

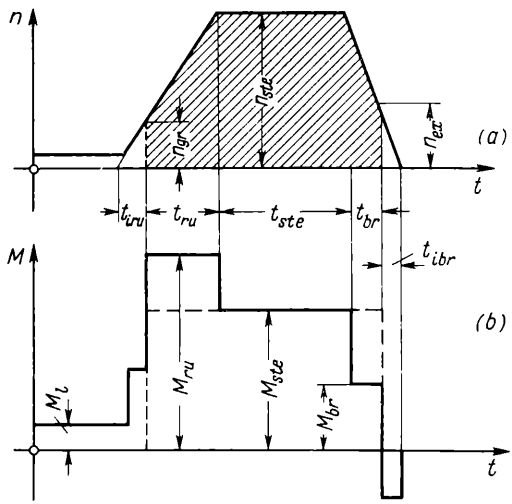

Fig. 235. Rolling velocity (*a*) and the load on the drive (*b*) during a pass with reversals

If we denote the acceleration of the motor, expressed in revolutions per minute per second, by ε_{ru} during the running up and by ε_{br} during the braking, then the driving torque during each of these periods is:

$$M_{ru} = M_{st} + \frac{GD^2}{375} \varepsilon_{ru} \qquad \text{(VI.63)}$$

during the running up,

$$M_{ste} = M_{st} \qquad \text{(VI.64)}$$

at steady state velocity, and

$$M_{br} = M_{st} - \frac{GD^2}{375} \varepsilon_{br} \qquad \text{(VI.65)}$$

during the braking.

Here GD^2 denotes the dynamic torque of the rotating parts of the mill and the rotor of the electric motor, referred to the shaft of the latter.

For shunt-wound electric motors—which, as a rule, are used for the drive of reversing rolling mills—the values of ε_{ru} and ε_{br} are

usually taken as constant. Then the load diagram during the pass will be made up of three rectangles (Fig. 235*b*). During the intermission period the load on the drive will also be different:

during the running up

$$M_{i\,ru} = M_l + \frac{GD^2}{375}\varepsilon_{ru} \tag{VI.66}$$

during the braking

$$M_{i\,br} = M_l - \frac{GD^2}{375}\varepsilon_{br} \tag{VI.67}$$

The values of the accelerations ε_{ru} and ε_{br} depend on the characteristics of the electric motor and its control arrangements. For large rolling mills, and, in particular, for blooming mills, the accelerations are usually taken as constant: $\varepsilon_{ru} \approx 30$ to 80 rpm sec and $\varepsilon_{br} \approx 60$ to 120 rpm sec.

To increase the capacity of the mill there is a tendency to increase these accelerations still further. In modern blooming mills they sometimes approach 100 rpm sec during the running up and 160 rpm sec during the braking.

Let us determine the duration of the above-mentioned load periods. If the times of running up, steady state velocity and braking are denoted by t_{ru}, t_{ste} and t_{br}, then the total time of the pass is

$$t = t_{ru} + t_{ste} + t_{br}$$

Designating the speed of the rolls during the gripping by n_{gr}, that at the steady state velocity by n_{ste}, and that at the exit by n_{ex}, we find t_{ru} and t_{br}:

$$t_{ru} = \frac{n_{ste} - n_{gr}}{\varepsilon_{ru}} \text{ and } t_{br} = \frac{n_{ste} - n_{ex}}{\varepsilon_{br}}$$

The length of the period of steady state velocity depends on the length L of the strip being rolled. Since the area of the shaded portion of the diagram shown in Fig. 235*a* corresponds to the length of the strip being rolled, we can set up the equation

$$L = \frac{\pi D}{60}\left(\frac{n_{gr} + n_{ste}}{2}t_{ru} + n_{ste}t_{ste} + \frac{n_{ste} + n_{ex}}{2}t_{br}\right)$$

where D is the working diameter of the rolls.

Hence the length of the period at steady state velocity is

$$t_{ste} = \frac{60L}{\pi D n_{ste}} - \frac{1}{n_{ste}}\left(\frac{n_{gr} + n_{ste}}{2}t_{ru} + \frac{n_{ste} + n_{ex}}{2}t_{br}\right) \tag{VI.68}$$

The running up and braking times during idling are

$$t_{i\,ru} = \frac{n_{gr}}{\varepsilon_{ru}} \text{ and } t_{i\,br} = \frac{n_{ex}}{\varepsilon_{br}}$$

VII

Forces During Die Rolling

1. DETERMINING THE CONTACT SURFACES DURING DIE ROLLING

In certain tube rolling mills (for example, Pilger, rockright, and the roller mills of the VNIIMETMASH system), in planetary mills, as well as in forging and rolling mills which serve for shaping various components, the reduction process is not performed continuously over the entire length of the component being rolled, but periodically, by working its separate portions.

In this method of rolling the metal is compressed in a groove which is shaped in such a way that its dimensions are gradually reduced by the motion of the rolls during the working period. The dimensions of the maximum groove, called the bite, are made slightly larger than the cross-sectional dimensions of the blank, whilst the dimensions of the minimum groove correspond to the dimensions of the rolled component.

Since in this method the metal is rolled in grooves of variable cross section, the contact area, and, consequently, the pressure on the rolls during the given pass is not held the same as in the usual method of rolling in grooves of constant cross section, but is varied with the variation of the cross sections of the groove and the blank to be rolled.

During the period when the metal is fed to the rolls the pressure on the rolls is obviously zero, since the dimensions of the bite receiving the blank are slightly larger than the dimensions of the initial cross section of this blank. During the subsequent motion of the rolls as a consequence of the reduction in the dimensions of the groove, the metal comes into contact with the rolls, and a pressure arises the value of which, depending on the subsequent roll pressure, will vary with the reduction.

It follows from this outline of die rolling that the essential feature in calculating the pressure of the metal in this method of rolling is the determination of the contact area. The magnitude of the reduction or reduction ratio during the entire working motion of the rolls must be known for this determination as well as the dimensions of the grooves.

Let us suppose that the grooves of the rolls for which the reduction or reduction ratio is to be determined are made so that the cross-sectional area of the blank being rolled varies as a certain curve AB (Fig. 236). The cross-sectional area of the blank to be rolled is plotted as the ordinate, whilst the motion of the rolls over which the cross section varies is plotted as the abscissa. This motion of the rolls obviously takes place with a certain mean diameter (varying as the rolls rotate) for which the peripheral velocity is equal to the velocity of the blank being rolled. We shall denote the area of the initial cross section of the blank by F_0 and that of the final one by F_1.

In order to determine the reduction ratio during the rolling of metal at a certain section of the groove, located, say, at a distance x from the vertical axis, it is necessary to find the size of the cross section of the blank entering the given section of the groove.

When the blank is fed by an amount s, the curve AB characterizing the variation of the cross-sectional area of the blank is obviously displaced relative to the grooves of the rolls by the magnitude of this feed, and thus assumes the position A_1B_1. The section CD of the blank is also correspondingly displaced by the amount of feed and assumes the position C_1D_1.

During the subsequent motion of the rolls from point A to point C, after this feed, the blank is reduced over the section x, and owing to this reduction the volume of the metal bounded by the curves AC and A_1E_1 is displaced towards the right. As a result of the displacement of the metal the length of the blank over the section x is correspondingly increased; the section C_1D_1 is displaced towards the right by a certain amount Δs, taking up the position C_2D_2. Hence it follows that the variation of the cross-sectional area of the blank on the portion not yet rolled will no longer be given by the curve E_1B_1, but by the curve H_2B_2, displaced relative to AB in the direction

of the horizontal axis by the amount

$$\Delta x = s + \Delta s \qquad \text{(VII.1)}$$

Thus at the given instant, i.e., after the reduction of the blank over the portion AC, the variation of the cross-sectional area of the blank is given by the broken curve ACH_2B_2.

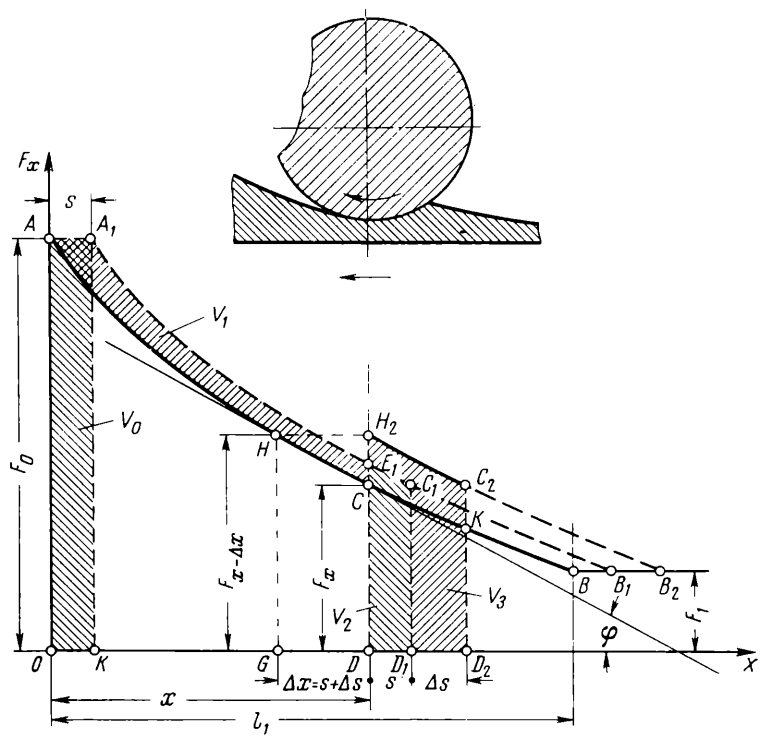

Fig. 236. Variation of the cross-sectional area of the blank being rolled with the motion of the rolls

It should be noted that the section E_1D of the blank does not enter the given section CD of the groove; a considerably larger section does, i.e., the section H_2D (the displaced section HG of the blank). Consequently, the reduction ratio in the groove section CD is

$$\lambda_x = \frac{H_2D}{CD} = \frac{F_{x-\Delta x}}{F_x} \qquad \text{(VII.2)}$$

Sometimes it is assumed that the reduction ratio equals the ratio of the area E_1D to the area CD, i.e., only the feed is taken into con-

sideration without allowing for the effect of the additional displacement of the rolled blank during the time when it is reduced. In view of the fact that the value of the displacement Δs increases with the motion of the rolls, and that at the end of the working motion of the rolls (the section l_1) it commonly exceeds several times the feed value (usually about 5 to 10 times), the error under this assumption becomes very considerable.

To calculate the reduction ratio from equation (VII.2) it is clearly necessary to find the value of $F_{x-\Delta x}$. This can be determined from the condition that the volume of the rolled blank remains constant.

The volume of the metal, V_0, fed into the rolls in a single feed, can be expressed, on a certain scale, as the area of the rectangle AA_1KO, i.e.,

$$V_0 = F_0 s \tag{VII.3}$$

From the diagram shown in Fig. 236 it follows that the volume V_0 is equivalent to the sum of the volumes V_1 and V_2, whence

$$F_0 s = V_1 + V_2 \tag{VII.4}$$

where V_1 and V_2 denote the volumes of the metal bounded by AA_1E_1C and $E_1C_1D_1D$.

When the blank is reduced by the rolls over the section AC the volume of the metal, as was mentioned above, is displaced. The volume $E_1H_2C_2D_2D_1C_1$, denoted by V_3, must equal this volume. Then, according to equation (VII.4),

$$F_0 s = V_2 + V_3 \tag{VII.5}$$

i.e., the volume of the metal bounded by $H_2C_2D_2D$ equals the volume of the metal entering the rolls at a single feed. As has been mentioned above, $H_2C_2D_2D$ is in fact $HCDG$ displaced during rolling from point A to point C. Consequently, the volume of the metal bounded by $HCDG$ must also be equal to the volume entering the rolls in a single feed (see Fig. 236):

$$F_0 s = \int_{x-\Delta x}^{x} F_x \, dx \tag{VII.6}$$

If the functional relationship $F_x = f(x)$ between the variation of the cross-sectional area of the blank and the length of the deformation region is known, then the value Δx can be determined from equation (VII.6). Substituting then the value $x - \Delta x$ of the abscissa into the given expression $F_x = f(x)$, we find the reduction ratio

from the equation

$$\lambda_x = \frac{F_{x-\Delta x}}{F_x} = \frac{f(x-\Delta x)}{f(x)} \qquad \text{(VII.7)}$$

When the variation of the cross-sectional area of the blank along the deformation region is given by a curve without an analytical expression, the area $HCDG$ is equated to a trapezium. Then the volume $F_0 s$ can be expressed thus:

$$F_0 s = \frac{F_{x-\Delta x} + F_x}{2} \Delta x \qquad \text{(VII.8)}$$

Subsequently drawing the tangent to the curve AB (a little to the left of the point C) and denoting the angle of inclination of this tangent to the horizontal axis by φ, we obtain

$$F_{x-\Delta x} = F_x + \Delta x \tan \varphi \qquad \text{(VII.9)}$$

After excluding the value Δx from equations (VII.8) and (VII.9)

$$F_{x-\Delta x} = \sqrt{F_x^2 - 2F_0 s \tan \varphi}$$

Dividing both sides of this equation by F_x [see equation (VII.2)] we find the formula for the reduction ratio in the different sections of the groove:

$$\lambda_x = \sqrt{1 - \frac{2F_0 \tan \varphi}{F_x^2} s} \qquad \text{(VII.10)}$$

Denoting the constant for the given section by

$$a = \frac{2F_0 \tan \varphi}{F_x^2} \qquad \text{(VII.11)}$$

we obtain a relatively simple expression for determining the reduction ratio in terms of the feed

$$\lambda_x = \sqrt{1 - as} \qquad \text{(VII.12)}$$

In practical calculations when it is required to determine the contact surface, and, consequently, the reduction ratio in different sections of the groove for the given dimensions of the latter, the working zone of the groove must be divided into a number of sections and the cross-sectional area calculated for each section of the blank. The graph giving the variation of the cross section along the length of the deformation zone (see Fig. 236) is afterwards plotted from these data. Hence we can determine the reduction ratio in any section of the groove over the region AB, using formulas (VII.10) and (VII.12).

After the determination of the reduction ratio the contact area and the pressure of the metal on the rolls are calculated in the same way as for the usual longitudinal rolling.

2. DETERMINATION OF THE REDUCTION RATIO AT THE END OF THE WORKING MOTION OF THE ROLLS

From the analysis of the die rolling process given above it follows that when the rolls reach the point B and the blank to be rolled has already been reduced over the basic section l_1, where the

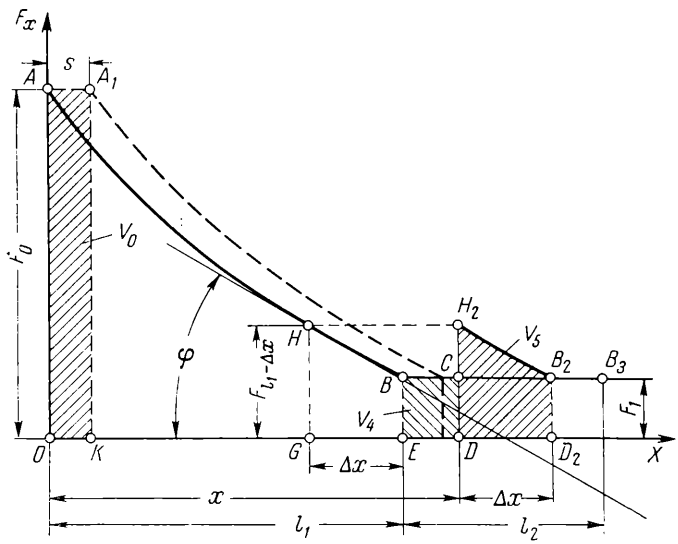

Fig. 237. Diagram showing the relation $F_x = f(x)$ (used to determine the reduction ratio at the end of the working cycle of the rolls)

cross-sectional area of the grooves decreases with the motion of the rolls, a considerable portion of the metal not yet reduced still remains in front of the rolls. This portion of the metal is obviously compressed by the next segment of the roll, having the groove of constant cross section. The reduction ratio during the subsequent motion of the rolls will gradually decrease, and, when the rolls reach the point B_3 (Fig. 237), where $BB_3 = l_2 = \frac{F_0}{F_1} s$, will become equal to unity.

To determine the reduction ratio at the end of the working motion of the rolls, i.e., over the section l_2, it is necessary to use a somewhat

different method of calculation, since equations (VII.10) and (VII.12) are applicable for calculating the reduction ratio only over the section l_1. Let us suppose that the blank has been rolled over the section x (see Fig. 237) and it is required to determine the reduction ratio at the section DC of the groove.

The reduction ratio at this section of the groove is given by

$$\lambda_x = \frac{H_2D}{CD} = \frac{F_{l_1-\Delta x}}{F_1} \qquad \text{(VII.13)}$$

The quantity $F_{l_1-\Delta x}$ is found from the condition that the volume of the rolled blank remains constant. From the diagram (Fig. 237) it follows that the volume V_0 of the metal supplied to the rolls in a single feed must be equal to the volume $(V_4 + V_5)$, i.e.,

$$V_0 = V_4 + V_5 \qquad \text{(VII.14)}$$

where V_4 and V_5 denote the volumes of the metal bounded by $BCDE$ and $H_2B_2D_2D$.

Owing to the fact that the line H_2B_2 corresponds to the portion HB of the curve AB, the equation for the volume V_5 can be written in the following form:

$$V_5 = \int_{l_1-\Delta x}^{l_1} F_x\, dx \qquad \text{(VII.15)}$$

Substituting the corresponding values of the volumes into equation (VII.14) we obtain

$$F_0 s = F_1 (x - l_1) + \int_{l_1-\Delta x}^{l_1} F_x\, dx \qquad \text{(VII.16)}$$

If the functional relationship between the variation of the cross-sectional area of the metal and the motion of the rolls is known, then using this equation, we can determine Δx. Knowing Δx from the given relation $F_x = f(x)$, we can subsequently find the reduction ratio from equation (VII.7).

In those cases where the variation of the cross-sectional area due to the motion of the rolls is in the form of a curve having no analytical expression, the same method can be used to calculate $F_{l_1-\Delta x}$ as for the section l_1.

Equating $H_2B_2D_2D$ to a trapezium, equation (VII.16) can be written in the following form:

$$F_0 s = F_1 (x - l_1) + \frac{F_{l_1-\Delta x} + F_1}{2} \Delta x \qquad \text{(VII.17)}$$

The quantity Δx is determined from the equation

$$F_{l_1-\Delta x} = F_1 + \Delta x \tan \varphi \qquad \text{(VII.18)}$$

where φ is the angle of inclination of the tangent drawn to the curve AB slightly to the left of the point B.

Solving these two equations simultaneously we find

$$F_{l_1-\Delta x} = \sqrt{F_1^2 + [F_0 s - F_1 (x - l_1)]\, 2 \tan \varphi}$$

Substituting this value of $F_{l_1-\Delta x}$ into equation (VII.13) we obtain the formula for determining the reduction ratio over the section l_2:

$$\lambda_x = \sqrt{1 + \frac{\lambda_{vol} s - (x - l_1)}{F_1} 2 \tan \varphi} \qquad \text{(VII.19)}$$

where $\lambda_{vol} = \frac{F_0}{F_1}$.

Using equation (VII.13) derived above when there exists a known functional relationship between the cross-sectional area of the metal and the motion of the rolls, and equation (VII.19) when the variation of the cross-sectional area of the metal over the length of the zone is given in the form of a curve without an analytical expression, we can find the reduction ratio at any section of the groove. After this the contact area and the pressure of the metal on the rolls are determined by the usual method.

3. MORE ACCURATE METHODS OF DETERMINING THE CONTACT SURFACES

The above method of determining the reduction ratio at different sections of the rolled blank during the working motion of the rolls is based on the fact that the dimensions of the transient portion of this blank are known, i.e., the curve AB (Fig. 236) is the actual variation of its cross-sectional area and not variation of the groove cross section. It is not difficult to see that when the above method is used, the effect of the elastic deformation of the roll stand (including the rolls) is taken into account together with that of the forward slip, since these phenomena are compensated for by the corresponding value of the feed. If, say, for each cycle of the rolls the point A returns by an amount x_{fs} as a result of the forward slip (Fig. 236), then the feed s must be increased by the amount

$$AA_1 = s + x_{fs}$$

In the case where the variation of the cross-sectional area of the groove, but not of the transient portion of the rolled blank, is known, the method of calculating the reduction ratio discussed in

the preceding two sections must be corrected for the elastic deformation of the working stand. Since the character of the deformation over the cycle of the rolls varies considerably, the pressure of the metal on the rolls and correspondingly the elastic deformation also change. At the beginning of the motion of the rolls, when they form a clearance, the elastic deformation is zero; it appears afterwards, attains a maximum and disappears at the end of the motion of the rolls. It follows that for an accurate calculation of the reduction ratio we must also know the variation of the pressure of the metal on the rolls during their motion. Then the curve characterizing the variation of the groove area during the motion of the rolls must be corrected, by allowing for the elastic deformation (Fig. 238):

$$F_x = F_{x\,gr} + \frac{P}{c} b_m \qquad \text{(VII.20)}$$

where F_x is the cross-sectional area of the rolled blank, calculated from equations (VII.10) and (VII.16)
$F_{x\,gr}$ is the area of the groove
P is the pressure of the metal on the rolls
c is the rigidity of the components of the stand
b_m is the mean width of the rolled article.

When thin-walled tubes are rolled it is necessary to consider also the effect of the local elastic deformation Δ of the mandrel, which can be calculated approximately from equation (V.21). In this case F_x is determined by the following equation (Fig. 239):

$$F_x = F_{x\,gr} + \frac{P}{c} b_m + 2\Delta b_m \qquad \text{(VII.21)}$$

When the ratio of the diameter of the rolls to their motion is large, it is advisable to consider the additional displacement of the metal due to the fact that part of the volume CH_2C_2K (Fig. 236) will be taken up by the roll. This problem has been considered in detail by R. Ritman and the author in relation to a planetary mill. It is solved in a similar manner for Pilger and rockright mills.

In determining this additional displacement of the volume we must consider two possible cases differing from each other in the extent of the displaced volume in the direction of the horizontal axis:

(1) the displaced volume is so small in relation to the distance between the rolls (Fig. 239*a*) that

$$s < \Delta x_1 < r(\sin\varphi + \sin\varphi_1)$$

where r is the radius of curvature of the working surface of the roll where it contacts the metal being rolled;

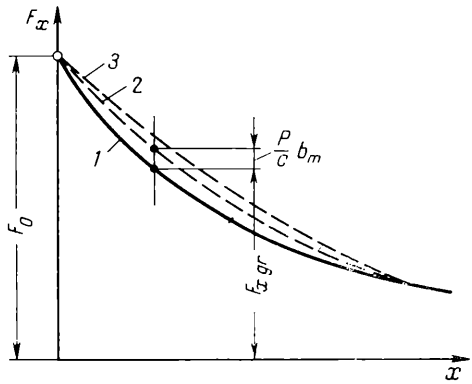

Fig. 238. Variation of the groove area $F_{x\,gr}$ (*1*) after correcting for the elastic deformation of stand (*2*) and mandrel (*3*)

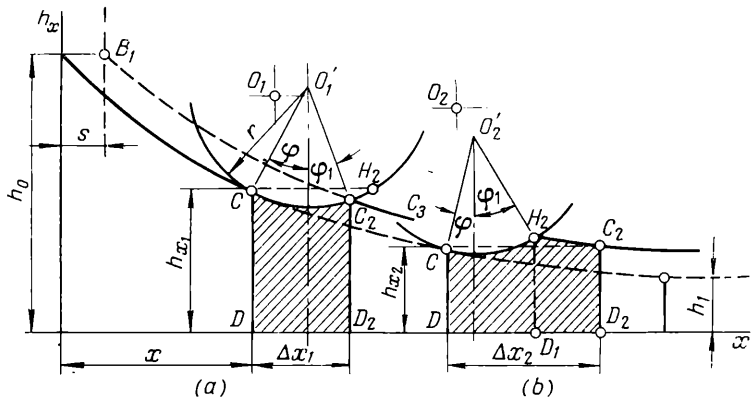

Fig. 239. Volumes displaced by the mandrel corrected for the volumes taken up by the rolls:

(*a*) $\Delta x_1 < 2r \sin \varphi$; (*b*) $\Delta x_2 > 2r \sin \varphi$; O_1 and O_2 are axes of rotation of the rolls; O_1' and O_2' are the centres of the mean curvature of the contact surfaces of the rolls

(2) the displaced volume extends outside the limits of the contact surface (Fig. 239*b*), where

$$\Delta x_2 > r(\sin\varphi + \sin\varphi_1)$$

The boundary between these two positions of the rolls is where the curve $B_1C_2C_3$ (Fig. 239*a*) of the displaced volume begins to cut the surface of the roll at a distance from the horizontal axis exceeding

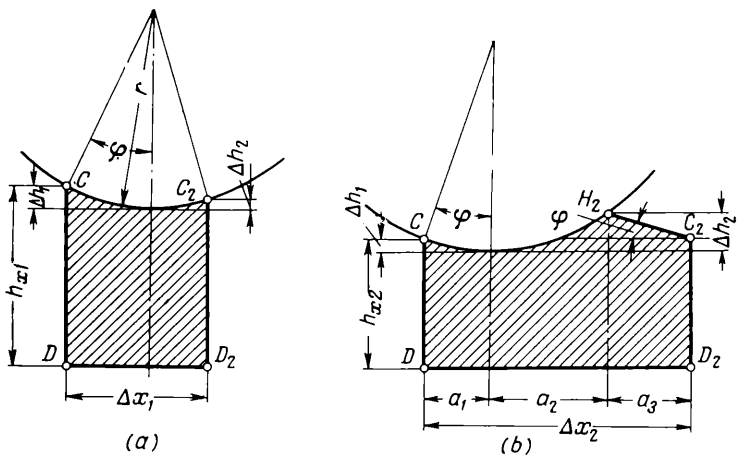

Fig. 240. Determination of the displaced volumes including the volumes taken up by the rolls:
(*a*) $\Delta x_1 < 2r \sin\varphi$; (*b*) $\Delta x_2 > 2r \sin\varphi$

h_x, i.e., the point C_2 reaches the point H_2 and will be displaced further towards the right. This case corresponds to the conditions

$$CD = C_2D_2$$

i.e., $\varphi = \varphi_1$ or

$$\Delta x_1 = 2r \sin\varphi$$

In the first case—if we assume the width of the blank to be equal to unity and if the arc of contact is replaced by a chord—the displaced volume can be expressed as (Fig. 240*a*):

$$V_0 = h_0 s = r \sin\varphi \left(h_{x1} - \frac{2}{3}\Delta h_1\right) + (\Delta x_1 - r \sin\varphi) \times \times \left(h_{x1} - \Delta h_1 + \frac{1}{3}\Delta h_2\right) \quad \text{(VII.22)}$$

where s is the feed;

Δh_1 and Δh_2 are determined from the equations:

$$r \sin \varphi \approx \sqrt{r \Delta h_1}$$

$$\Delta x_1 - r \sin \varphi \approx \sqrt{r \Delta h_2}$$

Substituting these values of Δh_1 and Δh_2 into equation (VII.22), we can determine Δx_1 and hence the contact area for the given h_{x1} and φ.

In approximate calculations, if the term $\frac{1}{3} \Delta h_2$ is neglected in equation (VII.22) in view of its smallness in comparison to h_{x1}, and if it is borne in mind that

$$\Delta h_1 = r \sin^2 \varphi$$

we obtain

$$\Delta x_1 = \frac{h_0 s - r \sin \varphi \left(h_{x1} - \frac{2}{3} r \sin^2 \varphi \right)}{h_{x1} - r \sin^2 \varphi} + r \sin \varphi \qquad \text{(VII.23)}$$

In the second case, when

$$\Delta x_2 > 2r \sin \varphi$$

the displaced volume is given by $DCH_2C_2D_2$ (Fig. 239*b*). Its value is (Fig. 240*b*):

$$V_0 = h_0 s = r \sin \varphi \left(h_{x2} - \frac{2}{3} \Delta h_1 \right) +$$

$$+ a_2 \left(h_{x2} - \Delta h_1 + \frac{1}{3} \Delta h_2 \right) + a_3 \left[h_{x2} + \frac{1}{2} (\Delta h_2 - \Delta h_1) \right] \qquad \text{(VII.24)}$$

This equation can be further supplemented by the equation

$$a_3 = \Delta x_2 - (r \sin \varphi + l_2) = \frac{\Delta h_2 - \Delta h_1}{\tan \varphi} \qquad \text{(VII.25)}$$

Taking into consideration that

$$\Delta h_1 = r \sin^2 \varphi \text{ and } \Delta h_2 = \frac{a_2^2}{r}$$

we can find Δx_2 and $(a_1 + a_2)$ from equations (VII.24) and (VII.25).

However, since the substitution leads to a complicated equation, it is advisable to use a simpler method. In this case the value Δx_2 is found by equating the area $DCH_2C_2D_2$ to the area of a triangle:

$$h_0 s = \Delta x_2 h_{x2}$$

Hence

$$\Delta x_2 = \frac{h_0 s}{h_{x2}} \qquad \text{(VII.26)}$$

After this the value l_2 is found from equation (VII.25), by assuming that $\tan \varphi \approx \sin \varphi$:

$$a_2 = -\frac{r \tan \varphi}{2} + \sqrt{\frac{r^2 \tan^2 \varphi}{4} + \Delta x_2 \tan \varphi} \qquad \text{(VII.27)}$$

or

$$a_1 + a_2 = a_2 + r \sin \varphi = \frac{r \tan \varphi}{2} \left(1 + \sqrt{1 + \frac{4h_0 s}{r h_{x2} \tan \varphi}}\right) \qquad \text{(VII.28)}$$

From formulas (VII.23) and (VII.28) we can find the contact surface not only on the basic section l_1 (see Fig. 237), but also at the end of the working motion on the section l_2.

4. THE DEPENDENCE OF THE EQUATIONS $F_x = f(x)$ ON THE REDUCTION CONDITIONS PREVALENT ON THE TRANSIENT PORTION OF THE BLANK

In many cases it is advisable to carry out die rolling under the given reduction conditions over the transient portion of the blank, i.e., involving the principal portion of the working motion of the rolls.

We consider first the nature of a curve showing the variation in the cross-sectional area F_x of the rolled article during the motion of the rolls for the reduction ratio to be constant.

In this case at all cross sections of the transient portion the following equation must hold

$$\lambda = \frac{F_{x-\Delta x}}{F_x} = \text{const.} \qquad \text{(VII.29)}$$

To determine the equation of the curve, which guarantees a constant reduction ratio, we use equation (VII.10) derived above. The quantity $\tan \varphi$ which in this equation can obviously be expressed as (see Fig. 236):

$$\tan \varphi = \frac{dF_x}{dx} \qquad \text{(VII.30)}$$

Substituting this value of $\tan \varphi$ into equation (VII.10) and dividing the variables, we obtain

$$-\frac{dF_x}{F_x^2} = \frac{\lambda^2 - 1}{2F_0 s} dx \qquad \text{(VII.31)}$$

After integration we have

$$\frac{1}{F_x} = \frac{\lambda^2 - 1}{2F_0 s} + C$$

The constant C is determined from the initial conditions when $x = 0$ and $F_x = F_0$. We obtain then:

$$C = \frac{1}{F_0}$$

$$\frac{1}{F_x} = \frac{1}{F_0}\left(\frac{\lambda^2 - 1}{2s}x + 1\right)$$

Hence

$$F_x = \frac{F_0}{\frac{\lambda^2 - 1}{2s}x + 1} \qquad \text{(VII.32)}$$

This formula gives the curve $F_x = f(x)$ for the variation of the cross-sectional area of the transient portion of the rolled metal along its length if the reduction ratio is to be constant over the entire section.

But formula (VII.32) is not quite accurate since in deriving it we took the derivative $\frac{dF_x}{dx}$ as constant over the section Δx (Fig. 236).

To derive the accurate equations two initial conditions must be satisfied:

(1) according to equation (VII.6) the area bounded by the curve $F_x = f(x)$ on the section from $x - \Delta x$ to x (see Fig. 236) is equal to the product of F_0 and the feed s, i.e.,

$$\int_{x-\Delta x}^{x} f(x)\,dx = F_0 s \qquad \text{(VII.33)}$$

(2) the ratio of the end ordinates of the section mentioned in the first condition is, in accordance with equation (VII.2), equal to the reduction ratio:

$$f(x) = \frac{f(x - \Delta x)}{\lambda} \qquad \text{(VII.34)}$$

To determine the required relationship $F_x = f(x)$ from these two conditions A. Iroshnikov proposed the use of the following method.

We suppose that the required relationship $F_x = f(x)$, as in the approximate method of calculation, is a hyperbola whose equation is similar in form to equation (VII.32):

$$F_x = f(x) = \frac{a}{bx + 1} \qquad \text{(VII.35)}$$

If the constant coefficients are found and they satisfy the conditions (VII.33) and (VII.34), then clearly the assumption made by us is correct and equation (VII.35) will be the required relationship $F_x = f(x)$. Proceeding from the initial conditions ($x = 0$ and

$F_x = F_0$) and using equation (VII.35) we find the coefficient a:

$$a = F_0$$

Then equation (VII.35) assumes the form

$$F_x = f(x) = \frac{F_0}{bx+1} \tag{VII.36}$$

Substituting the value of $f(x)$ from this equation into equation (VII.33), we obtain

$$\int_{x-\Delta x}^{x} \frac{F_0}{bx+1}\, dx = F_0 s \tag{VII.37}$$

or, after integration,

$$\frac{1}{b} \log_e \frac{bx+1}{b(x-\Delta x)+1} = s$$

from which

$$\frac{bx+1}{b(x-\Delta x)+1} = e^{bs} \tag{VII.38}$$

We further find that

$$x - \Delta x = \frac{1}{b}\left(\frac{bx+1}{e^{bx}} - 1\right) \tag{VII.39}$$

Substituting this value of $x - \Delta x$ for x into equation (VII.36), we obtain

$$f(x-\Delta x) = \frac{F_0 e^{bs}}{bx+1} \tag{VII.40}$$

The values of $f(x)$ and $f(x - \Delta x)$ obtained from equations (VII.36) and (VII.40) are substituted into equation (VII.34):

$$\frac{F_0}{bx+1} = \frac{F_0 e^{bs}}{bx+1} \frac{1}{\lambda}$$

Hence

$$e^{bs} = \frac{1}{\lambda}$$

or

$$b = \frac{\log_e \lambda}{s} \tag{VII.41}$$

Substituting this value of the coefficient into equation (VII.36), we obtain the required relationship:

$$F_x = \frac{F_0}{\frac{\log_e \lambda}{s} x + 1} \tag{VII.42}$$

This equation shows how the cross-sectional area of the blank being rolled must vary with the length of the transient portion if the reduction ratio is to be constant over the section l_1 (see Fig. 236).

To test the correctness of this equation let us calculate the reduction ratio using formula (VII.34).

We substitute the value of F_x into equation (VII.33):

$$F_0 s = \int_{x-\Delta x}^{x} F_x \, dx = \int_{x-\Delta x}^{x} \frac{F_0}{\frac{\log_e \lambda}{s} x + 1} \, dx$$

whence

$$\frac{\log_e \lambda}{s} (x - \Delta x) + 1 = \frac{1}{\lambda} \left(\frac{\log_e \lambda}{s} x + 1 \right)$$

The value of $x - \Delta x$, taken from this formula, is substituted for x into formula (VII.42) and $F_{x-\Delta x}$ is found as follows:

$$F_{x-\Delta x} = \frac{F_0}{\frac{1}{\lambda} \left(\frac{\log_e \lambda}{s} + 1 \right)}$$

The reduction ratio is determined from equation (VII.34):

$$\lambda_x = \frac{F_{x-\Delta x}}{F_x} = \frac{F_0}{\frac{1}{\lambda} \left(\frac{\log_e \lambda}{s} x + 1 \right)} : \frac{F_0}{\frac{\log_e \lambda}{s} x + 1} \quad \lambda$$

The reduction ratio for the entire section is found to be constant and equal to λ. Consequently, the assumption made in deriving formula (VII.42) is correct.

In a similar way we can derive equations which show how the cross-sectional area of the transient portion of the metal must vary for the reduction ratio over the section l_1 to be given by

$$\lambda_x = \lambda_0 + \alpha x \qquad \text{(VII.43)}$$

where λ_0 is the reduction ratio at the beginning of the motion of the rolls

α is the tangent of the angle of inclination of a straight line to the horizontal axis, characterizing the given variation of the reduction ratio (Fig. 241).

When the reduction ratio diminishes with the motion of the rolls (see the dash line in Fig. 241) a minus sign must be put in front of the coefficient α in this equation.

The equation for determining the required variation of the cross-sectional area for given rolling conditions, in accordance with equation (VII.43), is based on the same conditions as in the case of equation (VII.42).

The first condition [see equation (VII.33)] is also valid for this case. But the second condition [see equation (VII.34)] is

$$f(x) = \frac{f(x-\Delta x)}{\lambda_0 + \alpha x} \qquad \text{(VII.44)}$$

Using the same method as in deriving equation (VII.42), we obtain equations (VII.36) and (VII.40). Equation (VII.40) can be used in

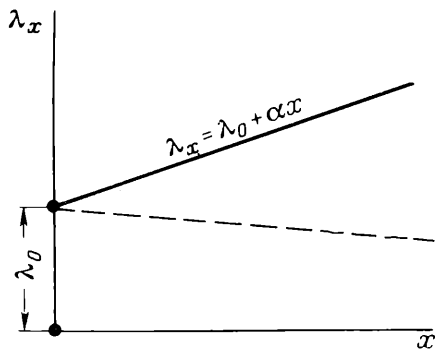

Fig. 241. A given linear variation of the reduction ratio over the transient portion of the blank

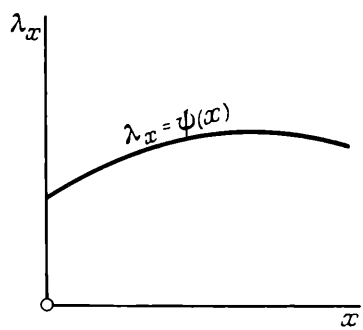

Fig. 242. A given non-linear variation $\lambda_x = \psi(x)$ of the reduction ratio on the transient portion of the blank

this case, if to simplify the calculation and the final results, the variation of λ_x over the section Δx is neglected. Then in integrating equation (VII.37) we can assume that b does not depend on x.

The values of $f(x)$ and $f(x - \Delta x)$ from equations (VII.36) and (VII.40) are substituted into equation (VII.44):

$$\frac{F_0}{bx+1} = \frac{F_0 e^{bs}}{bx+1} \frac{1}{\lambda_0 + \alpha x}$$

whence

$$e^{bs} = \lambda_0 + \alpha x$$

or

$$b = \frac{\log_e (\lambda_0 + \alpha x)}{s} \qquad \text{(VII.45)}$$

We substitute this value of the coefficient b into equation (VII.36):

$$F_x = \frac{F_0}{\frac{\log_e (\lambda_0 + \alpha x)}{s} x + 1} \qquad \text{(VII.46)}$$

The given formula shows how the cross-sectional area of the blank must vary over the transient section, if the reduction ratio over this section is to vary according to the linear law given by equation (VII.43).

For the same conditions, if the variation of the draught ratio is assumed arbitrarily (Fig. 242):

$$\lambda_x = \psi (x)$$

then the final formula, showing how the required law of the variation of the cross section over the transient section must be determined, has the form

$$F_x = \frac{F_0}{\frac{\log_e \psi (x)}{s} x + 1} \qquad \text{(VII.47)}$$

Equations (VII.42) and (VII.46) may be regarded as particular cases of this formula.

5. DIRECTION OF THE FORCES ACTING ON THE ROLLS OF PILGER MILLS

The direction of the forces acting on the rolls of Pilger mills is found in the same way as for the usual longitudinal rolling, when external longitudinal forces are applied to the metal being rolled (see Chapter IV, Section 2). In the present case this external force is furnished by R, the resistance of the mandrel (including the inertial force), which acts in the direction opposite to the direction of rotation of the rolls (Fig. 243).

Accordingly the resultant forces P on the rolls are slightly inclined to meet the metal being rolled. The angle θ between the direction of the forces P and the vertical plane depends on the ratio of the force R to the pressure of the metal on the rolls:

$$\sin \theta = \frac{R}{2P} \qquad \text{(VII.48)}$$

The force R is equal to the sum of the following quantities:

$$R = p_1F_1 - p_2F_2 + \mu G + U \qquad \text{(VII.49)}$$

where p_1 is the air pressure in the cylinder of the feeding mechanism
p_2 is the air pressure in the carriage
F_1 and F_2 are the piston areas
μ is the coefficient of friction
G is the weight of the moving parts (mandrel, piston, carriage, tube, etc.)
U is the inertial force, given by the formula

$$U = \frac{G}{g} j$$

where j is the acceleration of the tube
g is the acceleration of gravity.

The torque necessary to drive both rolls (Fig. 243), i.e., the rolling torque, is

$$M = 2Pa = 2Pr \sin(\beta + \theta) \qquad \text{(VII.50)}$$

where r is the radius of the working surface of the roll where the force P is applied, measured from the centre of its rotation
β is the angle characterizing the location of point of application of the force P.

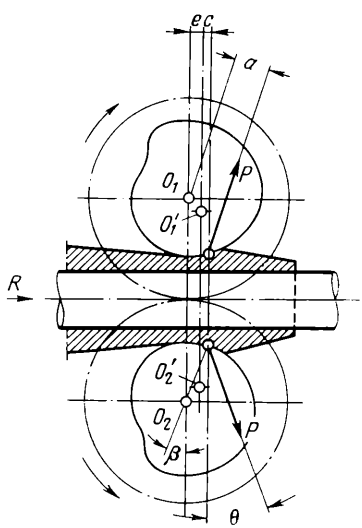

Fig. 243. Direction of the resultant forces applied to the rolls of a Pilger mill:
O_1 and O_2—axes of rotation of the rolls; O_1' and O_2'—centres of local curvature of the working surfaces of the rolls

We find the angle β from the condition that

$$r \sin \beta = e + c \qquad \text{(VII.51)}$$

where e is the distance between the planes passing through the axes O_1 and O_2 of rotation of the rolls and through the centres O_1' and O_2' of curvature of the working surfaces of the rolls at the point where they touch the metal
c is the distance from the planes passing through the points O_1' and O_2' to the point of application of the resultant of the pressure of the metal on the rolls.

If we neglect the effect that the asymmetry of the specific pressure distribution diagram has on the position of the resultant of the pressure of the metal on the rolls, then from Fig. 240, for the case where $\Delta x_1 < 2r \sin \varphi$, we obtain:

$$e = \frac{\Delta x_1}{2} - r \sin \varphi \qquad \text{(VII.52)}$$

and for the case where $\Delta x_1 > 2r \sin \varphi$:

$$e = \frac{a_1 + a_2}{2} - r \sin \varphi \qquad \text{(VII.53)}$$

where the values of Δx_1, a_1 and a_2 are found from equations (VII.23) and (VII.28).

6. PRESSURE OF THE METAL ON THE ROLLS OF ROCKRIGHT MILLS

In order to determine the magnitude and direction of the forces acting in mills of the rockright type for cold rolling of tubes, let us first analyze the kinematic diagram of the rolling process. Since the motion of the rolls is transmitted by shaft-mounted gear wheels being in constant engagement with stationary racks, the velocity of the individual points of the rolls can be expressed by the diagram shown in Fig. 244.

The velocity of the working surface of a roll, v_w, depends to a large extent on the distance y from the given point of the groove surface to the pitch line of the rack, CD (Fig. 244):

$$v_w = \frac{v_s}{r_0} y \qquad \text{(VII.54)}$$

where v_s is the velocity of the displacement of the roll stand
r_0 is the radius of the pitch circle of the gear in engagement with the rack.

Since r_0 is greater than the radius of the bottom of the groove and smaller than the nominal radius of the roll, i.e., the distance from the axis of the roll to the axis EF of the tube, three regions with different rolling conditions are possible on the contact surface, depending on the advance of the metal:

$$\left.\begin{aligned} v_w &= v_A \text{ to } v_B \\ v_w &> v_B \\ v_w &< v_A \end{aligned}\right\} \qquad \text{(VII.55)}$$

where v_A and v_B are the velocities of the metal at the sections passing through the points A and B (Fig. 244).

The first case corresponds to the usual conditions of longitudinal rolling, when slipping having two directions occurs over the arc of contact, i.e., the zones of backward and forward slip are observed.

In the second case the contact friction forces acting from the roll on to the metal over the entire arc AB are opposite to the direction

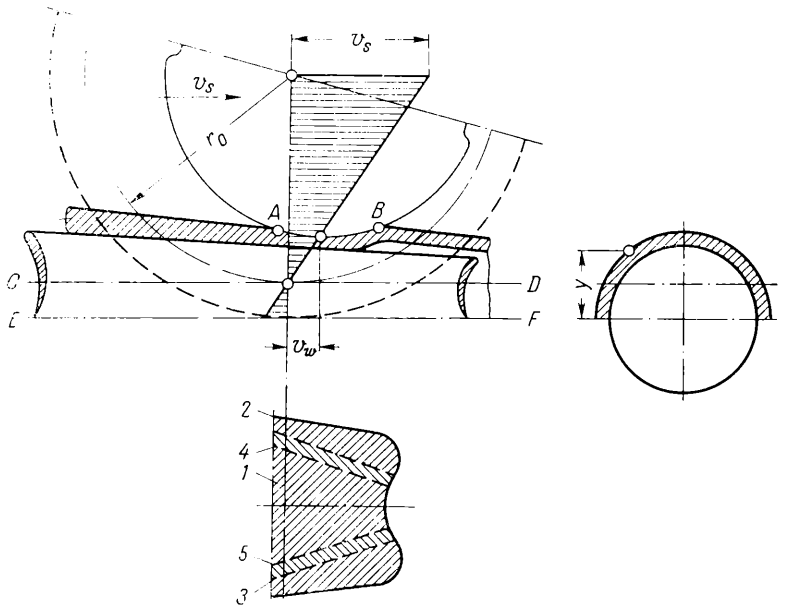

Fig. 244. Velocity diagram for different points of the rolls of mills for cold rolling of tubes and corresponding parts of the contact surface for different slipping conditions:

CD—stationary rack; EF—axis of the tube and mandrel; *1*—region of complete forward slip; *2* and *3*—regions of complete backward slip; *4* and *5*—regions where $v_w = v_A$ to v_B

of exit of the metal from the rolls. Consequently, the region where $v_w > v_B$ is a zone of continuous forward slip.

In the third case of rolling, when $v_w < v_A$, the contact friction forces are directed towards the exit of the metal from the rolls. In this case, too, the region of the contact surface is a continuous zone of backward slip.

If on the contact surface there is a region where the conditions of slipping predominate as in the first case, then the rolling process will be unstable, since over the displacement of the stand the diameter of the mandrel and the velocity of the rolled metal will vary.

In practice such rolling is usually used when the contact surface has a region characterized predominantly by the conditions of slip-

ping corresponding to the second case, i.e., the zone of forward slip. Then during the working motion of the rolls, longitudinal tensile stresses arise in the basic part of the rolled tube; these stresses promote a better deformation of the tube, and reduce the spreading.

Rolling with prevalence of regions on the contact surface characterized mainly by the conditions of slipping corresponding to the third case of rolling, i.e., the zone of backward slip, is less practicable than in the case where $v_w > v_B$, owing to the fact that during the forward motion of the rolls compressive stresses appear in the tube instead of the longitudinal tensile stresses, and these impede deformation.

In connection with what has just been said the regions with these three conditions of slipping must approximately be arranged as shown in the lower part of Fig. 244.

The relation between the three regions in question varies with the motion of the rolls. At the beginning of their motion the zone of forward slip must be larger than at the end, when both y and v_w are reduced. During the return motion of the rolls the directions of rolling and slipping are reversed. Since the velocity of working surface of the rolls relative to v_s remains unchanged, the contact surface, as in the forward motion, will consist of regions characterized by three different rolling conditions: a region of continuous forward slip over the entire arc of contact AB; two end regions of continuous backward slip, and two intermediate regions where the direction of slipping changes.

The velocity of slipping of the rolls along the metal changes not only during the motion, but also over the arc of contact AB (Fig. 244).

At the point A (Fig. 245*a*) the forward motion of the metal during the rolling can take place only at the beginning of the motion of the rolls, as a result of the elastic deformation of the tube and the action of the feed mechanism. The velocity v_A of this displacement is very small, and is much less than at the point B, where the metal is displaced as a result of its reduction, i.e.,

$$v_A < v_B$$

The variation of the slip over the arc of contact AB in the zone of forward slip during both forward and return motions can be expressed approximately as trapezoidal diagrams (Fig. 245*a* and *b*).

Analyzing the character of the slipping of the rolls and the mandrel along the metal during the forward and return motions, we notice that the conditions of deformation differ markedly in the two cases. In the first case the deformation of the metal in the zone of forward slip takes place between surfaces which move in different directions relative to the metal, whilst during the return motion they move in the same direction. Conversely, in the zone of backward slip the deformation during the forward motion takes place

between surfaces along which metal slips in the same direction, whilst during the return motion the slip is in different directions. In both cases, however, the contact surface of the metal and the rolls

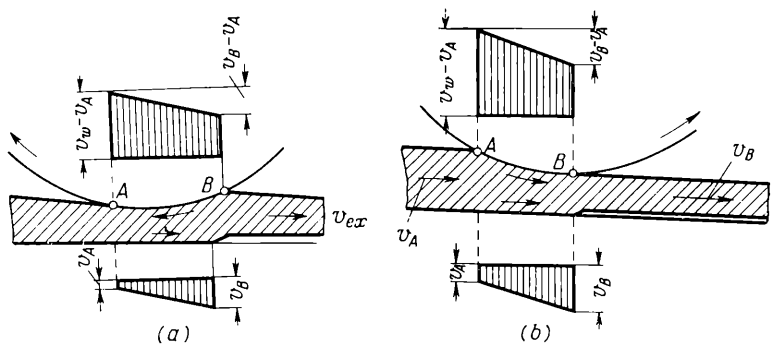

Fig. 245. Direction in which the metal being rolled slips along the roll in the zone of forward slip and along the mandrel, and the corresponding velocity diagrams:
(*a*) forward motion of the rolls; (*b*) return motion

and mandrel consists essentially of regions of continuous slipping, a neutral section being absent. Accordingly, no rise is observed in the specific pressure diagram over the middle portion of the contact surface.

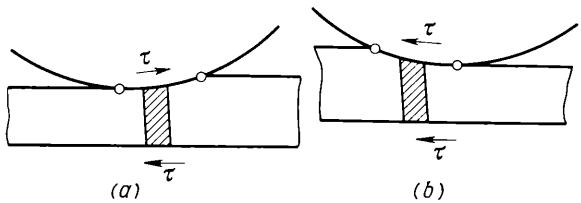

Fig. 246. Direction of the contact friction forces acting on the metal in the zone of forward slip in mills for cold rolling of tubes:
(*a*) forward motion of the rolls; (*b*) return motion

From these diagrams showing the direction of the contact friction forces (Fig. 246) we can determine the laws giving the distribution of the specific pressure. The specific pressure diagram over the portion where the friction forces have opposite directions can approximately be expressed for the forward motion by a trapezium (Fig. 247*a*). One side of this trapezium, when the deformation is assumed to be two-dimensional, is

$$p_A = 2k - \sigma_A$$

where σ_A is the tensile stress in the tube,
whilst the other side is

$$p_B = 2k$$

In this way the mean specific pressure in the zone of forward slip, over the region where wall thickness of the tube is reduced, can be determined from the expression

$$p_m = 2k - \frac{\sigma_A}{2} \qquad \text{(VII.56)}$$

We find the value of σ_A from the equation

$$\sigma_A = \xi \frac{P\mu}{Q_A} \qquad \text{(VII.57)}$$

where ξ is a coefficient indicating what part of the friction force $P\mu$ is taken up by the tube
P is the overall pressure of the metal on the roll
μ is the coefficient of friction between the roll and the tube being rolled
Q_A is the cross-sectional area of the tube in the plane passing through the point A.

The coefficient ξ depends on the ratio of the wall thickness of the tube to the angle of inclination γ of the generatrix of the mandrel

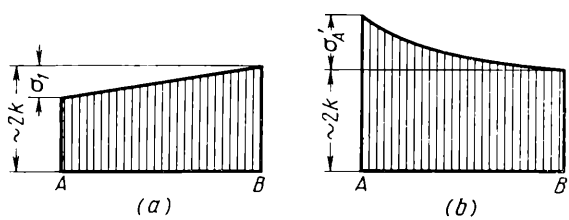

Fig. 247. Pressure distribution in zones where the wall thickness of the tube is reduced when it is rolled in a rockright mill:
(*a*) forward motion of the roll in the zone of forward slip; (*b*) return motion in the zone of forward slip, and forward motion in the zone of backward slip

to its axis. If we denote the pressure of metal on mandrel—acting from one roll perpendicularly to the axis of the mandrel—by Y, then clearly

$$\xi = 1 - \frac{Y(\mu_1 - \tan\gamma)}{P} \qquad \text{(VII.58)}$$

where μ_1 is the coefficient of friction between the mandrel and the metal being rolled.

During the return motion of the rolls, the friction forces acting in the zone of forward slip—both from the side of the rolls and from the side of the mandrel—are characterized by the same direction (see Fig. 246*b*), as in the usual rolling in the zone of forward slip.

If we assume that slipping takes place according to the law of dry friction, which is very likely, then obviously the specific pressure can be calculated from equation (II.35). Then the diagram of the distribution of the specific pressure is expressed by the curve (see Fig. 247*b*) plotted from this equation.

Clearly, the specific pressure at the point B is

$$p_B = 2k$$

whilst the pressure at the point A is found from equation (II.35), substituting $h_x = h_A$ in this equation, where h_A is the wall thickness of the tube at the section passing through the point A.

The increase of p_A above $2k$ shows that compressive stresses exist at the point A:

$$\sigma'_A = p_A - 2k$$

The mean specific pressure during the return motion is approximately given by:

$$p'_m = 2k + \frac{\sigma'_A}{2} \qquad \text{(VII.59)}$$

From the analysis just carried out into the pressure of the metal on the rolls we can conclude that during the forward motion of the rolls rolling is more effective than during the return motion, when compressive stresses arise in the tube increasing the specific pressure and the spreading.

The results of investigations by V. Sokolovsky are of the greatest interest among the available experimental data on the forces which arise in rockright mills. He established that the pressure of the metal on the rolls during the forward motion differs only slightly from the pressure during the return motion, in spite of the fact that the tube was fed only during the forward motion. The longitudinal forces arising in the mandrel were found to be in the main tensile during the forward motion, whilst during the return motion they were wholly compressive. These forces amounted on average to 3 to 15% of the pressure of the metal on the rolls. At the same time their absolute value was usually about 1.5 to 3 times greater during the return motion than during the forward motion.

7. DIRECTION OF THE FORCES ACTING ON THE ROLLS OF ROCKRIGHT MILLS

In order to determine the direction of the forces acting on the rolls and also that required to move the stand, let us first consider the conditions of equilibrium of the tube together with the mandrel, and then of the rolls.

For equilibrium of the tube and the mandrel the horizontal projection of the pressure P of the metal on the roll must clearly satisfy the following equation (for two rolls):

$$P \sin \theta = \frac{R}{2} \qquad \text{(VII.60)}$$

where θ is the angle of inclination of the force P to the line connecting the axes of the rolls, and

R is the axial force acting on the tube and the mandrel.

Setting up the equation of the moments of the forces relative to the axis of the top roll, engaged with the gear wheel of the bottom roll, we obtain (Fig. 248*a*):

$$Pa = Pr_r \sin (\theta - \beta) + T_g r_g \qquad \text{(VII.61)}$$

where a is the lever arm of the force P

r_r is the working radius of the roll

β is the angle characterizing the position of the point of application of the resultant of the pressure of the metal on the rolls

T_g is the peripheral force on the spur gear

r_g is the radius of the pitch circle of the spur gear engaged with the gear wheel of the bottom roll.

From this equation we find that

$$T_g = P \frac{r_r}{r_g} \sin (\theta - \beta) \qquad \text{(VII.62)}$$

If the influence of the friction forces in the bearings is neglected, then from the condition of equilibrium of the roll it follows that the resultant Q of the forces P and T_g passes through the axis of rotation of the roll, as shown by the dash line in Fig. 248*a*. When these forces are taken into account, the resultant Q touches the friction circle.

From the force diagram (Fig. 248*a*) and equation (VII.62) it follows that for $\theta = \beta$ the force P passes through the axis of the roll and is equal to the force Q. In this case the force on the spur gear becomes zero, and when $\beta > \theta$, its direction changes. To avoid unnecessary impacts on the gearing, it is advisable to use such a deformation scheme with which $\theta > \beta$.

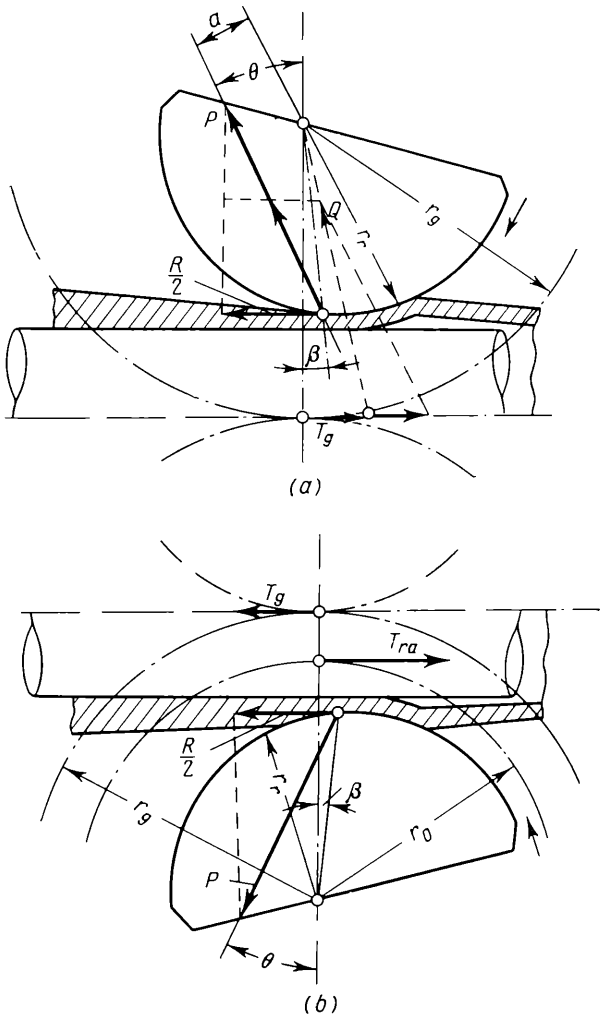

Fig. 248. Direction of the forces acting in mills for the cold rolling of tubes during the forward motion of the stand:
(*a*) top roll; (*b*) bottom roll geared to the rack

If the friction forces in the bearings are taken into account, then the direction of the forces changes when

$$r_r \sin(\theta - \beta) < \rho \qquad \text{(VII.63)}$$

where ρ is the radius of the friction circle of the journals of the rolls.

The direction of the forces acting on the bottom roll can be determined in the same way from the equation of moments, taking into account the force applied to the roll from the rack (Fig. 248*b*):

$$Pa = Pr_r \sin(\theta - \beta) = T_{ra} r_0 - T_g r_g \qquad \text{(VII.64)}$$

where T_{ra} is the force on the rack, and
r_0 is the radius of the pitch circle of the gear engaged with the rack.

Substituting into this equation the value of T_g from the expression (VII.62), we find the force on the rack:

$$T_{ra} = 2P \frac{r_r}{r_0} \sin(\theta - \beta) \qquad \text{(VII.65)}$$

It follows from this equation that the force on the rack (since $r_0 < r_g$) slightly exceeds double the force on the gear transmitting the motion to the top roll:

$$T_{ra} > 2T_g$$

The direction of the force on the rack, like the force T_g, changes when $\beta > 0$. If the friction forces in the bearings of the rolls are taken into account, then the change of direction takes place when

$$r_r \sin(\theta - \beta) < \rho \qquad \text{(VII.66)}$$

The static force required to displace the rolls, i.e., the roll stand without taking into account the friction losses in the bearings and guides, is determined as the horizontal projection of all the forces applied to both rolls. The force required to displace the top roll is

$$X_t = P \sin\theta - T_g = P \left[\sin\theta - \frac{r_r}{r_g} \sin(\theta - \beta) \right] \qquad \text{(VII.67)}$$

and for the bottom roll

$$X_b = P \left[\sin\theta - r_r \left(\frac{2}{r_0} - \frac{1}{r_g} \right) \sin(\theta - \beta) \right] \qquad \text{(VII.68)}$$

Since $r_0 < r_g$, the force necessary to displace the top roll is somewhat larger than that for the bottom roll. The total force necessary to displace both rolls is:

$$X_{tot} = X_t + X_b = 2P \left[\sin\theta - \frac{r_r}{r_0} \sin(\theta - \beta) \right] \qquad \text{(VII.69)}$$

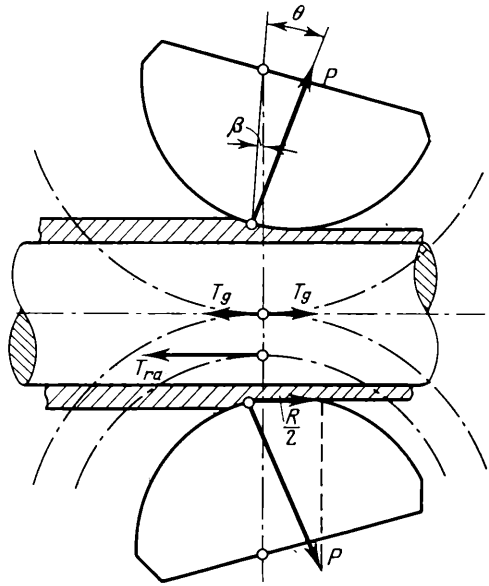

Fig. 249. Direction of the forces acting on the rolls during the return motion of the stand

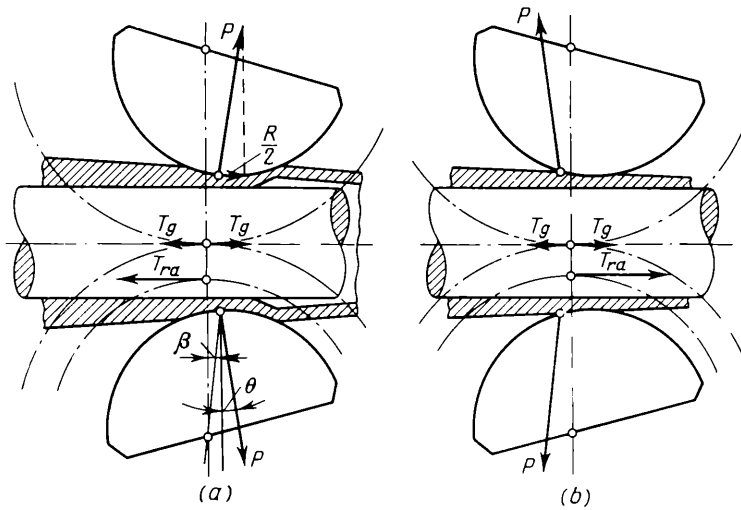

Fig. 250. Direction of the forces acting on the rolls for an excessively large diameter of the gear wheel engaging with the rack, when zones of backward slip predominate:
(*a*) forward motion; (*b*) return motion

During the return motion of the rolls the directions of the forces acting on them are found in a similar manner, with the only difference that the force R acts in the opposite direction (Fig. 249).

If rolling takes place with a predominance of zones of backward slip, then, as was mentioned above, the sign of the longitudinal stresses arising in the tube over the region from the feed chuck to the rolls is changed. The force P consequently will be inclined in the opposite direction, but its angle of inclination is still given by equation (VII.60). The direction and magnitude of the forces acting on the spur gears and the rack in this case of rolling can be found by the method given above, using equations (VII.62), (VII.65) and (VII.67) to (VII.69) and reversing the signs of the corresponding terms (Fig. 250).

8. THE KINEMATICS OF ROLLING IN PLANETARY MILLS

The relationship of the velocities of the working and support rolls and the cage (separator) is conveniently represented in the form of a diagram (Fig. 251) characterizing the variation of their velocities over a region from the centre of the support rolls to the point where the working rolls touch the metal being rolled.

During running idle when the slipping of the working rolls on the support rolls is absent, from this velocity diagram we find

$$v_l = 2v_{ca} - v_{sup} \qquad \text{(VII.70)}$$

where v_l is the velocity of the working roll where it touches the metal being rolled
v_{ca} is the velocity of the cage
v_{sup} is the peripheral velocity of the support roll.

It follows from this equation that the support rolls and the cage tend to impart a peripheral velocity to the working rolls which differs markedly from the velocity of the rolled metal. If during the exit of the metal from the rolls the peripheral velocity of the working roll is equal to or not less than the exit velocity v_1 of the metal, i.e., $v_l \approx v_1$, then, as the rolls approach the metal, a large difference between their velocities and the entry velocity v_0 of the metal will be observed:

$$v_l > v_0 \cos\varphi = \frac{v_1}{\lambda} \cos\varphi$$

where λ is the reduction ratio
φ is the angle characterizing the position of the working roll when it begins to contact the metal (Fig. 251).

Owing to this, an impact occurs at the beginning of the contact of the working roll with the metal, and then some slipping of this roll takes place along the metal being rolled, but most slipping

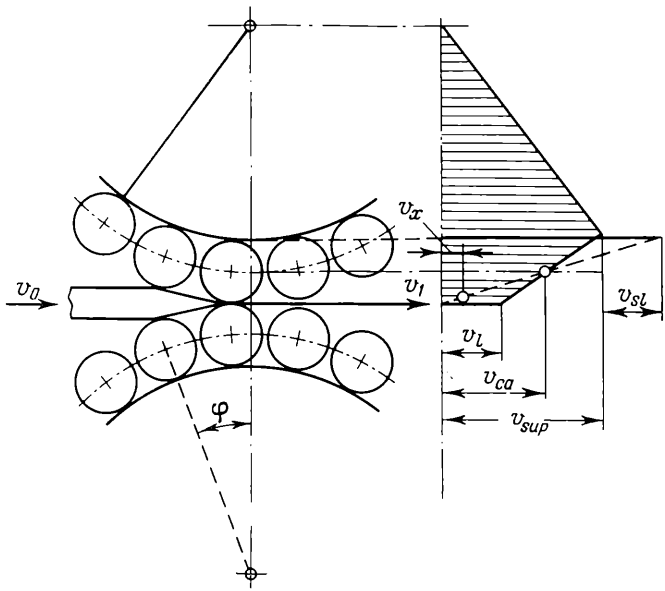

Fig. 251. Working arrangement of the rolls of a planetary mill and the corresponding velocity diagram

occurs on the support roll whose surface has a lower coefficient of friction than the rolled metal. This velocity of slipping can be calculated approximately from the equation

$$v_{sl} = v_0 \cos\varphi + 2(v_{ca} - v_0 \cos\varphi) - v_{sup} \qquad \text{(VII.71)}$$

As the rolling proceeds and the velocity of the motion of the metal increases, the velocity of slipping shown in the velocity diagram (Fig. 251) by the dash line decreases:

$$v_{sl} = 2v_{ca} - v_x \cos\varphi_x - v_{sup} \qquad \text{(VII.72)}$$

where v_x is the velocity of the forward motion of the metal being rolled in an arbitrarily chosen section

φ_x is the angle characterizing the position of the working roll at this section.

When $v_x = v_1$ the velocity of slipping approaches zero.

9. DETERMINATION OF THE CONTACT SURFACE IN PLANETARY MILLS

Each working roll will displace a volume of the metal, corresponding to the area $ABB'A'$ (Fig. 252), which is determined by the value of the feed for one working roll:

$$s = \frac{v_0}{n_{ca} z} \qquad \text{(VII.73)}$$

where v_0 is the feed velocity of the slab in the planetary stand
n_{ca} is the rotational speed of the cage
z is the number of working rolls.

The magnitude and direction of the resultant of the pressure of the metal on the rolls, and, consequently, the feed force from the side of the feed rolls vary for each working roll passing through the reduction zone. Correspondingly the feed velocity will vary also.

Neglecting this variation of the feed velocity, we assume that the magnitude of the feed s for any working roll remains constant over the entire reduction zone, and that the curves AB and $A'B'$ bounding the displaced volume are equivalent (Fig. 252).

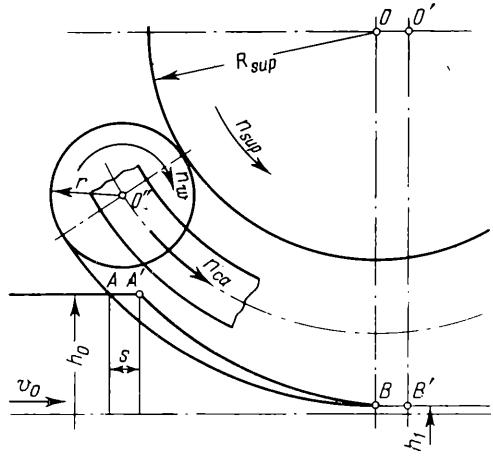

Fig. 252. The displaced volumes when rolling metal in a planetary mill

In this way the process of planetary rolling becomes analogous to the metal working process on Pilger mills, where the metal is fed at definite time intervals into the open grooves to shape the individual portions of the rolled article. Consequently, the results obtained in the analysis of the features of die rolling (see Section 1

of Chapter VII) may be used for calculating the forces arising when metal is rolled in a planetary mill.

The volume of the metal entering the reduction zone per working roll is determined from the equation

$$V_0 = h_0 s b \qquad \text{(VII.74)}$$

where h_0 is the initial thickness of the blank
b is the initial width of the blank.

The quantity b can be taken as constant, since spreading is not large when the metal is rolled in planetary mills.

In the following results the quantity b will be taken equal to unity.

It is obvious that, for any position of the working roll in the reduction zone, the volume V_0 is equivalent to the sum of the two volumes shown in Fig. 253:

$$V_0 = 2V_{AA'MEC} + 2V_{CC'E'E}$$

or

$$V_0 = 2V_{A'ACK} - 2V_{MEK} + 2V_{CC'E'E}$$

During rolling the volume $2V_{MEK}$ usually does not exceed $0.003V_0$; consequently this volume can be neglected. Then

$$V_0 = 2V_{A'ACK} + 2V_{CC'E'E}$$

The volume $V_{A'ACK}$ represents (if forward slip is neglected) the volume displaced when a working roll passes the reduction zone over a length x. As a result of this displacement the straight line EE' is displaced, by the amount Δs, together with all the metal located to the right of the roll.

From this it follows that

$$V_{A'ACK} = V_{EE'D'D}$$

or

$$V_0 = 2V_{EE'D'D} + 2V_{CC'E'E}$$

Then

$$V_0 = 2V_{CC'D'D}$$

i.e., the volume of the metal fed onto one working roll is equal to the volume bounded by $CC'DD'$ (the condition of constancy of the volume). Owing to this the cross section of the blank over the portion not yet rolled is given by the curve a, which is equivalent to AB, but is displaced to point N by the amount Δx:

$$\Delta x = s + \Delta s \qquad \text{(VII.75)}$$

The curve a is called *the displaced initial profile*, whilst the volume $2V_{CC'D'D}$ is called *the displaced volume.*

The quantity Δx serves as the starting point for determining the contact surface and the relative reduction; hence the first stage in solving the problem is to find this quantity. As seen from Fig. 253,

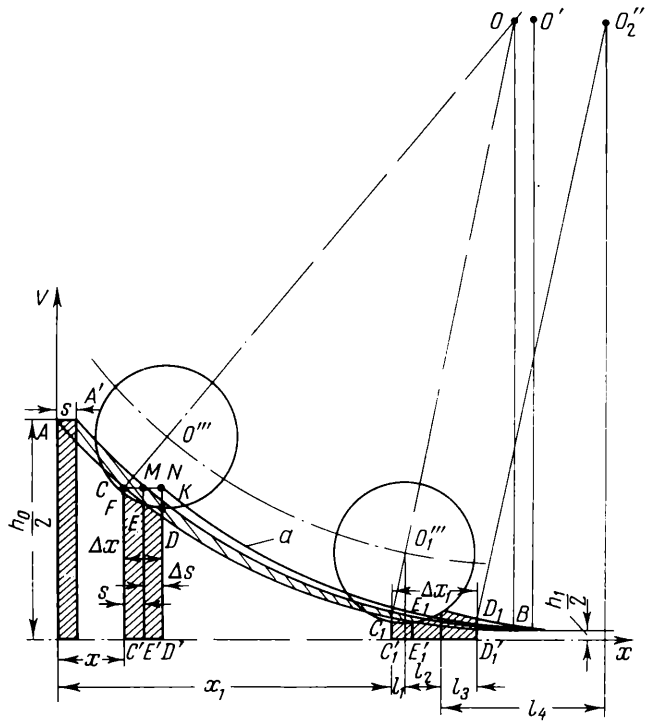

Fig. 253. The displaced volumes at the beginning and end of the reduction zone

over the whole reduction zone the displaced volume is bounded by outlines of different shapes (see, for example, $CC'D'D$ and $C_1C'_1D'_1D_1$), depending on the magnitude of the displacement and the distance between the working rolls. Accordingly the quantity Δx should be determined by different methods.

Case I. The displaced volume is so small in comparison with the distance between the working rolls (Fig. 253) that

$$s < \Delta x < 2r \sin \varphi$$

where r is the radius of the working roll.

Here the value of Δx can be found without a significant error (with accuracy up to 5%), from the usual formula for the reduction ratio:

$$\Delta x = \frac{h_0 s}{h_{ex}}$$

or

$$\Delta x \quad s\lambda$$

where h_{ex} is the thickness of the strip at the exit from the working rolls

λ is the reduction ratio.

Case II. The boundary of the displaced profile (Fig. 254) is given by the inequality:

$$\Delta x > 2r \sin \varphi$$

It is obvious that in this case the displaced volume is not bounded only by the two circular arcs of the working rolls, as in the preceding case.

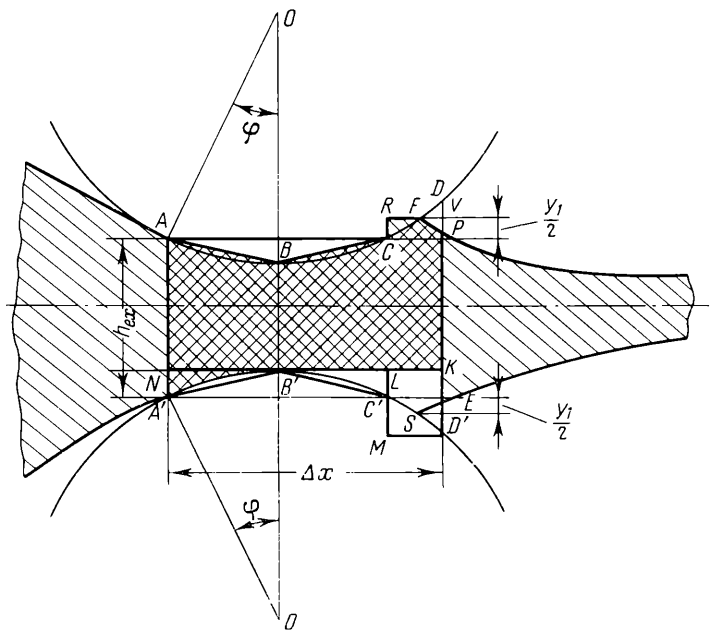

Fig. 254. The displaced volume when $\Delta x > 2r \sin \varphi$ (case II)

Indeed, if the displaced volume were located only between the circular arcs of the working rolls, then it would be bounded by the outline $ABCDD'C'B'A'$, corresponding to the length Δx. The quantity Δx characterizes, as was mentioned above, the displacement of the

initial profile, and hence

$$AA' = PE$$

Furthermore, at a distance Δx from AA' the displaced volume would be determined by the height $DD' > PE$, *which is not possible.*

The following rule may be deduced from this: from the instant when $\Delta x > 2r \sin \varphi$, *the displaced volume is described by a profile formed not only by the circular arcs of the working rolls but also by the displaced arcs of the initial profile, and is bounded by vertical line segments equal to the thickness of the strip at the exit.*

The magnitude of the displaced volume is

$$V_0 = V_{APEA'} - V_{A'NLC'} + V_{RCPV}$$

or

$$h_0 s = \Delta x h_{ex} - r(1 - \cos \varphi) 2r \sin \varphi + \frac{y_1}{2}(\Delta x - 2r \sin \varphi)$$

After a transformation we have

$$h_0 s = h_{ex} \Delta x + \frac{y_1}{2} \Delta x - r y_1 \sin \varphi - 2r^2 \sin \varphi (1 - \cos \varphi) \quad \text{(VII.76)}$$

where y_1 is the difference between the maximum thickness within the limits of the displaced volume and the thickness of the strip at the exit.

In setting up the second equation we assume that the initial profile is formed by the circle of the outer orbit of the planetary roll, with the radius

$$R = R_{sup} + 2r$$

where R_{sup} is the radius of the support roll
r is the radius of the working roll.

This will be true, if we neglect the forward slip of the metal and the feed velocity, which slightly distort the form of the initial profile:

$$\Delta x = r \sin \varphi + \sqrt{\left[(1 - \cos \varphi) r + \frac{y_1}{2}\right] 2r} + \\ + \sqrt{(h_{ex} + y_1 - h_1) R} - \sqrt{(h_{ex} - h_1) R} \quad \text{(VII.77)}$$

where h_1 is the final thickness of the strip.

Thus the value Δx can be determined from the two equations:

$$\left.\begin{aligned} h_0 s &= h_{ex} \Delta x + \frac{y_1}{2} \Delta x - r y_1 \sin \varphi - 2r^2 \sin \varphi (1 - \cos \varphi) \\ \Delta x &= r \sin \varphi + \sqrt{\left[(1 - \cos \varphi) r + \frac{y_1}{2}\right] 2r} + \\ &\quad + \sqrt{(h_{ex} + y_1 - h_1) R} - \sqrt{(h_{ex} - h_1) R} \end{aligned}\right\} \quad \text{(VII.78)}$$

Case III. The axes of the working rolls are located on a line connecting the centres of the support rolls. Here $\varphi = 0$ and $h_{ex} = h_1$. Equations (VII.78) assume the form:

$$\left.\begin{aligned} h_0 s &= h_{ex}\Delta x + \frac{y_1}{2}\Delta x \\ \Delta x &= \sqrt{y_1 r} + \sqrt{y_1 R} \end{aligned}\right\} \qquad \text{(VII.79)}$$

Case IV. The determination of the value of Δx after the working roll has intersected the line connecting the centres of the support rolls.

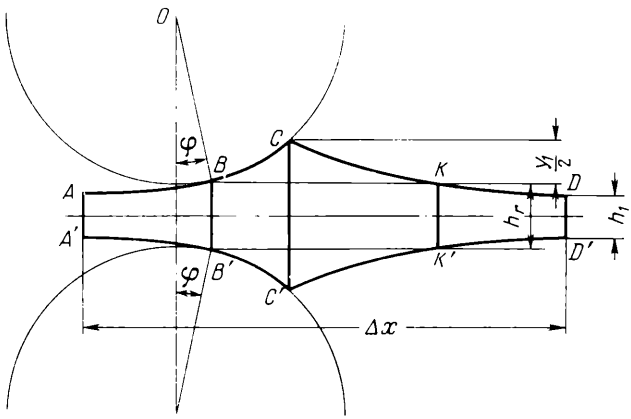

Fig. 255. The displaced volume, when the axes of the working rolls intersect the line connecting the centres of the support rolls

The working rolls, passing the extreme low position, begin to separate, deforming the displaced volume in such a way that its profile, in the greater part, is given by the radii of the outer orbit. It is obvious that when the working roll loses contact with the metal, the profile of the displaced volume will be determined solely by the radius of the outer orbit. In an intermediate case the magnitude of the displaced volume (Fig. 255) is:

$$V_0 = V_{AA'B'B} + V_{KK'D'D} + V_{BCKK'C'B'}$$

or

$$h_0 s = h_{ex}\Delta x + \frac{y_1}{2}\Delta x + R\sin\varphi\,(h_1 - h_{ex} - y_1)$$

Setting up the second equation we obtain the system of equations

$$\Delta x = R \sin \varphi + \sqrt{\left[r (1 - \cos \varphi) + \frac{y_1}{2} \right] 2r} - r \sin \varphi + \\ + \sqrt{(h_{ex} + y_1 - h_1) R}$$

$$\Delta x = \frac{h_0 s - R \sin \varphi (h_1 - h_{ex} - y_1)}{h_{ex} + \frac{y_1}{2}} \qquad \text{(VII.80)}$$

If the elastic deformation of the parts of the working stand is neglected, then the crests of the metal rolled in the planetary stand,

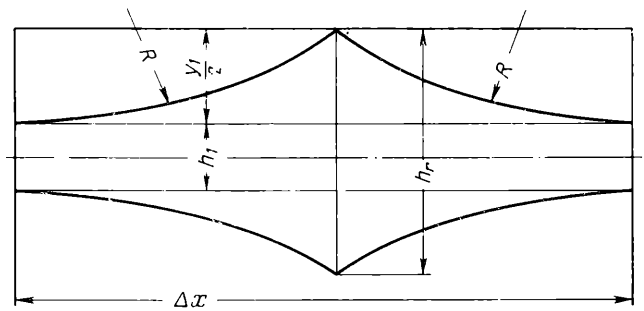

Fig. 256. Form of the strip emerging from a planetary stand

and the angle φ_c, at which the working roll ceases to be in contact with the metal (Fig. 256) can be determined from the equations

$$h_0 s = \Delta x [h_1 + R (1 - \cos \varphi_c)]$$

and

$$\Delta x = 2R \sin \varphi_c$$

Then the angle φ_c is found from the equation

$$h_0 s = 2R \sin \varphi_c [h_1 + R (1 - \cos \varphi_c)] \qquad \text{(VII.81)}$$

For small displaced volumes, when $\frac{h_0 s}{h_1} < 50$, the angle φ_c is determined, with a slight error, from the formula

$$\varphi_c = \frac{h_0 s}{2R h_1} \text{ radians} \qquad \text{(VII.82)}$$

The height of the crests is

$$\frac{(y_1)_c}{2} = R (1 - \cos \varphi_c) \qquad \text{(VII.83)}$$

The next stage in determining the magnitude of the contact area is to find the length and the position of the arc of contact. As a function

of the value of Δx, these quantities can be determined in the following manner.

Case I (Fig. 257, the left-hand position of the roll):

$$\Delta x < 2r \sin \varphi$$

In all the results which follow we again neglect the distortion of the initial profile and also the elastic compression of the rolls. The

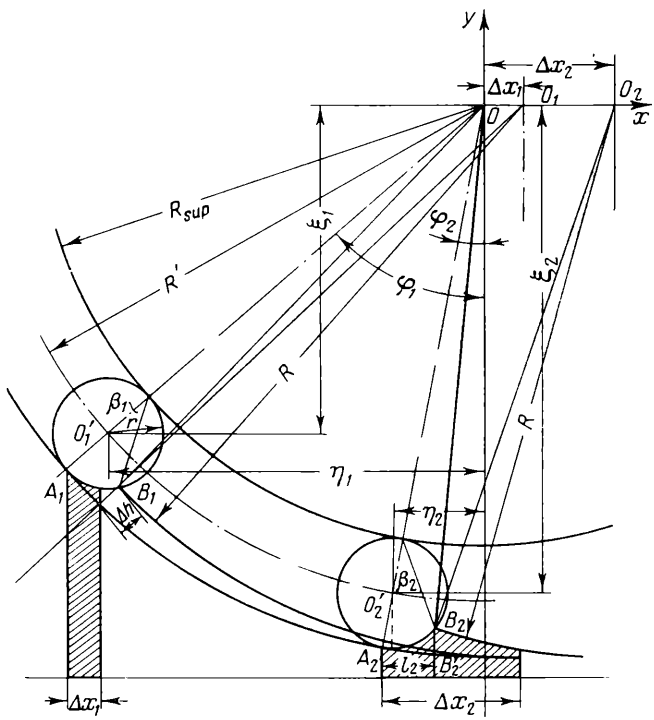

Fig. 257. Diagram showing two positions of the working rolls

position of the arc of contact is determined by the coordinates of the points A_1 and B_1.

The coordinates of the point A_1 are found from the following formulas (the origin of the coordinates being located at the centre of the support roll):

$$x_A = -(R_{sup} + 2r) \sin \varphi_1$$

$$y_A = -(R_{sup} + 2r) \cos \varphi_1$$

The coordinates of the point B_1 are found from the simultaneous equations of the two circles intersecting at this point. The first

circle, with the radius

$$R = R_{sup} + 2r$$

is drawn from the centre O_1 (Δx_1; O); the second, with the radius r, is drawn from the centre O_1' (η_1; $-\xi_1$), where

$$\left.\begin{aligned} \eta_1 &= (R_{sup} + r) \sin \varphi_1 \\ \xi_1 &= (R_{sup} + r) \cos \varphi_1 \end{aligned}\right\} \qquad \text{(VII.84)}$$

It is obvious that, in order to find the coordinates of the point B_1 (x_B and y_B'), we must solve the two equations:

$$\left.\begin{aligned} (x - \Delta x_1)^2 + y^2 &= R^2 \\ (x + \eta_1)^2 + (y + \xi_1)^2 &= r^2 \end{aligned}\right\} \qquad \text{(VII.85)}$$

If we subtract the first equation from the second and divide the variables, we obtain

$$2y\xi_1 = r^2 - R^2 - \eta_1^2 - \xi_1^2 + \Delta x_1^2 - 2x(\eta_1 + \Delta x_1)$$

or

$$y = \frac{r^2 - R^2 - (\eta_1^2 + \xi_1^2) + \Delta x_1^2}{2\xi_1} - x \frac{\eta_1 + \Delta x_1}{\xi_1}$$

where

$$\eta_1^2 + \xi_1^2 = (R_{sup} + r)^2$$

Denoting

$$A = \frac{r^2 - R^2 - (R_{sup} + r)^2 + x_1^2}{2\xi_1} \qquad \text{(VII.86)}$$

and

$$B = \frac{\eta_1 + \Delta x_1}{\xi_1} \qquad \text{(VII.87)}$$

we obtain the equation of a straight line

$$y = A - Bx$$

Substituting the value of y just obtained into the first equation of the system (II.85) we obtain

$$x^2 - 2\Delta x \times x + \Delta x^2 + A^2 - 2AB + B^2x^2 = R^2$$

or

$$x^2(1 + B^2) - 2x(\Delta x + AB) + \Delta x^2 + A^2 - R^2 = 0$$

Denoting

$$C = 1 + B^2 \qquad \text{(VII.88)}$$

$$K = \Delta x + AB \qquad \text{(VII.89)}$$

$$N = \Delta x^2 + A^2 - R^2 \qquad \text{(VII.90)}$$

we obtain the quadratic equation

$$Cx^2 - 2Kx + N = 0$$

We solve this equation:

$$x_{B1,2} = \frac{K \pm \sqrt{K^2 - CN}}{C} \tag{VII.91}$$

$$y_{B1,2} = A - Bx_{B1,2} \tag{VII.92}$$

Equating the arc of contact to the chord A_1B_1 (Fig. 257) we obtain the calculated length of this arc:

$$l_{calc} = \sqrt{(x_B - x_A)^2 + (y_B - y_A)^2} \tag{VII.93}$$

Case II (Fig. 257, the right-hand position of the working roll):

$$\Delta x > 2r \sin \varphi$$

In this case the difference in the abscissas of the points A_2 and B_2 is determined considerably more simply:

$$x_B - x_A = \Delta x' = r \sin \varphi_2 + \sqrt{\left[r(1 - \cos \varphi_2) + \frac{y_1}{2} \right] 2r} \tag{VII.94}$$

and the problem reduces to finding the difference in the ordinates of these points.

The ordinate of the point A_2 is found, as in the preceding case, from the equation

$$y_A = -(R_{sup} + 2r) \cos \varphi_2$$

whilst the ordinate of the point B_2 is found by solving the equation of the circle with radius r, drawn from the centre O_2' $(-\eta_2; -\xi_2)$, together with the equation of the straight line B_2B_2' which intersects this circle at the point B_2.

Thus the ordinate of the point B_2 is found from the system of equations:

$$\begin{aligned} &(x + \eta_2)^2 + (y + \xi_2)^2 = r^2 \\ &x = -\eta_2 - r \sin \varphi_2 + l_2 \end{aligned} \tag{VII.95}$$

We substitute the second equation into the first and express ξ_2 as given by the second formula (VII.84):

$$(l_2 - r \sin \varphi_2)^2 + [y + (R_{sup} + r) \cos \varphi_2]^2 = r^2$$

We expand the expression inside the brackets and group the terms with respect to y:

$$y^2 + 2y(R_{sup} + r) \cos \varphi_2 + l_2^2 - 2l_2 r \sin \varphi_2 + \\ + r^2 \sin^2 \varphi_2 + (R_{sup} + r)^2 \cos^2 \varphi_2 - r = 0$$

Hence

$$y_{B1,2} = -(R_{sup} + r)\cos\varphi_2 \pm \sqrt{2l_2 r \sin\varphi_2 + r^2\cos^2\varphi_2 - l_2^2}$$

Then

$$y_B - y_A = r\cos\varphi - \sqrt{2l_2 r\sin\varphi_2 + r^2\cos^2\varphi - l_2^2} \qquad \text{(VII.96)}$$

Equating the arc of contact to the chord A_2B_2 (Fig. 257), as in the preceding case, we obtain the calculated length of this arc:

$$l_{calc} = \sqrt{(x_B - x_A)^2 + (y_B - y_A)^2} \qquad .97)$$

We determine the angle characterizing the position of the working roll, using the simpler formulas (VII.94) and (VII.96) for the calculation.

It is obvious that for such an angle

$$\Delta x = 2r\sin\varphi_0 \text{ and } y_1 = 0$$

Let us substitute expression (VII.94) into the first equation of the system (VII.78):

$$h_0 s = h_{ex} 2r\sin\varphi_0 - 2r^2\sin\varphi_0(1 - \cos\varphi_0) \qquad \text{(VII.98)}$$

We determine h_{ex} from the formula

$$h_{ex} = 2R(1 - \cos\varphi_0) + h_1 \qquad \text{(VII.99)}$$

Substituting expression (VII.99) into (VII.98) we obtain

$$h_0 s = [2R(1 - \cos\varphi_0) + h_1]\, 2r\sin\varphi_0 - 2r^2\sin\varphi_0(1 - \cos\varphi_0)$$

or

$$h_0 s = 2r\sin\varphi_0[(2R - r)(1 - \cos\varphi_0) + h_1] \qquad \text{(VII.100)}$$

The angle φ_0 determined from this equation, even for the maximum feed, does not exceed 5°.

10. DIRECTION OF THE FORCES ACTING ON THE ROLLS OF PLANETARY MILLS

Let us first consider the direction of the forces acting on the working roll in the simplified case where the bearings of the roll are completely free of load, i.e., there are no forces acting from the cage.

It follows from the condition of equilibrium that in the case under consideration the resultant of the pressure of the metal on the roll

must pass through the centroid of the contact area between the working and support rolls.

If the effect of the rolling friction of the working roll on the support roll is neglected, then the angle θ (Fig. 258) between the direction

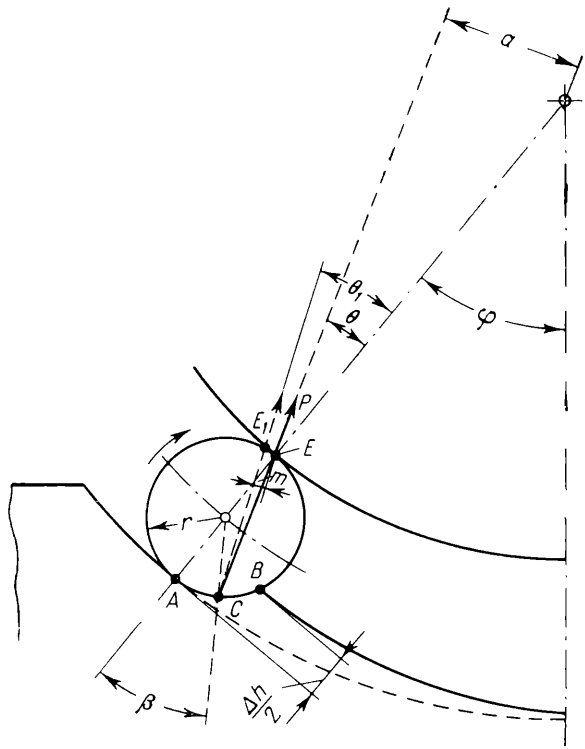

Fig. 258. Direction and point of application of the resultant of the pressure of the metal on the rolls for a single pair of working rolls

of the force P and the line connecting the centres of the working and support rolls is

$$\theta = \frac{\beta}{2}$$

where β is the angle characterizing the position of the point C (where the resultant of the pressure of the metal on the roll is applied) and is approximately equal to

$$\beta \approx \frac{AB}{2r}$$

Then the torque required to rotate the support roll, without con-

sidering the friction losses in its bearings, is

$$M_{sup} = Pa = PR_{sup} \sin \theta \qquad \text{(VII.101)}$$

If the effect of the rolling friction between the working and support rolls is taken into consideration, then the point where the force P is applied to the support roll is displaced in the direction opposite to the motion of the rolling surfaces by an amount m (equal to the

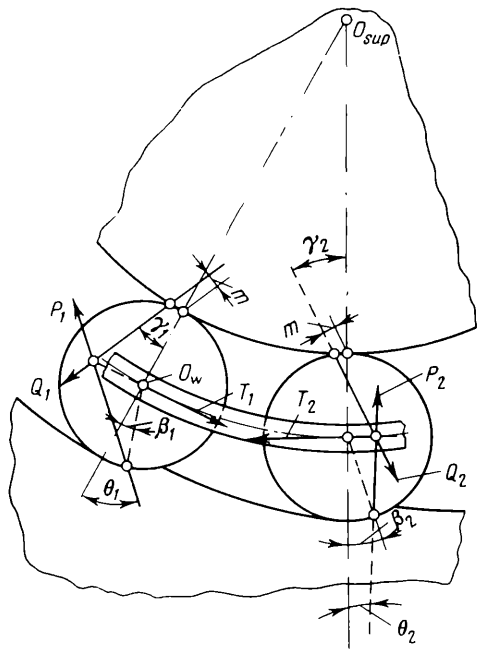

Fig. 259. Direction of the forces acting on the working rolls when two pairs of rolls are in the reduction zone

lever arm of friction), and it assumes the position of the point E_1 (Fig. 258). The resultant force P will be slightly inclined as shown by the dash line.

The angle θ_1 between the direction of the force P and the line connecting the centres of the working and support rolls can be determined from the expression

$$\theta_1 \approx \frac{\beta}{2} + \frac{m}{2r} \qquad \text{(VII.102)}$$

and correspondingly the moment of the force about the axis of the support roll is

$$M_{sup} = P(R_{sup} \sin \theta_1 + m) \qquad \text{(VII.103)}$$

A more characteristic case of rolling occurs when two pairs of working rolls are simultaneously in the reduction zone (Fig. 259). The direction of the forces acting on the rolls in this case was considered in detail by R. Ritman.

Since the support roll and the cage tend to impart to the working rolls a peripheral velocity which differs from the velocity of the metal being rolled, considerable friction forces arise on the contact surfaces. At the beginning of the reduction zone these friction forces are directed against the motion of the working roll, whilst at the end, on the other hand, they act in the same direction as this motion.

Consequently, at the beginning of the reduction zone, for the first pair of rolls the resultant P_1 of the pressure, exerted by the support roll on the working roll, is inclined against the direction of the motion of the metal (Fig. 259); the force P_2, for the second pair, is inclined in the direction of the motion of the metal. The same is true for the forces Q_1 and Q_2, applied to the working rolls from the support roll. If the friction in the bearings of the working roll is neglected, then these forces have the same moment about the axes of the working rolls as do the forces P_1 and P_2. Furthermore, the forces Q_1 and Q_2 intersect the forces P_1 and P_2 at the same points as do the forces T_1 and T_2, constituting the reactions of the bearings.

The angle of inclination θ_1 of the force P_1 to the line connecting the centres of the working and support rolls can be found from the equation of moments:

$$P_1 r \sin(\theta_1 - \beta_1) = Q_1 (r \sin \gamma_1 + m) \qquad \text{(VII.104)}$$

where β_1 is the angle characterizing the location of the point of application of the force P_1

γ_1 is the angle of inclination of the force Q_1 to the line $O_w O_{sup}$

m is the lever arm of the rolling friction.

The angle γ_1 in this equation can be found approximately from the condition at which the slipping of the working roll on the support roll will take place:

$$\tan \gamma_1 \approx \mu_1 \qquad \text{(VII.105)}$$

where μ_1 is the coefficient of friction when the working roll slips over the support roll.

For the sake of simplicity in the calculation it is assumed that

$$P_1 = Q_1 \quad \tan \gamma_1 \approx \sin \gamma_1$$

then from equation (VII.104) we obtain

$$\sin \theta_1 \approx \sin \beta + \mu_1 + \frac{m}{r} \qquad \text{(VII.106)}$$

The force T_1 is determined as the projection of the forces P_1 and Q_1:

$$T_1 = P_1 \sin\theta_1 + Q_1 \sin\gamma_1 \approx P_1 \left(\sin\beta + 2\mu_1 + \frac{m}{2} \right)$$

The direction of the forces applied to the second pair of working rolls is found in a similar manner, putting $T_1 = -T_2$.

The angle θ_2 is then found from the equation

$$T_2 = P_2 \sin\theta_2 + Q_2 \sin\gamma_2$$

Making the same assumptions as in deriving equation (VII.106), we obtain

$$\sin\gamma_2 = \frac{T_2}{2P_2} + \frac{m}{2r} - \frac{\sin\beta_2}{2} \qquad \text{(VII.107)}$$

Then the torque required to drive the support roll

$$M_{sup} = Q_2 (R_{sup} \sin\gamma_2 + m) - Q_1 (R_{sup} \sin\gamma_1 - m) \qquad \text{(VII.108)}$$

where the angles γ_2 and γ_1 are found from equations (VII.107) and (VII.105).

VIII

Forces During Cross and Helical Rolling

1. KINEMATICS OF CROSS ROLLING

During cross rolling as well as during helical rolling the reduction is carried out by making the contact surfaces of the rolls or some other tool approach each other as the body rotates whilst being shaped between these surfaces. In the case of cross rolling this approach takes place as a result of the relative displacement of the tool and the body being shaped in the direction perpendicular to the axis of rotation of the latter. During helical rolling, also called skew rolling, simultaneously with the approach of the contact surfaces the body being shaped also moves in the direction of its axis.

Let us consider the kinematics of these two rolling processes.

The relative displacement of the tool and the body being shaped, which for brevity will be called the blank, during cross rolling is effected by three methods:

(1) by reducing the centre distance of the rolls (Fig. 260*a*);

(2) by increasing the rolling radius of the rolls with their rotation (Fig. 260*b*);

(3) by moving the blank perpendicularly to its axis in the direction of the smaller distance between the surfaces of both rolls (Fig. 260*c*).

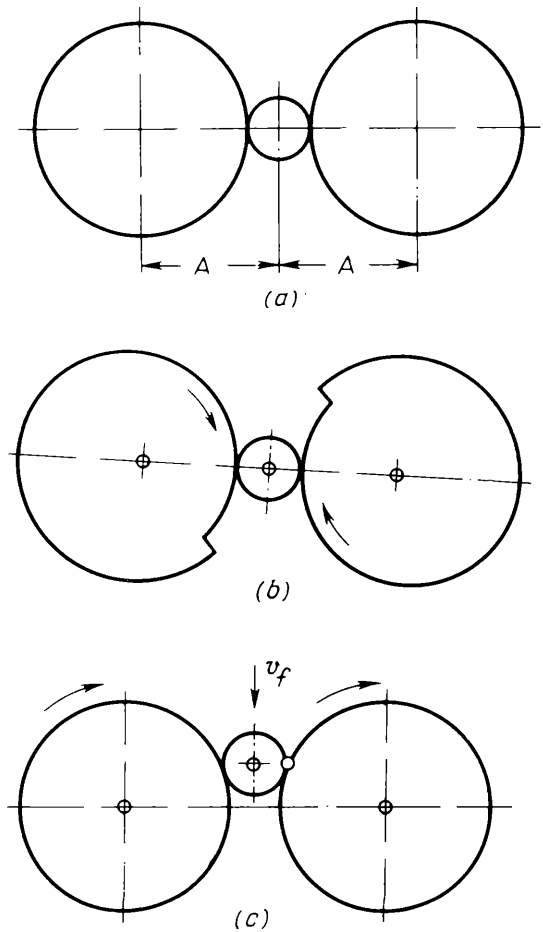

Fig. 260. Different methods of cross rolling:

(*a*) reduction of the centre distance of the rolls; (*b*) increase in the rolling radius of the rolls; (*c*) feed of the blank perpendicular to its axis in the direction of decreasing distance between the rolls

The reduction of the blank to radius Δr, effected by each roll or plate, i.e., in the case of two rolls per half a revolution, and in the case of three rolls per one third of a revolution, can be expressed by:

$$\Delta r = 60 \frac{v_A}{m n_{bl}} \tag{VIII.1}$$

where v_A is the velocity at which the distance A diminishes between the axes of the roll and the blank (see Fig. 260*a*)
m is the number of rolls
n_{bl} is the rotational speed of the blank.

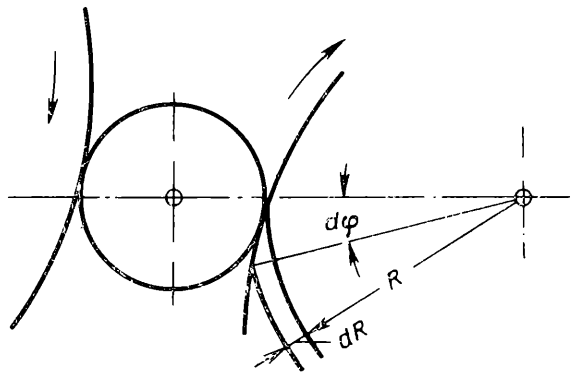

Fig. 261. Determination of v_A for a variable rolling radius

This formula is also applicable for the cases of rolling shown schematically in Fig. 260*b* and *c*, if we substitute the approximate value of v_A:

$$v_A = \frac{\pi n_r}{30} \frac{dR}{d\varphi} \tag{VIII.2}$$

for the case shown in Fig. 260*b*;

$$v_A = v_f \sin \alpha \tag{VIII.3}$$

for the case given in Fig. 260*c*.

Here $\frac{dR}{d\varphi}$ is the derivative of the radius of the roll with respect to its angle of rotation (Fig. 261)
v_f is the feed velocity of the blank (Fig. 262).
α is the angle determining the position of the blank relative to the rolls.

When the rotational speed of the blank is determined, it is necessary to consider the slipping taking place along the contact surfaces of the rolls and the blank. The magnitude of this slipping is usually

given by the tangential slipping coefficient:

$$\eta_t = \frac{v_{bl}}{v_r} \tag{VIII.4}$$

where v_{bl} is the peripheral velocity of the blank at the section passing through the axes of this blank and the rolls
v_r is the peripheral velocity of the rolls.

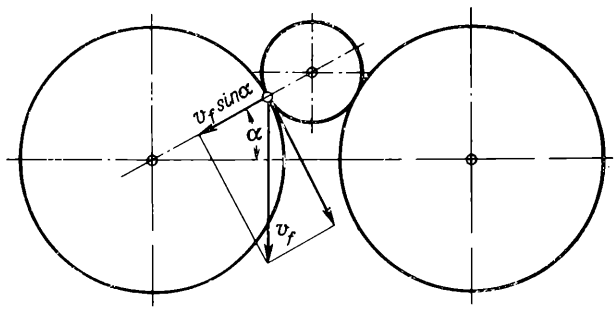

Fig. 262. Determination of v_A when a blank is fed in lateral direction

If we assume that at this section, where the velocity of the blank is v_{bl}, its radius equals r_{bl}, then the rotational speed of the blank is given by

$$n_{bl} = \frac{R_r}{r_{bl}} \eta_t n_r \tag{VIII.5}$$

where R_r is the radius of the rolls
n_r is the rotational speed of the rolls.

The first attempt to determine the coefficient of slipping during cross rolling was made by I. Pobedin and S. Granovsky. Subsequently this problem was considered by P. Teterin, P. Severdenko and L. Fyodorov. These authors arrived at different results depending on the direction of the velocity vector of the point A of the blank where it touches the roll (Fig. 263). In the writings of I. Pobedin and S. Granovsky, and also in those of P. Teterin this vector is directed tangentially to the contact surface (Fig. 263*a*), whilst in the writings of P. Severdenko and L. Fyodorov it is directed perpendicularly to the radius of the blank (Fig. 263*b*). As a result of this the character of the slipping of the metal along the surface of the rolls is different. In the first case, for a given rotational speed n_{bl} of the blank, the velocity is

$$v_A = \frac{\pi n_{bl}}{30} \frac{AD}{\cos(\alpha_r + \alpha_{bl})} \tag{VIII.6}$$

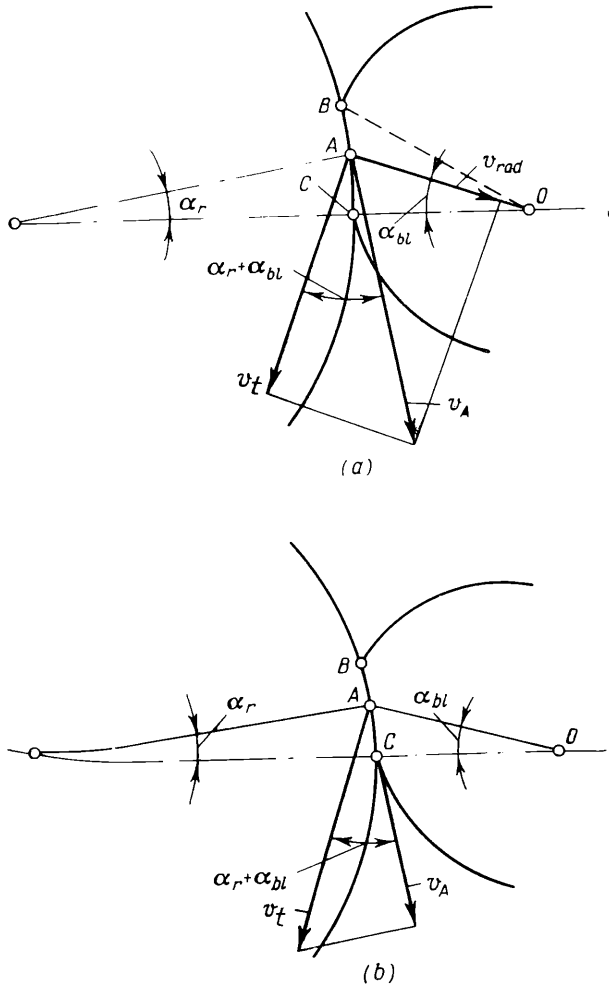

Fig. 263. Resolution of velocities in determining the coefficient of tangential slip:
(*a*) correct; (*b*) incorrect

whilst in the second case (Fig. 263*b*) it is

$$v_A = \frac{\pi n_{bl}}{30} \cos(\alpha_r + \alpha_{bl}) \qquad \text{(VIII.7)}$$

where α_r and α_{bl} are the angles characterizing the location of the point A on the blank and on the roll (Fig. 263) respectively.

It follows from these equations that in the first case (Fig. 263*a*) the velocity v_A decreases in the direction from the point B to the exit, whilst in the second case (Fig. 263*b*) it increases. If we assume that a neutral point exists on the contact surface, where the metal does not slip along the roll, then in the first case the velocity of the blank at the point B must be higher than the velocity of the rolls, whilst at the point C, conversely, the roll leads the blank. In the second case (Fig. 263*b*) the character of the slipping is the same as in longitudinal rolling, i.e., at the beginning of the arc of contact the metal lags behind the rolls, whilst at the end of the arc of contact it leads the rolls.

In order to shed some light on this problem, let us reconsider it, starting from the condition that the volume per second of the metal passing through each meridional cross section of the blank remains constant, beginning from the point B and finishing with the point C. The condition for the volume of the metal per second to remain constant can be expressed by the following equation for a rotating body:

$$OB\omega_B = OC\omega_C = r_x\omega_x = \text{const.}$$

where ω_B, ω_C and ω_x are the angular velocities of the sections characterized by the radii OB, OC and r_x respectively.

Thus, from the condition that the volume of metal per second remains constant, it follows that

$$r_x\omega_x = v_t = \text{const.} \qquad \text{(VIII.8)}$$

i.e., the peripheral velocity over the entire arc of contact BC must be constant.

Taking into consideration the fact that the absolute velocity of the point A must be directed tangentially to the contact surface of the rolls (Fig. 263*a*), we obtain

$$v_A = \frac{v_t}{\cos(\alpha_r + \alpha_{bl})} \qquad \text{(VIII.9)}$$

Since according to equation (VIII.8) $v_t = \text{const.}$, the velocity of the blank at the point B is a maximum, whilst at the point C, where $v_A = v_t$, it is a minimum. This serves to justify the results of P. Teterin relating to the nature of the slipping of the blank.

We shall assume that in cross rolling, as in longitudinal rolling, there exists a neutral point on the contact surface, where the metal of the blank moves with the same velocity as the rolls. Let us suppose that this point coincides with the point A (Fig. 263*a*); then from the results obtained above

$$v_t = v_r \cos(\alpha_r + \alpha_{bl})$$

Hence, according to equation (VIII.4),

$$\eta_t = \cos(\alpha_r + \alpha_{bl}) \qquad \text{(VIII.10)}$$

Experimental investigations into the coefficient of tangential slipping during cross rolling were carried out by V. Smirnov. According to these investigations, in the case of hot rolling of cylindrical blanks at 700 to 1,200°C, the coefficient of slipping lies within the limits 0.9 and 0.95.

2. KINEMATICS OF HELICAL ROLLING

The motion of metal in the direction of its axis during helical rolling is brought about by several methods. Of these the following are most widely used:

(1) arrangement of the rolls at a certain angle to the blank (Fig. 264*a*);

(2) displacement of the axis of the blank relative to the plane passing through the axes of the rolls (Fig. 264*b*).

When the rolls and the blank are parallel to each other, the motion of the metal in the direction of its axis can be secured by applying an axial force to the blank, or by providing the roll surfaces with helical grooves.

In the case where the rolls are set at an angle to the blank to be rolled, the components w_r and u_r of the peripheral velocity of the rolls in the tangential and axial directions are (Fig. 264*a*):

$$w_r = v_r \cos\beta = \frac{\pi n}{30} R_x \cos\beta \qquad \text{(VIII.11)}$$

$$u_r = v_r \sin\beta = \frac{\pi n}{30} R_x \sin\beta \qquad \text{(VIII.12)}$$

where v_r is the peripheral velocity of the rolls
β is the angle between the axes of the rolls and the blank
n is the speed of the rolls, rpm
R_x is the radius of the roll in the section x-x under consideration.

In tube rolling mills consisting of two disks which rotate in the same direction (Fig. 264*b*) the tube being rolled receives a translational motion as a result of the rolling plane being displaced relative

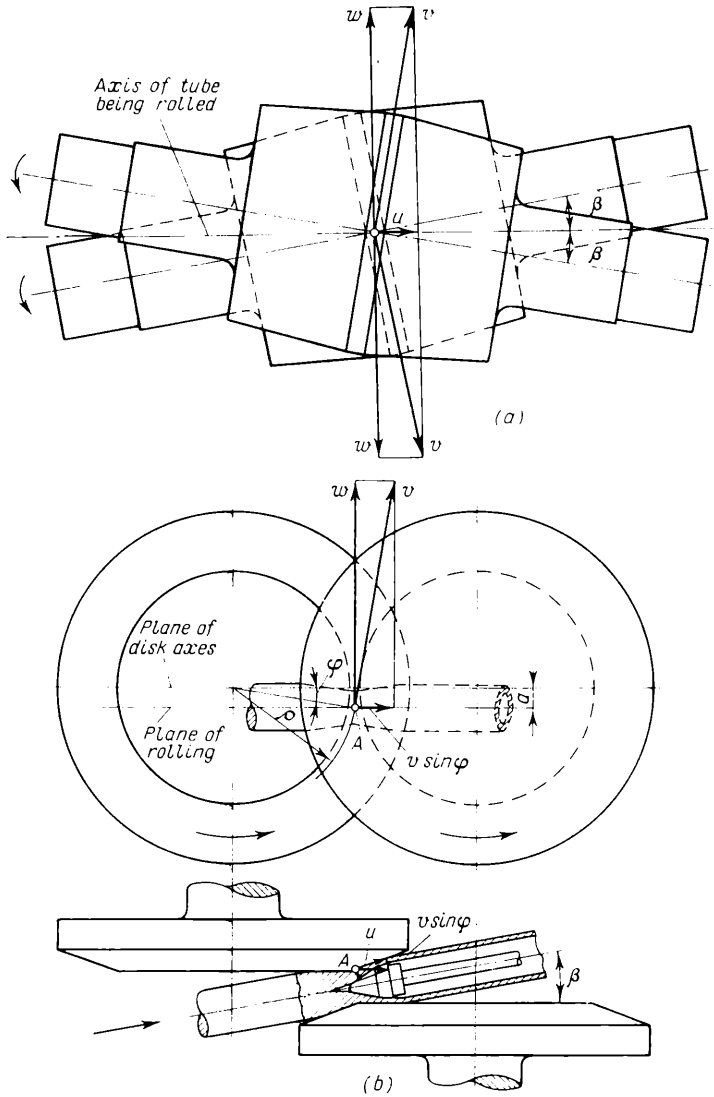

Fig. 264. Resolution of velocities in helical rolling:
(*a*) mill with skew rolls; (*b*) disk mill

to the axes of the disks. We denote the value of this displacement, i.e., the distance between the rolling plane and the axes of the disks, by a. The angle between the axis of the blank and the plane perpendicular to the axes of the disks is denoted by β (Fig. 264).

The velocity of the point A located, say, on the surface of the right-hand roll is denoted by v. Let us resolve this velocity into three mutually perpendicular directions, one of which is taken as the direction of the axis of the blank.

After we subtract the slipping between the disks and the blank, the component w of the velocity v represents the peripheral velocity of this blank. This projection equals

$$w_r = v_r \cos \varphi$$

or

$$w_r = \frac{\pi \rho n}{30} \cos \varphi \qquad \text{(VIII.13)}$$

where n is the speed of the disk in revolutions per minute.

The component u, causing the translational motion of the blank, is directed along the axis of the blank. Obviously this component is

$$u_r = v_r \sin \varphi \cos \beta \qquad \text{(VIII.14)}$$

From Fig. 264*b*

$$\sin \varphi = \frac{a}{\rho} \qquad \text{(VIII.15)}$$

Then equation (VIII.14) assumes the form

$$u_r = \frac{\pi n}{30} a \cos \beta \qquad \text{(VIII.16)}$$

It follows from this equation that all the points of the disk which touch the blank in a plane parallel to the axes of the disks tend to impart a translational motion to the blank which does not vary with the course of its motion.

In the case of conical rolls, the translational motion of the blank being rolled can be achieved by one of the methods previously considered: by arranging the rolls at an angle to the axis of the blank (Fig. 264*a*), or by displacing the roll axes relative to the plane passing through the axis of the article being rolled (Fig. 265). In the latter case the points of contact with the metal are located on the generatrices of the cone of the rolls which intersect with the axis of the blank; this results in maintaining the axial component of the velocity $v \sin \beta$.

In reality the translational motion of the blank during helical rolling, when passing through the deformation zone, varies considerably as its cross-sectional area is reduced.

If we neglect the possible variation in the density of the rolled metal, then the translational velocity of the individual cross sections

is given by the equation

$$Q_1u_1 = Q_2u_2 = \ldots\ Q_xu_x \qquad \text{(VIII.17)}$$

where $Q_1, Q_2, \ldots, Q_x$ are the cross-sectional areas of the blank
$u_1, u_2, \ldots, u_x$ are the translational velocities of the corresponding sections of the blank.

For large reductions in the cross-sectional area of the blank in the rolling process (in piercing mills, for example, the overall reduction ratio of the metal reaches four and more) the translational

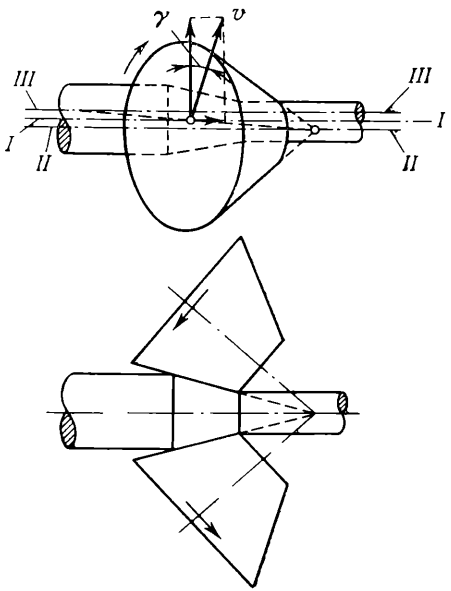

Fig. 265. Displacement of the axes of the conical rolls relative to the axis of the article to be rolled necessary to obtain a translational motion:
I-I—axis of the blank; *II-II*—axis of the front roll; *III-III*—axis of the back roll

velocities of the blank at entry and exit will differ markedly. Since the rolls tend to impart a translational motion to the rolled blank, in accordance with equation (VIII.12) or (VIII.16), a motion which in mills with skew rolls varies slightly with the course of the motion of the blank, and which in disk mills is constant, it can be seen that slipping between the rolls and blank is inevitable.

The translational velocity of any cross section of the blank is thus

$$u_x = \eta_{ax\,x}u_r$$

where $\eta_{ax\,x}$ is the coefficient of axial slipping in the case under consideration.

If we know the coefficient of axial slipping η_{ax} at the exit section, where the cross-sectional area of the blank is Q_1, then from equation (VIII.17) the translational velocity is

$$u_x = \eta_{ax} u_r \frac{Q_1}{Q_x} \tag{VIII.18}$$

or, for mills with skew rolls,

$$u_x = \eta_{ax} \frac{\pi n}{30} R_1 \sin\beta \frac{Q_1}{Q_x} \tag{VIII.19}$$

and for disk mills

$$u_x = \eta_{ax} \frac{\pi n}{30} a \cos\beta \frac{Q_1}{Q_x} \tag{VIII.20}$$

where Q_1 is the cross-sectional area of the blank at the exit
R_1 is the radius of the roll at the exit section.

According to experimental investigations into piercing mills, the exit velocity of the blank is usually less than the axial vector

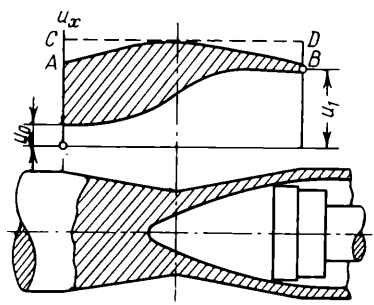

Fig. 266. Variation of the translational velocity of different sections of the rolled blank in piercing mills:
u_0—velocity of the blank entering the mill; u_1—velocity of the blank emerging from the mill; AB—the projection of the peripheral velocity of the rolls on to the axis of the blank in a mill with skew rolls; CD—the corresponding projection for a disk mill

of the peripheral velocity at the section, i.e., $\eta_{ax} < 1$. Therefore, over the entire deformation zone $u_x < u_r$, as shown in Fig. 266.

According to the investigations by N. Lomakin and A. Tselikov, during the piercing of tubes 112 to 235 mm in diameter in a 220 mill—the material being steels 1010, ШХ15, ЭЯ1Т, 38ХМЮА and 30ХГСА—the coefficients of slipping were found to lie within the following limits: $\eta_t = 0.6$ to 0.92; $\eta_{ax} = 0.68$ to 0.9.

Many factors have a marked effect on the coefficients of slipping, in particular, the reduction ratio of metal, an increase in which

results in a decrease in the coefficient of axial slipping (Fig. 267). The position of the mandrel nose also exerts a certain effect: as it moves forward the coefficient of axial slipping is reduced (Fig. 268).

The most detailed investigations into the coefficient of slipping have been carried out by S. Granovsky on a laboratory mill (VNIIMETMASH), by piercing tubes from a blank 40 mm in diameter heated up to 1,250 to 1,300°C. The material of the blank was steel Ст. 3.

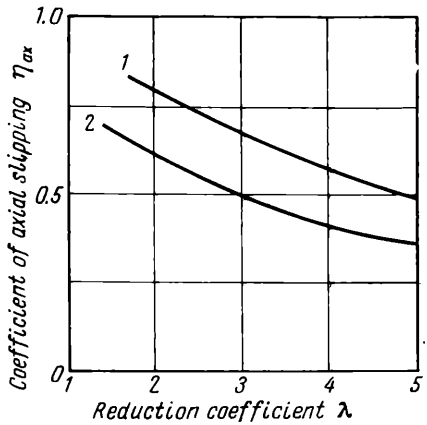

Fig. 267. Variation of the axial slipping coefficient with reduction ratio when piercing tubes of various outside diameters using steel 1020 (N. Lomakin and A. Tselikov):
1—135 to 173 mm; *2*—227 to 232 mm

From the data of these investigations S. Granovsky plotted graphs showing the variation of the coefficients of axial and tangential slipping with the angle of inclination β of the axes of the rolls to the axis of the blank (Fig. 269); a number of other factors were also studied. In these tests the coefficient of tangential slipping was more than unity, whilst that of axial slipping was less than unity. This indicates that the peripheral velocity of the tube at the exit from the rolls is higher than the velocity of the rolls, whilst in the axial direction, conversely, the tube lags behind the rolls.

Studying the angle of twist during piercing S. Granovsky arrived at the important conclusion that, depending on the nature of slipping of the blank along the rolls in the tangential direction, the whole deformation zone can be divided into three sections. In the two end sections at the beginning and end of the deformation zone the blank leads the rolls, whilst in the middle section it lags behind the rolls (Fig. 270). At the transition points, from the zones of for-

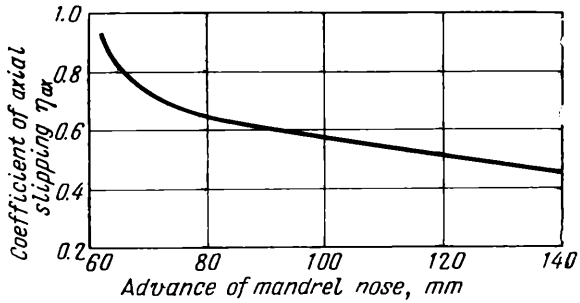

Fig. 268. Variation of the axial slipping coefficient with the advance of the mandrel nose beyond the middle zone of the rolls when piercing tubes 135 to 232 mm in diameter (N. Lomakin and A. Tselikov)

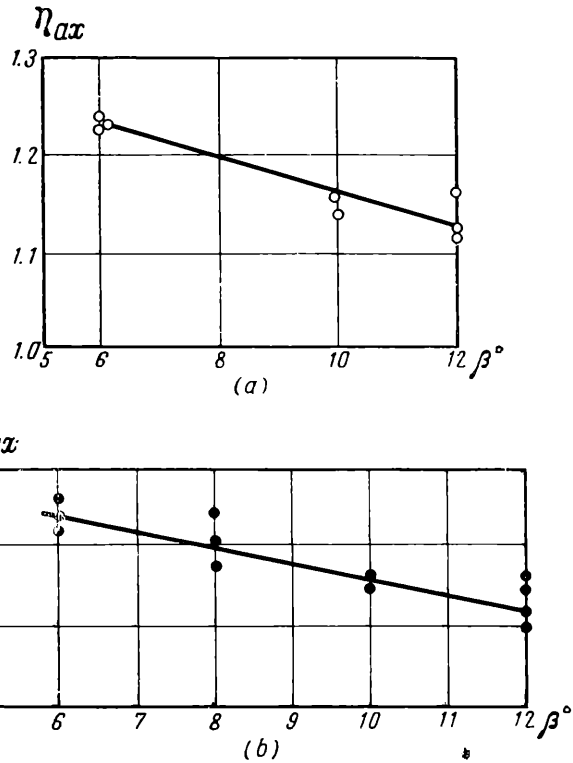

Fig. 269. Variation of coefficients of tangential and axial slipping with the angle of inclination β of the roll axes to the pierced blank axis (S. Granovsky):

(*a*) tangential slipping; (*b*) axial slipping

ward slip to the zone of backward slip, the blank moves with a peripheral velocity equal to the velocity of the rolls, and the coefficient of tangential slipping equals unity.

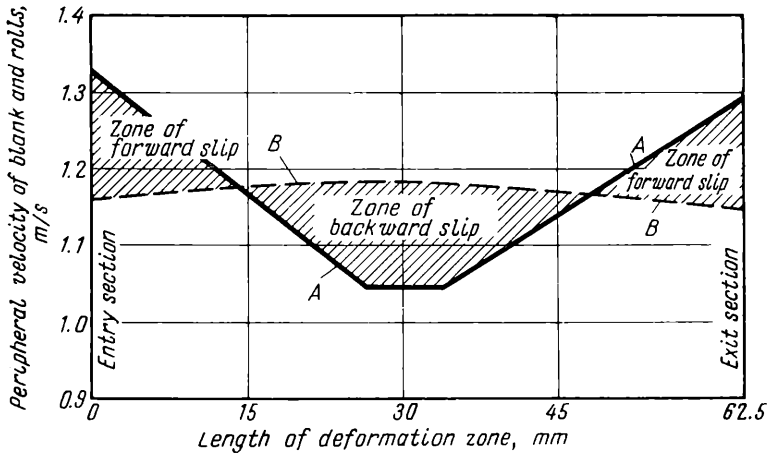

Fig. 270. Variation of the peripheral velocities of the blank (A) and the rolls (B) over the deformation zone during the piercing process (S. Granovsky)

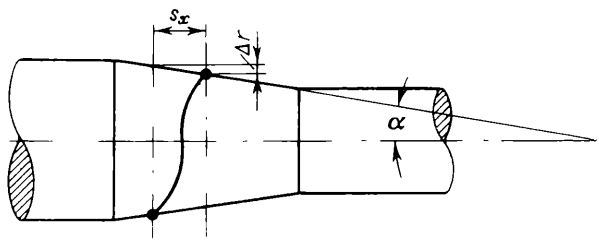

Fig. 271. Determination of radial reduction during helical rolling

The radial reduction Δr of the blank effected per roll during helical rolling—when the internal cavity is neither opened up nor widened—is given by the equation

$$\Delta r = s_x \tan \alpha \qquad \text{(VIII.21)}$$

where s_x is the axial displacement of the blank per revolution, divided by the number of the rolls

α is the angle between the tangent to the generatrix of the cone of the blank and its axis (Fig. 271).

The quantity s_x can be determined from the relationship between the translational and rotational velocities of the blank:

$$s_x = \frac{u_x}{n_x m} 60 \qquad \text{(VIII.22)}$$

where n_x is the average number of revolutions of the given section of the blank per minute

m is the number of rolls.

From equations (VIII.11) and (VIII.13) we find that

$$n_x = \frac{r_r \cos \beta}{\pi r_x} 30 \eta_{tx} = \frac{R_x}{r_x} \eta_{tx} n \cos \beta \qquad \text{(VIII.23)}$$

for mills with skew rolls, and

$$n_x = \frac{\pi \rho n \cos \varphi}{30 \pi r_x} 30 \eta_{tx} = \frac{\rho}{r_x} \eta_{tx} n \cos \varphi \qquad \text{(VIII.24)}$$

for disk mills,

where η_{tx} is the coefficient of tangential slipping for the given section.

After substituting the values of n_x and u_x from equations (VIII.19) and (VIII.20) into equation (VIII.22) we obtain

$$s_x = 2\pi \frac{R_1}{R_x} \frac{Q_1}{Q_x} r_x \frac{\eta_{ax}}{\eta_{tx}} \frac{\tan \beta}{m} \qquad \text{(VIII.25)}$$

for mills with skew rolls, and

$$s_x = 2\pi a \frac{r_x}{\rho} \frac{Q_1}{Q_x} \frac{\cos \beta}{m \cos \varphi} \frac{\eta_{ax}}{\eta_{tx}} \qquad \text{(VIII.26)}$$

for disk mills.

Substituting the value of s_x into equation (VIII.21), we find Δr.

The problem concerning the calculation of Δr when in the rolling process the internal cavity is either opened up or widened, as a result of the wall being reduced between the rolls and the mandrel, will be considered below.

3. DETERMINATION OF THE CONTACT SURFACE DURING CROSS AND HELICAL ROLLING IN THE ABSENCE OF A CAVITY

When a body of cylindrical form is cross rolled between smooth rolls, the contact surface can be calculated as the area of a rectangle the length of which equals the length of the rolls or that of the article being rolled. The width is dependent on the magnitude of the radial reduction Δr, as well as on the radius r of the blank and the

radius R of the rolls. From Fig. 272, with sufficient accuracy for practical purposes, we can assume that $AB \approx AC$.

Then

$$AB \approx \sqrt{(r+\Delta r)^2-(r+BC)^2} = \sqrt{R^2-(R-BC)^2} \quad b$$

If we neglect the squares of the quantities Δr and BC in this equation, we obtain

$$BC = \frac{r\Delta r}{r+R}$$

and

$$b \approx \sqrt{\frac{2Rr}{r+R}}\,\Delta r \qquad \text{(VIII.27)}$$

Using this equation we can find the ideal width of the contact area. Its actual width will be a little larger as a result of the metal being

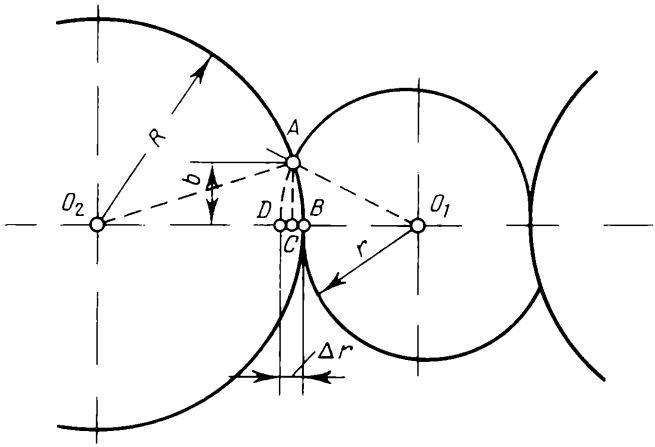

Fig. 272. Deformation during cross rolling

displaced to the other side of the line connecting the axes of the rolls, called the fin, and also as a result of the local elastic compression of the rolls and the blank being rolled.

The fin is apparently explained by the fact that at the point B (Fig. 273) the peripheral velocity of the rolls is somewhat higher than the velocity of the blank, and consequently the rolls tend to push out the part of the rolled metal close to this point, with an angular velocity slightly higher than the velocity of the remainder of the blank. The effect of the fin on the contact surface was first noticed by I. Pobedin and S. Granovsky. They measured the dimensions of the imprints left by the rolls on a large number

of cylindrical blanks, which during rolling were stopped under different conditions. According to the data provided by them, the ratio $b_2 : b_1$ (Fig. 273) ranges from 0.35 to 0.75.

We may, however, assume that these results giving the value of the fin are somewhat overestimated, since in the case where the rolling is suddenly stopped the rolls leave an imprint whose area is larger than the actual contact surface, owing to the recoil of the rolls after they have been stopped, i.e., a rotation through a very small angle in the opposite direction.

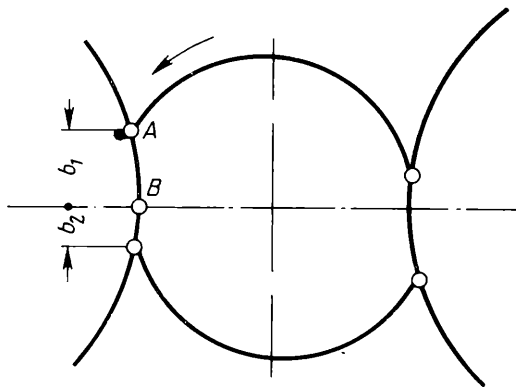

Fig. 273. The effect of fin on the contact surface

Let us now consider the problem concerning the effect of a local elastic compression of the blank and the rolls on the contact surface. The effect of this factor can be considerable in the case of rolling with small radial reductions Δr and high specific pressures (in particular, during cold rolling).

We denote the local elastic deformation of the roll in the radial direction by Δ_1 and that of the blank by Δ_2. For the blank to receive a permanent reduction by the required amount Δr, it is necessary to account for this by approaching the roll to the blank by an amount equal to the sum of these deformations, i.e., $\Delta_1 + \Delta_2$; the centre of the roll is then displaced from the point O_1 to the point O_2 (Fig. 274). As a result of the elastic compression the length of the line of contact is increased: its start is displaced from the point A_1 to the point A_2, and the contact segment B_2C emerges on the other side of the line connecting the centres of the roll and the blank.

Let us first find the extent of the contact segment $A_2B_2 \approx b_1$. From the diagram shown in Fig. 275 the length of the segment b_1 can be expressed as:

$$b_1 = \sqrt{R^2 - (R - DF)^2} = \sqrt{(r + \Delta r)^2 - (r + \Delta r - EF)^2}$$

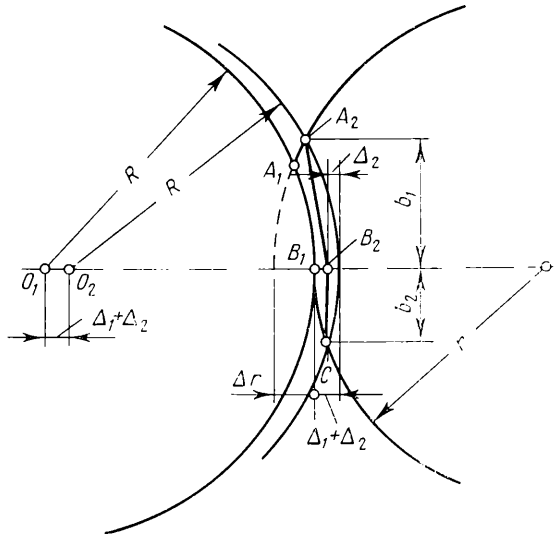

Fig. 274. Contact between the roll and the blank during cross rolling taking account of elastic compression of roll and blank

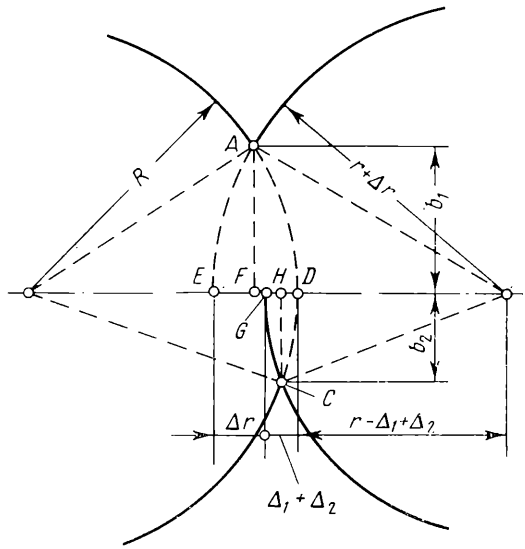

Fig. 275. Contact between the roll and the blank during cross rolling

After removing the parentheses we neglect the squares and products of the quantities DF, EF and Δr in view of their smallness in comparison with R and r. Also noting that

$$DF + EF = \Delta r + \Delta_1 + \Delta_2$$

we obtain

$$b_1 \approx \sqrt{\frac{2Rr}{R+r}(\Delta r + \Delta_1 + \Delta_2)} \qquad \text{(VIII.28)}$$

In an analogous manner we can find the length of the contact segment located on the other side of the line connecting the centres of the roll and the blank, i.e., the segment B_2C (Fig. 274), making use of the diagram shown in Fig. 275:

$$b_2 = B_2C \approx \sqrt{R^2 - (R - DH)^2} = \sqrt{r^2 - (r - GH)^2}$$

If we neglect the squares of GH and DH and note that $DH + GH = \Delta_1 + \Delta_2$, then

$$b_2 \approx \sqrt{\frac{2Rr}{R+r}(\Delta_1 + \Delta_2)} \qquad \text{(VIII.29)}$$

Deformations Δ_1 and Δ_2 can be found from the well-known results in the theory of elasticity, concerning the compression of two cylinders. If we neglect the fact that in the given case there is no symmetry in the compression of these cylinders about the line connecting their centres, and also assume that when the tube is rolled it closely fits the mandrel and that the deformation of its wall is very small, then the deformations Δ_1 and Δ_2 can be expressed as:

$$\left.\begin{aligned} \Delta_1 &= 2q\frac{1-\mu_1^2}{\pi E_1} \\ \Delta_2 &= 2q\frac{1-\mu_2^2}{\pi E_2} \end{aligned}\right\} \qquad \text{(VIII.30)}$$

where q is the pressure per unit length of the cylinders being compressed

μ_1 and E_1 denote Poisson's ratio and the modulus of elasticity of the roll

μ_2 and E_2 denote Poisson's ratio and the modulus of elasticity of the blank being rolled or of the mandrel when a thin-walled tube is rolled.

We express the quantity q in terms of the specific pressure on the contact surface:

$$q = 2b_2 p$$

and substitute the values of Δ_1 and Δ_2 from equations (VIII.30) into equation (VIII.29). Then

$$b_2 \approx 8p \left(\frac{1-\mu_1^2}{\pi E_1} + \frac{1-\mu_2^2}{\pi E_2} \right) \frac{Rr}{R+r} \qquad \text{(VIII.31)}$$

From equations (VIII.28) and (VIII.29), taking into consideration the elastic compression, we can express the overall width of the contact surface as:

$$b = b_1 + b_2 \approx \sqrt{\frac{2Rr}{R+r} \Delta r + b_2^2} + b_2 \qquad \text{(VIII.32)}$$

where b_2 is given by equation (VIII.31).

When bodies having the form of a cone or a sphere are cross rolled, the contact surface is determined in a similar manner, by dividing the given body into a number of segments and calculating Δr_x and b_x for each of them. The contact area is then

$$F = \sum \frac{b_x + b_{x+1}}{2} \Delta l \qquad \text{(VIII.33)}$$

where Δl is the length of the segment at the boundaries of which the widths of the contact area are b_x and b_{x+1}.

The contact surface during helical rolling can also be calculated from this formula, with the only difference that in determining b_x [see equation (VIII.27) or (VIII.32)] the quantity Δr should be found from formula (VIII.21).

4. DETERMINATION OF THE CONTACT SURFACE DURING THE HELICAL ROLLING OF HOLLOW BODIES

To determine the contact surface during the helical rolling of hollow bodies two different cases must be distinguished:

(1) rolling without a mandrel, or with a mandrel when the metal is in close contact with the mandrel over its entire surface;

(2) rolling with a mandrel, but with the metal being in contact with the mandrel only at points opposite the points of contact of the blank and the rolls.

The fundamental difference between these two cases of rolling is that in the first case reduction is effected only by the rolls, whilst in the second case the mandrel participates in the reduction of the metal, playing the same part as the internal roll during ring rolling (Fig. 276).

These two cases of rolling are differentiated by the pressure of the metal on the rolls and by the resistance of the tube wall to flexure. If the wall thickness of the tube is considerable and the pressure applied to the metal being rolled by one of the rolls is transmitted

to the other roll without the assistance of the mandrel, then the rolling process corresponds to the first case. If the wall thickness is reduced so that the tube begins to flatten as a result of the pressure

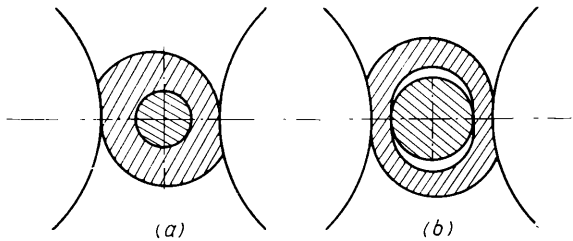

Fig. 276. Reduction diagram in the case of the helical rolling of hollow bodies:
(*a*) reduction is effected only by rolls (case I); (*b*) mandrel participates in reduction (case II)

exerted by the metal on the rolls (Fig. 276*b*), then the mandrel will begin to take part in reducing the wall of the tube; this will correspond to the transition from the first case of rolling to the second.

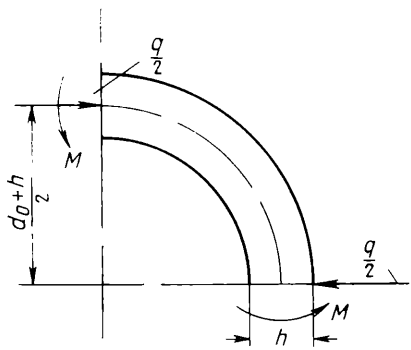

Fig. 277. Determination of the force which flattens the tube

The criterion for this transition is given by the resistance of the tube wall to flexure. The force q per unit length of the tube which causes plastic flexure of the tube wall, can be determined from the equation of equilibrium (Fig. 277):

$$\frac{q}{2} \times \frac{d_0 + h}{2} = 2M$$

where d_o is the outer diameter of the tube
h is the wall thickness
M is the maximum bending moment of the tube wall.

In the case of a large degree of flattening the value of this moment is found from the equation of plastic flexure:

$$M = \frac{\sigma_a h^2}{4}$$

from which the force required to flatten the tube is

$$q \approx \frac{\sigma_a h^2}{\frac{d_o + h}{2}} \qquad \text{(VIII.34)}$$

or the total force

$$P_{fl} \approx \frac{\sigma_a h^2}{\frac{d_o + h}{2}} (l + a)$$

where l is the length of the section of the tube subjected to the action of the force q

a is the assumed overall length of the outer regions involved in the flexure of the tube wall.

The contact surface in both cases of rolling considered is found to be dependent on the radial reduction effected by the roll whilst the blank is rotated.

We denote by s_x the displacement of an arbitrarily chosen section O-O of the blank per half a revolution in the axial direction (for a mill with two rolls) over the region *I* (Fig. 278). To determine the radial reduction carried out by the roll in the section x-x, we assume that the volume of metal per second passing through any meridional cross section during this half a revolution of the blank remains constant. If we neglect the deformation of the blank in the direction of its axis during this period, then we can write the equation

$$AB\omega = CD\omega = \text{const.}$$

where ω is the mean angular velocity of the given section.

It follows from this equation that for the first case of rolling the radial reduction effected in the section x-x can be expressed as:

$$\Delta r = AB - CE$$

or

$$\Delta r = r_{oO} - r_{iO} - (r_{ox} - r_{ix}) \qquad \text{(VIII.35)}$$

where r_{oO}, r_{ox} are the outer radii of the blank at the sections O-O and x-x

r_{iO}, r_{ix} are the inner radii.

Taking into account that

$$r_{oO} - r_{ox} = s_x \tan \alpha_x \quad r_{ix} - r_{iO} = s_x \tan \gamma_x$$

where α_x and γ_x are the angles between the axis of the blank and the tangents to the outer and inner surfaces of the blank respectively,

we obtain the formula suggested by the author in 1937:

$$\Delta r = s_x (\tan \gamma_x + \tan \alpha_x) \qquad \text{(VIII.36)}$$

The value s_x in this formula is determined from equations (VIII.25) and (VIII.26) or (VIII.22).

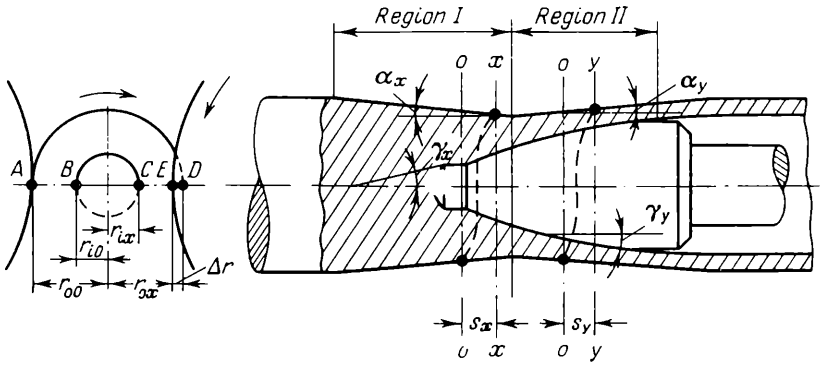

Fig. 278. Determination of the radial reduction in the case of helical rolling

In a similar manner we can find Δr at the beginning of the second region of deformation, where an increase in the outer radius takes place, but the flattening produced by the rolling has not commenced yet.

In this case the difference of the outer radii which appears in equation (VIII.35) is

$$r_{oO} - r_{ox} = -s_y \tan \alpha_y$$

Then the radial reduction for the second section is

$$\Delta r = s_y (\tan \gamma_y - \tan \alpha_y) \qquad \text{(VIII 37)}$$

where s_y is the axial displacement of the blank per revolution divided by the number of rolls located in the second section (Fig. 278).

We substitute the value of Δr obtained into equation (VIII.27) or (VIII.32) and find the quantity b; then from equation (VIII.33) we calculate F.

At the end of the second section, when the wall thickness is reduced so much that flattening of the tube takes place, the radial reduction effected by the roll should be determined from the conditions associated with the second case of rolling. As mentioned above, the fea-

ture of this case of rolling is that the mandrel begins to play the same role as the internal roll in ring rolling.

The radial reduction Δr_r effected by the roll, the value of which is needed to determine the contact surface by substituting in equation

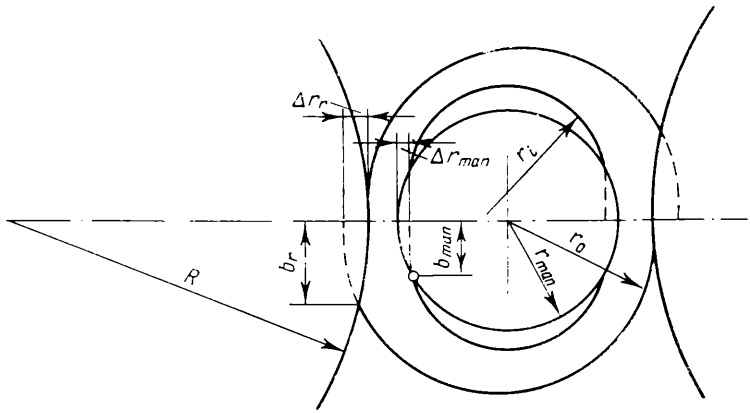

Fig. 279. Reduction of the tube wall between roll and mandrel

(VIII.27) or (VIII.32), is in this case determined with the following condition (Fig. 279) taken into account:

$$\Delta r_r = \Delta r_{tot} - \Delta r_{man} \qquad \text{(VIII.38)}$$

where Δr_{tot} and Δr_{man} are the total reduction and the reduction effected by the mandrel respectively.

The value Δr_{tot} in the right-hand side of this equation is found from equation (VIII.37), whilst Δr_{man} is found from equation (V.30), whence it follows that

$$\Delta r_{man} = \frac{r_i - r_{man}}{2 r_i r_{man}} b_{man}^2 \qquad \text{(VIII.39)}$$

where r_i is the inner radius of the tube
r_{man} is the radius of the cross section of the mandrel
b_{man} is the width of the contact surface between the mandrel and the tube.

The quantity b_{man} is determined from the condition that the pressure on the mandrel is equal to the pressure of the metal on the roll minus those forces which are transmitted through the tube walls to the other roll, bypassing the mandrel.

If we assume that the specific pressure on the roll and the mandrel is the same, then the width of the contact surface on the roll, b_r, and the corresponding width on the mandrel, b_{man}, should be deter-

mined from the equation

$$b_{man} = b_r - \frac{q}{p} \qquad \text{(VIII.40)}$$

where p is the mean specific pressure
q is the force necessary to flatten the tube, as given by equation (VIII.34).

Substituting this value of b_{man} into equation (VIII.39), we obtain

$$\Delta r_{man} = \frac{r_i - r_{man}}{2r_i r_{man}} \left(b_r - \frac{q}{p} \right)^2 \qquad \text{(VIII.41)}$$

Taking into account that from equation (VIII.27)

$$\Delta r_r = \frac{R + r_o}{2Rr_o} b_r^2$$

we have, by substituting the values of Δr_r and Δr_{man} into equation (VIII.38),

$$\frac{R + r_o}{2Rr_o} b_r^2 = \Delta r_{tot} - \frac{r_i - r_{man}}{2r_i r_{man}} \left(b_r - \frac{q}{p} \right)^2$$

Hence

$$b_r = \frac{B}{A + B} \frac{q}{p} + \sqrt{\left(\frac{B}{A + B} \right)^2 \left(\frac{q}{p} \right)^2 + \left[\Delta r_{tot} + B \left(\frac{q}{p} \right)^2 \right] \frac{1}{A + B}} \qquad \text{(VIII.42)}$$

where

$$A = \frac{R + r_o}{2Rr_o} \qquad B = \frac{r_i - r_{man}}{2r_i r_{man}}$$

If we neglect the effect of the stiffness of the tube wall and assume that $q = 0$, then this equation assumes the same form as the equation (V.31) derived earlier for the calculation of the contact surface during ring rolling.

The problem of determining the contact surface during the helical rolling of tubes on a mandrel of a plugging mill was considered in detail by V. Smirnov, whilst K. Gruber has done the same for expanding mills.

5. DETERMINATION OF THE STRESSES ON THE CONTACT SURFACE

In cross and helical rolling of solid or thick-walled bodies the contact surfaces are usually small in comparison with the distance between them, and accordingly the resistance to deformation, to a large extent, depends on the influence of the outer zones.

We shall first consider the case of the compression of a cylindrical body between parallel plates. The solution of this problem, in a closed form, was first given by A. Tomlenov, using the results of work by V. Sokolovsky and R. Hill.

This case of deformation is very close to cross rolling, if for simplicity we assume that the line of contact of the metal with the roll is rectilinear, and if we consider the process of cross rolling to be the result of the elementary processes of compression as the body turns through a small angle.

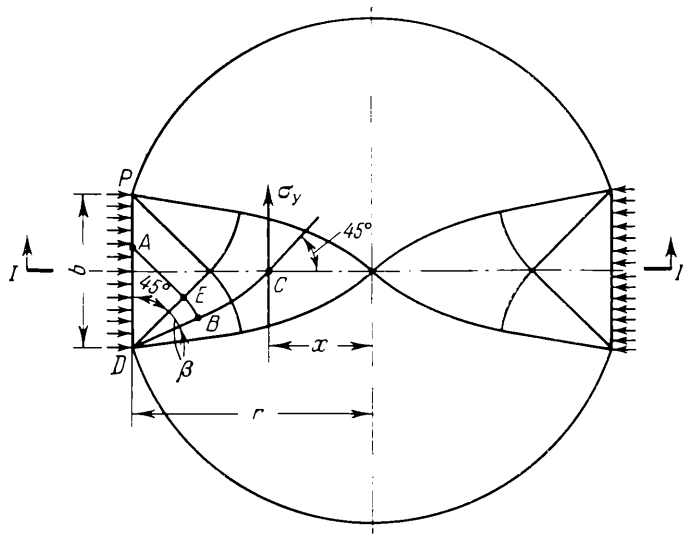

Fig. 280. Slip line field for a cylinder being compressed

If the strain in the direction of the axis of the cylinder is neglected the stress state for this process of compression can be represented by a field of slip lines (Fig. 280) consisting of an equilateral triangle, two fan zones and a curvilinear four-sided figure. The coordinates of the node points of this field can be determined by a number of different methods described in the literature. The boundaries of this field in a rigid-plastic material will determine the boundaries of the plastic region. In the case of a real material the boundaries of the field will determine the boundaries of the zone in which elastic deformations are very small in comparison with plastic deformations.

It should be noted that the field under consideration satisfies the kinematic boundary conditions, if we assume that the zone of sticking extends over the entire length of the arc of contact (this applies in the case where a long blank with a small contact length is deformed). Indeed, the magnitude of the displacement of the particles on the

contact surface is constant for the deformation described by the field; the components of displacement are v_x const. and $v_y = 0$, which corresponds to the case of sticking.

To obtain the magnitude of the specific pressure on the contact surface, let us consider the equilibrium of the half of the blank located on the right of the line I-I. From the condition of equilibrium we have

$$\int_0^r \sigma_y \, dx = 0 \tag{VIII.43}$$

where σ_y is the stress in the section I-I

r is the radius of the blank.

To determine the stress σ_y let us consider the two orthogonal slip lines AB and BC of Fig. 280; applying the first theorem of Hencky, we obtain

$$\left.\begin{aligned} \sigma_A - \sigma_B &= -2k\alpha_{AB} \\ \sigma_B - \sigma_C &= +2k\alpha_{BC} \end{aligned}\right\} \tag{VIII.44}$$

where σ_A, σ_B and σ_C are the mean stresses at the points A, B and C

k is the resistance to plastic deformation in pure shear

α_{AB} and α_{BC} are the angles of rotation of the slip lines between the points A and B, and B and C respectively.

Since the slip line BC forms an angle of 45° with the axis of the roll, the above angles of rotation are equal to the angle β between the slip lines DB and DE:

$$\alpha_{BC} = -\alpha_{AB} = \beta$$

Then from equations (VIII.44) it follows that

$$\sigma_A - \sigma_C = 2k(\alpha_{BC} - \alpha_{AB}) = 4k\beta$$

The mean stresses in these equations are determined from the plasticity equation:

$$\left.\begin{aligned} \sigma_A &= p - k \\ \sigma_C &= \sigma_y - k \end{aligned}\right\} \tag{VIII.45}$$

Hence it follows that for $x = 0$ to $r - \frac{b}{2}$

$$\sigma_y = p - 2k(1 + 2\beta) \tag{VIII.46}$$

Noting that on the section $x = r - \frac{b}{2}$ to r

$$\sigma_y = p - 2k$$

we obtain from equation (VIII.43)

$$\frac{b}{2}(p - 2k) + \int_0^{r-\frac{b}{2}} [p - 2k(1 + 2\beta)]\, dx = 0$$

We integrate this equation and then solve it for p:

$$p = 2k\left[1 + \frac{2}{r}\int_0^{r-\frac{b}{2}} \beta\, dx\right] \qquad \text{(VIII.47)}$$

In order to integrate equation (VIII.47) it is necessary to find $\beta = f(x)$. As shown by the investigations by V. Lugovskoi into the slip line field, this function can be expressed in the form of a series:

$$2\,\frac{r-x}{b} = I_0(2\beta) - 2I_1(2\beta) + 2I_3(2\beta) + 2I_5(2\beta) + \ldots \qquad \text{(VIII.48)}$$

where b is the width of the contact surface (see Fig. 280)

$I_n(2\beta)$ is the n-th order Bessel function of the imaginary argument 2β.

Following the suggestion of V. Lugovskoi, we can approximate the relation (VIII.48), within the limits $0 \leqslant \beta \leqslant \frac{\pi}{2}$, with accuracy up to $3^0{}_0$, by the function

$$2\,\frac{r-x}{b} = e^{1.6\beta} \qquad \text{(VIII.49)}$$

After taking logarithms we obtain the required expression:

$$\beta = 0.625 \log_e 2\,\frac{r-x}{b} \qquad \text{(VIII.50)}$$

Substituting (VIII.50) into (VIII.47) and integrating, we obtain after certain transformations

$$p = 2k\left(1.25 \log_e \frac{2r}{b} + 1.25\,\frac{b}{2r} - 0.25\right) \qquad \text{(VIII.51)}$$

The value $\frac{p}{2k}$ as a function of $\frac{b}{2r}$, calculated from this equation, is shown in Fig. 281.

The lower boundary of applicability of this field is the value $\frac{2r}{b}=1$, when the triangles under the contact surfaces touch with vertices and $p=2k$. The upper boundary is the value of $\frac{2r}{b}$ determined from the equation

$$p=2k\left(1.25\log_e\frac{2r}{b}+1.25\frac{b}{2r}-0.25\right)=2k\left(1+\frac{\pi}{2}\right) \quad \text{(VIII.52)}$$

where in the right-hand side of this equation there is the value of the specific pressure corresponding to a rigid die being indented into a half-space, for which the character of the field is altered.

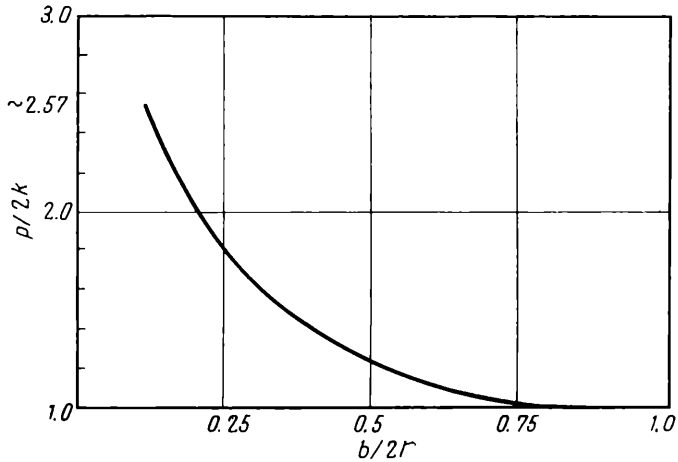

Fig. 281. Variation of $\frac{p}{2k}$ with $\frac{b}{2r}$, as given by equation (VIII.51) suggested by V. Lugovskoi

Solving this equation we find that $\frac{2r}{b_{max}}=8.5$. Thus formula (VIII.51) is valid within the limits $1\leqslant\frac{2r}{b}\leqslant 8.5$; when $\frac{2r}{b}>8.5$ the specific pressure is determined from Prandtl's formula:

$$p=2k\left(1+\frac{\pi}{2}\right)\approx 5.14k \quad \text{(VIII.53)}$$

A. Tomlenov has suggested that the value β over the interval $\beta=0$ to $\frac{\pi}{4}$ be approximated by the function

$$\beta=-0.535+0.6\eta-0.065\eta^2 \quad \text{(VIII.54)}$$

where $\eta=2\frac{r-x}{b}$,

whilst over the interval $\beta = \frac{\pi}{4}$ to $\frac{\pi}{2}$ it should be approximated by the function

$$\beta = 0.15 + 0.2\eta - 0.007\eta^2 \qquad \text{(VIII.55)}$$

As a result of these approximations he has obtained the following formulas for determining the specific pressure:

$$p \approx 2k\left[0.5\frac{b}{2r} + 0.6\frac{2r}{b} - 0.04\left(\frac{2r}{b}\right)^2\right] \qquad \text{(VIII.56)}$$

for the interval $1 < \frac{2r}{b} \leqslant 3.64$;

$$p \approx 2k\left[1.3 - \frac{b}{2r} + 0.2\frac{2r}{b} - 0.004\left(\frac{2r}{b}\right)^2\right] \qquad \text{(VIII.57)}$$

for the interval $3.64 < \frac{2r}{b} \leqslant 8.4$.

For values $\frac{2r}{b} > 8.4$, which corresponds to $\beta_{max} = 75.8°$, a displacement of the metal close to the contact surfaces begins, and in this case the pressure of the metal on the rolls should be determined from the formula (VIII.53).

Values of $\frac{p}{2k}$ as a function of $\frac{2r}{b}$, calculated from formulas (VIII.56) and (VIII.57), are presented in Table 21.

Table 21

The Specific Pressure $\frac{p}{2k}$ and the Maximum Tensile Stress $\frac{\sigma_y}{2k}$ During Cross Rolling, Calculated from Formulas (VIII.56) and (VIII.57)

$\frac{2r}{b}$	β, degrees	$\frac{p}{2k}$	$\frac{\sigma_y}{2k}$
1.0	0	1.0	0
1.6	15	1.17	0.35
2.44	30	1.43	0.61
3.64	45	1.80	0.75
5.42	60	2.08	0.92
8.15	75	2.54	1.08
12.40	90	2.57	—

Applying the method just considered to determine the effect of the outer zones on the specific pressure, and using equation (VIII.45), we can also establish the stress distribution over the entire meridional cross section of the blank.

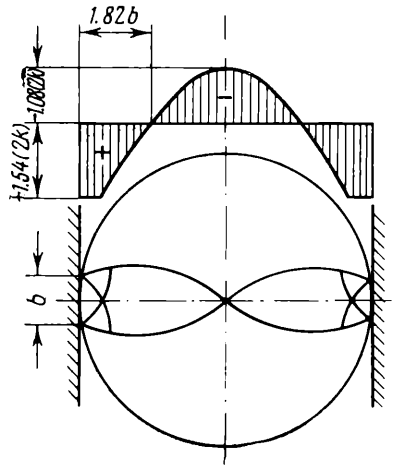

Fig. 282. Stress distribution during cross rolling when $\frac{b}{2r}=0.123$; $\beta=75°$ (A. Tomlenov)

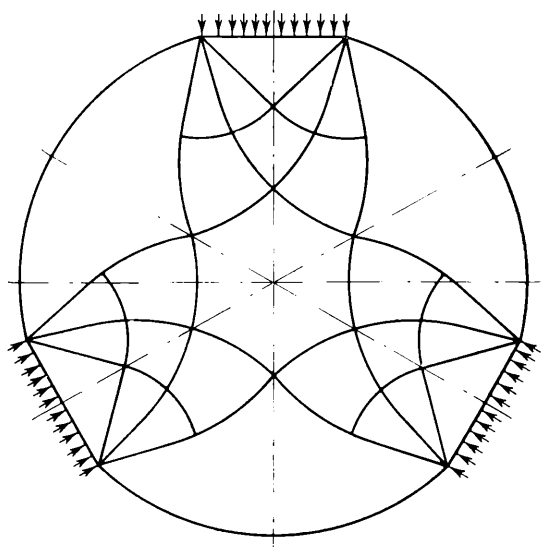

Fig. 283. Slip line field for metal being rolled in a three-roll mill

These calculations show that tensile stresses arise in the middle portion of the blank, whilst compressive stresses occur close to the contact surfaces (Fig. 282). The maximum values of the tensile stresses are given in Table 21.

When metal is rolled between three rolls, the layout of the plastic zones corresponds to the field shown in Fig. 283. Such an arrangement of the plastic zones, as in the case of the field shown in Fig. 280,

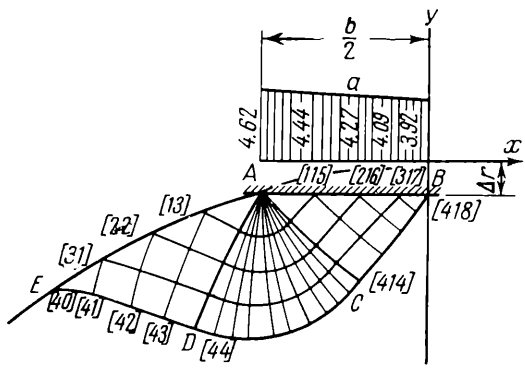

Fig. 284. Slip lines emerging from the contact surface to the cylindrical surface of the blank when $\frac{b}{2r} \approx 0.25$ ($a - p : k$ diagram) (M. Brovman)

satisfies the kinematic conditions on the boundary of the slip lines and, by virtue of a well-known theorem in the theory of plasticity, gives the upper value of the stress on the boundary.

In fact, the normal and tangential displacements on the contact surface are $v_r = \text{const.}$ and $v_t = 0$ respectively (which corresponds to the case of sticking), whilst the non-plastic zones are pressed out from the centre as a rigid body.

The method of calculating the contact pressure for this case of rolling is discussed in a work by A. Tselikov, V. Lugovskoi and E. Tretyakov.

In choosing formula (VIII.53) Prandtl assumed that the slip lines, whilst emerging from the contact surface to the free surface, rotate through an angle equal to $\frac{\pi}{2}$ (see Fig. 26*a*). But owing to the fact that in cross rolling the free surface is not a plane but the surface of a cylindrical blank, the angle of rotation of the slip line is somewhat smaller. The above slip lines have been constructed by M. Brovman; using them, he investigated the effect of the factor just mentioned on the contact stresses (Fig. 284). Since the slip lines do not conform to a plane but to a cylindrical surface

the specific pressure is slightly reduced; at the middle of the contact surface the pressure decreases a little more than at the edge, owing to a somewhat smaller angle of rotation of the slip line when it emerges to a free surface. If we assume that for $\frac{b}{2r} \approx 0.25$ the flow of the metal occurs close to the contact surfaces, then, as follows from Fig. 284, the specific pressure in this case is

$$p \approx (3.92 \text{ to } 4.62)\, k$$

i.e., approximately 0.76 to 0.9 of the pressure calculated from formula (VIII.53).

Results agreeing closely with this are also shown by the curve of Fig. 281.

6. DIRECTION OF THE FORCES ACTING ON THE ROLLS DURING CROSS ROLLING

Depending on the required change in the shape of the component being rolled, the axes of the rolls during cross rolling can be set either parallel to the axis of the component (Fig. 285) or inclined to

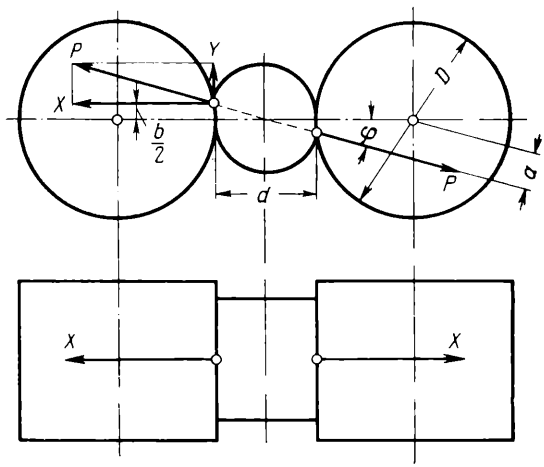

Fig. 285. Direction of the forces acting on the rolls during cross rolling when the axes of the rolls and the blank are parallel

it (Fig. 286). But at the same time they must be located in the meridional planes, i.e., in the planes passing through the axis of the component being rolled.

In both cases of rolling the direction of the forces acting on the rolls is determined from the condition of equilibrium of the blank

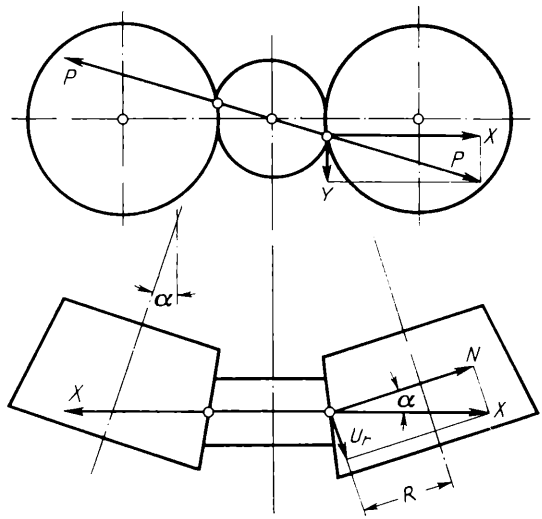

Fig. 286. Direction of the forces acting on the rolls during cross rolling when the roll axes are inclined to the blank axis in the meridional plane

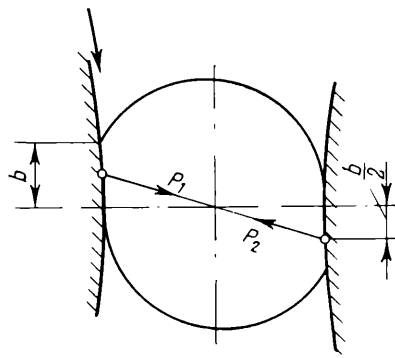

Fig. 287. Direction of the resultant forces applied to the rolled metal during the cross rolling process

being rolled. We replace the action of the rolls on the blank by corresponding forces: the resultant of the pressure of the left-hand roll on the blank is denoted by P_1, and that of the righ-hand roll by P_2. We assume that the point of application of these forces is located in the middle of the segment b (Fig. 287).

In view of the fact that, apart from the forces P_1 and P_2, there are no other forces acting on the blank, and that during the steady state rolling process the blank moves uniformly, the vector sum of the forces P_1 and P_2 must obviously be zero. It follows from this that the vectors of the forces P_1 and P_2 are equal and opposite. It follows from the symmetry condition that the forces P_1 and P_2 must pass through the axis of the blank.

The blank being rolled obviously exerts the same pressure on the rolls as plates or rolls exert on the blank, i.e., $P = P_1 = P_2$ (see Fig. 285).

We denote the angle of inclination of the force P to the line connecting the centres of the rolls by φ, and resolve the force P into horizontal and vertical components. The force acting on the roll in the horizontal direction is then

$$X = P \cos \varphi$$

whilst the force in the vertical direction is

$$Y = P \sin \varphi$$

The angle φ can be determined from the quantity b calculated previously

$$\tan \varphi = \frac{b}{d} \qquad \text{(VIII.58)}$$

The torque which must be applied to each roll to drive it, when the friction force in the bearings is not taken into account, equals (see Fig. 285):

$$M = Pa$$

or

$$M = P \frac{D+d}{2} \sin \varphi \approx P \frac{D+d}{2} \frac{b}{d} \qquad \text{(VIII.59)}$$

The results just obtained are valid when the rolls are inclined in the meridional plane to the axis of the blank (Fig. 286). Only in this case the axial force is given by

$$U_r = X \sin \alpha \qquad \text{(VIII.60)}$$

where α is the angle of inclination of the roll axis to the axis of the component being rolled.

The torque required to drive the roll is determined in this case by the equation

$$M = YR + X\frac{b}{2}\cos\alpha \qquad \text{(VIII.61)}$$

where R is the radius of the roll in the section where the resultant of the metal pressure is applied.

Substituting the values of X and Y given above into this equation we obtain

$$M = P\left(R\sin\varphi + \frac{b}{2}\cos\varphi\cos\alpha\right) \qquad \text{(VIII.62)}$$

In a similar manner we can find the equation of the forces and torques required to drive the rolls when metal is rolled between three

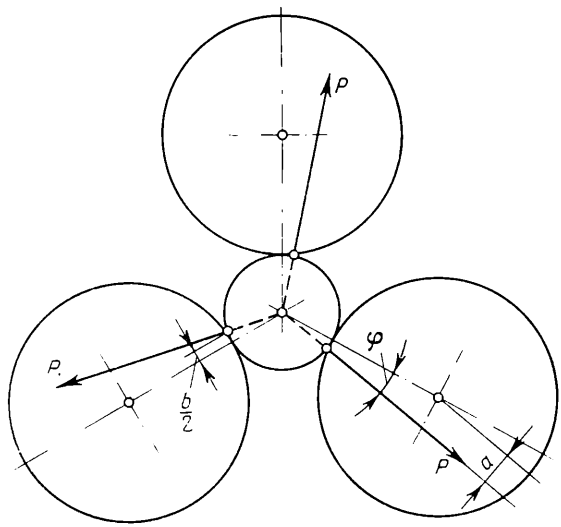

Fig. 288. Direction of the forces acting on the rolls during the cross rolling of metal in a three-roll mill

or more rolls. In all these cases the direction of the forces is determined from the condition that the resultant of the pressure exerted by the metal on the roll is found on the line passing through the axis of the rolled article and through the point where the resultant force P is applied to the roll (Fig. 288).

7. DIRECTION OF THE FORCES ACTING ON THE ROLLS DURING HELICAL ROLLING

There are two typical cases as regards the direction of forces during helical rolling: the metal being rolled does not meet any external resistance to its axial advance; and there is a resistance to the axial

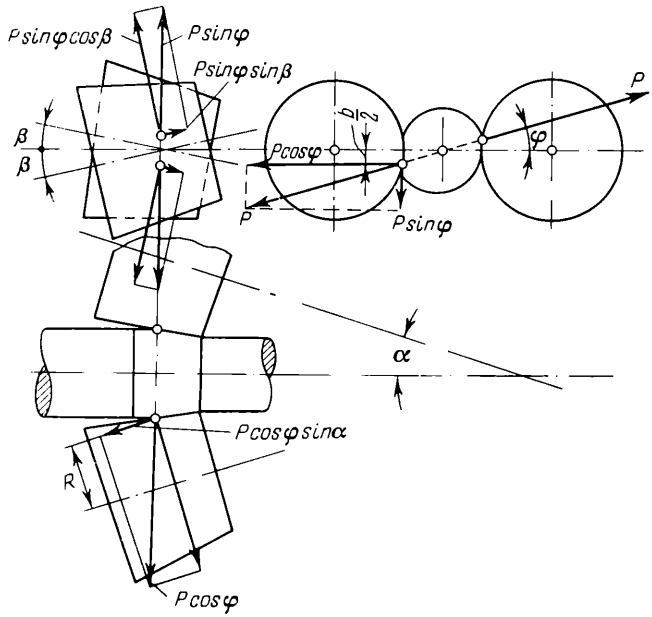

Fig. 289. Direction of the forces acting on the rolls for helical rolling in the absence of external axial resistance. Force vectors in the top left projection are scaled up

advance of the metal. The first case is possible when rolling is carried out without a mandrel or when rolling is carried out on a long mandrel which is free to move with the tube being rolled. The second case occurs when rolling on a short mandrel set against a bar (piercing or plugging mills).

The first case of rolling differs from the cases of cross rolling considered earlier in that the axes of the rolls are not located in the meridional plane but make an angle β with it (Fig. 289). Because of this inclination axial forces will act on the rolls. The magnitude and direction of these forces are determined from the condition that if there is no external axial resistance to the motion of the blank, then the resultants of the pressure of the metal on the rolls, i.e., the forces P, must lie in a plane perpendicular to the axis of the blank. The

projection of these forces on to the direction perpendicular to the principal meridional plane, equal to $P \sin \varphi$ (Fig. 289), provides the tangential force $P \sin \varphi \cos \beta$ on the roll, as well as the axial force $P \sin \varphi \sin \beta$.

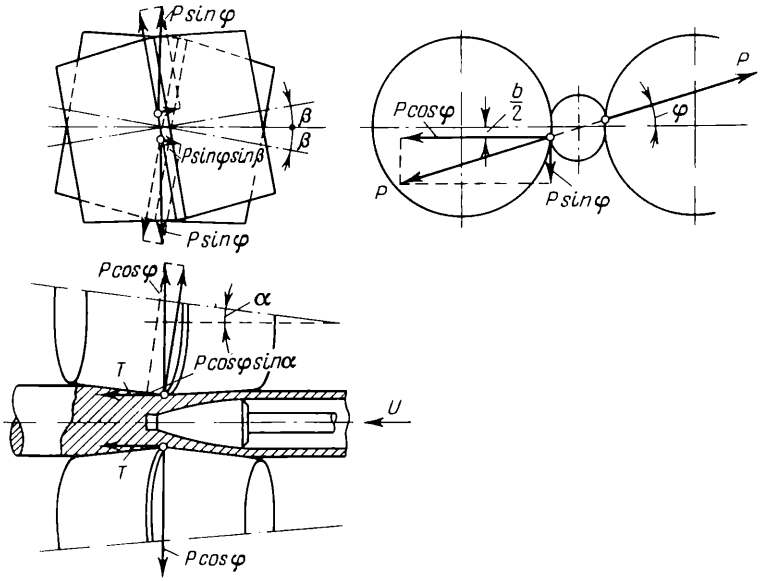

Fig. 290. Direction of the forces acting on the rolls of a piercing mill

If at the same time the rolls are set at an angle to the axis of the blank in the meridional plane, then the total axial force on each roll, from equation (VIII.60), is

$$U_r = P \cos \varphi \sin \alpha - P \sin \varphi \sin \beta \qquad \text{(VIII.63)}$$

The torque required to drive the roll is

$$M = P \left(R \sin \varphi \cos \beta + \frac{b}{2} \cos \varphi \cos \alpha \right) \qquad \text{(VIII.64)}$$

The second case of helical rolling, i.e., when the rolled metal is resisted by a short mandrel set against a bar, differs from the case just considered in that additional forces parallel to the axis of the blank act on the rolls. These forces are equal to the axial force arising in the mandrel. If this axial force in the mandrel is denoted by U_{man}, then in a mill with two rolls the following force acts on each roll (Fig. 290):

$$T = \frac{U_{man}}{2}$$

Then, from equation (VIII.63), the total axial force on the roll is

$$U_r = T\cos\alpha + P(\cos\varphi\sin\alpha - \sin\varphi\sin\beta) \qquad \text{(VIII.65)}$$

If we use equation (VIII.64), the torque required to drive the roll can be expressed as:

$$M = P\left(R\sin\varphi\cos\beta + \frac{b}{2}\cos\varphi\cos\alpha\right) + TR\sin\beta \qquad \text{(VIII.66)}$$

Let us consider the direction of the forces acting on the rolls when the axial displacement of the blank being rolled is secured not as

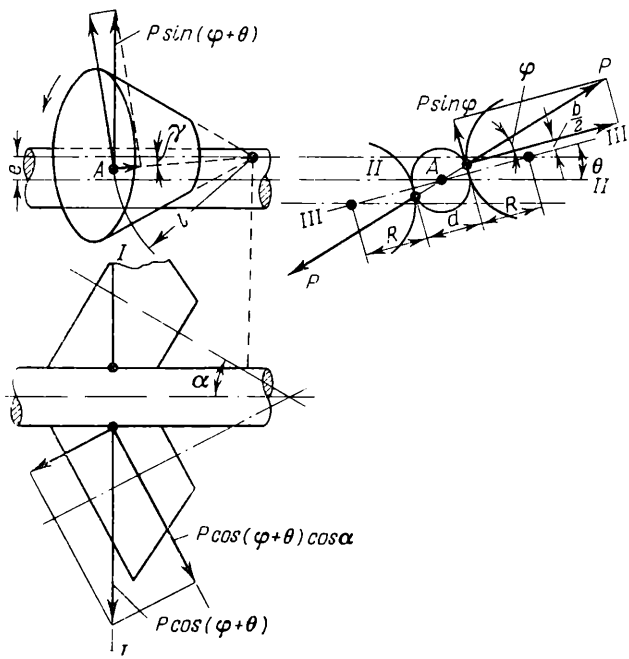

Fig. 291. Direction of the forces acting on the rolls during helical rolling when the roll axes are displaced relative to the blank axis

a result of the rolls' inclination to the meridional plane, but as a result of their axes being displaced relative to this plane (see Fig. 265).

In this case, when there is no axial resistance to the blank, the force acting on the roll is made up of two vectors (Fig. 291):

$$U_r \approx P\cos(\varphi + 0)\sin\alpha - P\sin(\varphi + 0)\sin\gamma \qquad \text{(VIII.67)}$$

where φ is the angle between the direction of the force P (resultant of the pressure of the metal on the rolls) and the line

connecting the centres of the rolls in the plane *I-I*, which is perpendicular to the axis of the blank and passes through the point *A* where the resultant of the pressure of the metal acting on the rolls is applied

θ is the angle between the meridional plane *II-II* drawn through the axis of the blank parallel to the axes of both rolls, and the line connecting the centres of the rolls in the plane *I-I* or the plane *III-III*

α is the angle of inclination of the axes of the rolls to the axis of the blank

γ is the angle between the axis of the blank and the generatrix of the cone of the roll which passes through the point *A*.

The angles φ, θ and γ can be found from the following expressions:

$$\left.\begin{aligned} \sin\varphi &= \frac{b}{d} \\ \sin\theta &= \frac{2e}{2R+d} \end{aligned}\right\} \qquad \text{(VIII.68)}$$

$$\sin\gamma = \frac{e - \frac{d}{2}\sin(\varphi+\theta)}{l} \qquad \text{(VIII.69)}$$

where e is the distance between the plane *II-II* and the plane drawn through the axis of the rolls parallel to the plane *II-II*

l is the distance from the vertex of the cone of the roll to the point *A*.

It is of interest to compare this case of the direction of the forces acting on the rolls with the preceding case (Fig. 289). If the forces acting on the rolls are projected on to the plane *III-III* and the plane perpendicular to it, then the direction of the forces can be represented by the diagram shown in Fig. 289. The angle β in the diagram in this case is analogous to the angle γ, and is only located in the plane perpendicular to the plane *III-III*. It can be determined from the equation

$$l\sin\beta = \frac{e}{\cos\theta} - \left(\frac{b}{2} + \frac{d}{2}\tan\theta\right) \qquad \text{(VIII.70)}$$

If in view of the smallness of the angle θ we assume that $\cos\theta \approx 1$, then $\beta \approx \gamma$.

In this case the force on the roll is

$$U_r \approx P\cos\varphi\sin\alpha - P\sin\varphi\sin\beta \qquad \text{(VIII.71)}$$

The torque required to drive the roll is determined from equation (VIII.64)

If on its way the blank meets a resistance in the form of a mandrel, then the effect of the force T must be considered in calculating U_r and M, as was done in deriving equations (VIII.65) and (VIII.66).

8. DIRECTION OF THE FORCES ACTING ON THE DISKS OF PIERCING DISK MILLS

From the condition of equilibrium of rolled blank and mandrel, considered above in the case of a piercing mill with skew rolls, it follows that the force acting on the blank due to each disk can be reduced to two resultant forces P and T, of which the first lies in a plane perpendicular to the axis of the blank, whilst the second is directed along its axis (Fig. 292).

Remembering that action equals reaction and that the blank being rolled exerts the same pressure on the disks as the disks exert on the blank, the pressure of the blank on each disk can also be expressed by the two forces P and T (Fig. 293) which are equal and opposite to the forces acting on the blank.

We resolve the forces P and T acting on the disks in three mutually perpendicular directions.

The horizontal pressure exerted by the blank on the disks, perpendicular to their axes, is:
on the first disk

$$X_1 = P_x + T_x$$

or

$$X_1 = P \cos \psi \sin \beta + \frac{U}{2} \cos \beta \qquad \text{(VIII.72)}$$

on the second disk

$$X_2 = P_x - T_x$$

or

$$X_2 = P \cos \psi \sin \beta - \frac{U}{2} \cos \beta \qquad \text{(VIII.73)}$$

where ψ is the angle between the force P and the horizontal plane, which can be determined (see Fig. 293) from the equation

$$\tan \psi = \frac{e}{r_0} \qquad \text{(VIII.74)}$$

where e is the distance from the plane of rolling to the point of application of the resultant of the pressure exerted by the disk on the blank

r_0 is the radius of the blank at the section where the resultant is applied.

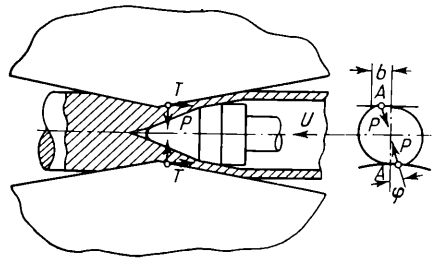

Fig. 292. Direction of the resultants of the pressure and friction forces applied by the rolls to a rolled blank in a piercing mill

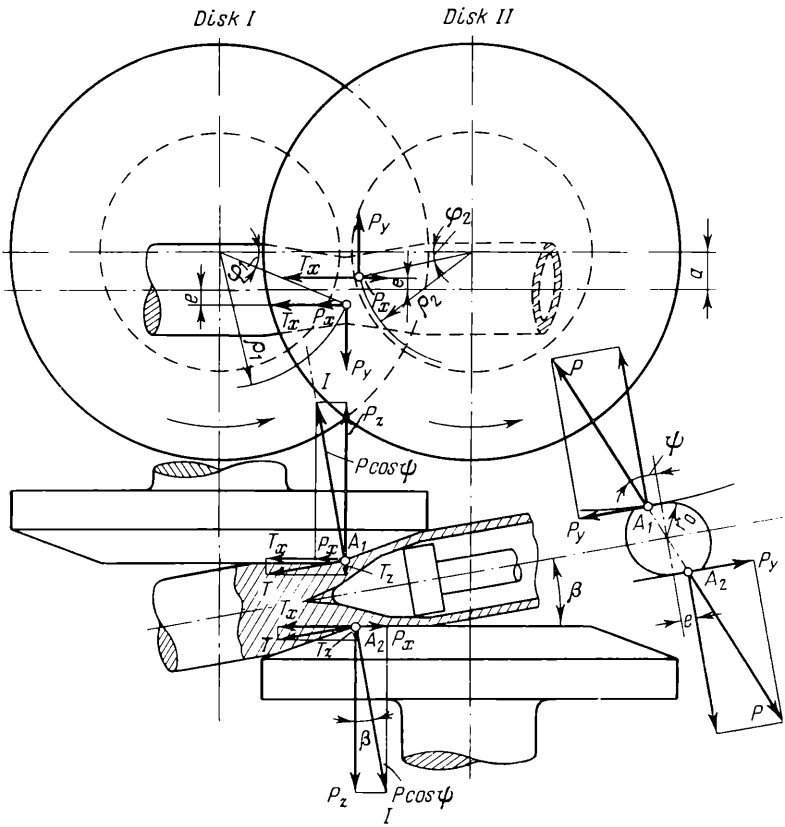

Fig. 293. Forces acting on the rolls in a piercing disk mill

The vertical pressure is the same for both disks, equalling

$$Y_1 = Y_2 = P_y$$

or

$$Y_1 = Y_2 = P \sin \psi$$

The axial pressure on the disk is:

$$Z_1 = P_z - T_z = P \cos \psi \cos \beta - \frac{U}{2} \sin \beta \qquad \text{(VIII.75)}$$

on the first disk, and

$$Z_2 = P_z + T_z = P \cos \psi \cos \beta + \frac{U}{2} \sin \beta \qquad \text{(VIII.76)}$$

on the second disk.

Knowing the pressure on the disks in all three directions we can easily calculate the torque required to drive the disks. It follows from Fig. 293 that the torque necessary to rotate the disks, neglecting the friction forces in the bearings, is:

$$M_1 = Y\rho_1 \cos \varphi_1 + X_1\rho_1 \sin \varphi_1$$

or

$$M_1 = P\rho_1 \sin \psi \cos \varphi_1 + P(a + e) \cos \psi \sin \beta + \frac{U}{2}(a + e) \cos \beta$$

for the first disk, and

$$M_2 = Y\rho_2 \cos \varphi_2 - X_2\rho_2 \sin \varphi_2$$

or

$$M_2 = P\rho_2 \sin \psi \cos \alpha_2 + P(a + e) \cos \psi \sin \beta + \frac{U}{2}(a - e) \cos \beta$$

for the second disk.

It follows from these equations that to drive the first disk, which is on the entry side of the blank, a larger torque is needed than for the second disk which is on the mandrel side.

9. EXPERIMENTAL DATA ON THE FORCES ACTING ON THE ROLLS DURING HELICAL ROLLING OF TUBES

A number of experimental investigations have been carried out during recent years into the forces and energy consumption during helical rolling of tubes in tube rolling mills of various designs.

One of the first and most detailed investigations into the forces in *piercing mills* under production conditions was made by N. Lomakin. He studied the effect of different factors on the pressure exerted by

the metal on the rolls, and on the axial force acting on the mandrel when tubes 124 to 235 mm in diameter, and of different steels, were rolled in a piercing mill with rolls 860 to 920 mm in diameter. Some typical data from these investigations are presented in Table 22.

Table 22

The Pressure of Metal on the Roll and the Axial Force Acting on the Mandrel During the Rolling of Tubes in Piercing Mills (After N. Lomakin)

Dimensions of tube, mm		Diameter of original blank, mm	Steel	Temperature, °C	Pressure of metal on roll, tons	Axial force on mandrel, tons
diameter	wall thickness					
124	11	115	1010	1,225-1,240	77-80	15-19
153	12	150	1010	1,200-1,215	62-72	21-22
170	10	150	1010	1,225-1,230	65-71	34-35
230	13	222	1010	1,200-1,220	108-115	—
131	22	130	ШХ15	1,130-1,140	84-100	—
162	27	170	ШХ15	1,120-1,140	95-97	—
208	47	193	30ХГСА	1,220	77-89	—
235	29	222	15М	1,190-1,220	125-134	—

Analyzing the results of these investigations N. Lomakin noted that, on average, the ratio of the axial force on the mandrel to the pressure exerted by the metal on the roll is

$$\frac{U}{P} \approx 0.37$$

Experimental investigations into the forces arising in a piercing mill are of great interest. Certain results of the investigations carried out by A. Geleji and others are given in Table 23.

Table 23

The Pressure of Metal on the Roll and the Axial Force Acting on the Mandrel in the Case of Tube Rolling in a Piercing Mill, Using Billets of Steel Ст. 35.29 at Temperature 1.230 to 1.260°C

Diameter of billet, mm	Diameter of tube, mm		Pressure on the roll, tons		Axial force on mandrel tons
	external	internal	principal	auxiliary (third)	
240-231	241	167	134	28	36
203	198	139	192	22	27
204	201	113	82	15	25

The energy consumption in piercing mills was investigated experimentally by I. Fomichev, Y. Vatkin, M. Sonkin and others. The results of the investigations by M. Sonkin are given in Fig. 294 in the form of curves of specific energy consumption depending on the reduction ratio in the process of piercing the blank into a tube.

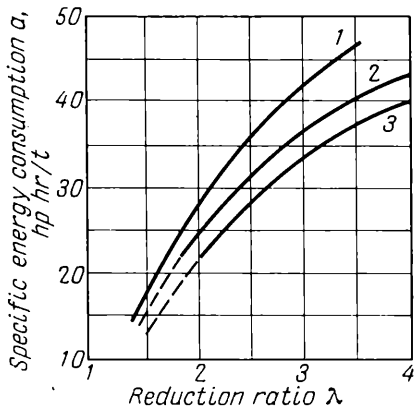

Fig. 294. Curves of specific energy consumption vs reduction ratio for the piercing of mild steel blanks having diameters of 130 mm (*1*), 170 mm (*2*) and 222 mm (*3*) using piercing mill 200

V. Osadchy and A. Gleiberg studied the distribution of the specific pressure on the roll during the rolling of blanks in a piercing mill. According to their data the mean specific pressure during the rolling of tubes of plain carbon steel was 7 to 13 kg/mm^2, whilst for stainless steel it reached 15 to 16 kg/mm^2.

Table 24

The Pressure of Metal on the Roll, the Power Used and the Axial Force Acting on the Mandrel During Tube Rolling on an Elongator

Diameter of initial tube, mm		Diameter of finished tube, mm		Reduction ratio	Maximum pressure on roll, tons	Maximum power used, kW	Maximum pressure on mandrel, tons
external	internal	external	internal				
385	230	385	370	1.48	318	1,945	—
500	375	490	475	1.75	305	3,430	46
550	390	547	531	2.0	290	3,000	60
620	435	615	600	1.9	350	3,810	54
625	100	638	435	1.87	303	2,550	44

Note. The material of the tube: steel Д; rolling temperature: 1,130 to 1,140°C; diameter of the rolls: 730 mm; speed of rotation of rolls: 27.5 to 34 rpm.

Experimental investigations into the forces in *elongators* during the rolling of thick-walled tubes and tubes with walls of smaller thickness were conducted by O. Plyatskovsky and others. Some results of these investigations are presented in Table 24.

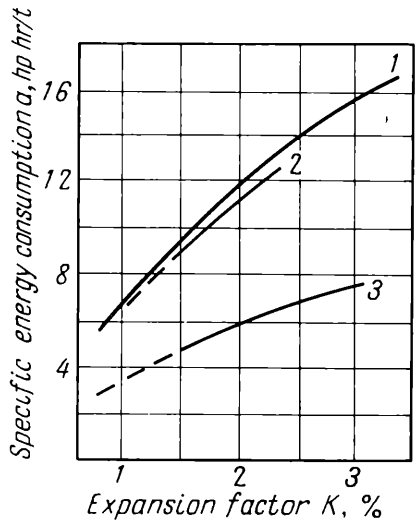

Fig. 295. Variation of specific energy consumption with the expansion factor of the outside tube diameter in the expansion rolling of tubes with diameters 127 to 140 mm and wall thicknesses 4.5 to 5 mm (*1*); 152 to 159 × 5 to 6 mm (*2*), and 219 × 8 to 10 mm (*3*):

$K = \frac{D_1 - D_0}{D_0} 100\%$, where D_0 and D_1 are the outside diameters of the tube before and after expansion. Tube material: steels 1010, 1020 and 1035

Experimental investigations into the forces in plugging mills were conducted by V. Buryanov, V. Osadchy and others. They measured the pressure of metal on the rolls under production conditions on a plugging mill of tube rolling unit 400. Some results from these investigations are given in Table 25.

The energy consumption during the rolling of tubes 127 to 219 mm in diameter, made of mild steels 1010, 1020 and 1035, was investigated by M. Sonkin. The results of this investigation are represented in the form of curves of the specific energy consumption as it depends on the pipe expansion factor (Fig. 295).

The forces arising in *three-roll plugging mills* working with a long mandrel were investigated by P. Teterin, F. Danilov and Y. Manegin. During the rolling of tubes of low carbon steel and ШХ15 steel—73 to 159 mm in diameter and with a wall thickness of 11 to 25 mm—

Table 25

The Pressure of Metal on the Roll During Tube Rolling in a Plugging Mill Following an Automatic Mill

Diameter and wall thickness of initial tube, mm	Diameter and wall thickness of tube after rolling, mm	Steel	Temperature of rolling, °C	Mean pressure of metal on roll, tons
242 × 7	255 × 7	10-20	860-835	18
242 × 17	254 × 17	10	1,000-985	20.5
266 × 7	280 × 7	20	870-830	14
268 × 17	279 × 17	20	1,020-990	20
270 × 45	277 × 45	20	1,070-1,040	20

the pressure exerted by the metal on the roll was found to be within the limits 8.7 to 34.4 tons. Here the diameter of the rolls was 320 to 489 mm, the height of the swell was 8 to 12 mm, and the peripheral velocity was 2 to 3.2 m/s.

The energy consumption in *an expanding mill* was investigated by K. Gruber. During the expansion of mild steel tubes, from an initial diameter of ~360 mm and a wall thickness of ~12 mm to a final diameter of ~450 to 460 mm and a wall thickness of ~9 mm, the mean loading on the drive shaft was 480 to 570 kW at the roll speed of 48 rpm. The temperatures at the beginning and end of the rolling process were 1,080 and 870°C respectively.

10. EXPERIMENTAL DATA ON THE FORCES ACTING ON THE ROLLS DURING CROSS AND HELICAL ROLLING OF SOLID COMPONENTS

The forces and energy consumption in *mills for rolling spheres*, designed by VNIIMETMASH, were investigated by S. Granovsky, I. Pobedin, V. Yefanov and others. According to these investigations the maximum pressure exerted by metal on the roll during the rolling of spheres of ШХ15 steel, at a temperature of 850°C, was within the following limits:

Diameter of sphere, mm	(inches)	Pressure, tons
28	(1 1/16)	6.5 to 10
53	(2)	16.5 to 22

In the first case the diameter of the rolls was 190 to 220 mm, and in the second it was 280 to 300 mm. The power consumed during the rolling of spheres 28 mm in diameter, at a rotational speed of 150 rpm, was 30 to 33 hp; during the rolling of spheres 53 mm in diameter, at a rotational speed of 100 rpm, it was 230 hp.

The results dealing with the pressure of metal on the roll and the power consumed during the rolling of mild steel spheres (for ball mills) 80 mm in diameter are presented in Table 26.

Table 26

The Pressure of Metal on the Roll During the Rolling of Spheres and the Power Consumed

Temperature of rolling, °C	Maximum pressure on roll, tons	Maximum power consumed, hp
840	40	246
920	35.5	210
1,100	28.5	152

Note. The speed of the rolls is 47 rpm.

Investigations into the forces and energy consumption in *a three-roll mill for helical rolling of periodic profiles* were carried out by G. Livshits, V. Anisiforov, I. Kazanskaya and V. Zhavoronkov. Certain results of the investigations by V. Zhavoronkov into the pressure of metal on the roll during the rolling of blanks 10 to 50 mm in diameter on three-roll mills 10 and 70 are presented in Table 27.

Table 27

The Pressure of Metal on the Roll During the Rolling of Periodic Profiles in a Three-Roll Mill

Diameter of initial blank, mm	The reduction factor of blank diameter, $\frac{d_0}{d_1}$	Steel	Pressure of metal on roll, tons
10	2.0	ШХ9	0.81
11	1.5	ШХ9	0.76
34	1.75	20	2.53
40	1.66	35	2.35
40	1.66	40ХН	5.50
50	1.47	50	5.16

The forces arising in *mills for rolling the teeth of gear wheels* were investigated by A. Kuzmin and M. Vasilchikov during hot rolling of helical teeth with a modulus of 1.5 mm, of steel 40XH, with an axial feed (using the bar method) of 1 to 3 mm per half a revolution of the blank (Table 28).

Table 28

Forces Arising During Hot Rolling of Gear Teeth

Diameter of blank, mm	Pressure of metal on roll, tons	Torque on roll, kgm
23.4	0.38-0.55	73-127
38.4	0.6-1.1	82-148
52.6	0.75-1.15	80-140
66	0.73-1.1	70-122

Note. Diameter of the pitch circle of the rolls is 184 mm; the number of teeth, 115.

During the rolling of straight teeth with a modulus of 3 mm with a radial feed (piece method), the number of teeth being 45 and the width being 30 mm, the pressure on the roll was 0.75 to 2.2 tons,

Table 29

Forces Acting on the Rolls During the Rolling of Screws with Different Threads

Type and dimensions of thread	Dimensions of rolls, mm		Material of rolls (steel)	Temperature of blank, °C	Pressure of metal on roll, tons	Torque, kgm
	outside diameter	length				
Trapezoidal:						
24 × 6	181.5	75	Ст. 5	20	12.7	~145
36 × 6	202	74	30	20	7-9.3	100-120
Semicircular 22 × 6	200	55	35	20	16-17	200-265
Trapezoidal:						
36 × 6	196	72	30	1,000	3.1-6.1	140-190
36 × 10	181	74	45	1,000	3.4-3.9	58-62
Rectangular 57 × × 6.35	168.5	80	30	850	3.1	35
Blank of hob cutter (t = 5 mm)	220	110	P18	1,100	17.8	264
Ditto	220	147	Ст. 3	1,000	20.4	350
Semicircular 104 × × 24	192	120	45	1,000	11	360

whilst the torque on the roll was 85 to 195 kgm (the pitch diameter of the rolls being 201 mm). The temperature at the beginning of rolling was 1,050 to 1,100°C; at the end of the rolling process it was 850 to 950°C.

During gear rolling the magnitude of the feed has an important effect on the force; as the feed increases the force increases as well.

The forces arising in *mills for rolling screws* with a large pitch, both during hot and cold rolling, were investigated in detail by M. Volkov and F. Kirpichnikov. A few of the results of these investigations, for rolling screws on a two-roll mill with an axial feed, by a method developed by VNIIMETMASH, are given in Table 29. During these investigations the velocity of cold rolling was within the limits 8 to 15 m/min, whilst the velocity of hot rolling was 20 to 40 m/min.

TO THE READER

Mir Publishers would be grateful for your comments on the content, translation and design of this book. We would also be pleased to receive any other suggestions you may wish to make.

Our address is: Mir Publishers, 2, Pervy Rizhsky Pereulok, Moscow, U.S.S.R.

Printed in the Union of Soviet Socialist Republics